



HAL
open science

Polypeptoids as simplified analogues of antimicrobial peptides

Pedro Javier Salas Ambrosio

► **To cite this version:**

Pedro Javier Salas Ambrosio. Polypeptoids as simplified analogues of antimicrobial peptides. Polymers. Université de Bordeaux, 2021. English. NNT : 2021BORD0185 . tel-03917120

HAL Id: tel-03917120

<https://theses.hal.science/tel-03917120>

Submitted on 1 Jan 2023

HAL is a multi-disciplinary open access archive for the deposit and dissemination of scientific research documents, whether they are published or not. The documents may come from teaching and research institutions in France or abroad, or from public or private research centers.

L'archive ouverte pluridisciplinaire **HAL**, est destinée au dépôt et à la diffusion de documents scientifiques de niveau recherche, publiés ou non, émanant des établissements d'enseignement et de recherche français ou étrangers, des laboratoires publics ou privés.

THÈSE PRÉSENTÉE
POUR OBTENIR LE GRADE DE

DOCTEUR DE

L'UNIVERSITÉ DE BORDEAUX

ÉCOLE DOCTORALE DES SCIENCES CHIMIQUES

SPÉCIALITÉ POLYMERES

Par Mr Pedro Javier SALAS AMBROSIO

**Polypeptoids as simplified analogues of
antimicrobial peptides**

Sous la direction du Dr. Colin BONDUELLE, Université de Bordeaux
co-directeur : Pr. Pierre VERHAEGHE, Université Paul Sabatier

Soutenue le 9 juillet 2021

Membres du jury :

M. TATON, Daniel	Professeur, Bordeaux INP	President
Mme. AMBLARD, Muriel	Directrice de recherche, IBMM, UMR CNRS 5247	Rapporteur
Mme. LEFAY Catherine	Maître de Conférences, Aix-Marseille Université	Rapporteur
Mme. ALVES Isabel	Directrice de recherche, Bordeaux CBMN CNRS 5248	Examineur
M. DUPUY Bruno	Directeur de recherche, Université de Paris, Institut Pasteur	Examineur
M. MORENO Abel	Professeur, UNAM Instituto de Química, Mexique	Examineur

Titre : Polypeptoides comme analogues simplifiés de peptides antimicrobiens naturels

Résumé :

Les peptides antimicrobiens (AMP) sont des biocides naturels produits notamment par les micro-organismes pour éliminer sélectivement leurs compétiteurs. L'efficacité des AMPs s'explique par leur capacité à déstabiliser les membranes, une propriété physicochimique liée à leur caractère amphiphile. Jusqu'à présent, le développement industriel des AMPs reste limité et leur sensibilité aux protéases empêche leur administration thérapeutique par voie orale. En reproduisant leur composition chimique ou certaines de leurs caractéristiques structurales, des analogues polymériques ont été proposés pour tenter de lever ces limitations, comme les polymères d'acides aminés qui sont biodégradables et biocompatibles.

Cette thèse présente la préparation de nouveaux copolypeptoïdes antimicrobiens par polymérisation par ouverture de cycle (ROP) de *N*-carboxyanhydrides-*N*-alkylés (NNCA) portant des substituants hydrophobes ou cationiques. Ces monomères NNCA portant des groupements alkyles hydrophobes (méthyle, isopropyle, cyclohexyle, benzyle, *p*-nitrobenzyle et méthylthioéthyle) ou des groupements alkyles précurseurs d'unités cationiques (*Cbz*-aminoéthyle et *Cbz*-aminobutyle) ont été préparés en deux étapes de synthèse : 1) amination réductrice avec de l'acide glyoxylique, 2) cyclisation en NNCA via la méthode de Leuchs grâce à l'introduction d'une protection *N*-Boc. Cette méthodologie a permis de préparer 9 monomères dont la polymérisation a été étudiée : nous avons d'abord déterminé les cinétiques de cette réaction dans le DMF et nous avons ensuite mis en œuvre des réactions de copolymérisation en mélangeant les NNCA. Cette approche nous a permis de préparer des copolypeptoïdes plus ou moins hydrophobes et d'inclure ces polymères dans des architectures différentes telles que des conjugués linéaires, des structures cycliques ou des structures étoilées.

Selon l'OMS, les infections bactériennes ont atteint des niveaux d'incidence très élevés dans le monde entier et sont responsables d'une mortalité inquiétante. Un des micro-organismes pathogènes particulièrement inquiétant est *Clostridioïdes difficile*, une bactérie Gram-positif responsable de colites pseudo-membraneuses, une infection nosocomiale fréquemment mortelle chez la personne âgée. L'objectif de cette thèse a été de développer une approche de chimie médicinale pour concevoir des copolypeptoïdes antimicrobiens capables de tuer cette bactérie. Dans un premier temps, nous avons préparé des bibliothèques de copolymères linéaires afin d'étudier les relations structure-activité antimicrobienne (RSA) en faisant varier la nature des chaînes latérales, la nature de l'initiateur, le degré de polymérisation, nous permettant de préparer des composés actifs dont les concentrations minimales inhibitrices (CMI) ont été déterminées vis-à-vis de *C. difficile*, parallèlement à leur cytotoxicité sur les cellules épithéliales intestinales Caco-2. Dans un deuxième temps, nous avons préparé des séries de copolypeptoïdes cycliques en développant une nouvelle méthodologie: la polymérisation par expansion de cycle en utilisant le LiHMDS. Cette nouvelle synthèse nous a permis de faire varier le contenu hydrophobe et la microstructure des copolymères peptoïdiques et de réaliser une seconde étude RSA par rapport

à des tests antimicrobiens. Finalement, les structures prometteuses et actives nous ont permis d'étendre notre approche de synthèse à d'autres architectures macromoléculaires: des structures dendritiques en étoile et des conjugués à des antibiotiques. Globalement, les études RSA ont montré que les copolymères linéaires et cycliques à microstructure aléatoire, contenant des groupements *N*-benzyle et *N*-aminobutyle présentaient l'activité antibactérienne la plus intéressante. Des tests antibactériens menés en parallèle sur d'autres germes nous ont enfin permis d'évaluer le spectre antibactérien.

Mots clés :

Polypeptoides, polymères antimicrobiens, polymérisation par ouverture de cycle, *N*-carboxyanhydrides, *C. difficile*, relations structure-activité, ingénierie macromoléculaire.

Title : Polypeptoids as simplified polymeric analogues of natural antimicrobial peptides

Abstract :

Antimicrobial peptides (AMP) are an interesting family of natural peptides mainly produced by microorganisms to eliminate their bacterial competitors. AMPs have demonstrated their effectiveness against all types of micro-organisms: the efficacy of AMPs is explained by their ability to destabilize membranes, a physicochemical property linked to their amphiphilic character. Until now, the industrial development of AMPs in pharmacy remains limited and their sensitivity to proteases prevents their therapeutic administration by oral route. By reproducing their chemical composition or certain structural characteristics, polymeric analogues have been proposed to try to overcome these limitations, such as amino acid polymers which are biodegradable and biocompatible.

This Ph.D. work presents the preparation of new antimicrobial copolypeptoids by ring-opening polymerization (ROP) of *N*-alkylated-*N*-carboxyanhydrides (NNCA) bearing hydrophobic and cationic substituents. These NNCA monomers bearing hydrophobic alkyl groups (methyl, isopropyl, cyclohexyl, benzyl, *p*-nitrobenzyl and methylthioethyl) or alkyl precursors of cationic units (*Cbz*-aminoethyl and *Cbz*-aminobutyl) were prepared in two synthetic steps: 1) reductive amination with glyoxylic acid, 2) cyclization into NNCA *via* the Leuchs method through the introduction of *N*-Boc protection. This methodology enabled us to prepare 9 monomers whose polymerization was studied: we first determined the kinetics of the ROP reactions in DMF and we implemented copolymerization reactions by mixing the NNCA monomers. Using this methodology, we developed a variety of copolypeptoids consisting of cationic and hydrophobic units at various ratios and designed copolymers with different macromolecular architectures such as linear-drug conjugates, cyclic structures or star-like structures.

According to the WHO, bacterial infections caused by resistant germs have reached very high levels of incidence worldwide, being responsible for a worrying mortality. One of the most problematic pathogens is *Clostridioides difficile*, a Gram-positive bacterium responsible for pseudomembranous colitis, a nosocomial infection that is frequently lethal in elderly patients. Current treatment consists in antibiotics that often present recurrences. The goal of this Ph.D. thesis was to develop a medicinal chemistry approach to design antimicrobial copolypeptoids capable of killing this pathogen. First, we prepared libraries of linear copolymers in order to study the structure-antimicrobial activity relationships (SAR) varying the nature of the side chains, the nature of the initiator, the degree of polymerization, enabling us to define a first series of active compounds whose minimum inhibitory concentrations (MIC) were determined towards *C. difficile* as well as their cytotoxicity on Caco-2 intestinal epithelial cells. In a second step, we prepared a series of cyclic copolypeptoids by developing a new methodology: the ring-expansion polymerization using LiHMDS. This new synthesis enabled us to access macrocyclic polymers and vary the hydrophobic content and microstructure of the peptoid copolymers, to perform a second SAR study with respect to antimicrobial tests on *C. difficile*. Finally, we extended our study to other macromolecular architectures: star-like copolymers and antibiotic drug conjugates.

Overall, SAR studies showed that linear and cyclic copolymers with random microstructure, containing *N*-benzyl and *N*-aminobutyl groups exhibited the most interesting antibacterial activity against *C. difficile*. Finally, antibacterial assays on other bacteria allowed us to evaluate a preliminary antibacterial spectrum of action.

Keywords:

Polypeptoids, antimicrobial polymers, ring-opening polymerization, *N*-carboxyanhydrides, *C. difficile*, structure-activity relationships, macromolecular engineering.

Unité de recherche

Laboratoire de Chimie des Polymères Organiques, UMR 5629

16 Avenue Pey-Berland, 33607

Pessac Cedex France

Acknowledgments

I would like to thank the members of the thesis jury for having accepted to evaluate my work. Thanks to the Consejo de Ciencia y Tecnología (CONACyT, México) for the scholarship to support my thesis.

I thank Sébastien Lecommandoux for having welcomed me to the LCPO as director of the laboratory and as leader of the Polymer Self-Assembly and Life Sciences team.

I thank very much to my thesis supervisors Colin Bonduelle and Pierre Verhaeghe for all your support since the beginning of the thesis project. Thank you for all the knowledge you share with me these years, I learned a lot from you during these three years, I will remember above all your vision of science, your discipline, your patience, your passion and your organization. I hope to have captured some of these qualities which I think are essential for a good researcher. I especially thank Colin for his advice, his dedication to me, his support, his mentorship, and our discussions about science and daily life.

I would like to thank all the permanent members of the team: Christophe, Bertrand, Jean-François, Olivier, Angela and Elisabeth. Thanks to you for allowing us to work in excellent conditions.

I thank all the people with whom I had the pleasure to collaborate: Bruno Dupuy and Antoine Tronnet for all the *C. difficile* tests, Marc Since for all the liposomal analyses, Sandra Bourgeade-Delmas for the cytotoxic assays and Jean-Luc Stigliani for the DFT calculations.

I thank all the teams of the LCPO, scientific or administrative, which allow us to work in optimal conditions. Many thanks to Amélie Vax-Weber, Anne-Laure Wirotius, Sylvain Bourasseau, Dominique Richard, Séverine Saint-Drenant, Corinne Goncalves-de-Carvalho, Claude Le Pierres, Bousquet Melanie and Loïc Petrault. And also I thank to Christelle Absalon and Yann Rayssac from the ISM.

This period of my life would not have been the same without the presence of great friends:

I want to thank to my dear friend Nadia M. for her friendship and for the amazing time we enjoy and for including me in her family, I will always treasure your friendship.

Dianita my friend, I will always remember your friendship and the crazy moments at party, beach, parks, Paris and Toulouse, I am sure we will meet later. Thank you also Vusalita the three of us we have unforgettable times.

I thank you Mostafa for the crazy time in the lab and also for helping me a lot during the last important moments and for your friendship.

I want to thank also to Pablo for his advices and long discussion in our lunch breaks, gracias hombre! Espero vernos pronto!

I thank my friends Antoine and Marion for those amazing moments in Toulouse and also I want to wish you a very happy life together including to your lovely coming baby!

I want to thanks to my friend Gerardo, one of the best mexicans I have met so far, we will meet later I am sure.

My friend Florent, it was one year that we met in Toulouse and for me that time is unfforgetable I thank you for your friendship and for all the happy moments we live together. I also want to thank Millad because of your friendship and joyful moments in our different trips the three of us.

My friend Iliana thank you very much for your advices about life and for all the happy moments in Toulouse and then in Paris, I will come to visit to you very soon to you and Gerardo. I want to thank Audrey, we met a short-time but it was enough to have a very nice moments, let's go to another party together with Gerardo!

My friend Tim it was a pleasure to meet you and have such a wonderful time sorrouded by beers, thank you for the happy moments, I wish you the best to you, Anna and your little shy cat.

Paul, than you for those amazing times in the lab sharing chemistry and after-work having some drinks, I am definetively going to Germany to see you again.

I want to thank to Samantha for those hapy moments in Bordeaux hanging out and having funny moments. This thanks also includes my friend, Julien, Sasha and Aime, for their friendship and lovely moments during this time in France.

I also want to thank to my friends Alfonso, Ray, Betsy, Monica, Angelita and much more friends in Mexico.

I thank also to all my colleagues: Samir, Pierre, Martin, Romane, Francis, Sifan, Boris, Leslie, Anouk, Ségolène, Marie, Esra, Chloé, Ting-ting, Hang, Manon, Florian, Christopher, Jérémy, Anne, David, Léa, Hanaé, Valentin, Clemence, Vaïana, Megi, Marie H., Clara, Miryam, Luzangel and all the others.

Me gustaría agradecer profundamente a toda mi familia que me ha apoyado durante todo este trayecto y que a pesar de la distancia los siento muy cerca de mí, en especial a mis padres Pedro Salas y Hormisdas Ambrosio, a mis hermanos Juan e Irene y a mi sobrino Santiago. Me gustaría agradecer también a mis tíos: Marcos, Juanita, Flavia, Ana, Rosita, Elías, Beto, Francisco por todo su apoyo. A mis primos Jorge, Josué, Edgar, por esas noches de diversión en línea.

Me gustaría agradecer especialmente a mi novia Angélica, hemos pasado mucho tiempo juntos, pero más separados y aun así seguimos en el mismo camino. Gracias por escucharme cuando lo necesitaba, apoyarme en los momentos difíciles y compartir esos momentos de felicidad.

This thesis was an important moment in my life, with a lot of investment, moments of happiness, enthusiasm but also moments of frustration, doubt or dejection. I firmly believe that I learned a lot and sincerely, thank you all!

TABLE OF CONTENTS

Objectif de la these	I
Aim of the thesis	VI
Abbreviations	XIII
Chapter 1 Synthetic polymers as simplified analogs of antimicrobial peptides	1
1 <i>Bacterial resistance to antibiotics</i>	1
2 <i>Clostridioides difficile</i>	4
3 <i>Antimicrobial Peptides (AMPs)</i>	10
3.1 AMPs modes of action.....	14
3.2 AMPs and membrane destabilization.....	15
3.3 Limitations of AMPs.....	17
4 <i>Synthetic antimicrobial polymers</i>	18
4.1 Synthetic polymers to mimic AMPs	19
4.2 Polymeric analogs of AMP as membrane disrupters and their related properties.....	22
5 <i>Polypeptide analogs of AMPs</i>	25
6 <i>Peptoids as analogs of AMPs with improved stability</i>	30
7 <i>Polypeptoids</i>	33
8 <i>References</i>	37
Chapter 2. Preparation of a small library of N-alkylated glycine N-carboxyanhydrides	64
1 <i>Bibliographical study</i>	64
1.1 NCA Preparation	64
1.1.1 Preparation of regular (non-alkylated) NCA	64
1.1.2 Preparation of N-alkylated NCA	66
1.2 Preparation of N-alkylated-N-Boc-glycine intermediates.....	69
2 <i>Preparation of N-alkylated-N-Boc-glycine intermediates</i>	71
2.1 Benzylation of glycine with benzyl bromide	71
2.2 2-Step synthesis of N-benzyl-N-Boc-glycine.....	71
2.3 Assays for the synthesis of N-benzyl-N-Boc-glycine from glyoxylic acid	73
2.3.1 Selection of the best operating procedure for the synthesis of 1	74
2.4 Synthesis of N-alkylated-N-Boc-glycine derivatives with hydrophobic character	75

2.5	Rotamers	76
2.6	Synthesis of <i>N</i> -alkylated- <i>N</i> -Boc-glycine derivatives as precursors of cationic building blocks 77	
3	<i>Preparation of the N-alkylated N-carboxyanhydrides (NNCA)</i>	78
3.1	Assays to produce NNCA	78
3.2	Synthesis of <i>N</i> -alkylated NCA with hydrophobic character	80
3.3	Synthesis of <i>N</i> -alkylated NCA with cationic character.....	81
3.4	Kinetics of the cyclization reactions of NNCA's	82
4	<i>Conclusion</i>	84
5	<i>Materials and methods</i>	85
5.1	Materials	85
5.2	Equipment and measurements	85
5.3	<i>N</i> -Alkylated-glycine derivatives	86
5.4	<i>N</i> -Alkylated- <i>N</i> -carboxyanhydrides	93
6	<i>References</i>	100
Chapter 3. Linear polypeptoid and their antimicrobial activity		105
1	<i>Preparation of polypeptoids by ROP from N-alkylated NCA</i>	106
1.1	Kinetics of the NNCA ROP	109
1.1.1	Influence of chloride impurities in polysarcosine	110
1.1.2	NCA: Influence of <i>N</i> -alkylation and <i>C</i> -alkylation.....	112
1.1.3	Influence of the <i>N</i> -alkyl group of NNCA's	114
1.1.4	Influence of bases to improve the kinetics in poly(sarcosine) synthesis	119
2	<i>Antimicrobial activity against C. difficile and structure-activity relationships of copolypeptoids with a controlled hydrophobic/cationic ratio</i>	122
2.1	Cationic poly(<i>N</i> -aminobutyl)glycine	123
2.2	Preparation of copolymers with varying hydrophobic/cationic ratio	127
2.3	Hydrophobic building block variation.....	131
3	<i>Optimization of the activity against C. difficile by implementing a macromolecular SAR approach</i> 138	
3.1	Nature of cationic side chain: <i>N</i> -(aminoethyl) versus <i>N</i> -(aminobutyl)	140
3.2	Polypeptoid vs polypeptide copolymers	142
3.3	M/I variation in poly(Nlys-Nphe) (DP 10, 20, 30) at 50% hydrophobic content	145
3.4	Initiator variation	149
3.5	Selectivity of the active compounds towards Caco-2 cells	152

3.6	Protease resistance of linear polypeptoids	154
4	<i>Conclusion</i>	156
5	<i>Materials and methods</i>	157
5.1	Materials	157
5.2	Equipment and measurements	157
5.3	Homopolypeptoids synthesis	159
5.4	Preparation of copolymers	168
5.4.1	Series of copolymers varying hydrophobic content	168
5.4.2	Hydrophobic side-chain variation	175
5.4.3	Series of copolymers varying hydrophobic content <i>N</i> -alkylated side chain and M/I	180
5.4.4	Cationic length variation	180
5.4.1	Copolymers synthesized by the ROP of NCA	181
5.4.2	Synthesis of copolymers varying the polymerization degree	183
5.4.3	Synthesis of copolymers varying the initiator	185
5.5	Antimicrobial assay	186
5.6	Cytotoxicity	187
5.7	Protease assay	188
5.8	Antimicrobial assay after trypsin treatment	188
6	<i>References</i>	190
Chapter 4. Macrocyclic polypeptoids and their antimicrobial activity		199
1	<i>Preparation of cyclic polymers using LiHMDS as a non-nucleophile strong base</i>	200
1.1	ROP of Sar-NCA with LiHMDS: kinetic study	203
1.2	Mechanisms insights and elucidation of the structure	207
1.3	Stability of cyclic polypeptoids with acidic conditions and propionylation	213
1.4	Comparison of LiHMDS initiated- versus <i>N</i> -heterocyclic carbene initiated-REP	218
1.5	Synthesis of polypeptoids varying the M/B ratio by LiHMDS-mediated REP	220
1.6	Preparation of cationic homopolymer	223
2	<i>Preparation of copolypeptoids</i>	225
2.1	Random copolymers varying the hydrophobicity	226
2.2	Block copolymers varying the hydrophobicity	228
3	<i>Antimicrobial assays</i>	230
4	<i>Liposome destabilization assay</i>	233
5	<i>Protease activity</i>	235
6	<i>Conclusion</i>	237

7	<i>Materials and methods</i>	238
7.1	Materials	238
7.2	Equipment and measurements	238
7.3	DFT calculations.....	239
7.4	Cyclic homopolypeptoids synthesis.....	243
7.4.1	Poly(Nme) kinetics studies	244
7.4.2	Mechanism study.....	245
7.4.3	Stability assays: HBr/TFA and Propionylation.....	246
7.4.4	Cationic cyclic polypeptoids	247
7.5	Copolypeptoid preparation.....	249
7.6	Antimicrobial assay.....	254
7.7	Cytotoxicity.....	255
7.8	Liposome destabilization	255
7.9	Protease assay.....	256
7.10	Antimicrobial assay after trypsin treatment.....	256
8	<i>References</i>	258
Chapter 5.	Macromolecular engineering of antimicrobial polypeptoids: star and drug-conjugate polymers	264
1	<i>Star-like polypeptoids as antimicrobial agents</i>	265
1.1	Preparation of star-like polypeptoids.	266
1.2	Star-like copolymers varying the arms number.....	269
1.3	Star copolypeptoids varying the hydrophobic content.....	275
1.4	Liposome destabilization assay	280
2	<i>Drug conjugates copolypeptoids as antimicrobial agents</i>	282
2.1	Preparation of polymer-drug conjugates	283
3	<i>Conclusions</i>	296
4	<i>Materials and methods</i>	297
4.1	Materials	297
4.2	Equipment and measurements	297
4.3	Star-like polysarcosine.....	298
4.4	Star-copolymers preparation.....	298
4.5	<i>Drug conjugates-copolymers preparation</i>	304
4.1	Antimicrobial assay.....	311
4.2	Cytotoxicity.....	311
5	<i>References</i>	312

General conclusions 317

Perspectives 320

Objectif de la these

Les peptides antimicrobiens (ou AMPs) sont des macromolécules composées d'acides aminés notamment produites par les micro-organismes pour lutter contre leurs compétiteurs.^{1,2} En tant que biocides naturels sélectifs, les AMPs sont potentiellement actifs contre tous les types de micro-organismes, notamment grâce à leurs propriétés de destabilisation membranaire.³ Jusqu'à présent, le développement industriel des AMPs reste limité pour diverses raisons, notamment leur coût de production^{4,5} et leur sensibilité aux protéases,^{6,7} empêchant par exemple leur administration par voie orale. Cette dernière limitation est un énorme inconvénient pour traiter les infections causées par des pathogènes du tube digestif tels que *Clostridioides difficile* (*C. difficile*).^{8,9}

Les polymères synthétiques sont certainement des candidats intéressants pour apporter une réponse efficace aux limites posées par la production et l'utilisation des AMPs. Dans cette perspective, la production de grandes quantités de substance active est un énorme avantage qu'apporte la chimie des polymères.¹⁰ Avec ces derniers, l'essor croissant de nouvelles méthodologies de synthèse permet de mimer de mieux en mieux les propriétés physico-chimiques des AMPs¹¹ et d'éviter la persistance des polymères dans l'environnement.¹⁰ Parmi ces polymères, ceux constitués d'acides aminés (appelés polypeptides) fournissent l'une des meilleures structures biomimétiques et bioactives pour de futures applications en science des matériaux.¹² En infectiologie, les polypeptides ont démontré des activités antimicrobiennes très prometteuses (y compris contre des bactéries résistantes aux médicaments) mais ils sont rapidement dégradés par les protéases.¹³

À cet égard, les "polypeptoïdes", également appelés poly(glycines *N*-substituées), sont des analogues *N*-alkylés des polypeptides pouvant offrir une résistance accrue aux protéases.¹⁴ La préparation des polypeptoïdes implique l'utilisation de monomères appelés *N*-carboxyanhydrides *N*-alkylés ou NNCAs qui sont polymérisés par un mécanisme d'ouverture de cycle (ROP) en utilisant des nucléophiles comme amorces.¹⁵ Cette voie de synthèse facilitée permet la préparation de copolymères bien définis^{16,17} dont on peut moduler la composition chimique, la taille et la topologie.

Dans ce travail de doctorat, l'objectif a été de préparer de nouveaux copolypeptoides antimicrobiens par ROP de NNCAs pour tuer sélectivement *C. difficile*. En préparant des copolymères amphiphiles constitués de glycine *N*-alkylées, afin de mimer la structure des AMPs,

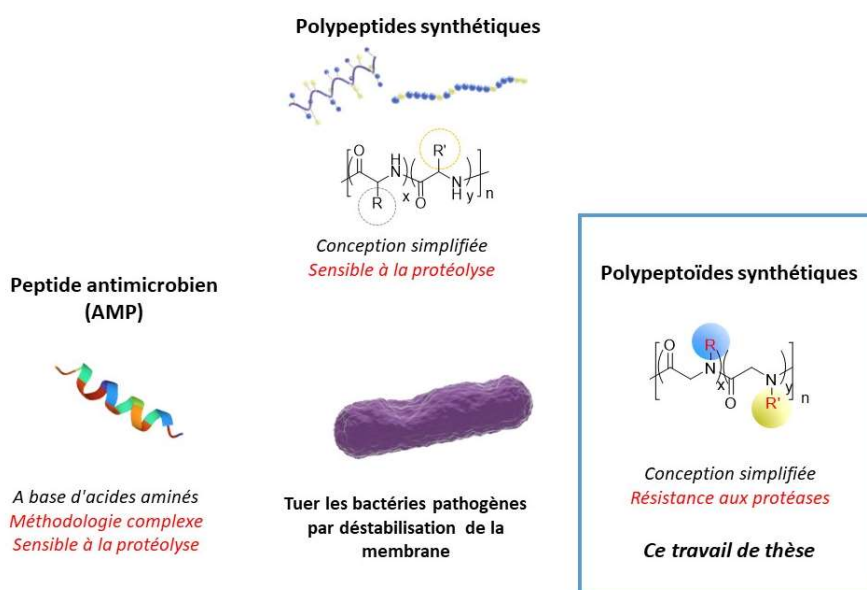
Objectif de la these

nous avons voulu combiner une résistance accrue aux protéases avec la capacité de déstabiliser la paroi de ce pathogène.

Nous avons émis l'hypothèse qu'étudier les relations structure-activité (RSA) de bibliothèques de copolymères (mélange d'unités hydrophobes et cationiques, degré de polymérisation, amorçage, masse molaire, topologie) pourrait permettre de concevoir des molécules actives par le biais d'une conception rationnelle.

Ce manuscrit est rédigé en anglais et composé de cinq chapitres.

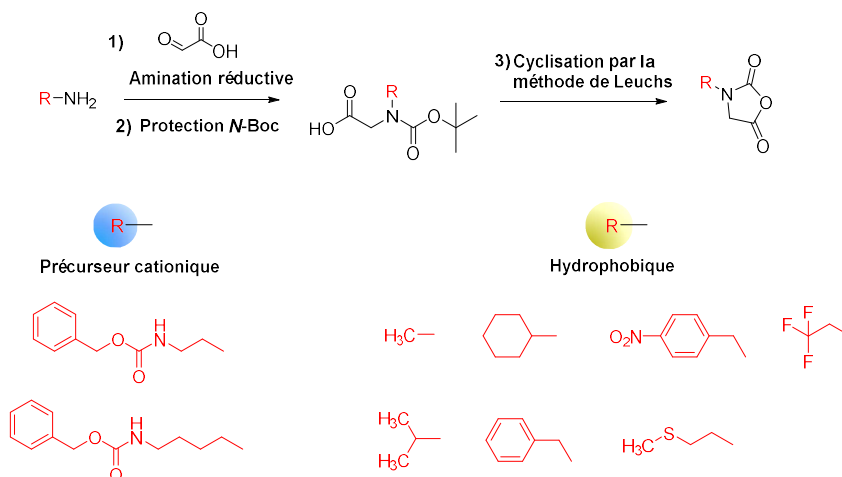
Dans le chapitre 1, nous avons d'abord décrit l'état de l'art concernant la bactérie *C. difficile* qui cause des infections nosocomiales mortelles chez les patients âgés. Cet état de l'art est ensuite associé à la présentation des AMPs et de leurs propriétés de déstabilisation membranaire. Nous décrivons ensuite comment les copolymères permettent de mimer les AMPs avant de fournir une bibliographie détaillée de l'utilisation des polypeptides comme agent antibactériens. Finalement, nous présentons comment les polypeptoïdes peuvent être une alternative aux limitations des polypeptides en infectiologie.



Dans le chapitre 2, nous avons développé la synthèse multi-étapes de nouveaux monomères NNCA en faisant varier les groupements hydrophobes (méthyle, isopropyle, cyclohexyle, benzyle, nitrobenzyle et méthylthioéthyle) et cationiques (*Cbz*-aminoéthyle et *Cbz*-aminobutyle) substituant l'atome d'azote de la glycine. La méthodologie comprend 2 étapes: 1)

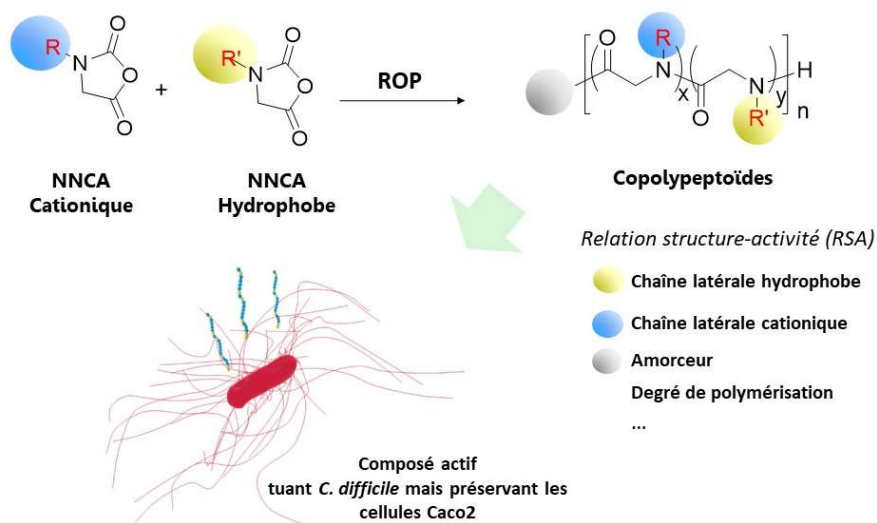
Objectif de la these

l'amination reductrice de l'acide glyoxylique 2) la cyclisation en monomère NNCA par la méthode de Leuchs à partir de dérivés *N*-Boc. Une brève étude cinétique de la dernière étape a été effectuée pour rationaliser l'influence de la *N*-alkylation sur l'étape de cyclisation en NNCA.

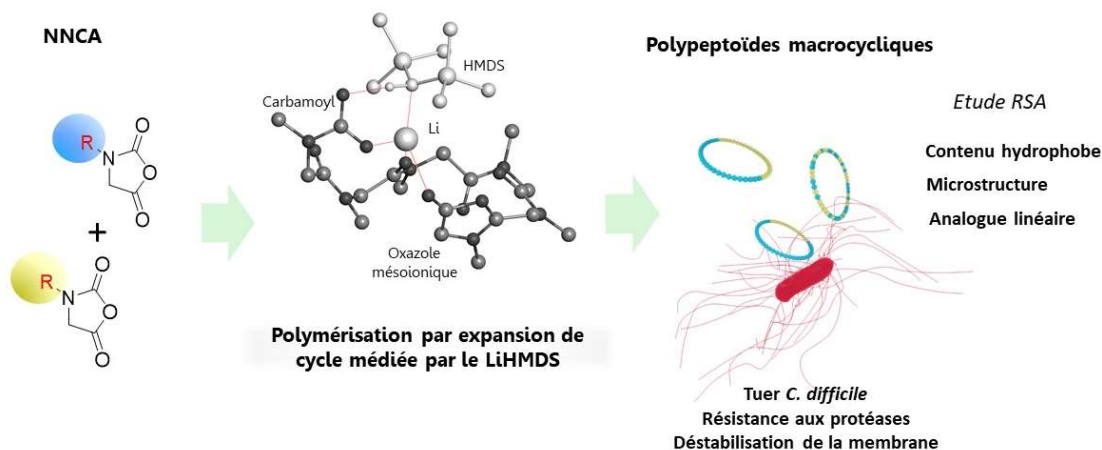


Le chapitre 3 est entièrement dédié à une étude mettant en œuvre la polymérisation par ouverture de cycle de NNCA. Nous avons d'abord établi les cinétiques de polymérisation par ouverture de cycle des différents NNCA en évaluant les effets de la *N*-alkylation: l'encombrement stérique ou les effets électroniques inductifs. Dans une deuxième étape, nous avons mené des réactions de copolymérisation pour préparer des polymères cationiques et hydrophobes que nous avons testés sur *C. difficile*. Une étude approfondie des relations structure/activité a été réalisée en modulant les paramètres macromoléculaires: contenu hydrophobe, nature du monomère (chaînes latérales hydrophobes et cationiques), degré de polymérisation, masse molaire et amorceur. Cette étude se termine par une évaluation de la sélectivité vis-à-vis des cellules épithéliales intestinales Caco-2.

Objectif de la these



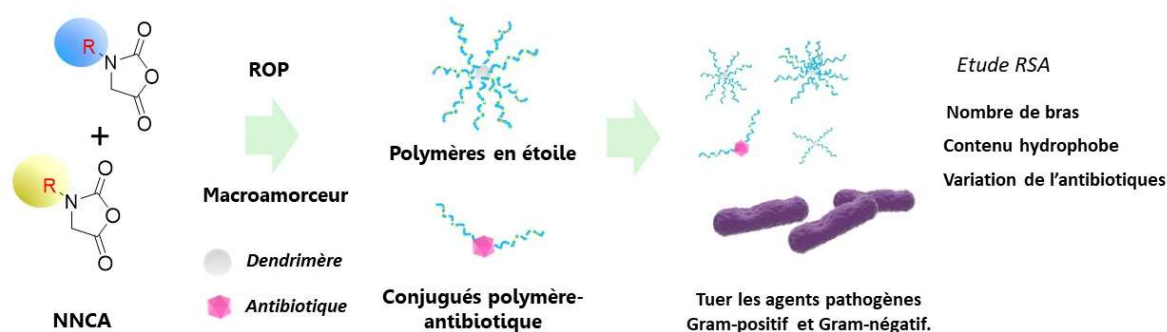
Dans le chapitre 4, nous avons effectué l'étude complète d'une nouvelle approche méthodologique permettant de préparer des polypeptoides cycliques en utilisant le LiHMDS. Nous avons d'abord étudié le mécanisme de cette nouvelle polymérisation par extension de cycle (REP) notamment en associant une approche théorique à nos résultats expérimentaux. Dans un deuxième temps, la mise en œuvre de réactions de copolymérisations nous a permis d'effectuer une étude des relations structure/activité de copolypeptoides cycliques en effectuant des tests avec *C. difficile*.



Enfin, dans le chapitre 5, nous avons développé de nouvelles approches d'ingénierie macromoléculaire permettant la préparation de polypeptoides en étoile ainsi que des polypeptoides conjugués à des molécules antibiotiques. L'étude de leurs RSA est encore en cours (nombre de bras, contenu hydrophobe, nature de la molécule antibiotique) sur diverses

Objectif de la these

bactéries Gram-positives et Gram-négatives. Les premiers résultats sont prometteurs.



Ce travail de doctorat a été réalisé sous la direction du Dr. Colin Bonduelle et la co-direction du Pr. Pierre Verhaeghe dans le cadre d'une collaboration entre cinq institutions: le Laboratoire de Chimie des Polymères Organiques (LCPO), le Laboratoire de Chimie de Coordination du CNRS (LCC), le Laboratoire de Pharmacochimie et Biologie pour le Développement (Pharmadev), le Centre d'Etudes et de Recherche sur le Médicament de Normandie (CERMN) et le laboratoire de pathogénèse des bactéries anaérobies de l'Institut Pasteur de Paris. Ce travail a bénéficié de l'appui d'une bourse du Consejo Nacional de Ciencia y Tecnología (CONACyT, Mexique), titulaire de la bourse n° 548662. Ce travail a été soutenu par l'agence nationale française française pour la recherche (ANR): ANR-17-CE07-0039-01.

Aim of the thesis

Antimicrobial peptides (or AMPs) are specific macromolecules made of amino acids that are produced by microorganisms to fight against bacteria.^{1,2} As selective natural biocides, AMPs are potentially active against all types of micro-organisms, thanks to their ability to destabilize cell membranes.³ This particular mechanism of action is due to various physicochemical properties including their amphiphilic character. So far, the pharmaceutical development of AMPs remains limited for various reasons including elevated cost of production,⁴ scalability⁵ and their sensitivity to proteases,^{6,7} preventing for instance their oral administration. This limitation is a tremendous drawback to treat infections caused by very dangerous pathogens such as *Clostridioides difficile* (*C. difficile*), which infects the digestive tract (an environment full of proteases) causing fatalities.^{8,9}

Synthetic polymers are certainly the best candidates to provide an effective response to the limitations posed by the production and use of AMPs. In this direction, access to large amounts of material is an enormous benefit of using polymer chemistry.¹⁰ Moreover, polymer chemistry enables to finely tune key parameters to mimic AMPs such as the cationic and hydrophobic ratio.¹¹ The growing development of biodegradable polymers also permits to avoid persistence in the environment.¹⁰ Among all polymeric analogs, our work focuses on those made of amino acids called polypeptide polymers: they are showing great potential by providing one of the best biomimetic and bioactive structures for further biomaterials science applications.¹² Although amino acid-based polymers demonstrated very efficient antimicrobial activity (including against drug resistance bacteria), they are susceptible to protease degradation.¹³

In this context, “polypeptoids”, also called poly(*N*-substituted glycines) are *N*-alkylated analogs of synthetic polypeptide polymers and thanks to this *N*-alkylation they can provide enhanced resistance to proteases.¹⁴ The simple preparation of polypeptoids involves the use of building blocks called *N*-alkylated-*N*-carboxyanhydrides or NNCAs that are polymerized through the ring-opening polymerization (ROP) using nucleophiles as initiators.¹⁵ This facile route of synthesis enables the preparation of well define copolymers^{16,17} whose chemical composition are can easily be adjusted.

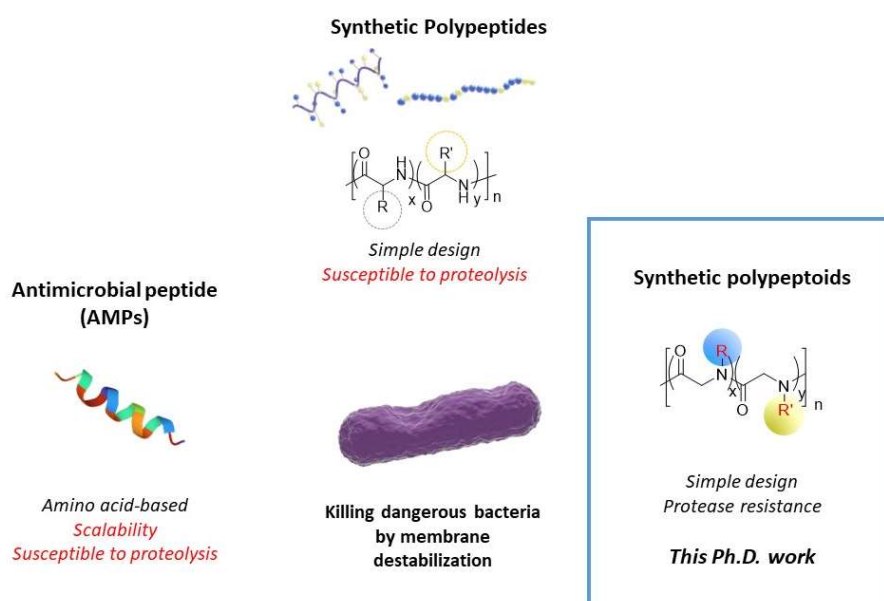
In this PhD work, the goal was to prepare novel antimicrobial copolypeptoids by ROP of NNCAs to selectively kill *C. difficile*. By preparing amphiphilic copolymers consisting of *N*-alkylated glycine, a chemical design aimed at mimicking the structure of AMPs, we sought to combine enhanced protease resistance with the ability to destabilize *C. difficile* membranes.

Aim of the thesis

We hypothesized that by studying the structure-activity relationships (SAR) of the copolymers (hydrophobic and cationic nature, hydrophobic content, polymerization degree, and initiator) we could design active molecules through a rational design.

This manuscript is composed of five chapters written in English and is organized as follows.

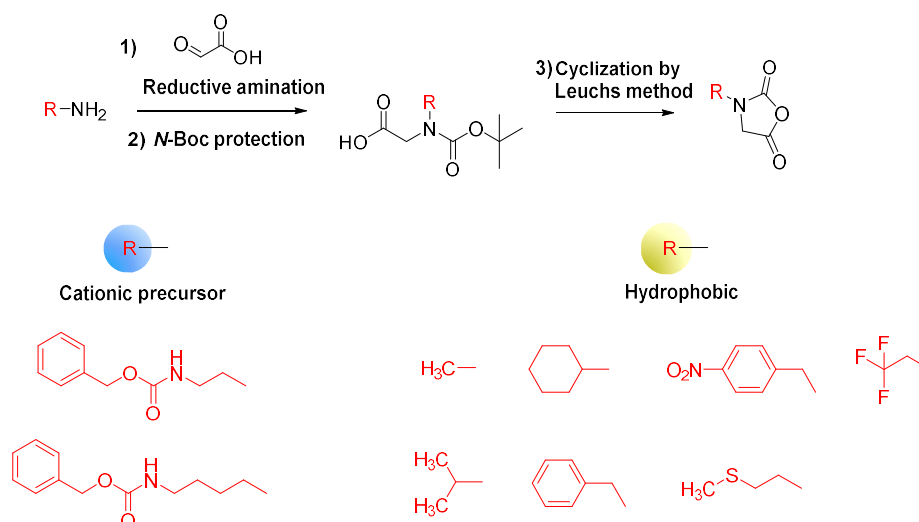
In chapter 1, we first described the state of the art concerning the nosocomial bacterium *C. difficile* that causes fatal infections in elderly patients. This state of the art was then complemented by a presentation of AMPs and their membrane destabilization properties. We then described how copolymers enable to mimic AMPs before providing a detailed bibliography of the use of



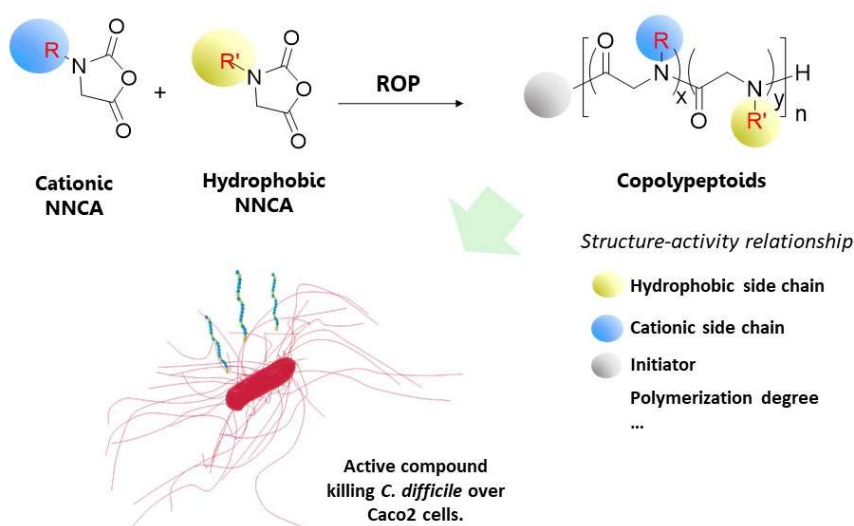
polypeptides as antibacterial agents. Finally, we presented how polypeptoids can be an alternative to polypeptides in infectious diseases.

In chapter 2, we developed the multi-step synthesis of new NNCA monomers by varying *N*-alkylated (methyl, isopropyl, cyclohexyl, benzyl, nitrobenzyl and methylthioethyl) and cationic (*Cbz*-aminoethyl and *Cbz*-aminobutyl) hydrophobic groups. The methodology included 2 steps: 1) reductive amination of glyoxylic acid 2) cyclization to NNCA monomer by Leuchs method from *N*-Boc derivatives. A brief kinetic study of the last step was performed to rationalize the influence of *N*-alkylation on the cyclization step to NNCA.

Aim of the thesis



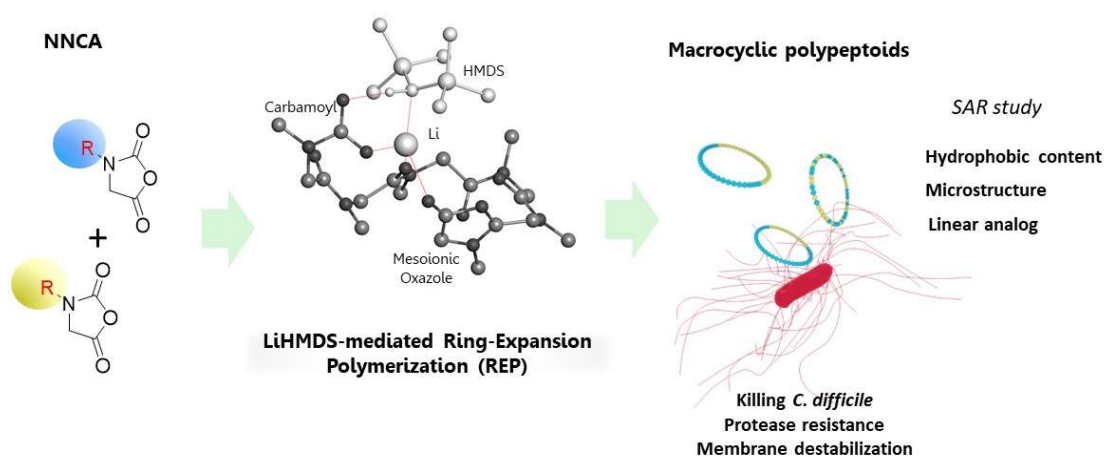
Chapter 3 is entirely dedicated to a study implementing the ring-opening polymerization of NNCA. We first established the ring-opening polymerization kinetics of different NNCA by evaluating the effects of *N*-alkylation: steric hindrance versus inductive electronic effects. In a second step, we conducted copolymerization reactions to prepare cationic and hydrophobic polymers that we evaluated against *C. difficile*. An in-depth study of the structure/activity relationship was performed by modulating the macromolecular parameters: hydrophobic content, nature of the monomer (hydrophobic and cationic side chains), degree of polymerization, molar mass and initiator. This study concluded with cytotoxic assays involving Caco-2 epithelial cells



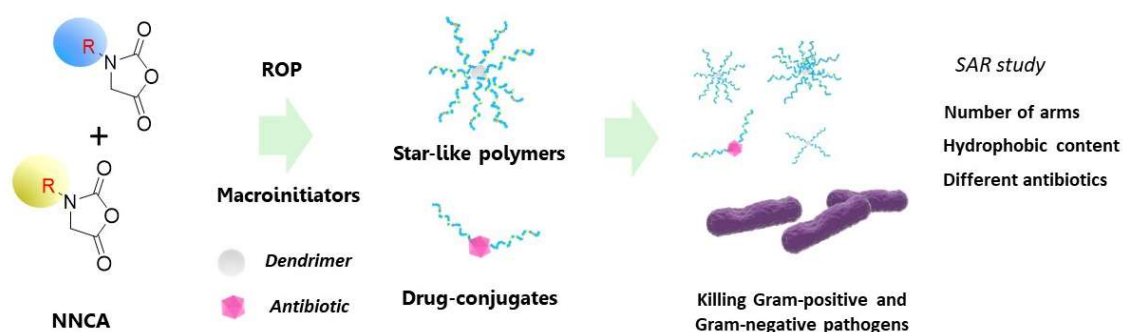
In chapter 4, we have performed a comprehensive study of a new methodological approach enabling the preparation of cyclic polypeptoids using LiHMDS. We have first studied the

Aim of the thesis

mechanism of this new ring expansion polymerization (REP) in particular by combining a theoretical approach with our experimental results. In a second step, the implementation of copolymerization reactions allowed us to study the structure/activity relationship of cyclic copolypeptoids by performing biological tests with *C. difficile*.



Finally, in chapter 5, we have developed new macromolecular engineering approaches enabling the preparation of star-like polypeptoids as well as drug-conjugated polypeptoids. The study of their structure-activity relationship is still in progress (number of arms, hydrophobic content, drug variation) toward several spectrum of Gram-positive and Gram-negative bacteria. The first results obtained are promising.



This PhD work was carried out under the joint supervision of Dr. Colin Bonduelle and Pr. Pierre Verhaeghe in the framework of a collaboration between five institutions: the University of Bordeaux to which belongs the Laboratoire de Chimie des Polymères Organiques (LCPO), the Laboratoire de Chimie de Coordination of the CNRS (LCC), the Laboratoire de Pharmacochimie et Biologie pour le Développement (Pharmadev), the Centre d'Etudes et de Recherche sur le

Aim of the thesis

Médicament de Normandie (CERMN), and the laboratory of Pathogenesis of Bacterial Anaerobes at the Institut Pasteur in Paris. This work was supported by a grant from the Consejo Nacional de Ciencia y Tecnología (CONACyT, Mexico), grant n° 548662. This work was also supported by the French national agency for research (ANR): grant No. ANR-17-CE07-0039-01.

Aim of the thesis

References

- (1) Zasloff, M. Antimicrobial Peptides of Multicellular Organisms. *Nature* **2002**, *415* (6870), 389–395.
- (2) Hancock, R. E. W.; Sahl, H. G. Antimicrobial and Host-Defense Peptides as New Anti-Infective Therapeutic Strategies. *Nat. Biotechnol.* **2006**, *24* (12), 1551–1557.
- (3) Schmidt, N. W.; Mishra, A.; Lai, G. H.; Davis, M.; Sanders, L. K.; Tran, D.; Garcia, A.; Tai, K. P.; McCray, P. B.; Ouellette, A. J.; Selsted, M. E.; Wong, G. C. L. Criterion for Amino Acid Composition of Defensins and Antimicrobial Peptides Based on Geometry of Membrane Destabilization. *J. Am. Chem. Soc.* **2011**, *133* (17), 6720–6727.
- (4) Gaglione, R.; Pane, K.; Dell'Olmo, E.; Cafaro, V.; Pizzo, E.; Olivieri, G.; Notomista, E.; Arciello, A. Cost-Effective Production of Recombinant Peptides in Escherichia Coli. *N. Biotechnol.* **2019**, *51*, 39–48.
- (5) Sun, B.; Wibowo, D.; Middelberg, A. P. J.; Zhao, C.-X. Cost-Effective Downstream Processing of Recombinantly Produced Pexiganan Peptide and Its Antimicrobial Activity. *AMB Express* **2018**, *8* (1), 6.
- (6) Hastings, J. W.; Sailer, M.; Johnson, K.; Roy, K. L.; Vederas, J. C.; Stiles, M. E. Characterization of Leucocin A-UAL 187 and Cloning of the Bacteriocin Gene from *Leuconostoc Gelidum*. *J. Bacteriol.* **1991**, *173* (23), 7491–7500.
- (7) Moncla, B. J.; Pryke, K.; Rohan, L. C.; Graebing, P. W. Degradation of Naturally Occurring and Engineered Antimicrobial Peptides by Proteases. *Adv. Biosci. Biotechnol.* **2011**, *02* (06), 404–408.
- (8) Centers for Disease Control and Prevention (CDC). Clostridioides Difficile (C. Diff). Clostridioides difficile (C. diff) <https://www.cdc.gov/cdiff/what-is.html> (accessed Feb 15, 2021).
- (9) Centers for Disease Control and Prevention (CDC). Antibiotic Resistance Threats in the United States. Antibiotic resistance threats in the United States <https://www.cdc.gov/drugresistance/biggest-threats.html> (accessed May 15, 2020).
- (10) Ergene, C.; Yasuhara, K.; Palermo, E. F. Biomimetic Antimicrobial Polymers: Recent Advances in Molecular Design. *Polym. Chem.* **2018**, *9* (18), 2407–2427.
- (11) Konai, M. M.; Bhattacharjee, B.; Ghosh, S.; Haldar, J. Recent Progress in Polymer Research to Tackle Infections and Antimicrobial Resistance. *Biomacromolecules* **2018**, *19* (6), 1888–1917.
- (12) Rasines Mazo, A.; Allison-Logan, S.; Karimi, F.; Chan, N. J. A.; Qiu, W.; Duan, W.; O'Brien-Simpson, N. M.; Qiao, G. G. Ring Opening Polymerization of α -Amino Acids: Advances in Synthesis, Architecture and Applications of Polypeptides and Their Hybrids. *Chem. Soc. Rev.* **2020**, *49* (14), 4737–4834.
- (13) Salas-Ambrosio, P.; Tronnet, A.; Verhaeghe, P.; Bonduelle, C. Synthetic Polypeptide Polymers as Simplified Analogues of Antimicrobial Peptides. *Biomacromolecules* **2021**, *22* (1), 57–75.
- (14) Miller, S. M.; Simon, R. J.; Ng, S.; Zuckermann, R. N.; Kerr, J. M. Comparison of the Proteolytic Susceptibilities of Homologous *L*-Amino Acid, *D*-Amino Acid and *N*-Substituted

Aim of the thesis

- Glycine Peptide and Peptoid Oligomers. *Drug Dev. Res.* **1995**, 32, 20–32.
- (15) Chan, B. A.; Xuan, S.; Li, A.; Simpson, J. M.; Sternhagen, G. L.; Yu, T.; Darvish, O. A.; Jiang, N.; Zhang, D. Polypeptoid Polymers: Synthesis, Characterization, and Properties. *Biopolymers* **2017**, 109 (1), 1–25.
- (16) Zhu, L.; Simpson, J. M.; Xu, X.; He, H.; Zhang, D.; Yin, L. Cationic Polypeptoids with Optimized Molecular Characteristics toward Efficient Nonviral Gene Delivery. *ACS Appl. Mater. Interfaces* **2017**, 9 (28), 23476–23486.
- (17) Fetsch, C.; Luxenhofer, R. Highly Defined Multiblock Copolypeptoids : Pushing the Limits of Living Nucleophilic. *Macromol. Rapid Commun.* **2012**, 33 (19), 1708–1713.

Abbreviations

%CF	Percentage of carboxyfluorescein released
5-OH-DHE	Münchnone moiety (5-hydroxy-2,3-dihydrooxazolium enolate)
ACN	Acetonitrile
<i>A. baumannii</i>	<i>Acinetobacter baumannii</i>
AMP	Antimicrobial peptide
<i>B. fragilis</i>	<i>Bacteroides fragilis</i>
Boc ₂ O	Di- <i>tert</i> -butyl dicarbonate
<i>C. difficile</i>	<i>Clostridioides difficile</i>
c-AMP	Cyclic antimicrobial peptide
CC ₅₀	50% cytotoxic concentration
CDI	<i>Clostridioides difficile</i> infections
Chol	Cholesterol
c-P(NIlys- <i>b</i> -Nphe)	Cyclic-poly[(<i>N</i> -aminobutylglycine)-block-(<i>N</i> -benzylglycine)]
c-P(ZNIlys- <i>b</i> -Nphe)	Cyclic-poly[(<i>Cbz-N</i> -aminobutylglycine)-block-(<i>N</i> -benzylglycine)]
Cy-NNCA	<i>N</i> -Cyclohexyl- <i>N</i> -carboxyanhydride
D ₂ O	Deuterium dioxide
DCM	Dichloromethane
dc-P(NIlys-Nphe)	Drug conjugate poly[(<i>N</i> -aminobutylglycine)-(<i>N</i> -benzylglycine)]
dc-P(ZNIlys-Nphe)	Drug-conjugate poly[(<i>Cbz-N</i> -aminobutylglycine)-(<i>N</i> -benzylglycine)]
Đ _M	Polymer dispersity
DMF	Dimethylformamide
DMSO	Dimethyl sulfoxide
DP	Polymerization degree
<i>E. coli</i>	<i>Escherichia coli</i>
equiv.	Equivalents
Et ₂ O	Diethyl ether
FTIR	Fourier-transform infrared spectroscopy
<i>H. pylori</i>	<i>Helicobacter pylori</i>
H/C%	Hydrophobic content
HBr	Hydrobromic acid
HMBC	Heteronuclear Multiple Bond Correlation
HSQC	Heteronuclear single quantum coherence spectroscopy
<i>L. monocytogenes</i>	<i>Listeria monocytogenes</i>
LiHMDS	Lithium bis(trimethylsilyl)amide
LS	Light-scattering
M/B	Monomer/Base ratio
M/I	Monomer/Initiator ratio or polymerization degree
MALDI-TOF	Matrix-assisted laser desorption/ionization Time-of-flight mass spectrometry
MeOH	Methanol
MET-NNCA	<i>N</i> -[2-(methylthio)ethyl]- <i>N</i> -carboxyanhydride
MIC	Minimum inhibitory concentration
M _n	Number average molar mass
MRSA	Methicillin-resistant <i>Staphylococcus aureus</i>
M _w	Weight average molar mass
MW	Molar mass
NaBH ₄	Sodium borohydride

NBDF	4-Fluoro-7-nitrobenzofurazan
NCA	<i>N</i> -carboxyanhydride
NGC	Negative Gaussian curve
NHC	<i>N</i> -Heterocyclic carbene
NMR	Nuclear magnetic resonance
NNCA	<i>N</i> -alkylated- <i>N</i> -carboxyanhydride
NPM-NNCA	<i>N</i> -(<i>p</i> -Nitrobenzyl)- <i>N</i> -carboxyanhydride
P(Gly)	Poly(glycine)
P(Me-Ala)	Poly(<i>N</i> -methyl)alanine
P(Nae)	Poly(2-aminoethyl)glycine
P(Ncy)	Poly(<i>N</i> -cyclohexyl)glycine
P(Nlys)	Poly(4-aminobutyl)glycine
P(Nlys-Nphe)	Poly[(<i>N</i> -aminobutylglycine)-(<i>N</i> -benzylglycine)]
P(Nme)	Poly(<i>N</i> -methyl)glycine or polysarcosine
P(Nmet)	Poly(2-(methylthio)ethyl)glycine
P(Nnpm)	Poly(4-nitrobenzyl)glycine
P(Nphe)	Poly(<i>N</i> -benzyl)glycine
P(Npr)	Poly(<i>N</i> -propyl)glycine
P(Nval)	Poly(<i>N</i> -isopropyl)glycine
P(ZNae)	Poly(<i>Cbz</i> (2-aminoethyl))glycine
P(ZNlys)	Poly(<i>Cbz</i> (4-aminobutyl))glycine
P(ZNlys-Nphe)	Poly[(<i>Cbz-N</i> -aminobutylglycine)-(<i>N</i> -benzylglycine)]
<i>P. aeruginosa</i>	<i>Pseudomonas aeruginosa</i>
PAMAM	Poly(amidoamine) dendrimer
PG	1,2-Dioleoyl-sn-glycero-3-phosphoglycerol
Phe-NNCA	<i>N</i> -Benzyl- <i>N</i> -carboxyanhydride
Poly(sar)	Polysarcosine
REP	Ring-expansion polymerization
RI	Refractive index
ROP	Ring-opening polymerization
RT	Room temperature
SAR	Structure-activity relationships
Sar-NCA	<i>N</i> -Methyl- <i>N</i> -carboxyanhydride
SEC	Size-exclusion chromatography
SOCl ₂	Thionyl chloride
S-P(Nlys-Nphe)	Star-like poly[(<i>N</i> -aminobutylglycine)-(<i>N</i> -benzylglycine)]
S-P(ZNlys-Nphe)	Star-like poly[(<i>Cbz-N</i> -aminobutylglycine)-(<i>N</i> -benzylglycine)]
SPC	Soybean phosphatidylcholine and cholesterol
SPPS	Solid-phase peptide synthesis
TFA	Trifluoroacetic acid
TFE-NNCA	<i>N</i> -Trifluoroethyl- <i>N</i> -carboxyanhydride
THF	Tetrahydrofuran
TLC	Thin-layer chromatography
Val-NNCA	<i>N</i> -Isopropyl- <i>N</i> -carboxyanhydride
WHO	World Health Organization
ZLys-NNCA	<i>N</i> - <i>Cbz</i> -aminobutyl- <i>N</i> -carboxyanhydride
ZNAE-NNCA	<i>N</i> - <i>Cbz</i> -aminoethyl- <i>N</i> -carboxyanhydride

Chapter 1 Synthetic polymers as simplified analogs of antimicrobial peptides

1 Bacterial resistance to antibiotics

Antibiotics are a class of drugs used to treat bacterial infections. The discovery of antibiotics was a major milestone in medicine that saved and continues to save millions of lives every year.¹ Unfortunately, their effectiveness is threatened by the capacity of bacteria to adapt and resist antibiotics.² Indeed, the antimicrobial resistance (AMR) is the ability of a microorganism to resist the action of one or more antimicrobial agents. AMR is one of the biggest public health challenges of our time.³⁻⁵ Worldwide, according to the World Health Organization (WHO), the leading problems are the misuse and overuse of antibiotics, both in human and veterinary medicine. Thus, the antibiotic consumption between 2000 and 2015, expressed in defined daily doses (DDD), grew by 65% (21 to 34.8 million DDDs) and the antibiotic consumption rate increased by 39% (11.3 to 15.7 DDDs per 1,000 inhabitants per day).⁶ As a consequence, more than 670,000 people die of resistant infections every year worldwide.⁷ In Europe, 33,000 deaths occurred annually with a burden of acquired antibiotic-resistant infections estimated to 170 DALYs (disability-adjusted life years per 100,000 inhabitants). This number is close to the one of combined burdens of influenza-tuberculosis-HIV (183 DALYs).⁸ Beyond this human burden, AMR has a strong impact on the health system budgets; for instance, the USA invest every year 20 billion USD to fight against AMR and their consequences⁹ while the European Union spends about 1.1 billion Euros against AMR.⁸

Another challenge related to AMR is the increase of hospital-acquired infections (HAIs) which are infections developed while receiving health care in hospitals (i.e. surgical procedures, use of medical devices or long-term treatment of drugs). The main reason is the antimicrobial exposure pressure over the different infectious agents leading to the exponential development of AMR.¹⁰⁻¹² Indeed, bacteria can contaminate and colonize almost all surfaces by biofilm formation, including medical devices. This bacteria biofilm represents a key factor responsible for bacteria spreading in hospital facilities since it ensures the growth and protection against antimicrobial agents. Biofilms resemble the tissues formed by eukaryotic cells, in their physiological

Chapter 1. Synthetic polymers as simplified analogs of antimicrobial peptides

cooperativity and in the extent to which they are protected from variations in bulk phase conditions by primitive homeostasis provided by the biofilm matrix.^{13,14} The antibiotics typically kill the planktonic bacteria, which are released from the biofilm but the treatment fails to penetrate the biofilm, allowing to protect and spread resistant bacteria.^{14–16}

It is important to mention that antibiotics generally involve mechanisms that consist of inhibiting bacterial cell wall synthesis, protein synthesis, or DNA replication.¹⁷ Addressing the problem of resistance in this context first requires a better understanding of the origin of these resistances. Thus, the development of AMR is a natural phenomenon that has two main possible origins: a) mutations in bacterial genes and b) acquisition of external resistance genes carried by mobile genetic elements that can spread between bacteria (**Figure 1**).^{2,3} Other resistance mechanisms are intrinsic such as, up or down expression of a normal gene due to the constant exposure of antibiotics. Certain species also possess efflux pumps.^{18–20} The first mechanism involves the chromosomal mutation or inductive expression of a latent chromosomal gene, while the second is due to an exchange of genetic material through transformation (the exchange of DNA), transduction (bacteriophage), or conjugation by plasmids (extrachromosomal DNA).^{21–23}

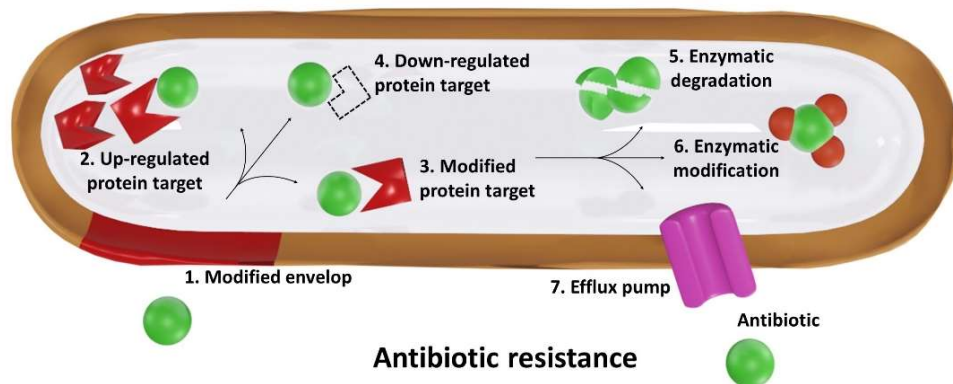


Figure 1. Antibiotic resistance. Bacteria develop resistance through mutations, by uptake of external mutated genes or intrinsic mechanism i.e. up and down-regulation causing: 1) modification on the bacterial envelope, 2) amplification, 3) modification, 4) quantitative decrease of the target (or activating enzymes for some prodrugs), 5) enzymatic degradation, 6) enzymatic modification of the antibiotic and 7) pumps that expulse antibiotics.

It is to note that resistance can be transferred horizontally by plasmids or by chromosomally located conjugative transposons that spread the resistance to other species i.e. Gram-positive species can transfer resistance to Gram-negative species, but the reverse is uncommon.²¹ This is the main reason that makes us vulnerable since the non-pathogenic bacteria that colonize us

Chapter 1. Synthetic polymers as simplified analogs of antimicrobial peptides

and make up our microbiome can also develop resistance, creating a reservoir of resistance genes that can then spread to pathogenic bacteria.² Once the resistance to an antibiotic is acquired for bacteria, the antimicrobial agents are rendered inactive by three major mechanisms: (i) inactivation of the antibiotic by destruction or modification, (ii) prevention of access to the target, and (iii) alteration of the antibiotic target site.^{21,24} Inactivation mediated by β -lactamases, efflux pumps, and single amino acid change in the targeted enzyme are examples of those mechanisms.²¹

Another problem is the lack of research to develop new antibiotics. In 2020, the WHO stated that the research of new antibiotics sorely lacks investment and technological developments to address the problem of resistance.²⁵ The new antibiotics under development do not bring spectacular benefits to existing drugs and only a few of these new treatments target Gram-negative bacteria. A priority pathogen list was published by the WHO (**Table 1**) and highlights pathogens that are posing an increasing risk to human health because they are resistant to most of existing anti-infective drugs.^{26,27}

Table 1. Biggest threats due to resistant pathogens reported by WHO in 2020.²⁷

	Microorganisms	Gram		Microorganisms	Gram
Urgent treats	Carbapenem-resistant <i>Acinetobacter</i>	-	Serious threats	Methicillin-resistant <i>Staphylococcus aureus</i> (MRSA)	+
	<i>Candida auris</i>	Fungi		Drug-resistant <i>Streptococcus pneumoniae</i>	+
	<i>Clostridioides difficile</i>	+		Drug-resistant <i>M. tuberculosis</i>	n.a.
	Carbapenem-resistant <i>Enterobacteriaceae</i>	-		Drug-resistant <i>Shigella</i>	-
	Drug-resistant <i>Neisseria gonorrhoeae</i>	-	Concerning threats	Erythromycin-Resistant Group A <i>Streptococcus</i>	+
Serious threats	Drug-resistant <i>Campylobacter</i>	-	Watch list	Clindamycin-resistant Group B <i>Streptococcus</i>	+
	Drug-resistant <i>Candida</i>	Fungi		Azole-resistant <i>Aspergillus fumigatus</i>	Fungi
	ESBL-producing <i>Enterobacteriaceae</i>	-		Drug-resistant <i>Mycoplasma genitalium</i>	+
	Vancomycin-resistant <i>Enterococci</i> (VRE)	+		Drug-resistant <i>Bordetella pertussis</i>	-
	Multidrug-resistant <i>Pseudomonas aeruginosa</i>	-			
	Drug-resistant <i>Salmonella</i>	-			

Currently, we are facing these new superbugs with a largely depleted armory.^{7,24} Thus, projects searching for new molecules displaying novel mechanisms of action must be developed in order to fight against the evolving resistance of bacteria.²⁸

2 *Clostridioides difficile*

Among those AMR superbugs listed by the WHO, *Clostridium difficile*/*Clostridioides difficile* or *C. difficile*²⁹ is one of the microorganisms that arises major concerns. This microorganism is responsible for more than 220,000 infections every year in the USA according to the Centers for Disease Control and Prevention (CDC).^{30,31} In 2018, with a current mortality rate of 9% in elderly people and 20% of recurrence, *C. difficile* caused 12,800 deaths according to the CDC.³² In Europe, more than 7,000 cases were reported during 2016 with a prevalence of 74.6% of HAIs³³ and the associated cost was estimated between 6,000 and 11,000 € per case.³⁴

C. difficile was first described in 1935 by I. Hall and E. O'Toole and classified as *Bacillus difficilis* since it was a bacillus difficult to isolate from the meconium and feces in infants.³⁵ Due to the microorganism growth in anaerobic conditions, it was classified into the genus *Clostridium*.³⁶ The pathogenic potential was discovered in 1969 when an absence of microbiota was induced in rats: infection evolved in diarrhea and occasionally death.³⁷

Nevertheless, this pathogenicity was not taken into account³⁸ until 1974 when two different reports provided information to demonstrate that *C. difficile* was an important cause of human disease, based on the following experiments and observations: i) the presence of cytotoxins in guinea pigs stools who developed the gut disease after receiving penicillin;³⁹ ii) significant association between patients receiving clindamycin and the development of pseudomembranous colitis (PMC);⁴⁰ iii) Further studies confirmed the clindamycin-induced colitis in hamsters,⁴¹ followed by the presence of the cytotoxins detected in stools of five out of six patients with histologically PMC⁴² and the confirmation of causal association of *C. difficile* and gut infection in man.^{43,44}

C. difficile can be found in aqueous sources being normally a harmless environmental organism, as it was reported in a study of 2580 environmental samples in South Wales, United Kingdom.⁴⁵ This study performed in 1996 included samples from water sources (river, sea, swimming pool), raw vegetables, soil, farm, and pet animal faces, in addition to general surfaces in homes, hospitals, and veterinary clinics. *Clostridioides difficile* and its spores were found in soils 21%, pets 7%, hospitals 20%, raw vegetables 2.4%, surfaces in private homes 2.2% and, more interestingly, river waters 87.5%, lake waters 46.7% and swimming pools 50%.³⁶

C. difficile is a 3-5 µm length bacterium presenting flagella which confer motility. It is a thin

Chapter 1. Synthetic polymers as simplified analogs of antimicrobial peptides

Gram-positive rod with oval terminal spores that do not markedly swell the rods (**Figure 2**).^{35,36,38} It is constituted of a complex cell envelope which is made of the cell wall and a lipid membrane (**Figure 3**). The cell wall is constituted of an S-layer formed of proteins of high molar mass (45-50 KDa) and low molar mass (22-38 KDa) that promote cell adhesion; a second layer constituted of polysaccharides (the most common is a polymer of hexaglycosylphosphate described as teichoic acid-like) and peptidoglycans whose polysaccharide backbone is formed of *N*-acetylglucosamine and *N*-acetylmuramic acid, and a lipid bilayer.⁴⁶ This biochemical architecture is responsible for a weak positive charge of the cell wall as determined by immuno-gold electron microscopy and by the fact that bacteria move to negatively charged fields determined by paper electrophoresis.⁴⁷



Figure 2. *Clostridioides difficile*: a spore-forming and flagellated Gram-positive bacterium.

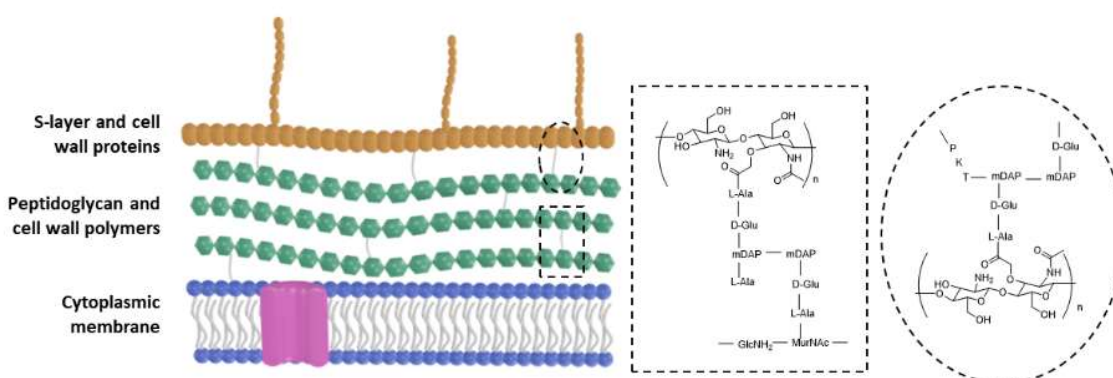


Figure 3. *Clostridioides difficile* envelope is mainly constituted of S-layer, polysaccharides, and a cytoplasmic membrane.

Chapter 1. Synthetic polymers as simplified analogs of antimicrobial peptides

The spore presents a more complex envelop architecture, constituted of an exosporium (layer of permeable carbohydrates), an outer lipid membrane, a cortex layer (containing enzymes that help for germination), a germ cell wall (during germination will become the cell wall) and an inner membrane.⁴⁸ The morphology of colonies is variable, typically at 24-48 h on blood-based media, colonies have 3-5 mm diameter with an irregular, lobate or rhizoidal edge, grey, opaque and non-hemolytic, although some strains have a greenish appearance due to *alpha*-type hemolysis on blood agar.^{38,49} The spore formation is more noticeable on agar cultures that have reached a stationary or decline phase in their growth around 48-72 h incubation, at that period colonies may develop a light grey or whitish center; a factor associated with sporulation that can have a “fried-egg” appearance.^{36,45} Smooth forms also may occur, especially on selective agars.⁴⁹ Spores of *C. difficile* are resistant to high temperatures, ultraviolet light, harsh chemicals, and antibiotics.⁵⁰ Spores increase the virulence of the microorganism since they can easily spread from human to human, especially in the hospital facilities when the disinfection process is inefficient, or proper handwashing is not respected.⁵¹ Furthermore, because spores are resistant to antibiotics, they can remain in the gastrointestinal tract and potentially contribute to a recurrent disease following treatment and eradication of vegetative forms.^{52,53}

The infections caused by *C. difficile* (CDI) embrace a wide number of clinical symptoms that can end in life-threatening diseases.⁵² The disease can start as asymptomatic colonization presented as regular watery diarrhea but rapidly can evolve into a massive colonic inflammation as a result of lesions that coalesce within the colon, creating a pseudomembrane of mucus constituted of immune cells and necrotic tissues. At this point, the disease is called pseudomembranous colitis and represents an advanced stage of the disease, which in some cases, leads to a deadly form of colonic distension, well known as toxic megacolon.^{33,54}

Generally, *C. difficile* colonizes the intestine (colon) after disruption of the normal intestinal flora and the spore germination is activated by the presence of bile acids.^{55,56} The presence of bile salts also increases the stability of *Clostridioides* biofilm formation.⁵⁷ Then, the virulence is potentiated by the production of two main toxins, Toxin A (TcdA) and Toxin B (TcdB) during the late log and stationary phases of the bacterial growth.^{58,59} TcdA binds to the apical side of the cell and, after internalization, causes actin cytoskeleton changes that result in disruption of tight junctions and loosening of the epithelial barrier, in cell death or in the production of inflammatory mediators that attract neutrophils (**Figure 4**). Disruption of tight junctions enables both TcdA and TcdB to cross the epithelium, affording the preferentially binding site of TcdB to the basolateral cell membrane. As a consequence of the cytotoxic effects, the host cells (epithelial cells,

Chapter 1. Synthetic polymers as simplified analogs of antimicrobial peptides

phagocytes, and mast cells) release various immunomodulatory mediators resulting in inflammation and the accumulation of neutrophils. Finally, TcdB prefers to enter the bloodstream, targeting cardiac tissues and being a deadly complication of the disease.⁵⁹ Despite the majority of *C. difficile* pathogenic strains produce both toxins,⁵¹ the emerging of hypervirulent strains is a global concern since i.e. PCR ribotype RT027/NAP1 overproduce TcdA and B with significant increases in the incidence of hospitalizations associated with CDI by the mid-2000s.^{60,61}

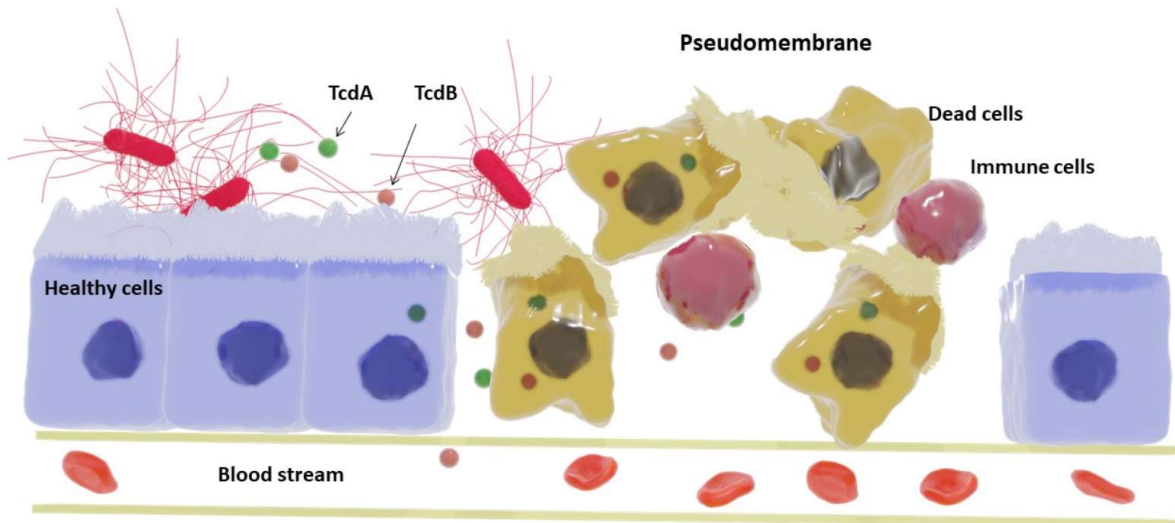


Figure 4. *Clostridioides difficile* colon pathogenesis. After spore germination, the release of toxins A (TcdA) and B (TcdB) and internalization in colon epithelium cells generate disruption, the formation of the pseudomembrane and TcdB enters into the bloodstream causing fatalities.⁵⁹

The virulence of *C. difficile* coupled with several risk factors in patients makes this disease a lethal health problem.⁶² One of these risk factors is the use of antibiotics that increases 7 to 10 times the appearance of CDI during the treatment and up to 2-3 months after.⁶³ Moreover, several antibiotics lead to the development of infection but some carry a higher risk than others, including amoxicillin, clavulanic acid, clindamycin, cefuroxime, and ciprofloxacin.^{64–67} This risk can be more important during the concomitant ingestion of proton-pump inhibitors.⁶⁸ A second important risk factor is age: elder people above 65 years old are 10 times more susceptible to acquire CDI than young people.^{52,60,69} This was demonstrated by high attributable mortality in an outbreak of the hypervirulent strain RT027/NAP1.⁷⁰ Finally, other risks involve the exposure to and acquisition of toxigenic strains that can be related to gastrointestinal surgery/manipulation, a serious underlying illness, immunocompromising conditions or healthcare.^{51,54,71,72}

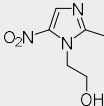
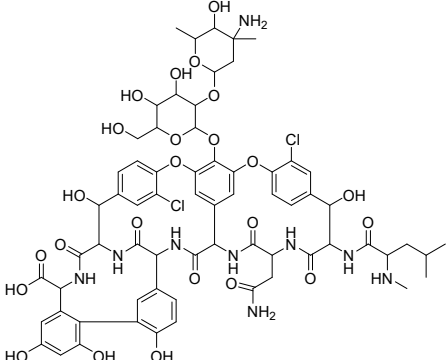
An opportune diagnosis of pseudomembrane colitis and the detection of the toxins or the

Chapter 1. Synthetic polymers as simplified analogs of antimicrobial peptides

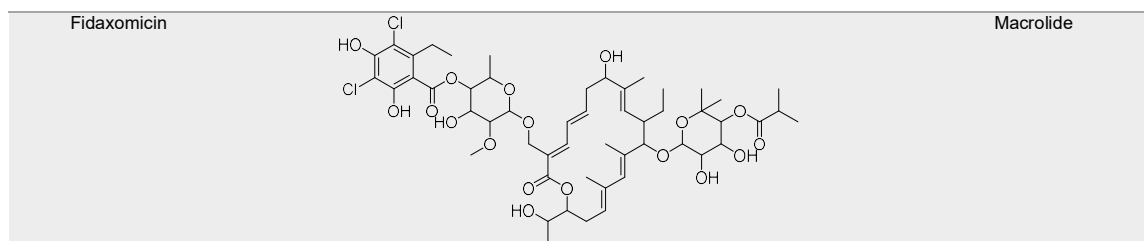
toxigenic strains decrease mortality.⁵¹ One of the treatments that can work against CDI and the recurrent infection is the fecal microbiota transplant.⁷³ However, several drawbacks are latent using this treatment i.e. lack of standardization of preparations, including quality control to minimize variations in bacterial counts during storage, and the possibility of inducing bacteremia or fungaemia.⁵⁹

The drug treatment of *C. difficile* infections is based on three molecules (**Table 2**): metronidazole, vancomycin and fidaxomicin.^{74,75} Metronidazole is a synthetic antibiotic belonging to the 5-nitroimidazole class, it is a nitroaromatic prodrug that, once is partially reduced, inhibits nucleic acid synthesis by forming covalent adducts to the DNA of microbial cells.⁷⁶ This antibiotic has been one of the first-line treatments for mild to moderate cases of CDI,⁷⁷ with a recommended oral dose of 500 mg, 3 times per day for 10-14 days.⁷⁴ It is the cheapest option with a cost of 18 euros for a 10-day treatment.⁷⁸ Nevertheless, the major disadvantage of this treatment is the antimicrobial resistance that has been reported through a decrease of the inhibitory concentration (MIC_{50}) from 0.21 mg/mL to 0.8 mg/mL in 10 *C. difficile* strains and a bigger increase in the strains RT027, RT106 and RT001 (0.8, 1.03 and 4.16 mg/mL).⁷⁹ Moreover, metronidazole presents systemic adverse effects because it is able to cross the gut barrier and penetrates into the blood and the nerve system.⁸⁰

Table 2. Current treatments against *Clostridioides difficile*.

Name	Structure	Antibacterial class
Metronidazole		5-Nitroimidazole
Vancomycin		Glycopeptide

Chapter 1. Synthetic polymers as simplified analogs of antimicrobial peptides



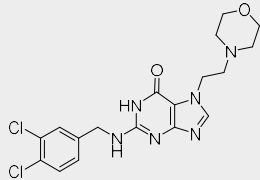
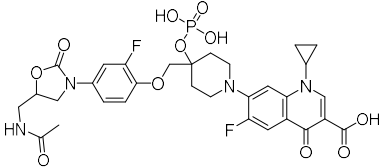
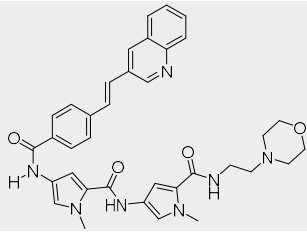
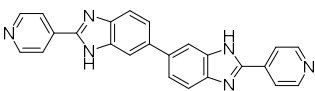
The second treatment, vancomycin, is a natural glycopeptide that inhibits the synthesis of the cell wall in Gram-positive bacteria by linking to the terminal *D*-alanyl-*D*-alanine moieties of the peptidoglycan precursors, avoiding the biosynthesis of the bacterial cell wall.⁸¹ The oral treatment for moderate CDI is 125 mg four times per day for 10 days with a higher cost (60 euros for 10 days treatment).⁷⁸ However, the potential appearance of AMR in vancomycin has started with a reported increase in the antimicrobial susceptibility from 0.66 mg/mL to 1 mg/mL.⁸² Moreover, the administration of vancomycin can also lead to a concomitant AMR of other bacteria such as the vancomycin-resistant *Enterococci* infections.⁸³

Fidaxomicin is a relatively novel macrocyclic lactone antibiotic with a narrow antibacterial spectrum against *C. difficile*. The mechanism of action consists in the inhibition of RNA polymerase, preventing transcription.⁷⁵ The treatment for moderate cases is the oral administration of 200 mg, two times per day for 10 days.⁷⁵ The major disadvantage is the cost of the treatment (about 1300 euros for a 10-day treatment).⁷⁸ The recurrence of CDI is known for all the different treatments and even if fidaxomicin promises the lowest value of recurrence (15%) in comparison to vancomycin (25%), the possibility to suffer a second CDI is still not solved. Moreover, between 2011 and 2016 it was found a resistant strain to fidaxomicin (RT344) presenting an increase of the MIC value from 0.04 mg/mL to 4 mg/mL evidencing that AMR would be also a problem for the coming days using this treatment.⁸²

The lack of treatment options in the face of the enormous threat posed by the infection motivates new treatments to be developed. According to the clinical trials database in 2020,⁸⁴ several novel antimicrobial entities are clinically studied against *C. difficile* infections (**Table 3**): Poly CAb is in clinical phase I; DNV3837, ACX-362E, MG-BP-3, and IMM-529 Cab are in phase II; bezlotoxuman and ridinilazole are in phase III; Teicoplanin is in phase IV. However the rapid evolution of AMR versus the therapeutic development is reaching a critical point and, more efforts should be done to produce other new entities displaying original mechanisms of action against *C. difficile* with, as much as possible, a narrow antibacterial spectrum.

Chapter 1. Synthetic polymers as simplified analogs of antimicrobial peptides

Table 3. New antimicrobial synthetic molecules in clinical development against *C. difficile* in 2020.⁸⁴

	Product name	Structure	Class	Clinical phase
Compound	ACX-362E (Ibezapolstat)		DNA polymerase II inhibitor	Phase II
	DNV3837		Oxazolidinone-quinolone hybrid	Phase II
	MGB-BP-3		DNA minor groove binder	Phase II
	Ridinilazole		Bis-benzimidazole	Phase III
	Teicoplanin		Glycopeptide mixture	Phase IV
Biologicals	IIM-529	n.a.	<i>C. difficile</i> polyclonal Ab	Phase II
	Bezlotoxuman	n.a.	Monoclonal antibody	Phase III
	PolyCAb	n.a.	<i>C. difficile</i> polyclonal Ab	Phase I

3 Antimicrobial Peptides (AMPs)

The adaptive immune system plays an important role to fight against microbes but this system is absent in plants, insects and microorganisms.⁸⁵ Alternatively, antimicrobial peptides or AMPs, also called host defense peptides (HDPs), are specific macromolecules made of amino acids and form part of the innate immune response against bacteria.^{85–87} The first evidence of AMPs was demonstrated through the growth inhibition of a variety of phytopathogens coming from wheat flour.⁸⁸ Further studies proved that a peptide isolated from the wheat endosperm *Triticum aestivum* was responsible for this event. The peptide was named purothionin and

Chapter 1. Synthetic polymers as simplified analogs of antimicrobial peptides

classified as a member of thionins that are distributed across the plant kingdom. Since then, AMPs have also been discovered in humans: Lysozyme was the first reported human AMP identified in 1922 from nasal mucus by A. Fleming⁸⁹ and its potency to kill bacteria established the occurrence of AMPs in humans.

The real importance of AMPs was recognized in prokaryotic cells in 1939 when R. Dubos isolated from *Bacillus brevis* a group of compounds called gramicidins, which demonstrated activity against a wide range of Gram-positive bacteria.^{90,91} Further study demonstrated that gramicidin S displayed wound healing properties on guinea pig skin.⁹² Then, gramicidin was the first AMP commercially manufactured as an antibiotic in 1944.^{93,94} Moreover, *Lactococcus lactis* produces an AMP called nisin A which has been used as a food preservative since 1950 and against which no significant development of resistance was detected.⁹⁵

With the rise of antibiotic resistance in the early 1960s, the interest of the scientific community toward AMPs re-emerged.⁸⁵ Since that breaking point, more than 3,000 AMPs were listed and several databases were created.^{85,96} AMPs can be isolated from a single-celled microorganism, insect and other invertebrates, plants, amphibians, birds, fish, and mammals, including humans.⁹⁷ The Antimicrobial Database (APD) of the University of Nebraska contains antimicrobial peptides from six kingdoms (343 bacteriocins/peptide antibiotics from bacteria, 5 from archaea, 8 from protists, 20 from fungi, 349 from plants, and 2307 from animals).⁹⁸ In humans, the three most representative groups of AMPs are defensins, cathelicidins and histatins.^{89,99–101}

AMPs are macromolecules made of amino acids. Their chemical structures are very diverse and some key structural features are identified as essential to their biological activity:¹⁰² the nature of the amino acids that constitute the peptidic backbone, the overall hydrophobicity and the global charge of the macromolecule.^{103,104} To simplify, AMPs can be organized into three main categories:

- *AMPs are tertiary folded and true proteins.* They are often enzymes with hydrolytic activities and this class of AMPs will not be developed further in this manuscript. These are the most complex structures and readers are invited to read more specific references on this topic (i.e. lysozyme, human-*beta*-defensin-3, subtilisins, etc.).^{105–107}

- *AMPs that are smaller in size than true proteins* (below 80 amino acids) but which still adopt a secondary structure that is associated to antimicrobial activity.⁹⁶ Typically, AMPs being

Chapter 1. Synthetic polymers as simplified analogs of antimicrobial peptides

part of this group have a minimum length of 22 residues for α -helical peptides (i.e. magainin 2, LL-37, Buforin, dermcidin, etc) or 8 residues for β -sheet peptides (defensins i.e., HNP-1).^{99,108}

- AMPs belonging to a third group corresponding to unstructured peptidic backbones which can be cyclic structures and are often conjugated with non-peptidic moieties. In this group, activity is usually directly linked to the primary sequence of the macromolecule. (i.e. darobactin, PR39, indolicidin, pyrrocoricin, etc.).^{109–113}

The chemical structure of oligomeric AMPs depends largely on six key features including amphipathy, charge, hydrophobicity, specific sequence, size, and secondary structure (**Figure 5**).^{103,104} Other parameters that are not always encountered can also play an important role: the presence of amino acids belonging to the *D* series, the presence of macrocyclic structures and the presence of unconventional amino acids (β -aminobutyric for instance).¹¹⁴ Despite their great chemical diversity, some specific amino acids are conserved in all the peptide sequences. In particular, lysine and arginine¹¹⁵ are strongly over-represented in AMPs as well as some hydrophobic residues (valine, phenylalanine, leucine and alanine, etc.,

Table 4).^{103,116} In most AMPs, the antibacterial activity does not depend on a single parameter but rather on a plural contribution including several chemical features within the same macromolecular backbones (**Figure 5**). In AMPs, there is no precise rule about the ideal number of hydrophobic residues or charged residues to maximize antimicrobial activity, as this balance varies widely and appears to be associated with some form of selective activity.^{104,116,117}

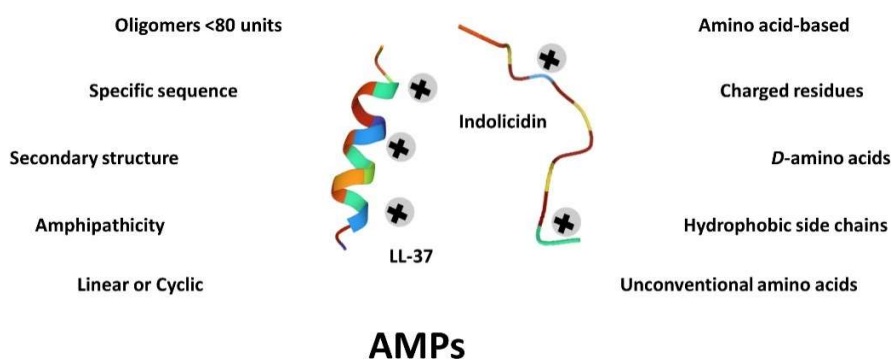


Figure 5. Main chemical structure features of AMPs using LL-37 (PDB ID: 5XNG)¹¹⁸ and indolicidin (PDB ID: 1G89)¹¹⁹ as models.

Chapter 1. Synthetic polymers as simplified analogs of antimicrobial peptides

Table 4. Representative antimicrobial peptides and key chemical features (APD, 2020).¹²⁰

AMP	Secondary structure	Sequence (No. of amino acid units) ^a	Net charge ^b	Hydrophobic content
Magainin ¹²¹	α -helix	GIGKFLHSAKKFGKAFVGEIMNS (23)	+3	43%
LL-37 ^{122,123}	α -helix	LLGDFFRKSKKIKGKFKRIVQRKDFLRNLVPRTE (37)	+6	35%
Buforin II ¹²⁴	α -helix	TRSSRAGLQFPVGRVHRLLRK (21)	+6	33%
θ -Defensin ^{125,126}	β -sheet	GFCRCLCRRGVCRICTR (18)	+5	55%
HNP-1 ¹²⁷	β -sheet	ACYCRIPACIAGERRYGTCTIYQGRWAFCC (30)	+3	53%
HNP-3 ^{126,128}	β -sheet	DCYCRIPACIAGERRYGTCTIYQGRWAFCC (30)	+2	50%
Nisin A ⁹⁵	Coil	ITSISLCTPGCKTGALMGCNMKTATCHCSIHVSK (34)	+3	44%
Indolicidin ^{112,129}	Coil	ILPWKWPWWPWRR (13)	+4	53%
Mersacidin ¹³⁰	Coil	CTFTLPGGGGVCTLTSECIC (20)	-1	45%
Daptomycin ^{131,132}	Coil	WNDTGKDADGSEY (13)	-3	15%
Darobactin ¹¹¹	Coil	WNWSKSF (7)	+1	42%

^a Cationic and hydrophobic amino acids. ^b Correspond to the amount of positively charged residues minus the amount of negatively charged residues.

Despite some exceptions where peptide structures are negatively charged or neutral (i.e. mersacidin, dermcidin, etc.),^{130,131,133} most AMPs are positively charged (

Table 4).^{103,134} The cationic nature of antimicrobial peptides is used to induce interaction with anionic bacterial membranes, often resulting in membrane destabilization.¹³⁵ Several studies have shown correlations between the net charge and its distribution with biological activity or selectivity towards certain bacteria.^{117,136–138} When the secondary structure is involved, the presence of an excessive amount of electrostatic charge can negatively affect biological activity by interfering with the structuring.¹³⁹ Importantly, the effectiveness of AMPs in killing bacteria also depends very much on pH and salt concentration: antimicrobial activities are often enhanced by a slightly acidic pH because the protonation of certain amino acids is promoted, such as histidine, aspartic acid or glutamic acid.^{140–142} Most AMPs contain around 50% hydrophobic residues in their primary sequences.¹⁰² This hydrophobicity can significantly modulate both the antibacterial activity and its specificity (spectrum of action).^{104,116,138} Overall, **hydrophobicity is a chemical leverage** to control the efficiency with which a peptide can penetrate bacterial lipid bilayers.^{102,138,143} In addition, an increase in the hydrophobicity of the peptide at the expense of the amount of net positive charges can significantly modulate the antimicrobial activity.¹⁴⁴ The effects observed are often empirical and the correlations observed are often dependent on the studied bacteria.¹⁴³ Above a certain level, hydrophobicity leads to a decreased antimicrobial activity and increased toxicity to eukaryotic cells.^{143,145} Overall, the hydrophobicity/load ratio is a key determining factor in the design of antimicrobial peptides.^{143–145} This ratio between hydrophobic and basic residues often ranges from 1:1 to 2:1.¹⁰³

The length of antimicrobial peptides most often ranges from 6 to about 60 amino acids,¹⁰³ but little is known about the correlation between size, charge density and antimicrobial activity. In this direction, peptide polymers would be perfect tools to shed light on these parameters. **The**

majority of AMPs are amphipathic: they are both hydrophilic (interaction with the phosphate heads of phospholipids) and hydrophobic (interaction with the lipid bilayer).¹⁴⁶ Quite often, antimicrobial peptides adopt amphipathic conformations when interacting with bacterial membranes (magainin 2, indolicidin, etc.) and are therefore stimuli-responsive backbones.^{135,147} They become active only upon membrane interaction, making them less toxic for other cell types for which the interaction is weaker.¹³³ Finally, it is to note that the incorporation of unconventional amino acids (or *D*-amino acids) or the fact that some AMPs are macrocyclic seem to be key chemical features to minimize the degradation of those peptides by bacteria that secrete proteases to defend themselves.^{148,149}

3.1 AMPs modes of action

There are two main modes of action that allow AMPs to kill bacteria (**Figure 6**): they can interact and disrupt the bacterial membrane, they can be internalized and target an important function of bacterial metabolism or stimulate the immune system to kill more effectively bacteria.⁹⁶ Among AMPs able to target the inner functions of the bacteria, the frog antimicrobial peptide buforin II, for instance, binds to both DNA and RNA to kill *E. coli*.¹²⁴ Similarly, in humans, defensin HNP1, PR-39 and indolicidin are other examples of DNA synthesis inhibitors.^{112,127,150} Targeting a more downstream metabolism, mersacidin peptides interfere with transglycosylation of lipid II, a necessary step in the synthesis of peptidoglycan of Gram-positive.¹³⁰ Overall, there are dozens, if not hundreds of potentially very selective inner metabolism to be targeted, many of which have not yet been studied. In this framework, the biological activity of AMPs can be a source

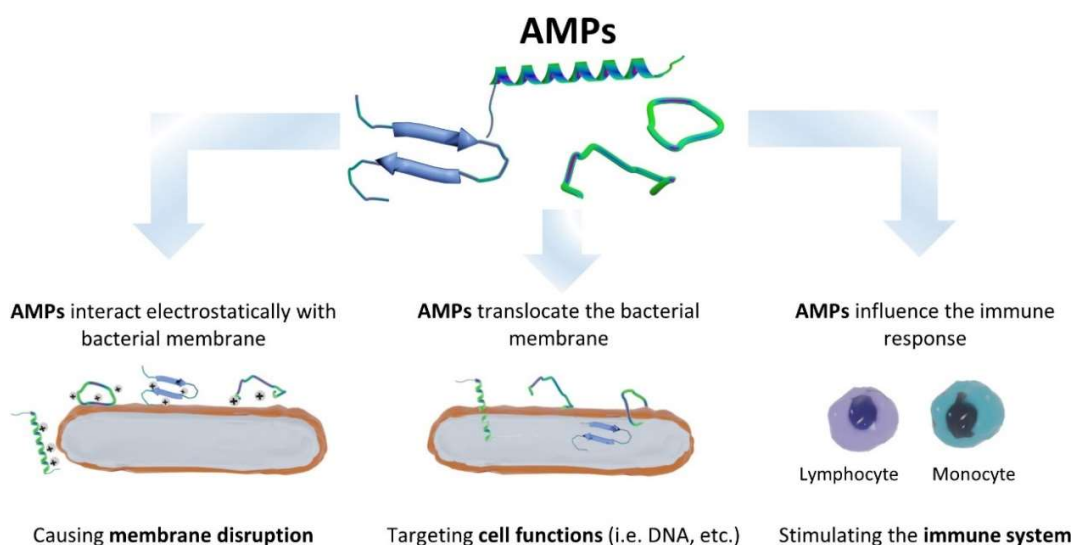


Figure 6. Mechanism of action of antimicrobial peptides: they can disrupt the bacterial membrane, inhibit cellular functions or stimulate the immune system.

Chapter 1. Synthetic polymers as simplified analogs of antimicrobial peptides

of inspiration in medicinal chemistry, with the aim of developing small drugs that are efficient synthetic analogs.^{151,152} For such inhibition, the possible contribution of polymer chemistry remains limited although major advances in sequence control could open the way for polymer science to achieve specific targeting in the future.

Much more interesting for polymer chemists, **the other mechanism implemented by AMPs to kill bacteria involves their ability to interact with bacterial membranes.** As presented above, AMPs exhibit a net positive charge and a high ratio of hydrophobic amino acids, allowing them to bind to negatively charged cytoplasmic membranes (**Figure 6**).⁸⁹ As a representative example, the human cathelicidin peptide LL-37 is an efficient AMP to bind bacterial membranes: it is cationic, α -helical and binds to membranes through electrostatic interactions, before inducing lysis of the bacteria by various mechanisms which are presented later.¹²³ This membrane destabilization mechanism is extensively developed in the following paragraphs.

3.2 AMPs and membrane destabilization

The specific features of AMPs and particularly the combined cationic and hydrophobic composition provide them with the ability to interact and perturb the bacterial membranes, which present anionic surfaces rich in lipids i.e. phosphatidylglycerol or cardiolipin, to the outside environment.¹³⁶ Several mechanisms were described to explain how AMPs destabilize the bacterial membrane (**Figure 7**) through the study of perturbation in artificial membranes, electrical

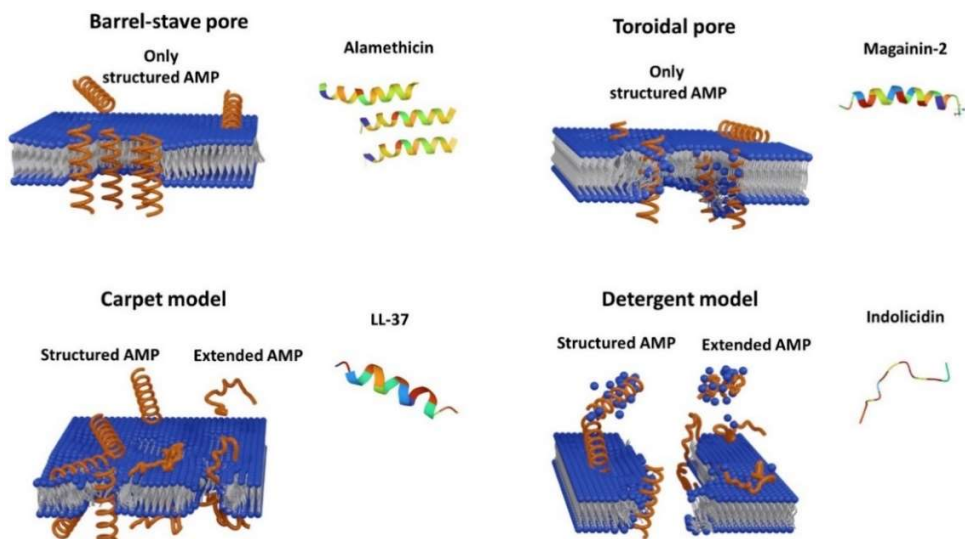


Figure 7. AMPs that display membrane disruption through different suggested mechanisms. Alamethicin (PDB ID: 1AMT),¹⁵³ magainin-2 (PDB ID: 2MAG),¹⁵⁴ LL-37 (PDB ID: 5XNG),¹¹⁸ and indolicidin (PDB ID: 1G89).¹¹⁹

Chapter 1. Synthetic polymers as simplified analogs of antimicrobial peptides

and configurational changes on the surface of membranes.¹⁵⁵

The barrel-stave mechanism describes the formation of channels or pores in the bacterial membrane through the perpendicular insertion of the AMPs causing bacterial leakage.⁹⁶ Magainins peptides, for instance, are folded due to the interaction with the anionic lipid membrane, and the resultant structure is stabilized by two to four disulfide bridges.^{147,155} Other features that are included in this category are a minimum length of 22 residues for α helical or 8 residues for β -sheet.⁹⁶

Another model is explained by the insertion and reorganization of the phospholipid bacterial membrane by interactions between the AMPs and the phospholipid head groups, the resultant structure is known as “toroidal pore”.¹⁰³ In comparison with the barrel-stave model the hydrophobic and hydrophilic arrangement of the lipids is maintained, whereas, in toroidal pores, the hydrophobic and hydrophilic arrangement of the bilayer is disrupted.⁹⁶ Some examples of this mechanism are magainin 2 and melittin.¹³⁵

In the carpet model, peptides are electrostatically attracted parallelly to the anionic phospholipid head groups and, at certain threshold concentration, they cover the membrane surface forming a carpet which leads to unfavorable interaction on the membrane surface with the consequent loss of the membrane integrity.¹⁵⁵ The carpet model does not require specific peptide-peptide interactions of the membrane-bound peptide monomers; it also does not require the peptide to insert into the hydrophobic core to form transmembrane channels or specific peptide structures. Examples of AMPs acting by the carpet model that also possesses amphiphilic character are indolicidin or LL-37.⁹⁶

AMPs also can act as a surfactant-like due to the strongly charged character of the amino acids, such as lysine or histidine, disrupting the bacterial membrane and forming micelles, this event takes part as a consequence of higher concentration on AMP in the carpet-like model. Examples of this mechanism are cathelicidin 1 and 2.¹⁵⁶

Although these models have a wide degree of acceptance, they do not include the importance of the cationic and hydrophobic relation that could explain the antimicrobial activity in AMPs that present an “extended” structure. Moreover, were rarely used to make specific molecular predictions, or drive engineering and design.¹³⁶ In this context, evidence associated to the cationic and hydrophobic relation with the lipid membrane was demonstrated through a phenomenon presented as an inductive saddle-splay effect by AMP over the lipid membrane,

Chapter 1. Synthetic polymers as simplified analogs of antimicrobial peptides

called as Negative Gaussian Curvature (NGC, **Figure 8**).¹⁵⁷ NGC was determined by the changes over the lipid membrane and the interaction with θ -defensins-1 or θ -defensins-7 through the small-angle X-ray scattering technique. The vesicles change drastically when they interact with AMPs displaying the formation of a cubic Pn3m “double diamond phase”, this form presents the NGC at every point of the surface since there is a positive curvature in one direction and a negative curve in the perpendicular direction producing the saddle-splay curvature (**Figure 8A**). Thus, the mechanism can be explaining due to the charged polymers induce electrostatic wrapping of membranes displaying NGC.¹⁵⁸ From the interior of the pores forming after the interaction with AMPs is possible to observe several manifestations such as blebs, buds and rod-like projections (**Figure 8B**).

The enlighten importance of cationic and hydrophobic relation was demonstrated in 2018 through the comparison between the defensin HBD-3 (sequence of 45 amino acids from which 13 are cationic and 2 anionic) and similarly charged peptide CHR01 with lower hydrophobic content (sequence of 14 amino acids from which 8 are cationic).¹⁵⁸ Confirming that high hydrophobic content decreases the membrane leakage due to an increase of positive Gaussian curve which can also lead to a decrease of antibacterial potency.

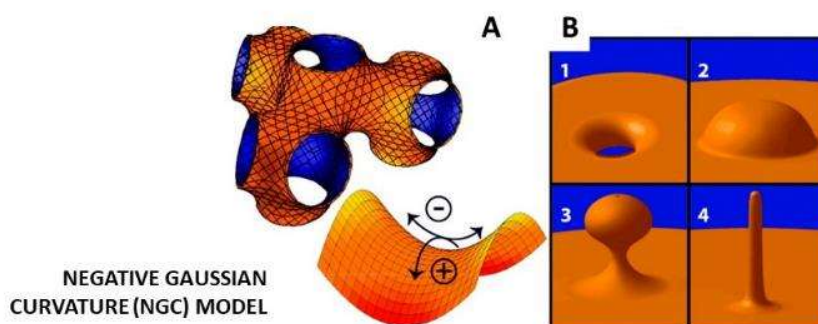


Figure 8. Generation of negative Gaussian curvature. A) Illustration of the Pn3m cubic phase (lower right: Negative Gaussian curvature requires positive curvature (+) in one direction and negative curvature (-) in the perpendicular direction to locally produce a saddle shape). B) Diagrams of different manifestations of saddle-splay curvature in the interior of a pore (1) and at the base of blebs (2), buds (3), and rod-like projections (4).¹⁵⁷

3.3 Limitations of AMPs

Although AMPs have an enormous potential to become commercially available therapeutics, several disadvantages limit their use. One of them is the high cost of production, as AMPs must be extracted and isolated from culture media of natural or genetically modified microorganisms.^{87,159} For example, modified *E. coli* can produce peptides with a cost of production

Chapter 1. Synthetic polymers as simplified analogs of antimicrobial peptides

that can reach 42 € per milligram in batches of 1,000 mg.¹⁶⁰ Another problem is the low recover of AMPs at the end of the production and the difficulties to work with living systems, for instance, the production of a pexiganan protein (DAMP4_{var}) with an optimized protocol demonstrated the production of 24 mg from 800 mL of cell culture.¹⁵⁹ Certainly, AMPs could be produced through a chemical approach, well known as the Merrifield method or solid-phase peptide synthesis (SPPS).¹⁶¹ However the inconvenient is that the scale-up is usually much too expensive to achieve acceptable industrial production costs and is definitely not competitive with the production of AMPs from microorganisms.¹⁶²

Despite cost and production are the main limitations, a shortlist of AMPs was approved in the USA (FDA) and Europe (EMA) including colistin and daptomycin, which are recommended for topic and intravenous administration.¹⁶³ However, the risk with intravenous administration of AMPs is that they can present high toxicity (nephrotoxicity and hepatic toxicity) and very serious adverse effects such as the high nephrotoxicity of colistin.¹⁶⁴

Another major problem of the AMPs is that they possess poor epithelial adsorption.¹¹⁰ Therefore, they become easy targets for proteolytic enzymes decreasing, inhibiting, or completely degrading the peptide resulting into the complete inhibition of antibacterial activity,¹⁰³ such as the case of Leucocin A-UAL 187¹⁶⁵ and LL-37.¹⁶⁶ Therefore, the oral administration limits the use of AMPs as an oral treatment against CDI despite promising applications.

4 Synthetic antimicrobial polymers

Synthetic polymers are certainly the best candidates to provide an effective response to the limitations posed by the production and use of AMPs. In this direction, access to large amounts of material is an enormous benefit of using polymer chemistry. Moreover, the growing development of biodegradable polymers makes it increasingly possible to create materials that can avoid persistence into the environment.¹⁶⁷ Similar to most of AMPs, polymers are macromolecules but unlike AMPs, they are constituted of monomer units whose sequence can be poorly controlled and they are polydisperse. Despite these fundamental differences, synthetic polymers have been extensively studied for decades to tackle bacteria as drug carriers, but also as antiseptic polymers.^{168–170}

Perhaps more difficult to conceive but also more challenging, polymers may intrinsically carry antimicrobial activity and become macromolecular antibiotic drug-compounds by

Chapter 1. Synthetic polymers as simplified analogs of antimicrobial peptides

themselves. Such antimicrobial polymers, also known as polymeric biocides, usually possess the structure of amphiphilic polycations and display biocidal activities or the ability to inhibit the growth of bacteria.^{171,172} As compared to AMPs, they could provide many advantages including low-cost and effective production, stable in long-term usage and storage, and biocidal or broad-spectrum activity against pathogenic microorganisms in brief times of contact.¹⁷⁰ Nevertheless, they often exhibit significant toxicity, at least comparable to the toxicity of AMPs and their use is today restricted to material sciences. It is necessary to note here the possible developments of formulations which enable to limit the toxicity of AMPs or synthetic polymers.¹⁷³ Areas that can benefit from the use of antimicrobial polymers are the manufacturing of fibers, textile sector, the design of water filtration systems, food packaging and biomedical and pharmaceutical industries, including the antibacterial coating of medical devices.^{174–177}

4.1 Synthetic polymers to mimic AMPs

Antimicrobial polymers, also known as polymeric biocides, have emerged as novel antimicrobial candidates to mimic AMPs. Following key chemical features of AMPs, antibacterial polymers incorporate at least two elements into their chemical structures: cationic groups and hydrophobic groups. The biological activity is influenced by the type, amount, location and distribution of these two components. Cationic groups are the essential building blocks that allow antimicrobial polymers to kill bacteria. They mainly include ammoniums,¹⁷⁸ sulfoniums¹⁷⁹ or phosphoniums (**Figure 9**).¹⁸⁰ There are two ways of introducing the hydrophobic chemical compo-

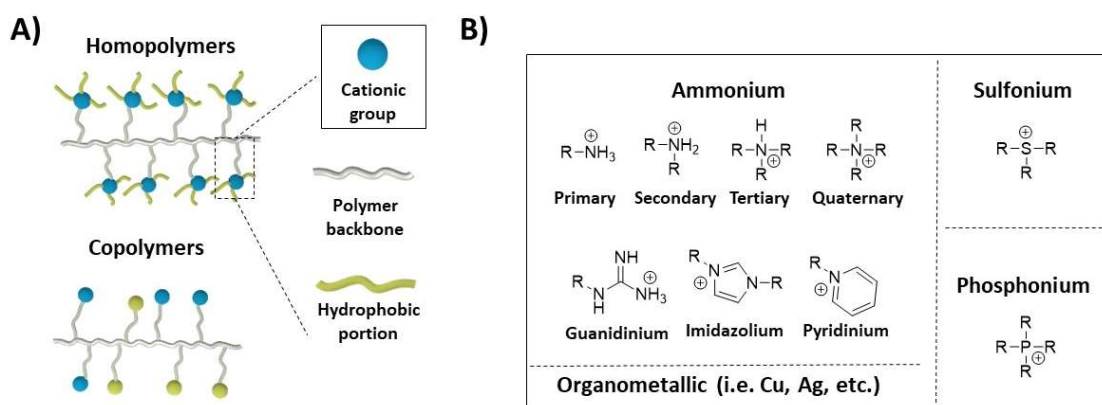


Figure 9. Antimicrobial polymers: essential elements for their chemical design. A) Cationic groups and other chemical functions are supported by either homo- or co-polymers; B) The main cationic groups that were used to develop antimicrobial polymers.

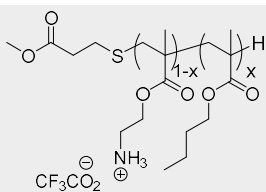
ment, either by carrying out the chemical design of quaternized homopolymers, or by controlling

Chapter 1. Synthetic polymers as simplified analogs of antimicrobial peptides

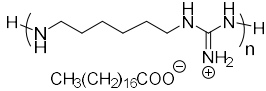
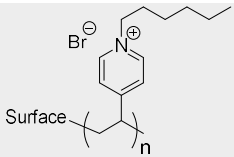
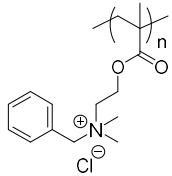
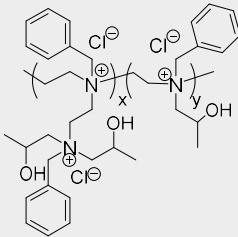
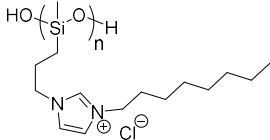
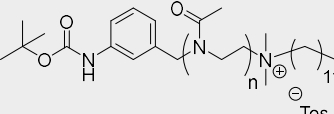
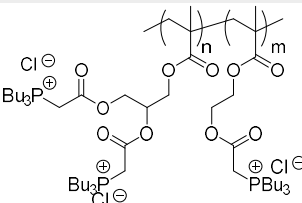
the topology of polymers by preparing copolymers mixing cationic monomer units with hydrophobic monomer units.¹⁸¹

Ammonium-based moieties are the most common cationic groups found in antimicrobial polymers (**Table 5**).¹⁸¹ The quaternary ammonium has a permanent positive charge, whereas primary, secondary and tertiary ammonium groups are pH-dependent, i.e. protonation state of polymers depends on the pKa of their constituent amine and the pH of the medium in which they will have to exert their antibacterial activity. K. Kuroda *et al.* proved that the pH-dependence characteristic is important to obtain less toxic antimicrobial polymers with a series of amphiphilic polymethacrylates.¹⁸² Moreover, they studied a series of polymers with primary, tertiary and quaternary ammonium groups and they showed that primary amine had substantially greater selectivity against *E. coli* than against red blood cells.¹⁸³ In addition to ammoniums, pyridinium or guanidinium salts, are also commonly used cationic groups found in antimicrobial polymers because of their high-water solubility and less-toxic properties.¹⁸¹ In these cations, the charge is delocalized through the π bonds or aromatic conjugated systems and plays a key role for the adsorption of the polymers on the bacterial membrane. In this direction, Y. Zhang *et al.* synthesized a series of polyhexamethylene guanidine stearate that demonstrated a broad spectrum of action against Gram-positive bacteria (*S. aureus*) and Gram-negative bacteria (*P. aeruginosa*).¹⁸⁴ Apart from chemical functions involving nitrogen atoms, antimicrobial cationic polymers carrying other cationic groups were also found effective against several bacteria: this mainly includes side chains bearing sulfur¹⁷⁹ or phosphorus atoms.¹⁸⁵ For instance, T. Endo *et al.* studied both sulfur- and phosphorus-containing polymers. The first was poly(*p*-vinylbenzyl-tetramethylenesulfonium tetrafluoroborate) and demonstrated antibacterial activity against *S. aureus* rather than *E. coli* whereas the second was poly(tributyl(4-vinylbenzyl)phosponium and demonstrated activity against *S. aureus* that was enhanced with a mixture of the analogous ammonium salt, highlighting the importance of the ammonium cation toward bactericidal activity.¹⁸⁰

Table 5. Examples of non-polypeptide antimicrobial polymers.

Group	Polymer class	Structure	Activity Gram (+/-)	Ref
Primary ammonium cation	Polymethacrylates; Poly (aminoethylmethacrylate-co-butylmethacrylate)		Negative	186

Chapter 1. Synthetic polymers as simplified analogs of antimicrobial peptides

	Polyguanidines; Polyhexamethylene guanidine stearate		Both	184
Quaternary ammonium cation	Polypyridines: Poly(4-vinylpyridine) quaternized with hexylbromide		Both	187
	Acrylamides: Poly(dimethylaminoethyl) methacrylate quaternized with benzyl chloride		Both	188
	Dendritic hyperbranched: Quaternized polyethyleneimine		Negative	189
	Siloxanes: Poly(3-N-imidazolopropyl) methylsiloxane quaternized with octylchloride		Both	178
	Polyoxazolines: Poly(2-methyl-1,3-oxazoline)		Positive	190
Phosphonium	Phosphorus salts: Poly(glycidyl methacrylate-co-2- hydroxyethyl methacrylate) tributyl phosphonium salt		Both	191

Overall, quaternization is an important chemical characteristic that greatly enhances the antimicrobial performance of antimicrobial polymers.¹⁹² This optimization is based on the simple inclusion of hydrophobicity on each side chain of the macromolecules. For instance, this characteristic can be easily modulated by the nature and the length of the alkyl lateral chains that are linked to the nitrogen atom in quaternized polymers.^{183,193} In this direction, J. Tiller *et al.* studied a series of poly(4-vinyl-*N*-alkylpyridinium bromide) with different linear alkyl chains from propyl to hexadecyl that killed *S. aureus* with the best activity for small alkyl chains.¹⁸⁷ Another study by G. Lu *et al.* evaluated the activity of dimethylaminoethylmethacrylate quaternized with benzyl, butyl, dodecyl or hexadecyl bromide and determined that benzyl and butyl chains had the

Chapter 1. Synthetic polymers as simplified analogs of antimicrobial peptides

best activities.¹⁸⁸ Although homopolymer synthesis is the simplest and most efficient way to produce antimicrobial polymer candidates, it is still nearly impossible to tune their activity, toxicity or to induce antimicrobial selectivity. Closer to AMPs in which cationic and hydrophobic units are carried by different monomer units, synthetic copolymers aim to solve these limitations. The emergence of free-radical polymerization and controlled polymerization reactions has greatly advanced the preparation of such copolymers and many approaches are now studied to generate these structures and better reproduce the membrane disruption properties of AMPs, regarding both effectiveness and selectivity.¹⁹⁴

4.2 Polymeric analogs of AMP as membrane disrupters and their related properties

The remarkable presence of cationic groups is the main feature of some antibiotic polymers because they can disturb the bacterial membrane similarly to most of the AMPs. In 2013, the characteristic behavior in AMPs, known as Negative Gaussian Curvature (NGC, **Figure 10**), was found in cationic polymers based on copolymers of methacrylate and aminoethyl methacrylate when interacting with lipid membranes, including the membrane pore formation, micellization, blebbing, and budding.¹⁹⁵ Other studies also proved that the membrane disruption that can be associated with NGC, i.e. quaternized poly(2-(dimethyl aminoethyl) methacrylate) initiated with bis(2-hydroxyethyl) disulfide which showed an increase of permeabilization in *Salmonella* species that led to deadly leakage.¹⁹⁶

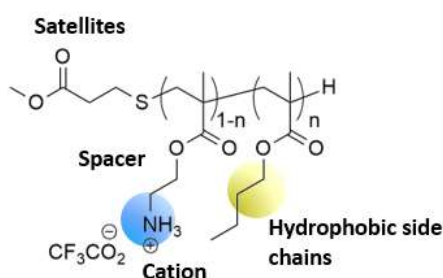


Figure 10. Parameters that may impact the antimicrobial activity using as an example poly (aminoethyl methacrylate-co-butyl methacrylate) that reports NGC behavior.¹⁹⁵

In order to promote the NGC and selective killing of bacteria, antimicrobial polymers should address better control of the structural features (**Figure 10**):

The molar mass of the polymer will involve different effects. For polymers that inhibit the

Chapter 1. Synthetic polymers as simplified analogs of antimicrobial peptides

biofilm formation, a high molar mass is desired, as M. Watanabe *et al.* demonstrated with copolymers bearing cationic biguanidine groups against *S. aureus* and *B. subtilis* using molar mass range from 42 kDa to 120 kDa.¹⁹⁷ However, when the goal is to kill bacteria for *in vivo* therapeutic applications, a high molar mass results in a potential decrease of both water solubility and antimicrobial activity, as it was demonstrated for poly(oxanorbornene) with propyl ammonium side chains.¹⁹⁸ Moreover, the molar mass can also affect the biocidal activities of antimicrobial polymers because it affects the size and net charge of the polymer.¹⁷²

Microstructure. Generally, random copolymers are reported in the literature but the sequence might be important in the design of antimicrobial polymers. K. Kuroda *et al.* demonstrated that no significant difference in antimicrobial activity exists comparing block and statistical copolymers of poly(2-aminoethyl vinyl ether) and poly(isobutyl vinyl ether). Nevertheless, the block copolymer presented higher selectivity against *E. coli* over human red blood cells.¹⁹⁹

The **effect of the counter-ions pair** is related to the solubility in water. When both anionic and cationic ions have a strong affinity, the solubility in water decreases i.e. tetrafluoroborate in poly(tributyl (4-vinyl benzyl) phosphonium) against *S. aureus*.²⁰⁰ The same effect takes part with hydrophobic counter ions using dodecanoate or hexadecanoate in poly(oxanorbornene).²⁰¹ However, in copolymers formed of *N*-vinylpyrrolidone and quaternized vinyl amines or aminoalkyl methacrylates there is no difference between Cl⁻, Br⁻ and I⁻ while killing *S. aureus* and *E. coli*.²⁰²

Importantly, the **amphiphilic balance**, the ratio between cationic and hydrophobic groups, significantly influences the biocidal activity of antimicrobial polymers.¹⁷² Related to this amphiphilic balance, the **cationic group** is a crucial parameter that can drastically modulate the antibacterial activity. E. Palermo *et al.* compared the biocidal behavior of ammonium cationic (poly(2-aminoethyl methacrylate), PAEMA), ternary ammonium cationic (PDMAEMA), and quaternary ammonium groups (alkylated PDMAEMA).¹⁸³ They found that polymers with primary and tertiary ammonium groups exhibited a higher biocidal effect and better selectivity than the quaternized counterpart, which required higher hydrophobicity to reach similar antibiotic performance, but may also induce more cytotoxicity.¹⁸³

Spacers, satellites, and alkyl side chains have an important function since they are related to the **hydrophobic content**. Spacers connect the cationic ion with the polymer backbone. They present a “snorkeling effect” which directly relates the spacer length and the biocidal activity. In

Chapter 1. Synthetic polymers as simplified analogs of antimicrobial peptides

this direction, E. Palermo *et al.* studied poly(amino methacrylate)-*co*-poly(ethyl methacrylate), using different lengths of the alkyl spacer chain from 2 to 8 carbons, to increase the selectivity against *E. coli* (the best copolymer possessed an amino octyl substituent).²⁰³ Satellite groups refer to the termini groups and probably assist the cationic group in disrupting the membrane by inserting into the lipid bilayer at the same site as the cationic group alkyl chain. C. Waschinski *et al.* demonstrated that an optimal antibacterial activity was found using decyl terminal group in comparison to methyl or hexadecyl groups in *N,N*-dimethyl dodecyl ammonium polyoxazoline.²⁰⁴ Finally, the structure of the **alkyl side chain** plays a crucial role during the interaction with bacterial membrane, as it was demonstrated by K. Lienkamp *et al.* through the activity against *E. coli* of oxanorbornene polymers.²⁰¹ They provide activity when side chains are propyl or butyl and deplete activity with methyl and ethyl substitutions. In another study, it was demonstrated activity and selectivity with a length of 4 carbons, when the length of the side chain was varied from 1 to 8 carbons in poly(*p*-methyl chloride-benzyl 2,2,-bis(methylol) propionate).¹⁶⁷ The biocidal activity decreased when increasing the length of the carbon chain, presumably, due to the decrease of aqueous solubility. Also, the effect of the structure between hexyl, cyclohexyl and benzyl groups was studied and the best activity corresponded to the hexyl group which is the less hydrophobic, as confirmed by the water-octanol test. The length of the alkyl chain, as well as the amphiphilic balance, were also tested by M. Ilker *et al.* by modification of different alkyl side chains in copolymers of cationic polynorbornenes constituted of isopropylene and isobutylene alkyl side chains, highlighting that selectivity can be improved by introducing a 10% of isobutylene alkyl substituent.²⁰⁵

All these structural parameters are powerful tools to design new antimicrobial macromolecules if one wants to mimic AMPs. However, polymers applications are so far more focused on biomaterial applications neglecting the development of antimicrobial polymers for therapeutical applications. Very often, the macromolecules are very large and thus may not act as fast as oligomers such as AMPs or small molecules.¹⁶⁹ Therefore, biocidal polymers that require contact times on the order of hours to provide substantial reductions in pathogen colonization, really have no practical value as therapeutics and fall into the category of antiseptic agents that are useful for medical devices. For a therapeutical approach, more efforts must be done to tune the polymer by more rigorously studying and defining the different structural and physicochemical parameters that are required to design specific (narrow-spectrum) and biocompatible antibacterial polymers.

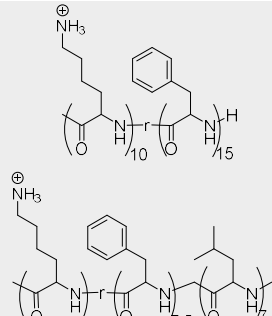
5 Polypeptide analogs of AMPS

Among polymers displaying antibacterial activity, some are chemically very close to AMPs: amino-acid polymers. Peptide polymers are designed to mimic the structure and function of natural peptides. They are showing great potential by providing one of the best biomimetic and bioactive structures for further biomaterials or therapeutic applications.¹⁸¹

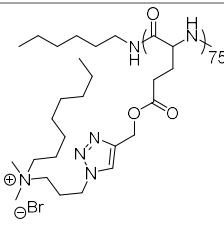
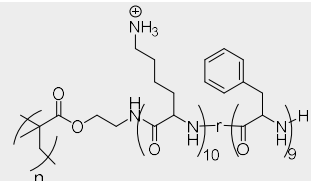
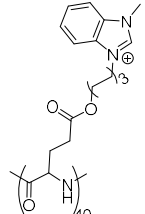
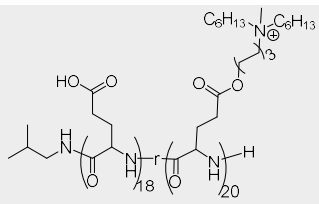
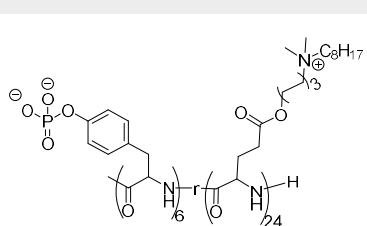
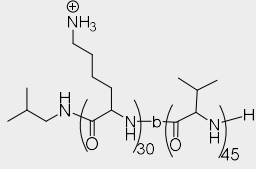
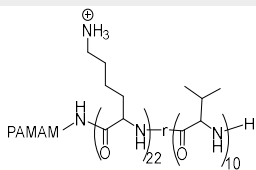
Very early, polypeptide copolymers have been used to induce membrane destabilization.^{206,207} The first fundamental studies on this subject showed that cationic polypeptide copolymers were able to bind to phospholipid membranes despite large distributions in chain lengths and a lack of control over the primary sequence of amino acids. Later, controlled polymerization was a decisive contribution to better study the macromolecular parameters involved in such membrane destabilization (amino acid composition, molar mass etc.).^{208,209}

An important foundational work involving antimicrobial polypeptide polymers was published by C. Zhou *et al.* in 2010.²¹⁰ This work reported the preparation of antibacterial and antifungal copolymers by ring-opening polymerization (ROP) of *N*-carboxyanhydrides (NCA) and using Ni(COD)₂ as initiator. By tuning the amphiphilic balance, two copolymers were highlighted, displaying a broad anti-infective spectrum against *C. albicans*, *E. coli*, *P. aeruginosa*, *S. marcescens* and *S. aureus* (**Table 6**). These copolymers were composed of 60% of hydrophobic units: poly(*L*-lysine)₁₀-*r*-(*L*-phenylalanine)₁₅ and poly(*L*-lysine)₁₀-*r*-(*L*-phenylalanine)_{7.5}-*r*-(*L*-leucine)_{7.5}. Their activities were better than the ones obtained with defensins LL-37, indolicidin and magainin I.

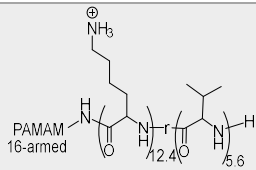
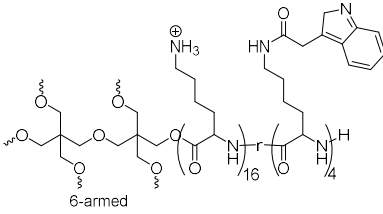
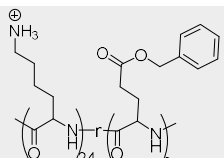
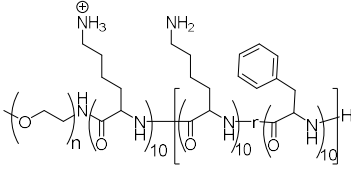
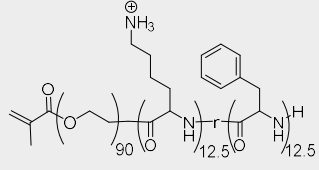
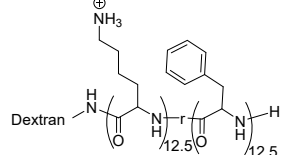
Table 6. Previously reported polypeptide polymers displaying anti-infective activity.

Feature	Polymer	Length (monomer units)	Active against	MIC ^a	Ref
Hydrophobic content variation		25	<i>E. coli</i> <i>P. aeruginosa</i> <i>S. marcescens</i> <i>S. aureus</i> <i>C. albicans</i>	31 µg/mL 31 µg/mL 250 µg/mL 31 µg/mL 125 µg/mL	210

Chapter 1. Synthetic polymers as simplified analogs of antimicrobial peptides

Quaternized ammonium cation		75	S. aureus E. coli	156-312 µg/mL	211
Alkyl side chain		10	E. faecalis S. aureus MRSA VRE K. pneumonia P. aeruginosa E. coli BL21 E. coli NDM1 E.coli lmiS	16 µg/mL	212
α-Helical pH-responsive		40	E. coli P. aeruginosa S. aureus B. toyonensis H. pylori MRSA	3-26 µg/mL 13 µg/mL 13 µg/mL 1-6 µg/mL 1.5 µg/mL	213
α-Helical pH-responsive		38	H. pylori	40 µg/mL (1 µM) at pH = 3	214
α-Helical enzymatic responsive		30	B. toyonensis S. aureus MRSA	40 µg/mL (4.1 µM) 20 µg/mL (2.1 µM) 20 µg/mL (2.1 µM)	215
Microstructure Hydrophobic content		75	E. coli ^b S. aureus P. aeruginosa S. marcescens	8 µg/mL 2 µg/mL 8 µg/mL 16 µg/mL	216
Star-shape architecture Hydrophobic content		32	E. coli P. aeruginosa K. Pneumoniae A baumannii CMDR A. baumannii ^b CMDR P. aeruginosa ^b	4.4 µg/mL (0.05 µM) ^c 1.7 µg/mL (0.02 µM) ^c 7.0 µg/mL (0.08 µM) ^c 1.7 µg/mL (0.02 µM) ^c 2.6 µg/mL (0.03 µM) ^c 2.6 µg/mL (0.03 µM) ^c	217

Chapter 1. Synthetic polymers as simplified analogs of antimicrobial peptides

Star-shape architecture	18	E. coli	218	4.4 µg/mL
Hydrophobic content				
Star-shape architecture	20	K. pneumoniae	219	1600 µg/mL (70 µM)
Hydrophobic content		E. coli		170 µg/mL (7.5 µM)
		P. aeruginosa		1600 µg/mL (70 µM)
		S. sonnei		1600 µg/mL (70 µM)
		S. typhimurium		200 µg/mL (8.7 µM)
		S. aureus		2050 µg/mL (90 µM)
Structure Linear	30	E. coli	220	1.7 µM
		B. subtilis		3.4 µM
Hinged	30	E. coli		1.58 µM
		B. subtilis		2.36 µM
Cyclic	30	E. coli		1.17 µM
		B. subtilis		1.78 µM
Star	30	E. coli		1.62 µM
		B. subtilis		3.23 µM
PEGylation	30	MRSA	221	55 µM
		B. subtilis ^b		2.5-5.5 µM
		K. Pneumoniae		27.5-55.3 µM
		P. eruginosa		>100 µM
PEGylation	25	S. aureus	222	125 µg/mL
		E. coli		
		P. aeruginosa		
Macroinitiator	25	MRSA	223	31.25 µg/mL
		S. epidermidis ^b		62.5 µg/mL
		E.coli		62.5 µg/mL
		P. aeruginosa		62.5 µg/mL
		C. albicans		62.5 µg/mL

^a Minimum inhibitory concentration; ^b multidrug multidrug-resistant bacteria including colistin resistance; ^c the values are given according to the minimum bactericidal concentration (MBC);

Later and to better study the influence of the cationic moiety, A. Engler *et al.* studied different

Chapter 1. Synthetic polymers as simplified analogs of antimicrobial peptides

poly(γ -(1-(3-(aminopropyl)-1H-1,2,3-triazol-4-yl)methoxy)-L-glutamate) bearing primary, secondary, tertiary and quaternary iminium pendant groups against Gram-positive and Gram-negative bacteria.²¹¹ The study demonstrated that quaternized compounds with a molar mass of 5 kDa have the best antibacterial activity. In another study, the nature of the alkyl side chain was also important to increase the antibacterial activity, as it was demonstrated with phenylalanine and leucine in copolymers containing lysine.²¹²

One important feature of polypeptide polymers is their secondary structuring. For instance, some studies reported the improvement of antimicrobial activity by designing polymers adopting an α -helical structure, such as poly(γ -(1-methyl-1H-imidazolium)-L-glutamate).²¹³ X. Xu *et al.* developed a copolymer based on poly(L-glutamic acid) and positively charged poly(γ -(6-N-(methyldihexylammonium)hexyl)-L-glutamate) (PGA)_m-r-(PHLG-MHH)_n.²¹⁴ This copolymer presented a pH-sensitive α -helical structure exhibiting remarkable activity against *H. pylori* at acidic pH (and not at neutral pH). Another study demonstrated that copolymers with phosphorylated tyrosine and (γ -(N-(dimethyloctyl hexylammonium)-L-glutamate) presented antibacterial activity against *S. aureus*, *B. cereus* and MRSA. Those polymers were less cytotoxic (cell viability > 80% at 70 μ M) as compared to non-phosphorylated analogs ones (cell viability < 40% at 70 μ M).²¹⁵

Besides secondary structure, C. Zhou *et al.* evaluated the efficacy between block copolypeptides and random copolymers based on lysine and phenylalanine, varying the hydrophobicity content from 30% to 60%.²¹⁶ All the copolymers presented a broad-spectrum antimicrobial activity but this activity was better with block copolymers, showing the typical membrane disruption found in AMPs. A cytotoxicity assay in L02 cells revealed that these copolymers were not cytotoxic (up to 1000 μ g/mL), even with a 60% hydrophobic side chain content. The enzymatic degradation demonstrated that the copolymer was degraded at 41% upon 3 hours.

Antimicrobial polypeptides were also prepared using dendritic cores to obtain star-shaped architectures, such as the work of G. Qiao *et al.* on structurally nanoengineered antimicrobial peptide polymers (SNAPPs).²¹⁷ This work involved the grafting-from synthesis of copolymers based on lysine and valine using poly(amidoamine) dendrimers. The length of the polymers ranged from 16 to 32 amino acid residues, the proportion of lysine valine was 2:1 and, the efficacy was demonstrated against Gram-negative and Gram-positive bacteria including multidrug-resistant *P. aeruginosa* and *A. baumannii*. Copolymers demonstrated superior activity in

Chapter 1. Synthetic polymers as simplified analogs of antimicrobial peptides

comparison with AMPs such as ovispirin, magainin II and melittin. SNAPPs with 16 amino acid residues also demonstrated *in vivo* activity against multidrug-resistant bacteria.²²⁴ In 2018, the same authors published a comprehensive study on the SNAPPs varying the arm numbers (4-16) and arm length (5-30 amino acid residues).²¹⁸ The study revealed that increasing arm number and length enhanced the antimicrobial activity, which can be related to higher local concentrations of polypeptide arms and an increase of *alpha*-helical content. However, the improvement of the antimicrobial activity was associated to more toxicity. According to flow cytometry studies, the mode of action of SNAPPs was established and based on the membrane disruption, an effect directly influenced by arm length and arm number. Another star-shaped polymer based on lysine and post-functionalized with indole (20% mol) was also developed by other authors but again, with significant toxicity.²¹⁹ The highest antimicrobial effect of star polymers was obtained by H. Liang *et al.* by comparing the activity of star polymers including 10 lysine and 5 phenylalanine residues with synthetic AMPs based on cecropin A and melittin.²²⁵ The study showed that star polymers interact strongly with a simulated dipalmitoylphosphatidylcholine bilayer in comparison to the peptides, which led to enhanced membrane disruption. A very interesting study involving copolymers of carboxybenzylglutamate and lysine (having a length of 30 amino acid residues and a hydrophobic content of approximately 20%) finally demonstrated good antibacterial activity against *E. coli* and *B. subtilis* with a remarkable low hemolysis $HC_{50} > 4000 \mu\text{g/mL}$, even varying the architecture between linear, hinged, cyclic and star polymers.²²⁰

Seeking for safer antimicrobial polypeptides, J. Cai *et al.* performed the synthesis of a lysine-phenylalanine copolymer using PEG-*b*-polylysine as macroinitiator.²²¹ The resulting polymers (constituted of 10 lysine and 15 phenylalanine monomer units) demonstrated a slight reduction of hemolytic activity from $HC_{50} = 3 \mu\text{M}$ to $HC_{50} = 9 \mu\text{M}$ due to the decrease of hydrophobicity allowed by PEGylation. Besides, the copolymers demonstrated antibacterial activity against Gram-positive and Gram-negative bacteria including methicillin-resistance species. In 2019, W. Huang *et al.* developed a copolymer based on dextran and poly(lysine-*r*-phenylalanine), both were copolymerized by click chemistry.²²³ Broad-spectrum antibacterial and antifungal activity were shown for the copolymers including multidrug-resistant bacteria and dextran 1) helped to decrease the hemolytic activity and 2) exhibited biocompatibility in murine myoblast (C21C12) cells.

In general, all the polypeptide polymers with antibacterial properties that were developed present 2 significant limitations.

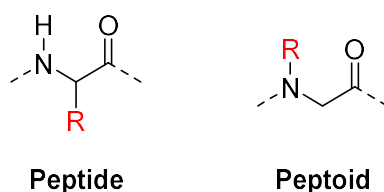
Chapter 1. Synthetic polymers as simplified analogs of antimicrobial peptides

- First, since polypeptides kill either both Gram-negative and Gram-positive bacteria or in the best of the cases, just one of these groups, the lack of selectivity is somehow an issue as compared to AMPs that are more specific.
- Second, the lack of selectivity towards humans cells has often to be improved. Both limitations could benefit from the design of libraries to better understand the different physico-chemical parameters improving the selectivity.

Finally, the fact that peptidic backbones rank polypeptides among biodegradable polymers, their high susceptibility to enzymatic hydrolysis can also result in a lack of effectiveness *in vivo*. For instance, polypeptides are hydrolyzed by proteases found along the digestive tube, such as trypsin²¹⁶ and carboxypeptidases.²²⁶ Therefore, this susceptibility to proteases could constraint to high doses treatment and increase the risk of adverse effects that AMPs are already presenting.¹⁶⁴

6 Peptoids as analogs of AMPs with improved stability

One of the most interesting approaches to mimics peptides is the use of *N*-alkylated analogs named “peptoids” in which the side chains of the *alpha*-amino acids found in peptides are linked to the nitrogen atom of the amide bond (**Scheme 1**). In peptides, the hydrogen in the *alpha* position helps to stabilize the formation of secondary structures, while in peptoids this hydrogen is replaced by an alkyl chain: this change prevents stabilizing conformations. Nevertheless, because of the presence of a tertiary amide function in their chemical structure, peptoids can easily adopt both *cis* and *trans* conformations (**Scheme 2**).²²⁷ This strongly reduces the protease recognition towards peptide bonds and decreases the proteolysis efficiency.



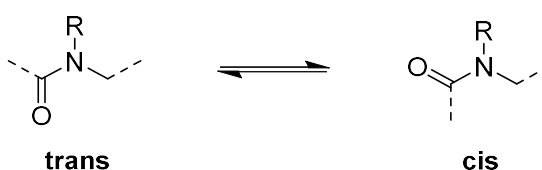
Scheme 1. General structures of Peptides and Peptoids.

In the late 1980s, peptoids were first introduced by a biotechnology company (the Chiron Corporation) and developed in 1992 by R. Zuckermann using stepwise synthesis.²²⁸ The first library was prepared by solid-phase peptide synthesis (SPPS), using the Merrifield-like

Chapter 1. Synthetic polymers as simplified analogs of antimicrobial peptides

strategy.²²⁹ Indeed, solid-phase synthesis is a technique employed worldwide to create sequence-specific oligomers such as oligopeptides, oligosaccharides or oligonucleotides.²³⁰ In a first step, a resin is prepared and will be the support for the synthesis then, several iterative routes can be followed: i) nucleophilic (R_2 -NH) attack to the carbonyl in Fmoc *N*-alkylated glycines followed by deprotection;²²⁸ ii) nucleophilic (R_2 -NH) attack to the carbonyl in Fmoc glycines followed by alkylation through reductive amination;²³¹ iii) nucleophilic (R_2 -NH) attack to haloacetic acid followed of primary amines addition by nucleophilic substitution;²³² iv) nucleophilic (R_2 -NH) attack to bromoacetic acid and *N*-alkylation assisted with *o*-nitrobenzenesulfonamides;²³³ v) acylation assisted with photolithographic synthesis and *N*-alkylation assisted with *o*-nitrobenzenesulfonamides.²³⁴ The advantage of the stepwise method is to control the sequence of the *N*-alkylated amino acids along the peptoid chain. In 1998, based on Zuckermann's developments, E. Cortez *et al.* introduced β -peptoids by analogy with β -peptides.²³⁵ Thereafter, C. Taillefumier *et al.* synthesized α,β -alternating peptoids.²³⁶

The characteristic tertiary backbone amide group in peptoids provides the flexibility of peptoid oligomers (**Scheme 2**). Due to its flexibility, a peptoid solution composed of *n* monomers



Scheme 2. *Cis/trans isomerism of peptoid (N,N-disubstituted amides).*

can exist in an equilibrium mixture of 2^{n-1} configurational isomers, or 2^n if the *N*-terminal amino acid is acetylated.²³⁷ This *cis/trans* isomerism can be observed by $^1\text{H-NMR}$ analysis by the appearance of signal multiplets, which are similar to $^1\text{H-NMR}$ signals of collagen in which proline residues are responsible of this multiplicity.^{237,238} Interestingly, peptoids can fold into helical secondary structures when they possess chiral pendant groups.²³⁸

The *N,N*-disubstituted amide linkage allows resistance toward protease hydrolysis as it was demonstrated in 1994 by S. Miller *et al.*²³⁹ This observation was established comparing *L*-peptides, *D*-peptides and peptoids using various proteases such as carboxypeptidase A, papain, pepsin, trypsin, elastase and chymotrypsin. The authors demonstrated that enzymes were not able to cleave, neither *D*-peptides nor *N*-substituted glycines. In 2010, S. Shin *et al.* indirectly corroborated this resistance to enzyme degradation by measuring the inhibition of bacterial

Chapter 1. Synthetic polymers as simplified analogs of antimicrobial peptides

growth.²⁴⁰ Thus, a synthetic AMP and its analogous antimicrobial peptoid were treated by a digesting protocol using trypsin and tested for their antimicrobial activity in *E. coli*. The study showed that, after digestion, the peptoid presented activity against *E. coli* similar to the one displayed before digestion while synthetic AMP lost most of its activity.

Previous studies have already reported antimicrobial properties with peptoids. In 1999, J. Winter *et al.* reported that peptoid dimers and trimers were effective against both Gram-negative and Gram-positive bacteria (minimum inhibitory concentration (MIC) = 5-40 μ M), these compounds also displayed hemolytic activity.²⁴¹ In 2008, A. Barron *et al.* reported the antibacterial activity of a library of peptoids and their selectivity for bacterial cells over mammalian cells.²⁴² The peptoids included in their sequence lysine-like (Nlys) and S-ethylphenyl (Nspe) moieties demonstrated optimal selectivity. Further studies focused on using bi-naphthyl structures to synthesize cyclic peptoids bearing antibacterial activity against *S. aureus*, *S. epidermis* and *Enterococcus* but the activity was not compared to reference drugs such as vancomycin.^{243,244} In 2012, K. Kirshenbaum *et al.* found a superior activity of cyclic peptoids against *E. coli* in comparison to the linear analogs but both presented hemolytic effects.²⁴⁵ The length of the *N*-hydrophobic substituent using pentyl, decyl and tridecyl alkyl side chains was also studied to resemble lipopeptides and, broad-spectrum antibacterial activity was higher using one decyl and tridecyl alkyl glycines in a peptide with 9 alkyl glycines.²⁴⁶

In 2015, R. Zuckerman *et al.* developed a library of antimicrobial peptoids and confirmed several of the previous findings.²⁴⁷ They evaluated the length of the spacer between the cationic Nlys carbon chain and *N*-2-aminoethyl glycine (Nae), observing that no significant effect was shown on the antibacterial activity. The same group also observed that hydrophobicity content affects the antibacterial activity by replacing the alkyl group *N*-(5-indene) for *N*-(2,2-diphenylethyl). The optimal antibacterial activity was found for the peptoid with a +4 net charge and a proportion of 5:9 for hydrophobic aminoacid-like units, which remained active over 6 hours against *E. coli*. In 2017, S. Cobb *et al.* explored the links between toxicity and biocidal activity.²⁴⁸ One of the parameters evaluated was the different cations Nlys, Narg (analogs of Lysine and Arginine) and Nae and it was found that Narg presented higher toxicity.

Despite, these promising biological properties, including multidrug resistance reversal properties^{242,249} and protease resistance,²³⁹ some important limitations are still limiting peptoid developments. One of them is the use of SPPS method that requires numerous reaction steps, leading to low yields and small amounts (a few milligrams) of the desired product.²¹⁰ Another

limitation is that this method is restricted in terms of chain length, usually less than 20 monomer units.^{230,250}

7 Polypeptoids

Peptoid polymers, also called poly(*N*-substituted glycines) or polypeptoids are *N*-alkylated analogs of synthetic polypeptide polymers: they are polypeptides with an *N*-substituted amide bond. The physicochemical properties of polypeptoids can be tailored by the *N*-alkylation, enabling control over 1) the hydrophilic to lipophilic balance, 2) the charge characteristics, 3) the backbone conformation, 4) the solubility, 5) the thermal and crystallization properties.²⁵¹ In contrast to polypeptides, they resist protease hydrolysis.

The direct way to prepare polypeptoids is to polymerize of *N*-alkylated-*N*-carboxyanhydrides monomers (NNCA). The NNCA monomers can be synthesized through several routes (**Figure 11**). Briefly, the Leuchs method involves the use of thionyl chloride (SOCl₂)²⁵² or other Lewis acid such as PCl₃ and PBr₃.^{253,254} Adaptation of the Leuchs method by Schlaad's and coworkers involved a mixture of acetyl chloride and acetic anhydride.²⁵⁵ Developed later, the main method to produce NNCA involves the use of phosgene or their derivatives diphosgene and triphosgene (The Fuchs Farthing method). The advantage of this approach is that there are fewer acid traces that can slow down the kinetics rate of polymerization.²⁵⁶

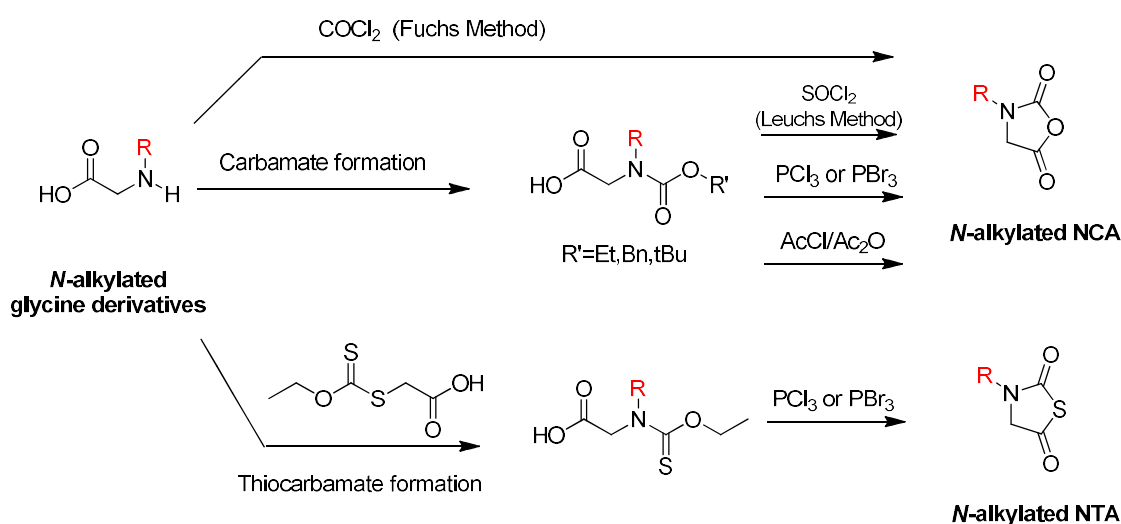


Figure 11. Synthesis of *N*-alkylated-*N*-carboxyanhydrides (NCA) and *N*-alkylated-*N*-thiocarboxyanhydrides (NTA).

Chapter 1. Synthetic polymers as simplified analogs of antimicrobial peptides

Generally, polypeptoids are synthesized from NNCA through a process called, ring-opening polymerization (ROP) that is commonly controlled using nucleophiles such as amines (primary or secondary), alcohols or *N*-heterocyclic carbenes.²⁵⁶ The most studied polypeptoid is obtained by polymerizing *N*-alkylated-*N*-carboxyanhydride, sarcosine (Sar-NCA). In 1906, H. Leuchs discovered this monomer by chance, attempting to purify *N*-ethoxycarbonyl or *N*-methoxycarbonyl aminoacid chlorides by distillation.²⁵⁷ Then, he reported the synthesis of sarcosine derivatives with high molar mass.^{252,258} In 1921 T. Curtis *et al.*²⁵⁹ and F. Wessely *et al.*²⁶⁰ assumed for the first time that the reaction products of NCAs were high-molar-mass polypeptoids. Nowadays, polysarcosine is well recognized and is one of the most investigated polypeptoids because of its comparable properties to PEG for biomedical applications and its degradability.^{261,262}

R. Luxenhofer *et al.* demonstrated that the polymerizations of Sar-NCAs proceeded in a controlled manner without chain transfer or termination events, producing polysarcosine with narrow Poisson distribution ($\bar{D}_M = 1.1-1.3$) and molar masses that can be controlled by the initial monomer to initiator feed ratios.²⁶³ The same author published other polypeptoids bearing *N*-ethyl, *N*-propyl, *N*-butyl and *N*-isobutyl side chains with narrow polymer dispersity ($\bar{D}_M = 1.14-1.31$).²⁵⁶ H. Schlaad *et al.* studied the polymerization of *N*-allyl-NNCA with molar masses in the range of 1.5-10.5 kg/mol and relatively narrow polymer dispersity ($\bar{D}_M = 1.1-1.4$) that allowed the post-functionalization with a protected saccharide.²⁶⁴ Moreover, R. Luxenhofer *et al.*, by pushing the limits of the polymerization process, prepared multiblock copolymers of polysarcosine with relatively narrow polydispersities ($\bar{D}_M = 1.52-1.10$).²⁶³ They also prepared penta-block copolypeptoids bearing *N*-methyl, *N*-ethyl, *N*-propyl, *N*-butyl and *N*-pentyl side chains with an increasing molar mass in agreement with each block synthesized and with polymer dispersity in the range of $\bar{D}_M = 1.89-1.12$.

Several interesting properties and applications were described for polypeptoid polymers. For instance, M. Barz *et al.* described the synthesis and application of bottlebrush copolymers between polylysine and sarcosine for gene delivery, taking advantage of poly sarcosine properties: water solubility, nonionic and nonimmunogenic.²⁶⁵ The cationic bottlebrush polymers were examined as effective carriers for siRNA delivery with a 70% knockdown efficiency in AM L-12 hepatocytes.

The thermal properties of the polypeptoid polymers are strongly dependent on the *N*-substituent structures, giving rise to amorphous and semicrystalline polymers according to D. Zhang *et al.* in 2013.²⁶⁶ Linear aliphatic *N*-substituents shorter than 4 carbons were amorphous,

Chapter 1. Synthetic polymers as simplified analogs of antimicrobial peptides

whereas polymers with longer linear aliphatic *N*-substituents ($n = 4, 5, 6, 8, 10, 12,$ and 14) tended to be highly crystalline and packed into the lamellar structure in the solid-state. The disappearance of crystallization was also observed with asymmetric branching onto the *N*-substituents (i.e. 2-ethylhexyl).

Because polypeptoids have a polar backbone, the overall hydrophilic and hydrophobic balance (HLB) can be tuned by controlling the *N*-substituent. This behavior is reflected in reversible temperature-induced cloud point transition due to a hydrophobic collapse, normally polypeptoids bearing methyl, ethyl or methoxyethyl substituents do not present this phenomenon because they are soluble in water.²⁵¹ C3 polypeptoids presented the lower critical solution temperatures (LCST) that can be tuned according to the molar mass and the nature of the monomer. This behavior can be controlled by copolymerization in cyclic and linear polypeptoids as D. Zhang *et al.* demonstrated.²⁵⁵ This LCST can be controlled in the range 20-60 °C by modifying the polymer composition and architecture. Cyclic polypeptoids exhibited lower clouding points than their linear counterparts by 5 °C, which is a result of cyclic polypeptoids forming soluble dimers in water.

Besides, polypeptoids and copolypeptoids present very interesting biological properties as also demonstrated D. Zhang *et al.*²⁵⁵ The cell viability on fibroblasts (HEL229) after contact with the cyclic poly(*N*-ethylglycine₇₄-*r*-butylglycine₁₅) was superior to 80% even at 5 mg/mL. The biocompatibility was also demonstrated by R. Luxenhofer *et al.* through the biocompatibility in human hepatoma (HepG2) cells up to the concentration of 2 mg/mL for different copolymers between sarcosine and, *N*-butyl-NNCA, *N*-propyl-NNCA and *N*-benzyl-NNCA.²⁶⁷ In the same year, J. Ling *et al.* studied the cytotoxicity of poly(sarcosine-*r*-butylglycine).²⁶⁸ The results showed hepatic cells (HepG2) still alive up to a concentration of 5 mg/mL for poly(sarcosine₄₈-*r*-butylglycine₂₆).

At the same time, D. Zhang *et al.* developed thermoreversible and injectable ABC polypeptoid hydrogels constituted of *N*-allyl-glycine (A), sarcosine (B) and *N*-decyl-glycine (C).²⁶⁹ The hydrogels presented transition gel temperatures in the range of 26-40 °C. The triblock copolymer A₉₂B₉₄C₁₂ presented minimal cytotoxicity up to 20 mg/mL in human adipose-derived stem cells (hASC). Furthermore, healthy spindle shape was observed on the cells which suggested that they can be used as scaffolds for engineering tissue.

In 2017, M. Barz *et al.* demonstrated that star-like sarcosine copolymers with lysine did not

Chapter 1. Synthetic polymers as simplified analogs of antimicrobial peptides

kill HeLa cells in a range of 0.1-1.0 mg/mL and also that the star polymers of sarcosine internalized into the cells which open the safety use for drug delivery.²⁷⁰ In the same year, D. Zhang *et al.* published a series of polymers bearing ethylene glycol side chains in which minimal cytotoxicity was found (>90% cell viability) in a range of 0.1-1.0 mg/mL in HepG2 cells. Also, they found that the copolymers presented minimal interaction with proteins using a lysozyme model.²⁷¹

The immunogenicity of polypeptoids was tested only for polysarcosine. The polymer did not cause any antigenic response in immunized rabbits.²⁷² Taking advantage of the nonimmunogenic response, the polymer was conjugated with grass pollen allergen extracts, demonstrating efficient suppression of the induction of immunoglobulin E (IgE) response in mice, opening the possibility to develop new treatments for allergies.²⁷³

Concerning the antibacterial activity that polypeptoids polymers could offer, only two reports were published by the group of M. Barz. The surface grafted with polymethacrylate was decorated with polysarcosine and poly(Lys-*r*-Phe).²⁷⁴ The designed material proved to be effective against *S. aureus*, *E. coli*, *P. aeruginosa* and *C. albicans*. However, the polypeptide itself demonstrated antimicrobial activity. The other report corresponds to a surface that contains silver nanoparticles and an ABC copolymer of glutamate, dopamine-glutamate and sarcosine.²⁷⁵ The material presented antibacterial activity against *E. coli*. In addition, no cytotoxic effect was observed over human dermal fibroblast.

8 References

- (1) World Health Organization. Antibiotic Resistance. Antibiotic resistance <https://www.who.int/news-room/fact-sheets/detail/antibiotic-resistance> (accessed May 15, 2020).
- (2) Pasteur Institute. Antibiotic Resistance. Antibiotic resistance <https://www.pasteur.fr/en/medical-center/disease-sheets/antibiotic-resistance> (accessed May 15, 2020).
- (3) European Centre for Disease Prevention and Control. Surveillance of Antimicrobial Resistance in Europe Annual Report of the European Antimicrobial Resistance Surveillance Network (EARS-Net) 2017. European Centre for Disease Prevention and Control: Stockholm, 2018.
- (4) Centers for Disease Control and Prevention (CDC). Antimicrobial Resistance (AR/AMR). Antimicrobial Resistance (AR/AMR) <https://www.cdc.gov/drugresistance/index.html> (accessed Jan 10, 2021).
- (5) World Health Organization. Antimicrobial Resistance. Antimicrobial resistance <https://www.who.int/news-room/fact-sheets/detail/antimicrobial-resistance> (accessed May 15, 2020).
- (6) Klein, E. Y.; Van Boeckel, T. P.; Martinez, E. M.; Pant, S.; Gandra, S.; Levin, S. A.; Goossens, H.; Laxminarayan, R. Global Increase and Geographic Convergence in Antibiotic Consumption between 2000 and 2015. *Proc. Natl. Acad. Sci. U. S. A.* **2018**, *115* (15), E3463–E3470.
- (7) O'Neill, J. Review on Antimicrobial Resistance. Tackling Drug-Resistant Infections Globally. Review on Antimicrobial Resistance. Tackling drug-resistant infections globally. <https://amr-review.org/> (accessed May 15, 2020).
- (8) Cassini, A.; Högberg, L. D.; Plachouras, D.; Quattrocchi, A.; Hoxha, A.; Simonsen, G. S.; Colomb-Cotinat, M.; Kretzschmar, M. E.; Devleeschauwer, B.; Cecchini, M.; Ouakrim, D. A.; Oliveira, T. C.; Struelens, M. J.; Suetens, C.; Monnet, D. L.; Strauss, R.; Mertens, K.; Struyf, T.; Catry, B.; Latour, K.; Ivanov, I. N.; Dobрева, E. G.; Tambic Andrašević, A.; Soprek, S.; Budimir, A.; Paphitou, N.; Žemlicková, H.; Schytte Olsen, S.; Wolff Sönksen, U.; Märtin, P.; Ivanova, M.; Lyytikäinen, O.; Jalava, J.; Coignard, B.; Eckmanns, T.; Abu

Chapter 1. Synthetic polymers as simplified analogs of antimicrobial peptides

- Sin, M.; Haller, S.; Daikos, G. L.; Gikas, A.; Tsiodras, S.; Kontopidou, F.; Tóth, Á.; Hajdu, Á.; Guólaugsson, Ó.; Kristinsson, K. G.; Murchan, S.; Burns, K.; Pezzotti, P.; Gagliotti, C.; Dumpis, U.; Liuimiene, A.; Perrin, M.; Borg, M. A.; de Greeff, S. C.; Monen, J. C.; Koek, M. B.; Elstrøm, P.; Zabicka, D.; Deptula, A.; Hryniewicz, W.; Caniça, M.; Nogueira, P. J.; Fernandes, P. A.; Manageiro, V.; Popescu, G. A.; Serban, R. I.; Schréterová, E.; Litvová, S.; Štefkovicová, M.; Kolman, J.; Klavs, I.; Korošec, A.; Aracil, B.; Asensio, A.; Pérez-Vázquez, M.; Billström, H.; Larsson, S.; Reilly, J. S.; Johnson, A.; Hopkins, S. Attributable Deaths and Disability-Adjusted Life-Years Caused by Infections with Antibiotic-Resistant Bacteria in the EU and the European Economic Area in 2015: A Population-Level Modelling Analysis. *Lancet Infect. Dis.* **2019**, *19* (1), 56–66.
- (9) Smith, R.; Coast, J. The True Cost of Antimicrobial Resistance. *BMJ* **2013**, *346*, f1493–f1493.
- (10) World Health Organization. Report on the Burden of Endemic Health Care-Associated Infection Worldwide Clean Care Is Safer Care. Report on the Burden of Endemic Health Care-Associated Infection Worldwide Clean Care is Safer Care <https://www.ncbi.nlm.nih.gov/books/NBK144030/> (accessed May 15, 2020).
- (11) Haque, M.; Sartelli, M.; McKimm, J.; Abu Bakar, M. Bin. Health Care-Associated Infections - an Overview. *Infect. Drug Resist.* **2018**, *Volume 11*, 2321–2333.
- (12) Centers for Disease Control and Prevention (CDC). Healthcare-Associated Infections. Healthcare-associated Infections <https://www.cdc.gov/hai/index.html> (accessed May 15, 2020).
- (13) Costerton, J. W.; Calkwell, D. E.; Kober, D. R.; M.Lappin-Scott, H.; Lewandowski, Z.; Caldwell, D. E.; Korber, D. R.; Lappin-Scott, H. M. Microbial Biofilms. *Annu. Rev. Microsc.* **1995**, *49*, 711–745.
- (14) Hall-Stoodley, L.; Costerton, J. W.; Stoodley, P. Bacterial Biofilms: From the Natural Environment to Infectious Diseases. *Nat. Rev. Microbiol.* **2004**, *2* (2), 95–108.
- (15) Thien Fah C, M.; A. O’Toole, G. Mechanisms of Biofilm Resistance to Antimicrobial Agents. *Trends Microbiol.* **2001**, *9* (1), 34–39.
- (16) Stewart, P. S.; Costerton, J. W. Antibiotic Resistance of Bacteria in Biofilms. *Lancet* **2001**, *358*, 135–138.

Chapter 1. Synthetic polymers as simplified analogs of antimicrobial peptides

- (17) Aslam, B.; Wang, W.; Arshad, M. I.; Khurshid, M.; Muzammil, S.; Rasool, M. H.; Nisar, M. A.; Alvi, R. F.; Aslam, M. A.; Qamar, M. U.; Salamat, M. K. F.; Baloch, Z. Antibiotic Resistance: A Rundown of a Global Crisis. *Infect. Drug Resist.* **2018**, Volume 11, 1645–1658.
- (18) Peterson, E.; Kaur, P. Antibiotic Resistance Mechanisms in Bacteria: Relationships between Resistance Determinants of Antibiotic Producers, Environmental Bacteria, and Clinical Pathogens. *Front. Microbiol.* **2018**, 9 (NOV), 1–21.
- (19) Chopra, I. Over-Expression of Target Genes as a Mechanism of Antibiotic Resistance in Bacteria. *J. Antimicrob. Chemother.* **1998**, 41 (6), 584–588.
- (20) Händel, N.; Schuurmans, J. M.; Feng, Y.; Brul, S.; Ter Kuile, B. H. Interaction between Mutations and Regulation of Gene Expression during Development of de Novo Antibiotic Resistance. *Antimicrob. Agents Chemother.* **2014**, 58 (8), 4371–4379.
- (21) Neu, H. C. The Crisis in Antibiotic Resistance. *Science* **1992**, 257 (5073), 1064–1073.
- (22) Alekshun, M. N.; Levy, S. B. Molecular Mechanisms of Antibacterial Multidrug Resistance. *Cell* **2007**, 128 (6), 1037–1050.
- (23) Levy, S. B.; Marshall, B. Antibacterial Resistance Worldwide: Causes, Challenges and Responses. *Nat. Med.* **2004**, 10 (S12), S122–S129.
- (24) Nikaido, H. Multidrug Resistance in Bacteria. *Annu. Rev. Biochem.* **2009**, 2, 119–146.
- (25) World Health Organization. Lack of New Antibiotics Threatens Global Efforts to Contain Drug-Resistant Infections. Lack of new antibiotics threatens global efforts to contain drug-resistant infections <https://www.who.int/news-room/detail/17-01-2020-lack-of-new-antibiotics-threatens-global-efforts-to-contain-drug-resistant-infections> (accessed May 15, 2020).
- (26) World Health Organization. Prioritization of Pathogens to Guide Discovery, Research and Development of New Antibiotics for Drug Resistant Bacterial Infections, Including Tuberculosis. *WHO, Press* **2017**.
- (27) World Health Organization. Biggest Threats and Data. Biggest Threats and Data <https://www.cdc.gov/drugresistance/biggest-threats.html#groupb> (accessed Apr 1, 2021).
- (28) Schein, C. H. Repurposing Approved Drugs on the Pathway to Novel Therapies. *Med. Res.*

Chapter 1. Synthetic polymers as simplified analogs of antimicrobial peptides

- Rev. **2020**, *40* (2), 586–605.
- (29) Lawson, P. A.; Citron, D. M.; Tyrrell, K. L.; Finegold, S. M. Reclassification of *Clostridium difficile* as *Clostridioides difficile* (Hall and O'Toole 1935) Prévot 1938. *Anaerobe* **2016**, *40*, 95–99.
- (30) Banaei, N.; Anikst, V.; Schroeder, L. F. Burden of *Clostridium difficile* Infection in the United States. *N. Engl. J. Med.* **2015**, *372* (24), 2368–2369.
- (31) Centers for Disease Control and Prevention (CDC). Antibiotic Resistance Threats in the United States. Antibiotic resistance threats in the United States <https://www.cdc.gov/drugresistance/biggest-threats.html> (accessed May 15, 2020).
- (32) Centers for Disease Control and Prevention (CDC). *Clostridioides difficile* (*C. diff*). *Clostridioides difficile* (*C. diff*) <https://www.cdc.gov/cdiff/what-is.html> (accessed Feb 15, 2021).
- (33) European Centre for Disease Prevention and Control (ECDC). Annual Epidemiological Report for 2016 *Clostridium difficile* Infections. Annual Epidemiological Report for 2016 *Clostridium difficile* infections <https://www.ecdc.europa.eu/en/publications-data/healthcare-associated-infections-clostridium-difficile-infections-annual> (accessed May 15, 2020).
- (34) Reigadas Ramírez, E.; Bouza, E. S. Economic Burden of *Clostridium difficile* Infection in European Countries. *Adv. Exp. Med. Biol.* **2018**, *1050*, 1–12.
- (35) HALL, I. C. INTESTINAL FLORA IN NEW-BORN INFANTS. *Am. J. Dis. Child.* **1935**, *49* (2), 390.
- (36) Aktories, K.; Wilkins, T. D. *Clostridium difficile*. Aktories, K., Wilkins, T. D., Eds.; Current Topics in Microbiology and Immunology; Springer Berlin Heidelberg: Berlin, Heidelberg, 2000; Vol. 250.
- (37) Hammarstrom, S. Autoantibodies to Colon in Germfree Rats Monocontaminated with *Clostridium difficile*. *J. Exp. Med.* **1969**, *129* (4), 747–756.
- (38) Smith, L. D.; King, E. O. Occurrence of *Clostridium difficile* in Infections of Man. *J. Bacteriol.* **1962**, *84*, 65–67.
- (39) Green, R. H. The Association of Viral Activation with Penicillin Toxicity in Guinea Pigs and

Chapter 1. Synthetic polymers as simplified analogs of antimicrobial peptides

- Hamsters. *Yale J. Biol. Med.* **1974**, *47* (3), 166–181.
- (40) Tedesco, F. J. Clindamycin-Associated Colitis. *Ann. Intern. Med.* **1974**, *81* (4), 429.
- (41) Bartlett, J. G.; Onderdonk, A. B.; Cisneros, R. L.; Kasper, D. L. Clindamycin-Associated Colitis Due to a Toxin-Producing Species of *Clostridium* in Hamsters. *J. Infect. Dis.* **1977**, *136* (5), 701–705.
- (42) Larson, H. E.; Parry, J. V.; Price, A. B.; Dolby, J.; Tyrrell, D. A. J.; Davies, D. R. Undescribed Toxin in Pseudomembranous Colitis. *Br. Med. J.* **1977**, *1* (6071), 1246–1248.
- (43) Bartlett, J. G.; Chang, T. W.; Gurwith, M.; Gorbach, S. L.; Onderdonk, A. B. Antibiotic-Associated Pseudomembranous Colitis Due to Toxin-Producing Clostridia. *N. Engl. J. Med.* **1978**, *298* (10), 531–534.
- (44) Lance George, W.; Goldstein, E. C.; Sutter, V.; Ludwig, S.; Finegold, S. Aetiology of Antimicrobial-Agent-Associated Colitis. *Lancet* **1978**, *311* (8068), 802–803.
- (45) Al Saif, N.; Brazier, J. S. The Distribution of *Clostridium difficile* in the Environment of South Wales. *J. Med. Microbiol.* **1996**, *45* (2), 133–137.
- (46) Kirk, J. A.; Banerji, O.; Fagan, R. P. Characteristics of the *Clostridium difficile* Cell Envelope and Its Importance in Therapeutics. *Microb. Biotechnol.* **2017**, *10* (1), 76–90.
- (47) Krishna, M. M.; Powell, N. B. L.; Boriello, S. P. Cell Surface Properties of *Clostridium difficile*: Haemagglutination, Relative Hydrophobicity and Charge. *J. Med. Microbiol.* **1996**, *44* (2), 115–123.
- (48) Kochan, T. J.; Foley, M. H.; Shoshiev, M. S.; Somers, M. J.; Carlson, P. E.; Hanna, P. C. Updates to *Clostridium difficile* Spore Germination. *J. Bacteriol.* **2018**, *200* (16), 1–12.
- (49) Hafiz, S.; Oakley, C. L. *Clostridium difficile*: Isolation and Characteristics (Plate VIII). *J. Med. Microbiol.* **1976**, *9* (2), 129–136.
- (50) Gerding, D. N.; Muto, C. A.; Owens, Jr., R. C. Measures to Control and Prevent *Clostridium difficile* Infection. *Clin. Infect. Dis.* **2008**, *46* (s1), S43–S49.
- (51) Ananthkrishnan, A. N. *Clostridium difficile* Infection: Epidemiology, Risk Factors and Management. *Nat. Rev. Gastroenterol. Hepatol.* **2011**, *8* (1), 17–26.
- (52) Heinlen, L.; Ballard, J. D. *Clostridium difficile* Infection. *Am. J. Med. Sci.* **2010**, *340* (3),

247–252.

- (53) Johnson, S.; Adelman, A.; Clabots, C. R.; Peterson, L. R.; Gerding, D. N. Recurrences of *Clostridium difficile* Diarrhea Not Caused by the Original Infecting Organism. *J. Infect. Dis.* **1989**, *159* (2), 340–343.
- (54) Dallal, R. M.; Harbrecht, B. G.; Boujoukas, A. J.; Sirio, C. A.; Farkas, L. M.; Lee, K. K.; Simmons, R. L. Fulminant *Clostridium difficile*: An Underappreciated and Increasing Cause of Death and Complications. *Ann. Surg.* **2002**, *235* (3), 363–372.
- (55) Theriot, C. M.; Bowman, A. A.; Young, V. B. Antibiotic-Induced Alterations of the Gut Microbiota Alter Secondary Bile Acid Production and Allow for *Clostridium difficile* Spore Germination and Outgrowth in the Large Intestine. *mSphere* **2016**, *1* (1), 1–16.
- (56) Pereira, F. C.; Saujet, L.; Tomé, A. R.; Serrano, M.; Monot, M.; Couture-Tosi, E.; Martin-Verstraete, I.; Dupuy, B.; Henriques, A. O. The Spore Differentiation Pathway in the Enteric Pathogen *Clostridium difficile*. *PLoS Genet.* **2013**, *9* (10).
- (57) Bouillaut, L.; Dubois, T.; Sonenshein, A. L.; Dupuy, B. Integration of Metabolism and Virulence in *Clostridium difficile*. *Res. Microbiol.* **2015**, *166* (4), 375–383.
- (58) Sullivan, N. M.; Pellett, S.; Wilkins, T. D. Purification and Characterization of Toxins A and B of *Clostridium difficile*. *Infect. Immun.* **1982**, *35* (3), 1032–1040.
- (59) Rupnik, M.; Wilcox, M. H.; Gerding, D. N. *Clostridium difficile* Infection: New Developments in Epidemiology and Pathogenesis. *Nat. Rev. Microbiol.* **2009**, *7* (7), 526–536.
- (60) Balsells, E.; Shi, T.; Leese, C.; Lyell, I.; Burrows, J.; Wiuff, C.; Campbell, H.; Kyaw, M. H.; Nair, H. Global Burden of *Clostridium difficile* Infections: A Systematic Review and Meta-Analysis. *J. Glob. Health* **2019**, *9* (1).
- (61) Kansau, I.; Barketi-Klai, A.; Monot, M.; Hoys, S.; Dupuy, B.; Janoir, C.; Collignon, A. Deciphering Adaptation Strategies of the Epidemic *Clostridium difficile* 027 Strain during Infection through in Vivo Transcriptional Analysis. *PLoS One* **2016**, *11* (6), 1–13.
- (62) HOPE. *Clostridium difficile* Infection in Europe. A CDI Europe Report. 2013.
- (63) Hensgens, M. P. M.; Goorhuis, A.; Dekkers, O. M.; Kuijper, E. J. Time Interval of Increased Risk for *Clostridium difficile* Infection after Exposure to Antibiotics. *J. Antimicrob. Chemother.* **2012**, *67* (3), 742–748.

Chapter 1. Synthetic polymers as simplified analogs of antimicrobial peptides

- (64) Bartlett, J. G.; Moon, N.; Chang, T. W.; Taylor, N.; Onderdonk, A. B. Role of *Clostridium difficile* in Antibiotic-Associated Pseudomembranous Colitis. *Gastroenterology* **1978**, *75* (5), 778–782.
- (65) Van Der Kooi, T. I. I.; Koningstein, M.; Lindemans, A.; Notermans, D. W.; Kuijper, E.; Van Den Berg, R.; Boshuizen, H.; Filius, P. M. G.; Van Den Hof, S. Antibiotic Use and Other Risk Factors at Hospital Level for Outbreaks with *Clostridium difficile* PCR Ribotype 027. *J. Med. Microbiol.* **2008**, *57* (6), 709–716.
- (66) Theriot, C. M.; Koenigsknecht, M. J.; Carlson, P. E.; Hatton, G. E.; Nelson, A. M.; Li, B.; Huffnagle, G. B.; Li, J. Z.; Young, V. B. Antibiotic-Induced Shifts in the Mouse Gut Microbiome and Metabolome Increase Susceptibility to *Clostridium difficile* Infection. *Nat. Commun.* **2014**, *5*.
- (67) Loo, V. G.; Poirier, L.; Miller, M. A.; Oughton, M.; Libman, M. D.; Michaud, S.; Bourgault, A.-M.; Nguyen, T.; Frenette, C.; Kelly, M.; Vibien, A.; Brassard, P.; Fenn, S.; Dewar, K.; Hudson, T. J.; Horn, R.; René, P.; Monczak, Y.; Dascal, A. A Predominantly Clonal Multi-Institutional Outbreak of *Clostridium difficile* –Associated Diarrhea with High Morbidity and Mortality. *N. Engl. J. Med.* **2005**, *353* (23), 2442–2449.
- (68) Kwok, C. S.; Arthur, A. K.; Anibueze, C. I.; Singh, S.; Cavallazzi, R.; Loke, Y. K. Risk of *Clostridium difficile* Infection with Acid Suppressing Drugs and Antibiotics: Meta-Analysis. *Am. J. Gastroenterol.* **2012**, *107* (7), 1011–1019.
- (69) Leffler, D. A.; Lamont, J. T. *Clostridium difficile* Infection. *N. Engl. J. Med.* **2015**, *372* (16), 1539–1548.
- (70) Pépin, J.; Valiquette, L.; Cossette, B. Mortality Attributable to Nosocomial *Clostridium difficile*-Associated Disease during an Epidemic Caused by a Hypervirulent Strain in Quebec. *Cmaj* **2005**, *173* (9), 1037–1041.
- (71) Dancer, S. J. Controlling Hospital-Acquired Infection: Focus on the Role of the Environment and New Technologies for Decontamination. *Clin. Microbiol. Rev.* **2014**, *27* (4), 665–690.
- (72) Slimings, C.; Riley, T. V. Antibiotics and Hospital-Acquired *Clostridium difficile* Infection: Update of Systematic Review and Meta-Analysis. *J. Antimicrob. Chemother.* **2014**, *69* (4), 881–891.
- (73) Bakken, J. S.; Borody, T.; Brandt, L. J.; Brill, J. V.; Demarco, D. C.; Franzos, M. A.; Kelly,

Chapter 1. Synthetic polymers as simplified analogs of antimicrobial peptides

- C.; Khoruts, A.; Louie, T.; Martinelli, L. P.; Moore, T. A.; Russell, G.; Surawicz, C. Treating *Clostridium difficile* Infection with Fecal Microbiota Transplantation. *Clin. Gastroenterol. Hepatol.* **2011**, 9 (12), 1044–1049.
- (74) McDonald, L. C.; Gerding, D. N.; Johnson, S.; Bakken, J. S.; Carroll, K. C.; Coffin, S. E.; Dubberke, E. R.; Garey, K. W.; Gould, C. V.; Kelly, C.; Loo, V.; Shaklee Sammons, J.; Sandora, T. J.; Wilcox, M. H. Clinical Practice Guidelines for *Clostridium difficile* Infection in Adults and Children: 2017 Update by the Infectious Diseases Society of America (IDSA) and Society for Healthcare Epidemiology of America (SHEA). *Clin. Infect. Dis.* **2018**, 66 (7), e1–e48.
- (75) Zhanel, G. G.; Walkty, A. J.; Karlowsky, J. A. Fidaxomicin: A Novel Agent for the Treatment of *Clostridium difficile* Infection. *Can. J. Infect. Dis. Med. Microbiol.* **2015**, 26 (6), 305–312.
- (76) Dingsdag, S. A.; Hunter, N. Metronidazole: An Update on Metabolism, Structure-Cytotoxicity and Resistance Mechanisms. *J. Antimicrob. Chemother.* **2018**, 73 (2), 265–279.
- (77) Zar, F. A.; Bakkanagari, S. R.; Moorthi, K. M. L. S. T.; Davis, M. B. A Comparison of Vancomycin and Metronidazole for the Treatment of *Clostridium difficile*-Associated Diarrhea, Stratified by Disease Severity. *Clin. Infect. Dis.* **2007**, 45 (3), 302–307.
- (78) Centre National Hospitalier d'Information sur le Médicament. Drugs against *C. difficile*. Drugs against *C. difficile* <http://www.theriaque.org/apps/contenu/accueil.php> (accessed Apr 20, 2020).
- (79) Baines, S. D.; O'Connor, R.; Freeman, J.; Fawley, W. N.; Harmanus, C.; Mastrantonio, P.; Kuijper, E. J.; Wilcox, M. H. Emergence of Reduced Susceptibility to Metronidazole in *Clostridium difficile*. *J. Antimicrob. Chemother.* **2008**, 62 (5), 1046–1052.
- (80) Hernández Ceruelos, A.; Romero-Quezada, L. C.; Ruvalcaba Ledezma, J. C.; López Contreras, L. Therapeutic Uses of Metronidazole and Its Side Effects: An Update. *Eur. Rev. Med. Pharmacol. Sci.* **2019**, 23 (1), 397–401.
- (81) Nagarajan, R. Antibacterial Activities and Modes of Action of Vancomycin and Related Glycopeptides. *Antimicrob. Agents Chemother.* **1991**, 35 (4), 605–609.
- (82) Freeman, J.; Vernon, J.; Pilling, S.; Morris, K.; Nicolson, S.; Shearman, S.; Clark, E.; Palacios-Fabrega, J. A.; Wilcox, M. Five-Year Pan-European, Longitudinal Surveillance of

Chapter 1. Synthetic polymers as simplified analogs of antimicrobial peptides

- Clostridium difficile* Ribotype Prevalence and Antimicrobial Resistance: The Extended ClosER Study. *Eur. J. Clin. Microbiol. Infect. Dis.* **2020**, *39* (1), 169–177.
- (83) Al-Nassir, W. N.; Sethi, A. K.; Li, Y.; Pultz, M. J.; Riggs, M. M.; Donskey, C. J. Both Oral Metronidazole and Oral Vancomycin Promote Persistent Overgrowth of Vancomycin-Resistant Enterococci during Treatment of *Clostridium difficile*-Associated Disease. *Antimicrob. Agents Chemother.* **2008**, *52* (7), 2403–2406.
- (84) National Institutes of Health (NIH). Clinical Trials.Gov. Clinical Trials.gov <https://clinicaltrials.gov/> (accessed Apr 13, 2021).
- (85) Phoenix, D. A.; Dennison, S. R.; Harris, F. Antimicrobial Peptides. Wiley-VCH Verlag GmbH & Co. KGaA: Weinheim, Germany, 2013.
- (86) Zasloff, M. Antimicrobial Peptides of Multicellular Organisms. *Nature* **2002**, *415* (6870), 389–395.
- (87) Hancock, R. E. W.; Sahl, H. G. Antimicrobial and Host-Defense Peptides as New Anti-Infective Therapeutic Strategies. *Nat. Biotechnol.* **2006**, *24* (12), 1551–1557.
- (88) Jago, W. Toxic Action of Wheat Flour to Brewer's Yeast. Allen, W., Ed.; The Chemical Catering Company: New York, 1926.
- (89) Zhang, L.; Gallo, R. L. Antimicrobial Peptides. *Curr. Biol.* **2016**, *26* (1), R14–R19.
- (90) Dubos, R. J. Studies on a Bactericidal Agent Extracted From a Soil *Bacillus*: I. Preparation of the Agent. Its Activity in Vitro. *J. Exp. Med.* **1939**, *70* (1), 1–10.
- (91) Dubos, R. J. Studies on a Bactericidal Agent Extracted from a Soil *Bacillus*: II. Protective Effect of the Bactericidal Agent against Experimental Pneumococcus Infections in Mice. *J. Exp. Med.* **1939**, *70* (1), 11–17.
- (92) Gause, G. F.; Brazhnikova, M. G. Gramicidin S and Its Use in the Treatment of Infected Wounds. *Nature* **1944**, *154* (3918), 703–703.
- (93) Van Epps, H. L. René Dubos: Unearthing Antibiotics. *J. Exp. Med.* **2006**, *203* (2), 259–259.
- (94) Nakatsuji, T.; Gallo, R. L. Antimicrobial Peptides: Old Molecules with New Ideas AMPs: A Diverse Group of Molecules. *J Invest Dermatol.* **2012**, *132* (302), 887–895.
- (95) Williams, G. C.; Delves-Broughton, J. NISIN. In *Encyclopedia of Food Sciences and*

Chapter 1. Synthetic polymers as simplified analogs of antimicrobial peptides

Nutrition; Elsevier, 2003; Vol. 182, pp 4128–4135.

- (96) Kumar, P.; Kizhakkedathu, J.; Straus, S. Antimicrobial Peptides: Diversity, Mechanism of Action and Strategies to Improve the Activity and Biocompatibility *In Vivo*. *Biomolecules* **2018**, *8* (1), 4.
- (97) Jenssen, H.; Hamill, P.; Hancock, R. E. W. Peptide Antimicrobial Agents. *Clin. Microbiol. Rev.* **2006**, *19* (3), 491–511.
- (98) Wang, G.; Li, X.; Wang, Z. APD3: The Antimicrobial Peptide Database as a Tool for Research and Education. *Nucleic Acids Res.* **2016**, *44* (D1), D1087–D1093.
- (99) Ganz, T. Defensins: Antimicrobial Peptides of Innate Immunity. *Nat. Rev. Immunol.* **2003**, *3* (9), 710–720.
- (100) Ganz, T.; Selsted, M. E.; Szklarek, D.; Harwig, S. S.; Daher, K.; Bainton, D. F.; Lehrer, R. I. Defensins. Natural Peptide Antibiotics of Human Neutrophils. *J. Clin. Invest.* **1985**, *76* (4), 1427–1435.
- (101) Zanetti, M.; Gennaro, R.; Romeo, D. Cathelicidins: A Novel Protein Family with a Common Proregion and a Variable C-Terminal Antimicrobial Domain. *FEBS Lett.* **1995**, *374* (1), 1–5.
- (102) Pasupuleti, M.; Schmidtchen, A.; Malmsten, M. Antimicrobial Peptides: Key Components of the Innate Immune System. *Crit. Rev. Biotechnol.* **2012**, *32* (2), 143–171.
- (103) Brogden, K. A. Antimicrobial Peptides: Pore Formers or Metabolic Inhibitors in Bacteria?. *Nat. Rev. Microbiol.* **2005**, *3* (3), 238–250.
- (104) Ahmed, T. A. E.; Hammami, R. Recent Insights into Structure–Function Relationships of Antimicrobial Peptides. *J. Food Biochem.* **2019**, *43* (1), 1–8.
- (105) Saurabh, S.; Sahoo, P. K. Lysozyme: An Important Defence Molecule of Fish Innate Immune System. *Aquac. Res.* **2008**, *39* (3), 223–239.
- (106) Harder, J.; Bartels, J.; Christophers, E.; Schröder, J.-M. Isolation and Characterization of Human β -Defensin-3, a Novel Human Inducible Peptide Antibiotic. *J. Biol. Chem.* **2001**, *276* (8), 5707–5713.
- (107) Thallinger, B.; Prasetyo, E. N.; Nyanhongo, G. S.; Guebitz, G. M. Antimicrobial Enzymes: An Emerging Strategy to Fight Microbes and Microbial Biofilms. *Biotechnol. J.* **2013**, *8* (1),

Chapter 1. Synthetic polymers as simplified analogs of antimicrobial peptides

- 97–109.
- (108) Shai, Y. Mechanism of the Binding, Insertion and Destabilization of Phospholipid Bilayer Membranes by α -Helical Antimicrobial and Cell Non-Selective Membrane-Lytic Peptides. *Biochim. Biophys. Acta - Biomembr.* **1999**, 1462 (1–2), 55–70.
- (109) Powers, J. P. S.; Hancock, R. E. W. The Relationship between Peptide Structure and Antibacterial Activity. *Peptides* **2003**, 24 (11), 1681–1691.
- (110) Nielsen, D. S.; Shepherd, N. E.; Xu, W.; Lucke, A. J.; Stoermer, M. J.; Fairlie, D. P. Orally Absorbed Cyclic Peptides. *Chem. Rev.* **2017**, 117 (12), 8094–8128.
- (111) Imai, Y.; Meyer, K. J.; Iinishi, A.; Favre-Godal, Q.; Green, R.; Manuse, S.; Caboni, M.; Mori, M.; Niles, S.; Ghiglieri, M.; Honrao, C.; Ma, X.; Guo, J. J.; Makriyannis, A.; Linares-Otoya, L.; Böhringer, N.; Wuisan, Z. G.; Kaur, H.; Wu, R.; Mateus, A.; Typas, A.; Savitski, M. M.; Espinoza, J. L.; O'Rourke, A.; Nelson, K. E.; Hiller, S.; Noinaj, N.; Schäberle, T. F.; D'Onofrio, A.; Lewis, K. A New Antibiotic Selectively Kills Gram-Negative Pathogens. *Nature* **2019**, 576 (7787), 459–464.
- (112) Subbalakshmi, C.; Sitaram, N. Mechanism of Antimicrobial Action of Indolicidin. *FEMS Microbiol. Lett.* **1998**, 160 (1), 91–96.
- (113) Baumann, A.; Démoulins, T.; Python, S.; Summerfield, A. Porcine Cathelicidins Efficiently Complex and Deliver Nucleic Acids to Plasmacytoid Dendritic Cells and Can Thereby Mediate Bacteria-Induced IFN- α Responses. *J. Immunol.* **2014**, 193 (1), 364–371.
- (114) Hwang, P. M.; Vogel, H. J. Structure-Function Relationships of Antimicrobial Peptides. *Biochem. Cell Biol.* **1998**, 76 (2–3), 235–246.
- (115) Salwiczek, M.; Qu, Y.; Gardiner, J.; Strugnell, R. A.; Lithgow, T.; McLean, K. M.; Thissen, H. Emerging Rules for Effective Antimicrobial Coatings. *Trends Biotechnol.* **2014**, 32 (2), 82–90.
- (116) Epand, R. M.; Vogel, H. J. Diversity of Antimicrobial Peptides and Their Mechanisms of Action. *Biochim. Biophys. Acta - Biomembr.* **1999**, 1462 (1–2), 11–28.
- (117) Findlay, B.; Zhanel, G. G.; Schweizer, F. Cationic Amphiphiles, a New Generation of Antimicrobials Inspired by the Natural Antimicrobial Peptide Scaffold. *Antimicrob. Agents Chemother.* **2010**, 54 (10), 4049–4058.

Chapter 1. Synthetic polymers as simplified analogs of antimicrobial peptides

- (118) Singh, S.; Datta, A.; Borro, B. C.; Davoudi, M.; Schmidtchen, A.; Bhunia, A.; Malmsten, M. Conformational Aspects of High Content Packing of Antimicrobial Peptides in Polymer Microgels. *ACS Appl. Mater. Interfaces* **2017**, *9* (46), 40094–40106.
- (119) Rozek, A.; Friedrich, C. L.; Hancock, R. E. W. Structure of the Bovine Antimicrobial Peptide Indolicidin Bound to Dodecylphosphocholine and Sodium Dodecyl Sulfate Micelles. *Biochemistry* **2000**, *39* (51), 15765–15774.
- (120) G., W.; X, L.; Z, W. The Antimicrobial Peptide Database (APD). The Antimicrobial Peptide Database (APD) <http://aps.unmc.edu/AP/main.php> (accessed May 15, 2020).
- (121) Zosloff, M. Magainins, a Class of Antimicrobial Peptides from *Xenopus* Skin: Isolation, Characterization of Two Active Forms, and Partial cDNA Sequence of a Precursor. *J. Occup. Environ. Med.* **1988**, *30* (6), 470.
- (122) Nijnik, A.; Hancock, R. E. W. The Roles of Cathelicidin LL-37 in Immune Defences and Novel Clinical Applications. *Curr. Opin. Hematol.* **2009**, *16* (1), 41–47.
- (123) Wang, G. Structures of Human Host Defense Cathelicidin LL-37 and Its Smallest Antimicrobial Peptide KR-12 in Lipid Micelles. *J. Biol. Chem.* **2008**, *283* (47), 32637–32643.
- (124) Park, C. B.; Kim, H. S.; Kim, S. C. Mechanism of Action of the Antimicrobial Peptide Buforin II: Buforin II Kills Microorganisms by Penetrating the Cell Membrane and Inhibiting Cellular Functions. *Biochem. Biophys. Res. Commun.* **1998**, *244* (1), 253–257.
- (125) Tang, Y.; Yuan, J.; Ösapay, G.; Ösapay, K.; Tran, D.; Miller, C. J.; Ouellette, A. J.; Selsted, M. E. A Cyclic Antimicrobial Peptide Produced in Primate Leukocytes by the Ligation of Two Truncated α -Defensins. *Science* **1999**, *286* (5439), 498–502.
- (126) Amerikova, M.; Pencheva El-Tibi, I.; Maslarska, V.; Bozhanov, S.; Tachkov, K. Antimicrobial Activity, Mechanism of Action, and Methods for Stabilisation of Defensins as New Therapeutic Agents. *Biotechnol. Biotechnol. Equip.* **2019**, *33* (1), 671–682.
- (127) Lehrer, R. I.; Barton, A.; Daher, K. A.; Harwig, S. S. L.; Ganz, T.; Selsted, M. E. Interaction of Human Defensins with *Escherichia Coli*. Mechanism of Bactericidal Activity. *J. Clin. Invest.* **1989**, *84* (2), 553–561.
- (128) Selsted, M. E.; Harwig, S. S. L.; Ganz, T.; Schilling, J. W.; Lehrer, R. I. Primary Structures of Three Human Neutrophil Defensins. *J. Clin. Invest.* **1985**, *76* (4), 1436–1439.

Chapter 1. Synthetic polymers as simplified analogs of antimicrobial peptides

- (129) Selsted, M. E.; Novotny, M. J.; Morris, W. L.; Tang, Y. Q.; Smith, W.; Cullor, J. S. Indolicidin, a Novel Bactericidal Tridecapeptide Amide from Neutrophils. *J. Biol. Chem.* **1992**, *267* (7), 4292–4295.
- (130) Brötz, H.; Bierbaum, G.; Reynolds, P. E.; Sahl, H. G. The Lantibiotic Mersacidin Inhibits Peptidoglycan Biosynthesis at the Level of Transglycosylation. *Eur. J. Biochem.* **1997**, *246* (1), 193–199.
- (131) Eliopoulos, G. M.; Willey, S.; Reiszner, E.; Spitzer, P. G.; Caputo, G.; Moellering, R. C. In Vitro and in Vivo Activity of LY 146032, a New Cyclic Lipopeptide Antibiotic. *Antimicrob. Agents Chemother.* **1986**, *30* (4), 532–535.
- (132) Cada, D. J.; Levien, T.; Baker, D. E. Daptomycin. *Hospital Pharmacy*. February 20, 2004, pp 161–171.
- (133) Schitteck, B.; Hipfel, R.; Sauer, B.; Bauer, J.; Kalbacher, H.; Stevanovic, S.; Schirle, M.; Schroeder, K.; Blin, N.; Meier, F.; Rassner, G.; Garbe, C. Dermcidin: A Novel Human Antibiotic Peptide Secreted by Sweat Glands. *Nat. Immunol.* **2001**, *2* (12), 1133–1137.
- (134) Hancock, R. E. W.; Lehrer, R. Cationic Peptides: A New Source of Antibiotics. *Trends Biotechnol.* **1998**, *16* (2), 82–88.
- (135) Lee, T.-H.; N. Hall, K.; Aguilar, M.-I. Antimicrobial Peptide Structure and Mechanism of Action: A Focus on the Role of Membrane Structure. *Curr. Top. Med. Chem.* **2015**, *16* (1), 25–39.
- (136) Wimley, W. C. Describing the Mechanism of Antimicrobial Peptide Action with the Interfacial Activity Model. *ACS Chem. Biol.* **2010**, *5* (10), 905–917.
- (137) Blazyk, J.; Wiegand, R.; Klein, J.; Hammer, J.; Epand, R. M.; Epand, R. F.; Maloy, W. L.; Kari, U. P. A Novel Linear Amphipathic β -Sheet Cationic Antimicrobial Peptide with Enhanced Selectivity for Bacterial Lipids. *J. Biol. Chem.* **2001**, *276* (30), 27899–27906.
- (138) Matsuzaki, K. Control of Cell Selectivity of Antimicrobial Peptides. *Biochim. Biophys. Acta - Biomembr.* **2009**, *1788* (8), 1687–1692.
- (139) Huang, H. W. Action of Antimicrobial Peptides: Two-State Model. *Biochemistry* **2000**, *39* (29), 8347–8352.
- (140) Walkenhorst, W. F.; Klein, J. W.; Vo, P.; Wimley, W. C. PH Dependence of Microbe

Chapter 1. Synthetic polymers as simplified analogs of antimicrobial peptides

- Sterilization by Cationic Antimicrobial Peptides. *Antimicrob. Agents Chemother.* **2013**, *57* (7), 3312–3320.
- (141) McDonald, M.; Mannion, M.; Pike, D.; Lewis, K.; Flynn, A.; Brannan, A. M.; Browne, M. J.; Jackman, D.; Madera, L.; Power Coombs, M. R.; Hoskin, D. W.; Rise, M. L.; Booth, V. Structure-Function Relationships in Histidine-Rich Antimicrobial Peptides from Atlantic Cod. *Biochim. Biophys. Acta - Biomembr.* **2015**, *1848* (7), 1451–1461.
- (142) Hitchner, M. A.; Santiago-Ortiz, L. E.; Necelis, M. R.; Shirley, D. J.; Palmer, T. J.; Tarnawsky, K. E.; Vaden, T. D.; Caputo, G. A. Activity and Characterization of a PH-Sensitive Antimicrobial Peptide. *Biochim. Biophys. Acta - Biomembr.* **2019**, *1861* (10), 182984.
- (143) Chen, Y.; Guarnieri, M. T.; Vasil, A. I.; Vasil, M. L.; Mant, C. T.; Hodges, R. S. Role of Peptide Hydrophobicity in the Mechanism of Action of α -Helical Antimicrobial Peptides. *Antimicrob. Agents Chemother.* **2007**, *51* (4), 1398–1406.
- (144) Stark, M.; Liu, L. P.; Deber, C. M. Cationic Hydrophobic Peptides with Antimicrobial Activity. *Antimicrob. Agents Chemother.* **2002**, *46* (11), 3585–3590.
- (145) Edwards, I. A.; Elliott, A. G.; Kavanagh, A. M.; Zuegg, J.; Blaskovich, M. A. T.; Cooper, M. A. Contribution of Amphipathicity and Hydrophobicity to the Antimicrobial Activity and Cytotoxicity of β -Hairpin Peptides. *ACS Infect. Dis.* **2016**, *2* (6), 442–450.
- (146) Bahar, A. A.; Ren, D. Antimicrobial Peptides. *Pharmaceuticals (Basel)*. **2013**, *6* (12), 1543–1575.
- (147) Wieprecht, T.; Dathe, M.; Krause, E.; Beyermann, M.; Maloy, W. L.; MacDonald, D. L.; Bienert, M. Modulation of Membrane Activity of Amphipathic, Antibacterial Peptides by Slight Modifications of the Hydrophobic Moment. *FEBS Lett.* **1997**, *417* (1), 135–140.
- (148) Hamamoto, K.; Kida, Y.; Zhang, Y.; Shimizu, T.; Kuwano, K. Antimicrobial Activity and Stability to Proteolysis of Small Linear Cationic Peptides with *D*-Amino Acid Substitutions. *Microbiol. Immunol.* **2002**, *46* (11), 741–749.
- (149) Lee, D. L.; Hodges, R. S. Structure-Activity Relationships of de Novo Designed Cyclic Antimicrobial Peptides Based on Gramicidin S. *Biopolym. - Pept. Sci. Sect.* **2003**, *71* (1), 28–48.
- (150) Boman, H. G.; Agerberth, B.; Boman, A. Mechanisms of Action on *Escherichia Coli* of

Chapter 1. Synthetic polymers as simplified analogs of antimicrobial peptides

- Cecropin P1 and PR-39, Two Antibacterial Peptides from Pig Intestine. *Infect. Immun.* **1993**, *61* (7), 2978–2984.
- (151) Rabanal, F.; Grau-Campistany, A.; Vila-Farrés, X.; Gonzalez-Linares, J.; Borràs, M.; Vila, J.; Manresa, A.; Cajal, Y. A Bioinspired Peptide Scaffold with High Antibiotic Activity and Low in Vivo Toxicity. *Sci. Rep.* **2015**, *5*, 1–11.
- (152) Lobo-Ruiz, A.; Tulla-Puche, J. Synthetic Approaches of Naturally and Rationally Designed Peptides and Peptidomimetics. Elsevier Ltd, 2017.
- (153) Fox, R. O.; Richards, F. M. A Voltage-Gated Ion Channel Model Inferred from the Crystal Structure of Alamethicin at 1.5-Å Resolution. *Nature* **1982**, *300* (5890), 325–330.
- (154) Gesell, J.; Zasloff, M.; Opella, S. J. Two-Dimensional ¹H NMR Experiments Show That the 23-Residue Magainin Antibiotic Peptide Is an α -Helix in Dodecylphosphocholine Micelles, Sodium Dodecylsulfate Micelles, and Trifluoroethanol/Water Solution. *J. Biomol. NMR* **1997**, *9* (2), 127–135.
- (155) Reddy, K. V. R.; Yedery, R. D.; Aranha, C. Antimicrobial Peptides: Premises and Promises. *Int. J. Antimicrob. Agents* **2004**, *24* (6), 536–547.
- (156) Banaschewski, B. J. H.; Veldhuizen, E. J. A.; Keating, E.; Haagsman, H. P.; Zuo, Y. Y.; Yamashita, C. M.; Veldhuizen, R. A. W. Antimicrobial and Biophysical Properties of Surfactant Supplemented with an Antimicrobial Peptide for Treatment of Bacterial Pneumonia. *Antimicrob. Agents Chemother.* **2015**, *59* (6), 3075–3083.
- (157) Schmidt, N. W.; Mishra, A.; Lai, G. H.; Davis, M.; Sanders, L. K.; Tran, D.; Garcia, A.; Tai, K. P.; McCray, P. B.; Ouellette, A. J.; Selsted, M. E.; Wong, G. C. L. Criterion for Amino Acid Composition of Defensins and Antimicrobial Peptides Based on Geometry of Membrane Destabilization. *J. Am. Chem. Soc.* **2011**, *133* (17), 6720–6727.
- (158) Arora, A.; Majhi, S.; Mishra, A. Antibacterial Properties of Human *Beta* Defensin-3 Derivative: CHR01. *J. Biosci.* **2018**, *43* (4), 707–715.
- (159) Sun, B.; Wibowo, D.; Middelberg, A. P. J.; Zhao, C.-X. Cost-Effective Downstream Processing of Recombinantly Produced Pexiganan Peptide and Its Antimicrobial Activity. *AMB Express* **2018**, *8* (1), 6.
- (160) Gaglione, R.; Pane, K.; Dell'Olmo, E.; Cafaro, V.; Pizzo, E.; Olivieri, G.; Notomista, E.; Arciello, A. Cost-Effective Production of Recombinant Peptides in *Escherichia coli*. *N.*

Chapter 1. Synthetic polymers as simplified analogs of antimicrobial peptides

- Biotechnol.* **2019**, *51*, 39–48.
- (161) Merrifield, R. B. Solid Phase Peptide Synthesis. I. The Synthesis of a Tetrapeptide. *J. Am. Chem. Soc.* **1963**, *85* (14), 2149–2154.
- (162) Andersson, L.; Blomberg, L.; Flegel, M.; Lepsa, L.; Nilsson, B.; Verlander, M. Large-Scale Synthesis of Peptides. *Biopolym. - Pept. Sci. Sect.* **2000**, *55* (3), 227–250.
- (163) Gomes, B.; Augusto, M. T.; Felício, M. R.; Hollmann, A.; Franco, O. L.; Gonçalves, S.; Santos, N. C. Designing Improved Active Peptides for Therapeutic Approaches against Infectious Diseases. *Biotechnol. Adv.* **2018**, *36* (2), 415–429.
- (164) Satlin, M. J.; Jenkins, S. G. Polymyxins. In *Infectious Diseases*; Elsevier, 2017; Vol. 1, pp 1285-1288.e2.
- (165) Hastings, J. W.; Sailer, M.; Johnson, K.; Roy, K. L.; Vederas, J. C.; Stiles, M. E. Characterization of Leucocin A-UAL 187 and Cloning of the Bacteriocin Gene from *Leuconostoc Gelidum*. *J. Bacteriol.* **1991**, *173* (23), 7491–7500.
- (166) Moncla, B. J.; Pryke, K.; Rohan, L. C.; Graebing, P. W. Degradation of Naturally Occurring and Engineered Antimicrobial Peptides by Proteases. *Adv. Biosci. Biotechnol.* **2011**, *02* (06), 404–408.
- (167) Chin, W.; Yang, C.; Ng, V. W. L.; Huang, Y.; Cheng, J.; Tong, Y. W.; Coady, D. J.; Fan, W.; Hedrick, J. L.; Yang, Y. Y. Biodegradable Broad-Spectrum Antimicrobial Polycarbonates: Investigating the Role of Chemical Structure on Activity and Selectivity. *Macromolecules* **2013**, *46* (22), 8797–8807.
- (168) Cheng, Y.; Qu, H.; Ma, M.; Xu, Z.; Xu, P.; Fang, Y.; Xu, T. Polyamidoamine (PAMAM) Dendrimers as Biocompatible Carriers of Quinolone Antimicrobials: An in Vitro Study. *Eur. J. Med. Chem.* **2007**, *42* (7), 1032–1038.
- (169) Muñoz-Bonilla, A.; Fernández-García, M. Polymeric Materials with Antimicrobial Activity. *Prog. Polym. Sci.* **2012**, *37* (2), 281–339.
- (170) Kenawy, E. R.; Worley, S. D.; Broughton, R. The Chemistry and Applications of Antimicrobial Polymers: A State-of-the-Art Review. *Biomacromolecules* **2007**, *8* (5), 1359–1384.
- (171) Siedenbiedel, F.; Tiller, J. C. Antimicrobial Polymers in Solution and on Surfaces: Overview

Chapter 1. Synthetic polymers as simplified analogs of antimicrobial peptides

- and Functional Principles. *Polymers (Basel)*. **2012**, 4 (1), 46–71.
- (172) Chen, A.; Peng, H.; Blakey, I.; Whittaker, A. K. Biocidal Polymers: A Mechanistic Overview. *Polym. Rev.* **2017**, 57 (2), 276–310.
- (173) Panja, S.; Bharti, R.; Dey, G.; Lynd, N. A.; Chattopadhyay, S. Coordination-Assisted Self-Assembled Polypeptide Nanogels to Selectively Combat Bacterial Infection. *ACS Appl. Mater. Interfaces* **2019**, 11 (37), 33599–33611.
- (174) Bucheńska, J. Polyamide Fibers (PA6) with Antibacterial Properties. *J. Appl. Polym. Sci.* **1996**, 61 (3), 567–576.
- (175) Tyagi, M.; Singh, H. Iodinated P(MMA-NVP): An Efficient Matrix for Disinfection of Water. *J. Appl. Polym. Sci.* **2000**, 76 (7), 1109–1116.
- (176) Goldberg, S.; Doyle, R. J.; Rosenberg, M. Mechanism of Enhancement of Microbial Cell Hydrophobicity by Cationic Polymers. *J. Bacteriol.* **1990**, 172 (10), 5650–5654.
- (177) Konradi, R.; Pidhatika, B.; Mühlebach, A.; Textor, M. Poly-2-Methyl-2-Oxazoline: A Peptide-like Polymer for Protein-Repellent Surfaces. *Langmuir* **2008**, 24 (3), 613–616.
- (178) Mizerska, U.; Fortuniak, W.; Chojnowski, J.; Hałasa, R.; Konopacka, A.; Werel, W. Polysiloxane Cationic Biocides with Imidazolium Salt (ImS) Groups, Synthesis and Antibacterial Properties. *Eur. Polym. J.* **2009**, 45 (3), 779–787.
- (179) Kanazawa, A.; Ikeda, T.; Endo, T. Antibacterial Activity of Polymeric Sulfonium Salts. *J. Polym. Sci. Part A Polym. Chem.* **1993**, 31 (11), 2873–2876.
- (180) Kanazawa, A.; Ikeda, T.; Endo, T. Polymeric Phosphonium Salts as a Novel Class of Cationic Biocides. X. Antibacterial Activity of Filters Incorporating Phosphonium Biocides. *J. Appl. Polym. Sci.* **1994**, 54 (9), 1305–1310.
- (181) Ergene, C.; Yasuhara, K.; Palermo, E. F. Biomimetic Antimicrobial Polymers: Recent Advances in Molecular Design. *Polym. Chem.* **2018**, 9 (18), 2407–2427.
- (182) Palermo, E. F.; Sovadinova, I.; Kuroda, K. Structural Determinants of Antimicrobial Activity and Biocompatibility in Membrane-Disrupting Methacrylamide Random Copolymers. *Biomacromolecules* **2009**, 10 (11), 3098–3107.
- (183) Palermo, E. F.; Kuroda, K. Chemical Structure of Cationic Groups in Amphiphilic Polymethacrylates Modulates the Antimicrobial and Hemolytic Activities.

Chapter 1. Synthetic polymers as simplified analogs of antimicrobial peptides

- Biomacromolecules* **2009**, *10* (6), 1416–1428.
- (184) Zhang, Y.; Jiang, J.; Chen, Y. Synthesis and Antimicrobial Activity of Polymeric Guanidine and Biguanidine Salts. *Polymer (Guildf)*. **1999**, *40* (22), 6189–6198.
- (185) Cuthbert, T. J.; Hisey, B.; Harrison, T. D.; Trant, J. F.; Gillies, E. R.; Ragona, P. J. Surprising Antibacterial Activity and Selectivity of Hydrophilic Polyphosphoniums Featuring Sugar and Hydroxy Substituents. *Angew. Chem, Int. Ed.* **2018**, *57* (39), 12707–12710.
- (186) Kuroda, K.; DeGrado, W. F. Amphiphilic Polymethacrylate Derivatives as Antimicrobial Agents. *J. Am. Chem. Soc.* **2005**, *127* (12), 4128–4129.
- (187) Tiller, J. C.; Liao, C. J.; Lewis, K.; Klibanov, A. M. Designing Surfaces That Kill Bacteria on Contact. *Proc. Natl. Acad. Sci. U. S. A.* **2001**, *98* (11), 5981–5985.
- (188) Lu, G.; Wu, D.; Fu, R. Studies on the Synthesis and Antibacterial Activities of Polymeric Quaternary Ammonium Salts from Dimethylaminoethyl Methacrylate. *React. Funct. Polym.* **2007**, *67* (4), 355–366.
- (189) Gao, B.; Zhang, X.; Zhu, Y. Studies on the Preparation and Antibacterial Properties of Quaternized Polyethyleneimine. *J. Biomater. Sci. Polym. Ed.* **2007**, *18* (5), 531–544.
- (190) Waschinski, C. J.; Tiller, J. C. Poly(Oxazoline)s with Telechelic Antimicrobial Functions. *Biomacromolecules* **2005**, *6* (1), 235–243.
- (191) Kenawy, E.-R.; Abdel-Hay, F. I.; El-Shanshoury, A. E.-R. R.; El-Newehy, M. H. Biologically Active Polymers. V. Synthesis and Antimicrobial Activity of Modified Poly(Glycidyl Methacrylate-Co-2-Hydroxyethyl Methacrylate) Derivatives with Quaternary Ammonium and Phosphonium Salts. *J. Polym. Sci. Part A Polym. Chem.* **2002**, *40* (14), 2384–2393.
- (192) Konai, M. M.; Bhattacharjee, B.; Ghosh, S.; Haldar, J. Recent Progress in Polymer Research to Tackle Infections and Antimicrobial Resistance. *Biomacromolecules* **2018**, *19* (6), 1888–1917.
- (193) Cheng, J.; Chin, W.; Dong, H.; Xu, L.; Zhong, G.; Huang, Y.; Li, L.; Xu, K.; Wu, M.; Hedrick, J. L.; Yang, Y. Y.; Fan, W. Biodegradable Antimicrobial Polycarbonates with *In Vivo* Efficacy against Multidrug-Resistant MRSA Systemic Infection. *Adv. Healthc. Mater.* **2015**, *4* (14), 2128–2136.
- (194) Lienkamp, K.; Madkour, A. E.; Musante, A.; Nelson, C. F.; Nüsslein, K.; Tew, G. N.; Nelson,

Chapter 1. Synthetic polymers as simplified analogs of antimicrobial peptides

- C. F.; Madkour, A. E.; Lienkamp, K.; Tew, G. N.; Madkour, A. E.; Musante, A.; Nelson, C. F.; Nüsslein, K.; Tew, G. N. Antimicrobial Polymers Prepared by ROMP with Unprecedented Selectivity: A Molecular Construction Kit Approach. *J. Am. Chem. Soc.* **2008**, *130* (30), 9836–9843.
- (195) Hu, K.; Schmidt, N. W.; Zhu, R.; Jiang, Y.; Lai, G. H.; Wei, G.; Palermo, E. F.; Kuroda, K.; Wong, G. C. L. L.; Yang, L. A Critical Evaluation of Random Copolymer Mimesis of Homogeneous Antimicrobial Peptides. *Macromolecules* **2013**, *46* (5), 1908–1915.
- (196) Rawlinson, L. A. B.; Ryan, S. M.; Mantovani, G.; Syrett, J. A.; Haddleton, D. M.; Brayden, D. J. Antibacterial Effects of Poly(2-(Dimethylamino Ethyl)Methacrylate) against Selected Gram-Positive and Gram-Negative Bacteria. *Biomacromolecules* **2010**, *11* (2), 443–453.
- (197) Ikeda, T.; Hirayama, H.; Yamaguchi, H.; Tazuke, S.; Watanabe, M. Polycationic Biocides with Pendant Active Groups: Molecular Weight Dependence of Antibacterial Activity. *Antimicrob. Agents Chemother.* **1986**, *30* (1), 132–136.
- (198) Ikeda, T.; Yamaguchi, H.; Tazuke, S. New Polymeric Biocides: Synthesis and Antibacterial Activities of Polycations with Pendant Biguanide Groups. *Antimicrob. Agents Chemother.* **1984**, *26* (2), 139–144.
- (199) Oda, Y.; Kanaoka, S.; Sato, T.; Aoshima, S.; Kuroda, K. Block versus Random Amphiphilic Copolymers as Antibacterial Agents. *Biomacromolecules* **2011**, *12* (10), 3581–3591.
- (200) Weight, M.; Salts, P. P.; Kanazawa, A.; Ikeda, T.; Endo, T. Polymeric Phosphonium Salts as a Novel Class of Cationic Biocides. II. Effects of Counter Anion and Molecular Weight on Antibacterial Activity of Polymeric Phosphonium Salts. *J. Polym. Sci. Part A Polym. Chem.* **1993**, *31* (6), 1441–1447.
- (201) Lienkamp, K.; Madkour, A. E.; Kumar, K. N.; Nüsslein, K.; Tew, G. N. Antimicrobial Polymers Prepared by Ring-Opening Metathesis Polymerization: Manipulating Antimicrobial Properties by Organic Counterion and Charge Density Variation. *Chem. - A Eur. J.* **2009**, *15* (43), 11715–11722.
- (202) Panarin, E. F.; Solovskii, M. V.; Zaikina, N. A.; Afinogenov, G. E. Biological Activity of Cationic Polyelectrolytes. *Die Makromol. Chemie* **1985**, *9* (S19851), 25–33.
- (203) Palermo, E. F.; Vemparala, S.; Kuroda, K. Cationic Spacer Arm Design Strategy for Control of Antibacterial Activity and Conformation of Amphiphilic Methacrylate Random

Chapter 1. Synthetic polymers as simplified analogs of antimicrobial peptides

- Copolymers. *Biomacromolecules* **2012**, *13* (5), 1632–1641.
- (204) Waschinski, C. J.; Barnert, S.; Theobald, A.; Schubert, R.; Kleinschmidt, F.; Hoffmann, A.; Saalwächter, K.; Tiller, J. C. Insights in the Antibacterial Action of Poly(Methyloxazoline)s with a Biocidal End Group and Varying Satellite Groups. *Biomacromolecules* **2008**, *9* (7), 1764–1771.
- (205) Ilker, M. F.; Nüsslein, K.; Tew, G. N.; Coughlin, E. B.; Nu, K.; Tew, G. N.; Coughlin, E. B. Tuning the Hemolytic and Antibacterial Activities of Amphiphilic Polynorbornene Derivatives. *J. Am. Chem. Soc.* **2004**, *126* (48), 15870–15875.
- (206) Katchalski, E.; Berger, A.; Bichowsky-Slomonicki, L.; Joseph, K. Antibiotically Active Amino-Acid Copolymers Related to Gramicidin S. *Nature* **1955**, *176* (4472), 118–119.
- (207) Katchalski, E.; Sela, M.; Silman, H. I.; Berger, A. Chapter 10 - Polyamino Acids as Protein Models. NEURATH Structure, and Function (Second Edition), H. B. T.-T. P. C., Ed.; Academic Press, 1964; pp 405–602.
- (208) Wyrsta, M. D.; Cogen, A. L.; Deming, T. J. A Parallel Synthetic Approach for the Analysis of Membrane Interactive Copolypeptides. *J. Am. Chem. Soc.* **2001**, *123* (51), 12919–12920.
- (209) Deming, T. J. Facile Synthesis of Block Copolypeptides of Defined Architecture. *Nature* **1997**, *390* (6658), 386–389.
- (210) Zhou, C.; Qi, X.; Li, P.; Chen, W. N.; Mouad, L.; Chang, M. W.; Leong, S. S. J.; Chan-Park, M. B. High Potency and Broad-Spectrum Antimicrobial Peptides Synthesized via Ring-Opening Polymerization of α -Aminoacid-*N*-Carboxyanhydrides. *Biomacromolecules* **2010**, *11* (1), 60–67.
- (211) Engler, A. C.; Shukla, A.; Puranam, S.; Buss, H. G.; Jreige, N.; Hammond, P. T. Effects of Side Group Functionality and Molecular Weight on the Activity of Synthetic Antimicrobial Polypeptides. *Biomacromolecules* **2011**, *12* (5), 1666–1674.
- (212) Zhen, J. Bin; Zhao, M. H.; Ge, Y.; Liu, Y.; Xu, L. W.; Chen, C.; Gong, Y. K.; Yang, K. W. Construction, Mechanism, and Antibacterial Resistance Insight into Polypeptide-Based Nanoparticles. *Biomater. Sci.* **2019**, *7* (10), 4142–4152.
- (213) Xiong, M.; Lee, M. W.; Mansbach, R. A.; Song, Z.; Bao, Y.; Peek, R. M.; Yao, C.; Chen, L. F.; Ferguson, A. L.; Wong, G. C. L.; Cheng, J. Helical Antimicrobial Polypeptides with

Chapter 1. Synthetic polymers as simplified analogs of antimicrobial peptides

- Radial Amphiphilicity. *Proc. Natl. Acad. Sci. U. S. A.* **2015**, *112* (43), 13155–13160.
- (214) Chen, J.; Peek, R. M.; Bao, Y.; Liu, Y.; Chen, L.-F.; Yin, L.; Wang, Z.; Song, Z.; Cheng, J.; Han, Z.; Wang, H.; Xiong, M.; Huang, S.; Xu, X. Selective Killing of *Helicobacter Pylori* with PH-Responsive Helix–Coil Conformation Transitionable Antimicrobial Polypeptides. *Proc. Natl. Acad. Sci.* **2017**, *114* (48), 12675–12680.
- (215) Xiong, M.; Han, Z.; Song, Z.; Yu, J.; Ying, H.; Yin, L.; Cheng, J. Bacteria-Assisted Activation of Antimicrobial Polypeptides by a Random-Coil to Helix Transition. *Angew. Chem, Int. Ed.* **2017**, *56* (36), 10826–10829.
- (216) Su, X.; Zhou, X.; Tan, Z.; Zhou, C. Highly Efficient Antibacterial Diblock Copolypeptides Based on Lysine and Phenylalanine. *Biopolymers* **2017**, *107* (11), 1–8.
- (217) Lam, S. J.; O'Brien-Simpson, N. M.; Pantarat, N.; Sulistio, A.; Wong, E. H. H.; Chen, Y.-Y.; Lenzo, J. C.; Holden, J. A.; Blencowe, A.; Reynolds, E. C.; Qiao, G. G. Combating Multidrug-Resistant Gram-Negative Bacteria with Structurally Nanoengineered Antimicrobial Peptide Polymers. *Nat. Microbiol.* **2016**, *1* (16162), 1–11.
- (218) Shirbin, S. J.; Insua, I.; Holden, J. A.; Lenzo, J. C.; Reynolds, E. C.; O'Brien-Simpson, N. M.; Qiao, G. G. Architectural Effects of Star-Shaped “Structurally Nanoengineered Antimicrobial Peptide Polymers” (SNAPPs) on Their Biological Activity. *Adv. Healthc. Mater.* **2018**, *7* (21), 1–12.
- (219) Chen, Y. F.; Lai, Y. Da; Chang, C. H.; Tsai, Y. C.; Tang, C. C.; Jan, J. S. Star-Shaped Polypeptides Exhibit Potent Antibacterial Activities. *Nanoscale* **2019**, *11* (24), 11696–11708.
- (220) Zhang, Y.; Song, W.; Li, S.; Kim, D. K.; Kim, J. H.; Kim, J. R.; Kim, I. Facile and Scalable Synthesis of Topologically Nanoengineered Polypeptides with Excellent Antimicrobial Activities. *Chem. Commun.* **2020**, *56* (3), 356–359.
- (221) Costanza, F.; Padhee, S.; Wu, H.; Wang, Y.; Revenis, J.; Cao, C.; Li, Q.; Cai, J. Investigation of Antimicrobial PEG-Poly(Amino Acid)S. *RSC Adv.* **2014**, *4* (4), 2089–2095.
- (222) Bevilacqua, M. P.; Huang, D. J.; Wall, B. D.; Lane, S. J.; Edwards, C. K.; Hanson, J. A.; Benitez, D.; Solomkin, J. S.; Deming, T. J. Amino Acid Block Copolymers with Broad Antimicrobial Activity and Barrier Properties. *Macromol. Biosci.* **2017**, *17* (10), 1600492.
- (223) Chen, Y.; Yu, L.; Zhang, B.; Feng, W.; Xu, M.; Gao, L.; Liu, N.; Wang, Q.; Huang, X.; Li,

Chapter 1. Synthetic polymers as simplified analogs of antimicrobial peptides

- P.; Huang, W. Design and Synthesis of Biocompatible, Hemocompatible, and Highly Selective Antimicrobial Cationic Peptidopolysaccharides via Click Chemistry. *Biomacromolecules* **2019**, *20* (6), 2230–2240.
- (224) Lam, S. J.; Wong, E. H. H.; O'Brien-Simpson, N. M.; Pantarat, N.; Blencowe, A.; Reynolds, E. C.; Qiao, G. G. Bionano Interaction Study on Antimicrobial Star-Shaped Peptide Polymer Nanoparticles. *ACS Appl. Mater. Interfaces* **2016**, *8* (49), 33446–33456.
- (225) Zhang, Y.; Chen, T.; Pan, Z.; Sun, X.; Yin, X.; He, M.; Xiao, S.; Liang, H. Theoretical Insights into the Interactions between Star-Shaped Antimicrobial Polypeptides and Bacterial Membranes. *Langmuir* **2018**, *34* (44), 13438–13448.
- (226) Green, M.; Stahmann, M. Synthesis and Enzymatic Hydrolysis of Glutamic Acid Polipeptides. *J. Biol. Chem.* **1952**, *197* (2), 771–782.
- (227) Zuckermann, R. N. Peptoid Origins. *Biopolymers* **2011**, *96* (5), 545–555.
- (228) Simon, R. J.; Kania, R. S.; Zuckermann, R. N.; Huebner, V. D.; Jewell, D. A.; Banville, S.; Ng, S.; Wang, L.; Rosenberg, S.; Marlowe, C. K.; Spellmeyer, D. C.; Tan, R.; Frankel, A. D.; Santi, D. V.; Cohen, F. E.; Bartlett, P. A. Peptoids: A Modular Approach to Drug Discovery. *Proc. Natl. Acad. Sci. U. S. A.* **1992**, *89* (20), 9367–9371.
- (229) Zuckermann, R. N.; Kerr, J. M.; Kent, S. B. H.; Moos, W. H. Efficient Method for the Preparation of Peptoids [Oligo(*N*-Substituted Glycines)] by Submonomer Solid-Phase Synthesis. *J. Am. Chem. Soc.* **1992**, *114* (26), 10646–10647.
- (230) Gangloff, N.; Ulbricht, J.; Lorson, T.; Schlaad, H.; Luxenhofer, R. Peptoids and Polypeptoids at the Frontier of Supra- and Macromolecular Engineering. *Chem. Rev.* **2016**, *116* (4), 1753–1802.
- (231) Meyer, J. P.; Davis, P.; Lee, K. B.; Porreca, F.; Yamamura, H. I.; Hruby, V. J. Synthesis Using a Fmoc-Based Strategy and Biological Activities of Some Reduced Peptide Bond Pseudopeptide Analogues of Dynorphin A. *J. Med. Chem.* **1995**, *38* (18), 3462–3468.
- (232) Tal-Gan, Y.; Freeman, N. S.; Klein, S.; Levitzki, A.; Gilon, C. Synthesis and Structure-Activity Relationship Studies of Peptidomimetic PKB/Akt Inhibitors: The Significance of Backbone Interactions. *Bioorganic Med. Chem.* **2010**, *18* (8), 2976–2985.
- (233) Vézina-Dawod, S.; Derson, A.; Biron, E. *N*-Substituted Arylsulfonamide Building Blocks as Alternative Submonomers for Peptoid Synthesis. *Tetrahedron Lett.* **2015**, *56* (2), 382–385.

Chapter 1. Synthetic polymers as simplified analogs of antimicrobial peptides

- (234) Li, S.; Bowerman, D.; Marthandan, N.; Klyza, S.; Luebke, K. J.; Garner, H. R.; Kodadek, T. Photolithographic Synthesis of Peptoids. *J. Am. Chem. Soc.* **2004**, *126* (13), 4088–4089.
- (235) Hamper, B. C.; Kolodziej, S. A.; Scates, A. M.; Smith, R. G.; Cortez, E. Solid Phase Synthesis of β -Peptoids: *N*-Substituted β -Aminopropionic Acid Oligomers. *J. Org. Chem.* **1998**, *63* (3), 708–718.
- (236) Hjelmgaard, T.; Faure, S.; Caumes, C.; De Santis, E.; Edwards, A. A.; Taillefumier, C. Convenient Solution-Phase Synthesis and Conformational Studies of Novel Linear and Cyclic α,β -Alternating Peptoids. *Org. Lett.* **2009**, *11* (18), 4100–4103.
- (237) Sui, Q.; Borchardt, D.; Rabenstein, D. L. Kinetics and Equilibria of *Cis/Trans* Isomerization of Backbone Amide Bonds in Peptoids. *J. Am. Chem. Soc.* **2007**, *129* (39), 12042–12048.
- (238) Kirshenbaum, K.; Barron, A. E.; Goldsmith, R. A.; Armand, P.; Bradley, E. K.; Truong, K. T. V.; Dill, K. A.; Cohen, F. E.; Zuckermann, R. N. Sequence-Specific Polypeptoids: A Diverse Family of Heteropolymers with Stable Secondary Structure. *Proc. Natl. Acad. Sci.* **1998**, *95* (8), 4303–4308.
- (239) Miller, S. M.; Simon, R. J.; Ng, S.; Zuckermann, R. N.; Kerr, J. M.; Moos, W. H. Proteolytic Studies of Homologous Peptide and *N*-Substituted Glycine Peptoid Oligomers. *Bioorganic Med. Chem. Lett.* **1994**, *4* (22), 2657–2662.
- (240) Bang, J. K.; Nan, Y. H.; Lee, E. K.; Shin, S. Y. A Novel Trp-Rich Model Antimicrobial Peptoid with Increased Protease Stability. *Bull. Korean Chem. Soc.* **2010**, *31* (9), 2509–2513.
- (241) Goodson, B.; Ehrhardt, A.; Ng, S.; Nuss, J.; Johnson, K.; Giedlin, M.; Yamamoto, R.; Moos, W. H.; Krebber, A.; Ladner, M.; Giacona, M. B.; Vitt, C.; Winter, J. Characterization of Novel Antimicrobial Peptoids. *Antimicrob. Agents Chemother.* **1999**, *43* (6), 1429–1434.
- (242) Chongsiriwatana, N. P.; Patch, J. A.; Czyzewski, A. M.; Dohm, M. T.; Ivankin, A.; Gidalevitz, D.; Zuckermann, R. N.; Barron, A. E. Peptoids That Mimic the Structure, Function, and Mechanism of Helical Antimicrobial Peptides. *Proc. Natl. Acad. Sci.* **2008**, *105* (8), 2794–2799.
- (243) Bremner, J. B.; Keller, P. A.; Pyne, S. G.; Boyle, T. R.; Brkic, Z.; David, D. M.; Garas, A.; Morgan, J.; Robertson, M.; Somphol, K.; Miller, M. H.; Howe, A. S.; Ambrose, P.; Bhavnani, S.; Fritsche, T. R.; Biedenbach, D. J.; Jones, R. N.; Buckheit, R. W.; Watson, K. M.; Baylis,

Chapter 1. Synthetic polymers as simplified analogs of antimicrobial peptides

- D.; Coates, J. A.; Deadman, J.; Jeevarajah, D.; McCracken, A.; Rhodes, D. I. Binaphthyl-Based Dicationic Peptoids with Therapeutic Potential. *Angew. Chem, Int. Ed.* **2010**, *49* (3), 537–540.
- (244) Bremner, J. B.; Keller, P. A.; Pyne, S. G.; Boyle, T. P.; Brkic, Z.; David, D. M.; Robertson, M.; Somphol, K.; Baylis, D.; Coates, J. A.; Deadman, J.; Jeevarajah, D.; Rhodes, D. I. Synthesis and Antibacterial Studies of Binaphthyl-Based Tripeptoids. Part 1. *Bioorg. Med. Chem.* **2010**, *18* (7), 2611–2620.
- (245) Benson, M. A.; Shin, S. B. Y.; Kirshenbaum, K.; Huang, M. L.; Torres, V. J. A Comparison of Linear and Cyclic Peptoid Oligomers as Potent Antimicrobial Agents. *ChemMedChem* **2012**, *7* (1), 114–122.
- (246) Chongsiriwatana, N. P.; Miller, T. M.; Wetzler, M.; Vakulenko, S.; Karlsson, A. J.; Palecek, S. P.; Mobashery, S.; Barron, A. E. Short Alkylated Peptoid Mimics of Antimicrobial Lipopeptides. *Antimicrob. Agents Chemother.* **2011**, *55* (1), 417–420.
- (247) Mojsoska, B.; Zuckermann, R. N.; Jensen, H. Structure-Activity Relationship Study of Novel Peptoids That Mimic the Structure of Antimicrobial Peptides. *Antimicrob. Agents Chemother.* **2015**, *59* (7), 4112–4120.
- (248) Bolt, H. L.; Eggimann, G. A.; Jahoda, C. A. B.; Zuckermann, R. N.; Sharples, G. J.; Cobb, S. L. Exploring the Links between Peptoid Antibacterial Activity and Toxicity. *Medchemcomm* **2017**, *8* (5), 886–896.
- (249) Masip, I.; Cortés, N.; Abad, M.-J.; Guardiola, M.; Pérez-Payá, E.; Ferragut, J.; Ferrer-Montiel, A.; Messeguer, A. Design and Synthesis of an Optimized Positional Scanning Library of Peptoids: Identification of Novel Multidrug Resistance Reversal Agents. *Bioorg. Med. Chem.* **2005**, *13* (6), 1923–1929.
- (250) Sun, J.; Zuckermann, R. N. Peptoid Polymers: A Highly Designable Bioinspired Material. *ACS Nano* **2013**, *7* (6), 4715–4732.
- (251) Chan, B. A.; Xuan, S.; Li, A.; Simpson, J. M.; Sternhagen, G. L.; Yu, T.; Darvish, O. A.; Jiang, N.; Zhang, D. Polypeptoid Polymers: Synthesis, Characterization, and Properties. *Biopolymers* **2017**, *109* (1), 1–25.
- (252) Leuchs, H.; Manasse, W. Über Die Isomerie Der Carbäthoxyl-Glycyl Glycinester. *Berichte der Dtsch. Chem. Gesellschaft* **1907**, *40* (3), 3235–3249.

Chapter 1. Synthetic polymers as simplified analogs of antimicrobial peptides

- (253) Kricheldorf, H. R.; Von Lossow, C.; Schwarz, G. Primary Amine-Initiated Polymerizations of Alanine-NCA and Sarcosine-NCA. *Macromol. Chem. Phys.* **2004**, *205* (7), 918–924.
- (254) Guo, L.; Zhang, D. Cyclic Poly(α -Peptoid)s and Their Block Copolymers from *N*-Heterocyclic Carbene-Mediated Ring-Opening Polymerizations of *N*-Substituted *N*-Carboxylanhydrides. *J. Am. Chem. Soc.* **2009**, *131* (50), 18072–18074.
- (255) Lahasky, S. H.; Hu, X.; Zhang, D. Thermoresponsive Poly(α -Peptoid)s: Tuning the Cloud Point Temperatures by Composition and Architecture. *ACS Macro Lett.* **2012**, *1* (5), 580–584.
- (256) Fetsch, C.; Grossmann, A.; Holz, L.; Nawroth, J. F.; Luxenhofer, R. Polypeptoids from *N*-Substituted Glycine *N*-Carboxyanhydrides: Hydrophilic, Hydrophobic, and Amphiphilic Polymers with Poisson Distribution. *Macromolecules* **2011**, *44* (17), 6746–6758.
- (257) Kricheldorf, H. R. Polypeptides and 100 Years of Chemistry of α -Amino Acid α -Carboxyanhydrides. *Angew. Chem, Int. Ed.* **2006**, *45* (35), 5752–5784.
- (258) Leuchs, H.; Geiger, W. Über Die Anhydride von α -Amino-*N*-Carbonsäuren Und Die von α -Aminosäuren. *Berichte der Dtsch. Chem. Gesellschaft* **1908**, *41* (2), 1721–1726.
- (259) Curtius, T.; Sieber, W. Umwandlung von Alkylierten Malonsäuren in Alpha Aminosäuren. *Ber. Dtsch. Chem. Ges. B* **1922**, *55*, 1543–1558.
- (260) Wessely, F.; Riedl, K.; Tuppy, H. Untersuchungen Über α -Amino-*N*-Carbonsäureanhydride VI. *Monatshefte für Chemie und verwandte Teile anderer Wissenschaften* **1950**, *81* (6), 861–872.
- (261) Secker, C.; Brosnan, S. M.; Luxenhofer, R.; Schlaad, H. Poly(α -Peptoid)s Revisited: Synthesis, Properties, and Use as Biomaterial. *Macromol. Biosci.* **2015**, *15* (7), 881–891.
- (262) Birke, A.; Ling, J.; Barz, M. Polysarcosine-Containing Copolymers: Synthesis, Characterization, Self-Assembly, and Applications. *Prog. Polym. Sci.* **2018**, *81*, 163–208.
- (263) Fetsch, C.; Luxenhofer, R. Highly Defined Multiblock Copolypeptoids: Pushing the Limits of Living Nucleophilic. *Macromol. Rapid Commun.* **2012**, *33* (19), 1708–1713.
- (264) Robinson, J. W.; Schlaad, H. A Versatile Polypeptoid Platform Based on *N*-Allyl Glycine. *Chem. Commun.* **2012**, *48* (63), 7835.
- (265) Hörtz, C.; Birke, A.; Kaps, L.; Decker, S.; Wächtersbach, E.; Fischer, K.; Schuppan, D.;

Chapter 1. Synthetic polymers as simplified analogs of antimicrobial peptides

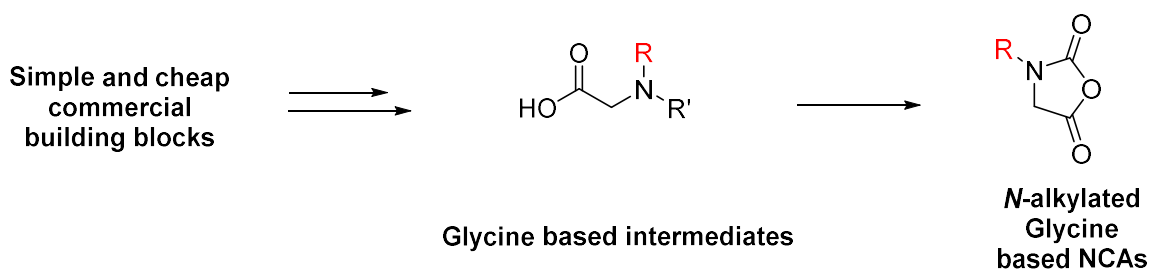
- Barz, M.; Schmidt, M. Cylindrical Brush Polymers with Polysarcosine Side Chains: A Novel Biocompatible Carrier for Biomedical Applications. *Macromolecules* **2015**, *48* (7), 2074–2086.
- (266) Lee, C.-U.; Li, A.; Ghale, K.; Zhang, D. Crystallization and Melting Behaviors of Cyclic and Linear Polypeptoids with Alkyl Side Chains. *Macromolecules* **2013**, *46* (20), 8213–8223.
- (267) Fetsch, C.; Flecks, S.; Gieseler, D.; Marschelk, C.; Ulbricht, J.; Van Pée, K. H.; Luxenhofer, R. Self-Assembly of Amphiphilic Block Copolypeptoids with C2-C5 Side Chains in Aqueous Solution. *Macromol. Chem. Phys.* **2015**, *216* (5), 547–560.
- (268) Tao, X.; Du, J.; Wang, Y.; Ling, J. Polypeptoids with Tunable Cloud Point Temperatures Synthesized from *N*-Substituted Glycine *N*-Thiocarboxyanhydrides. *Polym. Chem.* **2015**, *6* (16), 3164–3174.
- (269) Xuan, S.; Lee, C. U.; Chen, C.; Doyle, A. B.; Zhang, Y.; Guo, L.; John, V. T.; Hayes, D.; Zhang, D. Thermoreversible and Injectable ABC Polypeptoid Hydrogels: Controlling the Hydrogel Properties through Molecular Design. *Chem. Mater.* **2016**, *28* (3), 727–737.
- (270) Holm, R.; Weber, B.; Heller, P.; Klinker, K.; Westmeier, D.; Docter, D.; Stauber, R. H.; Barz, M. Synthesis and Characterization of Stimuli-Responsive Star-Like Polypept(o)ides: Introducing Biodegradable PeptoStars. *Macromol. Biosci.* **2017**, *17* (6), 1–14.
- (271) Xuan, S.; Gupta, S.; Li, X.; Bleuel, M.; Schneider, G. J.; Zhang, D. Synthesis and Characterization of Well-Defined PEGylated Polypeptoids as Protein-Resistant Polymers. *Biomacromolecules* **2017**, *18* (3), 951–964.
- (272) Maurer, P. H.; Subrahmanyam, D.; Katchalski, E.; Blout, E. R.; Maurer, H. P.; Subrahmanyam, D.; Katchalski, E.; Blout, E. R. Antigenicity of Polypeptides (Poly *Alpha* Amino Acids). *J. Immunol.* **1959**, *83* (2), 193–197.
- (273) Whittall, N.; Moran, D. M.; Wheeler, A. W.; Cottam, G. P. Suppression of Murine IgE Responses with Amino Acid Polymer/Allergen Conjugates. *Int. Arch. Allergy Immunol.* **1985**, *76* (4), 354–360.
- (274) Gao, Q.; Li, P.; Zhao, H.; Chen, Y.; Jiang, L.; Ma, P. X. Methacrylate-Ended Polypeptides and Polypeptoids for Antimicrobial and Antifouling Coatings. *Polym. Chem.* **2017**, *8* (41), 6386–6397.
- (275) Yoo, J.; Birke, A.; Kim, J.; Jang, Y.; Song, S. Y.; Ryu, S.; Kim, B. S.; Kim, B. G.; Barz, M.;

Chapter 1. Synthetic polymers as simplified analogs of antimicrobial peptides

Char, K. Cooperative Catechol-Functionalized Polypept(o)ide Brushes and Ag Nanoparticles for Combination of Protein Resistance and Antimicrobial Activity on Metal Oxide Surfaces. *Biomacromolecules* **2018**, 19 (5), 1602–1613.

Chapter 2. Preparation of a small library of *N*-alkylated glycine *N*-carboxyanhydrides

The simplest way to prepare polypeptoids is to polymerize *N*-alkylated glycine *N*-carboxyanhydrides monomers (NNCA). The NNCA monomers can be synthesized through the Leuchs method: this route involves the use of thionyl chloride (SOCl₂)¹ or other Lewis acids such as PCl₃ and PBr₃.^{2,3} The purpose of this chapter was to study the synthesis of various *N*-alkylated glycine in order to prepare NNCA monomers from cheap commercial building blocks, in good yields, using safe, simple and fast operating procedures, according to **Scheme 3**.



Scheme 3. Goal of chapter 2: Efficient and safe synthesis of *N*-alkylated-*N*-carboxyanhydrides based on glycine.

1 Bibliographical study

1.1 NCA Preparation

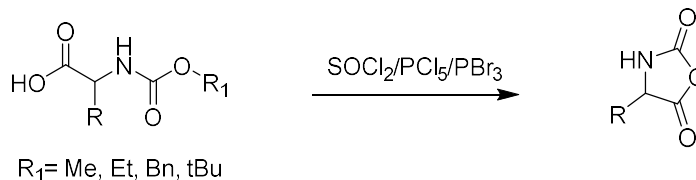
1.1.1 Preparation of regular (non-alkylated) NCA

In the literature, the synthesis of NCA from regular amino acids is extensively reported.⁴ The first examples of NCA synthesis were described by H. Leuchs between 1906-1908 while he was trying to purify, by distillation, the hypothetical halogenated product of the reaction of *N*-methoxycarbonyl- or *N*-ethoxycarbonyl-aminoacids with thionyl chloride (SOCl₂).^{1,5,6} Using this method he synthesized NCA compounds from amino acids such as glycine, *L*-phenylalanine and

Chapter 2. Preparation of a small library of *N*-alkylated glycine *N*-carboxyanhydrides

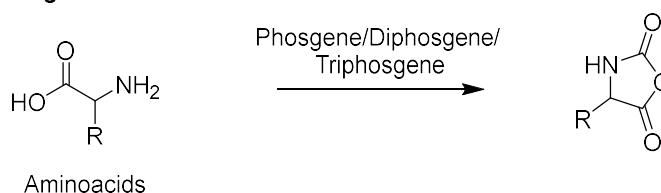
L-leucine (**Scheme 4**).

Leuchs method

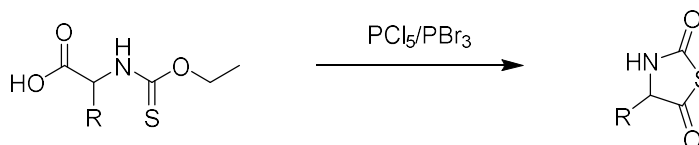


Carbamate Aminoacid Derivatives

Fuchs-Farthing method



Kricheldorf NTA method



Scheme 4. Main synthesis pathways reported for the preparation of NCA and NTA.

Following this approach, E. Katchalski *et al.* prepared different NCAs by reacting *N*-carboxybenzyl or *N*-carboxyethyl- substituted amino acids with other chlorinated or brominated electrophilic reagents, such as PCl_5 and PBr_3 , obtaining ornithine (60% yield), phenylalanine (82%), alanine (60-68%), lysine (85%) and valine (85-88%) NCAs.^{7,8}

Another method to synthesize NCA was developed by F. Fuchs⁹ and adapted by C. Farthing (**Scheme 4**).¹⁰ This method was extensively used because it allowed the synthesis of NCA directly through the reaction of amino acids with an excess of phosgene (COCl_2) in dioxane at 40°C , avoiding the preparation of intermediates contrary to Leuchs method.¹⁰ However, this method was dangerous because phosgene is a very toxic gas that is lethal in humans at a concentration of 500 ppm after 1 minute of contact (UN Hazard Class: 2.3; UN Subsidiary Risks: 8). In the Fuchs-Farthing approach, the risk was increased by the use of large amounts of phosgene (>2 equiv.). The use of phosgene dilutions in benzene facilitated the use of phosgene but did not solve the

Chapter 2. Preparation of a small library of *N*-alkylated glycine *N*-carboxyanhydrides

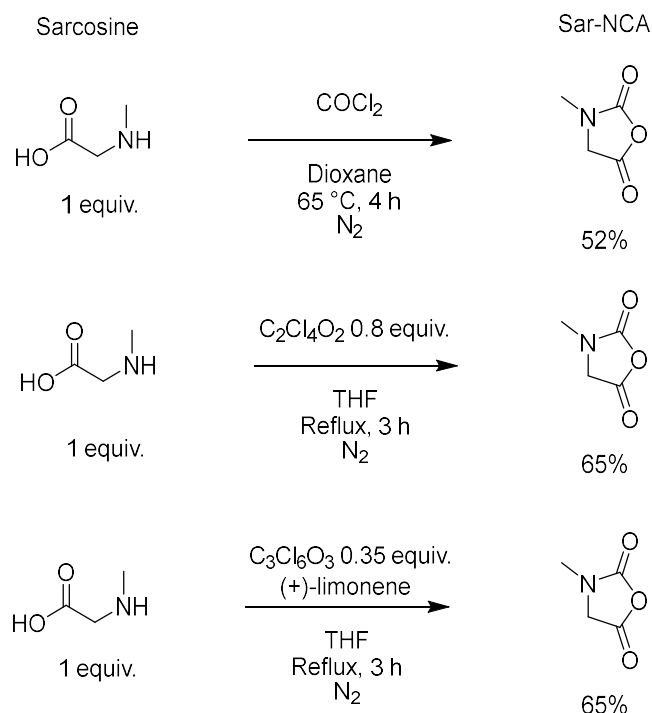
high toxicity issue.¹¹ In this direction, phosgene derivatives were later developed as safer alternatives such as diphosgene (C₂Cl₄O₂) and triphosgene (C₃Cl₆O₃). For instance, NCAs were synthesized by heating a mixture of diphosgene with amino acid solutions in anhydrous THF at 60 °C, obtaining the glycine (70% yield), *L*-alanine (59%), *L*-valine (70%), and γ -methyl-*L*-glutamate (84%) NCAs.¹² Synthesis of NCA using triphosgene, which is a solid, was demonstrated with several amino acids, such as *L*-alanine, *L*-leucine, *L*-phenylalanine, etc. in THF at 40-50 °C, giving the corresponding NCAs in 58-89% yields.¹³ However, triphosgene and diphosgene decompose into phosgene (active cyclization agent) during the reaction, calling for a very careful treatment of the reaction medium after completion of the reaction.¹⁴

As the efficacy of phosgene and its derivatives to produce NCA was balanced by its high toxicity, alternative methods were developed, for instance, nitrosation (O₂/NO) of *N*-carbamoyl aminoacids with diphenyl carbonate¹⁵, as well as the preparation of NCA using urethane derivatives with acetic acid (which can be included as part of the Leuchs method since it involves the reaction between carbamates and acids).¹⁶ Finally, *N*-thiocarboxyanhydrides (NTA) formed from aminoacids thioester derivatives have been reported as analogs of NCA, as Kricheldorf demonstrated (**Scheme 4**).¹⁷ However, the polymerization of NTAs released toxic carbonyl sulfide.

1.1.2 Preparation of *N*-alkylated NCA

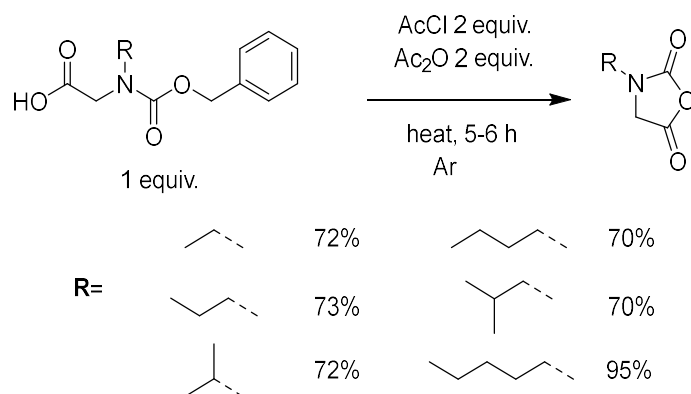
The knowledge developed with *N*-carboxyanhydrides can be extended to the synthesis of *N*-alkylated NCA (abbreviated as NNCA). In this paragraph, we briefly described various approaches that were reported for their preparation. The first examples are based on the use of phosgene and its derivatives diphosgene and triphosgene (**Scheme 5**). G. Fasman *et al.* reported the synthesis of *N*-methylated NCA (Sar-NCA) in 52% yield from the *N*-alkylated amino acid sarcosine (*N*-methylglycine) by reacting it with phosgene (bubbling under inert atmosphere).¹⁸ In another publication, M. Barz *et al.* reacted diphosgene with sarcosine in refluxing THF and isolated Sar-NCA in a 65% yield, after purification by sublimation.¹⁹ R. Luxenhofer *et al.* produced the same Sar-NCA in 76% yield from sarcosine, using triphosgene and (+)-limonene in THF.²⁰

Chapter 2. Preparation of a small library of *N*-alkylated glycine *N*-carboxyanhydrides



Scheme 5. Synthesis of sarcosine NCA (Sar-NCA) using phosgene and its derivatives.^{18–20}

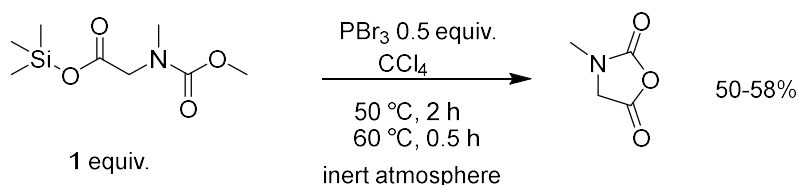
Outside phosgene and its derivatives, different routes were also investigated. For instance, R. Luxenhofer *et al.* (**Scheme 6**) reacted *N*-(benzyloxycarbonyl)glycine derivatives bearing various alkyl groups (ethyl, propyl, isopropyl, butyl, isobutyl and pentyl) on the nitrogen atom with acetyl chloride and acetic anhydride under argon atmosphere to afford the corresponding NNCA in 70–95% yield.^{20,21} Using the same protocol with slight changes, H. Schlaad *et al.* synthesized NNCA bearing *N*-isopropyl, *N*-allyl and *N*-propargyl groups in good yields (>80%).²²



Scheme 6. Synthesis of various *N*-alkylated NCA from Cbz-protected glycine derivatives according to Luxenhofer.^{20,21}

Chapter 2. Preparation of a small library of *N*-alkylated glycine *N*-carboxyanhydrides

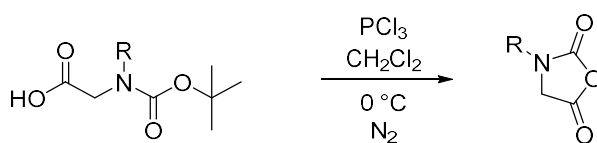
Chlorinated and brominated electrophilic reagents were also used for synthesizing Sar-NCA. For instance, PBr_3 reacted with a *O*-silylated carbamate sarcosine derivative in carbon tetrachloride, forming the corresponding NNCA in a yield 58% (**Scheme 7**).^{2,23}



Scheme 7. Synthesis of Sar-NCA from a trimethylsilylated carbamate.^{2,23}

Protocols involving phosphorus trichloride (PCl_3) and glycine derivatives were also frequently reported for preparing NNCA. With slight modifications, the protocol consisted of reacting *N*-alkylated-*N*-Boc-glycine derivatives and PCl_3 in dried aprotic solvents, at low temperature, under inert atmosphere, affording the corresponding NNCA in good yields (**Table 7**).

Table 7. *N*-alkylated NCAs obtained by cyclization reactions using PCl_3 .



R=	PCl_3	Solvent	Time	Purification	Yield	Reference
(equiv.)	(equiv.)		(h)		(%)	
Methyl	1	DCM	2	Sublimation	66	3
Ethyl	1	DCM	2	Sublimation	40	24–26
Propyl	1	DCM	2	Sublimation	55	24
Butyl	1	DCM	2	Sublimation	65	3
Isobutyl	1	DCM	2	Sublimation	21	24
Hexyl	1	DCM	2	Sublimation	40	25
Octyl						
2ethylhexyl	1	DCM	2	Sublimation	n.a	25
Dodecyl						
Tetradecyl						
Decyl	1	DCM	2	Sublimation	57	27
Allyl	1	DCM	4-5	Distillation	73	28
Propargyl	1	DCM	3	Recrystallization	55	29
MeOEt					85	
Me(OEt) ₂	1	DCM	2	Distillation	60-64	30
Me(OEt) ₃					61-64	

Chapter 2. Preparation of a small library of *N*-alkylated glycine *N*-carboxyanhydrides

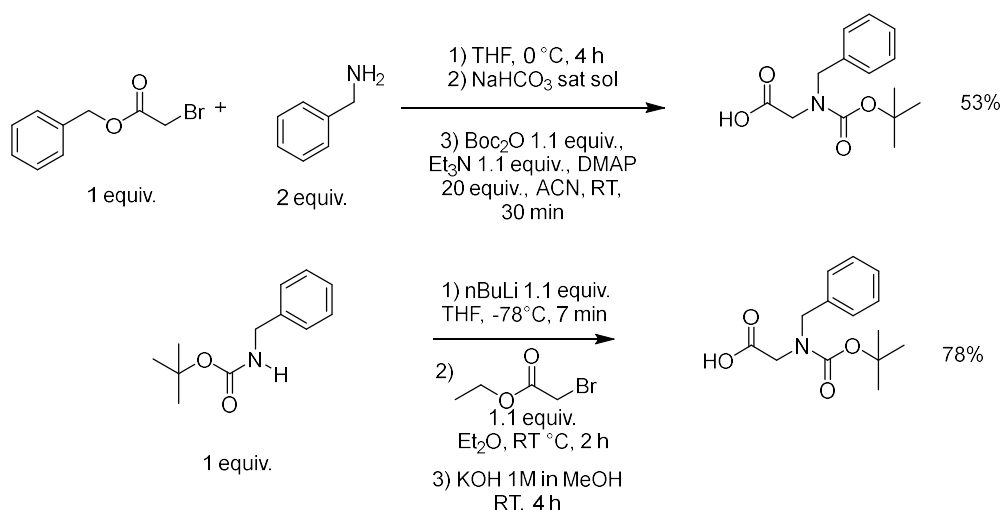
(<i>R</i>)Methylbenzyl							
(<i>S</i>)Methylbenzyl	1	1.2	DCM	2	Recrystallization and Sublimation	40	31

In this Ph.D. work, we aimed at preparing novel *N*-alkylated-glycine-based NCAs without using phosgene (and its derivatives). We focused our attention on a multi-step synthesis involving chlorinated electrophilic reagents: before operating the cyclization step into NNCA, we first studied the preparation of various *N*-alkylated-*N*-Boc-glycine intermediates.

1.2 Preparation of *N*-alkylated-*N*-Boc-glycine intermediates

To synthesize *N*-alkylated-*N*-Boc-glycine derivatives, three main routes are reported in the literature.

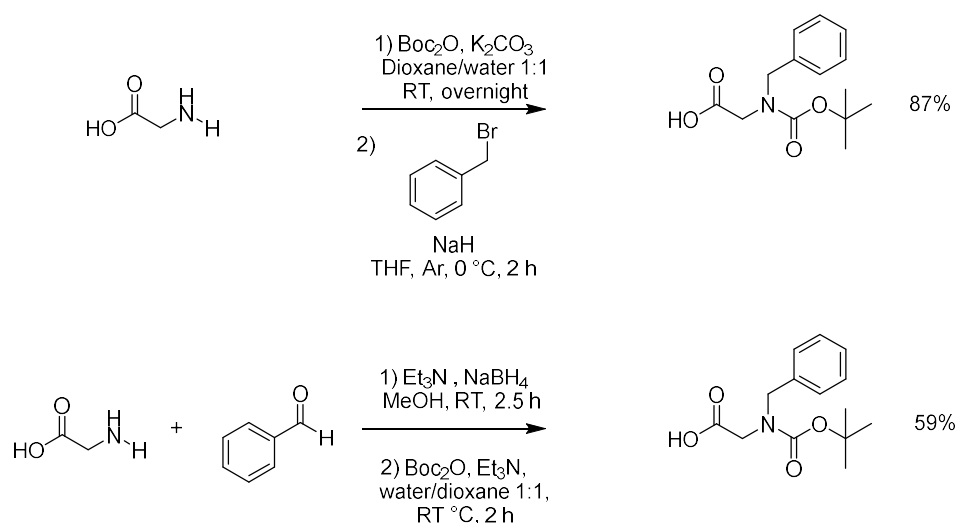
First, *N*-alkylated-*N*-Boc glycine intermediates have been prepared **from bromoacetate esters (Scheme 8)**. G. Bossler and D. Seebach proposed in 1994 a method to synthesize *N*-benzyl-*N*-Boc-glycine in three steps, starting with a nucleophilic substitution between benzylamine and benzyl bromoacetate, followed by the deprotection of the benzyl ester and the formation of a *N*-*tert*-butylcarbamate function (*N*-Boc-) with a global 53% yield.³² Later, P. Van Der Veken *et al.* reported the preparation of the same glycine derivative in three steps with a 78% global yield: deprotonation of *N*-Boc-benzylamine with *n*-butyllithium, acetylation using bromoethyl acetate and final deprotection of the carboxylic acid in basic medium.³³ The main disadvantage of the synthesis pathways from bromoacetate esters is that they require 3 steps which increases the production cost, in comparison with other simpler approaches.



Scheme 8. Synthetic routes to produce *N*-benzyl-*N*-Boc-glycine from bromoacetate esters.^{32,33}

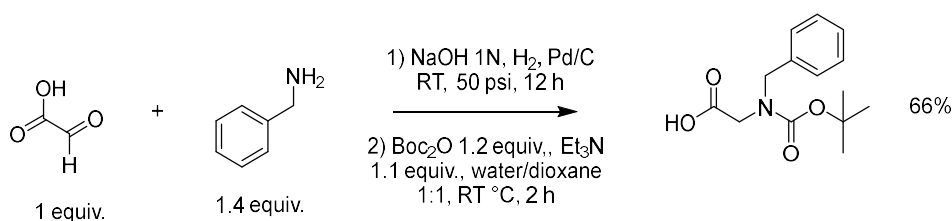
Chapter 2. Preparation of a small library of *N*-alkylated glycine *N*-carboxyanhydrides

Second, *N*-alkylated-*N*-Boc-glycine intermediates have been prepared from glycine (**Scheme 9**).³⁴ This strategy involved the formation of a *tert*-butylcarbamate between glycine and di-*tert*-butyl dicarbonate, isolating the *N*-Boc-glycine which was further *N*-deprotonated with sodium hydride and alkylated on the nitrogen atom with a benzyl group, using benzyl bromide (87% yield). This method seems attractive but the synthesis approach requires two reaction steps that cannot take place in a one-pot procedure, requiring an intermediate isolation/purification. The alternative strategy involved the reductive amination between glycine and benzaldehyde, followed by the formation of a *tert*-butylcarbamate with Boc₂O (global yield = 59%). However, this procedure is not very satisfying as the two reaction steps show limited yields.



Scheme 9. Main routes for synthesizing *N*-benzyl-*N*-Boc-glycine from glycine.³⁴

Another route towards *N*-alkylated-*N*-Boc-glycine derivatives was proposed by A. Mouna *et al.* in 1994.³⁴ It started by the reductive amination between glyoxylic acid and benzylamine, followed by the formation of an *N*-Boc-carbamate on the secondary amine, leading to *N*-benzyl-*N*-Boc-glycine in 66% global yield (**Scheme 10**). However, like the other procedures developed by A. Mouna *et al.*, this 2-step reaction procedure included an intermediate isolation/purification.



Scheme 10. Synthesis route to produce *N*-benzyl-*N*-Boc-glycine from glyoxylic acid.³⁴

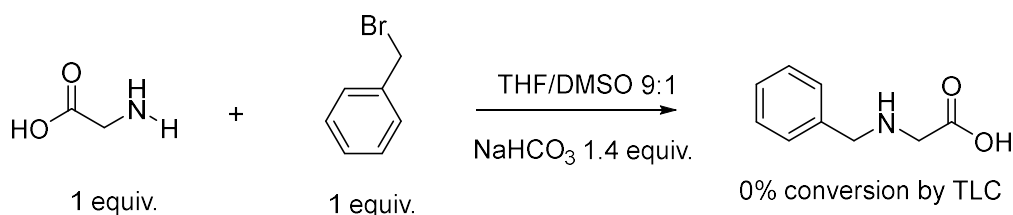
Chapter 2. Preparation of a small library of *N*-alkylated glycine *N*-carboxyanhydrides

In summary, three main strategies have been developed for synthesizing *N*-benzyl-*N*-Boc-glycine, starting from bromoacetate esters, glycine or glyoxylic acid. The procedure from bromoacetate ester required one more step than the two others, so we decided to focus our study on the routes starting from either glycine or glyoxylic acid, looking for an optimal procedure to first prepare the *N*-benzyl-*N*-Boc-glycine because the conversion of the aromatic compounds can be followed by thin-layer chromatography (TLC) and then, to apply this optimal procedure to the preparation of several *N*-Boc-glycine derivatives, bearing diverse alkyl groups on the nitrogen atom.

2 Preparation of *N*-alkylated-*N*-Boc-glycine intermediates

2.1 Benzylation of glycine with benzyl bromide

We first tried to alkylate glycine with benzyl bromide in THF/DMSO 9:1 (**Scheme 11**) at two different temperatures (20 and 60 °C). The reaction was followed by thin-layer chromatography (TLC). However, no conversion was observed after 4 h. This lack of reactivity could be explained by the poor solubility of glycine in the solvent mixture since a successful reaction was reported



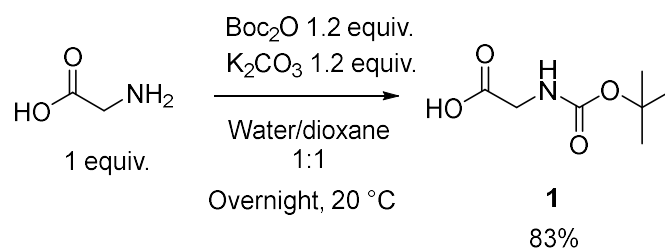
Scheme 11. Synthesis of *N*-benzyl glycine from glycine and benzyl bromide.

using the methyl glycinate ester and leading to the corresponding *N*-benzylated ester in 86% yield.³⁵ We did not perform more assays in this way as the use of methyl glycinate would lead to an extra synthesis step (ester hydrolysis) to provide the target compound.

2.2 2-Step synthesis of *N*-benzyl-*N*-Boc-glycine from glycine

We then explored an alternative route for the synthesis of *N*-Boc-*N*-benzylglycine from glycine in a 2-step procedure. Through an adaptation from Lake's synthesis method,³⁶ we first prepared *N*-Boc-glycine (**Scheme 12**). The reaction of glycine with 1.2 equiv. of Boc₂O in a mixture of water and dioxane provided *N*-Boc-glycine in 83% yield.

Chapter 2. Preparation of a small library of *N*-alkylated glycine *N*-carboxyanhydrides

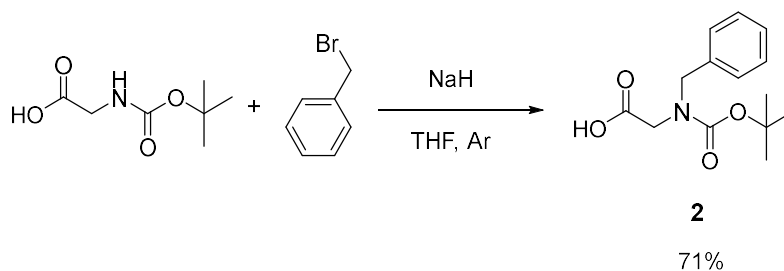


Scheme 12. Synthesis of *N*-Boc-glycine from glycine.

N-Boc-glycine was then alkylated with benzyl bromide, using a methodology that was reported by A. Mouna *et al.* with some modifications to avoid a chromatography purification step (**Table 8**).³⁴ The first trial consisted in the reaction between *N*-Boc-glycine, benzyl bromide and NaH under argon atmosphere, leading to a poor conversion of 10% that was increased to 20% by using 2 equiv. of benzyl bromide after 24 h (Entries 1 and 2). Varying other parameters such as temperature and NaH amount demonstrated conversion gain of 30% at $40\text{ }^\circ\text{C}$ and NaH (4 equiv.) and doubling the conversion ratio to 60% using 5 equiv. of NaH (Entries 3 and 4). Therefore, a large excess of NaH (12 equiv.) was used, varying reaction temperature: 20, 40 and $66\text{ }^\circ\text{C}$ (Entries 5, 6 and 7), providing good conversions in the $40\text{-}66\text{ }^\circ\text{C}$ range.

The operating procedure was optimized to avoid the chromatography purification step. First, THF was evaporated and the solid was resuspended in water. To eliminate the excess of benzyl bromide, cyclohexane extraction was performed to the aqueous phase. Finally, compound **2** was extracted with diethyl ether at pH = 3 in 71% yield.

Table 8. Synthesis of *N*-Boc-*N*-benzyl glycine **1** from *N*-Boc-glycine and benzyl bromide.



Entry	<i>N</i> -Boc glycine (equiv.)	Benzyl bromide (equiv.)	NaH (equiv.)	Temperature ($^\circ\text{C}$)	Time (h)	Conversion by TLC (visual estimation)
1	1	1	3	20	16	+/-
2	1	2	3	20	24	+

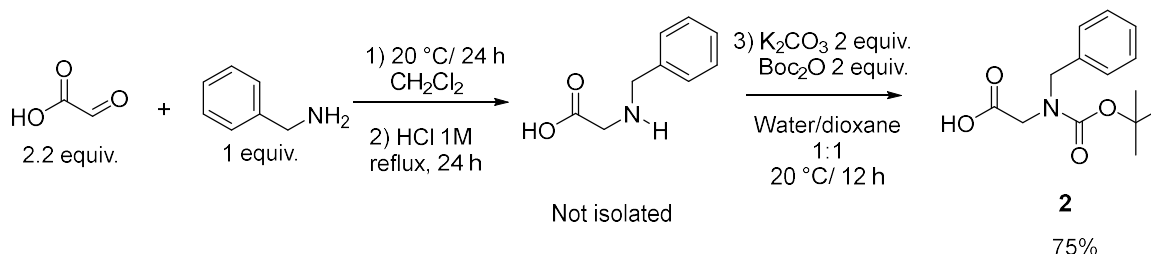
Chapter 2. Preparation of a small library of *N*-alkylated glycine *N*-carboxyanhydrides

3	1	2	4	40	24	+
4	1	2	5	40	24	++
5	1	2	12	20	24	++
6	1	2	12	40	24	+++
7	1	2	12	66	24	+++

In summary, it was possible to develop an efficient protocol to prepare *N*-Boc-*N*-benzyl glycine **2** in 2 steps from glycine in a global 53% yield. However, this protocol did not appear optimal as it a) was not a one-pot procedure, b) involved large amounts of a harsh base, NaH, c) required heating of the reaction medium and d) took a long time: 36 h.

2.3 Assays for the synthesis of *N*-benzyl-*N*-Boc-glycine from glyoxylic acid

Then we tried a one-pot procedure with some modifications of a previously reported method (**Scheme 13**).³ First, the methodology consisted in the formation of an intermediate *N*-benzyl-glycine (not isolated) from glyoxylic acid and benzylamine. The conversion of the reaction (consumption of benzylamine) was followed by TLC (DCM/MeOH 70:30). To reach full conversion, 2.2 equiv. of glyoxylic acid and a 24 h stirring were necessary. Then, reflux with HCl 1 M was performed, followed of *N*-Boc protection with 2 equiv. of Boc₂O. Upon liquid-liquid extraction from an aqueous solution at pH = 3 using Et₂O, compound **2** was isolated in 75% yield.



Scheme 13. Method A to produce *N*-benzyl-*N*-Boc-glycine from glyoxylic acid.

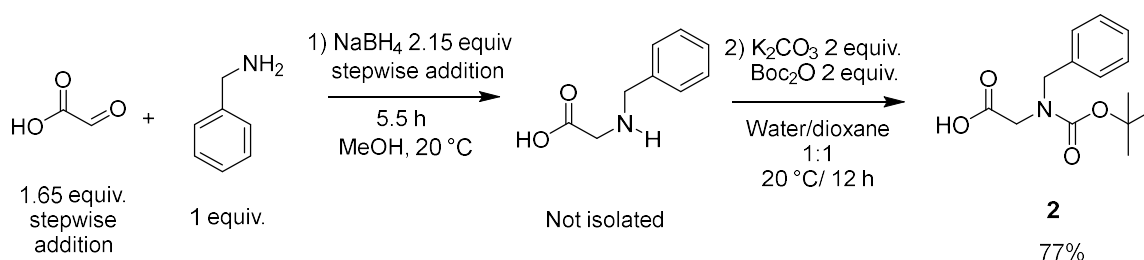
This procedure (method A) allowed the synthesis of the glycine-based derivatives in a one-pot reaction but the whole process lasts 60 h which increases the cost of the production. Moreover, this procedure has been ineffective due to a very uncommon method of reductive amination involving glyoxylic acid.³⁷

This procedure (method A) allows the synthesis of the glycine-based derivatives in a one-pot reaction but the whole process lasts 60 h, which increases the cost of the production. Moreover, this procedure lacks of good synthetic control due to a very uncommon method of

Chapter 2. Preparation of a small library of *N*-alkylated glycine *N*-carboxyanhydrides

reductive amination coming from glyoxylic acid.³⁷

Thus, we studied a second synthetic method (method B) starting with the reductive amination between primary amines and glyoxylic acid, using NaBH₄ (**Scheme 14**) as an alternative to H₂/Pd.³⁴ The conversion was improved by the step-wise addition of 1.65 equiv. of glyoxylic acid over 2.5 h, followed by the sequential addition of 2.15 equiv. of NaBH₄ over 3 h (**Table 9**). Thus, in only 18 h, without isolating intermediate benzylglycine, we prepared the compound **2** in 77% yield from glyoxylic acid, in two steps, through a 1-pot procedure.



Scheme 14. Method B to produce *N*-benzyl-*N*-Boc-glycine from glyoxylic acid.

Table 9. Optimization of the protocol to synthesize *N*-Boc-*N*-benzyl-glycine from glyoxylic acid and benzylamine: Method B.

	Glyoxylic acid (equiv.)	Time (h)	Conversion into imine intermediate by TLC*	NaBH ₄ (equiv.)	Time (h)	Reductive amination conversion by TLC*
	0.33	0.5	+/-	0.33	0.5	+/-
Feed 1	0.33	0.5	+	0.33	0.5	+
Feed 2	0.33	0.5	++	0.33	0.5	+
Feed 3	0.33	0.5	+++	0.33	0.5	++
Feed 4	0.33	0.5	+++	0.33	0.5	+++
Feed 5				0.50	0.5	complete

*Thin layer chromatography was eluted in DCM/MeOH (70:30) and revealed with ninhydrin R_fbenzylamine>0.9, R_fimine= 0.4 R_fN-benzylglycine= 0.5

2.3.1 Selection of the best operating procedure for the synthesis of 1

To select an optimal synthesis procedure, the costs of reagents and solvents were calculated for each synthesis pathway that was studied, considering the synthesis of 1 gram of *N*-benzyl-*N*-Boc-glycine **2**, and according to the Sigma-Aldrich and Fluorochem catalogs (**Table 10**). Among the three methods, the most expensive was the process starting from glycine (10.18 € from Sigma-Aldrich), mainly due to the cost of anhydrous conditions (solvent + Ar). Among the

Chapter 2. Preparation of a small library of *N*-alkylated glycine *N*-carboxyanhydrides

methods that we performed at 20 °C without anhydrous conditions, the cheapest was the synthetic pathway from glyoxylic acid “method B” (synthesis from glyoxylic acid involving NaBH₄) having a cost of 1.12 € (from Fluorochem), relatively close to the method A (1.20 €). Moreover, method B affords **2** in only 18 h and 77% yield. Therefore, this efficient and simple one-pot optimized method was selected for the preparation of all *N*-alkylated-*N*-Boc-glycines.

Table 10. Reagent cost evaluation of the three different synthesis methods to produce 1 gram of *N*-Boc-*N*-benzyl glycine **2** (3.8 mmol). Prices were extracted from commercial catalogs on march 2021 (bottles ranging 100 g - 500g). Yields are included in the calculations.

	Synthesis from Glycine		Synthesis from Glyoxylic acid Method A		Synthesis from Glyoxylic acid Method B			
	Cost (€)		Cost (€)		Cost (€)			
	Fluorochem	Sigma-Aldrich	Fluorochem	Sigma-Aldrich	Fluorochem	Sigma-Aldrich		
Glycine 99% (6.4 mmol, 0.48 g)	0.08	0.48	Glyoxylic acid 97% H ₂ O (11.1 mmol, 1.05 g)	0.44	0.89	Glyoxylic acid 97% H ₂ O (8.1 mmol, 0.57 g)	0.32	0.65
Boc ₂ O 97% (7.7 mmol, 1.73 g)	0.34	3.49	Benzylamine 98% (5.0 mmol, 0.55 g)	0.04	0.14	Benzylamine 98% (4.9 mmol, 0.41 g)	0.04	0.14
K ₂ CO ₃ 99% (7.7 mmol, 1.07 g)	0.05	0.25	Boc ₂ O 97% (10.1 mmol, 2.26 g)	0.45	4.57	NaBH ₄ 98% (10.5 mmol, 0.41 g)	0.26	0.37
NaH 60% (76.8 mmol, 3.07 g)	1.10	1.19	K ₂ CO ₃ 99% (10.1 mmol, 1.40 g)	0.07	0.33	Boc ₂ O 97% (9.8 mmol, 2.20 g)	0.43	4.45
Benzyl Bromide 98% (12.8 mmol, 2.23 g)	1.73	1.07	HCl (2 mL)	0.21 ^a	0.31	K ₂ CO ₃ 99% (9.8 mmol, 1.37 g)	0.07 ^a	0.32
THF anhydrous	1.73 ^a	3.70	Without anhydrous solvent		Without anhydrous solvent			
	Anhydrous conditions		Open-air		Open-air			
Total cost (€)	4.08	10.18	1.20	6.24	1.12	5.93		
Time consumption (h)	36		60		18			
Global yield (%)	53		75		77			

^a Prices calculated from Fisher Scientific website

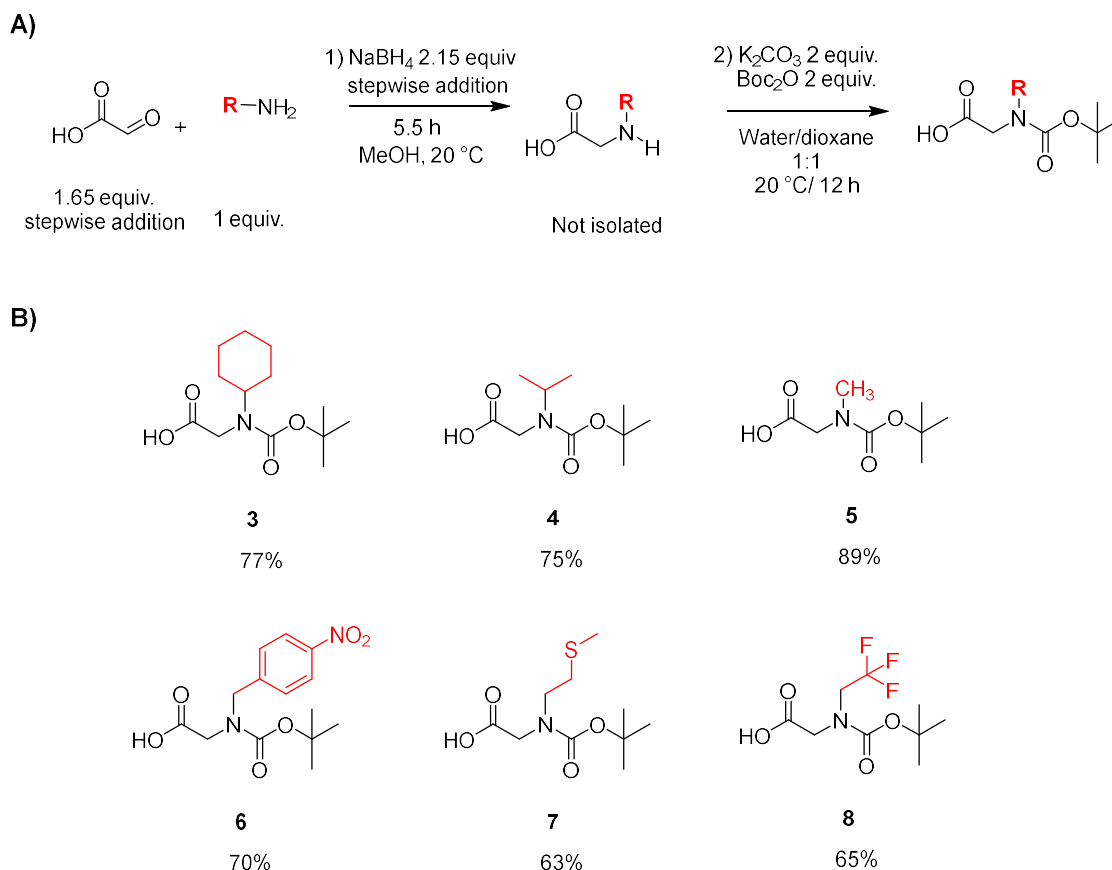
2.4 Synthesis of *N*-alkylated-*N*-Boc-glycine derivatives with hydrophobic character

Since the variation of the hydrophobic character of the side chains is one of the key parameters that can modulate the antimicrobial activity of the target amphiphilic copolymers,³⁸ we then decided to synthesize a series of 7 NNCA building blocks bearing alkyl chains with increasing lipophilicity, including methyl, *gem*-trifluoroethyl, isopropyl, methylthioethyl, cyclohexyl, benzyl and *p*-nitro-benzyl groups. For that purpose, we applied the previously described one-pot-protocol

Chapter 2. Preparation of a small library of *N*-alkylated glycine *N*-carboxyanhydrides

for the synthesis of **2** (Scheme 15a).

The compounds **3-8** were successfully synthesized and obtained the corresponding compounds in 63-77% yield (Scheme 15b). It is to note that all compounds were isolated with good purity after liquid-liquid extractions, avoiding the use of any chromatography purification step.



Scheme 15. Synthetic strategy to develop hydrophobic *N*-alkylated-*N*-Boc-glycines. A) General synthesis route and B) Series of prepared *N*-alkylated derivatives.

2.5 Rotamers

Carbamates adopt *cis* and *trans* conformations, a phenomenon also known as rotameric effect. The rotameric effect in carbamates happens due to the mesomeric effect between the carbonyl group and the nitrogen atom.³⁹ Indeed the presence of rotamers in some *N*-(arylsulfonylmethyl)-carbamates demonstrated to be temperature-dependent due to hindered internal rotations around the nitrogen to carbonyl bond that were bypassed by delivering energy

Chapter 2. Preparation of a small library of *N*-alkylated glycine *N*-carboxyanhydrides

to the molecule.⁴⁰ This *cis/trans* behavior was also observed in *N*-(benzyloxycarbonyl)-*L*-proline *tert*-butyl ester.⁴¹

As an example, in this work, the same rotameric effect was observed with *N*-benzyl-*N*-Boc-glycine **2**, as presented in **Figure 12**. Two rotamers were noted on the ¹H-NMR spectrum at 25 °C but all split signals merged into a single one when registering the spectrum at 70 °C.

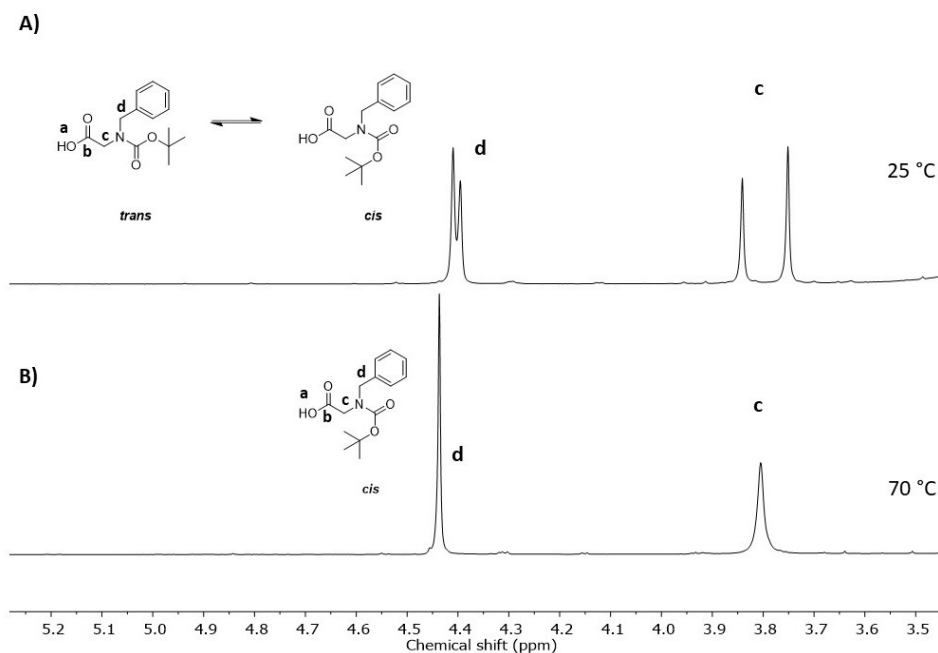
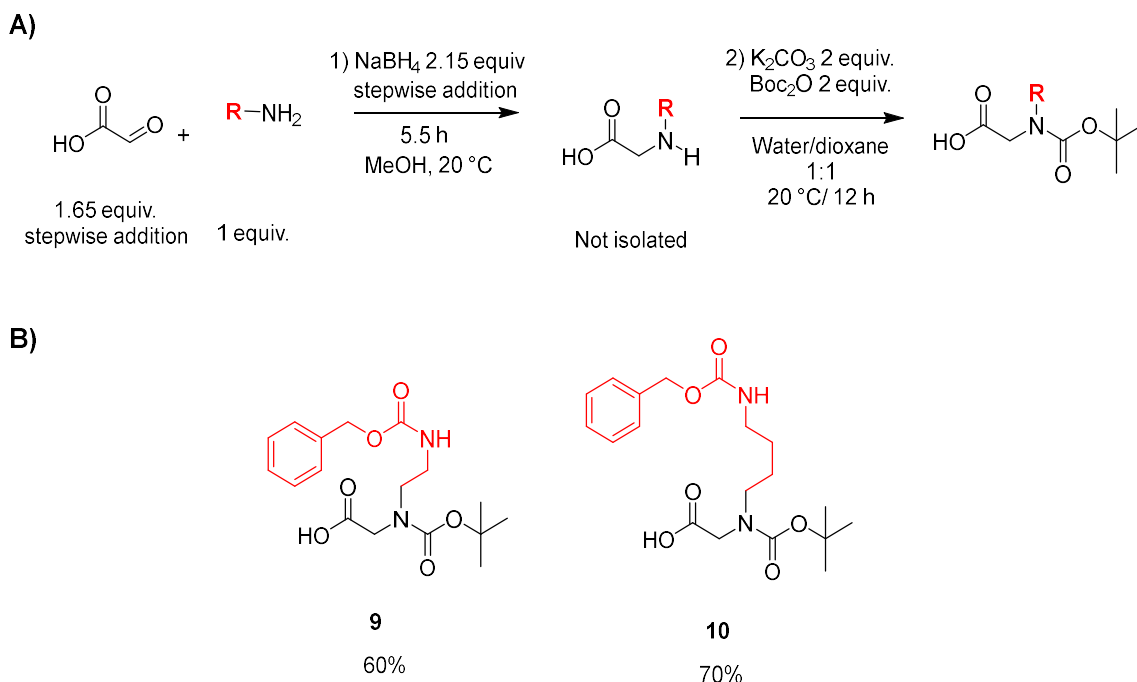


Figure 12. Representative signals on ¹H-NMR of carbamate rotamers and the effect of temperature in DMSO-*d*₆ of *N*-benzyl-*N*-Boc-glycine at a) 25 ° and b) 70 °C.

2.6 Synthesis of *N*-alkylated-*N*-Boc-glycine derivatives as precursors of cationic building blocks

To design amphiphilic antibacterial copolymers, we chose to include cationic charges in the structures of the target polymers.³⁸ To reach that goal and to study the influence of the size of the alkyl chain, two different precursors of glycine-based NNCA, bearing a protected aminoalkyl moiety on the nitrogen atom were prepared. The preparation was made according to the optimized procedure that was previously described (**Scheme 16a**), from commercial 1,2-diaminoethyl- or 1,4-diaminobutyl-containing reagents on which one amine function was protected by a benzyloxycarbamate (*Cbz* or *Z*) group. Upon the synthesis and corresponding purification by liquid-liquid extraction the two *Cbz*-amino-protected-*N*-Boc-glycine derivatives **9** and **10** were isolated in 60 and 70% yields, respectively.

Chapter 2. Preparation of a small library of *N*-alkylated glycine *N*-carboxyanhydrides



Scheme 16. Synthesis of Cbz-amino-protected-*N*-Boc-glycines. A) General synthesis route and B) Series of prepared *N*-alkylated derivatives.

3 Preparation of the *N*-alkylated *N*-carboxyanhydrides (NNCA)

From the *N*-alkylated-*N*-Boc-glycine derivatives that were synthesized, NNCA were prepared in one step by using Leuchs' method. To reach an efficient cyclization procedure, several electrophilic reagents were evaluated (PCl_3 or $SOCl_2$). To afford pure monomers, a filtration over celite was also carried out. Finally, the kinetics of the intramolecular cyclization reaction was also studied.

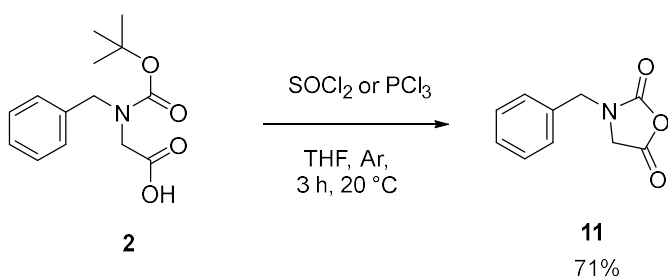
3.1 Assays to produce NNCA

As previously noted (section 1.1), PCl_3 was the most frequently used reagent to obtain NNCA from *N*-alkylated-*N*-carbamate-protected-aminoacids. Only one publication by T. Higashimura *et al.* reported the production of *N*-cyanoethylglycine NCA (63% yield) using thionyl chloride.⁴² Then, the reactions between *N*-benzyl-*N*-Boc-glycine **2** and thionyl chloride ($SOCl_2$) or phosphorus trichloride (PCl_3), affording *N*-benzyl-NCA **11** (or Phe-NNCA, as a position isomer of Phenylalanine NCA), were compared (**Table 11**). The formation of the NNCA was followed by the increase of the signal peaks around 1850 and $\approx 1776\text{ cm}^{-1}$ corresponding to the $NC=O$ and $OC=O$ stretchings until no change was observed (**Figure 13**). By operating the reaction in anhydrous

Chapter 2. Preparation of a small library of *N*-alkylated glycine *N*-carboxyanhydrides

THF under Ar atmosphere, we observed that SOCl_2 was a more efficient reagent than PCl_3 and that the use of an excess of these cyclization reagents was not necessary. After 3 h of reaction, compound **11** was then isolated in 71% yield.

Table 11. Assays to synthesize *N*-Benzyl-glycine-NCA (*Phe*-NNCA).



Entry	<i>N</i> -benzyl- <i>N</i> -Boc-glycine (equiv.)	SOCl_2 (equiv.)	PCl_3 (equiv.)	Yield (%)
1	1	2.5		70
2	1	1		71
3	1		1	23

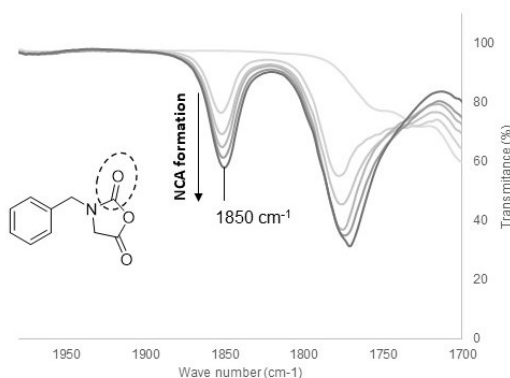
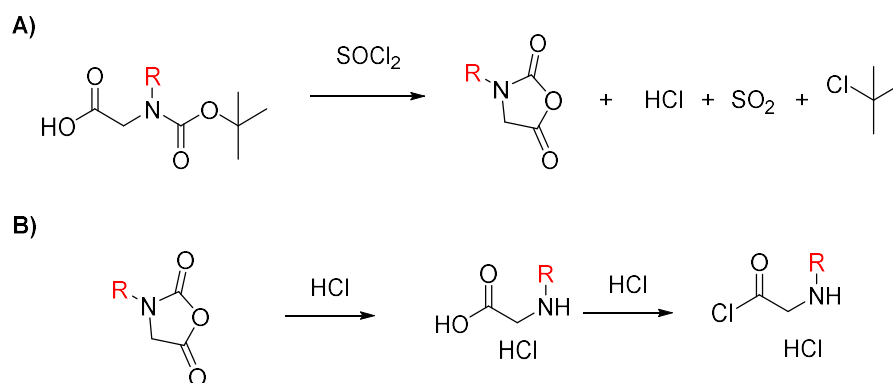


Figure 13. Demonstration of the evolution of the NCO stretching signal of NNCA formation at 1850 cm^{-1} followed by FTIR.

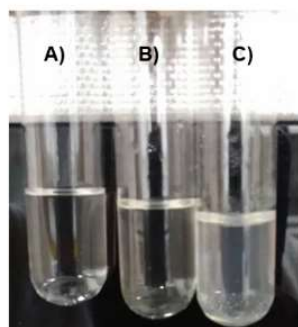
Then, we focused our efforts on the purification of *Phe*-NNCA **11**. Since electrophilic contaminants (i.e. HCl and HCl aminoacid salts formed during the reaction) can hinder or quench the polymerization process, highly pure monomers must be synthesized.⁴³ Indeed, during the NNCA synthesis, HCl can open the cycles leading to HCl-amino acid salts and HCl-acetyl chloride derivatives (**Scheme 17**).^{44–46} Traditionally, in the literature the purification methods that were reported are distillation, recrystallization or sublimation, depending on the physicochemical properties of the NNCA.

Chapter 2. Preparation of a small library of *N*-alkylated glycine *N*-carboxyanhydrides



Scheme 17. Byproducts formed during the NNCA synthesis. A) Cyclization of NNCA and B) NNCA ring opening mediated by HCl.

Recently, a method performing filtration over dried Celite demonstrated high efficacy in eliminating the chlorine contaminants in the synthesis of NCA.⁴⁷ Thus, we transposed this protocol to the purification of **11** and compared it with the recrystallization of **11** in a DCM/cyclohexane (1:6) mixture. The remaining traces of chloride anions after each purification procedure were evaluated by the addition of silver nitrate in a THF solution of **11** (formation of a silver chloride precipitate). As shown in **Figure 14**, the procedure involving a filtration over celite was not only more efficient than crystallization to eliminate chloride contaminants but also permitted to isolate **11** in higher yields (79%) versus 71%.



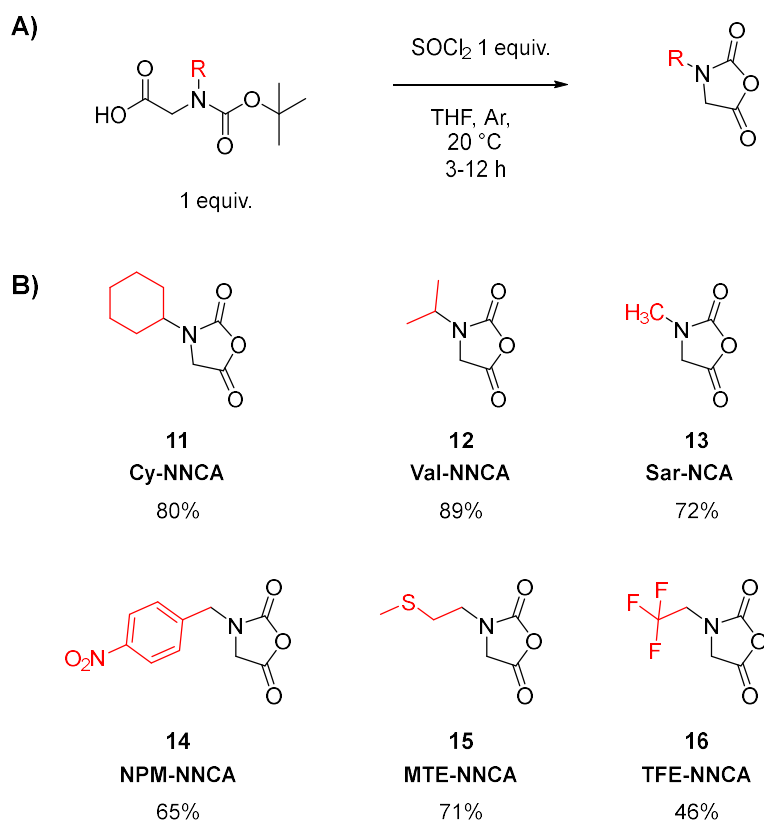
A)	Blank	n.a
B)	Filtration over Celite	79% yield
C)	Recrystallization	71% yield

Figure 14. Left: Chloride test after the purifications of *N*-benzyl-NCA. Chloride anion concentration was decreased after filtration over Celite compared to recrystallization by DCM/Cyclohexane (1 mM AgNO₃ assay in THF). Right: NNCA isolation yields after the two different purification methods

3.2 Synthesis of *N*-alkylated NCA with hydrophobic character

To prepare the *N*-alkylated-*N*-Boc-glycine we carried out the methodology according to **Scheme 18** including the purification by filtration over celite. The different NNCA **12-17** were

Chapter 2. Preparation of a small library of *N*-alkylated glycine *N*-carboxyanhydrides

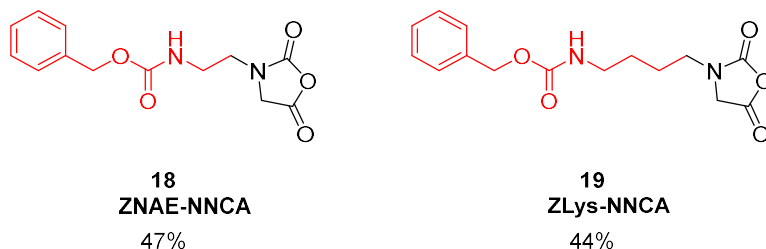


Scheme 18. Synthesis of *N*-alkylated NCA. A) General synthesis route and B) Series of prepared *N*-alkylated derivatives.

successfully prepared in a range of 46 to 89%.

3.3 Synthesis of *N*-alkylated NCA with cationic character

The synthesis of *N*-protected-aminoalkyl-NNCA is not reported. We carried out the cyclization of **9** and **10** through the Leuchs method using SOCl₂ described in section 3.2.

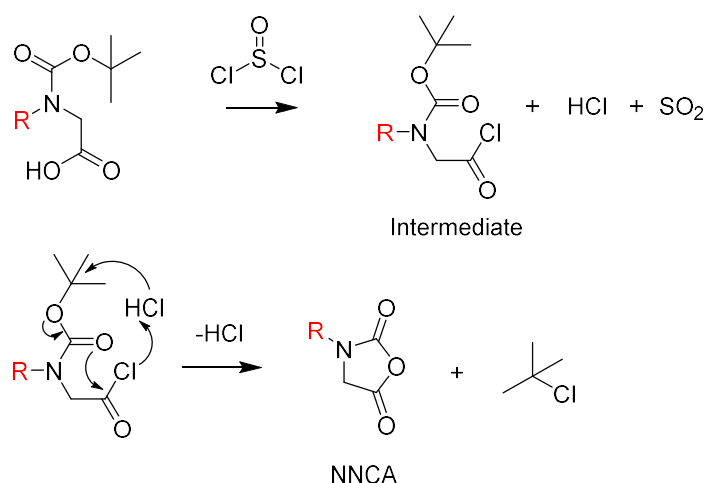


Scheme 19. Synthesis of ZNAE- and ZLys-NNCA

After purification over celite we obtained the *Cbz*-*N*-protected-aminoalkyl-NNCA **18** and **19** in a 47 and 44% yield, respectively (**Scheme 19**).

3.4 Kinetics of the cyclization reactions of NNCA

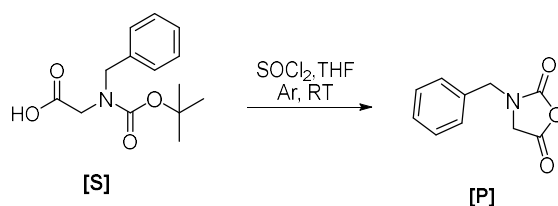
The mechanism of the cyclization of *N*-alkylated-*N*-Boc-glycine derivatives into the corresponding NNCA by Leuchs method was not studied but we hypothesized a mechanism presented in **Scheme 20**.⁴⁸ It could be decomposed into: 1) halogenation of the carboxylic acid function by SOCl_2 , leading to an acyl chloride intermediate that rapidly decomposes, releasing SO_2 and 2) cyclization into NNCA by an intramolecular nucleophilic attack mediated as a result of the acidic deprotection of the *tert*-butyl group by HCl .



Scheme 20. Proposed mechanism for the formation of NNCA when using Leuchs' method with SOCl_2

Despite the fact the NNCA preparation from carbamate derivatives has been well documented, there is no information regarding the effect of the *N*-alkyl side chains on the kinetics of the NNCA formation. Therefore, we evaluated the kinetic rates of the NNCA formation by the appearance of the signal peaks corresponding to the NCO ($\text{C}=\text{O}$ 1850 cm^{-1} stretching), measured by FTIR (**Figure 13**). Two different effects were evaluated including, steric hindrance and electron-withdrawing effect.

The kinetic rates (k) were obtained using the first-order kinetic rate from the slope of a plot of the $\ln(\text{S}_0/\text{S})$ vs time (**Equation 1**):



$$\ln \left[\frac{S_0}{S_t} \right] = k t \quad \text{Equation 1}$$

Where: $S_0 = I_0 - I_f$

I_0 was the intensity of the signal at initial time and I_f the intensity detected at the end of the experiment;

And: $S_t = I_t - I_f$

I_t was the intensity at the sampling time t . To calculate the kinetic constants, we assumed that the rate of appearance of [P] was equal to the disappearance of [S].

The effect of the steric hindrance was observed through a decrease of the kinetic rate values when we introduced a more bulky *N*-substituent for instance, Sar-NCA ($k = 4.97 \text{ h}^{-1}$) compared to Val-NNCA presented a 5-times smaller kinetic rate value ($k = 0.98 \text{ h}^{-1}$) followed by Cy-NNCA ($k = 1.48 \text{ h}^{-1}$) and Phe-NNCA ($k = 2.16 \text{ h}^{-1}$, **Figure 15a**).

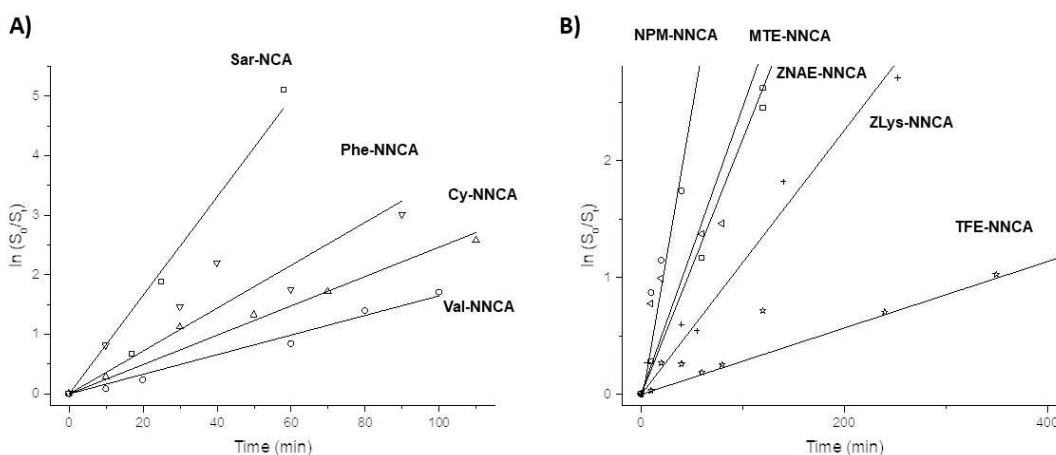


Figure 15. Kinetics of the ring-closing of *N*-alkylated-*N*-carboxyanhydrides in THF 0.4 M at 20 °C. A) steric hindrance effect using *N*-alkylated side chains and B) steric and electronic effects varying the *N*-substituent.

However, we were not able to associate an electronic effect with the changes observed with the different kinetic rates. We only observed that TFE-NNCA presented the slowest kinetic rate value ($k = 0.17 \text{ h}^{-1}$, **Figure 15b**), a low value we could attribute to the high electron-withdrawing effect. The rest of the NNCA's followed a decrease in the kinetic constant that was not necessarily related to steric or electronic effects: NPM-, MTE-, ZNAE-, ZLys-NNCA, respectively (**Table 12**).

Chapter 2. Preparation of a small library of *N*-alkylated glycine *N*-carboxyanhydrides

Table 12. Summary of the kinetic rates of the *N*-alkylated-NCA synthesized.

	R	k (h⁻¹)
Sar-NCA	Methyl	4.97
NPM-NCA	Nitrobenzyl	2.89
Phe-NNCA	Benzyl	2.16
Cy-NNCA	Cyclohexyl	1.48
MET-NNCA	Methylthioethyl	1.47
ZNAE-NNCA	Cbz-aminoethyl	1.31
Val-NNCA	Isopropyl	0.98
ZLys-NNCA	Cbz-aminobutyl	0.68
TFE-NNCA	Trifluoroethyl	0.17

4 Conclusion

In summary, we prepared a small library of NNCA's using an optimized protocol involving 2-steps of synthesis: 1) the reductive amination from primary amines and glyoxylic acid and consequent *N*-Boc protection in "one-pot" (yields > 70%) optimizing the method of purification through a simple liquid-liquid extraction; 2) cyclization using the Leuchs method with SOCl₂ in quantitative yields (>44%), optimizing the method of purification through a simple celite filtration. A comprehensive study of this second step involving kinetic experiments allowed to establish that more bulky *N*-substituents slowed down the NNCA formation, while the electronic effect did not influence this step.

5 Materials and methods

5.1 Materials

All the chemicals and solvents were purchased from Sigma Aldrich, Fluorochem, Acros, TCI, Strem and, unless otherwise described, were used without any purification. Dichloromethane (DCM), tetrahydrofuran (THF), diethyl ether (Et₂O), hexane were obtained from a solvent system purificator (PureSolv, Innovative Technology), kept under argon atmosphere and freshly used. MilliQ water was obtained from a (Purelab Prima, ELGA). Celite 545 was dried using the Schlenck line at 200 °C for 3 h and stored under argon atmosphere.

5.2 Equipment and measurements

Melting point

The melting points were determined with a Start Melting point determiner SMP3 at the Laboratoire de Chimie de Coordination (LCC, Toulouse, France).

Infrared (IR) spectroscopy

The IR spectra was recorded using the FTIR spectrometer (Fortier MIR spectrometer, Perkin Elmer), and the samples were measured with the ATR (GladiATR, Pike Technologies) from Fisher technologies performing 32 scans at the Laboratoire de Chimie de Coordination (LCC, Toulouse, France). The raw data was obtained with the Perkin Elmer spectrum 10 software and processed using the Originlab 2016 software.

Kinetic investigations using IR spectroscopy

The analyzed compounds were dissolved in the corresponding solvent in the Schleck vessel under an argon atmosphere at 20 °C. Subsequently, 50 µL sample was taken with an argon purged syringe. The sample was dropped onto the ATR unit of the IR spectrometer, dried with a current of air for 30 s and measured in the range from 400 cm⁻¹ to 4000 cm⁻¹. Using the band height of the C=O stretching at about 1850 cm⁻¹, the monomer conversion could be followed, since the increase is linear in the examined concentration range. After the addition of SOCl₂ for NCA synthesis, the initial value for the band at 0% conversion was corrected by a correction factor. Samples were taken at different reaction times until no change in peak height (1850 cm⁻¹) was noted. The analysis of results was carried out using the Origin lab 2016 software. .

Nuclear magnetic resonance spectroscopy (NMR)

Chapter 2. Preparation of a small library of *N*-alkylated glycine *N*-carboxyanhydrides

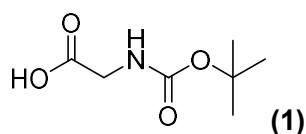
Most of the NMR spectra were recorded in a Bruker IconNMR 400 MHz at the LCC (Toulouse, France) to the exception of compounds **15-19** that were recorded in a Bruker Avance III 400 spectrometer at the LCPO (Bordeaux, France). The spectra were analyzed at 295 K and data were analyzed using Mestrenova 10.0 software. The chemical shifts of the signals are given in ppm. The spectra obtained were calibrated using the residual solvent signals (CHCl₃ 7.26 ppm, H₂O 4.79 ppm, dimethyl sulfoxide (DMSO) 2.50 ppm, trifluoroacetic acid (TFA) 11.50 ppm). The signals were categorized as follows: singlet (s), doublet (d), triplet (t), quartet (q), multiplet (m) and broad (br).

Mass spectrometry

The high resolution mass spectrometry analysis were performed at the Institut de Chimie de Toulouse at the Université Paul Sabatier (Toulouse, France). The spectra was registered in a GCT premier (DCI, CH₄, HR-MS) or Xevo G2 QTOF (Waters, ESI, HRMS).

5.3 *N*-Alkylated-glycine derivatives

***N*-Boc-glycine (1)**. The synthesis method was based on a previous report with some modifications.³⁶ Briefly, glycine 98.5% (65 mmol, 4.95 g 1 equiv.), Boc₂O 99% (78 mmol, 17.19 g, 1.2 equiv.) and K₂CO₃ 99% (78 mmol, 10.88 g, 1.2 eq) were stirred overnight at 20 °C in 150 mL of water-dioxane (1:1). Then, dioxane was evaporated, a saturated solution of Na₂CO₃ was added and 3 extractions with ethyl acetate were done. The pH of the aqueous phase was adjusted with 2 M HCl to pH = 3 followed by 3 extractions with EtOAc. The organic phase was dried over MgSO₄, filtered and evaporated, affording compound **1** as a white powder in 83% yield (9.45 g).



Chemical Name: (*tert*-butoxycarbonyl)glycine

Chemical Formula: C₇H₁₃NO₄

Molecular Weight: 175.18 g/mol

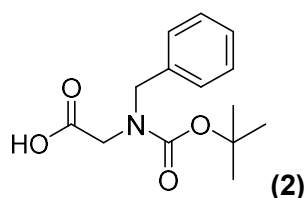
Melting Point: 87 °C (Lit 85-86 °C).⁴⁹

¹H-NMR (400 MHz, CDCl₃) δ: 1.48 (s, 9H, CH₃), 3.93-3.99 (m, 2H, CH₂), 5.05 (b, 1H, NH), 10.63 (br, 1H, COOH). In agreement with literature.³⁶ No data for ¹³C-NMR analysis is shown.

Chapter 2. Preparation of a small library of *N*-alkylated glycine *N*-carboxyanhydrides

***N*-Benzyl-*N*-Boc-glycine (2).** The method was based on Method B. In a round bottom flask, benzylamine 99% (11.04 mL, 100 mmol, 1 equiv.) was solubilized in 200 mL of methanol. Glyoxylic acid monohydrate 97% (3.13 g, 33 mmol, 0.33 equiv.) was added and the reaction mixture stirred for 30 minutes. Then, NaBH₄ 98% (1.27 g, 33 mmol, 0.33 equiv.) was added and the reaction mixture was stirred 30 min. The addition of glyoxylic acid and NaBH₄ was repeated 5 times until benzylamine was fully consumed, monitoring by TLC (CHCl₂-MeOH, 70-30). An additional amount of 0.5 equiv. of NaBH₄ was added to reduce the remaining imine intermediate and the solvent was evaporated.

Then, water (150 mL), potassium carbonate 99% (27.92 g, 200 mmol, 2 equiv.), dioxane (150 mL) and di-*tert*-butyldicarbonate 99% (44.09 g, 200 mmol, 2 equiv.) were successively added before the mixture was stirred for 12 h at RT. Then the solvent was evaporated *in vacuo*. To the crude residue, 100 mL of water were added and 3 extractions with 100 mL of diethyl ether were performed. The pH of the aqueous phase was decreased around pH = 3 using 6 M HCl, added drop by drop. Four extractions with 100 mL of diethyl ether were done and the organic phase was dried over sodium sulphate, filtered, and evaporated until a remaining volume of 25 mL. Then the temperature was decreased to 4 °C until a precipitate was formed and filtered off before the solvent was fully evaporated. To the viscous liquid, 200 mL of hexane were added and the mixture was kept at 4 °C overnight to allow precipitation of the product. The solid was washed 3 times with 25 mL of hexane, dried *in vacuo* and isolated as a yellowish powder in 77% yield (20.42 g).



Chemical Name: *N*-benzyl-*N*-(*tert*-butoxycarbonyl)glycine

Molecular Formula: C₁₄H₁₉NO₄

Molecular Weight: 265.31 g/mol

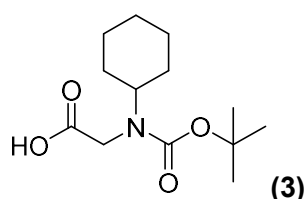
Melting Point: 102-103 °C (Lit. 103 °C)⁵⁰

¹H-NMR, CDCl₃ 400 MHz δ: 1.48 (s, 9H, CH₃), 3.90 (d, 2H, *J*=54.4 Hz, CH₂), 4.53 (d, 2H, *J*=14.2 Hz, CH₂), 7.22-7.36 (m, 5H, Ar). COOH missing in these experimental conditions. In agreement with the literature.^{33,50}

Chapter 2. Preparation of a small library of *N*-alkylated glycine *N*-carboxyanhydrides

^{13}C NMR, CDCl_3 100 MHz δ : 28.28 (d, $J=7.0$ Hz, 3CH_3), 47.60 (C), 51.26 (d, $J=71$ Hz, CH_2), 81.06 (d, $J=27.2$ Hz, CH_2), 127.55 (d, $J=6.8$ Hz, CH), 128.13 (CH), 128.65 (CH), 137.13 (d, $J=12.7$ Hz, C), 155.83 (d, $J=55$ Hz, COO), 175.36 (d, $J=56.4$ Hz, COOH).

***N*-Cyclohexyl-*N*-Boc-glycine (3).** The synthesis was performed similarly to the protocol described for compound **2**. The product was isolated as a white crystalline powder in 77% yield (19.81 g) starting from cyclohexylamine 99% (11.58 mL, 100 mmol).



Chemical name: *N*-(tert-butoxycarbonyl)-*N*-cyclohexylglycine

Molecular formula: $\text{C}_{13}\text{H}_{23}\text{NO}_4$

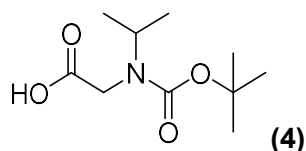
Molecular weight: 257.33 g/mol

Melting point: 99-101 °C (Lit. 103-104 °C)⁵¹

^1H -NMR, CDCl_3 400 MHz δ : 0.95-1.36 (m, 5H, CH_2), 1.37-1.54 (m, 9H, CH_3), 1.57-1.86 (m, 5H, CH_2), 3.64-4.17 (m, 3H, CH_2+CH), 9.09 (br, 1H, COOH). In agreement with the literature.³³

^{13}C -NMR, CDCl_3 100 MHz δ : 25.61 (d, $J=28.6$ Hz, 2CH_2), 28.42 (s, 3CH_3), 31.14 (2CH_2), 42.21 (CH_2), 54.39 (CH), 56.39 (C), 80.53 (CH_2), 154.97 (COO), 176.86 (s, COOH).

***N*-Isopropyl-*N*-Boc-glycine (4).** The synthesis was performed similarly to the protocol described for compound **2**. The product was isolated as a white crystalline powder in 75% yield (16.29 g) starting from isopropylamine 99% (8.27 mL, 100 mmol).



Chemical name: *N*-(tert-butoxycarbonyl)-*N*-isopropylglycine

Chapter 2. Preparation of a small library of *N*-alkylated glycine *N*-carboxyanhydrides

Molecular formula: C₁₀H₁₉NO₄

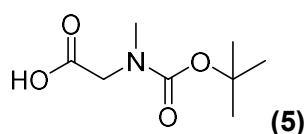
Molecular weight: 217.27 g/mol

Melting point: 94-95 °C (Lit. 98 °C)³⁴

¹H-NMR, CDCl₃ 400 MHz δ: 1.11 (br, 6H, 2CH₃), 1.46 (br, 9H, 3CH₃), 3.85 (d, 2H, *J*=37.4 Hz CH₂), 4.20-4.46 (m, 1H, CH), 9.75 (br, 1H), COOH. In agreement with the literature.³⁴

¹³C-NMR, CDCl₃ 100 MHz δ: 20.55 (2CH₃), 28.44 (3CH₃), 43.39 (d, *J*=68 Hz CH), 46.18-48.01 (d, *J*=180 Hz, C), 80.73 (d, *J*=40.7 Hz, CH₂), 150.03 (COO), 176.78 (COOH).

***N*-Methyl-*N*-Boc-glycine (5).** The synthesis was performed similarly to the protocol described for compound **2**. The product was isolated as a white powder in 89% yield (16.83 g) starting from sarcosine 98% (9.09 g, 100 mmol).



Chemical name: *N*-(*tert*-butoxycarbonyl)-*N*-methylglycine

Molecular formula: C₈H₁₅NO₄

Molecular weight: 189.21 g/mol

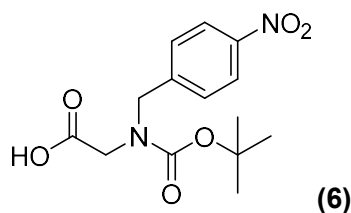
Melting point: 88-89 °C (Lit. 84-86 °C)⁵²

¹H-NMR, CDCl₃ 400 MHz δ: 1.43-1.46 (d, 9H, *J*=14.9 Hz, 3CH₃), 2.93 (d, 3H, *J*=3.1 Hz, CH₃), 3.98 (d, 2H, *J*=31.0 Hz, CH₂), 9.19 (br, 1H, COOH). In agreement with the literature.⁵³

¹³C-NMR, CDCl₃ 100 MHz δ: 28.41 (d, *J*=8.1 Hz, 3CH₃), 37.74 (d, *J*=13.5 Hz, C), 50.59 (d, *J*=51 Hz, CH₃), 80.77 (CH₂), 156.08 (d, *J*=89.1 Hz, COO), 175.35 (d, *J*=34.4 Hz, COOH). In agreement with the literature.⁵³

***N*-(*p*-Nitrobenzyl)-*N*-Boc-glycine (6).** The synthesis was performed similarly to the protocol described for compound **2**. The product was isolated as a yellowish crystalline powder in 70% yield (4.56 g) starting from *p*-nitrobenzylamine hydrochloride 97% (4.08 g, 21 mmol).

Chapter 2. Preparation of a small library of *N*-alkylated glycine *N*-carboxyanhydrides



Chemical name: *N*-(*tert*-butoxycarbonyl)-*N*-(4-nitrobenzyl)glycine

Molecular formula: C₁₄H₁₈N₂O₆

Molecular weight: 310.31 g/mol

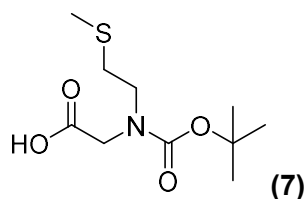
MS (CI⁺): *m/z*= 311.12 [M+H]⁺

Melting point: 93 °C

¹H-NMR, CDCl₃ 400 MHz δ: 1.46 (d, 9H, *J*=16.6 Hz, 3CH₃), 3.96 (d, 2H, *J*=54.8 Hz, CH₂), 4.61 (d, 2H, *J*=16.6 Hz, CH₂), 7.41 (m, 2H, Ar), 8.22 (m, 2H, Ar), COOH missing in these experimental conditions.

¹³C-NMR, CDCl₃ 100 MHz δ: 28.34 (3CH₃), 48.65 (d, *J*=13.8 Hz, C), 51.49 (d, *J*=71.1 Hz, CH₂), 81.89 (d, *J*=28.0 Hz, CH₂), 124.05 (2CH), 128.34 (d, *J*=67 Hz, 2CH), 145.15 (d, *J*=21.2 Hz, C), 147.60 (C), 155.52 (m, COO), 174.18 (d, *J*=33.7 Hz, COOH).

***N*-(2-(Methylthio)ethyl)-*N*-Boc-glycine (7).** The synthesis was performed similarly to the protocol described for compound **2**. The product was isolated as a yellow viscous oil in 63% yield (15.70 g) starting from 2-(methylthio)ethylamine 97% (9.59 mL, 100 mmol).



Chemical name: *N*-(*tert*-butoxycarbonyl)-*N*-(2-(methylthio)ethyl)glycine

Molecular formula: C₁₀H₁₉NO₄S

Molecular weight: 249.33 g/mol

Melting point: viscous liquid

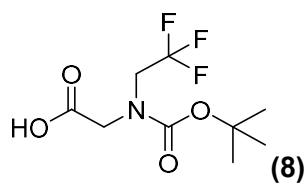
Chapter 2. Preparation of a small library of *N*-alkylated glycine *N*-carboxyanhydrides

MS (Cl⁺): $m/z = 250.11$ [M+H]⁺

¹H-NMR, CDCl₃ 400 MHz δ : 1.46 (d, 9H, $J=18.6$ Hz, 3CH₃), 2.13 (br, 3H, CH₃), 2.67 (dd, 2H, $J=12.2, 5.8$ Hz, CH₂), 3.47 (dt, 2H, $J=17.5, 7.2$ Hz, CH₂), 4.03 (d, 2H, $J=24.4$ Hz, CH₂), COOH missing in these experimental conditions.

¹³C-NMR, CDCl₃ 100 MHz δ : 15.64 (d, $J=8.5$ Hz, CH₃), 28.40 (d, $J=14.5$ Hz, 3CH₃), 32.52 (d, $J=24.0$ Hz, CH₂), 48.40 (d, $J=30.9$ Hz, C), 49.93 (d, $J=52.2$ Hz, CH₂), 81.18 (d, $J=22.9$ Hz, CH₂), 155.46 (d, $J=82.0$ Hz, COO), 175.32 (d, $J=59.4$ Hz, COOH).

***N*-(Trifluoroethyl)-*N*-Boc-glycine (8)**. The synthesis was performed similarly to the protocol described for compound **2**. The product was isolated as a white crystalline powder in 65% yield (16.71 g) starting from 2,2,2-trifluoroethylamine 99% (8.03 mL, 100 mmol).



N-(*tert*-butoxycarbonyl)-*N*-[2-(2,2,2-trifluoroethyl)glycine]

Molecular formula: C₉H₁₄ F₃NO₄

Molecular weight: 257.21 g/mol

Melting point: 82-85 °C

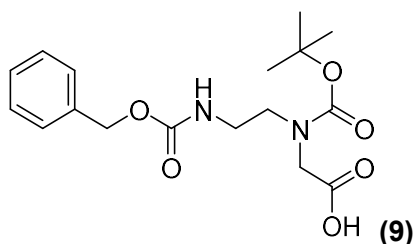
MS (Cl⁺): $m/z = 258.09$ [M+H]⁺

¹H-NMR, CDCl₃ 400 MHz δ : 1.46 (d, 9H, $J=9.2$ Hz, 3CH₃), 3.92 (oct, $J=17.5$ Hz CH₂), 4.10 (d, 2H, $J=23.4$ Hz, CH₂), 8.19 (br, 1H, COOH).

¹³C-NMR, CDCl₃ 100 MHz δ : 28.16 (d, $J=3.5$ Hz, 3CH₃), 48.25-49.99 (m, CH₂), 56.39 (C), 85.52 (d, $J=8.8$ Hz, CH₂), 124.57 (q, $J=280$ Hz, CF₃), 154.94 (d, $J=4.1$ Hz, COO), 174.97 (d, $J=28.2$ Hz, COOH).

***N*-(Cbz-aminoethyl)-*N*-Boc-glycine (9)**. The synthesis was performed similarly to the protocol described for compound **2**. The product was isolated as a white powder in 60% yield (9.16 g) starting from *N*-Cbz-1,4-diaminoethane hydrochloride 99% (10.09 g, 43 mmol).

Chapter 2. Preparation of a small library of *N*-alkylated glycine *N*-carboxyanhydrides



Chemical name: *N*-[2-(benzyloxycarbonylaminoethyl)]-*N*-(*tert*-butoxycarbonyl)glycine

Molecular formula: C₁₇H₂₄N₂O₆

Molecular weight: 352.39 g/mol

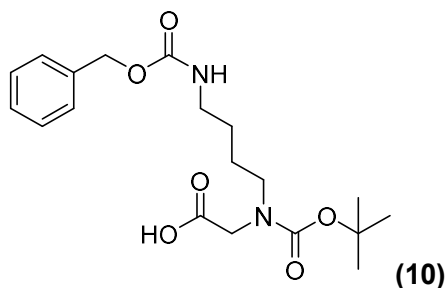
Melting point: 117 °C

MS (CI): *m/z*= 351.15 [M-H]⁻

¹H-NMR, CDCl₃ 400 MHz δ: 1.42 (d, 9H, *J*=6.2 Hz, 3CH₃), 3.21-3.50 (m, 4H, 2CH₂), 3.90 (m, 2H, CH₂), 5.05-5.21 (m, 2H, CH₂), 5.53 (s, 1H, NH), 7.30-7.36 (m, 5H, Ar), COOH missing in these experimental conditions.

¹³C-NMR, CDCl₃ 100 MHz δ: 28.31 (d, *J*=8.8 Hz, 3CH₃), 39.89 (d, *J*=22.3 Hz, C), 48.80 (d, *J*=58.2 Hz, CH₂), 49.97 (d, *J*=44.7 Hz, CH₂), 67.20 (d, *J*=64.1 Hz, CH₂), 81.13 (d, *J*=27.2 Hz, CH₂), 128.21 (d, *J*=9.8 Hz, 2CH), 128.40 (CH), 128.63 (2CH), 136.56 (C), 155.98 (d, *J*=41.3 Hz, COO), 156.87 (d, *J*=42.9 Hz, COO), 174.03 (d, *J*=31.7 Hz, COOH)

***N*-(*Cbz*-aminobutyl)-*N*-*Boc*-glycine (10)**. The synthesis was performed similarly to the protocol described for compound **2**. The product was isolated as a white powder in 70% yield (15.4 g) starting from *N*-*Cbz*-1,4-diaminobutane hydrochloride 99% (15.16 g, 58 mmol).



Chapter 2. Preparation of a small library of *N*-alkylated glycine *N*-carboxyanhydrides

Chemical name: *N*-(4-(((benzyloxy)carbonyl)amino)butyl)-*N*-(tert-butoxycarbonyl)glycine

Molecular formula: C₁₉H₂₈N₂O₆

Molecular weight: 380.44 g/mol

Melting point: 65 °C

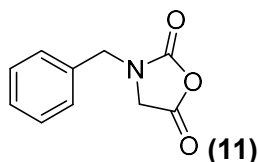
MS (Cl⁻): *m/z*= 379.18 [M-H]⁻

¹H-NMR, CDCl₃ 400 MHz δ: 1.44 (d, 9H, *J*=13.7 Hz, 3CH₃), 1.52 (br, 4H, 2CH₂), 3.15-3.33 (m, 4H, CH₂), 3.91 (d, 2H, *J*=30.2 Hz, CH₂), 4.75-5.23 (m, 3H, CH₂ and NH), 7.27-7.39 (m, 5H, Ar), COOH missing in these experimental conditions.

¹³C-NMR, CDCl₃ 100 MHz δ: 25.46 (d, *J*=22.6 Hz, CH₂), 25.98-27.17 (m, CH₂), 28.35 (d, *J*=12.9 Hz, 3CH₃), 41.00 (d, *J*=34.7 Hz, C), 48.07 (d, *J*=34.8 Hz, CH₂), 48.99 (d, *J*=34.7 Hz, CH₂), 67.01 (d, *J*=56.0 Hz, CH₂), 80.71 (d, *J*=13.7 Hz, CH₂), 128.14 (3CH), 128.57 (2CH), 136.63 (C), 155.83 (d, *J*=70.2 Hz, COO), 157.40 (d, *J*=126.5 Hz, COO), 174.04 (d, *J*=50.0 Hz, COOH)

5.4 *N*-Alkylated-*N*-carboxyanhydrides

***N*-Benzyl-*N*-carboxyanhydride (Phe-NNCA, 11).** In a dry Schlenk flask, *N*-benzyl-*N*-Boc-glycine (**2**, 1 g, 3.8 mmol, 1 equiv.) was dried for 10 min under vacuum. Then 9 mL of anhydrous THF were added, followed by thionyl chloride 99% (0.27 mL, 3.8 mmol, 1 equiv.). The reaction mixture was stirred 4 h under Ar at RT and the solvent was evaporated *in vacuo*. Then, the crude residue was washed 3 times with 18 mL of hexane and the suspension was filtered off using a cannula. The corresponding precipitate was dried under vacuum. Then 4 mL of DCM were added to the precipitate and the suspension was filtered over dry Celite using 5x15 mL of DCM. The product was dried under vacuum washed with 3x5 mL of diethyl ether, filtered off using a cannula, dried under vacuum and isolated as a yellowish crystalline powder in 79% yield (0.57 g).



Chemical name: 3-benzylloxazolidine-2,5-dione

Molecular formula: C₁₀H₉NO₃

Chapter 2. Preparation of a small library of *N*-alkylated glycine *N*-carboxyanhydrides

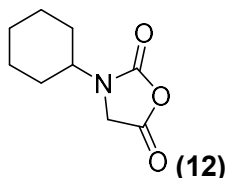
Molecular weight: 191.19 g/mol

MS (Cl⁺): m/z = 192.06 [M+H]⁺

¹H-NMR, CDCl₃ 400 MHz δ : 3.95 (s, 2H, CH₂), 4.57 (s, 2H, CH₂), 7.27-7.44 (m, 5H, Ar).

¹³C-NMR, CDCl₃ 100 MHz δ : 47.67 (CH₂), 48.40 (CH₂), 128.39 (2CH), 128.70 (CH), 129.34 (2CH), 133.85 (C), 152.29 (NCOO), 165.39 (COO). Both proton and carbon NMR were in agreement with a previously reported synthesis.⁵⁴

***N*-Cyclohexyl-*N*-carboxyanhydride (Cy-NNCA, 12).** The synthesis was performed similarly to the protocol described for compound **11**. The product was isolated as a white power in 80% yield (0.57 g) starting from *N*-cyclohexyl-*N*-Boc-glycine (**3**, 1 g, 3.9 mmol).



Chemical name: 3-cyclohexyloxazolidine-2,5-dione

Molecular Formula: C₉H₁₃NO₃

Molecular weight: 183.21 g/mol

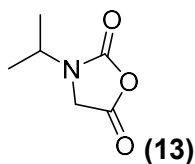
MS (Cl⁺): m/z = 184.09 [M+H]⁺

¹H-NMR, CDCl₃ 400 MHz δ : 1.02-1.19 (m, 1H, CH), 1.25-1.49 (m, 4H, 2CH₂), 1.65-1.76 (m, 1H, CH), 1.98-1.77 (m, 4H, 2CH₂), 3.72-3.97 (m, 1H, NCH), 4.04 (s, 2H, CH₂).

¹³C-NMR, CDCl₃ 100 MHz δ : 25.09 (CH₂), 25.18 (2CH₂), 30.47 (2CH₂), 45.63 (CH), 52.71 (CH₂), 151.44 (NCOO), 166.13 (COO).

***N*-Isopropyl-*N*-carboxyanhydride (Val-NNCA, 13).** The synthesis was performed similarly to the protocol described for compound **11**. The product was isolated as a white power in 89% yield (0.99 g) starting from *N*-isopropyl-*N*-Boc-glycine (**4**, 1.7 g, 7.8 mmol).

Chapter 2. Preparation of a small library of *N*-alkylated glycine *N*-carboxyanhydrides



Chemical name: 3-isopropylloxazolidine-2,5-dione

Molecular Formula: C₆H₉NO₃

Molecular weight: 143.14 g/mol

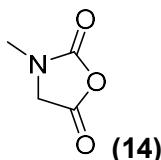
MS (Cl⁺): *m/z*= 144.06 [M+H]⁺

¹H-NMR, CDCl₃ 400 MHz δ: 1.25 (d, 6H, *J*=6.8 Hz, CH₃), 4.04 (s, 2H, CH₂), 4.27 (hept, 1H, *J*=6.8 Hz, CH).

¹³C-NMR, CDCl₃ 100 MHz δ: 20.05 (2CH₃), 44.89 (CH), 45.31 (CH₂), 151.35 (NCOO), 165.93 (COO).

Both ¹H- and ¹³C-NMR were in agreement with the literature.²²

***N*-Methyl-*N*-carboxyanhydride (Sar-NCA, 14).** The synthesis was performed similarly to the protocol described for compound **11**. The product was isolated as a white powder in 72% yield (0.99 g) starting from *N*-methyl-*N*-Boc-glycine (**5**, 2.27 g, 12 mmol).



Chemical name: 3-methylloxazolidine-2,5-dione

Molecular Formula: C₄H₅NO₃

Molecular weight: 115.09 g/mol

MS (Cl⁺): *m/z*= 116.03 [M+H]⁺

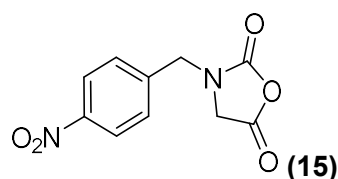
¹H-NMR, CDCl₃ 400 MHz δ: 3.03 (s, 3H, CH₃), 4.12 (s, 2H, CH₂).

¹³C-NMR, CDCl₃ 100 MHz δ: 30.41 (CH₃), 51.04 (CH₂), 152.45 (NCOO), 165.45 (COO).

Chapter 2. Preparation of a small library of *N*-alkylated glycine *N*-carboxyanhydrides

Both ^1H - and ^{13}C -NMR were in agreement with previously reported syntheses.^{3,20}

***N*-(*p*-Nitrobenzyl)-*N*-carboxyanhydride (NPM-NNCA, 15).** The synthesis was performed similarly to the protocol described for compound 11. The product was isolated as a yellowish powder in 65% yield (0.49 g) starting from *N*-(*p*-nitrobenzyl)-*N*-Boc-glycine (6, 1 g, 3.2 mmol).



Chemical name: 3-(4-nitrobenzyl)oxazolidine-2,5-dione

Molecular formula: $\text{C}_{10}\text{H}_8\text{N}_2\text{O}_5$

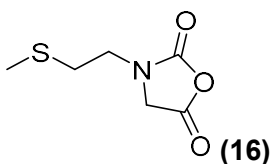
Molecular weight: 236.18 g/mol

MS (Cl^+): $m/z = 237.05$ [$\text{M}+\text{H}$] $^+$

^1H -NMR, CDCl_3 400 MHz δ : 4.03 (s, 2H, CH_2), 4.68 (s, 2H, CH_2), 7.43-7.55 (m, 2H, CH Ar), 8.20-8.37 (m, 2H, CH Ar).

^{13}C -NMR, CDCl_3 100 MHz δ : 47.71 (CH_2), 48.43 (CH_2), 128.42 (2CH), 128.89 (C), 129.36 (2CH), 133.85 (C), 152.29 (NCOO), 165.37 (COO).

***N*-[2-(methylthio)ethyl]-*N*-carboxyanhydride (MET-NNCA, 16).** The synthesis was performed similarly to the protocol described for compound 11. The product was isolated as a yellow viscous oil in 71% yield (0.49 g) starting from *N*-[2-(methylthio)ethyl]-*N*-Boc-glycine (7, 1 g, 4.0 mmol).



Chemical name: 3-[2-(methylthio)ethyl]oxazolidine-2,5-dione

Chapter 2. Preparation of a small library of *N*-alkylated glycine *N*-carboxyanhydrides

Molecular Formula: C₆H₉NO₃S

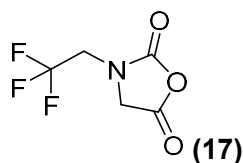
Molecular weight: 175.20 g/mol

MS (Cl⁺): *m/z*= 176.03 [M+H]⁺

¹H-NMR, CDCl₃ 400 MHz δ: 2.16 (s, 3H, CH₃), 2.76 (t, 2H, *J*=6.4 Hz, CH₂), 3.63 (t, 2H, *J*=6.4 Hz, CH₂), 4.24 (s, 2H, CH₂).

¹³C-NMR, CDCl₃ 100 MHz δ: 15.29 (CH₃), 32.00 (CH₂), 41.99 (CH₂), 49.70 (CH₂), 152.36 (NCOO), 165.34 (COO).

***N*-Trifluoroethyl-*N*-carboxyanhydride (TFE-NNCA, 17).** The synthesis was performed similarly to the protocol described for compound **11**. The product was isolated as a white powder in 46% yield (0.32 g) starting from *N*-(trifluoroethyl)-*N*-Boc-glycine (**8**, 1 g, 3.9 mmol).



Chemical name: 3-(2,2,2-trifluoroethyl)oxazolidine-2,5-dione

Molecular Formula: C₅H₄F₃NO₃

Molecular weight: 183.01 g/mol

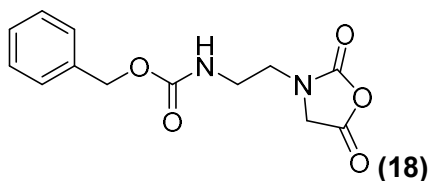
MS (Cl⁺): *m/z*= 184.02 [M+H]⁺

¹H-NMR, CDCl₃ 400 MHz δ: 4.03 (q, 2H, *J*=8.5 Hz, CH₂), 4.92 (s, 2H, CH₂).

¹³C-NMR, CDCl₃ 100 MHz δ: 45.17 (q, *J*=35.9 Hz, CH₂), 49.87 (CH₂), 123.43 (q, *J*=279 Hz, CH₂), 152.16 (NCOO), 163.74 (COO).

***N*-Cbz-aminoethyl-*N*-carboxyanhydride (ZNAE-NNCA, 18).** The synthesis was performed similarly to the protocol described for compound **11**. The product was isolated as a white powder in 47% yield (0.63 g) starting from *N*-(Cbz-aminoethyl)-*N*-Boc-glycine (**9**, 1.7 g, 4.8 mmol).

Chapter 2. Preparation of a small library of *N*-alkylated glycine *N*-carboxyanhydrides



Chemical name: benzyl-(2-(2,5-dioxooxazolidin-3-yl)ethyl)carbamate

Molecular Formula: C₁₃H₁₄N₂O₅

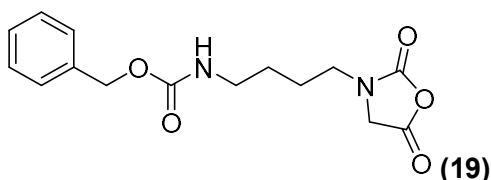
Molecular weight: 278.26 g/mol

MS (CI⁺): *m/z*= 279.09 [M+H]⁺

¹H-NMR, CDCl₃ 400 MHz δ: 3.36-3.48 (m, 4H, 2CH₂), 4.16 (s, 2H, CH₂), 5.07 (s, 2H, CH₂), 5.29 (s, 1H, NH), 7.31-7.37 (m, 5H, Ar).

¹³C-NMR, CDCl₃ 100 MHz δ: 38.41 (CH₂), 43.90 (CH₂), 49.39 (CH₂), 67.30 (CH₂), 128.21 (2CH), 128.46 (CH), 128.75 (2CH), 136.24 (C), 153.00 (NCOO), 157.09 (NCOO), 165.42 (COO).

***N*-Cbz-aminobutyl-*N*-carboxyanhydride (ZLys-NNCA, 19).** The synthesis was performed similarly to the protocol described for compound **11**. The product was isolated as a white powder in 44% yield (0.6 g) starting from *N*-(Cbz-aminobutyl)-*N*-Boc-glycine (**10**, 1.7 g, 4.5 mmol).



Chemical name: benzyl (2-(2,5-dioxooxazolidin-3-yl)butyl)carbamate

Molecular Formula: C₁₅H₁₈N₂O₅

Molecular weight: 306.32 g/mol

MS (CI⁺): *m/z*= 307.12 [M+H]⁺

¹H-NMR, CDCl₃ 400 MHz δ: 1.38-1.75 (br, 4H, 2CH₂), 3.25 (q, 2H, *J*=6.4 Hz, CH₂), 3.42 (t, 2H, *J*=7.1 Hz, CH₂), 4.04 (s, 2H, CH₂), 4.84 (s, 1H, NH), 5.09 (s, 2H, CH₂), 7.31-7.39 (m, 5H, Ar).

Chapter 2. Preparation of a small library of N-alkylated glycine N-carboxyanhydrides

^{13}C -NMR, CDCl_3 100 MHz δ : 24.39 (CH_2), 27.16 (CH_2), 40.24 (CH_2), 43.31 (CH_2), 49.05 (CH_2), 66.76 (CH_2), 128.11 (2CH), 128.25 (CH), 128.62 (2CH), 136.63 (C), 152.28 (NCOO), 156.69 (NCOO), 165.68 (s, COO).

6 References

- (1) Leuchs, H.; Manasse, W. Über Die Isomerie Der Carbäthoxyl-Glycyl Glycinester. *Berichte der Dtsch. Chem. Gesellschaft* **1907**, *40* (3), 3235–3249.
- (2) Kricheldorf, H. R.; Von Lossow, C.; Schwarz, G. Primary Amine-Initiated Polymerizations of Alanine-NCA and Sarcosine-NCA. *Macromol. Chem. Phys.* **2004**, *205* (7), 918–924.
- (3) Guo, L.; Zhang, D. Cyclic Poly(α -Peptoid)s and Their Block Copolymers from *N*-Heterocyclic Carbene-Mediated Ring-Opening Polymerizations of *N*-Substituted *N*-Carboxylanhydrides. *J. Am. Chem. Soc.* **2009**, *131* (50), 18072–18074.
- (4) Kricheldorf, H. R. Polypeptides and 100 Years of Chemistry of α -Amino Acid α -Carboxyanhydrides. *Angew. Chem, Int. Ed.* **2006**, *45* (35), 5752–5784.
- (5) Leuchs, H. Ueber Die Glycin-Carbonsäure. *Berichte der Dtsch. Chem. Gesellschaft* **1906**, *39* (1), 857–861.
- (6) Leuchs, H.; Geiger, W. Über Die Anhydride von α -Amino-*N*-Carbonsäuren Und Die von α -Aminosäuren. *Berichte der Dtsch. Chem. Gesellschaft* **1908**, *41* (2), 1721–1726.
- (7) Katchalski, E.; Spitnik, P. Ornithine Anhydride. *J. Am. Chem. Soc.* **1951**, *73* (6), 2946–2947.
- (8) Ben-Ishai, D.; Katchalski, E. Synthesis of *N*-Carboxy- α -Amino Acid Anhydrides from *N*-Carbalkoxy- α -Amino Acids by the Use of Phosphorus Tribromide. *J. Am. Chem. Soc.* **1952**, *74* (14), 3688–3689.
- (9) Fuchs, F. Über *N*-Carbonsäure-Anhydride. *Berichte der Dtsch. Chem. Gesellschaft (A B Ser.)* **1922**, *55* (9), 2943–2943.
- (10) Farthing, A. C. Synthetic Polypeptides. Part I . 3213 627. Synthetic Polypeptides. Part. *J. Chem. Soc.* **1950**, *resumed*, 3213–3217.
- (11) Fuller, W. D.; Verlander, M. S.; Goodman, M. A Procedure for the Facile Synthesis of Amino acid *N*-carboxyanhydrides. *Biopolymers*. September 1976, pp 1869–1871.
- (12) Oya, M.; Katakai, R.; Nakai, H.; Iwakura, Y. A Novel Synthesis of *N*-Carboxy- α -Amino Acid Anhydride. *Chem. Lett.* **1973**, *2* (11), 1143–1144.
- (13) Daly, W. H.; Poché, D. The Preparation of *N*-Carboxyanhydrides of α -Amino Acids Using

Chapter 2. Preparation of a small library of N-alkylated glycine N-carboxyanhydrides

- Bis(Trichloromethyl)Carbonate. *Tetrahedron Lett.* **1988**, 29 (46), 5859–5862.
- (14) Katakai, R.; Iizuka, Y. An Improved Rapid Method for the Synthesis of N-Carboxy α -Amino Acid Anhydrides Using Trichloromethyl Chloroformate. *J. Org. Chem.* **1985**, 50 (5), 715–716.
- (15) Boiteau, L.; Collet, H.; Lagrille, O.; Taillades, J.; Vayaboury, W.; Giani, O.; Schu e, F.; Commeyras, A. From Prebiotic Macromolecules to Synthetic Polypeptides: A New, Efficient Synthesis of α -Amino Acid N-Carboxyanhydrides(NCAs). *Polym. Int.* **2002**, 51 (10), 1037–1040.
- (16) Endo, T.; Sudo, A. Well-Defined, Environment-Friendly Synthesis of Polypeptides Based on Phosgene-Free Transformation of Amino Acids into Urethane Derivatives and Their Applications. *Polym. Int.* **2020**, 69 (3), 219–227.
- (17) Kricheldorf, H. R.; B osinger, K. Mechanismus Der NCA-Polymerisation, 3.  ber Die Amin Katalysierte Polymerisation von Sarkosin-NCA Und -NTA. *Die Makromol. Chemie* **1976**, 177 (5), 1243–1258.
- (18) Fasman, G. D.; Blout, E. R. Copolymers of L-proline and Sarcosine: Synthesis and Physical-chemical Studies. *Biopolymers* **1963**, 1 (2), 99–109.
- (19) Birke, A.; Huesmann, D.; Kelsch, A.; Weilb acher, M.; Xie, J.; Bros, M.; Bopp, T.; Becker, C.; Landfester, K.; Barz, M. Polypeptoid-Block-Polypeptide Copolymers: Synthesis, Characterization, and Application of Amphiphilic Block Copolypept(o)ides in Drug Formulations and Miniemulsion Techniques. *Biomacromolecules* **2014**, 15 (2), 548–557.
- (20) Fetsch, C.; Grossmann, A.; Holz, L.; Nawroth, J. F.; Luxenhofer, R. Polypeptoids from N-Substituted Glycine N-Carboxyanhydrides: Hydrophilic, Hydrophobic, and Amphiphilic Polymers with Poisson Distribution. *Macromolecules* **2011**, 44 (17), 6746–6758.
- (21) Fetsch, C.; Luxenhofer, R. Highly Defined Multiblock Copolypeptoids : Pushing the Limits of Living Nucleophilic. *Macromol. Rapid Commun.* **2012**, 33 (19), 1708–1713.
- (22) Robinson, J. W.; Secker, C.; Weidner, S.; Schlaad, H. Thermoresponsive Poly(N-C3 Glycine)S. *Macromolecules* **2013**, 46 (3), 580–587.
- (23) Kricheldorf, H. R.; Lossow, C. V.; Schwarz, G.; Fritsch, D. Chain Extension and Cyclization of Telechelic Polysarcosines. *Macromol. Chem. Phys.* **2005**, 206 (12), 1165–1170.

Chapter 2. Preparation of a small library of *N*-alkylated glycine *N*-carboxyanhydrides

- (24) Guo, L.; Lahasky, S. H.; Ghale, K.; Zhang, D. *N*-Heterocyclic Carbene-Mediated Zwitterionic Polymerization of *N*-Substituted *N*-Carboxyanhydrides toward Poly(α -Peptoid)s: Kinetic, Mechanism, and Architectural Control. *J. Am. Chem. Soc.* **2012**, *134* (22), 9163–9171.
- (25) Lee, C.-U.; Li, A.; Ghale, K.; Zhang, D. Crystallization and Melting Behaviors of Cyclic and Linear Polypeptoids with Alkyl Side Chains. *Macromolecules* **2013**, *46* (20), 8213–8223.
- (26) Lahasky, S. H.; Hu, X.; Zhang, D. Thermoresponsive Poly(α -Peptoid)s: Tuning the Cloud Point Temperatures by Composition and Architecture. *ACS Macro Lett.* **2012**, *1* (5), 580–584.
- (27) Lee, C. U.; Smart, T. P.; Guo, L.; Epps, T. H.; Zhang, D. Synthesis and Characterization of Amphiphilic Cyclic Diblock Copolypeptoids from *N*-Heterocyclic Carbene-Mediated Zwitterionic Polymerization of *N*-Substituted *N*-Carboxyanhydride. *Macromolecules* **2011**, *44* (24), 9574–9585.
- (28) Robinson, J. W.; Schlaad, H. A Versatile Polypeptoid Platform Based on *N*-Allyl Glycine. *Chem. Commun.* **2012**, *48* (63), 7835.
- (29) Lahasky, S. H.; Serem, W. K.; Guo, L.; Garno, J. C.; Zhang, D. Synthesis and Characterization of Cyclic Brush-Like Polymers by *N*-Heterocyclic Carbene-Mediated Zwitterionic Polymerization of *N*-Propargyl *N*-Carboxyanhydride and the Grafting-to Approach. *Macromolecules* **2011**, *44*, 9063–9074.
- (30) Xuan, S.; Gupta, S.; Li, X.; Bleuel, M.; Schneider, G. J.; Zhang, D. Synthesis and Characterization of Well-Defined PEGylated Polypeptoids as Protein-Resistant Polymers. *Biomacromolecules* **2017**, *18* (3), 951–964.
- (31) Guo, L.; Li, J.; Brown, Z.; Ghale, K.; Zhang, D. Synthesis and Characterization of Cyclic and Linear Helical Poly(α -Peptoid)s by *N*-Heterocyclic Carbene-Mediated Ring-Opening Polymerizations of *N*-Substituted *N*-Carboxyanhydrides. *Pept. Sci.* **2011**, *96* (5), 596–603.
- (32) Bossler, H. G.; Seebach, D. Peptide Enolates. *C*-Alkylation of Glycine Residues in Linear Tri-, Tetra-, and Pentapeptides via Dilithium Azadienediolates. *Helv. Chim. Acta* **1994**, *77* (4), 1124–1165.
- (33) Van Der Veken, P.; Senten, K.; Kertész, I.; De Meester, I.; Lambeir, A. M.; Maes, M. B.; Scharpé, S.; Haemers, A.; Augustyns, K. Fluoro-Olefins as Peptidomimetic Inhibitors of

Chapter 2. Preparation of a small library of *N*-alkylated glycine *N*-carboxyanhydrides

- Dipeptidyl Peptidases. *J. Med. Chem.* **2005**, *48* (6), 1768–1780.
- (34) Mouna, A. M.; Nguyen, C.; Rage, I.; Xie, J.; Nee, G.; Mazaleyrat, J. P.; Wakselman, M. Preparation of *N*-Boc *N*-Alkyl Glycines for Peptoid Synthesis. *Synth. Commun.* **1994**, *24* (17), 2429–2435.
- (35) Blacquiere, J. M.; Pegis, M. L.; Raugei, S.; Kaminsky, W.; Forget, A.; Cook, S. A.; Taguchi, T.; Mayer, J. M. Synthesis and Reactivity of Tripodal Complexes Containing Pendant Bases. *Inorg. Chem.* **2014**, *53* (17), 9242–9253.
- (36) Lake, F.; Linde, C. A Practical Synthesis of [¹³C₄] *N*-Benzylpiperazine from [¹³C₂] Glycine. *Tetrahedron Lett.* **2012**, *53* (30), 3927–3929.
- (37) Hoefnagel, A. J.; Peters, J. A.; Vanbekkum, H. The Reaction of Glyoxylic Acid with Ammonia Revisited. *J. Org. Chem.* **1992**, *57* (14), 3916–3921.
- (38) Salas-Ambrosio, P.; Tronnet, A.; Verhaeghe, P.; Bonduelle, C. Synthetic Polypeptide Polymers as Simplified Analogues of Antimicrobial Peptides. *Biomacromolecules* **2021**, *22* (1), 57–75.
- (39) Lee, C. M.; Kumler, W. D. The Dipole Moment and Structure of the Carbamate Group. *J. Am. Chem. Soc.* **1961**, *83* (22), 4596–4600.
- (40) van Est-Stammer, R.; Engberts, J. B. F. N. Hindered Internal Rotation in Carbamates: An NMR Study of the Conformations of Alkyl and Aryl *N*-(Alkylsulfonylmethyl)-*N*-Methylcarbamates and Aryl *N*-(Arylsulfonylmethyl)-*N*-Methylcarbamates. *Recl. des Trav. Chim. des Pays-Bas* **2010**, *90* (12), 1307–1319.
- (41) de Leer, E. W. B.; van der Toorn, J. M. A Proton Magnetic Resonance Study of the Influence of the Solvent on the Rotation about the Carbamate Amide Bond in *N*-(Benzyloxycarbonyl)-*L*-Proline *t*-Butyl Ester. *Recl. des Trav. Chim. des Pays-Bas* **2010**, *94* (6), 119–122.
- (42) Imanishi, Y.; Tsuchida, T.; Higashimura, T. Synthesis and Characterization of Poly(*N*-Cyanoethylglycine). *Polym. J.* **1978**, *10*, 287.
- (43) Dorman, L. C.; Shiang, W. R.; Meyers, P. A. Purification of γ -Benzyl and γ -Methyl *L*-Glutamate *N*-Carboxyanhydrides by Rephosgenation. *Synth. Commun.* **1992**, *22* (22), 3257–3262.

Chapter 2. Preparation of a small library of N-alkylated glycine N-carboxyanhydrides

- (44) Brenner, M.; Photaki, I. Zur Herstellung Der Chlorid-hydrochloride Der α -Aminosäuren. *Helv. Chim. Acta* **1956**, *39* (6), 1525–1528.
- (45) Kramer, J. R.; Deming, T. J. General Method for Purification of α -Amino Acid-*N*-Carboxyanhydrides Using Flash Chromatography. *Biomacromolecules* **2010**, *11* (12), 3668–3672.
- (46) Katchalski, E.; Sela, M. Synthesis and Chemical Properties of Poly- α -Amino Acids. *Adv. Protein Chem.* **1958**, *13* (C), 243–492.
- (47) Semple, J. E.; Sullivan, B.; Sill, K. N. Large-Scale Synthesis of α -Amino Acid-*N*-Carboxyanhydrides. *Synth. Commun.* **2017**, *47* (1), 53–61.
- (48) Bai, T.; Shen, B.; Cai, D.; Luo, Y.; Zhou, P.; Xia, J.; Zheng, B.; Zhang, K.; Xie, R.; Ni, X.; Xu, M.; Ling, J.; Sun, J. Understanding Ring-Closing and Racemization to Prepare α -Amino Acid NCA and NTA Monomers: A DFT Study. *Phys. Chem. Chem. Phys.* **2020**, *22* (26), 14868–14874.
- (49) Anderson, G. W.; McGregor, A. C. *t*-Butyloxycarbonylamino Acids and Their Use in Peptide Synthesis. *J. Am. Chem. Soc.* **1957**, *79* (23), 6180–6183.
- (50) Kessler, H.; Krämer, P.; Krack, G. Peptide Conformation, IX Conformational Studies on Cyclotriptides Containing *N*-Benzyl-Glycine. *Isr. J. Chem.* **1980**, *20* (1–2), 188–195.
- (51) Goodfellow, V. S.; Marathe, M. V.; Kuhlman, K. G.; Fitzpatrick, T. D.; Cuadrado, D.; Hanson, W.; Zuzack, J. S.; Ross, S. E.; Wieczorek, M.; Burkard, M.; Whalley, E. T. Bradykinin Receptor Antagonists Containing *N*-Substituted Amino Acids: In Vitro and in Vivo B₂ and B₁ Receptor Antagonist Activity. *J. Med. Chem.* **1996**, *39* (7), 1472–1484.
- (52) Emig, P.; Lichtenthaler, F. W.; Trummelitz, G. Synthesis of Dipeptidyl Aminosugar Nucleosides, Structurally Related to Gougerotin. *Tetrahedron Lett.* **1970**, 2061–2064.
- (53) Yoon, U. C.; Jin, Y. X.; Oh, S. W.; Park, C. H.; Park, J. H.; Campana, C. F.; Cai, X.; Duesler, E. N.; Mariano, P. S. A Synthetic Strategy for the Preparation of Cyclic Peptide Mimetics Based on SET-Promoted Photocyclization Processes. *J. Am. Chem. Soc.* **2003**, *125* (35), 10664–10671.
- (54) Fetsch, C. Polypeptide - Synthese Und Charakterisierung. Julius-Maximilians-Universität Würzburg, 2015.

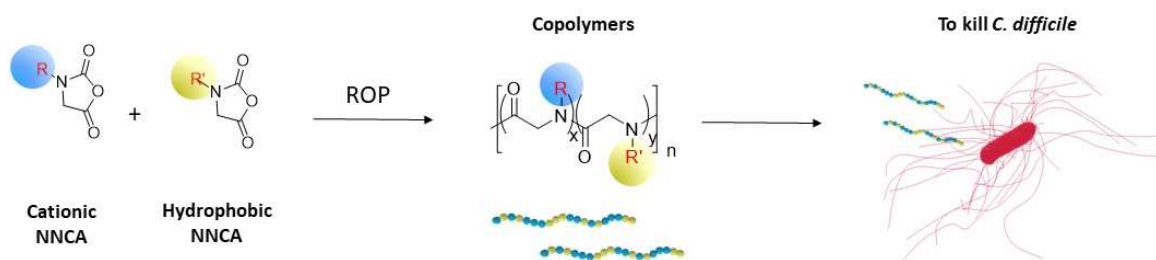
Chapter 3. Linear polypeptoid and their antimicrobial activity

Many peptides have demonstrated potent activity against pathogenic bacteria and are considered promising candidates for the treatment of bacterial infections.^{1,2} However their preparation is complex, involving either biosynthesis or supported multiple-step-synthesis, both approaches presenting important limitations such as consumption of many reagents, long time, isolation/purification problems and difficulties in scaling-up.^{3,4} In this context, polymer chemistry is an alternative methodology that could solve some of those drawbacks.⁵ Moreover, the use of polymer chemistry is a simple way to design backbones with cationic and hydrophobic side chains, a key structural parameter of antimicrobial peptides (AMPs).^{5,6} Among other polymers, polypeptides are one of the best polymer scaffolds to be used as an anti-infective agent because they finely mimic the peptidic structure of AMPs. Polypeptide polymers are obtained through the ring-opening polymerization (ROP) of *N*-carboxyanhydrides (NCAs): this controlled polymerization process involves simple reagents and allows the preparation of polymers made of amino acids in both good yields and large quantities.⁷ However, AMPs and polypeptide polymers share a common disadvantage: the susceptibility to proteases that breakdowns their peptide bonds, resulting in the loss of activity.⁸ This feature may limit the development of antimicrobial polypeptides, for instance, to design orally administered drugs.

Based on a polymeric approach, this research project focused on polypeptides analogs, the poly(*N*-alkylated-glycines) also called polypeptoids. The goal was to investigate the potential of polypeptoids as a new class of antimicrobial amino acid-based polymers, analogues of AMPs with low protease susceptibility. Antimicrobial peptoids were already prepared by solid-phase peptide synthesis (SPPS)⁹⁻¹⁶ and studied for their biological activity but this research work is a pioneering study concerning their development using polymer chemistry. In peptoids, the *N*-alkylation introduces a steric and conformational effect that strongly reduces protease recognition, therefore, decreasing the proteolysis of those backbones as compared to polypeptides.¹⁷ However, making these peptoids by iterative coupling on solid support requires high amounts of numerous reagents and long reaction times at high temperatures. Therefore, accessing polypeptoids through polymerization can result in a very powerful approach to prepare protease-resistant and antibacterial polymeric backbones in which no sequence control would be required.

Chapter 3. Linear polypeptoid and their antimicrobial activity

Indeed, polymer chemistry offers several advantages: first, it affords simple combinatorial optimization as compared to solid-phase synthesis, for instance by merging in a single step, cationic and hydrophobic units using copolymerization reactions. Second, the use of polymers allows to define new pharmacophores that we can call macromolecular pharmacophores (size, topology, initiator variation). In this chapter 3, the goal was to generate a copolypeptoid library by ROP of *N*-alkylated-*N*-carboxyanhydrides (NNCA). These copolymers aimed to provide a comprehensive study to define the best macromolecular parameters achieving antimicrobial properties with a particular pathogen, *Clostridioides difficile*, a drug-resistant bacteria that colonize the digestive tube (**Scheme 21**).



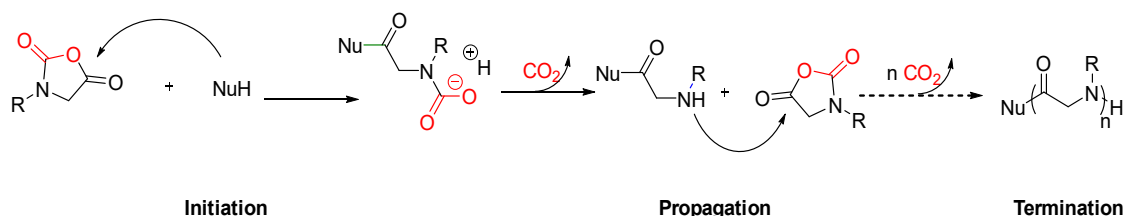
Scheme 21. Synthesis of antimicrobial copolypeptoids through ring-opening polymerization of hydrophobic and cationic NNCA.

1 Preparation of polypeptoids by ROP from *N*-alkylated NCA

Polypeptoids are synthesized from NNCA through ROP using nucleophiles as initiators (**Scheme 22**).¹⁸ The most common nucleophiles used in the ROP reaction are primary amines.¹⁹ First, the ROP mechanism of NNCA involves the initiation step: the nucleophilic attack of the initiator onto the "anhydride-like" carbonyl group of the NCA moiety that results in the ring-opening. Then, an unstable carbamic acid is formed that releases CO₂ to lead to a secondary amine formation: this new nucleophile will then induce the propagation step. The propagation is a repetition of nucleophilic attacks until the complete consumption of NNCA. The final polymer possesses a nucleophilic end group that can be re-engaged in other ROP of NNCA. Overall, the ROP of NNCA can be considered as a living polymerization process: the addition of more

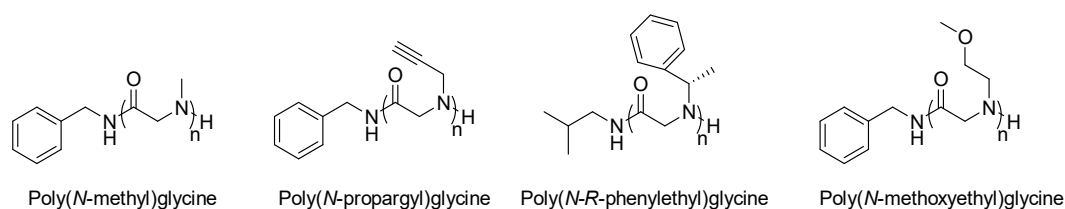
Chapter 3. Linear polypeptoid and their antimicrobial activity

monomers will increase stoichiometrically (and in a controlled fashion) the length of the polymer chain (the molar mass).²⁰ This behavior enables to design not only random²¹ but also block copolymers.²²



Scheme 22. Ring-opening polymerization mechanism for NNCA

So far, the most studied polypeptoid was polysarcosine^{23,24,25,26–30} but other polyglycines bearing different *N*-alkylated groups were synthesized and a summary of the most representative backbones is reported in **Table 13** and **Scheme 23**. The important parameters to take into account to set up a polymerization of NNCA are briefly described in the next paragraphs.



Scheme 23. Representative poly(*N*-alkylated)glycine structures

Table 13. Representative poly(*N*-alkylated)glycine synthesis taken from recent articles. BN stands for benzonitrile, NMP for *N*-methyl-2-pyrrolidone, DCM for dichloromethane and THF for tetrahydrofuran.

<i>N</i> -alkylated group	Concentration	Initiator	M/I	Solvent	Temp	Pressure	Ref
Methyl	1 M	Benzylamine	20,40,80	DCM, DMF, dioxane	20	-	23
Methyl, ethyl, propyl, butyl, isobutyl	0.5 M	Benzylamine	25, 50	BN, NMP	20	50 mbar	20
Butyl	1.0 M	Benzyl alcohol-TMG	25-400	THF	50	-	31
Hexyl, octyl, 2-ethyl-1-hexyl, decyl, dodecyl, tetradecyl	0.4 M	Benzylamine	100	THF	70	-	32
Isopropyl	NNCA melted	Benzylamine	50	-	160 °C	-	33
Allyl	1-2%	Benzylamine	100	DCM, BN	RT	20 mbar	34

Chapter 3. Linear polypeptoid and their antimicrobial activity

Propargyl	10%	Benzylamine	25, 50, 75	BN	RT	20 mbar	33
Cyanoethyl	0.5 M	<i>N</i> -cyanoethylglycine diethylamide	20	DMF	RT	-	35
Benzyl, phenylethyl, isopentyl	~0.4 M	Isobutylamine	25	DCM	RT	-	36
Benzylmethyl, benzylethyl	2%		25, 50, 100	NMP	56 °C		37
(R)/(S)- Phenylethyl	0.4 M	NHC	50, 100, 200, 400	Toluene	50 °C	-	38
Methoxyethyl, methoxyethoxyethyl, methoxy-di(ethoxy)ethyl	1 M	Benzylamine	25, 50, 100, 200	THF	50 °C	-	39

Generally, it was shown that ROP is a controlled polymerization process meaning that there is a correlation between molar masses and the ratio of the NNCA concentration (M) over the concentration of the initiator (I), denominated also as theoretical polymerization degree (M/I or DP). This control over the ROP was for instance fully demonstrated by R. Luxenhofer *et al.* studying various M/I in the ROP of *N*-methyl-*N*-carboxyanhydride (Sar-NCA): the molar masses were controlled by the initial monomer to initiator feed ratios and polymers showed narrow Poisson distribution ($\mathcal{D}_M = 1.1-1.3$).²²

To be used as initiators, several primary or secondary amines were reported in the literature such as benzylamine, which is one of the most common initiators, but also neopentylamine or hexylamine, etc.¹⁸ In addition to amines, other initiators were also reported, such as alcohols when *N*-butyl-NCA was polymerized with 1,1,3,3-tetramethylguanidine (TMG) used as a catalyst.³¹ The use of other nucleophiles such as *N*-heterocyclic carbenes⁴⁰ or DBU⁴¹ led to the formation of cyclic/linear structures.

To perform the polymerization and avoid NNCA hydrolysis, several anhydrous solvents have already been used including dichloromethane (DCM),³⁶ tetrahydrofuran (THF),³¹ benzonitrile (BN),³³ *N*-methyl pyrrolidone (NMP),³⁷ dioxane and dimethylformamide (DMF).²³

The kinetic rate of the ROP was influenced by the solvent: for instance, during the polymerization of Sar-NCA, the kinetics rate in NMP ($k_{app} = 23.11 \times 10^{-3} \text{ L/mol}\cdot\text{s}$) was slower than the one measured in benzonitrile ($k_{app} = 305 \times 10^{-3} \text{ L/mol}\cdot\text{s}$).²⁰ It appeared that highly polar solvents enhanced the kinetics of the ROP reaction of NNCA, contrary to what it was reported for the ROP of NCAs. The choice of a good solvent for both monomer and polymer leads to a controlled polymerization as demonstrated by H. Kricheldorf *et al.* with polysarcosine in a variety of solvents (CHCl₂, 1,4-dioxane or DMF).²³ However, if the solvent did not solubilize the growing oligomers, then smaller polymerization degrees were obtained: during the preparation of poly(*N*-phenylethyl)glycine, a polymerization degree of about 10 was determined when targeting M/I =

25 and this was observed in different solvents including DMF, NMP, toluene, DCM and THF.

On another hand, the vacuum was another important parameter: in some works, reduced pressure enhanced the kinetic of the ROP in benzonitrile and the polymers obtained followed Poisson distributions.²⁰ However, in some cases, the NNCA's reactivity was so low that using reduced pressure is not enough to allow the ROP reaction: H. Schlaad *et al.* observed that 100% conversion was achieved in 28 days while they were preparing poly(*N*-allyl)glycine at a targeted $M/I = 100$ and in benzonitrile at 0.05 mbar.

Finally, the chemical nature of the *N*-alkylation was an even more important parameter that reduced the propagation efficiency during the ROP. For some *N*-alkylated groups with very low kinetic rates of ROP, it was necessary to drastically increase the temperature. For instance, H. Schlaad *et al.* demonstrated that the steric hindered *N*-isopropyl-NCA required a high temperature during the polymerization (160 °C molten state)³³ but the use of such temperature resulted in an increase of molar mass polydispersity in SEC ($\bar{M}_w = 1.14-1.53$). This parameter has led to a specific study in this chapter (see section 1.1.2) to better distinguish the influence of steric hindrance and the electronic effects.

Overall, the synthesis of polypeptoids from NNCA's is still challenging and the NNCA conversion time is highly related to the chemical nature of the *N*-alkylated group, a parameter that cannot be tuned, contrary to temperature, solvent, or vacuum. The purpose of this section is to evaluate the synthesis of homopolypeptoids from the NNCA's prepared in chapter 2. We first optimized the ROP methodology and we then provided a comprehensive description of the kinetic behavior to better understand the way each polymerization proceeds. We finally compared and combined all these results to evaluate how *N*-alkylation modulates the ROP reaction (steric hindrance versus electronic effects).

1.1 Kinetics of the NNCA ROP

Similarly to non-alkylated NCA monomers, the kinetics rate of NNCA conversion can be followed using FTIR-ATR spectroscopy by monitoring the NC=O and OC=O stretching signals at 1850 and ≈ 1776 cm^{-1} : the peak intensity of these signals are linearly correlated to the concentration of NNCA, as already reported (**Figure 16**).²⁰ In the first part, we used these kinetic experiments with Sar-NCA to optimize the purification step before the ROP. Later, we used the kinetic experiments with all the NCA's from chapter 2, to evaluate how the chemical nature of the *N*-alkylation influences the kinetics.

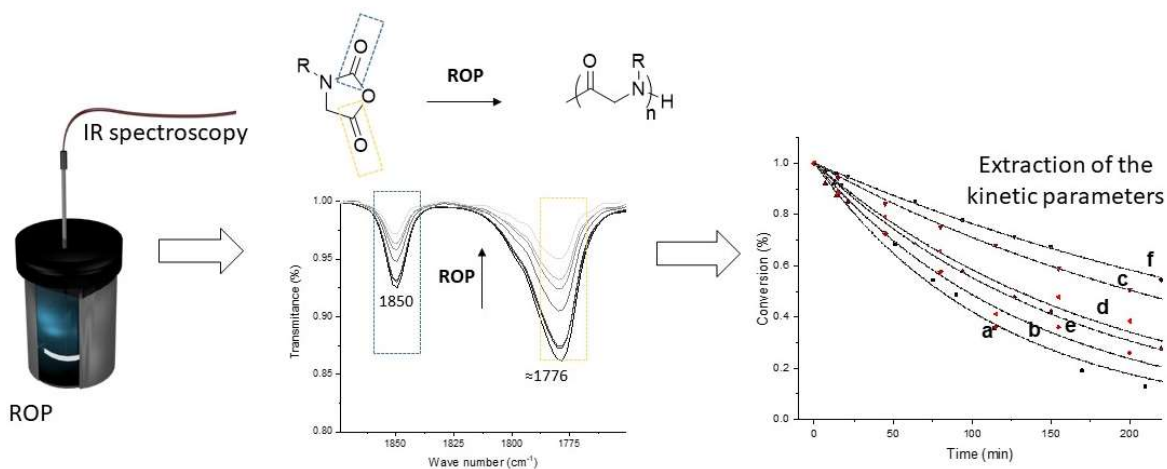
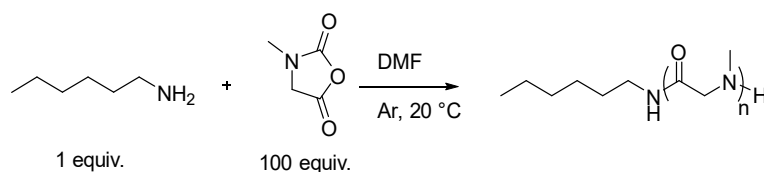


Figure 16. Schematic methodology to determine the NNCA ROP kinetics by FTIR-ATR.

1.1.1 Influence of chloride impurities in polysarcosine

After synthesizing NCA or NNCA (using either Fuchs or Leuchs method), purifying the monomer is a crucial step to well achieve their ring-opening polymerization. In particular, NNCA synthesis through Leuchs method releases HCl and chlorinated byproducts that stay persistent, even after recrystallization, thus compromising the monomer yield and purity.⁴² Moreover, HCl or other acidic contaminants are known to slow down the ROP process: a study done by R. Luxenhofer *et al.* reported that using trifluoromethanesulfonic acid decreased the apparent kinetics rate of the Sar-NCA (Sar-NCA) ROP from 23.1×10^{-3} to $2.36 \times 10^{-3} \text{ L} \cdot \text{mol}^{-1} \cdot \text{s}^{-1}$ when the concentration of the acid increased from 0 to 50%.²⁰ The reduction of acid traces is important to avoid the slow down of the NCA ROP kinetics, and in this direction, filtration over celite has already provided interesting results.⁴³ In this work, we studied the kinetics of the ROP reaction for *N*-methyl-NCA monomers (Sar-NCA, chapter 2, section 3.1) to optimize the monomer purification using celite filtration or recrystallization (**Scheme 24**). The NNCA monomer was used in anhydrous DMF, under argon and at $M/I = 100$ with hexylamine, the initiator of the ROP. Monomer without purification was used and compared to monomer purified by crystallization and/or celite filtration. The kinetic of the ROP were monitored by following the disappearance of the NC=O stretching at 1850 cm^{-1} by FTIR analyses (**Figure 17A**, we did not number the compounds described because we did not fully characterize them).



Scheme 24. Synthesis of polysarcosine using hexylamine as initiator in DMF 0.4 M.

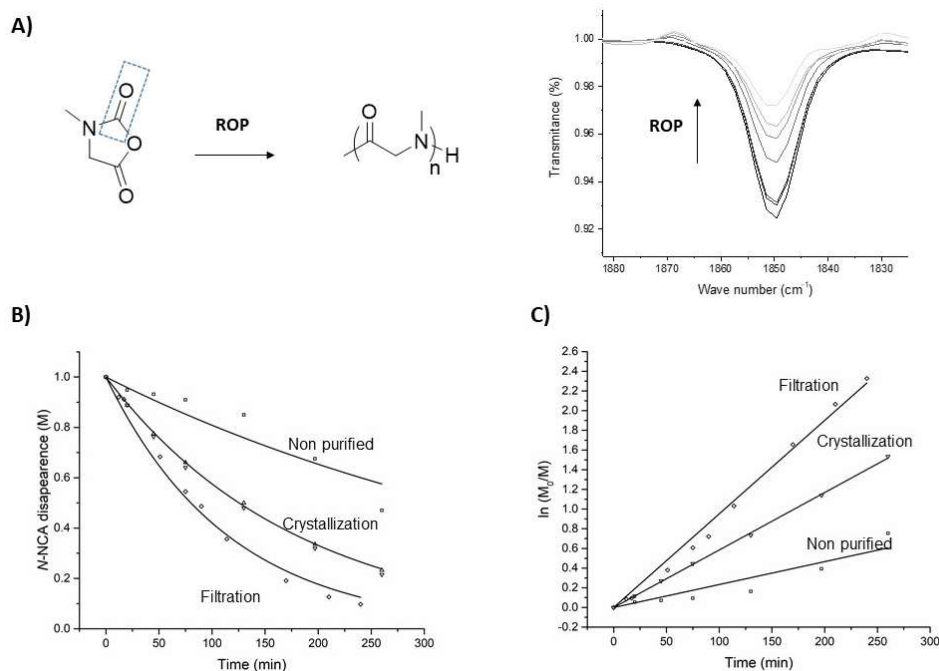


Figure 17. Kinetic experiments of Sar-NCA purified by Celite filtration, crystallization and without crystallization (ROP in DMF at 0.4 M and at M/I = 100). A) Disappearance over time of the stretching bond at 1850 cm⁻¹ during the ROP, B) Conversion plot and C) linear regression upon data treatment using the first-order model.

Plotting NNCA disappearance over time indicated that the reaction time was longer for non-purified NNCA: the ROP of the non-purified NNCA reached only 63% of conversion after 260 minutes whereas the ROP of the monomer purified by crystallization reached 77% after the same reaction time (**Figure 17 A and B**). Interestingly, the conversion was improved by replacing the crystallization step by the filtration over celite (>97% conversion after 260 min).

To determine the kinetic rates, the data were adjusted to the first-order equation through a plot of the $\ln(M_0/M)$ versus time, where the M_0 was the initial intensity peak and M was the intensity at a certain time: the slope of the curve was the kinetics constant value (**Figure 17C**). Previous studies confirmed that the ROP of Sar-NCA follows a first-order kinetics rate:⁴⁴ It indicates that

Chapter 3. Linear polypeptoid and their antimicrobial activity

the concentration of propagating species remains constant and it supports the living character of the polymerization process.²⁰ On **Figure 17B** and **C**, we clearly observed that the impurities generated during the NNCA synthesis are associated with lower kinetic rate constants. Interestingly, celite filtration showed a 2-4 fold improvement of the values of the kinetic constants, and this step of purification afforded the fastest polymerization of Sar-NCA (0.57 h^{-1} ,

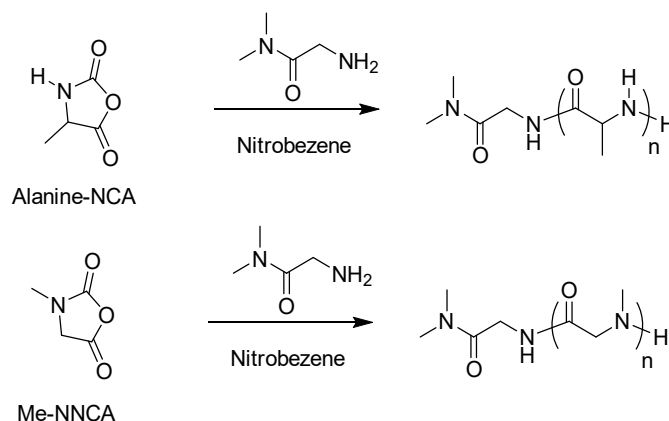
Table 4). Similar to NCAs, this method was the best to get rid of acid contaminants with NNCA. For the rest of this Ph.D. research work, we have thus decided to use this purification method to prepare all our NNCA monomers before polymerization.

Table 14. ROP kinetic rates of Sar-NCA purified by different methods.

Purification method of NNCA	M/I	Kinetics rate (h^{-1})
Non purified	100	0.14
Crystallization	100	0.35
Filtration over celite	100	0.57

1.1.2 NCA: Influence of N-alkylation and C-alkylation

The N-alkylation of NNCA or the C-alkylation of NCAs strongly influences the kinetics rate of the polymerization.⁴⁵ This observation was first made by C. Bamford *et al.* when they compared the reactivity between structural isomers of 2-amino-N,N-dimethylacetamide (**Scheme 25**).^{26,46} They observed that the position of methyl group modified the reactivity: they found a 2nd order kinetic rate of $k = 1.13 \text{ mol}^{-1} \cdot \text{l} \cdot \text{sec}^{-1}$ for alanine-NCA and $0.82 \text{ mol}^{-1} \cdot \text{l} \cdot \text{sec}^{-1}$ for Sar-NCA by monitoring the CO_2 release.



Scheme 25. Early studies of alkylation of NCAs.

Chapter 3. Linear polyeptoid and their antimicrobial activity

In this Ph.D. thesis, to go further, we have investigated the ROP kinetics of glycine NCA and other methylated derivatives in DMF at 0.4 M and using allylamine as initiator (polymerization degree (M/I) of 20). The kinetics were determined by FTIR thanks to the signal decrease of the carbonyl stretching band ($C=O$) at 1850 cm^{-1} . After almost 2 days, all the polymerization of glycine-NCA and their methylated derivatives sarcosine- and *N*-methyl-alanine-NNCAs were finished (we did not number the compounds described because we did not fully characterize them). As clearly depicted in **Figure 18**, the steric hindrance at both *C* or *N* location were influencing the ROP. In all cases, the ROP followed a first-order kinetics, a behavior generally expected when low DPs are targeted with NCAs.²⁰

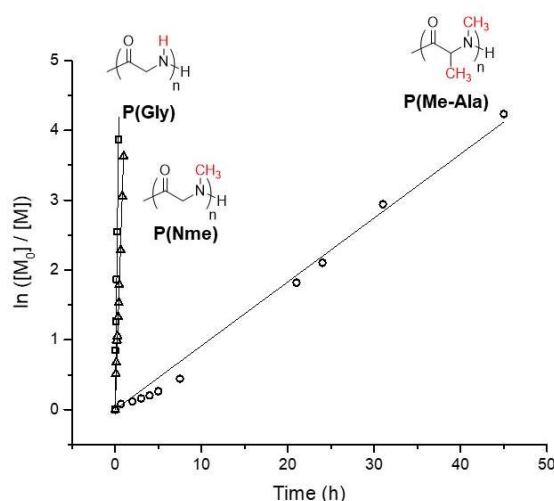


Figure 18. Kinetics of the ROP process for NNCA in DMF 0.4 M having an $M/I = 20$ varying the methylated position on different peptidomimetic polymers.

We found that a methyl group can drastically influence the kinetic rate but this influence strongly depends on its position. The simplest glycine-NCA provided the fastest polymerization rate (P(Gly), $k = 10.02\text{ h}^{-1}$). The kinetic rate decreased with the steric hindrance in the *N* position as we observed when a methyl group was positioned (P(Nme), $k = 3.72\text{ h}^{-1}$) with a 2.6 times lower value than P(Gly). Finally, when methyl group was positioned in *C* and in *N* position concomitantly, the kinetic rate was strongly decreased (P(Me-Ala), $k = 9.16 \times 10^{-2}\text{ h}^{-1}$) with a value that was 40.6 times lower than P(Nme). Overall, we can conclude that steric hindrance is bigger for *C*-methylation.⁴⁵ We also observed steric hindrance with *N*-methylation but this effect was much lower, counterbalanced by an electronic effect also influencing the ROP.

1.1.3 Influence of the *N*-alkyl group of NNCA

The short study presented in part 1.1.2 clearly shows that understanding the effect of *N*-alkylation toward the ROP reaction is more complex than just taking into account the steric hindrance effect. In the literature, it is possible to find a variety of poly(*N*-alkylated)glycines, bearing various alkyl groups.¹⁸ However, the way this *N*-alkylation influences the kinetics of the ROP is still poorly understood. Usually, people accept that steric hindrance is the main parameter explaining ROP kinetic decrease, as demonstrated experimentally by R. Luxenhofer *et al.*²⁰ and confirmed by J. Ling *et al.* through a computational study.⁴⁷ However, these previous studies are limited in practice because they only provide information on *N*-alkylations involving aliphatic groups. On the other hand, as we observed in **Figure 18**, a simple *N*-methylation produces both steric and electronic effects. In general, accessing more functional NNCA is difficult and it is rare to find *N*-substituted poly(glycines) bearing charged, aromatic or heteroatom-containing substituents. Very recently, some insights suggest that the electronic effect could be as strong as the steric hindrance in some cases.⁴⁸ In this context, this research work provided a unique opportunity to compare a wide range of different *N*-substitution to better rationalize its influence on the ROP of NNCA.

As presented in chapter 2, we developed the synthesis of a small library of *N*-alkylated NCA through an adaptation of the Leuchs method using thionyl chloride and filtration with celite. In this section, we have set up the ROP of these NNCA using allylamine as initiator (targeting a $M/I = 20$) in anhydrous DMF under inert conditions and at RT. To follow the ROP kinetics, the reaction mixtures were monitored by FTIR (**Figure 17a**). The direct observation of the disappearance of the NNCA stretchings indicated that the reaction time to reach full conversion was varying significantly with time, ranging from 3 h (Sar-NCA) to more than 12 days (Cy-NNCA, **Figure 19**).

As already reported in the literature for aliphatic groups, the kinetics of NNCA were highly influenced by steric hindrance.^{20,47} For instance, poly(*N*-propyl)glycine [P(Npr)] reached full conversion after 48 h with a kinetic constant of $k = 6.82 \times 10^{-2} \text{ h}^{-1}$ (**Table 15**) that was found 54 times lower than the kinetic constant of the ROP forming polysarcosine (PNme, $k = 3.72 \text{ h}^{-1}$).

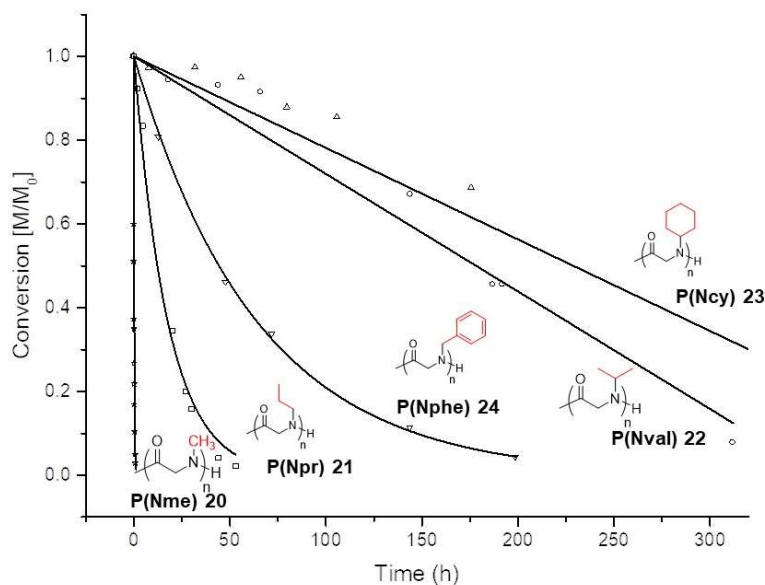


Figure 19. Steric influence over the kinetics of the ROP process for NNCA in DMF at 0.4 M having a $M/I = 20$ for all the monomers.

This influence was even more pronounced when we performed the ROP of more sterically hindered monomers such as Val-NNCA and Cy-NNCA. The full conversion into poly(*N*-isopropyl)glycine [P(Nval)] was reached upon 15 days ($k = 2.8 \times 10^{-3} \text{ mol} \cdot \text{L}^{-1} \cdot \text{h}^{-1}$) and into poly(*N*-cyclohexyl)glycine [P(Ncy)] upon 20 days ($2.1 \times 10^{-3} \text{ mol} \cdot \text{L}^{-1} \cdot \text{h}^{-1}$) respectively (**Figure 19**).

Table 15. ROP kinetics rate of the NNCA into the poly(*N*-alkylated)glycines. Experiments were performed in DMF at 0.4 M and 20 °C.

Polymer	R	Reaction order	k_{obs} (h^{-1})
P(Nme) 20	Methyl	first	3.72
P(Npr) 21	Propyl	first	6.82×10^{-2}
P(Nval) 22	Isopropyl	zero ^a	2.80×10^{-3}
P(Ncy) 23	Cyclohexyl	zero ^a	2.10×10^{-3}
P(Nphe) 24	Benzyl	first	1.56×10^{-2}
P(Nnpm) 25	Nitrobenzyl	first	6.40×10^{-3}
P(Nmet) 26	Methylthioethyl	first	2.72×10^{-2}
P(ZNae) 27	Cbz-aminoethyl	zero ^a	8.20×10^{-3}
P(ZNlys) 28	Cbz-aminobutyl	first	3.05×10^{-2}

^a Zero-order unit: $\text{mol} \cdot \text{L}^{-1} \cdot \text{h}^{-1}$.

Interestingly, the most hindered monomer conversions to corresponding polypeptoids P(Nval) and P(Ncy) were associated to zero-order kinetic profiles (**Figure 19** left and **Table 15**). According to **Scheme 22**, the ROP reaction involves two steps: a nucleophilic attack, and a CO_2 release. Here, we observed that the determining step was the nucleophilic attack, because of steric hindrance: we thus confirmed the study performed by T. Bai and J. Ling in which they calculated that Val-NNCA had a higher energetic barrier during the carbonyl addition ($\Delta G = 39.35$

Chapter 3. Linear polypeptoid and their antimicrobial activity

kcal/mol) than Me-NNCA ($\Delta G = 33$ kcal/mol).⁴⁷ This steric effect was reduced during the synthesis of poly(*N*-propyl)glycine increasing quantitatively the kinetic constant and associated to a first-order kinetic reaction [$P(Npr)$, $k = 6.8 \times 10^{-2} \text{ h}^{-1}$].

The effect of such steric hindrance was not necessarily found correlating the volume of the substituent because when we introduced a benzyl group on the NNCA, the formation of poly(*N*-benzyl)glycine **24**] was also associated to a first-order kinetic reaction ($k = 1.56 \times 10^{-2} \text{ h}^{-1}$, **Figure 19** right) reaching full conversion approximately after 13 days. These results showed that the steric hindrance is significantly counterbalanced by another effect, an electronic-inductive effect that activates the propagation.

To better determine how significant can be this inductive effect, we followed the ROP of more functional NNCA (meaning NNCA containing heteroatoms on their side chains, **Figure 20**). First, we studied the ROP kinetics of NPM-NNCA that possess a nitro electron-withdrawing group, to compare it with the benzyl side chain. Upon approximately 15 days of reaction, we reached a

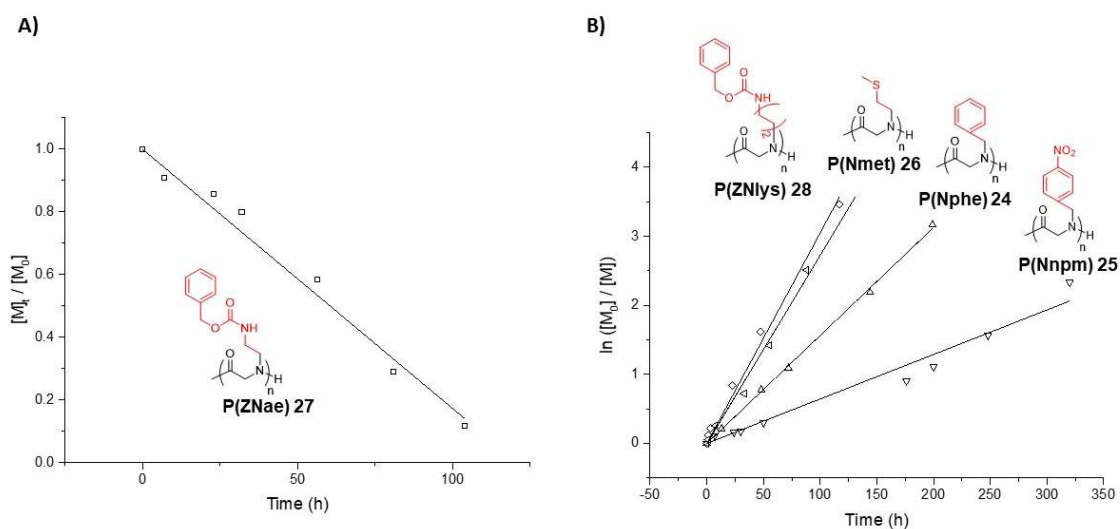


Figure 20. Influence of the electronic effect of the alkyl substituent during the ROP process for NNCA in DMF 0.4 M having a $M/I = 20$ for all the monomers. A) zero-order kinetics ROP and B) first-order kinetics ROP

full conversion and monitored a first-order kinetic rate of $k = 6.40 \times 10^{-3} \text{ h}^{-1}$ for poly(nitrobenzylglycine) [$P(Nnpm)$]. We noticed a 2.3 fold decrease between the kinetic constants of $P(Nnpm)$ **25** and $P(Nphe)$ **24**, confirming that the inductive electronic effect can strongly influence the ROP reactivity. This effect increases the electron density on the nitrogen atom and

Chapter 3. Linear polypeptoid and their antimicrobial activity

thus its nucleophilicity: it is this same effect that is at the origin of a higher pKa for secondary amines compared to primary amines.⁴⁹

To better understand this inductive effect we also compared the ROP of *N*-benzylated-NCAs with NNCA monomers bearing ethyl substituents with a methylthioether or a *gem*-trifluorinated functional group. When the ROP was monitored, the formation of poly(*N*-methylthioethyl)glycine (P(Nmet), $k = 2.72 \times 10^{-2} \text{ h}^{-1}$) was associated with 1.76 fold higher kinetics rate than P(Nphe). This result confirmed that the electronic inductive effect enhances the nucleophilicity of the secondary amine during the propagation. On another hand, the *N*-trifluoroethyl-NCA took more than two weeks to achieve less than 5% of conversion (as followed by FTIR, data not shown). Thus, electron-withdrawing groups (negative inductive effect) decreased the nucleophilicity during the propagation and consequently the CO₂ release.

Finally, to better understand the influence of the steric hindrance and electronic effect together we compared the ROP of *Cbz-N*-ethylamino- and *Cbz-N*-butylamino-NCAs (P(ZNae) & P(ZNlys), **Table 15**). Interestingly, P(ZNae) presented a zero-order kinetic profile whereas P(ZNlys) showed the characteristic of a first-order kinetic profile reaching full conversion in both cases at 135 h (**Figure 20**). Our hypothesis was the following: the steric hindrance contributed to a decrease of the reactivity during the nucleophilic attack and the electronic-inductive effect enhanced the nucleophilicity. Thus, the combination of both effects during ROP showed that NNCA is consumed at the same speed as the CO₂ is released, presenting an apparent zero-order for P(ZNae) ($k = 8.2 \times 10^{-3} \text{ mol} \cdot \text{L}^{-1} \cdot \text{h}^{-1}$) while in the case of P(ZNlys) is merely an inductive effect that enhanced the constant rate ($k = 3.05 \times 10^{-2} \text{ h}^{-1}$) when we compared with P(Nphe) (improvement of 1.95 fold).

After completing each kinetic experiment, all the homopolymers were purified by precipitation using diethyl ether. The yields were good for almost all polypeptoids (60 to 80% of the mass was recovered) except for poly(*N*-methylthioethyl)glycine that afforded a yield of 41%. This low yield was attributed to the several precipitation steps performed on an oily product for which a high affinity to DMF was observed. To get a deeper molecular understanding of their chemical structures, we performed ¹H-NMR analyses, size exclusion chromatography (SEC), and MALDI TOF analyses.

All the NMR characterizations are described in detail in the experimental part. We describe here only the ¹H-NMR analysis performed with poly(sarcosine) to underline the importance of this

technique to determine the polymerization degree (DP_{NMR}). First, the 1H -NMR analysis of poly(sarcosine) revealed the presence of characteristic broad signals at 2.50-3.10 ppm and 3.80-4.42 ppm (**Figure 21** protons *d*, *e*). As already observed with peptoids synthesized by SPPS, these multiplets are attributable to the different *cis/trans* configurations of the peptoid backbone.^{50,51} These signals and the protons belonging to allylamine, the initiator, (**Figure 21** protons *a*, *b*) allowed us to determine the polymerization degree by correlating the peak intensities

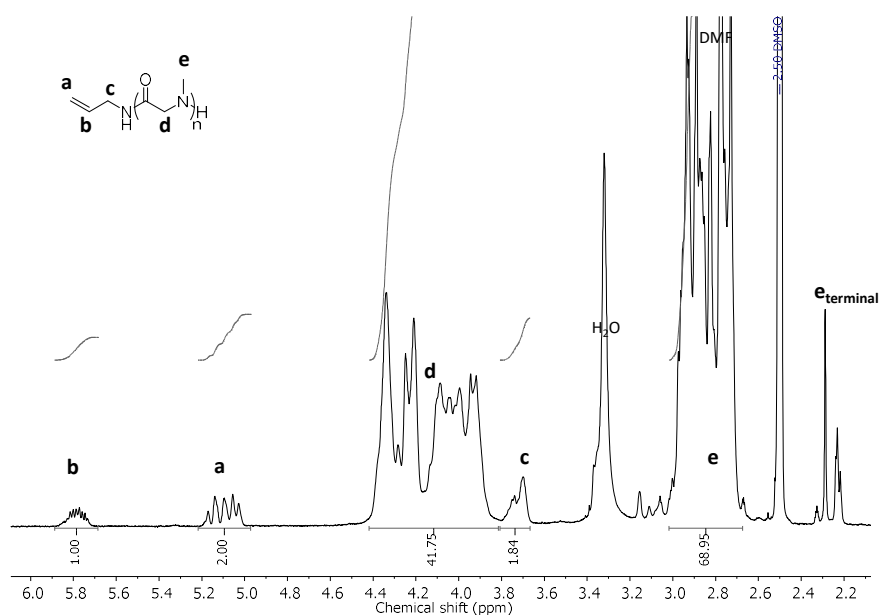


Figure 21. Representative 1H -NMR spectrum of poly(sarcosine) at $M/I = 20$ using allylamine as the initiator in $DMSO-d_6$. Characteristic multiplet-broad peaks were observed due to the *cis/trans* conformation and the possible combinations along the polymer backbone.

with the protons of the polymer backbones. Outside polysarcosine, 1H -NMR analyses of the other poly(*N*-alkylated)glycines were indicating polymerization degrees in agreement with the targeted $M/I = 20$ (**Table 16**). However, numbered molar masses (M_n) determined by SEC in DMF or HFIP showed a lower value than the theoretical one in most of the cases but presented low polydispersities in the range $D_M = 1.02$ -1.30, except in the case of P(Nnpm) with a value of $D_M = 1.90$. This deviation can be explained due to the small size of the polymers. We also tried to determine the molar masses using the calibration curve method with polystyrene standards but in most of the cases, we obtained values even lower than those reported in **Table 16** (data not shown).

Chapter 3. Linear polypeptoid and their antimicrobial activity

Table 16. Hydrophobic homopolypeptoids molar masses, M/I and yields. Polymers were synthesized using allylamine as initiator at $M/I = 20$.

	MW theoretical (g mol ⁻¹)	MW from ¹ H-NMR (g mol ⁻¹)	M_n from SEC (g mol ⁻¹)	M_w (g/mol)	\bar{D}_M	Yield (%)
P(Nme) 20	1477	1619	1000	800	1.03	60
P(Npr) 21	2037	2235	2400	2600	1.09	58
P(Nval) 22	2037	2433	1500	1800	1.16	63
P(Ncy) 23	2837	3810	800	1100	1.29	79
P(Nphe) 24	2997	2556	1600	2300	1.19	68
P(Nnpm) 25	3897	3897	4000	4600	1.90	69
P(Nmet) 26	2677	2939	5400	6700	1.22	41
P(ZNae) 27	4737	5205	4000	5100	1.29	64
P(ZNlys) 28	5297	6083	5600	6000	1.08	52

^a Determined in HFIP. ^b Calculated for a multiple peak distribution.

We performed matrix-assisted laser desorption/ionization time-of-flight mass spectrometry (MALDI TOF) analysis using α -cyano-4-hydroxycinnamic acid as matrix agent, revealing one population of poly(*N*-substituted)glycines that was initiated with allylamine with $\Delta \approx 71$ g/mol corresponding to sarcosine monomer unit (**Figure 22**, polysarcosine).

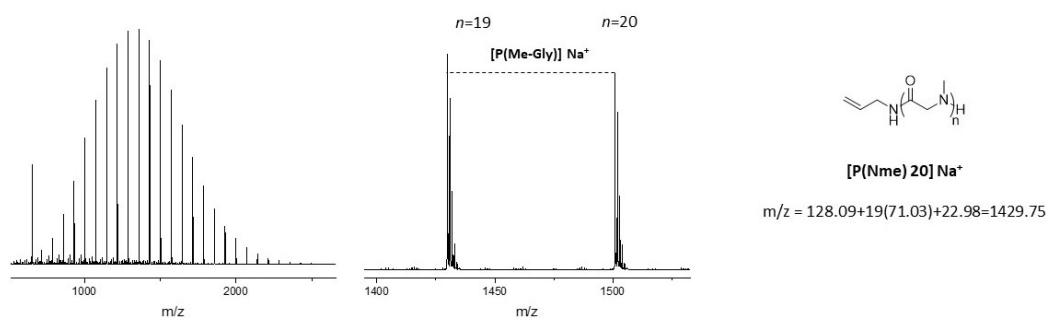


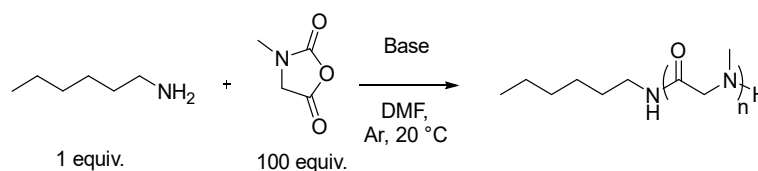
Figure 22. Representative MALDI TOF spectrum for poly(sarcosine) or P(Nme).

1.1.4 Influence of bases to improve the kinetics in poly(sarcosine) synthesis

Compared to NCAs, the ring-opening polymerization of NNCA is known to be a slow process as, previously mentioned (part 1.1.2 and 3). Moreover, we observed significant differences in NNCA ROP reactivities which may cause a problem when operating copolymerization reactions (since the monomers may not randomly incorporate into the polymer structure). To level out the reactivity, we decided to explore catalyst alternatives. Several conditions were already reported to enhance the ROP process, such as solvent, temperature, and vacuum.^{20,33} In this context, the use of bases could promote NCA polymerization kinetics, as shown using non-nucleophilic bases like triethylamine^{52,53} or lithium bis(trimethylsilyl)amide

Chapter 3. Linear polypeptoid and their antimicrobial activity

(LiHMDS).⁵⁴ Furthermore, other catalysts such as crown ethers were recently used to enhance the same ROP process of NCAs.⁵⁵ Few examples regarding catalysis during ROP of NNCA were developed such as the use of trimethylguanidinium as a catalyst to activate primary alcohols as initiators³¹ as well as the use of triethylamine (TEA) and diisopropylamine during the preparation of *N*-methylated polypeptides.³¹ In this Ph.D. thesis, we decided to study the effect of various bases or of crown ether (18 crown 6) on the ROP kinetics of Sar-NCA in DMF at 0.4 M, using allylamine as initiator (polymerization degree (*M/I*) of 100, **Scheme 26**). The kinetics were determined by FTIR thanks to the signal decrease of the carbonyl stretching band (C=O) at 1850 cm^{-1} (conversion plot is depicted in **Figure 23**, we did not number the compounds described because we did not fully characterize them at this stage).



Scheme 26. Base-activation experiment during Sar-NCA ring-opening polymerization (hexylamine was the initiator).

In comparison to non-alkylated NCAs, it is to note that base activating the ROP of NNCA do not suffer from deprotonation-induced side reactions.⁵⁶

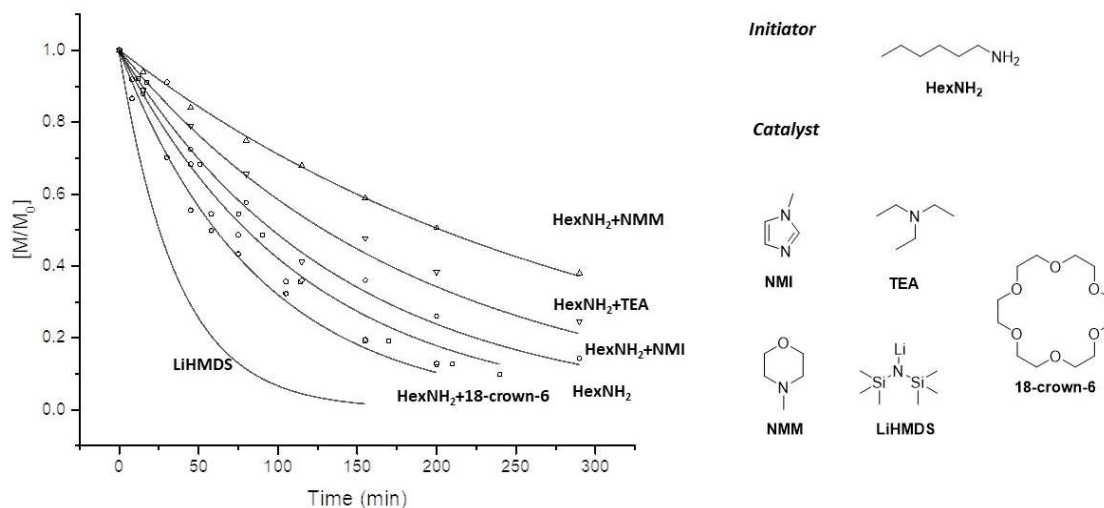


Figure 23. Kinetics using hexylamine as initiator having a *M/I* = 100 in DMF at 0.4 M and 20 °C and a variety of catalysts. LiHMDS kinetics was performed without hexylamine.

The results obtained with different bases are presented in **Table 17** and in **Figure 23**.

Chapter 3. Linear polypeptoid and their antimicrobial activity

Surprisingly, the use of bases such as *N*-methylimidazole (NMI), *N*-methyl morpholine (NMM), and triethylamine (TEA) slowed down the conversion. The kinetics rate decreased following the order NMM > TEA > NMI, as shown in **Table 17**. A possible explanation for this experimental observation could be that hydrogen bond formation helps to stabilize the carbamate upon ring opening (**Scheme 22**), the slope becomes close to zero-order kinetics. Another hypothesis could be that adding base makes the solvent having a higher affinity to CO₂.⁵⁷ The lowest kinetic constant was encountered using NMM (0.2 h⁻¹).

Table 17. First-order results of the *Sar*-NCA ROP kinetics using hexylamine as initiator having a *M/I* = 100 in DMF at 0.4 M and 20 °C.

Catalyst	Concentration (mM)	pKa in DMSO	Kinetic rates (h ⁻¹)
-	-	-	0.57
NMI	80	7.0	0.41
NMM	80	7.4	0.2
TEA	80	9.0	0.3
18-crown-6	4	-	0.64
LiHMDS	4	26.0 ^b	0.61
LiHMDS*	4	26.0 ^b	1.06

^aWithout hexylamine in the reaction pot. ^bIn THF

In contrast, we observed that hard (and non-nucleophilic) base LiHMDS could improve 1.85 fold the kinetic constant ($k=1.06$ h⁻¹, **Table 17**) as compared to hexylamine alone, an effect that we will fully describe in the next chapter, dedicated to cyclic polypeptoids.

Finally, when we employed 18-crown-6 as a catalyst, we observed a slight increase of the kinetic rate from 0.57 to 0.64·h⁻¹, which can be explained by the possible sequestration of positively charged species during the ROP process such as the proton of the carbamate, promoting an increase of the CO₂ release.⁵⁵ It is necessary to note that for this experiment, we used a low concentration of crown ether (4 mM), but the increase of concentration could probably have a more important effect on the kinetic rate.

In summary, it was possible to determine that the electronic effect is an important parameter that influences the kinetic behavior of NNCA during ROP. In some cases, electronic effects introduced by *N*-alkylation can counterbalance an expected steric hindrance effect. As it was not really possible to improve the reactivity of the polymerization by using a base, we established that the ROP can be implemented at *M/I* = 20 to afford hydrophobic or cationic homopolymers.

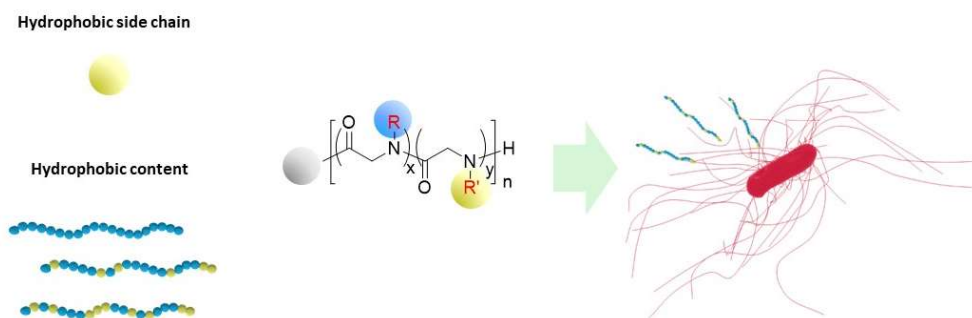
2 Antimicrobial activity against *C. difficile* and structure-activity relationships of copolypeptoids with a controlled hydrophobic/cationic ratio

In medicinal chemistry, the screening of chemical libraries is an efficient tool to direct the design of anti-infective agents through the study of their structure-activity relationships (SAR).⁵⁸ The use of polymer chemistry opens this concept to macromolecular pharmacophores which often remain to be studied for polymeric AMP analogs: size, dispersity, topology, monomer unit composition, nature of the initiator, etc.⁵⁹ Specifically, the macromolecular design of copolymers require to define key parameters, as already described in chapter 1. As a representative example of such a SAR approach, S. Gellman *et al.* optimized the design of nylon-3 copolymers against various bacteria^{60–63} including *C. difficile*.⁶⁴ They have reported SAR regarding the polymer length, head group, cationic/hydrophobic side-chain content, and influence of the chemical nature of the hydrophobic unit. In a study targeting *B. subtilis*, they showed for instance that the best design was to prepare copolymers having 50% of hydrophobic content to reach a bacterial minimal inhibitory concentration (MIC) below 0.78 µg/mL and they demonstrated, from determining the minimum hemolytic concentration (MHC), that the best copolymer displayed a selectivity index of 16.⁶⁰

The first key example of a macromolecular SAR approach involving polypeptides copolymers was published in 2001 by T. Deming *et al.* to design phospholipid membrane destabilizers.⁶⁵ In that study, they performed a screening of more than 60 different copolymers made of two different NCA monomers and varying the structural parameters such as length, nature of the building block, and hydrophobic content. They determined that a high hydrophobic content (>30%) generally increases the interaction with the bilayer membranes of liposomes. The liposomes contained dyacetylenic surfactant that changed the color from violet to orange upon interaction with peptides, an indirect way to follow membrane destabilization. Moreover, this study showed that a precise optimization of the copolymer composition allowed to achieve selective interactions with specific membrane compositions (phospholipid cocktails). The SAR approach of polypeptide polymers was further investigated by G. Qiao *et al.* taking advantage of the use of a polymerization reaction varying the topology of the polypeptides: they prepared star-like copolymers to develop unprecedented activity against multi-drug-resistance bacteria.⁶⁶ In their study they mentioned that the star-like design vs the linear polymer presented 40 fold higher antibacterial activity against *E. coli* and *S. aureus*.

Chapter 3. Linear polypeptoid and their antimicrobial activity

In this stimulating context, the macromolecular SAR approach was never investigated for the preparation of polypeptoid copolymers. In this section, we studied the preparation of several linear copolymers based on poly(*N*-alkylated-glycines), starting by varying the hydrophobic content *via* the cationic/hydrophobic monomer ratio along with the nature of the hydrophobic side chain and tested their activities against *Clostridioides difficile* (**Scheme 27**).



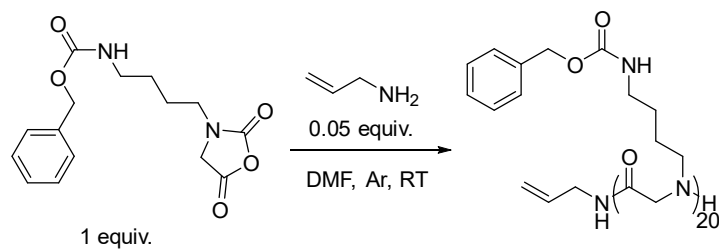
Scheme 27. Studied parameters for the preparation of copolypeptoids for further antibacterial SAR.

2.1 Cationic poly(*N*-aminobutyl)glycine

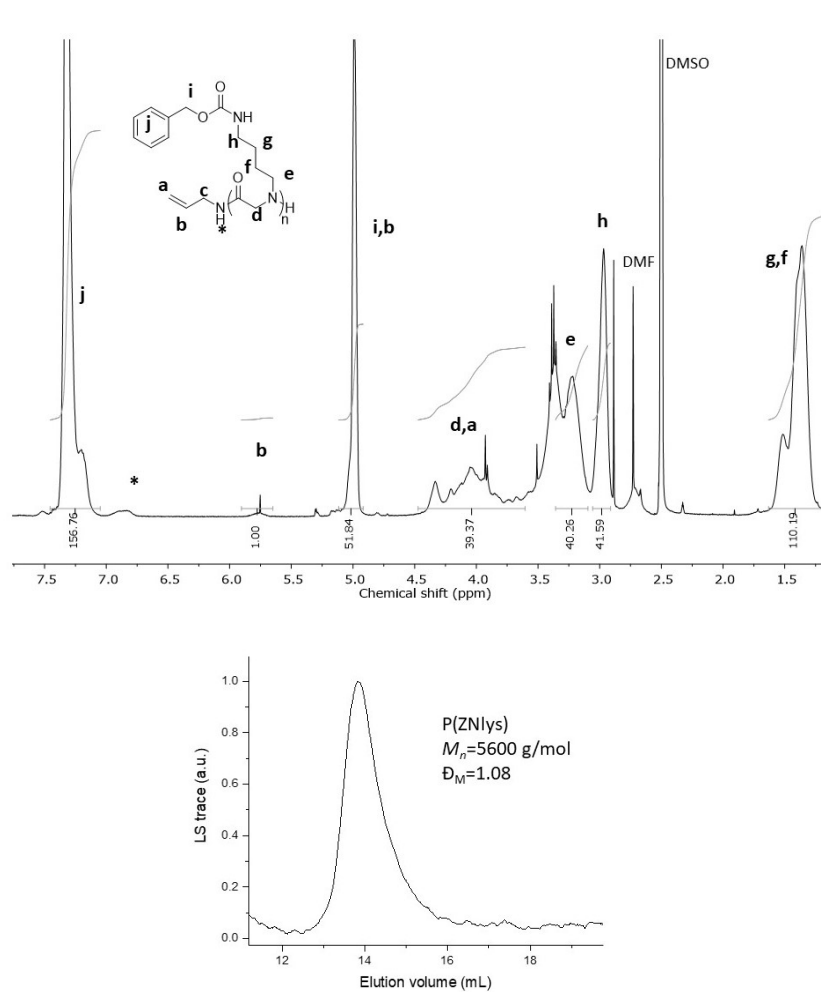
Previous reports involving poly(*N*-substituted)glycines bearing functional groups like nitrile,³⁵ allyl,³⁴ and propargyl²¹ have implemented post-polymerization coupling towards cationic backbones.²¹ However, the direct polymerization of monomers bearing cationic groups remains challenging: this would be useful for the proposed SAR approach. Accordingly, we have developed a new strategy to design a lysine-like NNCA (ZLys-NNCA) with *N*-carboxybenzoyl protection (*N*-Cbz group, see chapter 2). This monomer was designed to afford smooth deprotection of the polypeptoid backbone providing cationic polymers.

With polypeptides, the deprotection of *N*-Cbz groups is used to prepare poly(*L*-lysine) from poly(*Z*-*L*-lysine) in a mixture of trifluoroacetic acid and HBr at RT.⁶⁷ We first prepared poly(*N*-*Z*-aminobutyl)glycine [P(ZNlys)**28**] from this ZLys-NNCA monomer, using allylamine as initiator at M/I = 20, in anhydrous DMF and under argon (**Scheme 28**).

The progress of the chemical reaction was followed by FTIR and, at full conversion (7 days), the polymer was isolated by precipitation in diethylether as a yellowish powder in 64% yield. We analyzed the polymer by ¹H-NMR in DMSO-*d*₆ and SEC in DMF. By using the signals of the proton corresponding to the allylamine initiator (CH, 5.65 ppm, **Figure 24**) the polymerization degree



Scheme 28. Synthesis of *P*(ZNlys)**28** from ZLys-NNCA.

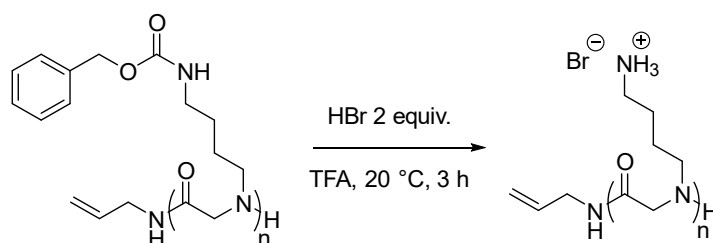


was determined from the averaged integrations of the signals belonging to the polymer backbone ($\text{DP}_{\text{NMR}} = 23$), a polymerization degree in agreement with the theoretical value.

Chapter 3. Linear polypeptoid and their antimicrobial activity

Then, we determined the numbered molar mass (M_n) by SEC in DMF through light-scattering detection. The homopolymer presented a $M_n = 5600$ g/mol with low dispersity ($D_M = 1.08$). This result ensured the preparation of protected cationic polypeptoids in agreement with the expected molar mass of $M_n = 5300$ g/mol.

With polypeptides, the deprotection of *N*-Cbz groups is already used to prepare poly(*L*-lysine) from poly(*Z*-*L*-lysine): the procedure implements a reaction in trifluoroacetic acid at room temperature with HBr as a deprotecting agent.⁶⁷ We accordingly carried out the side chain deprotection of P(ZNlys) by adapting this procedure: the polypeptoid was solubilized in trifluoroacetic acid (TFA) and 2 equiv. of HBr (based on the monomer unit MW = 262 g/mol) were added before stirring 3 h at RT to afford poly(*N*-aminobutyl)glycine [P(Nlys), **Scheme 29**].



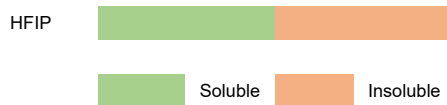
Scheme 29. Deprotection reaction to prepare P(Nlys) **28D**.

The poly(*N*-aminobutyl)glycine (**28D**) was purified by precipitation in diethyl ether, then dialysis and freeze-dried in 60% yield. We first evaluated its solubility and compared it to the polymer before deprotection (**Table 18**). In contrast to the *N*-Cbz-protected counterpart, PNlys was not soluble in organic solvents except in trifluoroacetic acid.

Table 18. Solubility test of the cationic homopolymers before and upon deprotection.

Solvent	PZNlys 28	PNlys 28D
Cyclohexane	Insoluble	Insoluble
Et ₂ O	Insoluble	Insoluble
Toluene	Insoluble	Insoluble
DCM	Soluble	Insoluble
THF	Soluble	Insoluble
ACN	Soluble	Insoluble
MeOH	Soluble	Insoluble
DMF	Soluble	Insoluble
DMSO	Soluble	Soluble
Water	Insoluble	Soluble
TFA	Soluble	Soluble

Chapter 3. Linear polypeptoid and their antimicrobial activity



Although the drastic change in solubility revealed that we certainly obtained cationic polypeptoids, further characterizations were conducted to verify that our deprotection strategy did not degrade the polymer backbone. We fully characterized P(Nlys) by $^1\text{H-NMR}$ analysis in D_2O and SEC analysis in acetate buffer (**Figure 25**). On the NMR spectrum, the characteristic signal peaks corresponding to the protons of both initiator and deprotected polymer backbone were found (signals *a-c* and *d-h*) and the protons of the *Cbz*-protecting group had all disappeared. This confirmed that the polymer was fully deprotected.

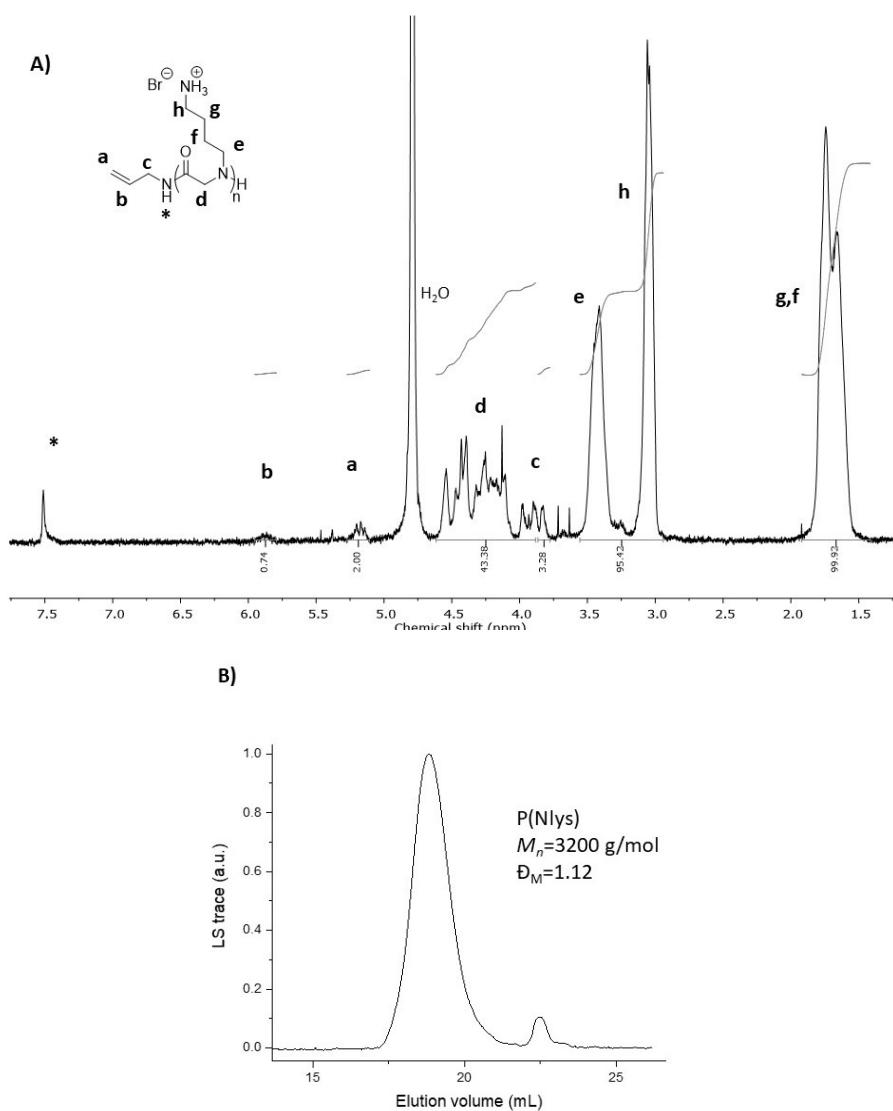


Figure 25. Characterization of poly(*N*-aminobutyl)glycine (**28D**): A) $^1\text{H-NMR}$ in D_2O (the star corresponds

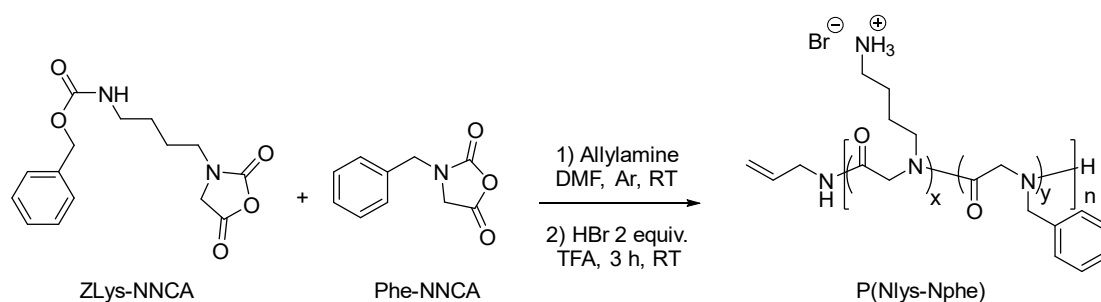
Chapter 3. Linear polypeptoid and their antimicrobial activity

to the terminal NH). B): Chromatogram from SEC in water acetate buffer pH = 4.0.

Using signals integrations, we determined the degree of polymerization (DP_{NMR}) which was in agreement with the theoretical $M/I = 20$ ($DP_{\text{NMR}} = 23$). On another hand, the SEC analysis allowed to characterize a polypeptoid having a molar mass M_n of 3200 g/mol and a narrow distribution D_M of 1.12. This decrease in molar mass upon deprotection was explained by the loss of the *Cbz*-protecting group and the calculated values were in relative agreement with the theoretical one ($MW = 2600$ g/mol without considering the HBr molar mass).

2.2 Preparation of copolymers with varying hydrophobic/cationic ratio

Previous macromolecular SAR approaches showed that varying the hydrophobic/cationic ratio is an important parameter that can be tuned through ring-opening copolymerization.⁶⁷ According to R. Luxenhofer *et al.*, polypeptoid copolymers can be obtained with narrow dispersity,²² however, a mixture of *N*-alkylated analogs of amino acid monomers mixing lysine-like side chains with a hydrophobic amino acid (we chose here phenylalanine-like) have never been implemented. To achieve this goal, we prepared a library of poly[*N*-(aminobutyl)glycine-*N*-(benzyl)glycine] [P(Nlys-Nphe)] in a 2-step process (**Scheme 30**). In the first step, we carried out the ROP of the NNCA mixtures, using allylamine as initiator, targeting a $M/I = 20$. Moreover, we varied the hydrophobic content through the stoichiometry ratio between ZLys- and Phe-NNCA monomers from 10% to 50%, to define a small library with increasing hydrophobic content. In the second step we deprotected the copolymer using HBr (2 equiv.) in TFA at RT.



The copolymerization conversions were followed using infrared spectroscopy, by taking small aliquots of the reaction mixture. At full conversion (about 15 days at RT), copolymers were isolated by precipitation in diethyl ether to afford yellowish powders with good yields (69-81%). Each copolymer was analyzed by SEC in DMF and ¹H-NMR in DMSO-d₆ (**Figure 26** and **Figure 27**).

Chapter 3. Linear polypeptoid and their antimicrobial activity

As shown in part 1.1.2 the kinetic constant of the ROP of P(Nlys) was 1.9 fold higher than the one of P(Nphe). This difference in reactivity would provide imperfect *statistical* copolymers and potentially, a heterogenous molar mass. Interestingly, despite these kinetic differences, the copolymers presented narrow dispersity ($\bar{M}_w = 1.04-1.07$, **Figure 26**) suggesting a controlled polymerization process.

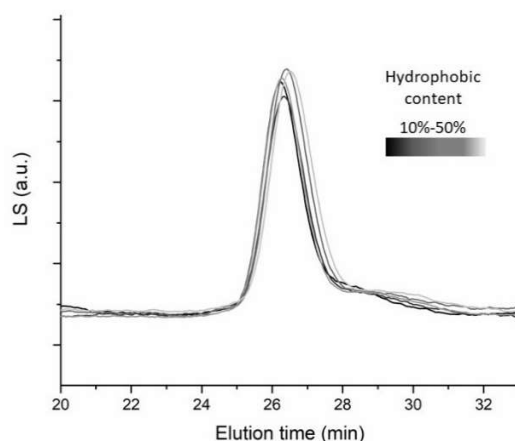


Figure 26. Light scattering chromatograms showing P(ZNlys-Nphe)**29-33** with increasing hydrophobic to Cbz-lysine content (10 to 50%). The LS traces were obtained from SEC analyses performed in DMF.

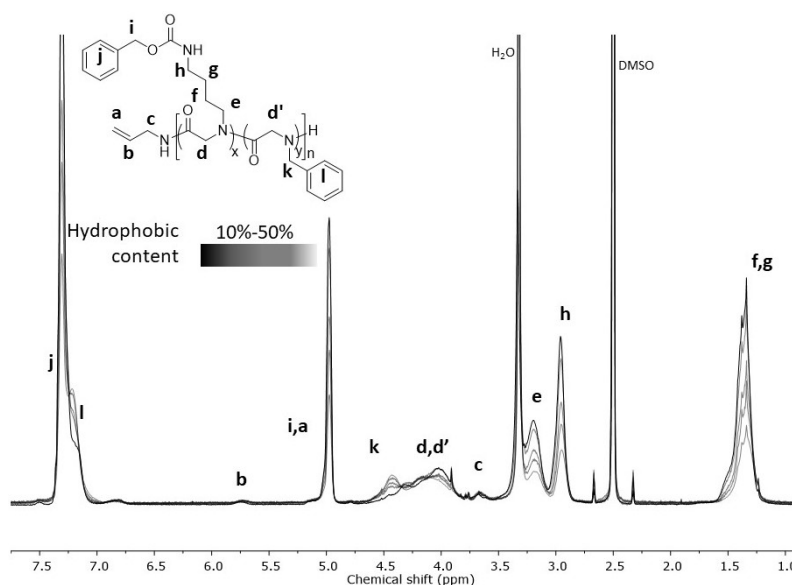


Figure 27. ¹H-NMR spectra in DMSO for P(ZNlys-Nphe)**29-33** varying the hydrophobic content from 10 to 50%.

As depicted in **Figure 27** for poly(Cbz-N-aminobutyglycine)-(N-benzylglycine) (P(ZNlys-

Chapter 3. Linear polypeptoid and their antimicrobial activity

Nphe)**29-33** varying the hydrophobic content, the $^1\text{H-NMR}$ spectrum obtained in DMSO-d_6 revealed i) the presence of a broad-multiplet signal attributable to glycine polymer backbone ($-\text{CH}_2-$, peak d, d' , 3.83-4.66 ppm), ii) the side chains of the polymer backbone: Nphe peak signal at 7.2 ppm (peak l) and Nlys peaks 0.96-1.82 ppm (f, g), 2.74-3.07 ppm (h), 3.06-3.26 ppm (e).

For all copolymers, we calculated the degree of polymerization (DP_{NMR}) using the signals of the glycine polymer backbone (3.83-4.66 ppm) and the signal of the allylamine initiator (peak b at ~ 5.8 ppm). In general, the DP_{NMR} was close to the theoretical $M/I = 20$ (**Table 19**). Those results corroborated well the results obtained by SEC in DMF (values of M_w found between 6000 and 6600 $\text{g}\cdot\text{mol}^{-1}$) and this last analysis also demonstrated that copolymers were obtained with low dispersity ($\text{Đ}_M = 1.04 - 1.07$).

Table 19. Library of $P(\text{ZNlys-Nphe})$ **29-33**: molar masses from SEC, DP_{NMR} , and yields.

Polypeptoid	ZLys NNCA (%)	Phe NNCA (%)	MW theo (g/mol)	M_n (g/mol) ^a	M_w (g/mol)	Đ_M	DP_{NMR}^b	Hydrophobic content (%) ^b	Yield (%)
29	90	10	5000	6100	6300	1.04	20	12	69
30	80	20	4800	6100	6300	1.04	23	20	76
31	70	30	4600	5800	6000	1.04	19	27	81
32	60	40	4300	6400	6600	1.03	22	38	77
33	50	50	4100	5100	5400	1.05	23	49	70

^a SEC performed in DMF using a $dn/dc=0.0819$. ^b Calculated from the $^1\text{H-NMR}$ spectrum in DMSO-d_6

We also determined the hydrophobic content using $^1\text{H-NMR}$ analysis by comparing the integrations of the signals of the glycine (peak d, d') to the integrations of the signals of the *N*-alkylated side chains. They confirmed the increasing hydrophobic content in the final copolymer structure (**Table 19**).

We then performed the deprotection procedure optimized for $P(\text{Nlys})$ **28D** in part 2.1. All copolymers were deprotected in TFA by adding 2 equivalents of HBr (relative to cationic side chains). Upon 3 h of deprotection the copolymers were purified by precipitation in diethyl ether, then dialyzed and freeze-dried. This step afforded “water-soluble and cationic copolymers” in good yields varying from 62 to 82%. We verified by $^1\text{H-NMR}$ (**Figure 28**) that the deprotection

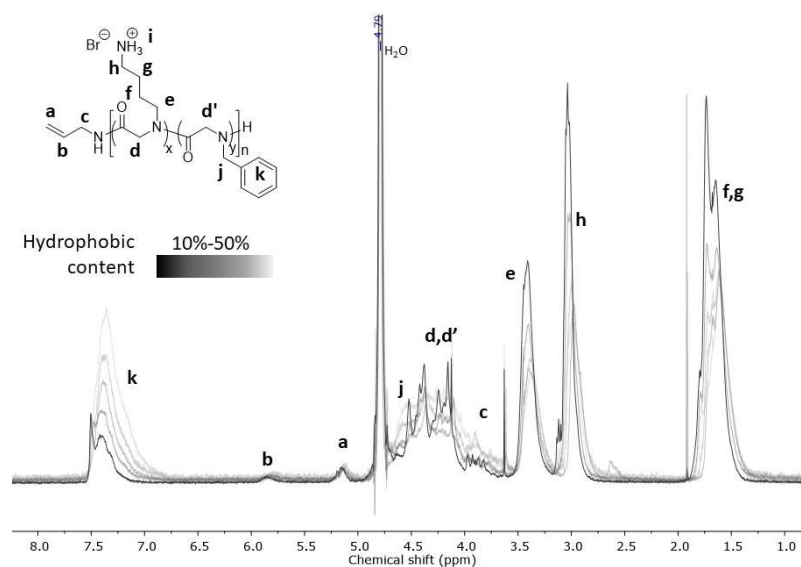


Figure 28. $^1\text{H-NMR}$ spectra in D_2O for $P(\text{Nlys-Nphe})\mathbf{29D-33D}$ varying the hydrophobic content from 10 to 50 % at $M/I = 20$.

step had not changed the hydrophobic content: the copolymers spectra indicated the expected increase of the signals belonging to the hydrophobic building block (signal *l*, 7.4 ppm), the expected decrease of the signals belonging to the cationic side-chains (**Figure 28**, signals *e-h*,) and disappearance of the *Cbz*-protecting group

By analyzing carefully the integration of the different signals (**Figure 27** and corresponding discussion), the polymerization degree, as well as the hydrophobic content, were precisely calculated and provided values in agreement with the values obtained before deprotection (**Table 20**). All these NMR characterizations confirmed that the copolymer did not suffer from chemical modifications during the deprotection step.

Table 20. Series of $P(\text{Nlys-Nphe})\mathbf{29D-33D}$: DP_{NMR} , and yields before deprotection.

Polypeptoid	Nlys NNCA (%)	Nphe NNCA (%)	$\text{DP}_{\text{NMR}}^{\text{b}}$	Hydrophobic content (%) ^b	Yield upon deprotection (%)
29D	90	10	25	13	75
30D	80	20	19	20	73
31D	70	30	19	26	80
32D	60	40	19	35	62
33D	50	50	21	51	82

^a SEC performed in DMF using a dn/dc. ^b Calculated from the $^1\text{H-NMR}$ spectrum in D_2O

We also performed size exclusion chromatography (SEC) on the different copolymers solubilized in sodium acetate buffer (pH = 4). However, these analyses failed to provide simple chromatograms (**Figure 29**): we attributed this observation to the significant hydrophobic content that introduced incompatibility with the aqueous medium (nano aggregation). Indeed, we observed that at 20% of hydrophobicity and above, the SEC peak split in different populations, and this splitting was more important when the hydrophobic content increased (**Figure 29 A**). The possible nano-aggregation was also confirmed with the light-scattering detection (**Figure 29 B**).

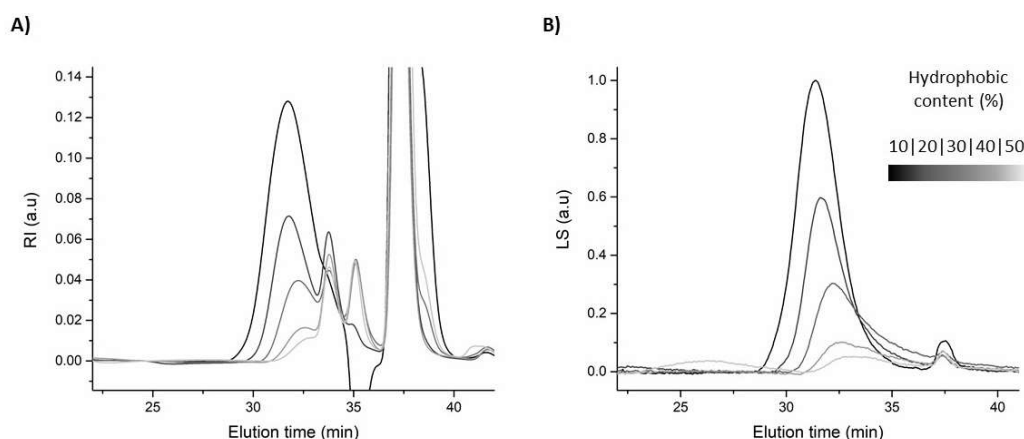


Figure 29. Chromatograms of the copolymers **29D-33D** with hydrophobic content variation performed in sodium acetate buffer 0.5 M pH = 4. A) Refractive index trace and B) Light scattering trace.

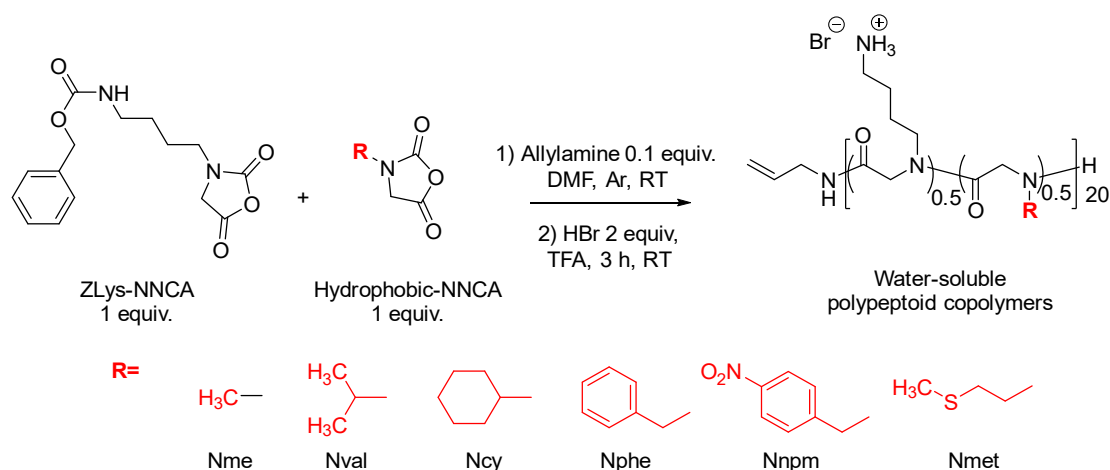
In summary, through a ring-opening copolymerization of NNCA methodology, we successfully prepared a library of water-soluble copolypeptoids with controlled hydrophobic content, polymerization degree and with narrow dispersity.

2.3 Hydrophobic building block variation

Structure-antimicrobial relationships are tools that allow the identification and the design of active macromolecules with enhanced properties.⁵ The hydrophobic content is a key parameter to kill bacteria because the cationic/hydrophobic balance allows membrane destabilization, leading to bacteria leakage and death. Moreover, the macromolecular SAR approach indicates that the chemical nature of the hydrophobic side chain also influences bioactivity.⁵⁹ As previously discussed in chapter 1 (for polypeptides), choosing the right hydrophobic monomer is crucial, as it was demonstrated by the screening of copolymers composed of *L*-lysine mixed with another amino acid (One of the following: *L*-alanine, *L*-leucine, *L*-isoleucine, *L*-phenylalanine and *L*-valine).⁶⁵ As presented in chapter 2, we developed the preparation of NNCA with various *N*-

Chapter 3. Linear polypeptoid and their antimicrobial activity

alkylation: different carbon lengths (methyl, isopropyl, cyclohexyl, benzyl) and containing heteroatoms (nitrobenzyl and methylthioethyl). In this part of the project, we decided to mix the lysine-like NNCA with all hydrophobic NNCA that were prepared. Our goal was to screen libraries of polypeptoid copolymers composed of various hydrophobic/cationic ratio (0 to 50%) at M/I = 20 (Allylamine was used as the initiator, **Scheme 31**).



Scheme 31. Synthesis diagram showing the synthesis of a library of copolymers varying the chemical nature of the hydrophobic side-chain.

All the ring-opening copolymerizations were carried out following the same procedure as the one which was developed in section 2.2 (all procedures and compound characterizations are given in the experimental section). We then performed the deprotection procedure optimized for P(Nlys)**28D**, as presented in section 2.1. All copolymers were deprotected in TFA by adding 2 equivalents of HBr (relative to cationic side chains). Upon 3 h of deprotection the copolymers were purified by precipitation in diethyl ether, then dialyzed and freeze-dried. This step afforded cationic copolymers in yields varying from 30 to 80%. We tested all copolypeptoids over *C. difficile*. The evaluations were performed in the framework of a collaborative effort with the Pasteur Institute (Dr. Bruno Dupuy and Antoine Tronnet did all the antimicrobial evaluations on this pathogen). We first implemented a fast screening of the libraries of copolypeptoids using a 96-well plate using brain-heart infusion (BHI) culture medium: in each well, approximately 10^5 colony-forming units per mL (CFU/mL) of *C. difficile* were inoculated with increasing concentrations of polypeptoids and incubated under CO₂ atmosphere for 24 h at 37 °C. We calculated the percentage of the optical density ($\lambda = 580$ nm) at initial time and after 24 h, reported as percentage of the inhibition of *C. difficile* growth (**Figure 30**).

Chapter 3. Linear polypeptoid and their antimicrobial activity

We observed that both the chemical nature of the nitrogen alkyl substituent and the hydrophobic content were key parameters to inhibit the growth of *C. difficile* (**Figure 30**). For instance, copolymers made with phenylalanine-like units demonstrated a clear decrease in turbidity at H/C > 30%. At H/C = 50%, the decrease in turbidity was observed down to 12.5 µg/mL: the antimicrobial activity of the copolymers augmented when we increased the hydrophobic content up to 50%.

Regarding the less hydrophobic side-chains *N*-methyl (Nme) and *N*-isopropyl (Nval), we were not able to detect any antimicrobial activity while we increased the hydrophobic content up

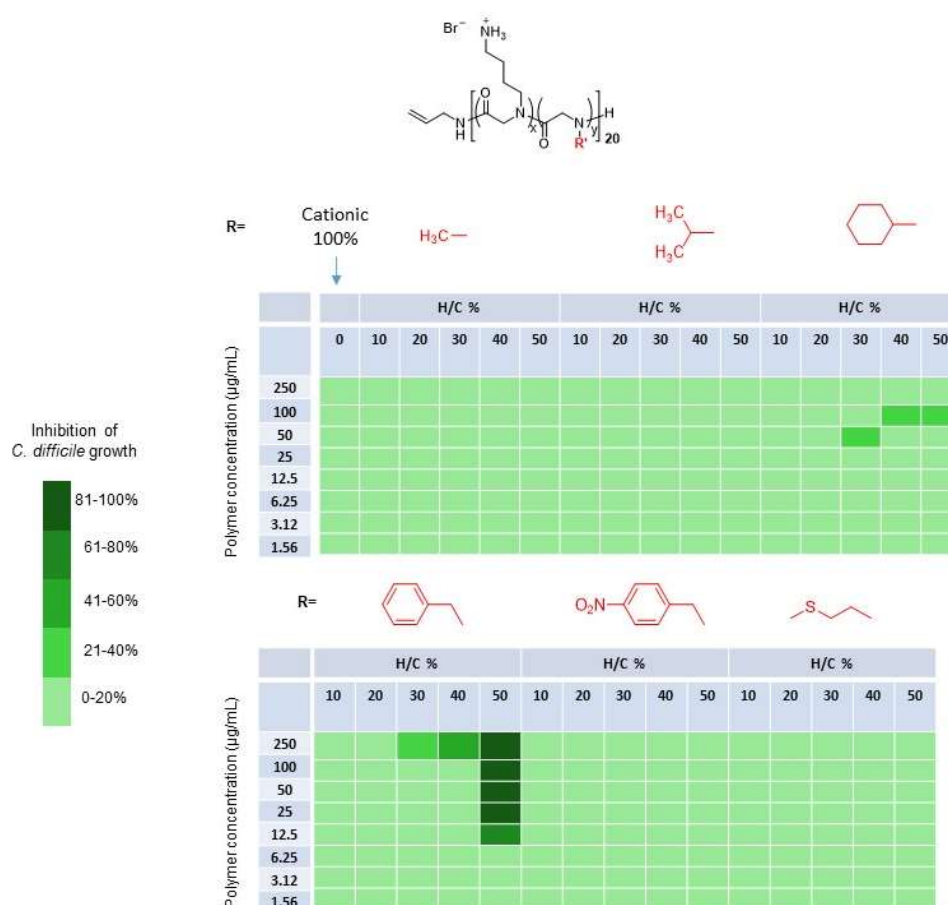


Figure 30. Hydrophobic influence on the inhibition of the growth of *C. difficile*. The increase of the color intensity represents a higher inhibition of bacterial growth (H/C % is the hydrophobic/cationic ratio or hydrophobic content).

to 50%. However, a slight decrease in turbidity was observed with copolymers composed of monomer units bearing cyclohexyl side chains: we observed a possible activity above 40-50% of hydrophobic content, the best parameters for copolymers composed of phenylalanine-like units.

The turbidity changes observed at the H/C ratio of 50% prompted us to examine carefully the characterization of the corresponding copolymers. First, we performed NMR and SEC analyses on the copolymers before deprotection (**Figure 31, Table 21**). We evaluated the DP_{NMR} and hydrophobic content by 1H -NMR in $DMSO-d_6$ (**Figure 31**). We determined the polymerization degree (DP_{NMR}) by comparing the integration of the signals corresponding to the initiator peak (*b*, 5.8 ppm) to the integration of the signals of the polymer backbone (~3.6-4.7 ppm). Overall, we

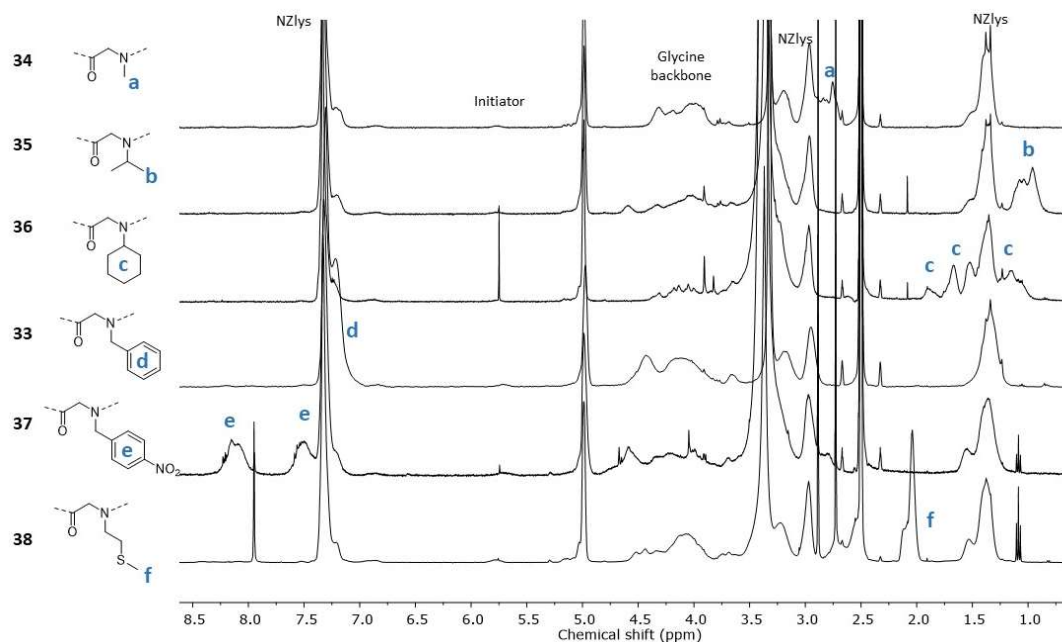


Figure 31. 1H -NMR spectra in $DMSO-d_6$ for the characteristic signals of the hydrophobic side chains in copolymers with ZNlys at 50% hydrophobic content and $M/I = 20$.

determined DP_{NMR} in agreement with the expected values ($DP_{NMR} = 18-27$, **Table 30**). The highest DP_{NMR} for poly(Nlys-Nme) was in agreement with a higher molar mass and attributed to an inaccuracy during this specific experiment. Because the antimicrobial activity was inexistent, we did not redo the experiment. We also verified the hydrophobic content of all the copolymers by comparing the integrations of the signal of the polymer backbone (CH_2 , peak *d, d'*, 3.83-4.66 ppm) to the integration of the signal of the side chains (*e-f*, **Figure 31**). We found hydrophobic content in agreement with the expected ratio (46-53%, **Table 21**).

On another hand, SEC characterization showed that we prepared copolymers with molar masses in the range of 3200-5900 g/mol that were in agreement with the targeted size (**Table 21**). The isolated copolymers followed a relatively wide range of polymer dispersity (\bar{D}_M) from 1.04 to 1.32. The samples that presented higher \bar{D}_M values were the copolymers incorporating

Chapter 3. Linear polypeptoid and their antimicrobial activity

hydrophobic monomer units with more sterically hindered *N*-alkylation (*N*-isopropyl and *N*-cyclohexyl), the ROP reaction exhibiting zero order kinetic rates (see section 1.2). The copolymer with the highest \bar{D}_M value of 1.32 was the one made of Nnpm units and this dispersity was corroborating the already broad dispersity encountered when the homopolymer was synthesized (see section 1.1.3, P(Nnpm)).

Table 21. Series of copolymers varying the hydrophobic side chain before deprotection (**33**, **34-38**): molar masses from SEC, DP_{NMR} , hydrophobic content from NMR and yields

Hydrophobic side-chain	MW theo (g/mol)	M_n (g/mol) ^a	M_w (g/mol)	\bar{D}_M	DP_{NMR} ^b	Hydrophobic content (%) ^b	Yield (%)
Nme (34)	3300	5300	5600	1.06	27	47	59
Nval (35)	3600	3200	3900	1.26	22	45	35
Ncy (36)	4000	2800	3400	1.19	23	51	40
Nphe (33)	4100	5100	5400	1.05	23	49	70
Nnpm (37)	4600	4200	5600	1.32	18	43	59
Nmet (38)	3900	5900	6200	1.04	22	53	53

^a SEC performed in DMF using a $dn/dc=0.0819$. ^b Calculated from the ¹H-NMR spectrum in DMSO-*d*₆

Second, we performed NMR and SEC analyses on the copolymers after deprotection (**Table 22**). The copolymers were fully characterized by ¹H-NMR in D₂O: the spectra revealed in each case the presence of the protons attributable to the initiator (5.8 ppm), *N*-substituents, and glycine backbone (**Figure 32**). To evaluate the DP_{NMR} we use the integration of the initiator signals and we compared it with the integration of the peak of the glycine backbone (~3.6-4.6 ppm). They were all in agreement with the values before deprotection ($DP_{NMR} = 20-27$). Further comparison between integrations of the peaks attributed to glycine backbone and to the hydrophobic side-chain provided the hydrophobic content (**Figure 32**). Overall, a good correlation between expected and calculated hydrophobic content was observed (43-54%, **Table 22**). Therefore, ¹H-NMR confirmed that we successfully prepared a small library of copolypeptoids with variable target hydrophobic contents.

Table 22. Copolymers varying the *N*-alkylated side chain (**33D**, **34D-38D**): molar masses from SEC, DP_{NMR} , and yields upon deprotection.

Hydrophobic side-chain	DP_{NMR} ^b	Hydrophobic content (%) ^b	Yield upon deprotection (%)
Nme (34D)	27	50	57
Nval (35D)	22	50	48
Ncy (36D)	23	54	72
Nphe (33D)	21	51	82
Nnpm (37D)	19	52	31
Nmet (38D)	22	43	38

^a SEC performed in DMF using a $dn/dc=0.0819$. ^b Calculated from the ¹H-NMR spectrum in D₂O

Chapter 3. Linear polypeptoid and their antimicrobial activity

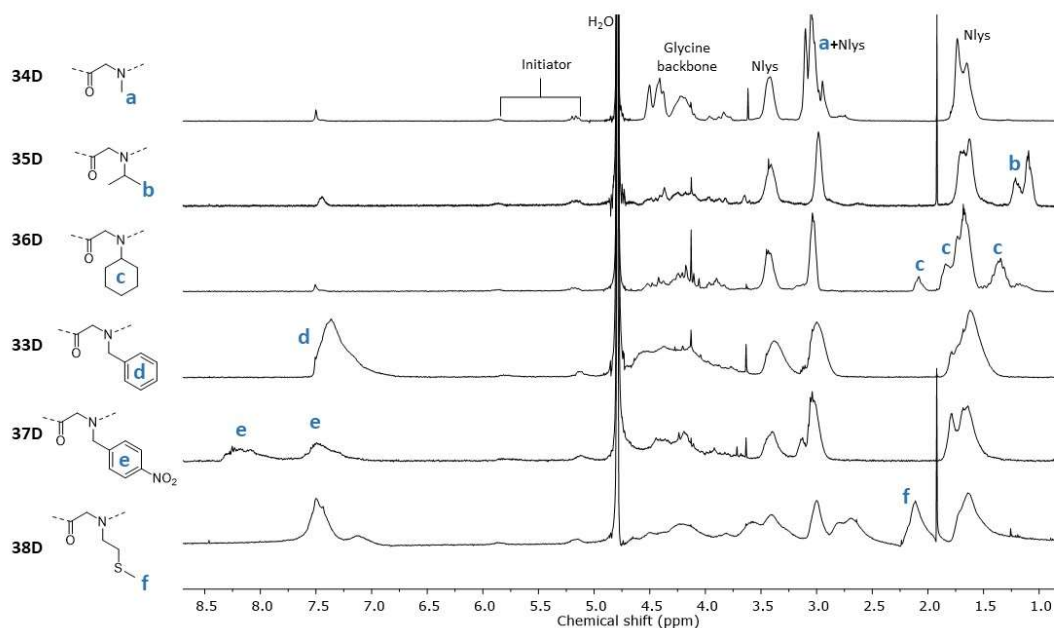


Figure 32. $^1\text{H-NMR}$ spectra in D_2O for the characteristic signals of the hydrophobic side chains in copolymers with Nlys at 50% hydrophobic content and $M/I = 20$.

We finally calculated the minimum inhibitory concentration (MIC) from the microdilution method (**Figure 33**) for the copolymers bearing different *N*-alkylated hydrophobic groups at $H/C = 50\%$. In this study, the bacteria (approximately 10^5 CFU/mL) were incubated in a brain-heart infusion medium (BHI) for 24 h under CO_2 atmosphere with increasing concentrations of polypeptoids, to determine the concentration at which no bacterial growth was observed, commonly named as minimal inhibitory concentration (MIC).

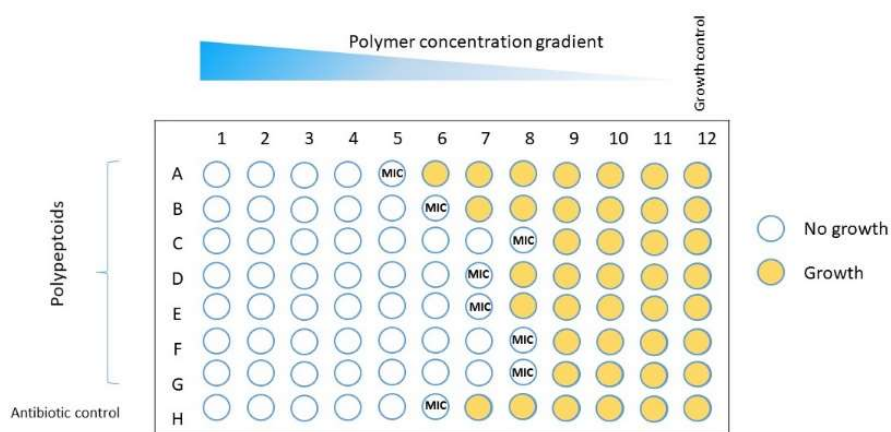


Figure 33. Microdilution methodology to determine the MIC against *C. difficile*.

Chapter 3. Linear polypeptoid and their antimicrobial activity

A MIC value of 15.6 $\mu\text{g/mL}$ (4.2 μM , using $\text{MW} = 3700 \text{ g/mol}$ from DP_{NMR} in D_2O) was calculated for poly(Nlys-Nphe)₂₀ the most active compound (**Table 23**). Unfortunately, the results showed that we could not observe MIC values below 100 $\mu\text{g/mL}$ for the other polymers containing alkylated side chains such as Nme, Nval, Ncy, Nnpm, or Nmet (**34D-38D**). The result of a poor MIC > 100 $\mu\text{g/mL}$ corresponding to poly(Nlys-Nme) **34D** is not surprising since P(Nme) homopolymers are already soluble in water meaning that the hydrophobicity of the *N*-methylated unit was very low. However, we were surprised that copolymers having either Nval or Ncy in our design did not present MIC < 100 $\mu\text{g/mL}$. Moreover, it was also surprising that copolymers having Nnpm moieties were inactive while Nphe presented a good activity. Therefore, we selected a hydrophobic content of 50% because its superior antimicrobial activity (**Table 23**)

Table 23. Antimicrobial activity determination against *C. difficile* of copolymers varying the hydrophobic side-chain at $M/I = 20$.

Polypeptoid	Hydrophobic content (%) ^a	MIC ($\mu\text{g/mL}$)	Polypeptoid	Hydrophobic content (%) ^a	MIC ($\mu\text{g/mL}$)
34D	51	>100	33D	46	15.6
35D	54	>100	37D	52	>100
36D	52	>100	38D	43	>100

^a Calculated from the ¹H-NMR spectrum in D₂O

At this stage of the research project, we identified an active macromolecular compound poly(Nlys-Nphe)₂₀ (**33D**): the targeted M/I was 20 and the targeted hydrophobic content was 50%. Moreover, the copolymer was composed of phenylalanine-like units, and the aromaticity of the side chain was an important pharmacophore to inhibit *C. difficile* growth.

3 Optimization of the activity against *C. difficile* by implementing a macromolecular SAR approach

SAR approaches have been often developed with peptides using SPPS (solid-phase synthesis). One of the most representative examples of such SAR study is the work of M. Inoue *et al.* about the preparation of gramicidin analogs with improved selectivity.⁶⁸ They performed a screening of 4096 peptides through a multidimensional design varying 6 of 15 amino acid residues using *D*-Leu, *D*-Val, *D*-Asm, and *D*-Thr (design 4⁶). Ten active molecules incorporating leucine and valine were finally selected (13-54% yields) to kill *S. pyogenes* (MIC = 16 nM): they showed a similar mechanism of action as compared to gramicidin (membrane-pore formation) but an improved selectivity (SI = 1.06 instead of 0.17). More recent works showed that the selectivity of other AMPs can be enhanced by varying the sequence⁶⁹ or the hydrophobic content (18%)⁷⁰ when the goal was to kill Gram-positive and Gram-negative bacteria.

Similarly to peptides, SAR approaches have already been developed with peptoids prepared through SPPS.⁷¹ A. Barron *et al.* used the SAR approach to prepare antimicrobial molecules composed of lysine-like units (Nlys) mixed with a variety of hydrophobic units: *N*-(*S*)-phenylethylglycine (Nspe), (*S*)-*N*-(1-naphthylethyl)glycine, (*S*)-*N*-(1-methylbutyl)glycine, (*S*)-*N*-(*sec*-butyl)glycine, *N*-(methylimidazole)glycine, (*R*)-*N*-(1-phenylethyl)glycine and *N*-(2-carboxyethyl)glycine.¹⁰ The peptoids that included in their sequence lysine-like (Nlys) and *S*-ethylphenyl moieties demonstrated optimal selectivity with a broad-spectrum activity (MIC = 1.7-28 μ M). Several important findings were also demonstrated:

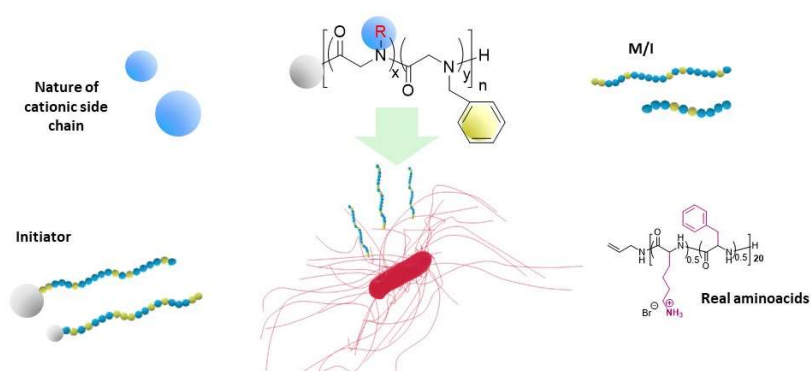
- the helical structure was not necessary to the activity;
- a +3 net charge was present in all the active compounds and generally, the increase of hydrophobicity was directly related to increased hemolytic activity.

The hydrophobicity of the side-chains was further explored by introducing binaphthyl substituents^{11,12} or through the length variation of the *N*-hydrophobic substituent using pentyl, decyl, and tridecyl alkyl side chains.¹³ In both cases, these modifications resulted in higher activity against bacteria but also in higher hemolytic effects. Another SAR study was performed by Zuckermann who varied the sequence, length, and hydrophobicity of oligomers composed of *N*-(aminoethyl)glycine (Nae), Nlys, *N*-(isobutyl)glycine, *N*-(1-isobutyl)glycine (Nleu), *N*-(2-methylbutyl)glycine, *N*-(phenylmethyl)glycine (Nphe), *N*-(2-phenylethyl)glycine, *N*-(2,2-

Chapter 3. Linear polypeptoid and their antimicrobial activity

diphenylethyl)glycine, *N*-(5-indenyl)glycine, *N*-(2-indolethyl)glycine and Nspe.¹⁵ The optimal antibacterial activity was found for the peptoid with a +4 net charge and a proportion of 5:9 for hydrophobic aminoacid-like units, which remained active over 6 h against *E. coli* (MIC = 16 µg/mL). In order to decrease the cytotoxicity and increase the antibacterial properties Cobs and co-authors evaluated the influence of the cationic side chains using Nae, Nlys, *N*-(aminohexyl)glycine, *N*-(4-guanidylbutyl)glycine (Narg), and the hydrophobic side chains Nleu, Nphe, Nspe, *N*-(*p*-fluorobenzyl)glycine, *N*-(*m*-fluorobenzyl)glycine, *N*-(*p*-chlorobenzyl)glycine, *N*-(*p*-methoxybenzyl)glycine, *N*-(pentyl)glycine.¹⁶ They found that Narg presented higher toxicity over HepG2 and HaCaT cells. Moreover, the peptoids having a length of 12 units, +5 charge, and fluorinated substituents presented an improved activity against *E. coli* (MIC = 6 µM), *S. aureus* (MIC = 2 µM), and *S. epidermidis* (MIC < 1 µM). Finally, they also pointed out that hydrophobicity was not always an important parameter to kill the Gram-negative bacterium *E. coli*.

Despite, the fascinating promises of antimicrobial peptoids, including multidrug resistance properties^{9,10} and protease resistance,⁷² no study has reported yet activities against the deadly nosocomial bacteria *C. difficile*. The use of polypeptoids to fight against this worldwide threat is however promising since they can have a longer bioavailability in the digestive tract in comparison to AMPs.^{73,74} Furthermore, in previous reports, polypeptides demonstrated activity against multidrug-resistant bacteria.⁵⁹ However, antimicrobial copolymers based on lysine and phenylalanine are not commonly found in the literature.⁶⁷ Therefore, in this section we will describe the design optimization of copolymers based on Nlys and Nphe through the anti-*C. difficile* structure-antimicrobial relationships (**Scheme 32**). We have investigated different macro-

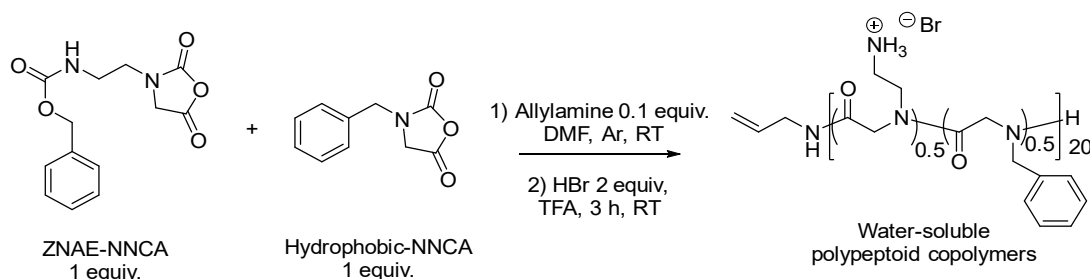


Scheme 32. Structure-antimicrobial relationship design against *C. difficile*.

molecular parameters (nature of cationic building block, polymerization degree, amino acid-based copolymers and initiator) to explore and render the antibacterial activity.

3.1 Nature of cationic side chain: *N*-(aminoethyl) versus *N*-(aminobutyl)

As reported with polymers based on acrylates, the way the nature of the cationic charge is an important parameter that strongly modifies the antibacterial activity.^{75,76} In this direction, SAR approach recently showed that polypeptide copolymers based on ornithine (a not human cationic amino acid with a carbon chain length of 3 atoms) have a better long-term and biofilm disruptive action in comparison to lysine analogs.⁷⁷ As presented in chapter 2, we have developed the preparation of NNCA's bearing a *N*-protected-2-aminoethyl group in ZNAE-NNCA to be compared to *N*-protected-4-aminobutyl group in ZLys-NNCA. Our goal was to prepare a copolymer in which ZLys-NNCA is replaced by ZNAE-NNCA to compare the antimicrobial activity with a controlled hydrophobic content when mixing with Phe-NNCA. We carried out the copolymerization using Phe-NNCA as hydrophobic block at M/I = 20 and 50% of hydrophobic content using allylamine as the initiator (**Scheme 33**).



Scheme 33. Strategy to prepare copolymers varying the hydrophobic side-chain.

Upon full conversion (~15 days), the copolymer P(ZNae-Nphe) (**39**) was isolated by precipitation, obtained as a yellowish powder in a 74% yield and characterized by SEC (**Table 24**). The copolymer presented a molar mass in agreement with the theoretical value ($M_n=3800$ g/mol versus an expected 4100 g/mol) and narrow dispersity $\mathcal{D}_M = 1.11$

Table 24. Results for P(ZNae-Nphe) (**39**) copolymers: molar mass from SEC, DP_{NMR} , and yield before deprotection.

Hydrophobic side-chain	M/I	Hydrophobic content theoretical (%)	MW theo (g/mol)	M_n (g/mol) ^a	M_w (g/mol)	\mathcal{D}_M	DP_{NMR} ^b	Hydrophobic content (%) ^p	Yield (%)
Nphe	20	50	3800	4600	5100	1.11	22	49	74

^a SEC performed in DMF. ^b Calculated from the ¹H-NMR spectrum in DMSO-d₆

The copolymer was then characterized by $^1\text{H-NMR}$ in DMSO-d_6 (**Figure 34a**). We determined the DP_{NMR} by calculating the polymerization degree from the integrations of the initiator peak (*b*, 5.8 ppm) and the polymer backbone (*d*, *d'*): a DP_{NMR} value of 22 was obtained that was close to the *M/I*. Then, we determined the hydrophobic content by comparing integrations of the signals of the polymer backbone (CH_2 , peak *d*, *d'*, 3.83-4.66 ppm) to the signals from the side chains (*e-h*) and we found a hydrophobic content of 49% similar to the 50% expected.

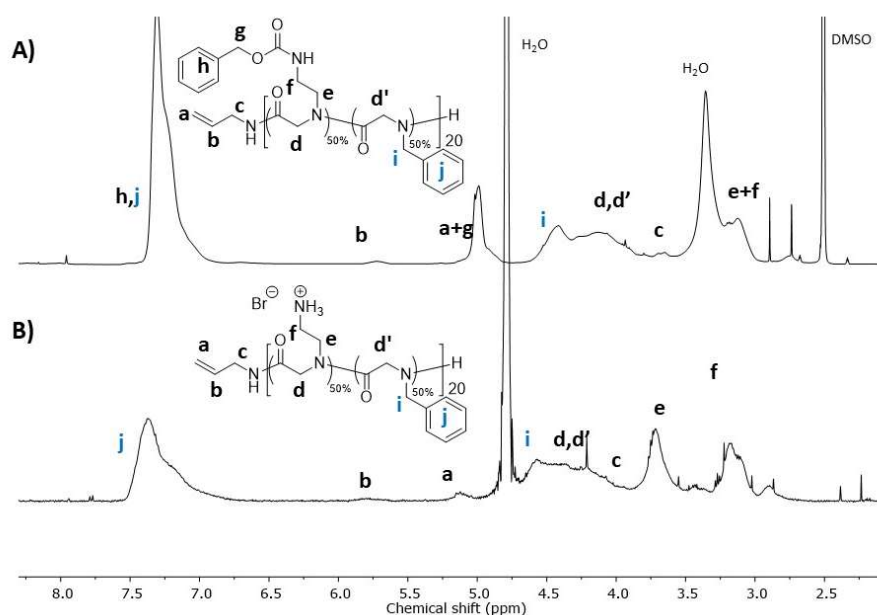


Figure 34. $^1\text{H-NMR}$ spectra for the characteristic signals of the hydrophobic side chains in copolymers with *N*-2-aminoethyl glycine at 50% hydrophobic content and *M/I* = 20. A) spectrum before deprotection in DMSO-d_6 (**39**) and B) spectrum upon deprotection in D_2O (**39D**).

Upon deprotection (HBr 2 equiv. in TFA for 3 h) the copolymer was isolated by precipitation in diethyl ether, dialyzed, and freeze-dried (yield of 44%). The resulting powder was analyzed by $^1\text{H-NMR}$ using D_2O . On the spectrum, we observed the presence of the protons corresponding to the cationic and hydrophobic side-chains (*j*, **Figure 34b**), as well as protons attributable to the polymer backbone (*d*, *d'*, 4.52-3.91 ppm) and initiator (*b*, 5.87-5.67 ppm). We then calculated the polymerization degree using the integration of the signal of initiator (*b*) and polymer backbone (*d*, *d'*) and we found a $\text{DP}_{\text{NMR}} = 18$ in agreement with the one found before deprotection (**Table 25**). Moreover, we determined the hydrophobic content using the signals of the polymer backbone and side chains (*j*, *e*, *f*, **Figure 34b**) and we found a value of 44% in agreement with the one found before deprotection. Interestingly, we prepared copolymers using ZNAE-NNCA and Phe-NNCA by ROP with controlled hydrophobic content, polymerization degree and with narrow dispersity.

Chapter 3. Linear polypeptoid and their antimicrobial activity

Table 25. Results for P(Nae-Nphe) (**39D**) copolymers: DP_{NMR} , and yield upon deprotection.

Hydrophobic side-chain	M/I	Hydrophobic content theoretical (%)	DP_{NMR}^a	Hydrophobic content (%) ^a	Yield upon deprotection (%)
Nphe	20	50	18	45	44

^a Calculated from the ¹H-NMR spectrum in D₂O upon deprotection

The nature of the cationic side chain is reported as a relatively important parameter for the SAR approach of peptoids.^{14,15} Therefore, we determined the MIC value using the microdilution method (**Figure 33** and corresponding discussion) for the copolymer P(Nae-Nphe) H/C = 50% **39D**. Unfortunately, we could not find a MIC value for P(Nae-Nphe) lower than 100 µg/mL (**Table 26**). This result was in agreement with previous studies where a decrease in carbon length of cationic side-chains did not improve the antibacterial activity.^{14,15} From this short study, we demonstrated that between P(Nae-Nphe) and P(Nlys-Nphe) copolymers the optimal carbon length corresponded to the lysine analog at the DP = 20 studied 15.6 µg/mL (4.2x10⁻⁶ M, using MW = 3700 g/mol from DP_{NMR} in D₂O).

Table 26. Antimicrobial activity of copolypeptoids varying the carbon chain length of the cationic residue

Polypeptoid	Hydrophobic content from ¹ H-NMR ^a	MIC (µg/mL)	MIC (M)
33D	51	15.6	4.2X10 ⁻⁶
39D	45	>100	>2.5x10 ⁻⁵

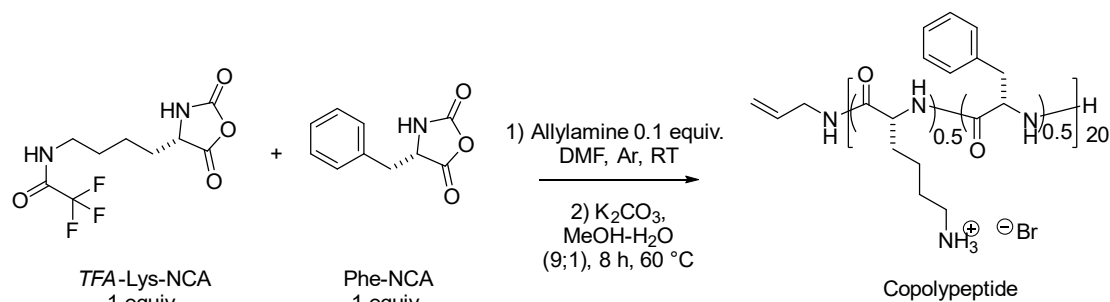
^aCalculated from H-NMR in D₂O

3.2 Polypeptoid vs polypeptide copolymers

As discussed in the introduction of this chapter, polypeptide polymers made of L-lysine and L-phenylalanine can induce the membrane destabilization of liposomes. However, the innate limited aqueous solubility of phenylalanine limits this design, even though antibacterial properties against *E. coli*, *P. aeruginosa*, *S. marcescens*, *S. aureus* and *C. albicans* were reported for a DP = 25 (30-60% hydrophobic content).⁶⁷ Therefore, as part of the structure activity-relationship

Chapter 3. Linear polypeptoid and their antimicrobial activity

approach, we prepared the copolypeptide analog of our best anti-*C. difficile* copolypeptide targeting a DP = 20 and 50% of hydrophobic content using TFA-Lys- and Phe-NCAs, and allylamine as initiator (**Scheme 34**).



Scheme 34. Synthesis of *P(Lys-Phe)*40D from TFA-Lys-NCA and Phe-NCA in two steps.

Upon full conversion (24 h), the copolymer *P(TFA-Lys-Phe)*40 was isolated by precipitation in diethyl ether, dried under vacuum and obtained as a white powder in a low yield (29%). Then the copolymer was characterized by SEC in DMF (**Table 27**). The calculated molar masses were higher than the expected values and we observed a bimodal population that provided us a dispersity of $\bar{D}_M = 1.76$. We attributed this high dispersity to the difficult use of phenylalanine NCA in ROP: oligomers of phenylalanine tend to form beta-sheets, thus such aggregates will elude at higher elution volume.

Table 27. Results for *P(TFA-Lys-Phe)* copolymers (40): molar mass from SEC, DP_{NMR} , and yield before deprotection.

	M/I	Hydrophobic content theo.l (%)	MW theo (g/mol)	M_n (g/mol) ^a	M_w (g/mol)	\bar{D}_M	DP_{NMR} ^b	Hydrophobic content (%) ^b	Yield (%)
<i>P(TFA-Lys-Phe)</i> (40)	20	50	3700	5200	12090	1.76	24	55	29

^a SEC performed in DMF. ^b Calculated from the ¹H-NMR spectrum in DMSO-d₆

Then, we characterized the copolymer by ¹H-NMR in DMSO-d₆ (**Figure 35a**). We determined the DP_{NMR} by calculating the polymerization degree from the integrations of the initiator peak (*b*, ~5.8 ppm) and the polymer backbone (*d*, *d'*, 3.65-4.64 ppm): a DP_{NMR} value of 25 was obtained that was close to the theoretical M/I. Then, we determined the hydrophobic content by comparing integrations of the signals of the polymer backbone (*d, d'*) to the signals from the side chains (*e-l*) and we found a hydrophobic content of 55% close to the 50% expected.

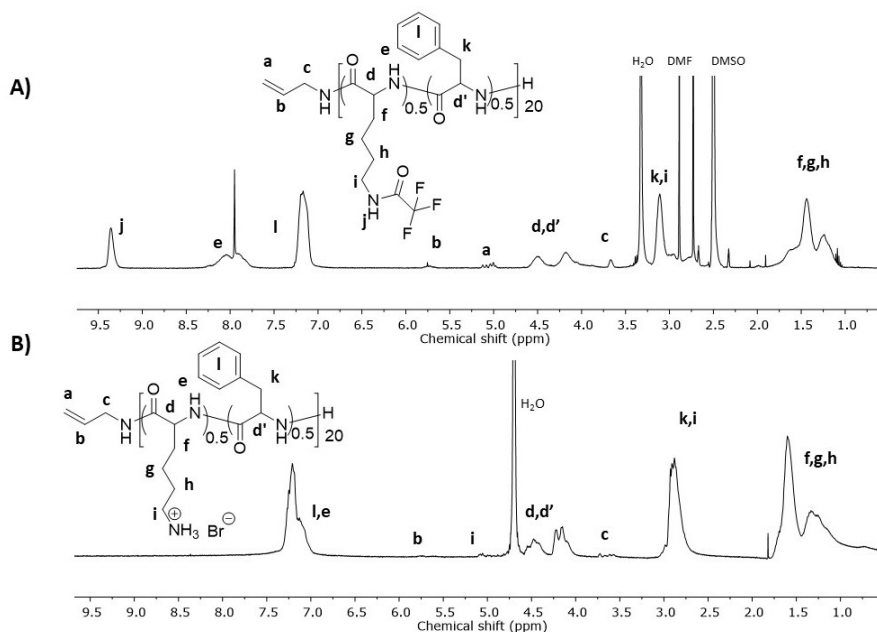


Figure 35. $^1\text{H-NMR}$ spectra for the characteristic signals of $P(\text{TFA-Lys-Phe})$ at 50% hydrophobic content and $M/I = 20$. A) spectrum before deprotection in $\text{DMSO-}d_6$ (**40**) and B) spectrum upon deprotection in D_2O (**40D**).

We then deprotected the copolymer using an adapted procedure⁷⁸ by refluxing the $P(\text{TFA-Lys-Phe})$ in a solution of K_2CO_3 (1:1 w/w) in methanol:water (9:1) for 8 h, the polymer became soluble with the progression of the deprotection. The polymer **40D** was recovered after evaporation, dialysis and freeze-drying in a 36% yield. The resulting powder was analyzed by $^1\text{H-NMR}$ using D_2O (**Figure 35b**). In the spectrum, we observed the presence of the protons corresponding to the cationic ($f-i$) and hydrophobic side-chains (k,l), as well as protons attributable to the polymer backbone (d,d' , 4.52-3.91 ppm) and initiator (b , 5.87-5.67 ppm). We then calculated the polymerization degree using the integration of the signal of initiator (b) and polymer backbone (d,d') and we found a $\text{DP}_{\text{NMR}} = 25$ in agreement with the one found before deprotection (**Table 28**). Moreover, we determined the hydrophobic content using the signals of the polymer backbone and side chains ($f-l$) and we found a value of 54% in agreement with the one found before deprotection. Therefore, we prepared the analog of the copolypeptoid $P(\text{Nlys-Nphe})$ with 50% of hydrophobic content and $\text{DP} = 20$.

Table 28. Results for $P(\text{Nae-Nphe})$ (**40D**) copolymers: DP_{NMR} , and yield upon deprotection.

Hydrophobic side-chain	M/I	Hydrophobic content theoretical (%)	DP_{NMR}^a	Hydrophobic content (%) ^a	Yield upon deprotection (%)
Nphe	20	50	25	54	36

^a Calculated from the $^1\text{H-NMR}$ spectrum in D_2O upon deprotection

Chapter 3. Linear polypeptoid and their antimicrobial activity

We then compared the anti-*C. difficile* activity of poly(Nlys_{0.5}-Nphe_{0.5})₂₀ (**33D**) to the one of the polypeptide analog (**40D**) made of lysine and phenylalanine (M/I = 20 and 50% hydrophobic content). We were able to evaluate the antimicrobial activity of the fully-aminoacid-based polymer that presented a MIC = 100 µg/mL (2.5x10⁻⁵ M, **Table 29**). However, this value was 6.4 times higher than the MIC of its polypeptoid analog. This result is particularly interesting because it demonstrated the enhanced potency that polypeptoids can present against bacteria.

Table 29. Antimicrobial activity of copolypeptoids vs copolypeptide against *C. difficile*.

Polypeptoid	Hydrophobic content from ¹ H-NMR ^a	MIC (µg/mL)	MIC (M)
33D	51	15.6	4.2x10 ⁻⁶
40D	48	100	^b 2.5x10 ⁻⁵

^a Calculated from H-NMR in DMSO-6d, ^b Calculated with MW = 4000 g/mol from DP_{NMR} = 25

3.3 M/I variation in poly(Nlys-Nphe) (DP 10, 20, 30) at 50% hydrophobic content

The macromolecular SAR approach indicates that the molar mass is a critical parameter to fight against bacteria. Many AMPs are known to induce membrane destabilization, especially small peptidic structures composed of 7 to 50 amino acid units.⁷⁹ The peptide/peptoid size can be easily modulated in one step using copolymerization. Therefore, we explored the synthesis of three different polymerization degrees for copolymers composed of Lys-like and Phe-like monomer units. We followed a procedure similar to the methodology developed in 2.1 for P(Nlys-Nphe)**28D** (**Scheme 30**). In the first step, we carried out the ROP of the NNCA mixture using allylamine as initiator, targeting a M/I = 10, 20, and 30.

The conversion was followed by FTIR (~20 days for the highest M/I). Then the copolymers were isolated by precipitation in diethyl ether and dried under vacuum in 61-70% yields (**Table 30**). The polymers were analyzed by SEC in DMF revealing molar masses (M_n) with narrow

Chapter 3. Linear polypeptoid and their antimicrobial activity

distributions and in agreement with the targeted M/I 10 and 20. For DP = 10 we observed a dispersity of $\bar{D}_M = 1.15$ and the presence of small peaks with lower molar mass that we did not observe at higher DP and we related to small oligomers (**Figure 36**).

Table 30. Series of *P(Nlys-Nphe)* varying the polymerization degree, M/I: molar masses from SEC, DP_{NMR} and yields before deprotection.

Polypeptoid	M/I theoretical	MW theo (g/mol)	M_n (g/mol) ^a	M_w (g/mol) ^a	\bar{D}_M	DP_{NMR} ^b	Hydrophobic content (%) ^b	Yield (%)
41	10	2000	2500	2900	1.15	12	47	51
33	20	4100	5100	5400	1.05	23	49	70
42	30	6100	5200	5800	1.12	35	46	61

^a SEC performed in DMF. ^b Calculated from the ¹H-NMR spectrum in DMSO-d₆

The copolymer at DP = 30 displayed a similar molar mass to DP = 20 and we related to a more compacted structure since it displayed a small hydrodynamic volume eluting at a similar elution volume (**Figure 37**). This compacted structure was attributed to a hydrophobic effect. It is to note that the dispersity was slightly increased for the sample targeted at M/I = 30: we attributed

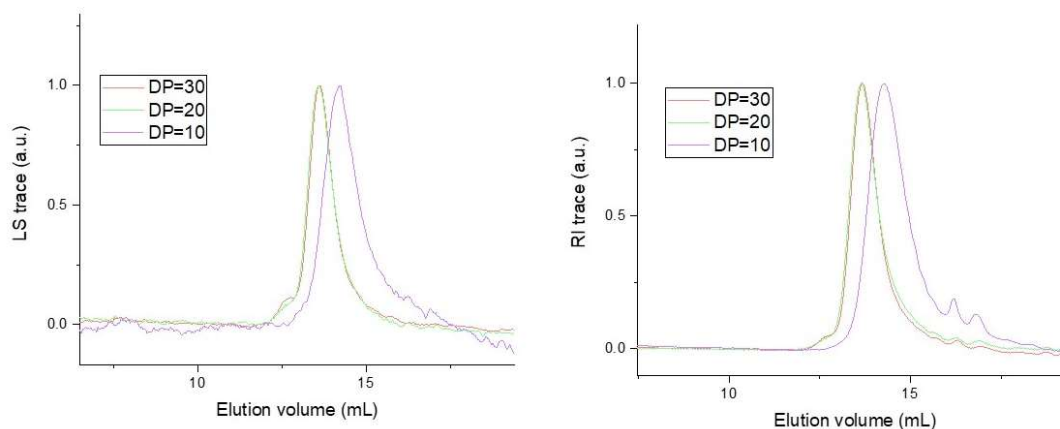


Figure 36. SEC chromatograms of the *P(Nlys-Nphe)* at different DP in DMF using MALS detection (left) and RI detection (right).

this observation to the appearance of slight turbidity during the polymerization (visually, the turbidity appeared at 90% of conversion).

Then we evaluated the DP_{NMR} and hydrophobic content by ¹H-NMR in DMSO-d₆ (**Figure 37**). First, we determined the polymerization degree by comparing the integration of the signal corresponding to the initiator peak (*b*, 5.8 ppm) to the integration of the polymer backbone peaks (*d,d'*, 3.83-4.66 ppm). DP_{NMR} were in agreement with the theoretical M/I values (**Table 30**).

Second, we determined the hydrophobic content by comparing the integration of the signals attributable to the polymer backbone and the integration of the signal attributable to hydrophobic side chains (*e-l*, **Figure 37**). We found hydrophobic content in agreement with the target values (46-51%, **Table 30**).

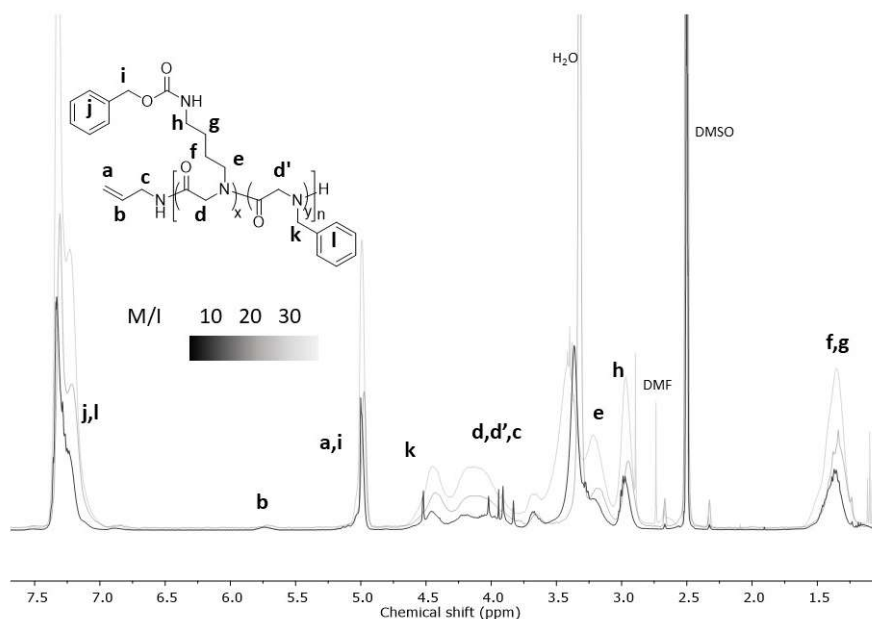


Figure 37. $^1\text{H-NMR}$ spectra in DMSO-d_6 for the characteristic signals of the hydrophobic side chains in copolymers with Nlys at 50% hydrophobic content varying the M/I (10, 20, 30).

We then performed the deprotection procedure optimized for P(Nlys)**28D** in section 2.1. All our copolymers were deprotected in TFA by adding 2 equivalents of HBr (relative to cationic side chains). Upon deprotection, the copolymers were isolated by precipitation in diethyl ether, dialyzed, and lyophilized (yields 72-90%). Upon dialysis, we observed transparent solutions for copolymer with a M/I of 10 or 20, while the copolymers with a M/I = 30 formed a cloudy solution.

To evaluate the polymerization degree and the copolymer composition, we analyzed the samples by $^1\text{H-NMR}$ in D_2O (**Figure 38**). We indeed calculated the DP_{NMR} and the hydrophobic content (as it is described in section 2.2) by carefully comparing the integration of the different signals of the initiator (*b*, 5.8 ppm) polymer backbone (*d,d'*) and side-chains (*e-k*, **Figure 38**). In general, we calculated and provided values of polymerization degree, as well as the hydrophobic content (**Table 31**) in agreement with the values obtained before deprotection. All these NMR characterizations confirmed that the copolymer did not suffer from chemical modifications during

the deprotection step.

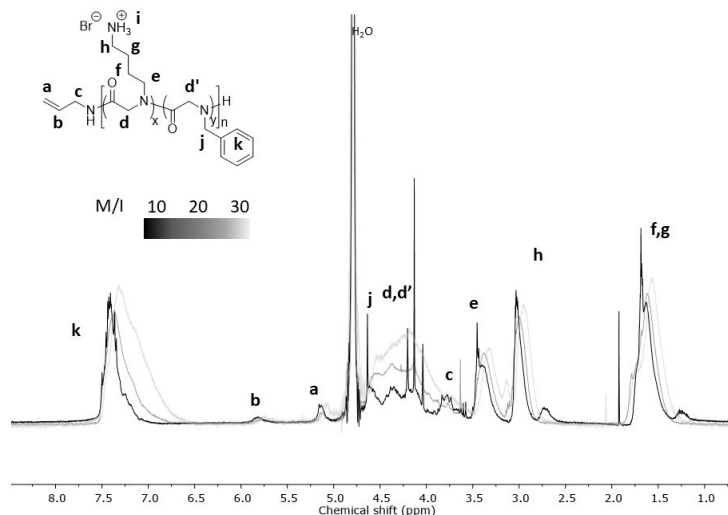


Figure 38. $^1\text{H-NMR}$ spectra in DMSO-d_6 for the characteristic signals of the hydrophobic side chains in copolymers with Nlys at 50% hydrophobic content varying the M/I (10, 20, 30).

Table 31. Series of $P(\text{Nlys-Nphe})$ varying the M/I (10, 20, 30): DP_{NMR} and yields upon deprotection.

Polypeptoid	M/I theoretical	$\text{DP}_{\text{NMR}}^{\text{b}}$	Hydrophobic content (%) ^b	Yield upon deprotection (%)
41D	10	10	50	72
33D	20	21	51	82
42D	30	35	50	90

^a SEC performed in DMF using a dn/dc. ^b Calculated from the $^1\text{H-NMR}$ spectrum in D_2O

Once we successfully prepared the copolymers $P(\text{Nlys-Nphe})$ with different polymerization degrees, we evaluated their antibacterial activity. We observed that between a $\text{DP} = 10$ and 20 the anti-*C. difficile* activity increased with a higher DP from a MIC value >100 to $15.6 \mu\text{g/mL}$, respectively (**Table 32**). In contrast with peptoids obtained by SPPS where less than 20 amino acid-like residues are necessary to produce antibacterial activity,⁸⁰ we observed that $\text{DP} = 30$ showed similar MIC values ($15.6 \mu\text{g/mL}$) to $\text{DP} = 20$. These results suggested that a minimum of 20 units were necessary to kill *C. difficile* and that the length of the polymer did not influence the antimicrobial activity from 20 to 30 aminoacid-like residues.

Chapter 3. Linear polypeptoid and their antimicrobial activity

Table 32. Antimicrobial activity of copolypeptoids varying the polymerization degree (M/I) against *C. difficile*.

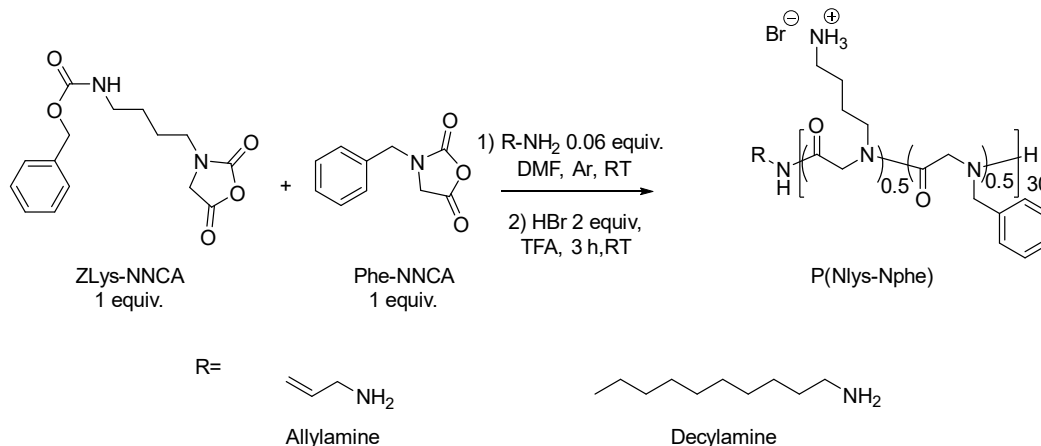
Polypeptoid	Hydrophobic content from ¹ H-NMR ^a	MIC (μg/mL)	MIC (M)
41D	50	>100	^b >2.5x10 ⁻⁵
33D	51	15.6	^c 4.2x10 ⁻⁶
42D	50	15.6	^d 2.5x10 ⁻⁶

^aCalculated from ¹H-NMR in D₂O. ^cCalculated using MW = 1800 g/mol. ^cCalculated using MW = 3700 g/mol. ^dCalculated using MW = 6200 g/mol.

3.4 Initiator variation

A polymerization reaction that implements an initiation step allows to introduce chemical moieties that can influence the antimicrobial activity. Previous work involving polyoxazolines and initiators with different carbon length showed that the best activity was obtained using hexylamine initiators.⁸¹ Therefore, as part of the SAR approach we decided to use a longer alkyl initiator. We prepared the copolymer using decylamine as initiator in the ROP of ZNlys- and Phe-NNCAs targeting a DP = 30 (DecylNH-P(Nlys-Nphe), **Scheme 35**) to compare the antimicrobial activity with P(Nlys-Nphe) initiated with allylamine at DP = 30 (prepared in 3.3).

The conversion was followed by FTIR (~20 days). Then, the copolymers were isolated by precipitation in diethyl ether and dried under vacuum in a 57% yield (**Table 33**). The results carried out by SEC in DMF revealed molar masses M_n =4500 g/mol that were lower than the expected value (similar effect described in 3.5) having a dispersity of \mathcal{D}_M = 1.18.



Scheme 35. 2-Step synthesis route to prepare DecylNH-P(Nlys-Nphe)**43D** and **42D**.

Table 33. Results for decylNH-Poly(ZNlys-Nphe) at 50% hydrophobic content: molar mass from SEC, DP_{NMR} and yields

Polypeptoid	Initiator	MW theo (g/mol)	M_n (g/mol) ^a	M_w (g/mol)	\bar{D}_M	DP_{NMR}^b	Hydrophobic content (%) ^b	Yield (%)
43l	Decylamine	6300	4500	5000	1.18	31	49	57

^a SEC performed in DMF. ^b Calculated from the ¹H-NMR spectrum in DMSO-*d*₆

Then we evaluated the DP_{NMR} and hydrophobic content by ¹H-NMR in DMSO-*d*₆ (**Figure 39a**). We determined the polymerization degree by correlation of the integration of the corresponding to the initiator peak (*a*, 0.84 ppm) and the integration of the polymer backbone peaks. We observed DP_{NMR} in agreement with the expected values ($DP_{\text{NMR}}=31$, **Table 33**).

Second, we determined the hydrophobic content by correlation of signal integration of polymer backbone and the signal integration of the side chains (*Nlys* and *Nphe*, **Figure 39a**). We found hydrophobic content in agreement with the theoretical values (49%,).

Upon deprotection (HBr 2 equiv. in TFA for 3 h), the copolymers were isolated having yields between 97%. We confirmed the existence of copolymers [P(Nlys-Nphe)] initiated with the different primary amines by ¹H-NMR in D₂O (**Figure 39b**).

Then we calculated the polymerization degree using the integration of the signals corresponding to the initiators (*a*, 0.83 ppm) and the polymer backbone (glycine backbone, CH₂, 3.69-4.45 ppm) that were in agreement with the values before deprotection (**Table 34**). Then, we determined the hydrophobic content correlating the integration of the *Nlys* and *Nphe* moieties as

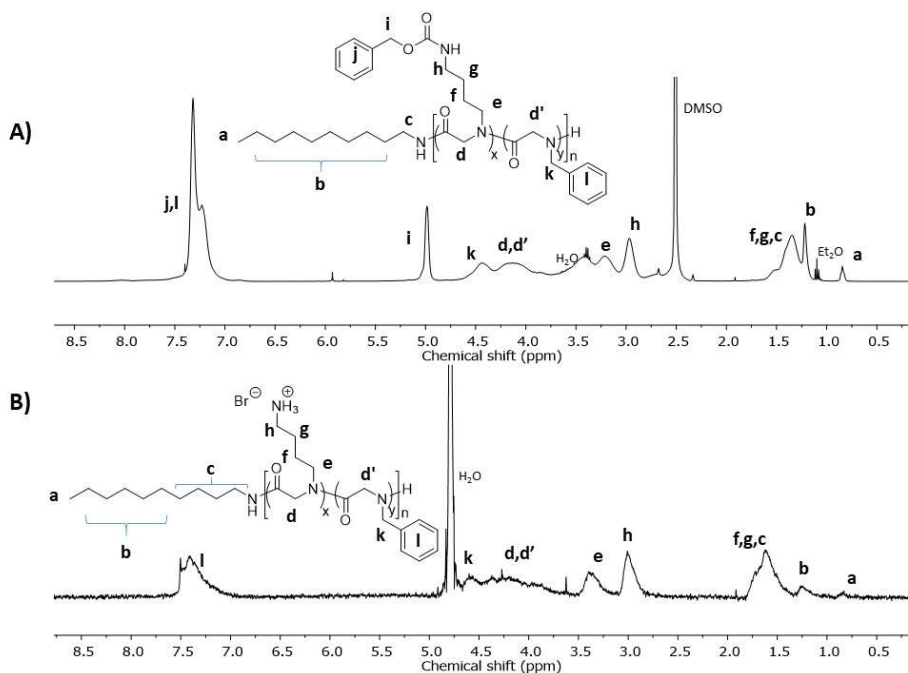


Figure 39. $^1\text{H-NMR}$ spectra for decylamine initiated ROP of ZLys- and Phe-NNCAs at $DP = 30$ and 50 % hydrophobic content: a) before deprotection in $\text{DMSO-}d_6$ and b) upon deprotection in D_2O .

it was discussed previously. We found values in agreement with the theoretical ones and with the results before deprotection (54% hydrophobic content).

Table 34. DecylINH-Poly(NIys-Nphe)**43D** characterization: DP_{NMR} and yield upon deprotection.

Polypeptoid	Initiator	DP_{NMR}^b	Hydrophobic content (%) ^a	Yield upon deprotection (%)
43D	Decylamine	30	54	97

^a Calculated from the $^1\text{H-NMR}$ spectrum in D_2O

The initiator can contribute to the hydrophobic content depending of the length of the carbon chain.⁸¹ Once we successfully prepared the copolymers DecylINH-P(NIys-Nphe)**43D** using decylamine as initiator, we determined its MIC on *C. difficile*. We evaluate two different copolymers initiated with allylamine and decylamine against *C. difficile*. We observed similar activity in both copolypeptoids (MIC=15.6 $\mu\text{g/mL}$, **Table 35**). These results indicated that the carbon length of the initiator did not seem to influence the antimicrobial activity against *C. difficile*.

Chapter 3. Linear polypeptoid and their antimicrobial activity

Table 35. Antimicrobial activity of copolypeptoids varying the initiator against *C. difficile*.

Polypeptoid	Hydrophobic content from $^1\text{H-NMR}^a$	MIC ($\mu\text{g/mL}$)	MIC (M)
42D	45	15.6	2.5×10^{-6}
43D	49	15.6	2.8×10^{-6}

^a Calculated from H-NMR in DMSO- d_6 . ^b Calculated with MW = 5500 g/mol from $\text{DP}_{\text{NMR}} = 30$

Through the ROP of NNCAs initiated by primary amines, we could successfully prepare a series of compounds that were further studied against bacteria. The structure-antimicrobial relationships allowed to select the optimal parameters to fight against *C. difficile*, observing that 50% of hydrophobic content and Nphe moieties were necessary to inhibit bacterial growth. Then, we observed that the structural parameters such as the length of the carbon chain of the cationic unit permitted to choose the copolymers bearing Nlys cationic moiety due to a higher anti-*C. difficile* activity (MIC = 15.6 $\mu\text{g/mL}$) in comparison to Nae moieties (MIC > 100 $\mu\text{g/mL}$). Indeed these peptoid polymer backbones ($\text{P}(\text{Nlys}_{0.5}\text{-Nphe}_{0.5})_{20}$) were more active than the peptide-based polymers ($\text{P}(\text{Lys}_{0.5}\text{-Phe}_{0.5})_{20}$). Furthermore, a polymerization degree in the range of 20 – 30 monomer units was necessary to exhibit a similar antibacterial activity (MIC = 15.6 $\mu\text{g/mL}$). Finally, by replacing the initiator allylamine for a longer one (decylamine) we preserved the same anti-*C. difficile* properties.

3.5 Selectivity of the active compounds towards Caco-2 cells

In the preparation of new therapeutic agents, particularly anti-infective ones, the cytotoxicity evaluation is part of the requirements to ensure that new chemical entities are really active *via* a selective mechanism and are not only unselective poisons. In past years, a parameter that was widely used to describe the cytotoxicity of AMPs and the biomimetic polymer analogs was the

Chapter 3. Linear polypeptoid and their antimicrobial activity

hemolytic activity because is a simple, cheap and fast test but now these evaluations tend to be done on mammalian cell lines or even *in vivo*.^{5,82,83} Here we evaluated the cytotoxicity over a Caco2-cell line which are intestinal epithelial cells used as a model of the intestinal barrier.⁸⁴ From a dose-response curve we determined the half-cytotoxic concentration (CC₅₀). The evaluations were performed in the framework of a collaborative effort with Pharmadev (Dr. Sandra Bourgeade-Delmas did all the evaluations).

The best molecules resulting from the structure-antimicrobial relationships were evaluated and are summarized in **Table 36**. We found that all the compounds presented a cytotoxicity value CC₅₀ > 143 µg/mL over the Caco2 cell line. The cytotoxicities of the copolypeptoids were comparable to the ones of commercial antibiotics vancomycin and metronidazole or the natural antimicrobial peptide LL-37.

In order to determine how selective were the copolypeptoids, we determined the selectivity index (SI) by the division of the CC₅₀ over the MIC values. Although the selectivity of all our copolypeptoids was lower in comparison to the commercial controls, we demonstrated that they were superior to the one presented for the peptide LL-37. Interestingly, we observed an improvement of the cytotoxicity, as well as SI, when we increased the M/I from 20 to 30 monomer units which demonstrated that also we improved the cytotoxicity simultaneously through the SAR. However, an increase of the initiator carbon length increased the cytotoxicity (CC₅₀ = 89.6 µg/mL). Moreover, when we analyzed carefully the MIC value we observed that molecule **42D** (2.5 µM) was in the same range of vancomycin (0.6 µM) or metronidazole (4.7 µM), demonstrating the potential use for therapeutic applications.

Table 36. Selectivity of copolypeptoids towards Caco-2 cells and comparison with drug controls.

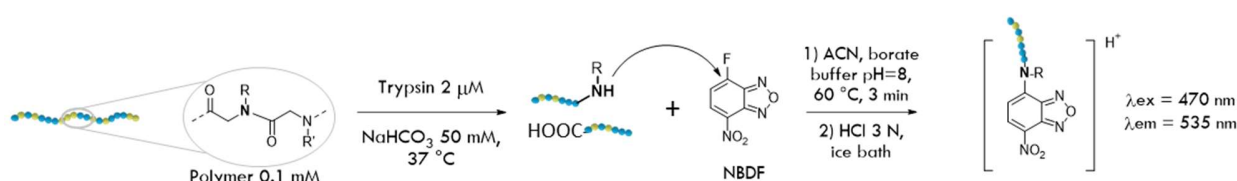
	MIC (µM)	MIC (µg/mL)	Caco2 CC ₅₀ (µg/mL)	SI (CC ₅₀ /MIC)
33D	4.2	15.6	143±13	9.2

Chapter 3. Linear polypeptoid and their antimicrobial activity

	MIC (μM)	MIC ($\mu\text{g/mL}$)	Caco2 CC ₅₀ ($\mu\text{g/mL}$)	SI (CC ₅₀ /MIC)
	2.5	15.6	211.2 \pm 20	13.5
42D				
	2.8	15.6	89.6 \pm 1	5.7
43D				
Vancomycin	0.6	0.8	>250	>312
Metronidazole	4.7	0.8	>250	>312
Fidaxomicin	0.05	0.05	141	2820
Doxorubicin	-	-	7.3	-
LL-37	2.4	12.5	213 \pm 7	17

3.6 Protease resistance of linear polypeptoids

Peptoids are known to resist proteolytic degradation mediated by proteases.⁷² This characteristic made them as an attractive strategy to develop therapeutic agents administered orally, especially for *C. difficile* that infects the digestive tract. However, proteolysis of cationic polypeptoids is scarcely documented. Here, we carried out proteolysis experiments using trypsin (one of the main proteases presented in the digestive tube), in our first experiment we measured the proteolytic activity implementing a methodology developed for small peptoids,⁷² that consisted of reacting 4-Fluoro-7-nitrobenzofurazan (NBDF) with secondary amines (S_NAr reaction) resulting from the proteolysis of the amide bonds upon digestion of the polymer (0.1 mM in NaHCO₃ buffer 50 mM pH = 7.8) at 37 °C (see the experimental section for a detailed protocol, **Scheme 36**).



Scheme 36. Proteolysis evaluation using NBDF as fluorophore precursor. “R” is either a cationic or hydrophobic group.

Chapter 3. Linear polypeptoid and their antimicrobial activity

The analysis was performed with P(Nlys-Nphe)**42D** that presented good activity against *C. difficile* and we employed a linear polypeptide (poly(lysine-phenylalanine) M/I = 200 and 9% hydrophobic content, synthesis not shown) as a polymeric reference. We followed the progression of the reaction by taking aliquots at a certain time and upon NBDF treatment we measured the fluorescence ($\lambda_{em} = 535$ nm, **Figure 40**). We observed that the linear copolypeptoid **42D** was not degraded by trypsin within 50 minutes, while the linear polypeptide was rapidly degraded in the first 20 min, thus, we concluded that linear polypeptoids presented resistance to trypsin.

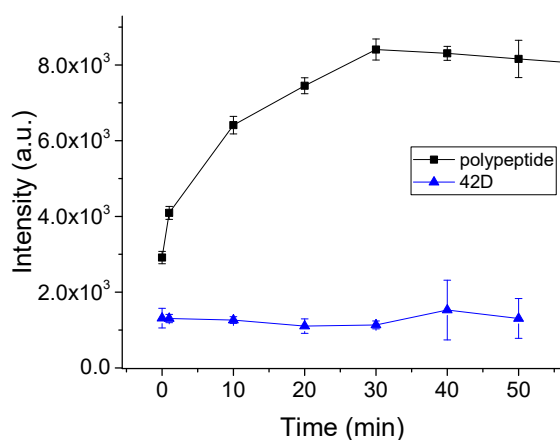


Figure 40. Linear polypeptoids resist protease activity using trypsin 2 μ M and polymer concentration 0.1 mM.

We then evaluated the antimicrobial activity (MIC) upon trypsin exposure of the AMP LL-37 and the most active P(Nlys-Nphe)**42D** (1 h at 37 °C, **Table 37**). We observed a decrease in the antimicrobial potency of LL-37 of MIC > 200 μ g/mL upon trypsin treatment, while the linear polypeptoid **42D** remained active before or upon trypsin digestion with a MIC = 15.6 μ g/mL. Therefore, we also demonstrated the trypsin resistance of linear polypeptoids in a simulated protease environment.

Table 37. Antimicrobial comparison of linear polypeptoids versus LL-37 with and without trypsin digestion.

Entry	MIC (μ g/mL)
P(Nlys-Nphe) 42D	15.6
P(Nlys-Nphe) 42D + trypsin	15.6
LL-37	12.5
LL-37 + trypsin	>200

4 Conclusion

Overall, we prepared anti-*C. difficile* polypeptoid polymers through the ROP synthesis by finely tuning the macromolecular parameters based on the structure-activity relationship. First, we studied the ROP kinetics of the small library of NNCA's reported in chapter 2 and we found different kinetic rates associated with electronic and steric effects during the ROP with a faster process in which electron-donating or less hindered *N*-alkylated groups were found. Moreover, we prepared the *Z*-protected polymer analogs of lysine (P(Nlys)) with a controlled polymerization degree, molar mass and narrow distribution ($\mathcal{D}_M = 1.08$), that we successfully deprotected with HBr (2 equiv.) in TFA preserving the polymer structure. Then, we prepared amphiphilic copolymers with controlled hydrophobic content, polymerization degree and narrow polymer dispersity ($\mathcal{D}_M < 1.4$). Then, from a first screening of the libraries of copolymers based on the SAR by varying the H/C% and the hydrophobic monomer we found the copolymer bearing phenylalanine-like moieties with a 50% of hydrophobic content P(Nlys-Nphe)₂₀ presenting good antibacterial activity. Indeed following a more detailed SAR studying structural parameters such as nature of cationic side-chain, amino acid-based polymer, polymerization degree and initiator carbon length, we concluded that optimal MIC values of 15.6 $\mu\text{g/mL}$ were encountered in copolymers with a DP = 20-30, using either allyl or decyl amine as initiator, and 50% H/C, copolymers: P(Nlys-Nphe)₂₀, P(Nlys-Nphe)₃₀ and decylNH-P(Nlys₅-Nphe)₃₀. Furthermore, from the cytotoxicity evaluation in Caco-2 cells, we determined that the best molecule with the lowest cytotoxicity ($\text{CC}_{50} = 211.2 \mu\text{g/mL}$) was P(Nlys-Nphe)₃₀ with the highest selectivity index SI = 13.5. Finally, we demonstrated that linear polypeptoids are resistant to protease activity, specifically for trypsin.

5 Materials and methods

5.1 Materials

All the chemicals and solvents in this work were purchased from Sigma Aldrich, Fluorochem, Acros, TCI, Strem and, unless otherwise described, were used without any purification. Dimethylformamide (DMF), tetrahydrofuran (THF) were obtained from a solvent system purificator at the Laboratoire de Chimie des Polymères Organique (PureSolv, Innovative Technology, LCPO Bordeaux), kept under argon atmosphere and freshly used. MiliQ water was obtained from a (Purelab Prima, ELGA).

5.2 Equipment and measurements

Glovebox

The monomers synthesized were stored at 4 °C under argon atmosphere and weighted in the glovebox Jacomex GP13 No. 2675 at the LCPO (Bordeaux, France).

Infrared (IR) spectroscopy

The IR spectra we recorded using the FTIR spectrometer (Vertex 70, Bruker), and the samples were measured with the ATR (GladiATR, Pike Technologies) from Fisher technologies performing 32 scans (LCPO, Bordeaux, France). The raw data was obtained with the Opus7.5 software and processed using the Originlab 2016 software.

Kinetic investigations using IR spectroscopy

The analyzed compound was dissolved in the anhydrous solvent in the Schleck vessel under an argon atmosphere at 20 °C at 0.4 M. At a certain time, 50 μ L sample was taken with an argon purged syringe. The sample was dropped onto the ATR unit of the IR spectrometer and measured in the range from 400 cm^{-1} to 4000 cm^{-1} . Using the band height of the C=O stretching at about 1850 cm^{-1} , the monomer conversion could be followed, since the increase is linear in the examined concentration range. The initial value for the band at 100% conversion was corrected by a correction factor using DMF as blank. Samples were taken at different times until no change in height was present, to determine the band height, the resulting monomer conversion and the corresponding reaction time. Data analysis was carried out using the Origin lab 2016 software.

Size-exclusion chromatography (SEC)

Chapter 3. *Linear polypeptoid and their antimicrobial activity*

Molar masses were determined using three different SEC systems, depending on the polymer solubility.

-Samples that were soluble in DMF were analyzed using the system DMF/LiBr (1%), in an Ultimate 3000 HPLC System (Thermo Fisher Scientific, France) equipped with Asahipack gel columns (GF310 7.5x300 mm + GD510 7.5x300 mm) for extended temperature organic-based separations coupled to a Wyatt-756rEX Refractive Index detector and to a Dawn Helos II MALS detector. The samples were dissolved in DMF (5 mg/mL) and were run at a flow rate of 0.5 mL/min at 50°C. The chromatograms were recorded with the Chromeleon 7.2 software and Astra 7.1.0 software and analyzed using the Originlab 2016 software. Either the molar mass was calculated using a calibration curve or the dn/dc value. The calibration curve was performed with polystyrene standards with molar masses in the range 0.9-364 kg/mol. The dn/dc was determined from the injection of samples dissolved in DMF at 5 mg/L.

- Samples soluble in hexafluoro-2-propanol (HFIP+ 0,05% KTFA) were analyzed on an Ultimate 3000 system from Thermoscientific equipped with PL HFIP gel columns (300 x 7.5 mm) (exclusion limits from 100 Da to 150 000 Da), a diode array detector DAD, a multi-angle light scattering detector MALS and a differential refractive index detector dRI from Wyatt technology. The samples were dissolved in HFIP (5 mg/mL) and the analysis was carried out using a flowrate of 0.8 mL/min at 40°C. The chromatograms were recorded with the Chromeleon 7.2 and Astra 7.1.0 softwares and analyzed using the Originlab 2016 software. Either the molar mass or the dn/dc value was calculated using a calibration curve. Easivial kit of PMMA from Agilent was used as the calibration curve. The dn/dc were determined from the injection of samples dissolved in DMF at 5 mg/L.

Samples soluble in water were analyzed in an Ultimate 3000 HPLC System (Thermo Fisher Scientific) equipped with TOSOH G4000PWXL (7.8 x 300 mm) and G3000PWXL (7.8 x 300 mm) columns for extended temperature aqueous-based separations coupled to a Wyatt-756rEX Refractive Index detector and a Dawn Helos II MALS detector. The samples were dissolved in acetate buffer 0.3 M and were run at a flow rate of 0.6 mL/min at 50°C. The chromatograms were recorded with the Chromeleon 7.2 and Astra 7.1.0 softwares and analyzed using the Originlab 2016 software. Either the molar mass or the dn/dc value was calculated using a calibration curve. The calibration curve was performed with PEG standards with molar masses in the range 0.3-43.5 kg/mol.

Matrix-Assisted Laser Desorption Ionization-Time of Flight (MALDI TOF)

MALDI-MS spectra were performed at CESAMO facility (Bordeaux, France) on an Autoflex maX TOF mass spectrometer equipped with a frequency tripled Nd:YAG laser emitting at 355 nm. Spectra were recorded in the negative-ion mode using the reflectron and with an accelerating voltage of 19 kV. For MALDI-MS analyses, polysarcosine deposits were prepared according to the following recipe: polysarcosines and the cationic agent (NaI) were dissolved in methanol at 10 mg/mL. The α -CHCA matrix (α -cyano-4-hydroxycinnamic acid) solution was prepared by dissolving 10 mg in 1 mL of methanol and the solutions were combined in a 10:1:1 volume ratio (matrix: sample: salt). One microliter of this solution was deposited onto the grid and vacuum-dried before analysis. For MALDI-MS analyses, Poly(ZNlys) deposits were prepared according to the following recipe: the polymer and the cationic agent (NaI) were dissolved in methanol at 10 mg/mL. The dithranol matrix solution was prepared by dissolving 10 mg in 1 mL of dichloromethane and the solutions were combined in a 10:1:1 volume ratio (matrix: sample: salt).

5.3 Homopolypeptoids synthesis

Isolation of homopolymers by precipitation. The small library of synthesized monomers includes a variety of *N*-allylated NNCA and the homopolymers of some of them are already reported, such as PSar, PNval and PNphe and, typically, the procedures for their isolation are either precipitation⁴⁷ or dialysis.³³ Precipitation is a technique that allows the isolation of polymers in a short time while dialysis can last several days. Therefore, the solubility test was performed in different solvents for the homopolymers synthesized at M/I = 20 using allylamine as initiator to select the best solvent for precipitation.

The solubility in water and organic solvents is an important issue in most for the homopolypeptides obtained from the ROP of NCA. The homopolymers synthesized in this work presented different solvent affinity due to the nature of the *N*-alkyl-substituent and were soluble in many organic solvents. For instance, P(Nmte), P(ZNae) and P(ZNlys) presented good solubility in a variety of organic solvents including, dichloromethane, tetrahydrofuran, etc. (**Table 38**). However, this solubility was reduced in the case of polymers prepared from Cy and Phe-NNCAs, an effect that comes from strong hydrophobic interactions. The comparison between PNnpm and PNphe demonstrated that the solubility issue was possible to improve in polar organic solvents by introducing the nitro group in PNnpm. On another side, poly(*N*-valine) and poly(sarcosine) were soluble in water, as previously reported.^{20,33} Despite the differences in solubility, it was possible to find a universal solvent where all the polymers were insoluble. The universal solvent

Chapter 3. Linear polypeptoid and their antimicrobial activity

for the homopolymers was HFIP, a solvent that is well known to solubilize proteins, while the non-solvents were diethyl ether and cyclohexane. Therefore, Et₂O was chosen to isolate the different polymers presented in this thesis work.

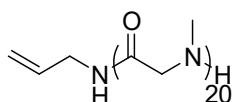
Table 38. Solubility test of the homopolymers synthesized using the small library of NNCAs, allylamine as initiator and with a *M/I* = 20.

Solvent	P(Nme)	P(Nval)	P(Ncy)	P(Nphe)	P(Nnpm)	P(Nmte)	P(ZNae)	P(ZNlys)
Cyclohexane	Insoluble	Insoluble	Insoluble	Insoluble	Insoluble	Insoluble	Insoluble	Insoluble
Et ₂ O	Insoluble	Insoluble	Insoluble	Insoluble	Insoluble	Insoluble	Insoluble	Insoluble
Toluene	Insoluble	Insoluble	Insoluble	Insoluble	Insoluble	Insoluble	Insoluble	Insoluble
DCM	Soluble	Insoluble	Insoluble	Insoluble	Insoluble	Soluble	Soluble	Soluble
THF	Soluble	Insoluble	Insoluble	Insoluble	Insoluble	Soluble	Soluble	Soluble
ACN	Soluble	Soluble	Insoluble	Insoluble	Insoluble	Soluble	Soluble	Soluble
MeOH	Soluble	Soluble	Insoluble	Insoluble	Insoluble	Soluble	Soluble	Soluble
DMF	Soluble	Insoluble	Insoluble	Insoluble	Soluble	Soluble	Soluble	Soluble
DMSO	Soluble	Soluble	Insoluble	Insoluble	Insoluble	Soluble	Soluble	Soluble
Water	Soluble	Soluble	Insoluble	Insoluble	Insoluble	Insoluble	Insoluble	Insoluble
TFA	Soluble	Soluble	Soluble	Soluble	Insoluble	Insoluble	Soluble	Soluble
HFIP	Soluble	Soluble	Soluble	Soluble	Soluble	Soluble	Soluble	Soluble

Legend: Soluble (Green), Insoluble (Orange)

Synthesis of poly(*N*-methyl)glycine [P(Nme) 20]. *N*-Methyl-NCA monomer (Sar-NCA, 0.2 g, 1.74x10⁻³ mol) was weighted in a glovebox under pure argon, introduced in a flame-dried Schlenk vessel, and dissolved with 4.3 mL of anhydrous DMF. A solution of allylamine (0.5 M in DMF) was prepared and 174 μL (8.69x10⁻⁵ mol) were added with an argon purged syringe. The solution was stirred at room temperature under argon until completion. The polymer was then recovered as a white solid by precipitation in diethyl ether and dried under high vacuum. Yield: 60% (0.074 g)

P(Nme) 20



Molecular weight: 1477 g/mol

Molar mass (SEC in DMF, dn/dc = 0.0942): $M_n=1000$ g/mol $\bar{M}_w = 1.03$

Chapter 3. Linear polypeptoid and their antimicrobial activity

The DP_{NMR} was calculated from:

$$DP_{\text{NMR}} = \frac{\sum I_H}{\frac{\sum nH}{X}}$$

where I_H is the intensity of the peak, nH is the number of protons of each peak and X is the number of signals

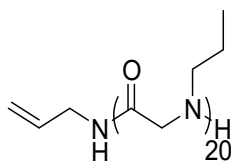
$$DP_{\text{NMR}} = 22$$

$$MW_{\text{NMR}} = (DP_{\text{NMR}} * 71 \text{ g/mol} + 57 \text{ g/mol}) = 1619 \text{ g/mol}$$

$^1\text{H-NMR}$ DMSO- d_6 400 MHz δ (ppm): 2.50-3.10 (m, 69H, CH_3), 3.62-3.80 (m, 2H, CH_2 allylamine), 3.80-4.42 (m, 42H, CH_2), 5.0-5.20 (m, 2H, CH_2 allylamine), 5.64-5.82 (m, 1H, CH allylamine). In agreement with the literature (except for the initiator peaks). NH terminal missing in these experimental conditions.

Synthesis of poly(*N*-propyl)glycine [P(Npr) 21]. *N*-propyl-NCA monomer (propyl-NNCA, 200 mg, 1.40×10^{-3} mol) was weighted in a glovebox under pure argon, introduced in a flame-dried Schlenk, and dissolved with 3.5 mL of anhydrous DMF. A solution of allylamine (0.5 M in DMF) was prepared and 140 μL (6.99×10^{-5} mol) were added with an argon purged syringe. The solution was stirred at RT under argon until completion. The polymer was then recovered as a white solid by dialysis in water (MWCO 500 Da) and freeze-dried. Yield: 58%. (0.08 g, white solid)

P(Npr) 21



Molecular weight: 2037 g/mol

Molar mass (SEC in DMF, $dn/dc = 0.0827$): $M_n = 2400$ g/mol $\bar{M}_w = 1.09$

$$DP_{\text{NMR}} = 22$$

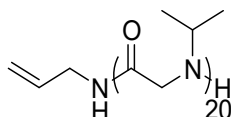
$$MW_{\text{NMR}} = (DP_{\text{NMR}} * 99 \text{ g/mol} + 57 \text{ g/mol}) = 2235 \text{ g/mol}$$

Chapter 3. Linear polypeptoid and their antimicrobial activity

$^1\text{H-NMR}$ D_2O , 400MHz δ (ppm): 0.77-1.05 (m, 38H, CH_2), 1.37-1.94 (m, 59H, CH_3), 3.10-3.54 (m, 40H, CH_2), 3.80-3.91 (m, 2H, CH_2 allylamine), 3.97-4.62 (m, 39H, CH_2), 5.16 (s, 2H, CH_2 allylamine), 5.86 (s, 1H, CH allylamine), 7.49 (s, 1H, NH terminal).

Synthesis of poly(*N*-isopropyl)glycine [P(Nval) 22]. *N*-isopropyl-NCA monomer (Val-NNCA, 174 mg, 1.22×10^{-3} mol) was weighted in a glovebox under pure argon, introduced in a flame-dried Schlenk, and dissolved with 3 mL of anhydrous DMF. A solution of allylamine (1 M in DMF) was prepared and 61 μL (6.08×10^{-5} mol) were added with an argon purged syringe. The solution was stirred at RT under argon until completion. The polymer was then recovered as a white solid by precipitation in diethyl ether and dried under a high vacuum. Yield: 60%. (0.072 g)

P(Nval) 22



Molecular weight: 2037 g/mol

Molar mass (SEC in DMF, PMMA calibration curve): $M_n = 1500$ g/mol $D_M = 1.16$

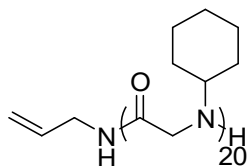
$DP_{\text{NMR}} = 24$

$MW_{\text{NMR}} = (DP_{\text{NMR}} \times 99 \text{ g/mol} + 57 \text{ g/mol}) = 2433$ g/mol

$^1\text{H-NMR}$ TFA- d 400 MHz δ (ppm): 1.03-1.57 (m, 150H, CH_3), 3.16-4.14 (m, 24H, CH), 4.52-4.15 (m, 55H, CH_2), 4.78-4.91 (m, 2H, CH_2 allylamine), 5.25 (m, 1H, CH allylamine). NH terminal missing in these experimental conditions.

Synthesis of poly(*N*-cyclohexyl)glycine [P(Ncy) 23]. *N*-cyclohexyl-NCA monomer (Cy-NNCA, 0.2 g, 1.09×10^{-3} mol) was weighted in a glovebox under pure argon, introduced in a flame-dried Schlenk, and dissolved with 2.7 mL of anhydrous DMF. A solution of allylamine (1 M in DMF) was prepared and 55 μL (5.46×10^{-5} mmol) were added with an argon purged syringe. The solution was stirred at RT under argon until completion. The polymer was then recovered as a white solid by precipitation in diethyl ether and dried under high vacuum. Yield: 79%. (0.12 g)

P(Ncy) 23



Molecular weight: 2837 g/mol

Molar mass (SEC in HFIP, PMMA calibration curve): $M_n = 800$ g/mol $D_M = 1.30$

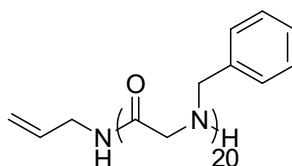
$DP_{NMR} = 27$

$MW_{NMR} = (DP_{NMR} * 139 \text{ g/mol} + 57 \text{ g/mol}) = 3810 \text{ g/mol}$

$^1\text{H-NMR}$ TFA-d 400 MHz δ (ppm): 1.08-2.32 (m, 275H, CH_2), 3.27-3.69 (m, 26H, CH), 3.76-3.86 (m, 2H, CH_2 allylamine), 4.08-4.59 (m, 57H, CH_2), 5.14-5.40 (m, 2H, CH_2 allylamine), 5.90-5.71 (m, 1H, CH allylamine). NH terminal missing in these experimental conditions.

Synthesis of poly(*N*-benzylglycine [P(Nphe) 24]. *N*-Benzyl-NCA monomer (Phe-NNCA, 0.126 g, 6.59×10^{-4} mmol) was weighted in a glovebox under pure argon, introduced in a flame-dried Schlenk, and dissolved with 1.6 mL of anhydrous DMF. A solution of allylamine (1 M in DMF) was prepared and 33 μL (3.3×10^{-5} mol) were added with an argon purged syringe. The solution was stirred at RT under argon until completion. The polymer was then recovered as a yellowish solid by precipitation in diethyl ether and dried under high vacuum. Yield: 68% (0.066 g).

P(Nphe) 24



Molecular weight: 4047 g/mol

Molar mass (SEC in HFIP, PMMA calibration curve): $M_n = 1600$ g/mol $D_M = 1.20$

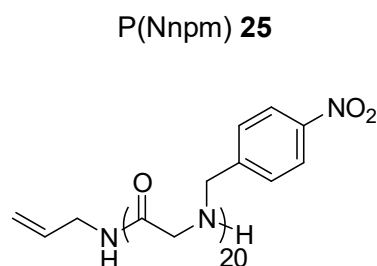
$DP_{NMR} = 17$

$MW_{NMR} = (DP_{NMR} * 147 \text{ g/mol} + 57 \text{ g/mol}) = 2556 \text{ g/mol}$

Chapter 3. Linear polypeptoid and their antimicrobial activity

$^1\text{H-NMR}$ TFA- d_4 400 MHz δ (ppm): 3.71-3.91 (m, 2H, CH_2 allylamine), 3.96-4.81 (m, 70H, $\text{CH}_2+\text{CH}_2\text{Ar}$), 5.00-5.20 (m, 2H, CH_2 allylamine), 5.57-5.76 (m, 1H, CH allylamine), 6.73-7.51 (m, 85H, Ar). NH terminal missing in these experimental conditions. In agreement with the literature (except for initiator peaks).³⁶

Synthesis of poly(4-nitrobenzyl)glycine [P(Nnpm) 25]. *p*-Nitrobenzyl-*N*-carboxyanhydride (NPM-NNCA, 157 mg, 6.62×10^{-4} mol) was weighted in a glovebox under pure argon, introduced in a flame-dried Schlenk, and dissolved with 1.7 mL of anhydrous DMF. A solution of allylamine (1 M in DMF) was prepared and 33 μL (3.31×10^{-5} mol) were added with an argon purged syringe. The solution was stirred at RT under argon until completion. The polymer was then recovered as a yellowish solid by precipitation in diethyl ether and dried under high vacuum. Yield: 69%. (0.088 g)



Molecular weight: 3897 g/mol

Molar mass (SEC in DMF, PS calibration curve): $M_n = 4000$ g/mol $D_M = 1.90$

$DP_{\text{NMR}} = 20$

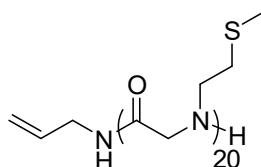
$MW_{\text{NMR}} = (DP_{\text{NMR}} \times 192 \text{ g/mol} + 57 \text{ g/mol}) = 3897 \text{ g/mol}$

$^1\text{H-NMR}$ DMSO- d_6 400 MHz δ (ppm): 3.53-3.71 (m, 2H, CH_2 allylamine), 3.78-4.84 (m, 72H, $\text{CH}_2+\text{CH}_2\text{Ar}$), 4.91-5.15 (m, 2H, CH_2 allylamine), 5.56-5.78 (m, 1H, CH allylamine), 7.23-8.37 (m, 92H, Ar). NH terminal missing in these experimental conditions.

Synthesis of poly(2-(methylthio)ethyl)glycine [P(Nmet) 26]. *N*-methylthioethyl-NCA monomer (Nmet-NCA, 400 mg, 2.28×10^{-3} mol) was weighted in a glovebox under pure argon, introduced in a flame-dried Schlenk, and dissolved with 5.7 mL of anhydrous DMF. A solution of allylamine (1 M in DMF) was prepared and 114 μL (1.14×10^{-4} mol) were added with an argon purged syringe. The solution was stirred at RT under argon until completion. The polymer was then recovered as a brownish solid by precipitation in diethyl ether and dried under high vacuum.

Yield: 41%. (0.123 g)

P(Nmet) **26**



Molecular weight: 2677 g/mol

Molar mass (SEC in DMF, PS calibration curve): 5449 g/mol $\bar{M}_n = 1.22$

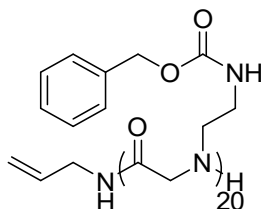
$DP_{\text{NMR}} = 22$

$MW_{\text{NMR}} = (DP_{\text{NMR}} \cdot 131 \text{ g/mol} + 57 \text{ g/mol}) = 2939 \text{ g/mol}$

$^1\text{H-NMR}$ DMSO- d_6 400 MHz δ (ppm): 1.98-2.23 (m, 86H, CH_3), 2.53-2.72 (m, 47H, CH_3), 3.67-3.79 (m, 2H, CH_2 allylamine), 3.86-4.70 (m, 49H, CH_2), 4.97-5.29 (m, 2H, CH_2 allylamine), 5.66-5.93 (m, 1H, CH allylamine). NH terminal missing in these experimental conditions.

Synthesis of poly(Cbz(2-aminoethyl))glycine [P(ZNae) 27]. *N*-Cbz aminoethyl-*N*-carboxy anhydride (ZNAE-NNCA, 185 mg, 6.65×10^{-4} mol) was weighted in a glovebox under pure argon, introduced in a flame-dried Schlenk, and dissolved with 1.7 mL of anhydrous DMF. A solution of allylamine (1 M in DMF) was prepared and 33 μL (3.32×10^{-5} mol) were added with an argon purged syringe. The solution was stirred at RT under argon until completion. The polymer was then recovered as a yellowish solid by precipitation in diethyl ether and dried under high vacuum, analyzed by $^1\text{H-NMR}$ (DMSO- d_6). Yield: 52%. (0.081 g).

P(ZNae) **27**



Molecular weight: 4737 g/mol

Molar mass (SEC in DMF, $dn/dc=0.0920$): $M_n = 4000$ g/mol $\bar{M}_n = 1.29$

Chapter 3. Linear polypeptoid and their antimicrobial activity

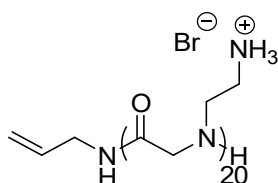
$$DP_{\text{NMR}} = 22$$

$$MW_{\text{NMR}} = (DP_{\text{NMR}} * 234 \text{ g/mol} + 57 \text{ g/mol}) = 5205 \text{ g/mol}$$

$^1\text{H-NMR}$ DMSO- d_6 400 MHz δ (ppm): 2.92-3.60 (m, 86H, 2CH₂), 3.78-4.50 (m, 34H, CH₂) 4.84-5.21 (m, 40, CH₂), 5.59-5.90 (m, 1H, CH₂ allylamine), 7.04-7.49 (m, 104H, Ar+NHCO). NH terminal missing in these experimental conditions.

Deprotection of PZNae to afford poly(2-aminoethyl)glycine [P(Nae) 27D]. In a test tube, 50 mg of PZNae (2.1×10^{-4} mol, MW = 234.26 g/mol monomer unit) were completely dissolved with 0.5 mL of trifluoroacetic acid. To the polymer solution, 77 μL of HBr 33% (4.3×10^{-4} mol, 2 equiv.) were added and the solution was stirred at 20 °C for 3 h. Then, the polymer was precipitated on diethyl ether, centrifuged at 4000 rpm, the supernatant was removed, the solid was resuspended in 1 mL of water and the pH was adjusted to pH = 7 with a NaHCO₃ saturated solution. The solutions were dialyzed using regenerated cellulose membranes (MWCO 500Da), the first time with Milli-Q water, followed by phosphates buffer pH = 7 (0.05 M) and two replacements with Milli-Q water. The solutions were freeze-dried (BenchTop Pro, SP Scientific). Yield 60% (0.023 g, yellowish solid).

P(Nae) 27D



Molecular weight: 3677 g/mol

$$DP_{\text{NMR}} = 18$$

$$MW_{\text{NMR}} = (DP_{\text{NMR}} * 181 \text{ g/mol} + 57 \text{ g/mol}) = 3315 \text{ g/mol}$$

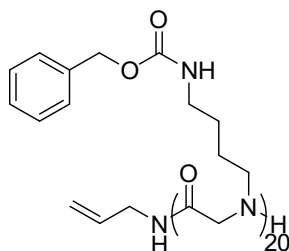
$^1\text{H-NMR}$ D₂O 400 MHz, δ : 3.42-3.63 (m, 35H, CH₂), 3.92-4.16 (m, 38H, CH₂), 4.39-4.92 (m, 35H, CH₂), 5.35-5.60 (m, 2H, CH₂ allylamine), 6.08-6.26 (m, 1H, CH allylamine), 7.61-7.85 (m, 1H, NH terminal). NH₃⁺ missing in these experimental conditions.

Synthesis of poly(Cbz(4-aminobutyl))glycine [P(ZNlys) 28]. Cbz aminobutyl-*N*-carboxyanhydride (ZLys-NNCA, 0.203 g, 6.63×10^{-4} mol) was weighted in a glovebox under pure argon, introduced in a flame-dried Schenck, and dissolved with 1.7 mL of anhydrous DMF. A

Chapter 3. Linear polypeptoid and their antimicrobial activity

solution of allylamine (1 M in DMF) was prepared and 33 μL (3.31×10^{-5} mol) were added with an argon purged syringe. The solution was stirred at RT under argon until completion. The polymer was then recovered by precipitation in diethyl ether and dried under high vacuum. Yield: 64%. (0.11 g, yellowish solid)

P(ZNlys) 28



Molecular weight: 5297 g/mol

Molar mass (SEC in DMF, $dn/dc = 0.0816$): $M_n = 5600$ g/mol $D_M = 1.08$

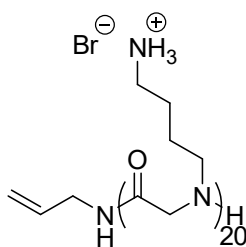
$DP_{NMR} = 23$

$MW_{NMR} = (DP_{NMR} * 262 \text{ g/mol} + 57 \text{ g/mol}) = 6083$ g/mol

$^1\text{H-NMR}$ DMSO- d_6 400 MHz δ (ppm): 1.20-1.63 (m, 110H, 2CH_2), 2.91-3.06 (m, 41H, CH_2), 3.10-3.36 (m, 40H, CH_2), 3.60-4.47 (m, 39H, CH_2), 4.92-5.12 (m, 51H, CH_2), 5.65-5.90 (m, 1H, CH allylamine), 7.05-7.46 (m, 156H, Ar+NHCO). NH terminal missing in these experimental conditions.

Deprotection of PZNlys to afford poly(4-aminobutyl)glycine [P(Nlys) 28D]. In a test tube, 100 mg of PZNlys (3.8×10^{-4} mol, MW = 262.32 g/mol monomer unit) were completely dissolved with 1.0 mL of trifluoroacetic acid. To the polymer solution, 138 μL of HBr 33% (7.6×10^{-4} mol) were added and the solution was stirred at 20 $^\circ\text{C}$ for 3 h. Then, the polymer was precipitated on diethyl ether, centrifuged at 4000 rpm the supernatant was removed, the solid was resuspended in 1 mL of water and the pH was adjusted to pH = 7 with a NaHCO_3 saturated solution. The solutions were dialyzed using regenerated cellulose membranes (MWCO 500Da), the first time with Milli-Q water, followed by phosphates buffer pH = 7 (0.05 M) and two replacements with Milli-Q water. The solutions were freeze-dried (BenchTop Pro, SP Scientific) Yield = 60% (0.048 g, yellowish solid)

P(Nlys) **28D**



Molecular weight: 4237 g/mol

Molar mass (SEC in water acetic acid, PEG calibration curve): $M_n = 1100$ g/mol, $D_M = 1.37$

$DP_{NMR} = 24$

$MW_{NMR} = (DP_{NMR} * 209 \text{ g/mol} + 57 \text{ g/mol}) = 5073 \text{ g/mol}$

$^1\text{H-NMR}$ D_2O 400 MHz, δ : 1.41-1.92 (m, 99H, 2CH₂), 2.94-3.56 (m, 95H, 2CH₂), 3.79-4.62 (m, 45H, CH₂), 5.11-5.27 (m, 2H, CH₂ allylamine), 5.79-5.95 (m, 1H, CH allylamine), 7.42-7.52 (m, 1H, NH terminal). NH₃⁺ missing in these experimental conditions.

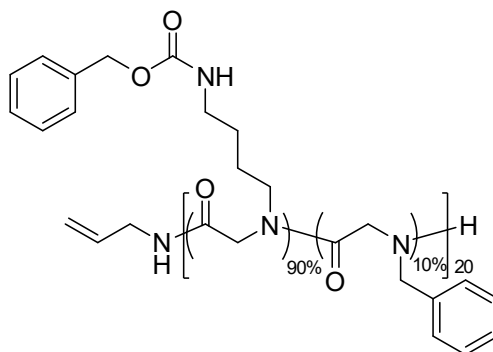
5.4 Preparation of copolymers

5.4.1 Series of copolymers varying hydrophobic content

Copolymer libraries were prepared using hydrophobic NNCAs and ZLys-NNCA. As a representative example, the synthesis of *poly[(Z-N-aminobutylglycine)-(N-benzylglycine)]* [*P(ZNlys-Nphe)*] by ROP is described at $M/I = 20$ and 10% of hydrophobic content (**29**). *N*-(Cbz-(2-aminobutyl))-NCA (ZLys-NNCA, 183.5 mg, 5.99×10^{-4} mol) and *N*-benzyl-NCA (Phe-NNCA, 12.7 mg, 6.66×10^{-5} mol) were weighted in a glovebox under argon, introduced in a flame-dried Schlenck vessel, and dissolved with 2 mL of anhydrous DMF. Then, allylamine (33.3 μL , 3.33×10^{-5} mol) in DMF at a concentration of 1.0 M was added to the monomer solution with an argon purged syringe. The solution was stirred at RT under argon until completion of the reaction. The polymer was then recovered by precipitation in diethyl ether, dried under vacuum and recovered as a yellowish powder in a 69% yield (0.115 g)

P(ZNlys_{90%}Nphe_{10%})₂₀ (29)

Chapter 3. Linear polypeptoid and their antimicrobial activity



SEC (DMF, $dn/dc = 0.0819$): 6100 g/mol, $D_M = 1.040$

The polymerization degree ($PD_{NMR} = 20$) and hydrophobic content (12%) were calculated according to the **Table 39**.

Table 39. *M/I and hydrophobic content determination*

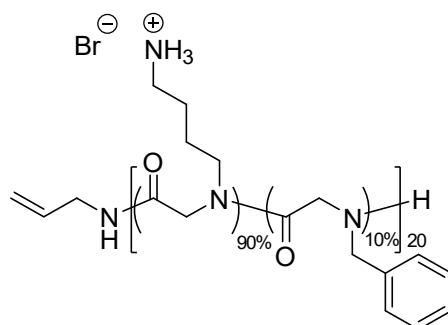
Chemical shift	Integration	Calculated M/I	%cationic content
1.13-1.65	76H/4H	19	95
2.79-3.07	38H/2H	19	95
3.07-3.26	30H/2H	15	75
3.53-4.36	39H/2H	20	-
4.8-5.24	38H/2H	19	95
5.6-5.92	1H	-	-
7.07-7.21	14H/5H	3	85
7.23-7.6	96H/6H	16	80
		%average cationic	88
		hydrophobic content (%)	12

$^1\text{H-NMR}$ DMSO- d_6 400 MHz δ (ppm): 0.96-1.82 (m, 76H, 2CH_2), 2.74-3.07 (m, 38H, CH_2), 3.06-3.26 (m, 30H, CH_2), 3.54-4.36 (m, 39H, CH_2), 4.39-4.58 (m, 4H, CH_2), 4.8-5.24 (m, 38H, CH_2), 5.6-5.92 (m, 2H, CH allylamine), 7.07-7.21 (m, 14H, Ar), 7.26-7.60 (m, 96H, Ar+NHCO). NH terminal missing in these experimental conditions.

Chapter 3. Linear polypeptoid and their antimicrobial activity

Deprotection of the copolymers was carried out similarly to P(ZNlys) deprotection method. The representative example of deprotection is given as follows: for *poly[(-N-aminobutylglycine)-(N-benzylglycine)] [P(Nlys-Nphe)]* at M/I = 20 and 10% (**29D**). In a test tube, 50 mg of P(ZNlys-Nphe) (1.7×10^{-4} mol, MW = 262.32 g/mol monomer unit and taking into account as 90% mol) were completely dissolved with 0.5 mL of trifluoroacetic acid. To the polymer solution, 62.3 μ L of HBr 33% (3.4×10^{-4} mol) were added and the solution was stirred at 20 °C for 3 h. Then, the polymer was precipitated on diethyl ether, centrifuged at 4000 rpm the supernatant was removed, the solid was resuspended in 1 mL of water and the pH was adjusted to pH = 7 with a NaHCO₃ saturated solution. The solutions were dialyzed using regenerated cellulose membranes (MWCO 500Da), the first time with Milli-Q water, followed by phosphate buffer pH = 7 (0.05 M) and two replacements with Milli-Q water. The solutions were freeze-dried (BenchTop Pro, SP Scientific). Upon freeze-drying, the copolymer was recovered as a yellowish viscous oil in 75% yield. (0.0387 g).

P(Nlys_{90%}Nphe_{10%})₂₀ (29D)

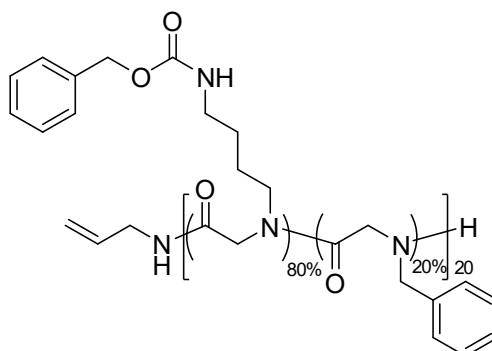


Calculated $DP_{NMR} = 25$ and hydrophobic content = 13%

¹H-NMR D₂O 400 MHz δ (ppm): 1.34-1.92 (m, 85H, 2CH₂), 2.86-3.14 (m, 46H, CH₂), 3.17-3.55 (m, 38H, CH₂), 3.83-4.55 (m, 49H, CH₂), 4.55-4.66 (m, 4H, CH₂), 5.07-5.25 (m, 2H, CH allylamine), 5.74-5.96 (m, 1H, CH allylamine) 7.12-7.58 (m, 12H, Ar+NH terminal). NH₃⁺ missing in these experimental conditions.

By using the previously described protocol, a series of copolymers (M/I = 20) was synthesized, displaying a hydrophobic content varying from 20 to 50%.

P(ZNlys_{80%}Nphe_{20%})₂₀ (30)



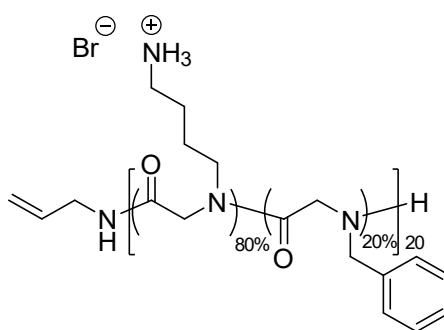
Yield=76% (0.12 g, yellowish solid)

SEC (DMF, dn/dc = 0.0819): 6100 g/mol, $D_M = 1.04$

Calculated $DP_{NMR} = 23$ and hydrophobic content = 20%

1H -NMR DMSO- d_6 400 MHz δ (ppm): 1.13-1.65 (m, 79H, 2CH₂), 2.79-3.07 (m, 41H, CH₂), 3.06-3.26 (m, 34H, CH₂), 3.54-4.36 (m, 46H, CH₂), 4.39-4.58 (m, 10H, CH₂), 4.8-5.24 (m, 43H, CH₂), 5.6-5.92 (m, 1H, CH allylamine), 7.07-7.21 (m, 33H, Ar), 7.26-7.60 (m, 118H, Ar+NHCO). NH terminal missing in these experimental conditions.

P(Nlys_{80%}Nphe_{20%})₂₀ (30D)



Yield: 73% (0.059 g, yellowish viscous oil)

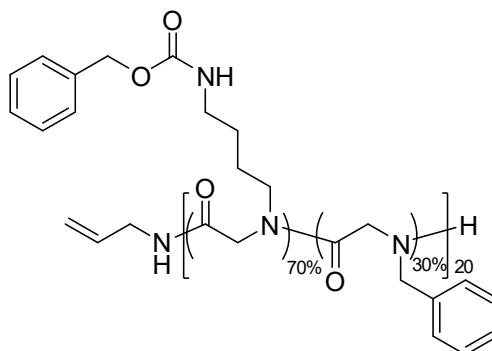
Calculated $DP_{NMR} = 19$ and hydrophobic content = 20%

1H -NMR D₂O 400 MHz δ (ppm): 1.34-1.92 (m, 54H, 2CH₂), 2.86-3.14 (m, 30H, CH₂), 3.17-3.55 (m, 25H, CH₂), 3.83-4.55 (m, 37H, CH₂), 4.55-4.66 (m, 8H, CH₂), 5.07-5.25 (m, 2H, CH

Chapter 3. Linear polypeptoid and their antimicrobial activity

allylamine), 5.74-5.96 (m, 1H, CH allylamine) 7.12-7.58 (m, 18H, Ar+NH terminal). NH₃⁺ missing in these experimental conditions.

P(ZNlys_{70%}Nphe_{30%})₂₀ (31)



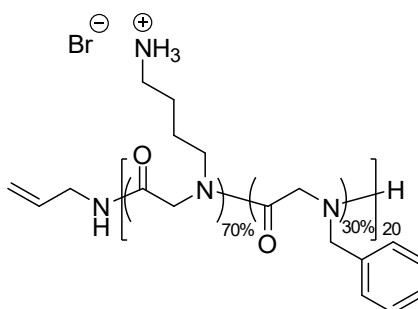
Yield: 81% (0.123 g, yellowish solid)

SEC (DMF, dn/dc = 0.0819): 5800 g/mol, $\bar{M}_n = 1.04$

Calculated DP_{NMR} = 19 and hydrophobic content = 27%

¹H-NMR DMSO-d₆ 400 MHz δ (ppm): 1.13-1.65 (m, 60H, 2CH₂), 2.79-3.07 (m, 28H, CH₂), 3.06-3.26 (m, 25H, CH₂), 3.54-4.36 (m, 37H, CH₂), 4.39-4.58 (m, 10H, CH₂), 4.8-5.24 (m, 27H, CH₂), 5.6-5.92 (m, 1H, CH allylamine), 7.07-7.21 (m, 28H, Ar), 7.26-7.60 (m, 69H, Ar+NHCO). NH terminal missing in these experimental conditions.

P(Nlys_{70%}Nphe_{30%})₂₀ (31D)



Yield: 80% (0.08 g, yellowish viscous oil)

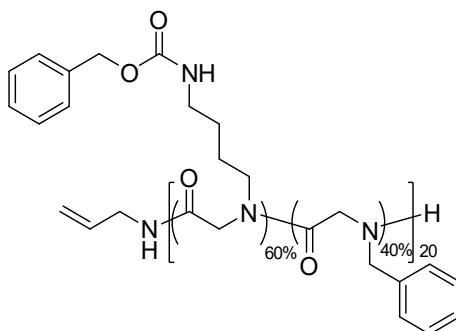
Calculated DP_{NMR} = 19 and hydrophobic content = 26%

¹H-NMR D₂O 400 MHz δ (ppm): 1.34-1.92 (m, 55H, 2CH₂), 2.86-3.14 (m, 29H, CH₂), 3.17-3.55 (m, 28H, CH₂), 3.83-4.55 (m, 39H, CH₂), 4.55-4.66 (m, 9H, CH₂), 5.07-5.25 (m, 2H, CH

Chapter 3. Linear polypeptoid and their antimicrobial activity

allylamine), 5.74-5.96 (m, 1H, CH allylamine) 7.12-7.58 (m, 31H, Ar+NH terminal). NH₃⁺ missing in these experimental conditions.

P(ZNlys_{60%}Nphe_{40%})₂₀ (32)



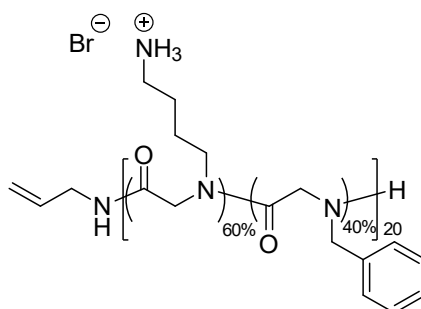
Yield: 77% (0.11 g, yellowish solid)

SEC (DMF, dn/dc = 0.0819): 6400 g/mol, $\bar{M}_w = 1.03$

Calculated DP_{NMR} = 22 and hydrophobic content = 38%

¹H-NMR DMSO-d₆ 400 MHz δ (ppm): 1.13-1.65 (m, 57H, 2CH₂), 2.79-3.07 (m, 30H, CH₂), 3.06-3.26 (m, 22H, CH₂), 3.54-4.3 (m, 44H, CH₂), 4.39-4.58 (m, 15H, CH₂), 4.8-5.24 (m, 24, CH₂), 5.6-5.92 (m, 1H, CH allylamine), 7.07-7.21 (m, 35H, Ar), 7.26-7.60 (m, 63H, Ar+NHCO). NH terminal missing in these experimental conditions.

P(Nlys_{60%}Nphe_{40%})₂₀ (32D)



Yield: 62% (0.05 g, yellowish viscous oil)

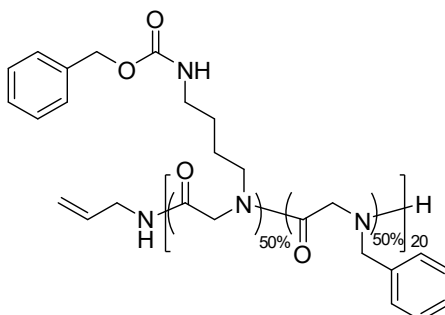
Calculated DP_{NMR} = 19 and hydrophobic content = 35%

¹H-NMR D₂O 400 MHz δ (ppm): 1.34-1.92 (m, 47H, 2CH₂), 2.86-3.14 (m, 28H, CH₂), 3.17-3.55 (m, 23H, CH₂), 3.83-4.55 (m, 38H, CH₂), 4.55-4.66 (m, 10H, CH₂), 5.07-5.25 (m, 2H, CH

Chapter 3. Linear polypeptoid and their antimicrobial activity

allylamine), 5.74-5.96 (m, 1H, CH allylamine) 7.12-7.58 (m, 33H, Ar+NH terminal). NH₃⁺ missing in these experimental conditions.

P(ZNlys_{50%}Nphe_{50%})₂₀ (33)



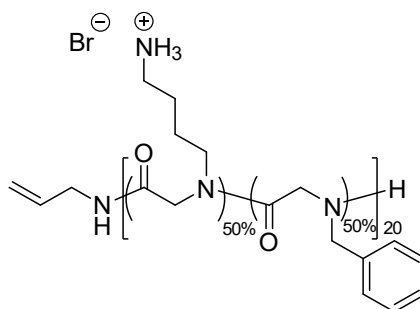
Yield: 70% (0.096 g, yellowish solid)

SEC (DMF, dn/dc = 0.0819): 5100 g/mol, $\bar{M}_w = 1.05$

Calculated DP_{NMR} = 23 and hydrophobic content = 49%

¹H-NMR DMSO-d₆ 400 MHz δ (ppm): 1.13-1.65 (m, 48H, 2CH₂), 2.79-3.07 (m, 24H, CH₂), 3.06-3.26 (m, 23H, CH₂), 3.55-4.32 (m, 46, CH₂), 4.33-4.69 (m, 22H, CH₂), 4.84-5.18 (m, 25, CH₂), 5.6-5.92 (m, 1H, CH allylamine), 7.07-7.60 (m, 128H, 2Ar+NHCO). NH terminal missing in these experimental conditions.

P(Nlys_{50%}Nphe_{50%})₂₀ (33D)



Yield: 82% (0.06 g, yellowish viscous oil)

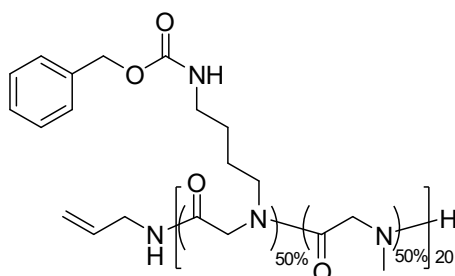
Calculated DP_{NMR} = 21 and hydrophobic content = 51%

¹H-NMR D₂O 400 MHz δ (ppm): 1.34-1.92 (m, 44H, 2CH₂), 2.86-3.14 (m, 25H, CH₂), 3.17-3.55 (m, 20H, CH₂), 3.83-4.55 (m, 41H, CH₂), 4.55-4.66 (m, 17H, CH₂), 5.07-5.25 (m, 2H, CH allylamine), 5.74-5.96 (m, 1H, CH allylamine) 7.12-7.58 (m, 47H, Ar+NH terminal). NH₃⁺ missing in these experimental conditions.

5.4.2 Hydrophobic side-chain variation

Using the protocol described in 5.4.1 for P(ZNlys-Nphe) and P(Nlys-NPhe), ROP and deprotection steps, we synthesized the following compounds:

P(ZNlys_{50%}Nme_{50%})₂₀ (34)



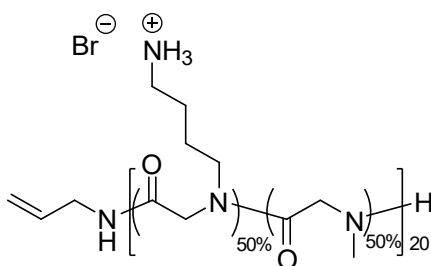
Yield: 59% (0.065 g, yellowish solid)

SEC (DMF, dn/dc = 0.0819): 5300 g/mol, $\bar{M}_w = 1.06$

Calculated $DP_{NMR} = 27$ and hydrophobic content = 47%

¹H-NMR DMSO-d₆ 400 MHz δ (ppm): 1.01-1.65 (m, 68H, 2CH₂), 2.61-3.12 (m, 75H, CH₂+CH₃), 3.80-4.57 (m, 54H, CH₂), 4.90-5.10 (m, 30, CH₂), 5.80 (br, 1H, CH allylamine), 6.91-7.41 (m, 84H, Ar+NHCO). NH terminal missing in these experimental conditions.

P(Nlys_{50%}Nme_{50%})₂₀ (34D)



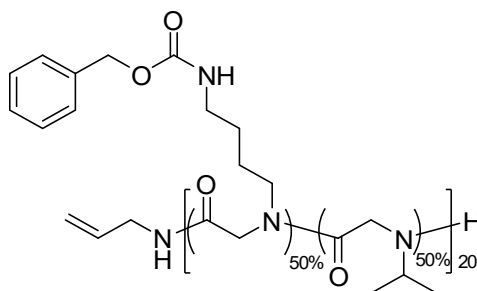
Yield: 57% (0.058 g, yellowish viscous oil)

Calculated $DP_{NMR} = 27$ and hydrophobic content = 50%

¹H-NMR D₂O 400 MHz δ (ppm): 1.34-1.85 (m, 60H, 2CH₂), 2.86-3.19 (m, 71H, CH₂+CH₃), 3.27-3.59 (m, 26H, CH₂), 3.98-4.66 (m, 41H, CH₂), 5.10-5.24 (m, 2H, CH₂ allylamine), 5.87 (br, 1H, CH allylamine). NH terminal and NH₃⁺ missing in these experimental conditions.

P(ZNlys_{50%}Nval_{50%})₂₀ (35)

Chapter 3. Linear polypeptoid and their antimicrobial activity



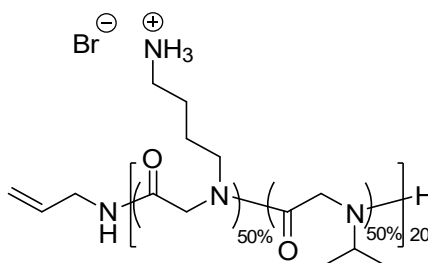
Yield: 35% (0.042 g, yellowish solid)

SEC (DMF, $dn/dc = 0.0819$): 3200 g/mol, $D_M = 1.26$

Calculated $DP_{NMR} = 22$ and hydrophobic content = 45%

1H -NMR DMSO- d_6 400 MHz δ (ppm): 0.80-1.21 (m, 39H, 2CH₃), 1.22-1.58 (m, 57H, 2CH₂), 2.88-3.07 (m, 29H, CH₂), 3.72-4.73 (m, 44, CH₂), 4.92-5.08 (m, 27, CH₂), 5.80 (m, 1H, CH allylamine), 6.98-7.98 (m, 77H, Ar+NHCO). We could not identify the CH of isopropyl nor CH₂ from the Nlys because of interference with H₂O. NH terminal missing in these experimental conditions.

P(Nlys_{50%}Nval_{50%})₂₀ (35D)



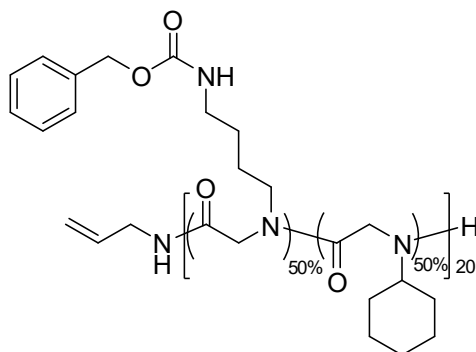
Yield: 48% (0.019 g, yellowish viscous oil)

Calculated $DP_{NMR} = 22$ and hydrophobic content = 50%

1H -NMR D₂O 400 MHz δ (ppm): 0.96-1.30 (m, 33H, 2CH₃), 1.89-1.34 (m, 59H, 2CH₂), 2.79-3.08 (m, 32H, CH₂), 3.26-3.56 (m, 28H, CH₂), 3.72-4.57 (m, 43H, CH₂), 5.07-5.29 (m, 2H, CH₂ allylamine), 5.85 (br, 1H, CH allylamine). We could not identify the CH of isopropyl. NH terminal and NH₃⁺ missing in these experimental conditions.

P(ZNlys_{50%}Ncy_{50%})₂₀ (36)

Chapter 3. Linear polypeptoid and their antimicrobial activity



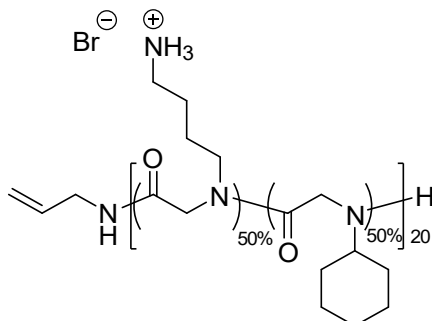
Yield: 40% (0.053 g, yellowish solid)

SEC (DMF, $dn/dc = 0.0819$): 2800 g/mol, $D_M = 1.19$

Calculated $DP_{NMR} = 23$ and hydrophobic content = 51%

1H -NMR DMSO- d_6 400 MHz δ (ppm): 0.90-1.81 (m, 125H, 7CH₂), 2.88-3.04 (m, 29H, CH₂), 3.61-4.41 (m, 46H, CH₂), 4.89-5.07 (m, 26, CH₂), 5.85 (br, 1H, CH allylamine), 7.14-7.46 (m, 72H, Ar+NHCO). We could not distinguish the CH₂ from the Nlys nor CH from Ncy because of interference with H₂O. NH terminal missing in these experimental conditions.

P(Nlys_{50%}Ncy_{50%})₂₀ (36D)

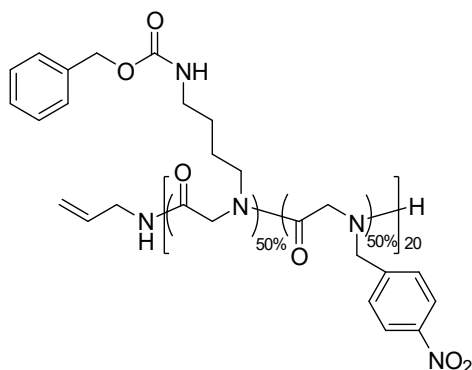


Yield: 72% (0.028 g, yellowish viscous oil)

Calculated $DP_{NMR} = 23$ and hydrophobic content = 54%

1H -NMR D₂O 400 MHz δ (ppm): 0.91-2.23 (m, 118H, 7CH₂), 2.95-3.16 (m, 30H, CH₂), 3.28-3.58 (m, 26H, CH₂), 3.79-4.60 (m, 46, CH₂), 5.08-5.36 (m, 2H, CH₂ allylamine), 5.86 (br, 1H, CH allylamine). We could not identify the CH of cyclohexyl. NH terminal and NH₃⁺ missing in these experimental conditions.

P(ZNlys_{50%}Nnpm_{50%})₂₀ (37)



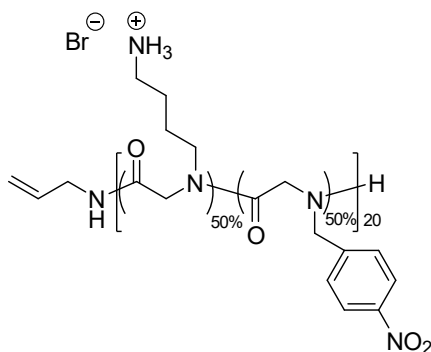
Yield: 59% (0.088 g, yellowish solid)

SEC (DMF, $dn/dc = 0.0819$): 4200 g/mol, $D_M = 1.32$

Calculated $DP_{NMR} = 18$ and hydrophobic content = 43%

1H -NMR DMSO- d_6 400 MHz δ (ppm): 1.17-1.72 (m, 44H, 2CH₂), 2.90-3.01 (m, 20H, CH₂), 3.75-4.47 (m, 36H, CH₂), 4.49-4.80 (m, 13H, CH₂), 4.92-5.09 (m, 21, CH₂), 5.56-5.90 (br, 1H, CH allylamine), 7.09-7.41 (m, 59H, Ar+NH), 7.43-8.32 (m, 34H, Ar). We could not distinguish the CH₂ from the Nlys because of interference with H₂O. NH terminal missing in these experimental conditions.

P(Nlys_{50%}Nnpm_{50%})₂₀ (37D)

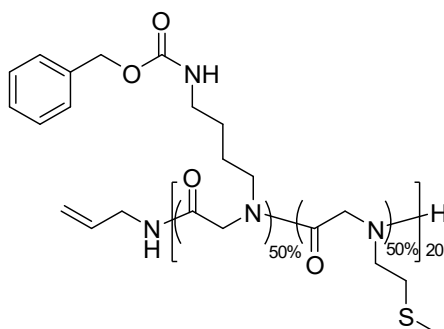


Yield: 31% (0.02 g, yellowish viscous oil)

Calculated $DP_{NMR} = 19$ and hydrophobic content = 52%

1H -NMR D₂O 400 MHz δ (ppm): 1.27-1.95 (m, 52H, 2CH₂), 2.86-3.16 (m, 35H, CH₂), 3.29-3.49 (m, 20H, CH₂), 3.60-4.36 (m, 38H, CH₂), 4.41-4.66 (m, 16H, CH₂), 4.98-5.20 (m, 2H, CH₂ allylamine), 5.80 (br, 1H, CH allylamine). 7.07-8.40 (m, 37H, Ar). NH terminal and NH₃⁺ missing in these experimental conditions.

P(ZNlys_{50%}Nmet_{50%})₂₀ (38)



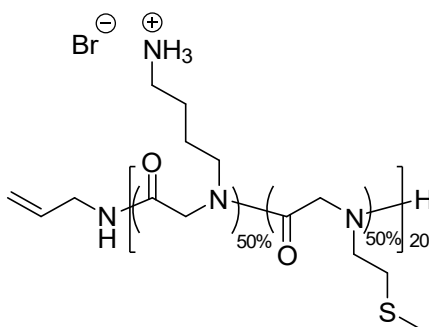
Yield: 53% (0.066 g, brownish solid)

SEC (DMF, $dn/dc = 0.0819$): 5900 g/mol, $D_M = 1.04$

Calculated $DP_{NMR} = 22$ and hydrophobic content = 53%

1H -NMR DMSO- d_6 400 MHz δ (ppm): 1.19-1.68 (m, 46H, 2CH₂), 1.97-2.25 (m, 33H, CH₃), 2.95-3.10 (m, 19H, CH₂), 3.11-3.31 (m, 22H, CH₂), 3.62-4.63 (m, 45, CH₂), 4.89-5.23 (m, 24H, CH₂), 5.79 (br, 1H, CH allylamine), 6.97-7.46 (m, 64H, Ar+NH). We could not identify the CH₂ from the Nmet. NH terminal missing in these experimental conditions.

P(Nlys_{50%}Nmet_{50%})₂₀ (38D)



Yield: 38% (0.033 g, brownish viscous oil)

Calculated $DP_{NMR} = 22$ and hydrophobic content = 43%

1H -NMR D₂O 400 MHz δ (ppm): 1.28-1.82 (m, 55H, 2CH₂), 1.93-2.25 (m, 26H, CH₃), 2.42-2.86 (m, 30H, CH₂), 2.88-3.12 (m, 22H, CH₂), 3.16-3.51 (m, 28H, CH₂), 3.51-3.74 (m, 19H, CH₂), 3.94-4.70 (5.23, 44H, CH₂), 5.72-7.97 (m, 2H, CH₂ allylamine), 5.97-5.72 (m, 1H, CH allylamine)

Chapter 3. Linear polypeptoid and their antimicrobial activity

5.4.3 Series of copolymers varying hydrophobic content *N*-alkylated side chain and M/I

Using the protocols described in 5.4.1, we synthesized the following copolymers **Table 40** in which the yields before and after deprotection are provided.

Table 40. Library of synthesized copolymers varying the hydrophobic NNCA content and using ZLys-NNCA as cationic precursor monomer (allylamine = initiator).

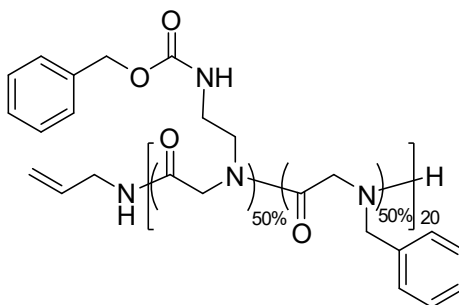
Hydrophobic NNCA	H/C _{theo} (%)	DP _{theo}	^a DP _{NMR}	^a H/C % _{NMR}	Yield (%)	
					Before deprotection	Upon deprotection
Sar-NNCA	10	20	26	7	72	66
Sar-NNCA	20	20	24	15	69	63
Sar-NNCA	30	20	25	24	44	55
Sar-NNCA	40	20	23	39	57	67
Val-NNCA	10	20	25	9	75	64
Val-NNCA	20	20	30	19	61	61
Val-NNCA	30	20	28	24	38	51
Val-NNCA	40	20	29	36	49	55
Cy-NNCA	10	20	18	10	54	66
Cy-NNCA	20	20	20	23	49	64
Cy-NNCA	30	20	18	27	48	62
Cy-NNCA	40	20	16	36	67	30
NPM-NNCA	10	20	21	12	61	53
NPM-NNCA	20	20	23	26	57	40
NPM-NNCA	30	20	21	31	63	37
NPM-NNCA	40	20	19	45	47	29
MTE-NNCA	10	20	^b 18	^b 12	18	16
MTE-NNCA	20	20	^b 16	^b 20	18	35
MTE-NNCA	30	20	^b 17	^b 29	31	37
MTE-NNCA	40	20	-	-	61	-

^a Calculated from the ¹H-NMR spectrum in DMSO-d₆

5.4.4 Cationic length variation

Using the protocols described in 5.4.1, we synthesized the following copolymer using ZNAE-NNCA as cationic precursor monomer.

P(ZNae_{50%}Nphe_{50%})₂₀ (39)



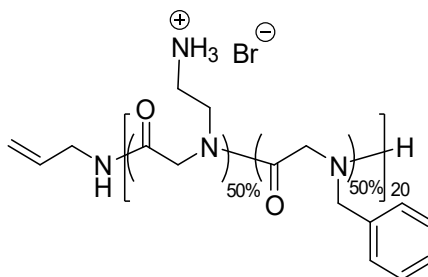
Yield: 74% (0.094 g, yellowish solid)

SEC (DMF, dn/dc = 0.0819): 4600 g/mol, $\bar{M}_n = 1.11$

Calculated $DP_{NMR} = 22$ and hydrophobic content = 49%

1H -NMR DMSO- d_6 400 MHz δ (ppm): 2.93-3.22 (m, 25H, CH₂), 4.32-4.68 (m, 24H, CH₂), 4.79-5.18 (m, 25H, CH₂), 5.58-5.60 (m, 1H, CH₂), 6.95-7.27 (m, 63H, Ar), 7.27-7.43 (m, 64H, Ar+NHCO). NH terminal missing in these experimental conditions.

P(Nae_{50%}Phe_{50%})₂₀ (39D)



Yield: 44% (0.023 g, yellowish viscous oil)

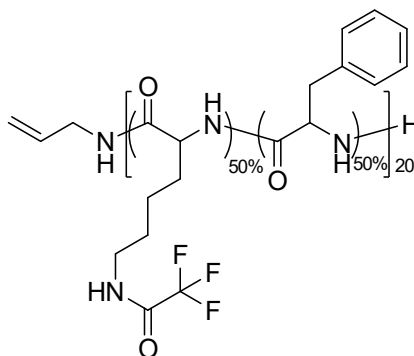
Calculated $DP_{NMR} = 18$ and hydrophobic content = 45%

1H -NMR D₂O 400 MHz δ (ppm): 2.69-3.26 (m, 32H, CH₂), 3.34-3.88 (m, 28H, CH₂), 3.91-4.52 (m, 35H, CH₂), 4.52-4.70 (m, 15H, CH₂), 5.00-5.26 (m, 2H, CH₂), 5.67-5.87 (m, 1H, CH₂), 7.24-7.56 (m, 74H, Ar). NH terminal and NH₃⁺ missing in these experimental conditions.

5.4.1 Copolymers synthesized by the ROP of NCA

Synthesis of poly(Cbz-Lysine-phenylalanine_{0.5}) having M/I = 20 and 50% hydrophobic content: Cbz-Lysine-NCA (ZLys-NCA, 357 mg, 1.3x10⁻³ mol) and Phenylalanine-NCA (Phe-NCA, 254 mg, 1.3x10⁻³ mol) were weighted in a glovebox under argon, introduced in a flame-dried Schlenk vessel, and dissolved with 5 mL of anhydrous DMF. Then, allylamine (133 μL, 1.3x10⁻⁴ mol) in DMF at a concentration of 1.0 M was added to the monomer solution with an argon purged syringe. The solution was stirred at RT under argon until completion. The polymer was then recovered by precipitation in diethyl ether and dried under high vacuum having a 29% yield (0.143 g, white solid).

P(ZLys_{50%}Phe_{50%})₂₀ (40)



Molar mass (SEC in DMF, PS calibration curve): M_n 5200 g/mol, $D_M = 1.76$

¹H-NMR DMSO-d₆ 400 MHz δ (ppm): 0.96-1.86 (m, 85H, 3CH₂), 3.04-3.20 (m, 30H, 2CH₂), 3.65-4.64 (m, 24H, CH), 4.79-5.30 (m, 2H, CH₂ allylamine), 5.60-5.90 (b, 1H, CH allylamine), 6.90-7.33 (m, 53H, Ar), 7.95-8.22 (m, 17H, NHCO), 9.23-9.49 (m, 11H, NHCO).

Polymerization degree (M/I) was calculated from the intensity of the CH peaks (3.65-4.64 ppm) and the hydrophobic content from the intensity of the aromatic protons (6.90-7.33 ppm) as follows:

$$\%H/C = \frac{\frac{I_{Ar}}{5}}{DP_{NMR}}$$

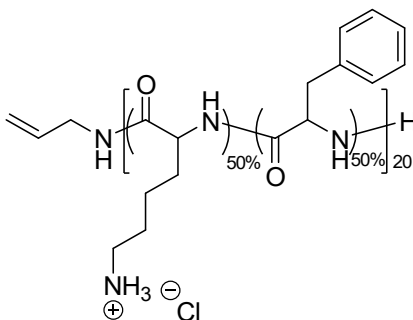
Calculated DP_{NMR} = 24, hydrophobic content: 55%

Deprotection. In a round bottom flask, 125 mg of the copolymer were added followed by 25 mL of methanol:water (9:1) and 125 mg of K₂CO₃. The mixture was refluxed for 8 h, then the solvent was evaporated and the copolymer was acidified with HCl 1 M until a pH = 7. The polymer

Chapter 3. Linear polypeptoid and their antimicrobial activity

was dialyzed (MWCO 500 Da), lyophilized and recovered as a white powder in a 36% yield (0.052 g).

P(Lys_{50%}Phe_{50%})₂₀ (40D)



Yield: 36% (white solid)

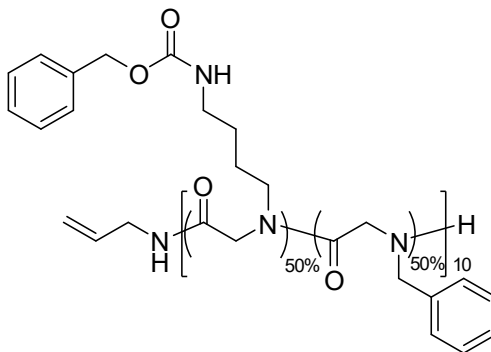
Calculated M/I = 25 and hydrophobic content = 54%

¹H-NMR D₂O 400 MHz δ (ppm): 0.82-1.59 (m, 122H, 3CH₂), 2.88 (b, 55H, 2CH₂), 4.07-4.52 (m, 25H, CH), 5.05 (m, 2H, CH₂ allylamine), 5.68 (m, 1H, CH allylamine), 7.21 (b, 66H, Ar). NH terminal and NH₃⁺ missing in these experimental conditions.

5.4.2 Synthesis of copolymers varying the polymerization degree

Using the protocols described in 5.4.1, we synthesized the following copolymer varying the polymerization degree (M/I ratio):

P(ZNlys_{50%}Nphe_{50%})₁₀ (41)



Chapter 3. Linear polyepitoid and their antimicrobial activity

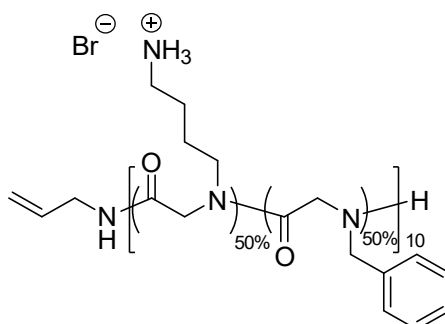
Yield: 51% (0.07 g, yellowish solid)

SEC (DMF, $dn/dc = 0.0819$): 2500 g/mol, $D_M = 1.15$

Calculated $DP_{NMR} = 12$ and hydrophobic content = 47%

1H -NMR DMSO- d_6 400 MHz δ (ppm): 1.19-1.58 (m, 25H, 2CH₂), 2.82-3.07 (m, 13H, CH₂), 3.08-3.26 (m, 11H, CH₂), 3.75-4.32 (m, 20, CH₂), 4.36-4.69 (m, 9H, CH₂), 4.9-5.11 (m, 13, CH₂), 5.6-5.85 (m, 1H, CH allylamine), 7.07-7.53 (m, 62H, 2Ar+NHCO). NH terminal missing in these experimental conditions.

P(Nlys_{50%}Nphe_{50%})₁₀ (41D)

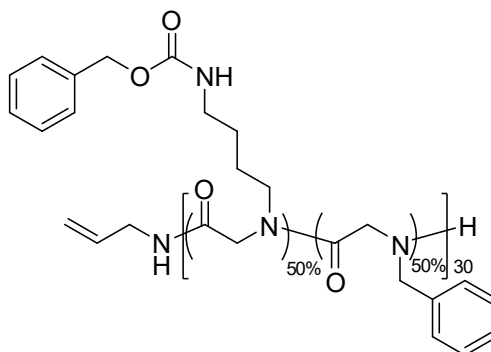


Yield: 72% (0.033 g, yellowish viscous oil)

Calculated $DP_{NMR} = 10$ and hydrophobic content = 50%

1H -NMR D₂O 400 MHz δ (ppm): 1.31-1.79 (m, 24H, 2CH₂), 2.79-3.09 (m, 12H, CH₂), 3.16-3.56 (m, 11H, CH₂), 3.71-4.45 (m, 20H, CH₂), 4.45-4.69 (m, 7H, CH₂), 5.05-5.22 (m, 2H, CH allylamine), 5.91-5.67 (m, 1H, CH allylamine) 7.05-7.59 (m, 21H, Ar). NH terminal and NH₃⁺ missing in these experimental conditions.

P(ZNlys_{50%}Nphe_{50%})₃₀ (42)



Yield: 61% (0.52 g, yellowish solid)

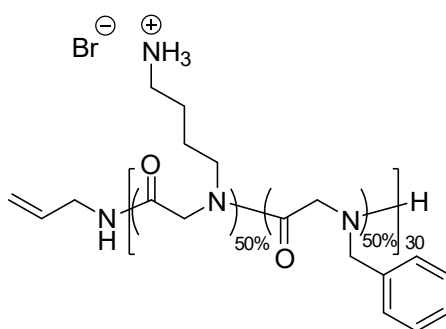
Chapter 3. Linear polypeptoid and their antimicrobial activity

SEC (DMF, $dn/dc = 0.0819$): 5200 g/mol, $D_M = 1.12$

Calculated $DP_{NMR} = 35$ and hydrophobic content = 46%

1H -NMR DMSO- d_6 400 MHz δ (ppm): 1.17-1.62 (m, 75H, 2CH₂), 2.89-3.05 (m, 39H, CH₂), 3.08-3.29 (m, 40H, 2CH₂), 3.66-4.28 (m, 70, CH₂), 4.30-4.69 (m, 36H, CH₂), 4.84-5.14 (m, 39, CH₂), 5.63-5.85 (m, 1H, CH allylamine), 6.89-7.47 (m, 198H, 2Ar+NHCO). NH terminal missing in these experimental conditions.

P(NIys_{50%}Nphe_{50%})₃₀ (42D)



Yield: 90% (0.354 g, yellowish solid)

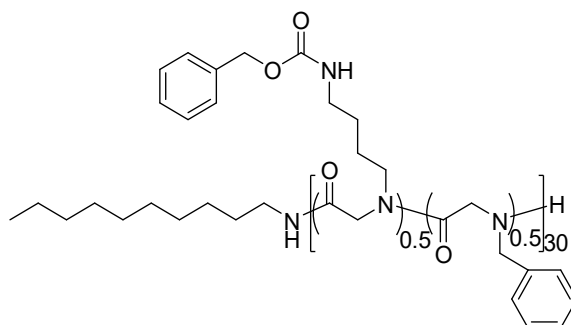
Calculated $DP_{NMR} = 35$ and hydrophobic content = 50%

1H -NMR D₂O 400 MHz δ (ppm): 1.19-1.85 (m, 84H, CH₂), 2.63-3.08 (m, 47H, CH₂), 3.12-3.44 (m, 36H, CH₂), 3.53-4.65 (m, 141H, 2CH₂), 5.03-5.22 (m, 2H, CH allylamine), 5.64-5.84 (m, 1H, CH allylamine), 6.66-7.54 (m, 124H, Ar). NH terminal and NH₃⁺ missing in these experimental conditions.

5.4.3 Synthesis of copolymers varying the initiator

Using the protocols described in 5.4.1, we synthesized the following copolymers using decylamine as initiator:

DecyINH-P(ZNIys_{50%}Nphe_{50%})₃₀ (43)



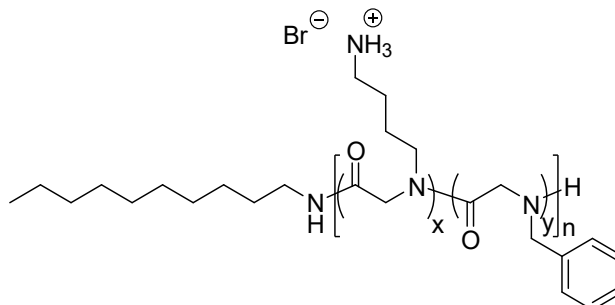
Yield: 57% (0.156 g, yellowish solid)

SEC (DMF, dn/dc = 0.0819): 4500 g/mol, $D_M = 1.18$

$DP_{NMR} = 31$, calculated hydrophobic content = 49%

¹H-NMR DMSO-d₆ 400MHz δ (ppm): 0.84 (s, 3H, CH₃), 1.13-1.27 (br, 18H, CH₂ decylamine), 1.27-1.58 (m, 58H, 2CH₂), 2.85-3.09 (m, 37H, CH₂), 3.09-3.31 (m, 34H, CH₂), 3.82-4.41 (m, 62H, CH₂), 4.41-4.62 (m, 18H, CH₂), 4.87-5.157 (br, 30H, CH₂), 6.98-7.58 (m, 152H, Ar+NHC=O). NH terminal missing in these experimental conditions.

DecylNH-P(Nlys_{50%}Nphe_{50%})₃₀ (43D)



Yield: 97% (0.111 g, yellowish solid)

Calculated $DP_{NMR} = 18$ and hydrophobic content = 45%

¹H-NMR D₂O 400 MHz δ (ppm): 0.83 (s, 3H, CH₃), 1.10-1.13 (s, 10H, 5CH₂ decylamine), 1.91-1.33 (m, 53H, 2CH₂+4CH₂ decylamine), 3.10-2.82 (m, 29H, CH₂), 3.15-3.49 (m, 25H, CH₂), 3.69-4.45 (m, 59H, CH₂), 4.45-4.74 (m, 26H, CH₂), 7.62-7.92 (m, 57H, Ar). NH terminal and NH₃⁺ missing in these experimental conditions.

5.5 Antimicrobial assay

The analyses were performed at the Pasteur Institute (Paris, France) by PhD candidate

Chapter 3. Linear polypeptoid and their antimicrobial activity

Antoine Tronnet and Dr. Bruno Dupuy. The procedure is described as follows.

Clostridioides difficile strain 630Δerm used in this study is described by H. Hussain *et al.* in 2005.⁸⁵ *C. difficile* strain was cultured in an anaerobic chamber with an atmosphere of 5% H₂, 5% CO₂, 90% N₂. Cells were cultured on a brain-heart infusion medium at 37 °C. The Minimal Inhibitory Concentration (MIC) of tested polymers and control drugs (metronidazole (Sigma-Aldrich), vancomycin (Sigma-Aldrich), fidaxomicin (Carbosynth), and LL-37 (sb-peptide)) were determined using the microdilution method.⁸⁶ A twofold serial dilution of tested polymers and control drugs were prepared in highly purified water to give a final concentration range from 1000 to 8 µg/mL and 20 µL of each concentration was added to a 96-well plate. Then, an overnight bacterial solution of *C. difficile* having an OD₆₀₀ between 0.450 and 0.600 (10⁷-10⁸ CFU/mL) was diluted in Brain Heart Infusion (BHI) at 10⁵ CFU/mL, each well was inoculated anaerobically with 180 µL and incubated at 37°C.

MIC reported is the minimal drug concentration that totally suppressed the growth of bacteria after 24 h at 37 °C, by visual determination. The experiments were performed by triplicates. The uninoculated medium was used as a negative control to test for contamination of the growth medium. The positive control consisted of a well inoculated with *C. difficile* but no antimicrobial compound was added.

5.6 Cytotoxicity

The analyses were performed at the Pharmacochemistry and Biology for Development (Pharmadev, Toulouse, France) by Dr. Sandra Bourgeade-Delmas. The procedure is described as follows.

The evaluation of the tested peptides cytotoxicity by MTT assay on the Caco-2 cell line (human epithelial cell line) was done according to Mosmann with slight modifications. The experiments were performed by Sandra Bourgeade-Delmas at PHARMA-DEV in Toulouse, France. Briefly, cells (1.10⁵ cells/mL) in 100 µL of the complete medium [DMEM High Glucose supplemented with 10% fetal calf serum (FCS), 2 mM L-glutamine, antibiotics (100 U/mL penicillin, 100 µg/mL streptomycin) and 1X NEAA] were seeded into each well of 96-well plates and incubated at 37 °C in a humidified 5% CO₂ with 95% air atmosphere. After a 24 h incubation, various concentrations of peptides and appropriate controls were then added (100 µL) and the plates were incubated for 72 h at 37 °C. Each well was then microscope-examined for detecting possible precipitate formation before aspiration of the medium. MTT solution (0.5 mg/mL in

Chapter 3. Linear polypeptoid and their antimicrobial activity

complete DMEM High Glucose, 100 μ l) was then added to each well. Cells were incubated for 2 h at 37 °C. The MTT solution was then removed and DMSO (100 μ L) was added to dissolve the resulting formazan crystals. Plates were shaken vigorously (300 rpm) for 5 min. The absorbance was measured at 570 nm with a microplate spectrophotometer (Eon Bio Tek). Water was used as blank and doxorubicin (Sigma Aldrich) as a positive control. CC_{50} were calculated by non-linear regression analysis processed on dose-response curves, using TableCurve 2D V5 software. CC_{50} values represent the mean value calculated from three independent experiments.

5.7 Protease assay

The protocol was adapted from a known method for peptoid analysis.⁷² A polymer solution was prepared (0.1 mM) in 1 mL of NaHCO_3 buffer 50 mM pH = 7.8 equilibrated at 37 °C for 10 min and 47 μ L of trypsin 42 μ M (1 mg/mL) was added. At a certain time, 2.3 μ L of the reaction mixture were taken, placed in an Eppendorf tube, quenched with 200 μ L acetonitrile and 200 μ L sodium borate buffer 0.1 M and kept in an ice bath. 4-Fluoro-7-nitro-benzofurazan (NBDF) (10 μ L, acetonitrile solution 10 mM) was added, immediately the solution was incubated at 60 °C for 3 min and 500 rpm in the Eppendorf thermomixer R. The sample was placed on ice and 20 μ L of 3 N HCl were added to stabilize the 4-amino-7-nitro-benzofurazan product. The fluorescence was measured in a Spectra max M2 (Molecular devices) with $\lambda_{\text{ex}} = 470$ nm and $\lambda_{\text{em}} = 540$ nm. The values were adjusted using the appropriate blank. The raw data was obtained from SoftMaxPro V5 and analyzed in Origin2016 software.

5.8 Antimicrobial assay after trypsin treatment.

The analyses were performed at the Pasteur Institute (Paris, France) by PhD candidate Antoine Tronnet and Dr. Bruno Dupuy. The procedure is described as follows.

Solution of **P(NIys-Nphe) 42D** was prepared in carbonate buffer 50 mM pH = 7.8 at 1 mg/mL with 0.3 mg/mL of trypsin (Sigma-Aldrich). Solution of LL-37 was prepared in sodium carbonate buffer 50 mM pH = 7.8 at 2 mg/mL with 0.6 mg/mL of trypsin. After 1h at 37°C, a twofold serial dilution of **42D** and LL-37 were prepared in carbonate buffer 50 mM pH = 7.8 to give a final concentration range of 1000 to 8 μ g/mL for **42D** and 2000 to 16 μ g/mL for LL-37 and 20 μ L of each concentration was added to a 96-well plate. Solutions of **42D** and LL-37 in carbonate buffer 50 mM pH = 7.8 were also prepared without trypsin as control. Then, an overnight bacterial solution of *C. difficile* having an OD_{600} between 0.450 and 0.600 (10^7 - 10^8 CFU/mL) was diluted in Brain Heart Infusion (BHI) at 10^5 CFU/mL, each well was inoculated anaerobically with 180 μ L and incubated at 37°C. MIC reported are the minimal drug concentration that suppressed totally

Chapter 3. Linear polypeptoid and their antimicrobial activity

the growth of bacteria after 24 h at 37°C and determined visually. The experiments were performed by triplicates. The uninoculated medium was used as a negative control to test for contamination of the growth medium. The positive control was inoculated with *C. difficile* but no antimicrobial compound was added.

6 References

- (1) Brogden, K. A. Antimicrobial Peptides: Pore Formers or Metabolic Inhibitors in Bacteria?. *Nat. Rev. Microbiol.* **2005**, *3* (3), 238–250.
- (2) Magana, M.; Pushpanathan, M.; Santos, A. L.; Leanse, L.; Fernandez, M.; Ioannidis, A.; Giulianotti, M. A.; Apidianakis, Y.; Bradfute, S.; Ferguson, A. L.; Cherkasov, A.; Seleem, M. N.; Pinilla, C.; de la Fuente-Nunez, C.; Lazaridis, T.; Dai, T.; Houghten, R. A.; Hancock, R. E. W.; Tegos, G. P. The Value of Antimicrobial Peptides in the Age of Resistance. *Lancet Infect. Dis.* **2020**.
- (3) Boman, H. G. Peptide Antibiotics and Their Role in Innate Immunity. *Annu. Rev. Immunol.* **2003**, *13* (1), 61–92.
- (4) Gaglione, R.; Pane, K.; Dell’Olmo, E.; Cafaro, V.; Pizzo, E.; Olivieri, G.; Notomista, E.; Arciello, A. Cost-Effective Production of Recombinant Peptides in Escherichia Coli. *N. Biotechnol.* **2019**, *51*, 39–48.
- (5) Ergene, C.; Yasuhara, K.; Palermo, E. F. Biomimetic Antimicrobial Polymers: Recent Advances in Molecular Design. *Polym. Chem.* **2018**, *9* (18), 2407–2427.
- (6) Yang, Y.; Cai, Z.; Huang, Z.; Tang, X.; Zhang, X. Antimicrobial Cationic Polymers: From Structural Design to Functional Control. *Polym. J.* **2018**, *50* (1), 33–44.
- (7) Rasines Mazo, A.; Allison-Logan, S.; Karimi, F.; Chan, N. J. A.; Qiu, W.; Duan, W.; O’Brien-Simpson, N. M.; Qiao, G. G. Ring Opening Polymerization of α -Amino Acids: Advances in Synthesis, Architecture and Applications of Polypeptides and Their Hybrids. *Chem. Soc. Rev.* **2020**, *49* (14), 4737–4834.
- (8) Moncla, B. J.; Pryke, K.; Rohan, L. C.; Graebing, P. W. Degradation of Naturally Occurring and Engineered Antimicrobial Peptides by Proteases. *Adv. Biosci. Biotechnol.* **2011**, *02* (06), 404–408.
- (9) Masip, I.; Cortés, N.; Abad, M.-J.; Guardiola, M.; Pérez-Payá, E.; Ferragut, J.; Ferrer-Montiel, A.; Messeguer, A. Design and Synthesis of an Optimized Positional Scanning Library of Peptoids: Identification of Novel Multidrug Resistance Reversal Agents. *Bioorg. Med. Chem.* **2005**, *13* (6), 1923–1929.
- (10) Chongsiriwatana, N. P.; Patch, J. A.; Czyzewski, A. M.; Dohm, M. T.; Ivankin, A.; Gidalevitz,

Chapter 3. Linear polypeptoid and their antimicrobial activity

- D.; Zuckermann, R. N.; Barron, A. E. Peptoids That Mimic the Structure, Function, and Mechanism of Helical Antimicrobial Peptides. *Proc. Natl. Acad. Sci.* **2008**, *105* (8), 2794–2799.
- (11) Bremner, J. B.; Keller, P. A.; Pyne, S. G.; Boyle, T. P.; Brkic, Z.; David, D. M.; Robertson, M.; Somphol, K.; Baylis, D.; Coates, J. A.; Deadman, J.; Jeevarajah, D.; Rhodes, D. I. Synthesis and Antibacterial Studies of Binaphthyl-Based Tripeptoids. Part 1. *Bioorg. Med. Chem.* **2010**, *18* (7), 2611–2620.
- (12) Bremner, J. B.; Keller, P. A.; Pyne, S. G.; Boyle, T. R.; Brkic, Z.; David, D. M.; Garas, A.; Morgan, J.; Robertson, M.; Somphol, K.; Miller, M. H.; Howe, A. S.; Ambrose, P.; Bhavnani, S.; Fritsche, T. R.; Biedenbach, D. J.; Jones, R. N.; Buckheit, R. W.; Watson, K. M.; Baylis, D.; Coates, J. A.; Deadman, J.; Jeevarajah, D.; McCracken, A.; Rhodes, D. I. Binaphthyl-Based Dicationic Peptoids with Therapeutic Potential. *Angew. Chem, Int. Ed.* **2010**, *49* (3), 537–540.
- (13) Chongsiriwatana, N. P.; Miller, T. M.; Wetzler, M.; Vakulenko, S.; Karlsson, A. J.; Palecek, S. P.; Mobashery, S.; Barron, A. E. Short Alkylated Peptoid Mimics of Antimicrobial Lipopeptides. *Antimicrob. Agents Chemother.* **2011**, *55* (1), 417–420.
- (14) Benson, M. A.; Shin, S. B. Y.; Kirshenbaum, K.; Huang, M. L.; Torres, V. J. A Comparison of Linear and Cyclic Peptoid Oligomers as Potent Antimicrobial Agents. *ChemMedChem* **2012**, *7* (1), 114–122.
- (15) Mojsoska, B.; Zuckermann, R. N.; Jenssen, H. Structure-Activity Relationship Study of Novel Peptoids That Mimic the Structure of Antimicrobial Peptides. *Antimicrob. Agents Chemother.* **2015**, *59* (7), 4112–4120.
- (16) Bolt, H. L.; Eggimann, G. A.; Jahoda, C. A. B.; Zuckermann, R. N.; Sharples, G. J.; Cobb, S. L. Exploring the Links between Peptoid Antibacterial Activity and Toxicity. *Medchemcomm* **2017**, *8* (5), 886–896.
- (17) Zuckermann, R. N. Peptoid Origins. *Biopolymers* **2011**, *96* (5), 545–555.
- (18) Chan, B. A.; Xuan, S.; Li, A.; Simpson, J. M.; Sternhagen, G. L.; Yu, T.; Darvish, O. A.; Jiang, N.; Zhang, D. Polypeptoid Polymers: Synthesis, Characterization, and Properties. *Biopolymers* **2017**, *109* (1), 1–25.
- (19) Kricheldorf, H. R. Polypeptides and 100 Years of Chemistry of α -Amino Acid α -

Chapter 3. Linear polypeptoid and their antimicrobial activity

- Carboxyanhydrides. *Angew. Chem, Int. Ed.* **2006**, *45* (35), 5752–5784.
- (20) Fetsch, C.; Grossmann, A.; Holz, L.; Nawroth, J. F.; Luxenhofer, R. Polypeptoids from *N*-Substituted Glycine *N*-Carboxyanhydrides: Hydrophilic, Hydrophobic, and Amphiphilic Polymers with Poisson Distribution. *Macromolecules* **2011**, *44* (17), 6746–6758.
- (21) Zhu, L.; Simpson, J. M.; Xu, X.; He, H.; Zhang, D.; Yin, L. Cationic Polypeptoids with Optimized Molecular Characteristics toward Efficient Nonviral Gene Delivery. *ACS Appl. Mater. Interfaces* **2017**, *9* (28), 23476–23486.
- (22) Fetsch, C.; Luxenhofer, R. Highly Defined Multiblock Copolypeptoids : Pushing the Limits of Living Nucleophilic. *Macromol. Rapid Commun.* **2012**, *33* (19), 1708–1713.
- (23) Kricheldorf, H. R.; Von Lossow, C.; Schwarz, G. Primary Amine-Initiated Polymerizations of Alanine-NCA and Sarcosine-NCA. *Macromol. Chem. Phys.* **2004**, *205* (7), 918–924.
- (24) Kricheldorf, H. R.; Böisinger, K. Mechanismus Der NCA-Polymerisation, 3. Über Die Amin Katalysierte Polymerisation von Sarkosin-NCA Und -NTA. *Die Makromol. Chemie* **1976**, *177* (5), 1243–1258.
- (25) Kricheldorf, H. R.; Lossow, C. V.; Schwarz, G.; Fritsch, D. Chain Extension and Cyclization of Telechelic Polysarcosines. *Macromol. Chem. Phys.* **2005**, *206* (12), 1165–1170.
- (26) Ballard, D. G. H.; Bamford, C. H. Reactions of *N*-Carboxy- α -Amino-Acid Anhydrides Catalysed by Tertiary Bases. *J. Chem. Soc.* **1956**, 381–387.
- (27) Bamford, B. C. H.; Block, H.; Pugh, A. C. P. The Polymerization of 3-Substituted Oxazolidine-2,5-Diones. **1960**, 2057–2063.
- (28) Kricheldorf, H. R.; Von Lossow, C.; Schwarz, G. Tertiary Amine Catalyzed Polymerizations of α -Amino Acid *N*-Carboxyanhydrides: The Role of Cyclization. *J. Polym. Sci. Part A Polym. Chem.* **2006**, *44* (15), 4680–4695.
- (29) Kricheldorf, H. R.; Von Lossow, C.; Schwarz, G. Cyclic Polypeptides by Solvent-Induced Polymerizations of α -Amino Acid *N*-Carboxyanhydrides. *Macromolecules* **2005**, *38* (13), 5513–5518.
- (30) Kricheldorf, H. R.; Lossow, C. V.; Lomadze, N.; Schwarz, G. Cyclic Polypeptides by Thermal Polymerization of α -Amino Acid *N*-Carboxyanhydrides. *J. Polym. Sci. Part A Polym. Chem.* **2008**, *46* (12), 4012–4020.

Chapter 3. Linear polypeptoid and their antimicrobial activity

- (31) Chan, B. A.; Xuan, S.; Horton, M.; Zhang, D. 1,1,3,3-Tetramethylguanidine-Promoted Ring-Opening Polymerization of *N*-Butyl *N*-Carboxyanhydride Using Alcohol Initiators. *Macromolecules* **2016**, *49* (6), 2002–2012.
- (32) Lee, C.-U.; Li, A.; Ghale, K.; Zhang, D. Crystallization and Melting Behaviors of Cyclic and Linear Polypeptoids with Alkyl Side Chains. *Macromolecules* **2013**, *46* (20), 8213–8223.
- (33) Robinson, J. W.; Secker, C.; Weidner, S.; Schlaad, H. Thermoresponsive Poly(*N*-C3 Glycine)*S*. *Macromolecules* **2013**, *46* (3), 580–587.
- (34) Robinson, J. W.; Schlaad, H. A Versatile Polypeptoid Platform Based on *N*-Allyl Glycine. *Chem. Commun.* **2012**, *48* (63), 7835.
- (35) Imanishi, Y.; Tsuchida, T.; Higashimura, T. Synthesis and Characterization of Poly(*N*-Cyanoethylglycine). *Polym. J.* **1978**, *10*, 287.
- (36) Fetsch, C. Polypeptide - Synthese Und Charakterisierung. Julius-Maximilians-Universität Würzburg, 2015.
- (37) Fu, X.; Li, Z.; Wei, J.; Sun, J.; Li, Z. Schiff Base and Reductive Amination Reactions of α -Amino Acids: A Facile Route toward: *N*-Alkylated Amino Acids and Peptoid Synthesis. *Polym. Chem.* **2018**, *9* (37), 4617–4624.
- (38) Guo, L.; Li, J.; Brown, Z.; Ghale, K.; Zhang, D. Synthesis and Characterization of Cyclic and Linear Helical Poly(α -Peptoid)s by *N*-Heterocyclic Carbene-Mediated Ring-Opening Polymerizations of *N*-Substituted *N*-Carboxyanhydrides. *Pept. Sci.* **2011**, *96* (5), 596–603.
- (39) Xuan, S.; Gupta, S.; Li, X.; Bleuel, M.; Schneider, G. J.; Zhang, D. Synthesis and Characterization of Well-Defined PEGylated Polypeptoids as Protein-Resistant Polymers. *Biomacromolecules* **2017**, *18* (3), 951–964.
- (40) Guo, L.; Zhang, D. Cyclic Poly(α -Peptoid)s and Their Block Copolymers from *N*-Heterocyclic Carbene-Mediated Ring-Opening Polymerizations of *N*-Substituted *N*-Carboxyanhydrides. *J. Am. Chem. Soc.* **2009**, *131* (50), 18072–18074.
- (41) Li, A.; Lu, L.; Li, X.; He, L. L.; Do, C.; Garno, J. C.; Zhang, D. Amidine-Mediated Zwitterionic Ring-Opening Polymerization of *N*-Alkyl *N*-Carboxyanhydride: Mechanism, Kinetics, and Architecture Elucidation. *Macromolecules* **2016**, *49* (4), 1163–1171.
- (42) Dorman, L. C.; Shiang, W. R.; Meyers, P. A. Purification of γ -Benzyl and γ -Methyl *L*-

Chapter 3. Linear polypeptoid and their antimicrobial activity

- Glutamate *N*-Carboxyanhydrides by Rephosgenation. *Synth. Commun.* **1992**, 22 (22), 3257–3262.
- (43) Semple, J. E.; Sullivan, B.; Sill, K. N. Large-Scale Synthesis of α -Amino Acid-*N*-Carboxyanhydrides. *Synth. Commun.* **2017**, 47 (1), 53–61.
- (44) Sisido, M.; Imanishi, Y.; Toshinobu, H. Molecular Weight Distribution of Polysarcosine Obtained by NCA Polymerization. *Macromol. Chem. Phys.* **1977**, 178, 3107–3114.
- (45) Muhl, C.; Zengerling, L.; Groß, J.; Eckhardt, P.; Opatz, T.; Besenius, P.; Barz, M. Insight into the Synthesis of: *N*-Methylated Polypeptides. *Polym. Chem.* **2020**, 11 (43), 6919–6927.
- (46) Liu, J.; Ling, J. DFT Study on Amine-Mediated Ring-Opening Mechanism of α -Amino Acid *N*-Carboxyanhydride and *N*-Substituted Glycine *N*-Carboxyanhydride: Secondary Amine versus Primary Amine. *J. Phys. Chem. A* **2015**, 119 (27), 7070–7074.
- (47) Bai, T.; Ling, J. Polymerization Rate Difference of *N*-Alkyl Glycine NCAs: Steric Hindrance or Not? *Biopolymers* **2019**, 110 (4), e23261.
- (48) Zhang, D.; Barrett, B.; Sternhagen, G. Controlled Ring-Opening Polymerization of *N*-(3-*Tert*-Butoxy-3-Oxopropyl) Glycine Derived *N*-Carboxyanhydrides towards Well-Defined Peptoid-Based Polyacids. *Polym. Chem.* **2021**, 547–563.
- (49) Hall, H. K. Correlation of the Base Strengths of Amines. *J. Am. Chem. Soc.* **1957**, 79 (20), 5441–5444.
- (50) Bradley, E. K.; Kerr, J. M.; Richter, L. S.; Figliozzi, G. M.; Goff, D. a; Zuckermann, R. N.; Spellmeyer, D. C.; Blaney, J. M. NMR Structural Characterization of Oligo-*N*-Substituted Glycine Lead Compounds from a Combinatorial Library. *Mol. Divers.* **1997**, 3 (1), 1–15.
- (51) Sui, Q.; Borchardt, D.; Rabenstein, D. L. Kinetics and Equilibria of *Cis/Trans* Isomerization of Backbone Amide Bonds in Peptoids. *J. Am. Chem. Soc.* **2007**, 129 (39), 12042–12048.
- (52) Vacogne, C. D.; Schlaad, H. Controlled Ring-Opening Polymerization of α -Amino Acid *N*-Carboxyanhydrides in the Presence of Tertiary Amines. *Polymer (Guildf)*. **2017**, 124, 203–209.
- (53) Vacogne, C. D.; Schlaad, H. Primary Ammonium/Tertiary Amine-Mediated Controlled Ring Opening Polymerisation of Amino Acid *N*-Carboxyanhydrides. *Chem. Commun.* **2015**, 51

Chapter 3. Linear polypeptoid and their antimicrobial activity

- (86), 15645–15648.
- (54) Wu, Y.; Zhang, D.; Ma, P.; Zhou, R.; Hua, L.; Liu, R. Lithium Hexamethyldisilazide Initiated Superfast Ring Opening Polymerization of *Alpha*-Amino Acid *N*-Carboxyanhydrides. *Nat. Commun.* **2018**, *9* (1), 5297.
- (55) Xia, Y.; Song, Z.; Tan, Z.; Xue, T.; Wei, S.; Zhu, L.; Yang, Y.; Fu, H.; Jiang, Y.; Lin, Y.; Lu, Y.; Ferguson, A. L.; Cheng, J. Accelerated Polymerization of *N*-Carboxyanhydrides Catalyzed by Crown Ether. *Nat. Commun.* **2021**, *12* (1).
- (56) Guo, L.; Lahasky, S. H.; Ghale, K.; Zhang, D. *N*-Heterocyclic Carbene-Mediated Zwitterionic Polymerization of *N*-Substituted *N*-Carboxyanhydrides toward Poly(α -Peptoid)s: Kinetic, Mechanism, and Architectural Control. *J. Am. Chem. Soc.* **2012**, *134* (22), 9163–9171.
- (57) Welge, H. J. Absorption of Carbon Dioxide in Aqueous Alkalies. *Ind. Eng. Chem.* **1940**, *32* (7), 970–972.
- (58) Guha, R. On Exploring Structure–Activity Relationships. In *Methods in Molecular Biology*; 2013; Vol. 993, pp 81–94.
- (59) Salas-Ambrosio, P.; Tronnet, A.; Verhaeghe, P.; Bonduelle, C. Synthetic Polypeptide Polymers as Simplified Analogues of Antimicrobial Peptides. *Biomacromolecules* **2021**, *22* (1), 57–75.
- (60) Mowery, B. P.; Lindner, A. H.; Weisblum, B.; Stahl, S. S.; Gellman, S. H. Structure-Activity Relationships among Random Nylon-3 Copolymers That Mimic Antibacterial Host-Defense Peptides. *J. Am. Chem. Soc.* **2009**, *131* (28), 9735–9745.
- (61) Mowery, B. P.; Lee, S. E.; Kissounko, D. A.; Epand, R. M. R. F.; Epand, R. M. R. F.; Weisblum, B.; Stahl, S. S.; Gellman, S. H. Mimicry of Antimicrobial Host-Defense Peptides by Random Copolymers. *J. Am. Chem. Soc.* **2007**, *129* (50), 15474–15476.
- (62) Chakraborty, S.; Liu, R.; Hayouka, Z.; Chen, X.; Ehrhardt, J.; Lu, Q.; Burke, E.; Yang, Y.; Weisblum, B.; Wong, G. C. L.; Masters, K. S.; Gellman, S. H. Ternary Nylon-3 Copolymers as Host-Defense Peptide Mimics: Beyond Hydrophobic and Cationic Subunits. *J. Am. Chem. Soc.* **2014**, *136* (41), 14530–14535.
- (63) Liu, L.; Courtney, K. C.; Huth, S. W.; Rank, L. A.; Weisblum, B.; Chapman, E. R.; Gellman, S. H. Beyond Amphiphilic Balance: Changing Subunit Stereochemistry Alters the Pore-

Chapter 3. Linear polypeptoid and their antimicrobial activity

- Forming Activity of Nylon-3 Polymers. *J. Am. Chem. Soc.* **2021**.
- (64) Liu, R.; Suárez, J. M.; Weisblum, B.; Gellman, S. H.; McBride, S. M. Synthetic Polymers Active against *Clostridium difficile* Vegetative Cell Growth and Spore Outgrowth. *J. Am. Chem. Soc.* **2014**, *136* (41), 14498–14504.
- (65) Wyrsta, M. D.; Cogen, A. L.; Deming, T. J. A Parallel Synthetic Approach for the Analysis of Membrane Interactive Copolypeptides. *J. Am. Chem. Soc.* **2001**, *123* (51), 12919–12920.
- (66) Lam, S. J.; O'Brien-Simpson, N. M.; Pantarat, N.; Sulistio, A.; Wong, E. H. H.; Chen, Y.-Y.; Lenzo, J. C.; Holden, J. A.; Blencowe, A.; Reynolds, E. C.; Qiao, G. G. Combating Multidrug-Resistant Gram-Negative Bacteria with Structurally Nanoengineered Antimicrobial Peptide Polymers. *Nat. Microbiol.* **2016**, *1* (16162), 1–11.
- (67) Zhou, C.; Qi, X.; Li, P.; Chen, W. N.; Mouad, L.; Chang, M. W.; Leong, S. S. J.; Chan-Park, M. B. High Potency and Broad-Spectrum Antimicrobial Peptides Synthesized via Ring-Opening Polymerization of α -Aminoacid-*N*-Carboxyanhydrides. *Biomacromolecules* **2010**, *11* (1), 60–67.
- (68) Takada, Y.; Itoh, H.; Paudel, A.; Panthee, S.; Hamamoto, H.; Sekimizu, K.; Inoue, M. Discovery of Gramicidin A Analogues with Altered Activities by Multidimensional Screening of a One-Bead-One-Compound Library. *Nat. Commun.* **2020**, *11* (1), 1–10.
- (69) Zhu, N.; Zhong, C.; Liu, T.; Zhu, Y.; Gou, S.; Bao, H.; Yao, J.; Ni, J. Newly Designed Antimicrobial Peptides with Potent Bioactivity and Enhanced Cell Selectivity Prevent and Reverse Rifampin Resistance in Gram-Negative Bacteria. *Eur. J. Pharm. Sci.* **2021**, *158* (November 2020), 105665.
- (70) Liu, P.; Zeng, X.; Wen, X. Design and Synthesis of New Cationic Antimicrobial Peptides with Low Cytotoxicity. *Int. J. Pept. Res. Ther.* **2020**, No. 0123456789.
- (71) Goodson, B.; Ehrhardt, A.; Ng, S.; Nuss, J.; Johnson, K.; Giedlin, M.; Yamamoto, R.; Moos, W. H.; Krebber, A.; Ladner, M.; Giacona, M. B.; Vitt, C.; Winter, J. Characterization of Novel Antimicrobial Peptoids. *Antimicrob. Agents Chemother.* **1999**, *43* (6), 1429–1434.
- (72) Miller, S. M.; Simon, R. J.; Ng, S.; Zuckermann, R. N.; Kerr, J. M.; Moos, W. H. Proteolytic Studies of Homologous Peptide and *N*-Substituted Glycine Peptoid Oligomers. *Bioorganic Med. Chem. Lett.* **1994**, *4* (22), 2657–2662.

Chapter 3. Linear polypeptoid and their antimicrobial activity

- (73) Korbmacher, M.; Fischer, S.; Landenberger, M.; Papatheodorou, P.; Aktories, K.; Barth, H. Human α -Defensin-5 Efficiently Neutralizes Clostridioides Difficile Toxins TcdA, TcdB, and CDT. *Front. Pharmacol.* **2020**, *11* (August), 1–10.
- (74) Suárez, J. M.; Edwards, A. N.; McBride, S. M. The Clostridium difficile Cpr Locus Is Regulated by a Noncontiguous Two-Component System in Response to Type A and B Lantibiotics. **2013**, *195* (11), 2621–2631.
- (75) Judzewitsch, P. R.; Nguyen, T. K.; Shanmugam, S.; Wong, E. H. H.; Boyer, C. Towards Sequence-Controlled Antimicrobial Polymers: Effect of Polymer Block Order on Antimicrobial Activity. *Angew. Chem, Int. Ed.* **2018**, *57* (17), 4559–4564.
- (76) Palermo, E. F.; Vemparala, S.; Kuroda, K. Cationic Spacer Arm Design Strategy for Control of Antimicrobial Activity and Conformation of Amphiphilic Methacrylate Random Copolymers. *Biomacromolecules* **2012**, *13* (5), 1632–1641.
- (77) Pan, M.; Lu, C.; Zheng, M.; Zhou, W.; Song, F.; Chen, W.; Yao, F.; Liu, D.; Cai, J. Unnatural Amino-Acid-Based Star-Shaped Poly(L -Ornithine)s as Emerging Long-Term and Biofilm-Disrupting Antimicrobial Peptides to Treat *Pseudomonas Aeruginosa* -Infected Burn Wounds. *Adv. Healthc. Mater.* **2020**, *9* (19), 2000647.
- (78) Rodríguez-Hernández, J.; Gatti, M.; Klok, H. A. Highly Branched Poly(L-Lysine). *Biomacromolecules* **2003**, *4* (2), 249–258.
- (79) Lee, E. Y.; Lee, M. W.; Fulan, B. M.; Ferguson, A. L.; Wong, G. C. L. What Can Machine Learning Do for Antimicrobial Peptides, and What Can Antimicrobial Peptides Do for Machine Learning?. *Interface Focus* **2017**, *7* (6), 20160153.
- (80) Bicker, K.; Cobb, S. L. Recent Advances in the Development of Anti-Infective Peptoids. *Chem. Commun.* **2020**.
- (81) Waschinski, C. J.; Barnert, S.; Theobald, A.; Schubert, R.; Kleinschmidt, F.; Hoffmann, A.; Saalwächter, K.; Tiller, J. C. Insights in the Antibacterial Action of Poly(Methyloxazoline)s with a Biocidal End Group and Varying Satellite Groups. *Biomacromolecules* **2008**, *9* (7), 1764–1771.
- (82) Greco, I.; Molchanova, N.; Holmedal, E.; Jenssen, H.; Hummel, B. D.; Watts, J. L.; Håkansson, J.; Hansen, P. R.; Svenson, J. Correlation between Hemolytic Activity, Cytotoxicity and Systemic in Vivo Toxicity of Synthetic Antimicrobial Peptides. *Sci. Rep.*

Chapter 3. *Linear polypeptoid and their antimicrobial activity*

2020, 10 (1), 1–13.

- (83) Bonduelle, C.; Verhaeghe, P.; Dupuy, B.; Tronnet, A.; Salas-Ambrosio, P. Antimicrobial Cationic Peptoid and *N*-Substituted Peptidic Copolymers, Preparation and Uses Thereof. EP 21305198.0, 2021.
- (84) Lea, T. Caco-2 Cell Line. In *The Impact of Food Bioactives on Health*; Springer International Publishing: Cham, 2015; pp 103–111.
- (85) Hussain, H. A.; Roberts, A. P.; Mullany, P. Generation of an Erythromycin-Sensitive Derivative of *Clostridium difficile* Strain 630 (630 Δ erm) and Demonstration That the Conjugative Transposon Tn916 Δ E Enters the Genome of This Strain at Multiple Sites. *J. Med. Microbiol.* **2005**, 54 (2), 137–141.
- (86) EUCAST. Determination of Minimum Inhibitory Concentrations (MICs) of Antibacterial Agents by Broth Dilution. *Clin. Microbiol. Infect.* **2003**, 9 (8), ix–xv.

Chapter 4. Macrocyclic polypeptoids and their antimicrobial activity

In biology, cyclic macromolecules are important: they allow the living systems to fine-tune certain physicochemical properties or specific biological functions. For instance, cyclic lipids are one of the main constituents along the membranes of extremophiles providing resistance to high temperatures or high salts concentrations.¹ Many living organisms produce cyclic structures from amino acids, structures that have an interesting therapeutic value.²³ In this regard, more than 20 cyclic peptides are in clinical trials and some of them are already in the market.^{2,4} This includes the cyclic peptide ziconotide, a potent non-opioid analgesic drug that is isolated from the venom of the fish-eating marine snail, *Conus magus*, to treat severe and chronic pain.⁵ In general, the cyclic structure is formed by coupling the head of a peptide to the end extremity through different chemical bonds: amide, lactone, ether, thioether, and disulfide.² Cyclic peptides provide interesting features as compared to linear counterparts. The most important is the greater rigidity (decreased entropy as compared to linear analogs) resulting in higher binding affinity and selectivity.⁶ Moreover, because they lack a terminal amino acid, cyclic peptides are much less susceptible to exopeptidases.

In infectiology, many research works have investigated the antibacterial properties of cyclic antimicrobial peptides (*c*-AMPs). Like other antimicrobial peptides (AMPs), *c*-AMPs are produced by bacteria to protect themselves from other bacteria.⁷ A representative example of *c*-AMP, gramicidin S, is composed of 10 amino acids (including 2 positively charged) and has demonstrated high activity against drug-resistant bacteria.⁸ Its mechanism of action is not fully elucidated but it has been demonstrated that gramicidin S destabilizes bacterial membranes by inducing pore formation.⁹ The key structural features of *c*-AMPs are similar to the ones of linear AMPs: specific length, amino acid sequence, amino acid composition, etc. (see chapter 1). Even if some of them are negatively charged, like daptomycin,¹⁰ most of them are cationic macrocycles, including:

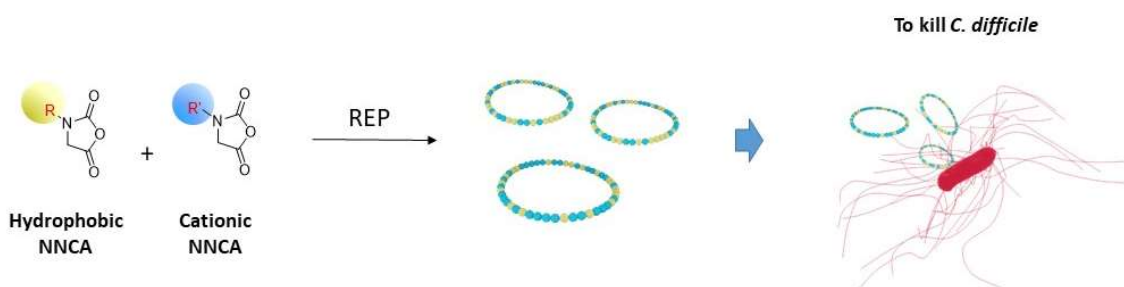
- Bacitracin, a 12 amino acid long AMP with a +1 net charge that interacts with bacterial membranes to interfere with the synthesis of the cell wall in Gram-positive bacteria.¹¹

- Colistin, a 10 amino acid AMP containing 5 positively charged residues: it is the last resort line in chemotherapy killing Gram-negative bacteria by inserting in the bilayer membrane and causing membrane leaking.¹²

Chapter 4. Macrocyclic polypeptoids and their antimicrobial activity

Despite interesting antibacterial properties, c-AMPs are generally restricted to clinic uses because they are often highly toxic and some of them are exclusively used for topical diseases.^{8,13} To improve their biocompatibility, SAR approaches currently explore new pharmacophores by developing synthetic peptides through solid-phase synthesis.⁹ Despite these efforts, endoprotease susceptibility, scale-up limitations and production costs are important factors limiting their development in therapy.

Using a polymeric approach, the goal in this chapter 4 was to design analogs of c-AMPs with low protease susceptibility by preparing cyclic poly(*N*-alkylated-glycines) also called cyclic polypeptoids. Cyclic peptoids are already known structures that can be obtained using solid-phase synthesis (SPPS).^{14,15} So far, the use of SPPS for the production of cyclic polypeptoids is limited by the numerous preparation steps and by the low reaction yields. Accessing cyclic polypeptoids through polymerization would be an interesting improvement in this field. Moreover, the use of polymer chemistry affords a simple route to combine, in a single step, cationic and hydrophobic units *via* copolymerizations. In this chapter, the goal was to prepare cyclic polypeptoids by copolymerizing *N*-alkylated-*N*-carboxyanhydrides (NNCA) using a ring-expansion copolymerization (REP) reaction promoted by lithium bis(trimethylsilyl)amide (LiHMDS). This unique access to cyclic peptoids enabled a comprehensive study of their antimicrobial properties against *Clostridioides difficile* (**Scheme 37**).



Scheme 37. Synthesis of cyclic polypeptoids for antimicrobial purposes.

1 Preparation of cyclic polymers using LiHMDS as a non-nucleophile strong base

Cyclic polymers are unique macromolecules that have different physical properties than

Chapter 4. *Macrocyclic polypeptoids and their antimicrobial activity*

their linear counterparts due to the “double constraint” related to cyclization. For instance, cyclic polyesters demonstrated modified solubility,^{16,17} crystallinity,^{17,18} and improved degradation profile toward against chemical hydrolysis.¹⁹ In solution, cyclic polymers possess a ring-like topology displaying smaller hydrodynamic volume. Also, it is known that cyclization concentrates spatial distribution of the side chains to achieve unique biological properties.^{20,21} For these reasons, efficient syntheses of cyclic polymers have attracted great interest in recent years.

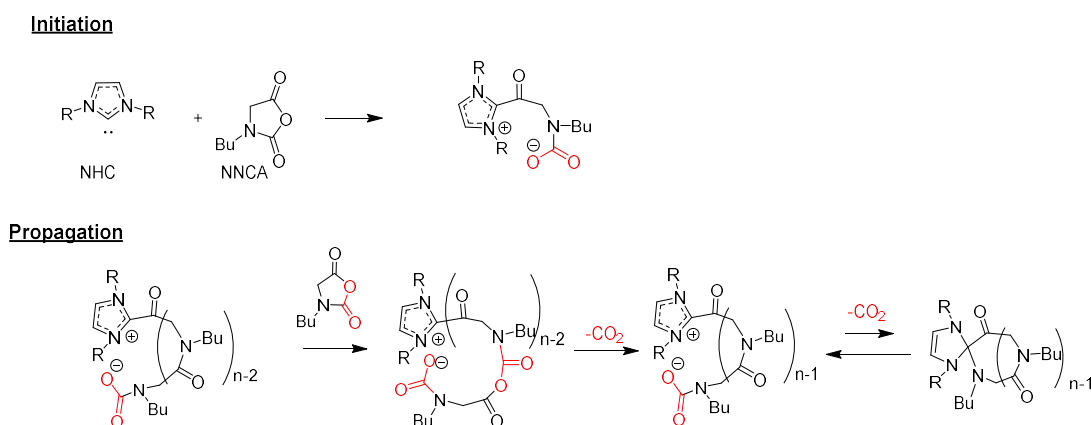
So far, three main routes have been proposed to synthesize cyclic polymers.^{20,22,23} Two of these routes involve post-polymerization grafting using tailored extremities of linear polymers and uni- or bi-molecular couplings.^{24–27} The bimolecular cyclization consists of using two activated moieties at the chain ends of two macromolecules that ensure the cyclization,^{20,28} similarly, the unimolecular cyclization occurs between the head and tail of a linear polymer to afford the cyclic structure: several approaches were investigated such as nucleophilic SnCl₄ assisted substitution²⁹ or click chemistry.³⁰ For these methods: a) the cyclization must be carried out at a high diluted concentration to avoid intermolecular condensation and b) access to cyclic polymers having high molar masses and low polymer dispersity is often complicated because of entropy.²⁰

In addition to these strategies, a third route is emerging in polymers science: the ring-expansion polymerization (REP). This methodology involves the insertion of cyclic monomers, (often *via* ring-opening polymerization reaction) using a cyclic catalyst/initiator. One of the first development of this approach was made with ring-expansion metathesis using cyclic ruthenium initiator/catalyst to produce cyclic olefins.²⁷ Since then, many other chain-growth processes have afforded REP as the zwitterionic ring-expansion polymerization developed by Hedricks and Waymouth to prepare cyclic polyesters from *N*-heterocyclic carbenes (NHCs).^{16,31} Based on similar zwitterionic mechanisms, other authors prepared recently cyclic polypeptides using various imidazolium hydrogen carbonate [NHC(H)(HCO₃)] initiators and *N*-carboxyanhydride monomers (NCAs).³² The scope of this last work included the preparation of cyclic copolymers bearing cationic precursor side chains (copolymers bearing *Cbz*-Lysine side chains).

Closer to this Ph.D. project, cyclic polypeptoids have already been prepared from Sar-NCA and Bu-NCA, using 2,6-diisopropylphenylimidazol-2-ylidene (NHC initiator).³³ D. Zhang *et al.* prepared macrocyclic structures which molar masses were controlled by the initial monomer/initiator ratio and with a dispersity $\mathcal{D}_M < 1.2$. These authors demonstrated possible access to both linear and cyclic copolymers by treatment with acetyl chloride or sodium bis(trimethylsilyl)amide, respectively.³⁴ The comparison of molar masses between linear and

Chapter 4. Macrocyclic polypeptoids and their antimicrobial activity

cyclic polypeptoids confirmed that cyclic structures exhibited a smaller hydrodynamic radius than linear polymers, thus eluting at a higher time. Later, D. Zhang *et al.* confirmed that REP followed a zwitterionic ring-opening polymerization when initiated by the nucleophilic attack of 1,3-Bis[2,6-bis(1-methylethyl)phenyl]-1,3-dihydro-2*H*-imidazol-2-ylidene on *N*-butyl-*N*-carboxyanhydrides (**Scheme 38**).³⁴ They described the mechanism by FTIR, matrix-assisted laser desorption/ionization analysis (MALDI TOF), and kinetics revealing that the mechanism followed a zwitterionic mechanism stabilized by the carbamate head and the NHC tail.



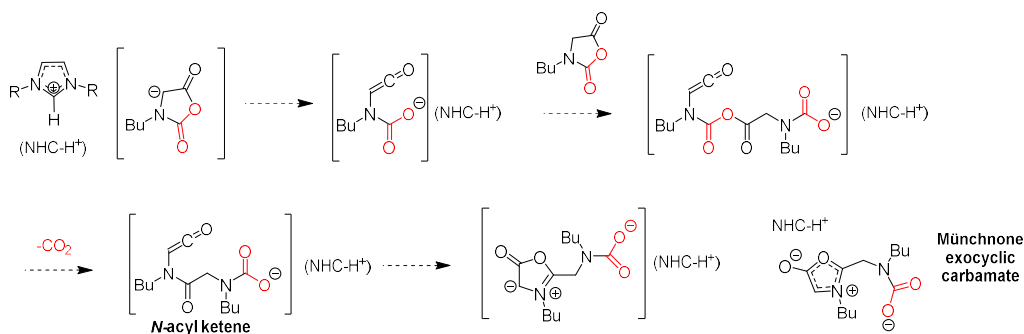
Scheme 38. Proposed mechanisms of the formation of cyclic polypeptoids by REP mediated with NHCs.³⁴

Overall, D. Zhang *et al.* showed that the REP needed to be carried out in low constant dielectric solvents, such as toluene, to access polymers in a controlled fashion (molar mass in agreement with M/I and low dispersity). The use of zwitterionic REP was a versatile approach, various NNCA monomers were used (with the limitation of toluene solubility) and the production of cyclic random copolymers was demonstrated including ones with amphiphilic character by varying the length of the *N*-substitutions using *N*-decyl-NNCA.³⁵

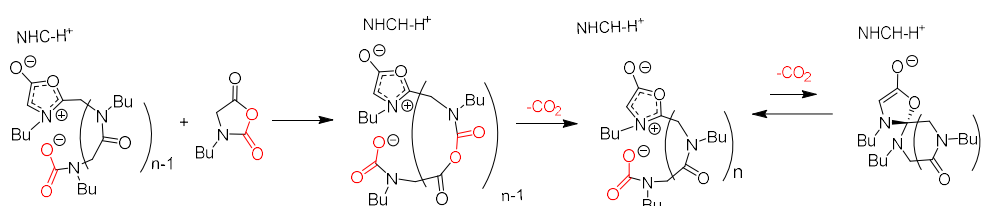
However, simple access to cyclic polymers with more functionalities, in particular bearing cationic precursor side chains, was still challenging because most of NNCA monomers (for instance those synthesized in chapter 2) are not soluble in toluene (**Table 38**). Interestingly, D. Zhang *et al.* also observed that in more polar solvents such as DMSO, a secondary mechanism was competing with the nucleophilic pathway presented in **Scheme 38**: a mechanism based on the formation of Münchnone carbamate complexes (**Scheme 39**).³⁴ This suggested that the use of strong bases could also lead to cyclic structures in more polar solvents with strong bases.

Chapter 4. Macrocyclic polypeptoids and their antimicrobial activity

Initiation



Propagation



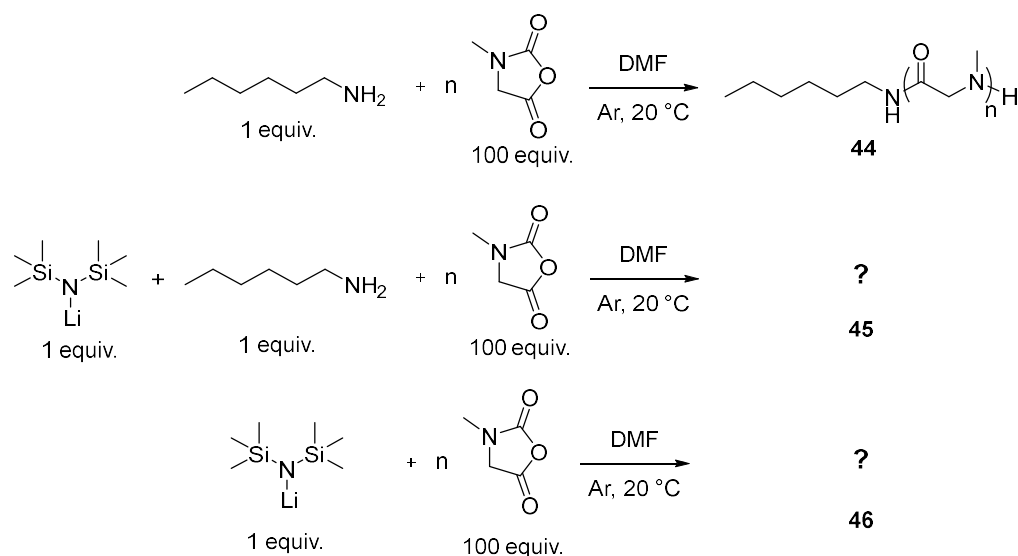
Scheme 39. The basic mechanism proposed for the formation of cyclic polypeptoids by NHC-induced REP.³⁴

For this reason, in the catalysis tests that are presented in chapter 3, we studied LiHMDS, a strong base already known to promote the superfast ROP of non-alkylated NCA monomers.³⁶ The results corresponding to these attempts are presented in the following paragraphs.

1.1 ROP of Sar-NCA with LiHMDS: kinetic study

As part of a catalytic study aiming at synthesizing polysarcosine (poly(sar)), we first implemented the ROP of Sar-NCA at 0.4 M in DMF from hexylamine (poly(sar)**44**), with or without a stoichiometric amount of LiHMDS (poly(sar)**45** and poly(sar)**46** as compared to hexylamine) at a monomer/LiHMDS ratio (M/B; B stands for base) = 100 (**Scheme 40**). The kinetics were followed by a decrease of the signal corresponding to the NCO stretching of the NCA at 1850 cm⁻¹ (as it was described in chapter 3 during the kinetics assays). Monitoring the disappearance of the NNCA peak by FTIR revealed that all polymerizations followed a first-order kinetics rate. Interestingly, a superior kinetics rate was found during the synthesis using LiHMDS (poly(sar)**46**, $k = 18 \times 10^{-3} \text{ min}^{-1}$) as compared to the polymerization initiated with hexylamine ($k = 9.5 \times 10^{-3} \text{ min}^{-1}$) (**Figure 41**) while the mixture LiHMDS + Hexylamine resulted in a similar kinetic rate to hexylamine initiated polymers ($10 \times 10^{-3} \text{ min}^{-1}$).

Chapter 4. Macrocyclic polypeptoids and their antimicrobial activity



Scheme 40. Catalytic experiments to enhance ROP kinetics of Sar-NCA using hexylamine (**44**), LiHMDS + Hexylamine (**45**) and LiHMDS (**46**) in DMF at 0.4 M.

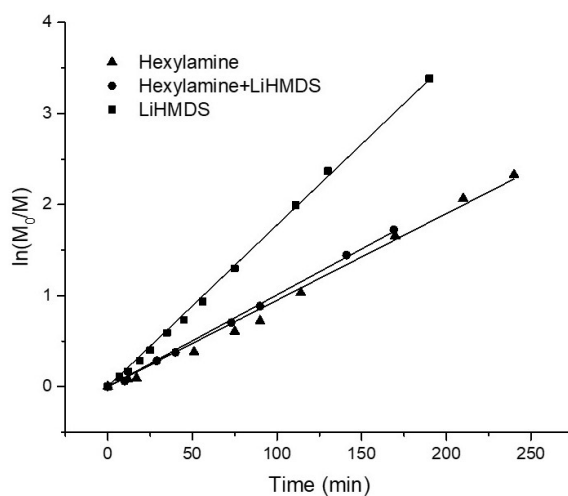


Figure 41. Comparison of the kinetics for the ROP reactions of poly(sar) using hexylamine (**44**), hexylamine + LiHMDS (**45**) and LiHMDS (**46**) at M/B=100 in DMF 0.4M

Although we observed a two-fold increase of the kinetics when we used LiHMDS, it is to note that the same initiator already provided a 20-fold kinetics difference with non-alkylated NCAs.³⁶ With NCAs, LiHMDS substracts the proton of the NCA ring which leads to the formation of a negatively charged species that initiates the ROP. This deprotonation cannot take place with NNCAs but with a very strong base like LiHMDS, the subtraction of the proton can take place in the *alpha* position (**Scheme 39**).^{33,34} Therefore we characterized the resultant product upon

precipitation in Et₂O and analyzed it by spectroscopy techniques such as SEC, MALDI TOF, and ¹H-NMR.

SEC analysis revealed a shift in the elution volume profiles between poly(sar)**46** and poly(sar)**44** having weighted-average molar masses (M_w) of 3500 g/mol ($\bar{D}_M = 1.06$) and 6100 g/mol ($\bar{D}_M = 1.06$), respectively (**Figure 42**). This particular feature is commonly presented in cyclic polymers due to the smaller hydrodynamic radius of cyclic polymers and consequent higher

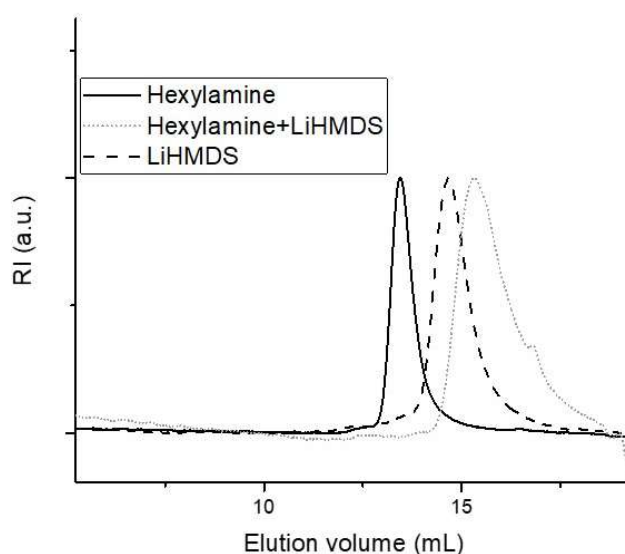


Figure 42. SEC chromatograms of the polymers obtained from the ROP initiated with hexylamine (poly(sar)**44**), with LiHMDS + hexylamine (poly(sar)**45**) and LiHMDS (poly(sar)**46**) at $M/B=100$.

elution volume in contrast with the linear counterpart, as reported in other studies about cyclic polypeptoids using NHCs.³³ Unexpectedly, poly(sar)**45** presented a lower molar mass of $M_w = 2300$ g/mol but a marked polydispersity $\bar{D}_M = 1.29$ that we attributed to a concomitant mechanism of initiation involving both hexylamine and LiHMDS.

The ¹H-NMR spectra showed the typical multiplet-broad peaks related to poly(sarcosine) for the three synthesized polymers (**Figure 43**). Interestingly, we observed that the NMR spectrum of the LiHMDS-initiated-polymer presented a signal at 2.24 ppm corresponding to the terminal methyl group that we first attributed to a cyclic species based on the basic mechanism³⁴ proposed by D. Zhang *et al.* (**Scheme 38c**). On another hand, the ¹H-NMR spectra of the two other polymers revealed the signals of hexylamine (CH₃, 0.85 ppm) and in concomitant mixture with the suggested cyclic structure (CH₃, 2.33 ppm, **Figure 43b**). Because of the dispersity value and the

presence of mixture of several compounds revealed by $^1\text{H-NMR}$, no more investigation was performed with poly(sar)**45**.

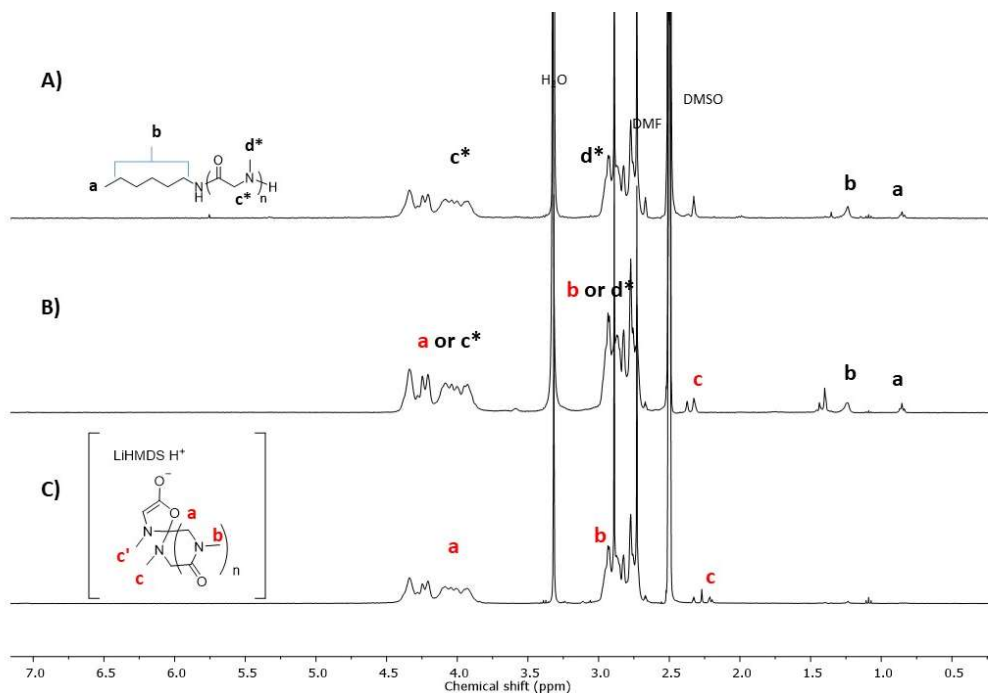


Figure 43. Comparison of $^1\text{H-NMR}$ spectra of poly(sarcosine) initiated with a) hexylamine, leading to (poly(sar)**44**) b) hexylamine and LiHMDS, leading to (poly(sar)**45**) and c) LiHMDS alone, leading to (cyclic, poly(sar)**46**)

To clarify the presence of cyclic structures from SEC and $^1\text{H-NMR}$ we performed MALDI TOF analysis of poly(sar)**46** using α -CHCA matrix (α -cyano-4-hydroxycinnamic acid) (**Figure 44**). The analysis revealed the presence of three sets of ions that matched with a $\Delta = 71$ g/mol, corresponding to the sarcosine building block (Nme), with an initiation attributable to previously observed spirocyclic structures thus confirming the formation of cyclic poly(peptoids).

From these results, we observed that cyclic structures were synthesized using LiHMDS as initiator in a polar solvent, DMF. At this stage, more information was necessary to understand how the polymerization proceeded.

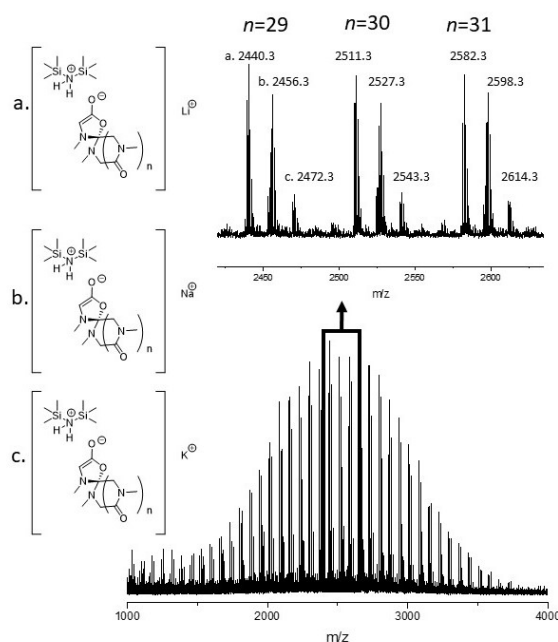


Figure 44. Full MALDI-ToF spectra with the assignment of the individual peaks from poly(sar)46.

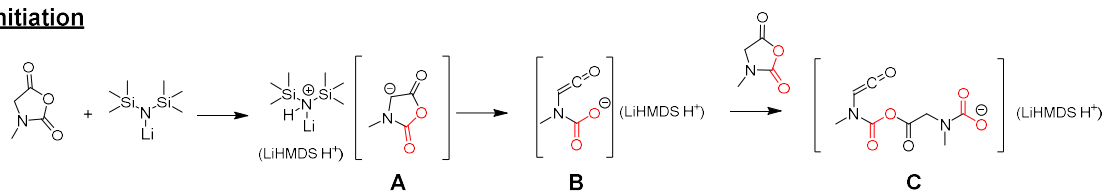
1.2 Mechanisms insights and elucidation of the structure

Previous mechanistic studies involving NHCs showed the formation of cyclic structures from two possible routes: a) nucleophilic attack by NHC and b) deprotonation of the NNCA.³⁴ Since LiHMDS is a non-nucleophilic molecule, we hypothesized a REP mechanism initiated by a deprotonation stage (**Scheme 41**). To demonstrate this possible mechanism, we implemented two new reactions by using Sar-NCA and LiHMDS with very low monomer/LiHMDS ratio (M/B ratio, where B stands for base) of 1 and 2 in DMF (0.4 M at 0°C). The goal was to catch the intermediates from the initiation steps of the mechanism proposed by D. Zhang *et al.*³⁴ Upon full conversion (~5 min) followed by FTIR, we isolated the product by precipitation in diethyl ether and drying under vacuum. We isolated a powder that was analyzed by electrospray ionization mass spectrometry ESI-MS and FTIR (**Figure 45** and **Figure 46**).

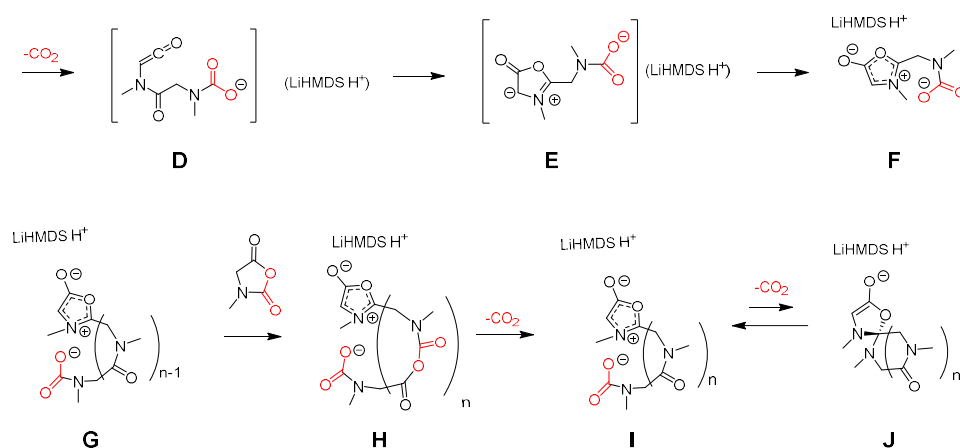
ESI-MS was used in negative mode (**Figure 45**) and we first analyzed the ESI-MS spectrum at M/B = 2 to provide full information about the REP initiation steps since M/B = 1 spectrum was too noisy (data not shown). Although the signal was too weak at $m/z = 185.06$, we observed the presence of the exocyclic Münchnone carbamate **F** matching with the theoretical value ($m/z = 185.05$). Since the process was very fast at early stages, and this even at low temperature, we also identified intermediates corresponding to the incorporation of more *N*-methylglycine units

Chapter 4. Macrocyclic polypeptoids and their antimicrobial activity

Initiation



Propagation



Scheme 41. Proposed mechanism for the formation of cyclic poly(sarcosine) initiated by LiHMDS based on the previously reported basic catalyzed route using NHCs.³⁴

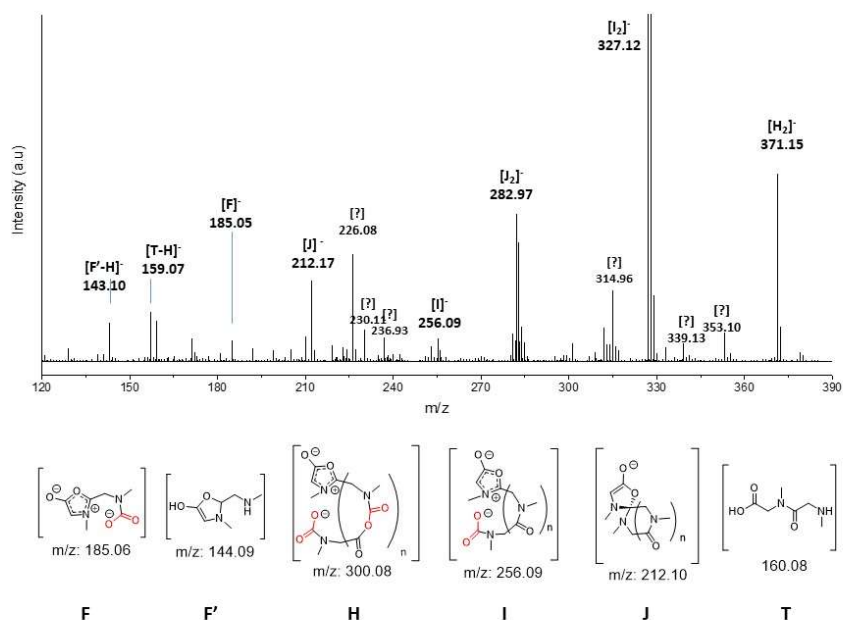


Figure 45. ESI-MS spectra of poly(sarcosine) initiated by LiHMDS at M/B=2 recorded in negative mode.

Chapter 4. Macrocyclic polypeptoids and their antimicrobial activity

such as the structures **H-J** (Scheme 41). The m/z values of each of these intermediates were found at expected m/z theoretical values. Other small signals were also observed that were attributed to fragmentation during the analysis **F'**, **T**, and others.

In the literature, mesoionic compounds (Münchnone) have been characterized through specific IR band signals: a doublet in the region comprised between 1630-1800 cm^{-1} for the carbonyl groups.^{37,38} Therefore, we performed FTIR analysis on the reaction performed at $M/B = 1$, thinking that we could observe these characteristic bands at low M/B . However, when we analyzed the reaction mixture, we did not observe the Münchnone species but the carbamate and the amide bonds instead (1500 and 1652 cm^{-1} , **Figure 46**). We attributed this observation to the premature formation of cyclic polymers as we already observed by ESI-MS at $M/B=2$ (**Figure 45**).

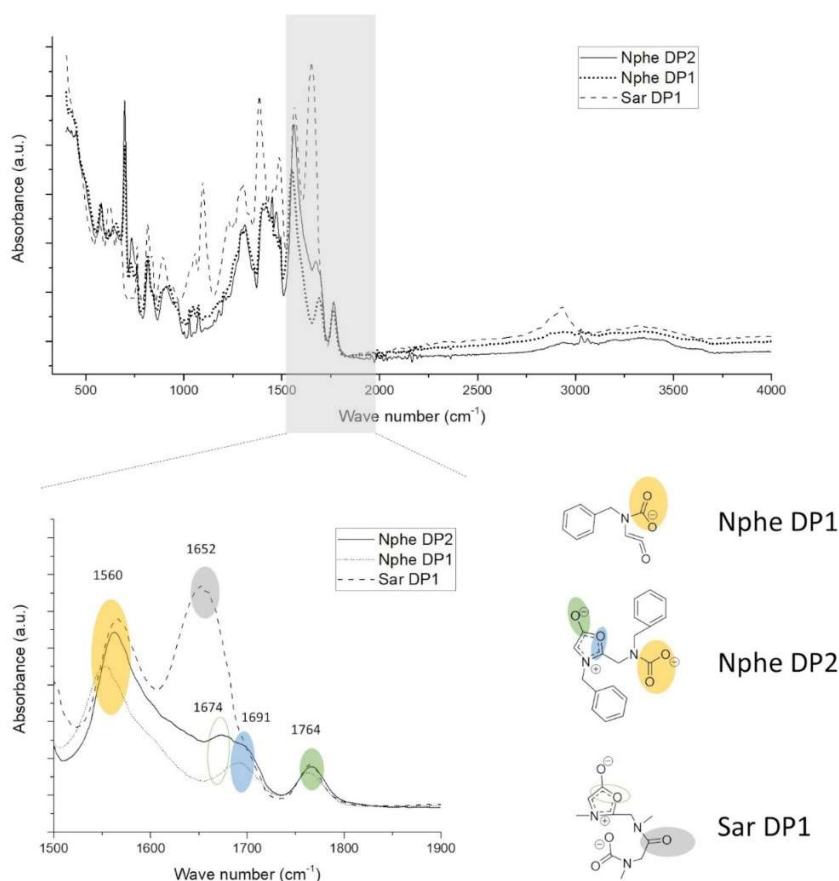


Figure 46. FTIR spectrum of *N*-benzyl-NCA reacted with LiHMDS at $M/I = 1$ and 2.

To slow down the reactivity, we then decided to repeat the reaction with more bulky groups using Phe-NNCA, and the reaction was performed again at $M/B = 1$ and 2. Upon precipitation and

drying under vacuum, we analyzed the compound by FTIR. This time, we successfully observed two peaks at 1691 and 1764 cm^{-1} that we clearly attributed to the carbonyl of Münchonone species, at both M/B = 1 & 2 (**Figure 46**). Furthermore, we observed a signal at 1560 cm^{-1} corresponding to the carbonyl stretching of the carbamate head group, similarly to other carbamates that presented a peak at 1570 cm^{-1} .³⁹

The spectroscopy studies revealed that we formed cyclic structures through a basic mechanism, however, it was difficult to characterize experimentally the zwitterionic intermediates responsible for the ring-expansion polymerization. Therefore, we performed molecular modeling studies on model peptoids composed of 5 monomer units (see the experimental section for a full description).⁴⁰ **Figure 47** shows the optimized structures we obtained upon DFT calculations of zwitterionic linear DP5 stabilized by LiHMDS (A), cyclic DP5 stabilized by LiHMDS (B), and cyclic DP5 stabilized by Li-DMF (C) structures. The computed relative energies showed that the cyclic

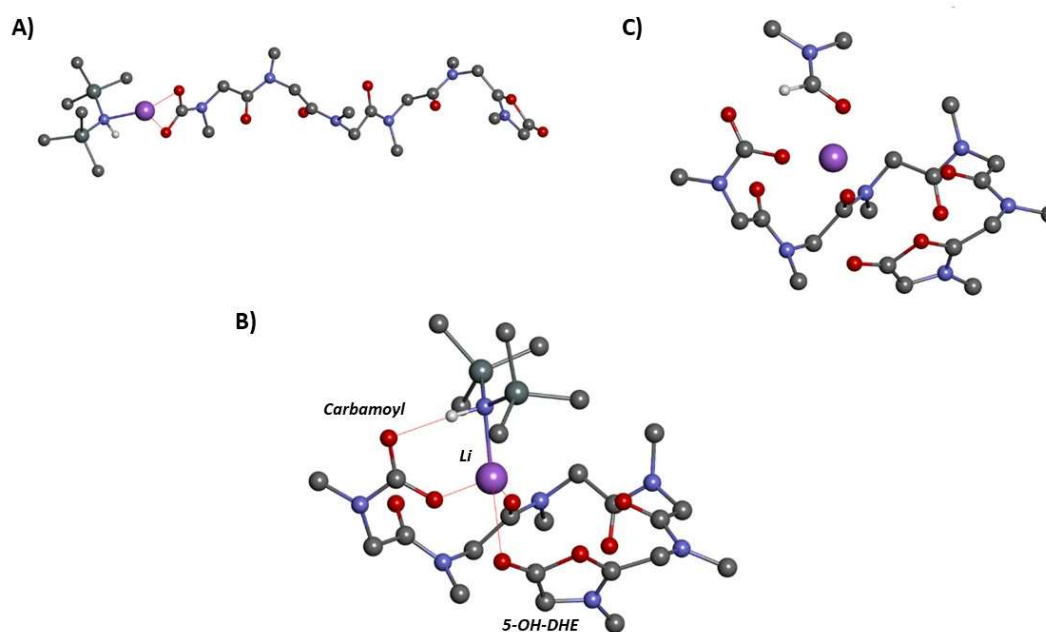


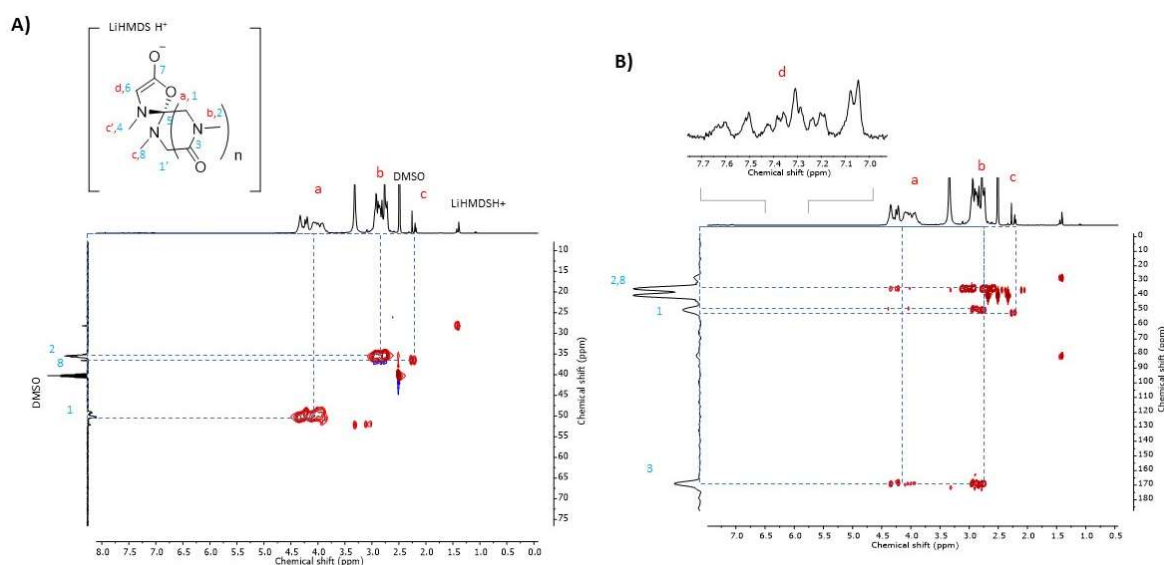
Figure 47. A) Structure of the zwitterionic DP5-LiHMDS (linear form). B) Structure of the zwitterionic DP5-LiHMDS (cyclic form). C) Structure of DP5-Li-DMF (cyclic form). For clarity, apolar hydrogens are omitted. The red lines show the interactions between LiHMDS and the peptoid.

zwitterionic form (B) was energetically more stable than the linear zwitterionic form (A) with an energy gap of $\Delta = -18.6 \text{ kJ/mol}^{-1}$. This result demonstrated that thermodynamically, cyclic polymers were more accessible than linear counterparts. In the same way, the cyclic zwitterionic

Chapter 4. Macrocyclic polypeptoids and their antimicrobial activity

form (B) was found energetically more stable than the cyclic DP5-Li-DMF form (C), with an energy gap of $\Delta = -16.0 \text{ kJ/mol}^{-1}$. From this study we could conclude that LiHMDS favored the stabilization of a cyclic intermediate in which three stabilizing interactions are created between the polymer and the Li^+ cation, allowing spatial proximity between the anionic carbamoyl extremity and the positive charge of the Münchnone moiety (5-hydroxy-2,3-dihydrooxazolium enolate = 5-OH-DHE in **Figure 47b**).

The presence of the 5-OH-DHE initiator was then investigated by performing new REP reactions to allow its NMR characterization (synthesis of lower molar mass). We carried out the REP of Sar-NCA at M/B = 35 in DMF 0.4 M (poly(sar)**47**). Upon full conversion followed by FTIR (2 h), we isolated the polymer by precipitation in diethyl ether in a 95% yield and characterized it by NMR (**Figure 48**). First, we observed broad and multiple peaks due to the *cis/trans* conformation of peptoid backbones⁴¹ that affected the whole structure (see for instance signals of the methyl group of the polymer backbone, **Figure 48, b and 2**). Nevertheless, we successfully observed 2D correlations involving the signals corresponding to the methyl group located right before the Münchnone exocyclic species *c*, **8** (2.21, 36.84 ppm) in HSQC (**Figure 48a**), the same



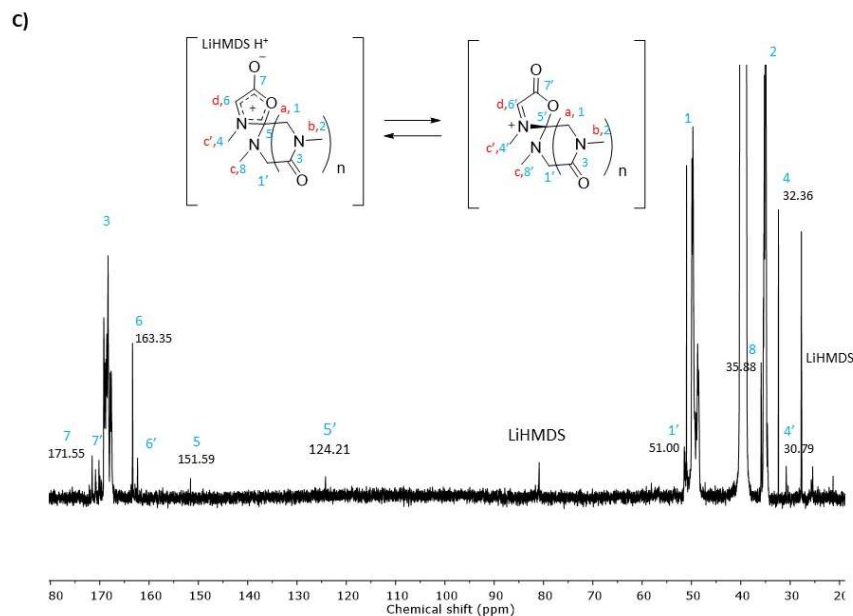


Figure 48. NMR spectra of poly(sar)47 showing the main characteristic peaks of the polypeptoid performed in DMSO- d_6 . a) HSQC, b) HMBC and c) ^{13}C -NMR.

signal also correlated with carbon 1 (2.21, 52.46 ppm) in HMBC (**Figure 48b**). Signals of the Münchnone were also observed as a multiplet signal attributed to the methine group *d* (7.0-7.7 ppm) in ^1H -NMR that was attributed to isomerism (**Figure 48b**). This isomerism was observed by ^{13}C -NMR through the signals 6 and 6' (163.35 and 162.33 ppm), 5 and 5' (151.29 and 124.21 ppm), 7 and 7' (170-171 ppm) corresponding to the Münchnone species. Overall, the analysis performed by NMR (^{13}C , HSQC and HMBC) in DMSO- d_6 corroborated the presence of Münchnone species.

As complementary studies, we characterized the compound by MALDI TOF and FTIR (**Figure 49**). By MALDI TOF using α -CHCA matrix we were able to identify the set of three ions matching with the cyclic structure bearing the Münchnone species and having $\Delta = 71$ g/mol indicating polymer formation by REP with LiHMDS. Finally, the FTIR spectrum showed both the carbonyl stretchings of both the zwitterionic structure and the Münchnone initiation species at 1568 and 1759 cm^{-1} as well as the polymer backbone at 1639 cm^{-1} .³⁷

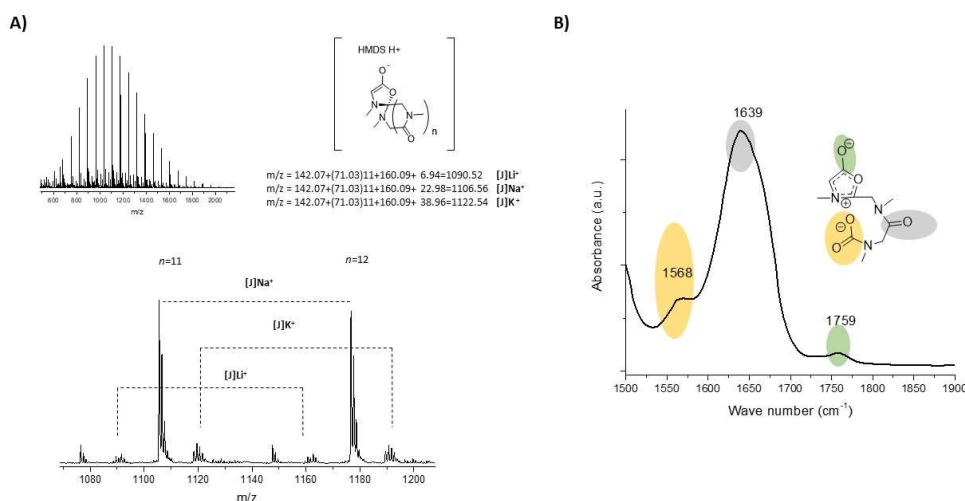
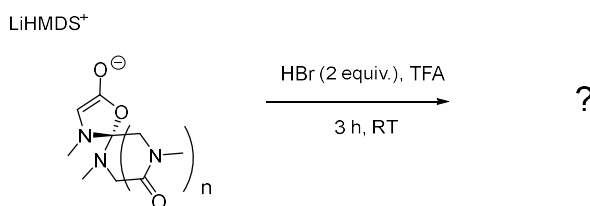


Figure 49. Complementary characterization of poly(sar) **47**. a) MALDI TOF spectrum showing the characteristic set of ions and b) FTIR spectrum showing the main characteristic peaks of the polypeptoid.

In conclusion, all these experimental and theoretical studies fully supported the hypotheses developed in section 1.1. The mechanism proposed by D. Zhang involving the formation of Münchnone species was therefore consistent with our observations and allowed us to explain the polymerization process initiated by LiHMDS working in a polar solvent (DMF).

1.3 Stability of cyclic polypeptoids with acidic conditions and propionylation

The mesoionic oxazole moiety (Münchnone species) is known to ring-open in acidic conditions.³⁸ Thus, the reactivity of the 5-OH-DHE ring from the cyclic structure was evaluated by exposing poly(Nme) poly(sar)**47** to HBr (2 equiv.) in TFA for 3 h at RT (**Scheme 42**).



Scheme 42. Acidic treatment of poly(sar)**47**.

We isolated the polymer by precipitation in diethyl ether and recovered it in a 75% yield upon drying. Then, we evaluated the structural changes on the chemical structure by NMR analyses in DMSO- d_6 (^1H , ^{13}C , HSQC and HMBC). First, we observed broad and multiple peaks on ^1H -NMR analyses due to the *cis/trans* conformation encountered in peptoids⁴¹ that affected

Chapter 4. Macrocyclic polypeptoids and their antimicrobial activity

the whole structure, meaning that the polymer resisted the acidic treatment (see for instance signals of the methyl group of the polymer backbone *b* and 2 in **Figure 50a** and **b**).

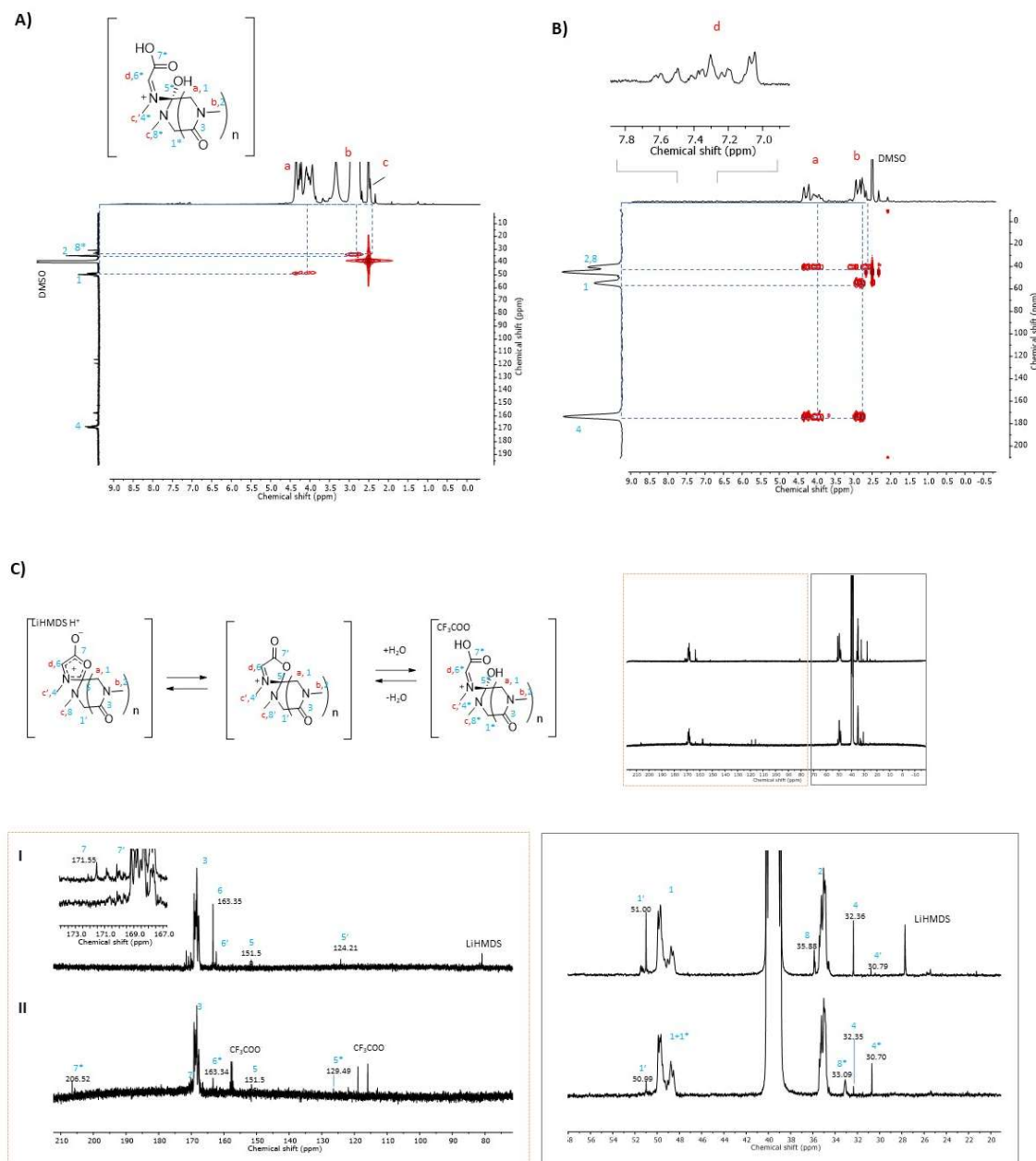


Figure 50. NMR characterization of poly(sar)47 upon acidic (HBr/TFA) treatment. 2D NMR showing the main characteristic peaks of the polypeptoid: A) HSQC and B) HMBC. C) ¹³C-NMR spectra of poly(sar)47 before (I) and upon acidic (HBr/TFA) treatment (II) showing the main characteristic peaks of the polypeptoid and the dynamic behavior of the exocyclic species performed in DMSO-d₆.

We then observed that the methyl group *c* shifted to 2.43 ppm and this new chemical shift was correlated with the carbon 8* (33.09 ppm) in the HSQC spectrum (**Figure 50a**). Moreover, a

Chapter 4. Macroyclic polypeptoids and their antimicrobial activity

comparison before and upon acid treatment of the poly(sar)**47** by ^{13}C -NMR revealed the concomitant presence of opened and closed forms of the Münchnone species (**Figure 50c**). Indeed, we observed a decrease of the signal of the carbon 4 (32.36 ppm), 8 (35.88 ppm) 6 (163.35 ppm) and 7 (171.51 ppm) of the mesoionic species and appearance of signals 4* (30.70 ppm), 8* (33.09 ppm), 6* (163.34 ppm) and 7* (206.52 ppm) corresponding to the ring-opening (**Scheme 42**).

In a second time, we performed MALDI TOF analysis using α -CHCA matrix and we confirmed that the polymer was preserved as we observed the typical $\Delta = 71$ g/mol corresponding to the *N*-methylglycine repeating unit (**Figure 51**). Moreover, the peak at $m/z = 110.54$ revealed that the 5-OH-DHE ring turned into an imino-acid group, as the opening form upon acidic treatment.

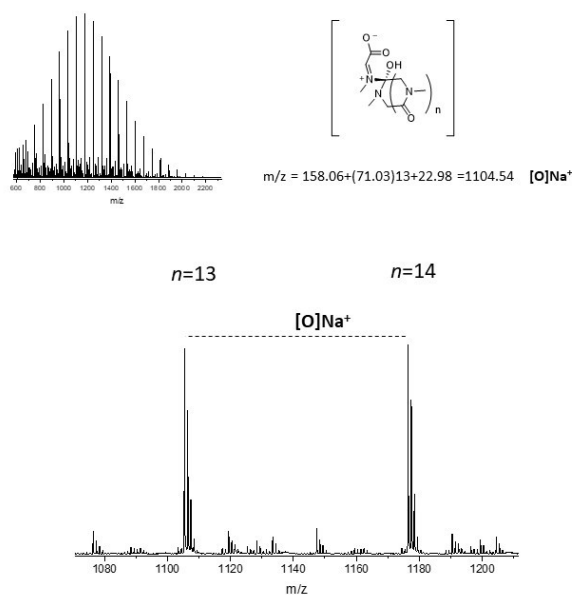


Figure 51. MALDI TOF spectrum for poly(*Nme*) M/B=35 upon acidic treatment (HBr/TFA).

In addition to the previous studies, we carried out SEC analysis to confirm that macrocyclic structures did not suffer structural modification upon the acid treatment. For that, we performed SEC analysis in DMF comparing poly(sar)**47** before and upon acid treatment (**Figure 52**). Interestingly, we observed a similar elution trace on the chromatogram as depicted in **Figure 52**. Therefore, we demonstrated that acidic treatment did not affect the overall macrocyclic structure and only resulted in ring-opening of the imino-acid function of the exocyclic group. These results

were important since the investigated reactivity with HBr was used to prepare cyclic polypeptoids bearing cationic side chains.

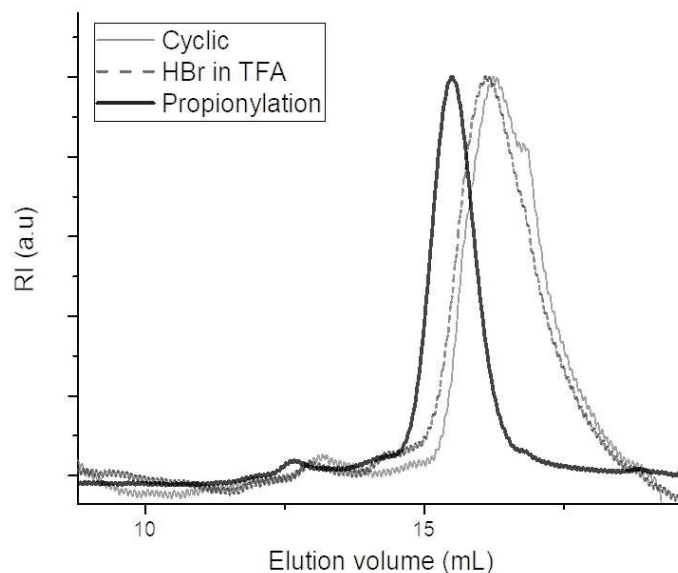


Figure 52. SEC chromatogram comparison of poly(Nme) $M/B = 35$ upon ring-opening polymerization initiated with LiHMDS (cyclic), propionylation, and acidic treatment (HBr 2 equiv. in TFA) in DMF.

Cyclic polypeptoids prepared with NHCs were already reported to react with acyl chlorides to yield linear counterparts.³⁴ Similarly, we found that treating poly(sar)**47** with propionic anhydride (1.8 equiv.) in anhydrous DMF for 12 h at RT yielded macrocycle opening into linear polypeptoid. Upon precipitation in diethyl ether (92% yield), we fully analyzed the propionylated polymer poly(sar)**47'** by SEC, NMR and MALDI TOF (**Figure 52** and **Figure 53**). The SEC analysis revealed a lower elution volume for poly(sar)**47'**, thus a linear polymer (**Figure 52**) with a higher molar mass ($M_w = 2200$ g/mol, $D_M = 1.15$) in comparison to the cyclic polymer ($M_w = 1800$ g/mol, $D_M = 1.03$). Moreover, according to previous studies,^{33,42,43} the ratio of the M_w values obtained with cyclic and linear counterparts ($M_{w\ cyclic} / M_{w\ linear}$ ratio = $\langle G \rangle$) provides information regarding the hydrodynamic radius ratio. Thus, we determined the $\langle G \rangle$ value of 0.81 that is similar to other cyclic polymers ($\langle G \rangle \sim 0.7-0.8$).^{33,42,43}

Then, we characterized poly(sar)**47'** by NMR and MALDI TOF analyses to verify the propionylation (**Figure 53**). First, 2D-NMR in DMSO- d_6 revealed that a signal attributable to the methyl extremity of the propionyl group was correlating the signals *g* and *6* (0.94 and 9.64 ppm in HSQC) and the signals *g* was found correlating the carbon 5 and 9 (0.94, 26.18, 173.71 ppm in HMBC). Moreover, the protons of the methylene group (signal *f*, 2.32 ppm) were correlating

Chapter 4. Macrocyclic polypeptoids and their antimicrobial activity

with carbon 5 (25.88 ppm in HSQC) and the *f* signal was found in correlation with carbon 6 and 9

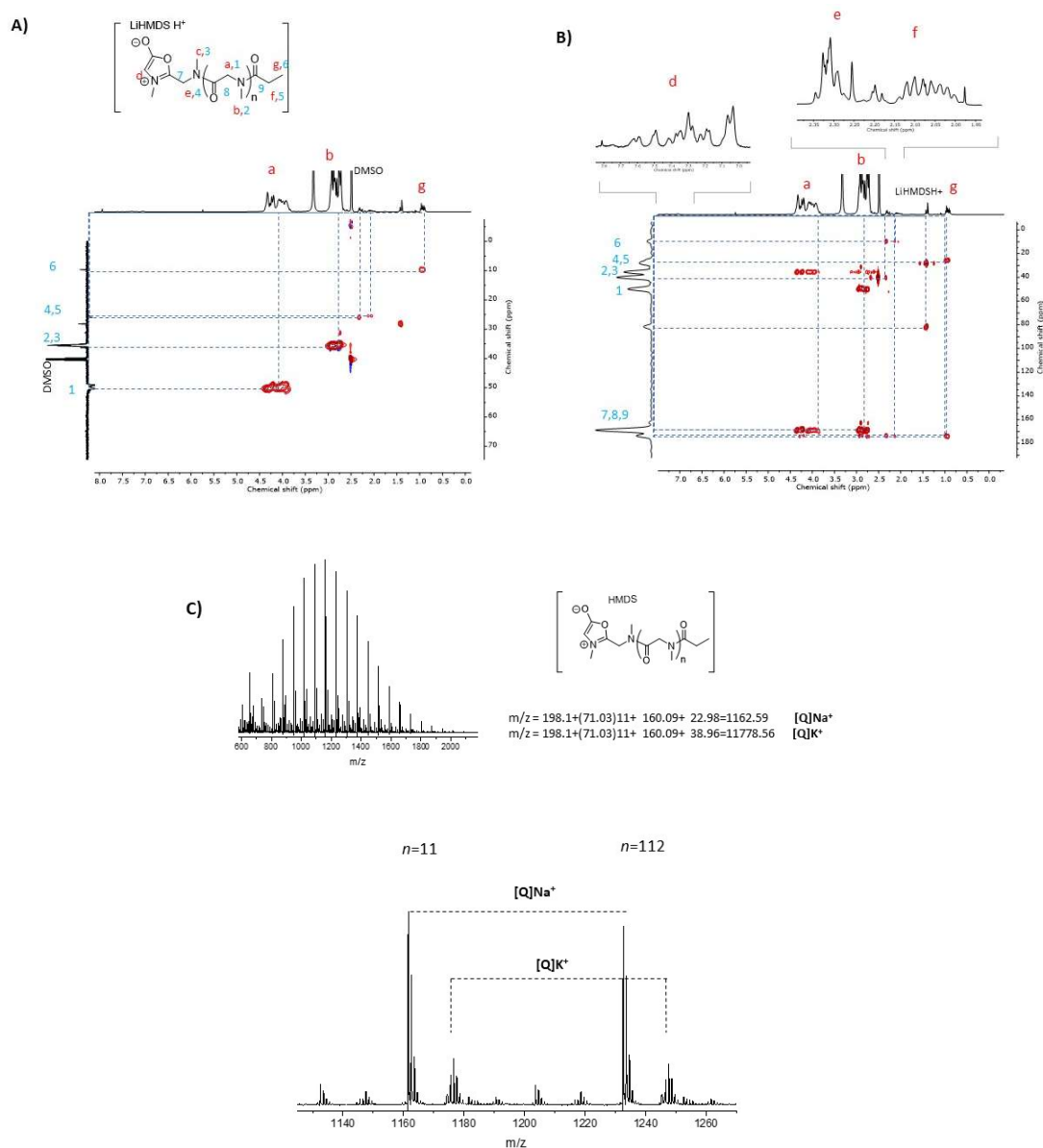


Figure 53. Characterization of poly(sar)47' showing the main characteristic peaks of the polypeptoid. A) HSQC and B) HMBC NMR spectra performed in DMSO-*d*₆. C) MALDI TOF spectrum.

(chemical shifts 2.32, 9.64, 173.71 ppm in HMBC). Besides, we observed the methine proton *d* corresponding to the Münchone extremity (7.2-7.8 ppm, **Figure 53**). Moreover, by using integrations of the signal attributable to a methyl group (CH₃, 0.94 ppm) and the integration of the signals of polymer backbone (CH₂, 3.84-4.44 ppm), we determined a polymerization degree of

21. This value was 10 units far from the theoretical one but matched perfectly with the M_w obtained by SEC (**Table 41**). Finally, we also performed MALDI TOF analysis using α -CHCA matrix to verify the propionylation. From this study, we corroborated the presence of linear structures bearing Münchone and propionylated extremities through the signal peaks corresponding to a set of ions with a $\Delta = 71$ g/mol typical of the monomer unit (**Figure 53c**).

Therefore, we found key informations regarding the reactivity of the cyclic polypeptoids: macrocyclic structures resisted acidic treatment and were opened by using propionic anhydride.

1.4 Comparison of LiHMDS initiated- versus *N*-heterocyclic carbene initiated-REP

Zhang and her collaborators carried out pioneer works about cyclic polypeptoids: they showed that NHC^{33,34,44} and 1,8-diazabicycloundec-7-ene (DBU)⁴⁵ can afford macrocycles *via* REP of NNCA. Although being quite efficient, these approaches remain sensitive to solvent effects, limiting the scope of the monomers that can be used for solubility reasons. In this section, to evaluate the benefit of our new methodology, we have conducted comparative experiments using LiHMDS-mediated REP and NHC-mediated REP.

N-heterocyclic carbenes are efficient initiators towards cyclic polypeptoids but their use is limited in polar solvents, such as DMF, as those solvents induce REP with two mechanisms: nucleophilic and basic.³⁴ To verify this statement, we challenged the polymerization performed in DMF by replacing LiHMDS with 3-dihydro-1,3-bis(2,4,6-trimethylphenyl)-2*H*-imidazol-2-ylidene, one of the best NHC to afford cyclic polypeptoids in toluene from *N*-butyl-NNCA.³⁴ We set up a REP experiment with Sar-NCA ($M/B = 100$, inert conditions and RT) in DMF with this NHC. The reaction was followed by FTIR until the disappearance of the peak at 1850 cm^{-1} . Upon full conversion, the polymer was precipitated in diethyl ether and dried under vacuum affording the poly(sar)**46 using NHC** in a 57% yield. Then, we characterized the polymer by SEC in DMF (**Figure 54**). A significantly broader peak was detected by this analysis (M_w was not possible to calculate) and was associated to much higher dispersity than the one from poly(sar)**46** ($D_M > 1.06$). These results confirmed that LiHMDS indeed better controlled the REP process occurring in DMF.

To better understand this difference in reactivity, additional theoretical calculations were carried out: we performed molecular modeling on model peptoids composed of 5 monomer units (see the experimental section for a full description). **Figure 54b** shows the optimized structures we obtained upon DFT calculations of zwitterionic cyclic DP5-LiHMDS (A) and cyclic DP5-NHC

(B, **Figure 55**). The computed relative energies of the simulated reactant and products showed

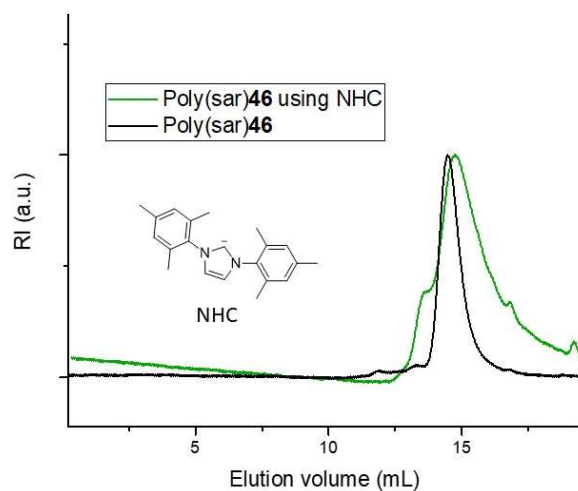


Figure 54. SEC comparison of cyclic poly(sar) **46** prepared by LiHMDS-REP and NHC-REP in DMF.

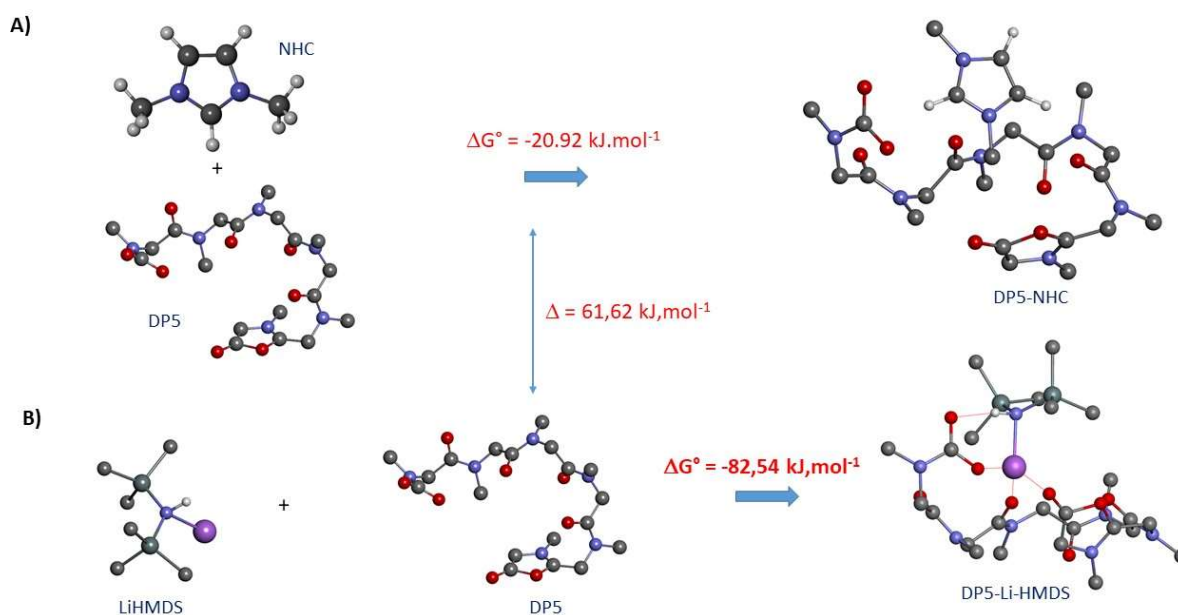


Figure 55. DFT comparative study of macrocyclic structures: a) DP5-NHC and b) DP5-LiHMDS (cyclic form, for clarity, apolar hydrogens are omitted).

that the cyclic zwitterionic species stabilized by LiHMDS (A) was more stable than the structure stabilized by NHC (B), with an energy gap of 61.6 kJ/mol⁻¹. This theoretical study indicated that, in both cases, the basic mechanism was favorable, but that it was much more favorable in the

case of LiHMDS. On the other hand, LiHMDS is not able to induce a nucleophile-like mechanism as NHCs do. Taken together, these results could explain why we were able to promote a clean and efficient REP in DMF.

In this Ph.D. work, it was important to demonstrate the access to cyclic cationic polymers for an antimicrobial design. Therefore, we studied briefly the use of NHCs to prepare cationic polymers using ZLys-NNCA monomers. For this purpose, we performed the reaction in a less polar solvent, THF, the solvent reported for the synthesis of cyclic polypeptoids with *N*-heterocyclic carbenes.⁴⁶ The reaction was performed at M/B = 30 using 3-dihydro-1,3-bis(2,4,6-trimethylphenyl)-2*H*-imidazol-2-ylidene (NHC) under inert conditions at RT.

Upon full conversion (24 h) followed by the disappearance of the NCO signal at 1850 cm⁻¹ by FTIR, we isolated the compound by precipitation in Et₂O, we dried under vacuum affording poly(ZNlys) using NHC in a 55% yield. Then, we characterized the polymer by SEC in DMF (**Figure 56**). We observed a significantly broader peak ($M_w = 4900$ g/mol) and was associated with much higher dispersity ($D_M > 2$). These results confirmed that LiHMDS can be a better controlled REP process in the preparation of cationic and cyclic polymers

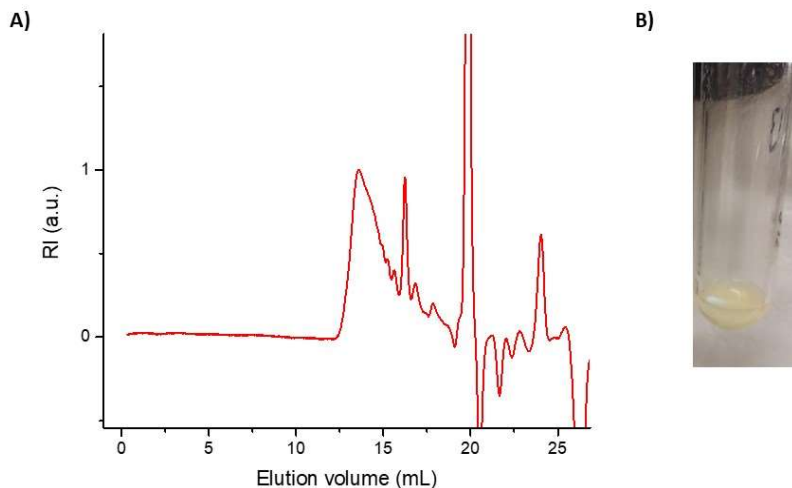


Figure 56. Synthesis of cyclic poly(ZNlys) from NHC: A) chromatogram by SEC in DMF and B) reaction mixture upon full conversion in THF.

1.5 Synthesis of polypeptoids varying the M/B ratio by LiHMDS-mediated REP

To further develop a comprehensive study of the LiHMDS-induced polymerization, several REP reactions using Sar-NCA as a monomer were carried out varying the M/B ratio from 35 to

Chapter 4. Macrocyclic polypeptoids and their antimicrobial activity

400 in DMF (0.4 M monomer concentration and under inert gas conditions, **Table 41**). The kinetics were followed by a decrease of the signal corresponding to the NCO stretching of the NCA at 1850 cm^{-1} (as described in chapter 3 during the kinetic assays). At full conversion (maximum 48 h for an M/B = 400) and after precipitation in Et_2O , the compounds were recovered in good yields ranging from 89 to 97% (**Table 41**). We first analyzed all these new polysarcosines by SEC in DMF: they presented increasing M_w values with controlled dispersity ($\mathcal{D}_M < 1.1$, **Figure 57a**): the lower the amount of LiHMDS added, the higher the weighted-average molar mass (M_w). An unexplained deviation was observed, especially for the higher ratios. Indeed, we generally observed a deviation that corresponded approximately to half of the theoretical values (**Table 41**).

Table 41. Poly(sarcosine)s upon REP (cyclic polymers, poly(sar)**46-52**) and upon propionylation (linear polymers, poly(sar)**46'-50'**). Molar masses were determined by SEC in DMF using $dn/dc_{\text{cyclic}} = 0.0978$ and $dn/dc_{\text{linear}} = 0.0861$.

Item	M / B	MW_{theo} (g/mol) ^a	M_n (g/mol)	M_w (g/mol)	\mathcal{D}_M	$\langle G \rangle^b$	DP_{NMR}^c	Yield	Full conversion (h)
Poly(sar) 46	100	7100	3300	3500	1.06	0.81	-	97%	5
Poly(sar) 47	35	2500	1700	1800	1.03	0.88	-	92%	2
Poly(sar) 48	60	4200	2000	2100	1.04	0.89	-	95%	3
Poly(sar) 49	75	5300	2400	2600	1.08	0.88	-	93%	4
Poly(sar) 50	200	14200	4700	5000	1.06	0.83	-	95%	24
Poly(sar) 51	400	28400	7900	8200	1.04	-	-	94%	48
Poly(sar) 52	50+50	7100	2900	3200	1.10	-	-	89%	-
Poly(sar) 46'	100	7100	3800	4000	1.07	-	52	90%	-
Poly(sar) 47'	35	2500	1900	2200	1.15	-	21	92%	-
Poly(sar) 48'	60	4200	2300	2400	1.06	-	32	92%	-
Poly(sar) 49'	75	5300	2800	2900	1.05	-	38	98%	-
Poly(sar) 50'	200	14200	5500	6000	1.09	-	127	90%	-

^aTheoretical M_w taking B as initiator and 71 g/mol for monomer unit; ^b $\langle G \rangle = M_w_{\text{cyclic}} / M_w_{\text{after propionylation}}$; ^c Calculated from $^1\text{H-NMR}$ using the CH_3 terminal group signal as a reference.

For each polymer, a part of the sample was then engaged in a propionylation reaction (see section 1.3) in order to compare the M_w values before and after linearization. We prepared the linear analogs from poly(sarcosines)**46-51** by using propionic anhydride (1.8 equiv.) in DMF at RT. After 12 h, the reaction was complete and the polymer was purified by precipitation in diethyl ether and dried under vacuum: the linear polymers were finally recovered in 90-98% yields. For all polymers, the $(M_w_{\text{cyclic}} / M_w_{\text{after propionylation}})$ from SEC analyses were close to 0.8, the value

established with cyclic polypeptoids when formed from NHCs promoted REP.³³ In fact this hydrodynamic volume difference was also observed on the plot of the elution volume obtained by SEC in DMF versus the logarithm of the weighted-averaged molar mass ($\log M_w$) of poly(sar)**46** before and upon propionylation. The plot revealed that poly(sar)**46** displayed a higher molar mass eluting a higher volume than the propionylated analog, thus, poly(sar)**46** had a lower hydrodynamic volume in comparison to linear counterparts in agreement with our calculation of $\langle G \rangle$.

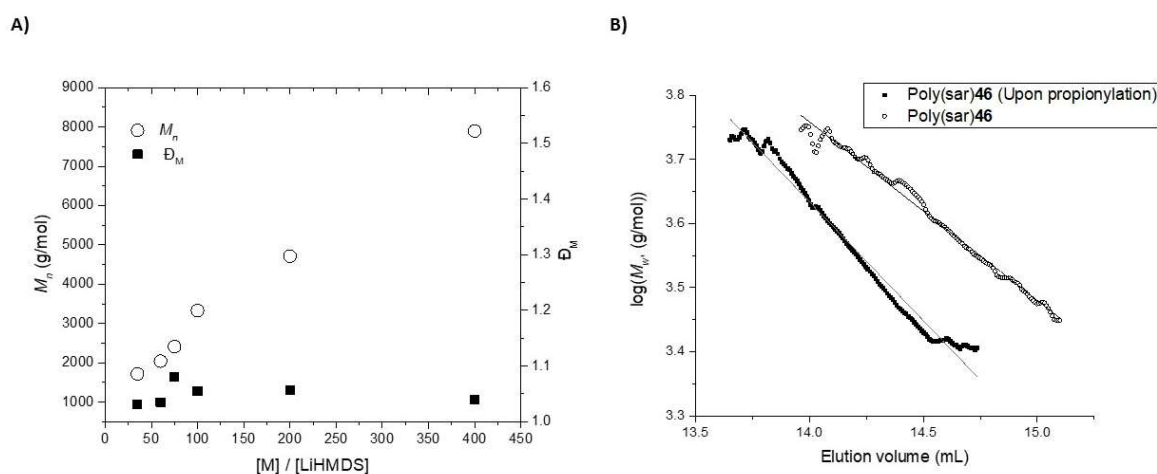


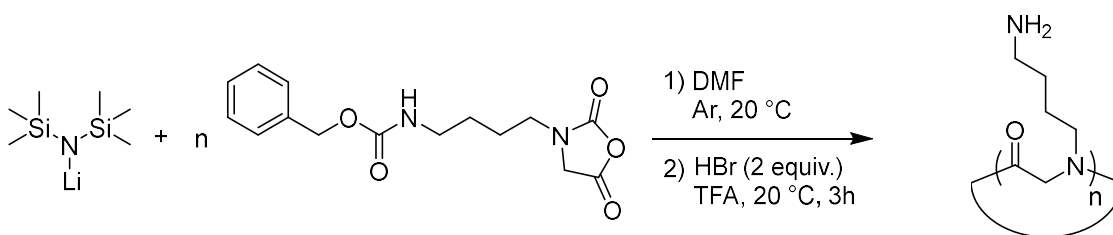
Figure 57. LiHMDS-mediated REP of Sar-NCA. A) Evolution of $\log M_w$ and \bar{D}_M (M_w/M_n) with M/B ratio. B) Difference of elution profiles of polymer **46** before or after propionylation versus the $\log M_w$ (g/mol).

The linear polypeptoids (cyclic + propionylated) were also characterized by ¹H-NMR in DMSO-d₆ and DP_{NMR} were calculated using the terminal methyl group (CH₃, 0.94 ppm) and the signals of polymer backbone (CH₂, 3.84-4.44 ppm, **Figure 53**). The calculated DP_{NMR} for **46'**-**50'** confirmed the deviation observed by SEC and we attributed hypothetically to the fact that during the REP process LiHMDS is needed to stabilize the zwitterionic macrocycle as we saw by DFT (section 1.2) thus presenting molecular masses lower than the theoretical value (**Table 41**).

Ultimately, the living nature of the REP was evaluated. Synthesis of poly(sar) at M/B = 50 was first performed and, at full conversion, another feed of Sar-NCA (M/B = 50) was added to the reaction until it was also consumed (FTIR monitoring of the NCA at 1850 cm⁻¹). The resulting poly(sar)**52** presented an M_w = 3200 g/mol, close to the M_w of poly(sar)**46**, associated with a low dispersity of $\bar{D} = 1.1$ (**Table 41**). This result indicated that diblock copolymers could be designed using LiHMDS.

1.6 Preparation of cationic homopolymer

The synthesis of cyclic polymers bearing aliphatic *N*-alkylated groups was already reported using NHC's.⁴⁷ However, this REP methodology is limited due to solvent incompatibility: for instance, cyclic polysarcosine was insoluble in toluene.³³ The use of a simple REP methodology, working in DMF, opens up interesting prospects to design polymers from new monomers (such as those developed in chapter 2), in particular positively charged cyclic polypeptoids that could pave the way to simplified analogues of *c*-AMPs. Therefore, we employed our REP methodology to synthesize cyclic polypeptoid from ZLys-NNCA. Our purpose was to prepare cyclic polymers bearing cationic side chains (*c*-poly(Nlys)) in two steps and at a targeted M/B = 30 (**Scheme 43**). The first step consisted of the REP of ZLys-NNCA using LiHMDS as initiator in DMF (0.4 M in DMF under inert conditions at RT) followed by deprotection in acid conditions (HBr 2 equiv. in TFA).



Scheme 43. Synthesis of cyclic cationic poly((*N*-aminobutyl)glycine) [*c*-(PNlys)]**53D** in DMF 0.4 M.

The conversion of the reaction was followed by a decrease of the signal corresponding to the NCO stretching of the NCA at $\sim 1850\text{ cm}^{-1}$. At full conversion, we isolated the *Cbz*-protected polymer (**53**) by precipitation (58% yield) and characterized it by NMR and MALDI TOF analyses (**Figure 58**). The formation of a polypeptoid backbone was first revealed by $^1\text{H-NMR}$ in CDCl_3 in which we observed the signals of polymer backbone (peak *a*, 3.6-4.6 ppm), and the side chains (peaks *b-e*), including the protecting group (peaks *g-h*). The $^{13}\text{C-NMR}$ allowed us to identify the carbons on the polymer backbone corresponding to the CH_2 (peaks 1, 48.19 ppm), the signal of the amide bonds (peak 6,9, 165.85 NCO) and the signals for the side chains (peaks 2-8). Then, we performed HSQC-NMR as depicted in **Figure 58a** and we observed correlation with the different signals present in the polymer, for instance, the CH_2 of the polymer backbone correlated with signals *a* and 1 (~ 4 and 48.19 ppm), thus, indicating the presence of a polypeptoid. However, we could neither observe the Münchnone species by this analysis nor LiHMDS: Münchnone species could be overlapped with the signal *h*. To better characterize the polymer structure, we also performed MALDI TOF analysis using dithranol matrix and confirmed the cyclic structure be-

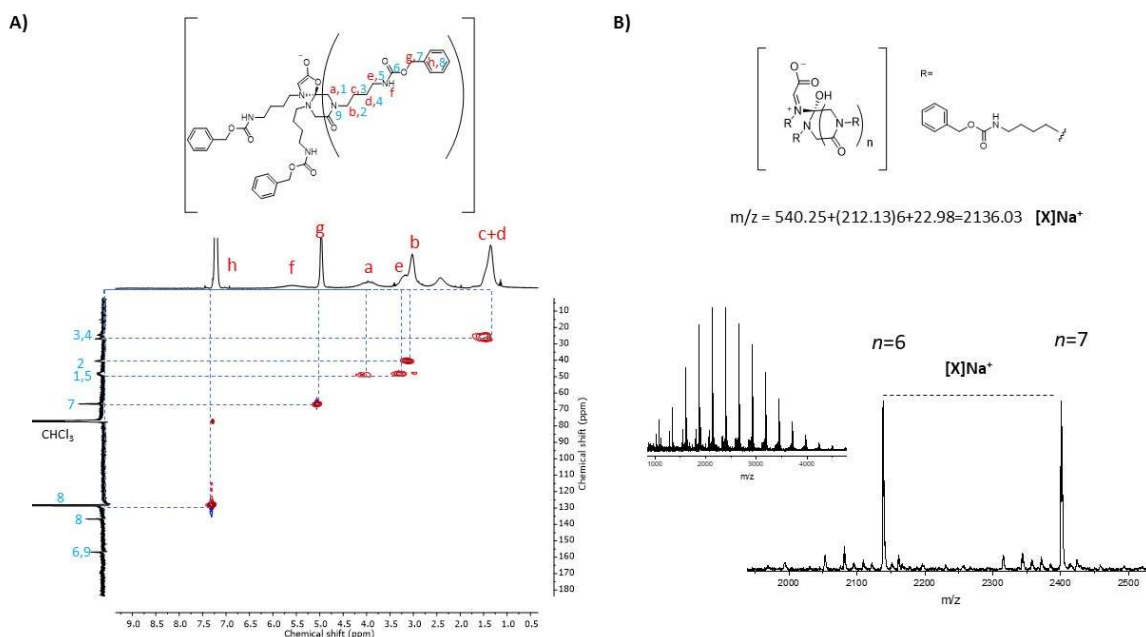


Figure 58. Cyclic poly(ZNlys) $M/I = 30$ (**53**): A) HSQC NMR spectrum in $CDCl_3$ and B) MALDI TOF spectrum

aring an imino-acid as exocycle group by the presence of a Na^+ adduct that has a $\Delta = 262$ g/mol attributed to the *Cbz*-aminobutyglycine (ZNlys). The MALDI TOF indicated that LiHMDS was lost during the purification step and the Münchone moiety was characterized in its opened form (addition of water) (**Figure 58b**).

The second step consisted of deprotecting the carboxybenzoyl group using HBr (2 equiv.) in TFA for 3 h at 20 °C. Precipitation in Et₂O then afforded the deprotected polymer **53D** in 62% yield. The cationic polymer (**53D**) was water-soluble (in marked contrast to the polypeptoid before deprotection **53**) and the deprotection was evaluated by performing ¹H-NMR analysis in D₂O (**Figure 59**).

The ¹H-NMR evidenced broad peak signals belonging to the polymer backbone (peak *a*, ~3.7-4.4 ppm) and to the lysine-like side chain (peaks *b-e*, **Figure 59a**) but without *Cbz*-group attributable signals. Further MALDI TOF analysis using α -CHCA matrix demonstrated the expected cyclic poly(Nlys) structure: the imino-acid as exocycle initiator group covalently attached to the polymer backbone composed of deprotected *N*-(aminobutyl)glycine monomer unit ($\Delta \approx 128$, **Figure 59b**).

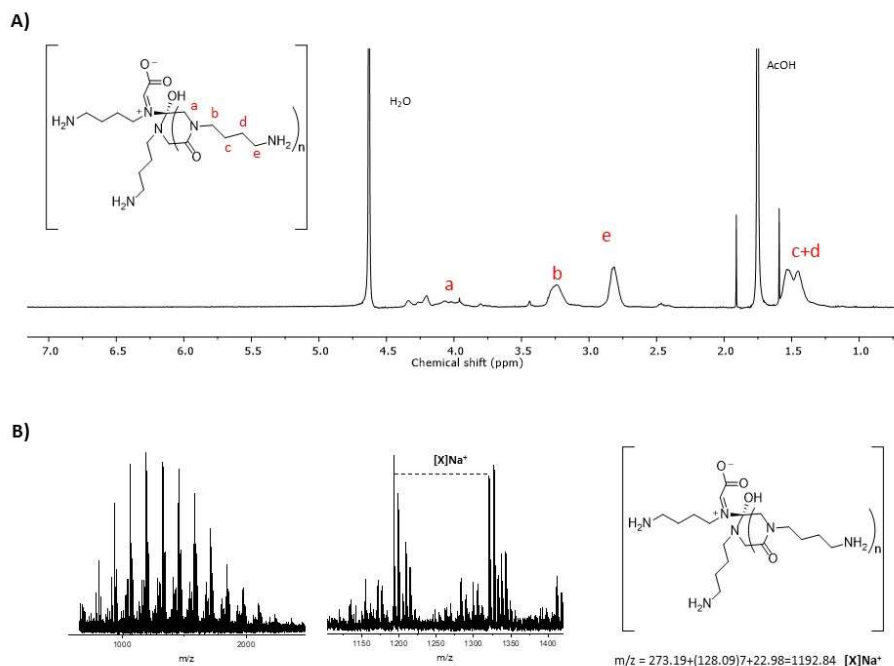


Figure 59. Cationic cyclic poly(Nlys) $M/I = 30$ upon deprotection (**53D**): A) $^1\text{H-NMR}$ spectrum in D_2O and B) MALDI TOF spectra.

Overall, these results showed that the polymerization of ZLys-NNCA mediated by LiHMDS allowed easy access to cyclic and cationic peptoid structures.

2 Preparation of copolypeptoids

Cyclic structures are used by living systems to achieve specific bioactivities.¹ This encompasses cyclic antimicrobial peptides (c-AMP) that are cationic and broad-spectrum anti-infective backbones.⁴⁸ The use of a simple REP methodology, working in DMF, opens up interesting prospects to design simplified analogs of such c-AMPs. Up to now, only a few monomers have been used in REP because of some limitations related to the solvents used (in which, for example, poly(sarcosine) was not soluble).^{46,47} Considering that both the hydrophobic and cationic characters are key structural features to design antimicrobial polymers,⁴⁹ we consequently prepared copolymers by mixing *N*-Z-protected-lysine-like NNCA (ZLys-NNCA) and phenylalanine-like NNCA (Phe-NNCA), since the mix of these two monomers presented interesting antibacterial properties, as described in chapter 3.

D. Zhang *et al.* were among the first authors to report the synthesis of cyclic polypeptoids

copolymers,³³ specifically block copolymers based on *N*-decyl and *N*-methyl NNCAs by sequential monomer addition using NHCs.³⁵ Following a similar strategy, other copolymers were reported: 1) copolymer bearing *N*-butyl and *N*-ethyl functions⁵⁰ and displaying tuneable cloud points or 2) copolymer bearing *N*-propargyl and *N*-butyl functions that were grafted with PEG by click chemistry, demonstrating the access to brush-like architectures from the cyclic structures.⁴⁶ However, the synthesis of cationic copolymers was still challenging. Here, we investigated the synthesis of such copolymers varying the hydrophobic content through LiHMDS-mediated REP in DMF.

2.1 Random copolymers varying the hydrophobicity

Using LiHMDS, our first objective was to prepare copolymers by mixing the two NNCAs simultaneously to obtain random copolymers bearing cationic and hydrophobic side chains. We carried out the synthesis of random cyclic copolypeptoids at M/B = 50 varying the hydrophobic content (10-50%) using Phe-NNCA and ZLys-NNCA (as hydrophobic and cationic building blocks, respectively). The copolymerizations were achieved in 0.4 M DMF under inert conditions at RT.

We monitored the conversion by FTIR following the decrease of the signal at 1859 cm⁻¹, and upon full conversion (~15 days) the cyclic Z-protected copolymers c-P(ZNlys-*r*-Nphe)**55-59** were isolated in 42-92% yields. They were characterized by SEC and ¹H-NMR (**Figure 60** and **Table 42**).

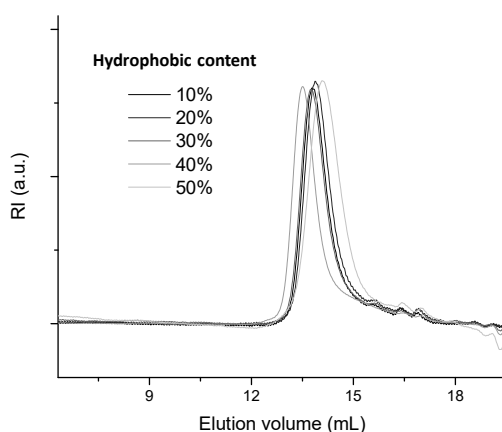


Figure 60. SEC chromatograms (DMF) of the series of cyclic P(Nlys-*r*-Nphe)**55-59** at M/I = 50, varying the hydrophobic content from 10% to 50%.

The protected copolymers showed molar masses ranging from $M_w = 4100$ to 6000 g/mol with narrow dispersity $D_M < 1.07$. We observed that those values were lower than the theoretical

Chapter 4. Macrocylic polypeptoids and their antimicrobial activity

ones (Table 42) but in agreement with the observation previously described for polysarcosines (section 1.4).

Then we characterized the copolymers by $^1\text{H-NMR}$ in DMSO-d_6 , as depicted in Figure 61a for c-P(ZNlys-r-Nphe)59. The spectra revealed the signals corresponding to the polymer backbone (CH_2 , peak a), the signals corresponding to ZNlys moiety (peaks b-g) and the signals of Nphe moiety (peaks h,i). Using the integrations of the peaks corresponding to the Nlys side chain (peaks c,d, Figure 61a) and the integrations of the signals of the copolymer (CH_2 , signals a,h), we determined the hydrophobic content and we found values in agreement with the theoretical ones Table 42.

Table 42. Random cyclic copolymers characterization before deprotection: molar masses from SEC, hydrophobic content from $^1\text{H-NMR}$ and yields.

Polypeptoid	Hydrophobic content (%)	MW_{Theo} (g/mol)	M_n (g/mol) ^a	M_w (g/mol)	D_M	Hydrophobic content (%) ^b	Yield (%)
c-P(ZNlys-r-Nphe)55	10	12500	5100	5500	1.08	7	47
c-P(ZNlys-r-Nphe)56	20	12000	4100	4400	1.07	15	42
c-P(ZNlys-r-Nphe)57	30	11400	4100	4300	1.05	31	57
c-P(ZNlys-r-Nphe)58	40	10800	5000	5300	1.05	39	81
c-P(ZNlys-r-Nphe)59	50	10200	5700	6000	1.06	50	92

^a SEC performed in DMF. ^b Calculated from the $^1\text{H-NMR}$ spectrum in DMSO-d_6

Then, the copolymers were deprotected using HBr (2 equiv. in TFA for 3h at RT). We isolated the copolymers by precipitation in Et_2O , dialysis, and freeze-drying and we characterized them by $^1\text{H-NMR}$ in D_2O as depicted in Figure 61b for c-P(Nlys-b-Nphe)59D. The spectra re-

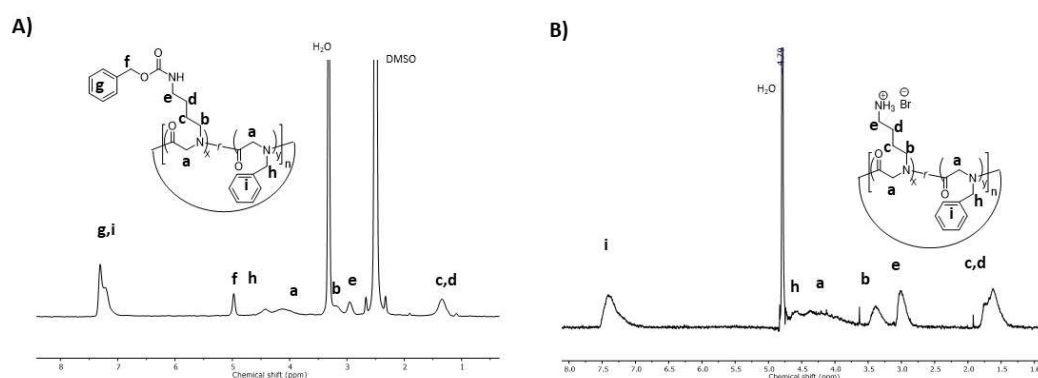


Figure 61. $^1\text{H-NMR}$ spectra of random cyclic poly(Nlys-Nphe) $M/I = 50$ at 50% of hydrophobic content: A) $^1\text{H-NMR}$ spectrum in DMSO-d_6 before deprotection (59) and B) $^1\text{H-NMR}$ spectrum in D_2O upon deprotection (59D).

Chapter 4. Macrocyclic polypeptoids and their antimicrobial activity

led the expected signals of the polypeptoid backbone (peak *a*) and the side chains (peaks *b-i*). Using the integrations of the peaks corresponding to the Nlys side chain (peaks *c,d*, **Figure 61b**) and the integrations of the signals of Nphe (peak *l*), we determined the hydrophobic content of the copolymers that were in agreement with the values before deprotection (**Table 43**).

Table 43. Random cyclic copolymers characterization upon deprotection: hydrophobic content ¹H-NMR and yields.

	Hydrophobic content (%)	Hydrophobic content (%) ^a	Yield (%)
c-P(NIys- <i>r</i> -Nphe)55D	10	6	65
c-P(NIys- <i>r</i> -Nphe)56D	20	21	65
c-P(NIys- <i>r</i> -Nphe)57D	30	29	58
c-P(NIys- <i>r</i> -Nphe)58D	40	40	37
c-P(NIys- <i>r</i> -Nphe)59D	50	50	46

^a Calculated from the ¹H-NMR spectrum in D₂O

2.2 Block copolymers varying the hydrophobicity

Using LiHMDS, our second objective was to prepare copolymers by mixing the two NNCA's sequentially to obtain block copolymers, combining cationic and hydrophobic blocks. We already verified that accessing block copolymers was possible through the feeding assay (section 1.5). We prepared in this section a series of block copolypeptoids at M/B = 50 varying the hydrophobic content from 10% to 50%. We first prepared a block with ZLys-NNCA (45 to 25 equiv.) following the conversion by FTIR, and at full conversion, we added Phe-NNCA (5 to 25 equiv.).

Then the cyclic protected copolymers (c-P(ZNIys-*b*-NPhe)**60-64**) were precipitated in diethyl ether and dried under vacuum and recovered in 37-51% yields. Then, we characterized **60-64** by SEC and ¹H-NMR (**Figure 62** and **Table 44**). All the copolymers exhibited monomodal distributions by SEC ($\mathcal{D}_M < 1.09$, **Figure 62**). Also, the molar masses were in the range of $M_w = 4100-5800$ g/mol, which was similar to those encountered for random copolypeptoids.

Then, we characterized the copolymers by ¹H-NMR in DMSO-*d*₆ as depicted for c-P(ZNIys-*b*-Nphe)**64** in **Figure 63a**. In agreement with the copolymers described in section 2.1, NMR spectra revealed peaks corresponding to the polymer backbone (peaks *a*) and the side chains (peaks *b-i*). Using the integrations of the peaks corresponding to the Nlys side chain (peaks *c,d*,) and the integrations of the signals of polymer (CH₂ *a,h*), we determined the hydrophobic content and we found values in agreement with the theoretical ones.

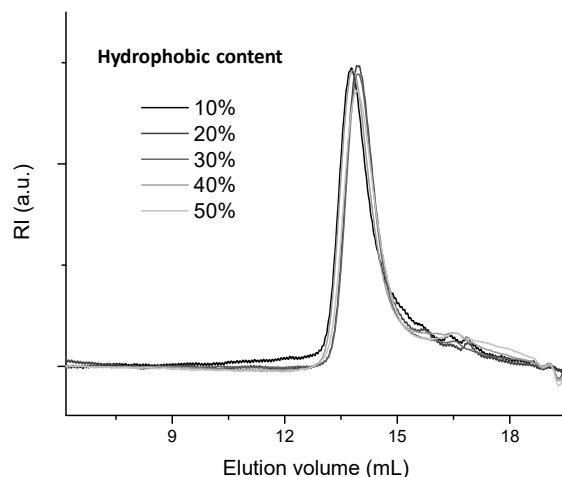


Figure 62. SEC chromatograms of the library of cyclic poly(Nlys-*b*-Nphe)**60-64** at *M/I* = 50 varying the hydrophobic content from 10% to 50%.

Table 44. Block cyclic copolymers characterization before deprotection: molar masses from SEC, hydrophobic content from ¹H-NMR and yields.

Polypeptoid	Hydrophobic content (%)	MW_{Theo} (g/mol)	M_n (g/mol)	M_w (g/mol)	\overline{D}_M	Hydrophobic content (%) ^a	Yield (%)
c-P(ZNlys- <i>b</i> -Nphe) 60	10	12500	3900	4100	1.03	5	51
c-P(ZNlys- <i>b</i> -Nphe) 61	20	12000	5300	5800	1.09	21	37
c-P(ZNlys- <i>b</i> -Nphe) 62	30	11400	4600	4800	1.05	32	37
c-P(ZNlys- <i>b</i> -Nphe) 63	40	10800	4700	5000	1.07	41	47
c-P(ZNlys- <i>b</i> -Nphe) 64	50	10200	4900	5200	1.06	51	49

^a SEC performed in DMF. ^b Calculated from the ¹H-NMR spectrum in DMSO-*d*₆

In a final step, the copolymers were deprotected using HBr (2 equiv. in TFA for 3 h at RT), precipitated in Et₂O, dialyzed and freeze-dried. Then, we characterized them by ¹H-NMR in D₂O as depicted for c-P(Nlys-*b*-Nphe)**64D** in **Figure 63b**. NMR spectra revealed typical signals attributable to the polymer backbone (peak *a*) and the side chains (peaks *b-i*). Using the integrations of the peaks corresponding to the Nlys side chain (peaks *c,d* **Figure 63b**) and the integrations of the signals of Nphe (peak *l*), we determined the hydrophobic contents that were in agreement with the values calculated before deprotection (**Table 45**).

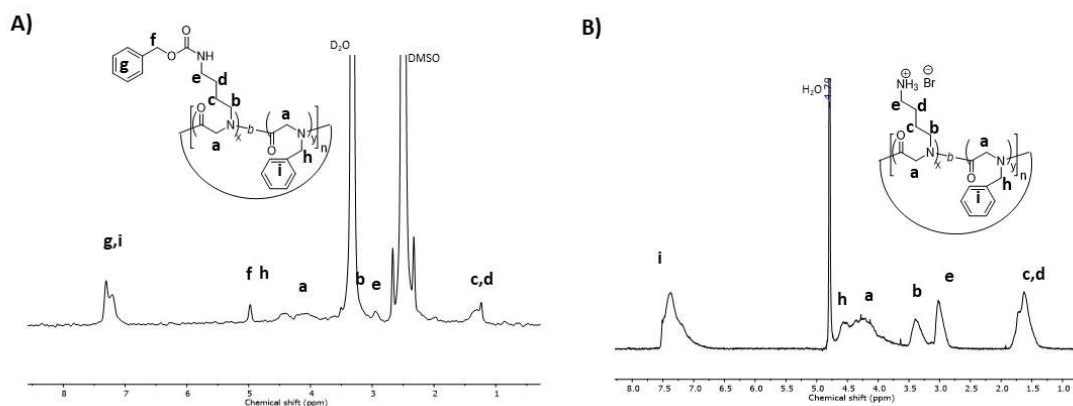


Figure 63. $^1\text{H-NMR}$ spectra of block-cyclic poly(Nlys-Nphe) $M/I = 50$ at 50% of hydrophobic content: A) $^1\text{H-NMR}$ spectrum in DMSO-d_6 (**64**) and B) $^1\text{H-NMR}$ spectrum in D_2O (**64D**).

Table 45. Block-cyclic copolymers characterization before deprotection: hydrophobic content from $^1\text{H-NMR}$ and yields

Polypeptoid	Hydrophobic content (%)	Hydrophobic content (%) ^a	Yield (%)
c-P(Nlys- <i>b</i> -Nphe) 60D	10	5	68
c-P(Nlys- <i>b</i> -Nphe) 61D	20	23	82
c-P(Nlys- <i>b</i> -Nphe) 62D	30	32	93
c-P(Nlys- <i>b</i> -Nphe) 63D	40	41	90
c-P(Nlys- <i>b</i> -Nphe) 64D	50	48	92

^a Calculated from the $^1\text{H-NMR}$ spectrum in D_2O

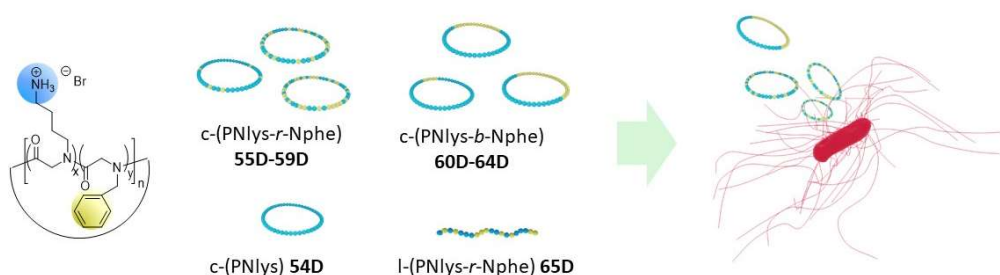
In summary, we prepared a series of random and block copolypeptoids through REP using LiHMDS. They were prepared from lysine-like and phenylalanine-like monomer units, a promising combination towards antimicrobial activities (see chapter 3).

3 Antimicrobial assays

Cyclic peptoids are promising scaffolds to design anti-infective agents,^{14,51} but antibacterial copolymers have never been developed on the basis of this chemical design: macrocyclic polypeptoids bearing cationic and hydrophobic side chains. Cyclic peptoids already demonstrated activity against Gram-positive and Gram-negative bacteria at MIC as low as 7.8 $\mu\text{g/mL}$ and with

Chapter 4. Macrocyclic polypeptoids and their antimicrobial activity

non-hemolytic activity.¹⁴ Furthermore, previous studies also reported that membrane destabilization could be achieved by choosing the right hydrophobic content.¹⁵ In this PhD project, we targeted a pathogenic Gram-positive bacterium responsible for severe hospital-acquired intestinal infections: *Clostridioides difficile* (*C. difficile*)^{52,53} and the cyclic copolymers synthesized through REP were evaluated *in vitro* against this pathogen (**Scheme 44**). In this biological study, the bacteria were incubated for 24 h under CO₂ atmosphere at 37 °C with increasing concentrations of cyclic polypeptoids, to determine the corresponding minimum inhibitory concentrations (MICs, **Table 46**). In parallel, the *in vitro* cytotoxicity of the best polymers was tested on a human intestinal epithelial cell line (Caco-2), allowing to measure the 50% cytotoxic concentrations (CC₅₀) and calculate the selectivity indices (SI = CC₅₀/MIC).



Scheme 44. Antimicrobial evaluation of polypeptoids developed by the LIHMDS-mediated REP.

Regarding the MIC results, we observed that the hydrophobic content was a crucial parameter to inhibit the *C. difficile* growth (**Table 46**). Indeed, the higher the hydrophobic content, the better the MIC for random copolymers **55D-59D**, including P(Nlys)**54D**, reaching the best value for c-P(Nlys-r-Nphe)**59D** with a MIC = 12.5 µg/mL. Then, we evaluated the MIC for block copolymers **60D-64D** and we found a relatively similar influence of the hydrophobic content over the inhibition growth of *C. difficile* with a maximum antimicrobial activity for copolymer **63D** (40% hydrophobic content, MIC = 12.5 µg/mL).

Table 46. Antimicrobial potency of the cyclic copolymers at M/I = 50, random and block copolymers against *C. difficile*.

Entry	Hydrophobic content from ¹ H-NMR (%) ^a	MIC (µg/mL)	MIC (µM)	Caco-2 CC ₅₀ (µg/mL)	SI (CC ₅₀ /MIC)
c-P(Nlys) 54D	0	>100	-	-	-
c-P(Nlys-r-Nphe) 55D	7	>100	-	-	-
c-P(Nlys-r-Nphe) 56D	15	>100	-	-	-
c-P(Nlys-r-Nphe) 57D	31	>100	-	-	-

Chapter 4. Macrocylic polypeptoids and their antimicrobial activity

c-P(Nlys- <i>r</i> -Nphe) 58D	39	>100	-	-	-
c-P(Nlys- <i>r</i> -Nphe) 59D	50	12.5	1.7 ^b	208±9	17
c-P(Nlys- <i>b</i> -Nphe) 60D	5	>100	-	-	-
c-P(Nlys- <i>b</i> -Nphe) 61D	21	>100	-	-	-
c-P(Nlys- <i>b</i> -Nphe) 62D	32	>100	-	-	-
c-P(Nlys- <i>b</i> -Nphe) 63D	41	12.5	-	77±6	6
c-P(Nlys- <i>b</i> -Nphe) 64D	51	100	-	105±8	<1
I-P(Nlys- <i>r</i> -Nphe) 65D	48	25	-	47±1	2
LL-37 (5229 g/mol)	-	12.5	2.4	213±7	17
Doxorubicin	-	-	-	8.1	-
Metronidazole (171 g/mol)	-	0.8	4.7	>250	>312
Vancomycin (1449 g/mol)	-	0.8	0.6	>250	>312
Fidaxomicin (1058 g/mL)	-	0.05	0.05	141	2820

^a Form ¹H-NMR before deprotection. ^b Calculated using M/B=50

Later, we evaluated the cytotoxicity over Caco-2 cells for the best copolymers **59D**, **63D** and **64D** (Table 46). We observed that diblock copolymer **64D** (CC₅₀ = 105 µg/mL), at the same hydrophobic content of 50%, presented a 2 fold higher cytotoxicity in comparison to c-P(Nlys-*r*-Nphe)**59D** and even higher cytotoxicity at 40% hydrophobic content (**63D**). Indeed, the calculated selectivity indices confirmed the influence of the microstructure and the hydrophobic content over the inhibition growth of *C. difficile*. We observed that c-P(Nlys-*r*-Nphe)**59D** presented a superior value of SI = 17, while block copolymers **63D** and **64D** showed SI < 6. Therefore, a random microstructure and 50% of hydrophobic content were the best parameters for this architectural design, regarding selective anti-*C. difficile* activity.

We then prepared the linear analog of the c-P(Nlys-*r*-Nphe)**59D** by propionylation as described in section 1.3 (see experimental section) and we evaluated its MIC, CC₅₀ and SI values (Table 46). Interestingly, the MIC value for I-P(Nlys-*r*-Nphe)**65D** (25 µg/mL) demonstrated a 2 fold decrease in antimicrobial activity, as compared to its cyclic counterpart. Moreover, we observed that the linear copolymer **65D** showed an increase of cytotoxicity and thus, a lower selectivity index (SI = 2). This revealed the importance of the cyclization regarding structure-activity relationships.

Also, we determined the MIC values of commercial antibiotics to use them as references (Table 46). To compare the potency with the best polymer **59D**, we calculated the MIC value in molarity units using a calculated molar mass of 7200 g/mol, resulting in a MIC = 1.7 µM. This MIC value was comparable with the anti-*C. difficile* activity of metronidazole MIC = 4.77 µM. However, the selectivity of **59D** was much lower in comparison to all the antibiotics tested.

Chapter 4. Macrocylic polypeptoids and their antimicrobial activity

Even though the copolymer **59D** was not superior to the current treatments, we observed that it was as effective as the antimicrobial peptide LL-37, with similar cytotoxic properties and selective index. This result encouraged us to investigate the selectivity of c-P(Nlys-r-Nphe)**59D** over a variety of Gram-positive (*S. aureus*, *E. faecalis*, *L. monocytogenes* and *S. pneumoniae*), and Gram-negative bacteria (*E. coli*, *P. aeruginosa*, *A. baumannii*) and anaerobic bacteria (*B. fragilis*). We determined the MIC values for **59D** using the microdilution method (the studies were performed by FONDEREPHAR in Toulouse).

Interestingly, we observed that c-P(Nlys-r-Nphe)**59D** had a superior activity over the different Gram-positive and negative bacteria tested (**Table 47**). Moreover, we observed that the copolymer was active against the Gram-positive *L. monocytogenes* with a MIC = 31.25 µg/mL. To better understand the potency over the Gram-negative and Gram-positive tested, we calculated the selectivity towards *C. difficile* (SB) by dividing the MIC of bacteria with the MIC of *C. difficile*. Overall, we observed that **59D** required a 5-fold higher concentration to kill other Gram-negative and Gram-positive bacteria (SB > 5), except for *L. monocytogenes* where the activity was very close (SB = 2.5). Thus, a relatively narrow spectrum was observed.

Table 47. Antimicrobial activity of polypeptoid **59D** against a variety of Gram-positive and Gram-negative bacteria..

	Gram	MIC (µg/mL)	SB* (MIC _{pathogen} /MIC _{C. difficile})
<i>C. difficile</i>	+ anaerobic	12.5	-
<i>S. aureus</i> CIP 4.83	+	62.5	5
<i>S. aureus</i> ATCC33591	+	62.5	5
<i>E. faecalis</i> CIP 103015T	+	125	10
<i>L. monocytogenes</i> CIP 82110T	+	31.25	2.5
<i>S. pneumoniae</i> CIP 104471	+	250	20
<i>E. coli</i> CIP 53.126	-	62.5	5
<i>P. aeruginosa</i> CIP 82.118	-	62.5	5
<i>Acinetobacter baumannii</i> CIP 70.34T	-	62.5	5
<i>B. fragilis</i> CIP 77.16	- anaerobic	65.5	5

* SB = selectivity against other bacteria

4 Liposome destabilization assay

The cyclic polypeptoids prepared in this Ph.D. work are made of cationic and hydrophilic side chains: they can kill bacteria by destabilizing the bacterial membrane, as sorts of cationic surfactants.⁴⁹ To verify this possible mechanism, we used an *in vitro* model: the destabilization of neutral or negatively charged liposomes containing carboxyfluorescein (CF). Indeed, to particularly focus on the influence of cationic copolymers side chains over negative charges in

Chapter 4. Macroyclic polypeptoids and their antimicrobial activity

bacterial membranes, we used two different liposome models: 1) neutral liposome membranes constituted of soybean phosphatidylcholine and cholesterol (SPC:Chol, 8:2) with a zeta potential of $\zeta = -3.9 \pm 0.9$ mV and 2) negatively charged liposome membranes constituted of 1,2-dioleoyl-sn-glycero-3-phosphoglycerol (PG) and cholesterol (PG:Chol, 8:2) with a zeta potential of $\zeta = -33.3 \pm 2.2$ mV. The evaluations were performed in the framework of a collaborative effort with the CERMN (Dr. Marc Since did all the evaluations).

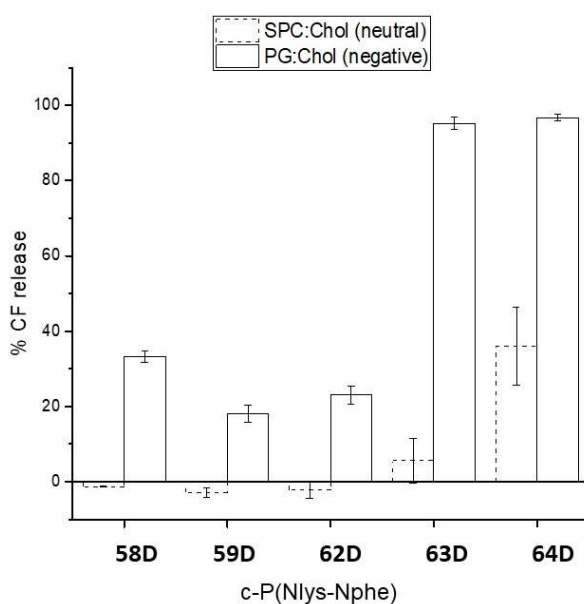


Figure 64. Membrane destabilization by active cyclic copolypeptoids using two different liposome models. SPC:Chol (8:2); PG:Chol (8:2).

The liposomes were first loaded with the fluorophore. Then, the copolymers c-P(Nlys-Nphe) **58D**, **59D**, **62D**, **63D** and **64D** were prepared at a concentration of 90 $\mu\text{g/mL}$ and mixed with the liposomes. Upon incubation (1.5 h), the concentration of released carboxyfluorescein was measured by fluorimetry ($\lambda_{\text{ex}} = 485$ nm and $\lambda_{\text{em}} = 528$ nm) and reported in percentage of release (%CF release, **Figure 64**). CF release was particularly significant for copolymers **58D** and **59D**: we found 33.3% and 18.1% of release, respectively, using the negatively charged liposome model, while in the neutral model the values were found <1%. These results demonstrated that the cyclic copolymers could significantly destabilize negatively charged membranes at 90 $\mu\text{g/mL}$ with some selectivity (versus neutral membranes).

On another hand, we observed that the copolymers **62D**, **63D** and **64D** displayed an increasing membrane destabilization in correlation to the hydrophobic content with %CF release

Chapter 4. Macrocylic polypeptoids and their antimicrobial activity

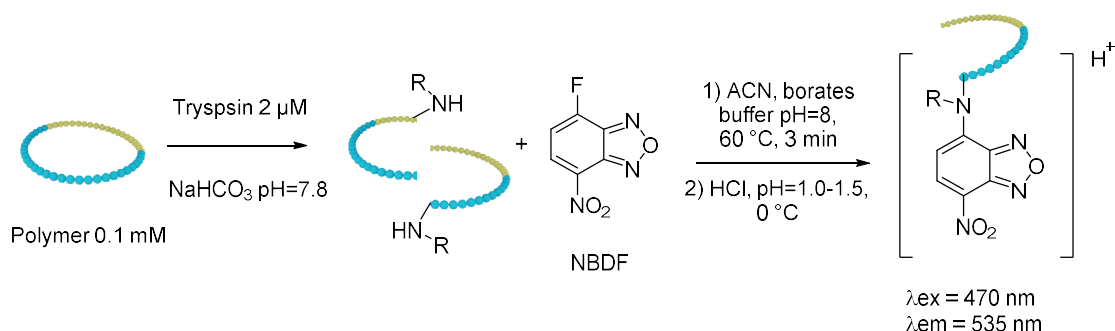
values of 23.1, 95.2, and 96.7%, respectively in the PG:Chol model. The same behavior was observed for the neutral liposome model having values of <1, 5.6 and 36%.

Interestingly, when we compared the values for block copolymers **63D** and **64D** with the random copolymers **58D** and **59D** we observed a higher membrane destabilization in both liposome models for block copolymers suggesting a higher interaction with the liposomes membranes even if the negative character was low ($\zeta = -3.9 \pm 0.9$ mV). Indeed, these results were in agreement with the higher cytotoxicity encountered in block copolymers **63D** and **64D** as we reported in section 3.

Thus, by using artificial membranes, we showed that the cyclic polypeptoids destabilized the lipid membranes in liposomes with a preference for negatively charged ones.

5 Protease activity

Peptoids are known to resist proteolytic degradation mediated by proteases,⁵¹ and in the chapter 3 section 3.6 we demonstrated that linear polypeptoids are also resistant. However cyclic polypeptoids remain unknown to this proteolytic activity. Therefore, we carried out proteolysis experiments using trypsin (2 μ M, one of the main proteases presented in the digestive tract) in NaHCO₃ buffer (50 mM pH = 7.8) and polymer solutions (0.1 mM) at 37 °C. To measure the proteolytic degradation we implemented a methodology developed for small peptoids,⁵¹ that consisted of reacting 4-Fluoro-7-nitrobenzofurazan (NBDF) with secondary amines (S_NAr reaction) resulting from the proteolysis of the amide bonds (see the experimental section for a detailed protocol, **Scheme 45**).



Scheme 45. Proteolysis evaluation using NBDF as fluorophore precursor. “R” is either a cationic or hydrophobic group.

Chapter 4. Macroyclic polypeptoids and their antimicrobial activity

The analysis was performed with c-P(Nlys-Nphe)**59D**, **62D**, **63D** and **64D** that presented good activity against *C. difficile* and we employed a linear polypeptide (poly(lysine-phenylalanine) M/I = 200 and 9% hydrophobic content, synthesis not shown) as a polymeric reference. We followed the progression of the reaction by taking aliquots at a certain time and upon NBDF treatment we measured the fluorescence ($\lambda_{em} = 535$ nm, **Figure 65**). We observed that the different cyclic copolypeptoids were not degraded by trypsin within 80 minutes, while the linear polypeptide was rapidly degraded in the first 20 min, thus, we concluded that cyclic polypeptoids presented resistance to trypsin.

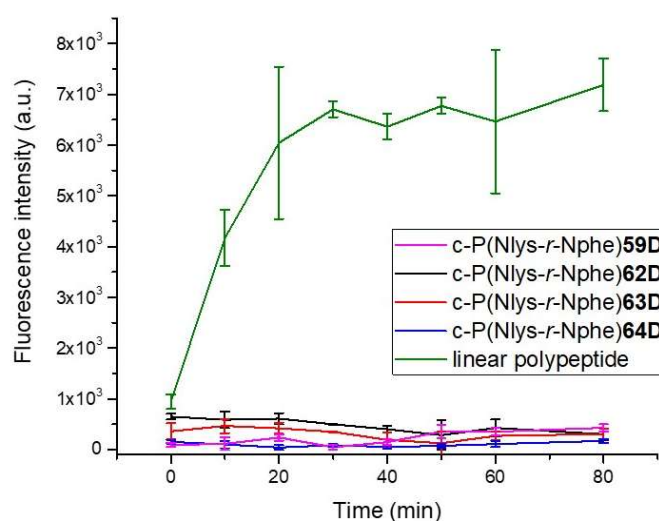


Figure 65. Cyclic polypeptoids resist protease activity using trypsin 2 μ M and polymer concentration 0.1 mM.

We then evaluated the antimicrobial activity (MIC) upon trypsin exposure of the AMP LL-37 and the most active c-P(Nlys-r-Nphe)**59D** (1 h at 37 °C, **Table 48**). We observed a decrease in the antimicrobial potency of LL-37 of MIC > 200 μ g/mL upon trypsin treatment, while the cyclic polypeptoid remained active before or upon trypsin digestion with a MIC = 12.5 μ g/mL. Therefore, we also demonstrated the trypsin resistance of cyclic polypeptoids in a simulated protease environment.

Table 48. Antimicrobial comparison of cyclic polypeptoids versus LL-37 with and without trypsin digestion.

Entry	MIC (μ g/mL)
c-P(Nlys-r-Nphe) 59D	12.5

Chapter 4. Macrocyclic polypeptoids and their antimicrobial activity

c-P(Nlys-r-Nphe) 59D + trypsin	12.5
LL-37	12.5
LL-37 + trypsin	>200

6 Conclusion

In summary, the use of a LiHMDS-mediated REP of NNCA in DMF was a versatile and facile route to cyclic polypeptoids allowing fine-tuning over their chemical composition. We first prepared cyclic poly(sarcosine) to provide a comprehensive study of the REP mechanism including the possibility to ring-open the structure using propionic anhydride. This new REP methodology allowed us to design cationic macrocycles, an important step forward in the design of antimicrobial polymers. We prepared series of cyclic copolymers based on lysine and phenylalanine analogs at M/B = 50 with random, and block microstructures and controlled hydrophobic content. By studying the structure-activity relationships of these parameters, we found that random copolymers at 50% of hydrophobic content demonstrated superior antimicrobial activity in comparison to the block copolymers and the linear counterpart. This particular combination was necessary to selectively kill *C. difficile*, demonstrating membrane destabilization in artificial membranes and a strong protease resistance that permitted to preserve the anti-infective activity in a simulated protease environment.

7 Materials and methods

7.1 Materials

All the chemicals and solvents in this work were purchased from Sigma Aldrich, Fluorochem, Acros, TCI, Strem and, unless otherwise described, were used without any purification. Dimethylformamide (DMF), tetrahydrofuran (THF) were obtained from a solvent system purificator (PureSolv, Innovative Technology), kept under argon atmosphere, and freshly used. MiliQ water was obtained from a (Purelab Prima, ELGA).

7.2 Equipment and measurements

Glovebox

The monomers synthesized were stored at 4 °C under an argon atmosphere and weighted in the glovebox Jacomex GP13 No. 2675 at the LCPO (Bordeaux, France).

Infrared (IR) spectroscopy

The IR spectra we recorded using the FTIR spectrometer (Vertex 70, Bruker), and the samples were measured with the ATR (GladiATR, Pike Technologies) from Fisher technologies performing 32 scans at the Laboratoire de Chimie des Polymères Organique (LCPO, Bordeaux, France). The raw data was obtained with the Opus7.5 software and processed using the Originlab 2016 software.

Size exclusion chromatography

Molar masses were determined using two different SEC systems according to the solubility as it is described in chapter 3 (pp 157).

Matrix-Assisted Laser Desorption Ionization-Time of Flight (MALDI TOF)

MALDI-MS spectra were performed at CESAMO facility (Bordeaux, France) on an Autoflex maX TOF mass spectrometer equipped with a frequency tripled Nd:YAG laser emitting at 355 nm. Spectra were recorded in the positive-ion mode using the reflectron and with an accelerating voltage of 19 kV. For MALDI-MS analyses, polysarcosine deposits were prepared according to the following recipe: polysarcosines and the cationic agent (NaI) were dissolved in methanol at 10 mg/mL. The α -CHCA matrix (α -cyano-4-hydroxycinnamic acid) solution was prepared by dissolving 10 mg in 1 mL of methanol and the solutions were combined in a 10:1:1 volume ratio

(matrix: sample: salt). One microliter of this solution was deposited onto the grid and vacuum-dried before analysis. For MALDI-MS analyses, Poly(ZNlys) deposits were prepared according to the following recipe: the polymer and the cationic agent (NaI) were dissolved in methanol at 10 mg/mL. The dithranol matrix solution was prepared by dissolving 10 mg in 1 mL of dichloromethane and the solutions were combined in a 10:1:1 volume ratio (matrix: sample: salt). One microliter of this solution was deposited onto the grid and vacuum-dried before analysis. For MALDI-MS analyses, deprotected poly(Nlys) deposits were prepared according to the following recipe: the polymer was dissolved in water at 10 mg/mL. The α -CHCA matrix solution was prepared by dissolving 10 mg in 1 mL of methanol. A sandwich technique was employed that consisted of matrix-sample-matrix layers by dropping: 3 μ L of matrix solution, 1 μ L of poly(Nlys) solution, and 1 μ L of the matrix solution. Every layer was dried previous to the next addition. Electrospray mass spectra (ESI-MS) were performed by the CESAMO (Bordeaux, France) on a Qexactive mass spectrometer (Thermo). The instrument is equipped with an ESI source and spectra were recorded in the negative mode. The spray voltage was maintained at 3200 V and capillary temperature set at 320 °C. Samples were introduced by injection through a 20 μ L sample loop into a 300 μ L/min flow of methanol from the LC pump.

7.3 DFT calculations

Computations were performed on peptoids with a degree of polymerization of 5 (DP5). The structures were built and pre-optimized with the Discovery Studio visualizer package.⁴⁰ For the extended form of the linear structure, the initial torsional angles were: 180° (NCC(=O)N) ; 180° (CC(=O)NC) ; 75° (C(=O)NCC(=O)). From the linear structure, a curved form was prepared so that the end of the peptide should be in close proximity to generate the cyclic structure. The cation LiHMDS was then manually positioned. Geometry optimizations of the resulting structures were performed with the the M06-2X density functional⁵⁴ and the 6-31+G(d,p) basis set with the GAUSSIAN 09.D01 program.⁵⁵ The bulk solvent effects were described with the integral equation formalism polarizable continuum Model (IEFPCM) with DMF as solvent.⁵⁶ In addition, Grimme dispersion correction (GD3) was used to include the noncovalent effects.⁵⁷ Vibrational frequencies were computed to confirm the convergence to local minima and to calculate the unscaled zero-point-energy (ZPE) and the Gibb's free energy at 298 K.

The Cartesian coordinates of the optimized geometries of cyclic and linear structures are given below.

Chapter 4. Macrocyclic polypeptoids and their antimicrobial activity

Table 49. Cartesian coordinates of the optimized DP5-LiHMDS linear structure.

C	-9.848767	1.630952	1.571349
Si	-8.952297	1.510038	-0.073974
C	-9.998347	2.299715	-1.424979
C	-7.301890	2.399113	-0.013326
N	-8.646573	-0.203331	-0.395505
Li	-6.869888	-0.883337	0.621235
H	-8.051527	-0.306095	-1.222294
Si	-9.860560	-1.487475	-0.304709
C	-10.067491	-2.007424	1.488436
C	-11.531409	-0.950762	-0.982092
C	-9.184315	-2.918127	-1.314076
C	2.556559	-2.272169	1.446101
N	2.130737	-1.462509	0.309275
C	1.086183	-0.596311	0.375051
C	0.177025	-0.696311	1.606419
N	-0.879362	0.287174	1.540374
C	-0.531684	1.647255	1.938290
C	-1.914628	0.013993	0.698687
C	-2.879141	1.165117	0.390549
N	-3.885182	0.788800	-0.566715
C	-4.955088	0.031853	-0.124308
O	-5.707026	-0.535438	-0.975795
O	-5.183012	-0.024828	1.127125
C	-3.468379	0.701182	-1.955993
O	-2.082294	-1.103850	0.215060
O	0.862128	0.228343	-0.508444
C	3.120393	-1.196910	-0.709757
C	4.013439	-0.018317	-0.300726
N	4.970271	0.363103	-1.186554
C	5.351625	-0.448634	-2.338197
C	5.938540	1.326384	-0.717118
C	6.992703	0.649066	0.165198
N	7.978077	1.434985	0.668905
C	8.197204	2.822579	0.267182
C	9.036875	0.756435	1.409100
C	9.974915	0.046745	0.489361
O	10.752797	0.744700	-0.324315
C	11.531728	-0.169492	-1.129782
O	12.319990	0.296586	-1.952482
C	11.122241	-1.421018	-0.694104
N	10.159085	-1.235220	0.294703
C	9.503734	-2.334673	1.002004
O	6.943449	-0.556249	0.403682
O	3.847856	0.553203	0.774391
H	-9.278980	1.143759	2.369439
H	-10.842422	1.171614	1.529217
H	-9.982830	2.683725	1.842027
H	-11.009893	1.884007	-1.456890
H	-9.537141	2.148294	-2.407003
H	-10.080787	3.378977	-1.254223
H	-6.656431	2.006313	0.779093
H	-7.457298	3.469619	0.159456
H	-6.769786	2.282520	-0.964644
H	-10.435010	-1.185839	2.110792
H	-9.114978	-2.350724	1.906243
H	-10.786109	-2.831056	1.559787
H	-12.227684	-1.796511	-0.961242
H	-11.971930	-0.144020	-0.386126
H	-11.446231	-0.603363	-2.016930
H	-9.864889	-3.774835	-1.275765
H	-9.056133	-2.634153	-2.363933
H	-8.211480	-3.240872	-0.927704
H	3.174552	-1.688289	2.137260
H	3.139919	-3.114750	1.071179
H	1.694888	-2.676234	1.976109
H	0.766375	-0.527530	2.512914

Chapter 4. Macrocyclic polypeptoids and their antimicrobial activity

H	-0.261265	-1.695188	1.662456
H	0.089348	1.596264	2.834227
H	0.025922	2.162186	1.147817
H	-1.426666	2.216358	2.187151
H	-2.308853	2.013289	-0.005068
H	-3.363057	1.484769	1.316567
H	-4.350713	0.622103	-2.588863
H	-2.920022	1.609881	-2.219268
H	-2.820642	-0.167196	-2.131758
H	3.732684	-2.091867	-0.855542
H	2.616371	-0.967969	-1.651363
H	5.840031	0.197508	-3.069336
H	6.043327	-1.246793	-2.046732
H	4.472318	-0.881198	-2.813644
H	5.425384	2.101693	-0.143522
H	6.420848	1.797569	-1.578659
H	8.698548	3.345692	1.082330
H	8.817596	2.886692	-0.632671
H	7.245702	3.320591	0.086761
H	9.597014	1.506263	1.972003
H	8.598431	0.049309	2.113154
H	11.435948	-2.401536	-1.004780
H	10.147791	-2.677155	1.812569
H	9.345777	-3.141099	0.286910
H	8.541030	-1.992790	1.375582

Table 50. Cartesian coordinates of the optimized DP5-LiHMDS cyclic structure.

C	-1.426385	3.238557	-2.455707
Si	-2.639757	2.236144	-1.423903
C	-4.283195	3.149028	-1.318654
C	-2.939768	0.578560	-2.254238
N	-1.973804	1.990367	0.190538
Li	-1.010160	0.111653	0.499538
H	-2.714616	1.565026	0.776351
Si	-1.118089	3.231328	1.108639
C	0.595323	3.500230	0.385978
C	-2.041297	4.875010	1.111516
C	-0.976395	2.613304	2.876698
C	0.305134	-2.588909	-4.043655
N	0.112073	-1.564022	-3.021182
C	-0.403177	-1.830443	-1.803962
C	-1.037465	-3.205548	-1.591995
N	-1.591425	-3.341220	-0.266321
C	-0.660221	-3.546937	0.842377
C	-2.878128	-2.946576	-0.082366
C	-3.479396	-3.031038	1.321893
N	-4.228314	-1.828175	1.631514
C	-3.504668	-0.636384	1.562113
O	-4.128842	0.454084	1.528955
O	-2.235772	-0.770960	1.548620
C	-5.650382	-1.801559	1.332707
O	-3.581325	-2.562903	-1.020070
O	-0.371489	-0.992644	-0.896816
C	0.867268	-0.338222	-3.158170
C	2.260030	-0.486334	-2.536578
N	3.074519	0.597947	-2.602886
C	2.584235	1.929202	-2.949156
C	4.286192	0.529311	-1.818513
C	3.954578	0.668236	-0.327467
N	4.959146	0.498838	0.566738
C	6.372589	0.365763	0.230868
C	4.623927	0.642691	1.976348
C	3.475404	-0.222504	2.389480

Chapter 4. Macrocyclic polypeptoids and their antimicrobial activity

O	2.546706	0.251981	3.196312
C	1.545058	-0.778403	3.417384
O	0.596381	-0.523305	4.159825
C	2.004844	-1.842995	2.661950
N	3.207551	-1.459126	2.061136
C	3.955793	-2.304785	1.132659
O	2.804377	0.892953	0.043271
O	2.613216	-1.544738	-2.021115
H	-0.423880	2.797286	-2.437956
H	-1.344669	4.276042	-2.114449
H	-1.768188	3.255389	-3.496599
H	-4.164276	4.140936	-0.871311
H	-4.987842	2.580595	-0.701558
H	-4.724553	3.271765	-2.313828
H	-2.015228	0.156340	-2.661833
H	-3.646774	0.699159	-3.082975
H	-3.354656	-0.157086	-1.555065
H	0.555680	4.021659	-0.575619
H	1.123858	2.550821	0.245806
H	1.187212	4.116197	1.073191
H	-1.516333	5.600926	1.742799
H	-2.117667	5.302266	0.105490
H	-3.055675	4.751980	1.506219
H	-0.480530	3.366619	3.499009
H	-1.968075	2.423964	3.302692
H	-0.399591	1.684177	2.946868
H	1.232448	-3.144134	-3.867282
H	0.359924	-2.099430	-5.016636
H	-0.537920	-3.277603	-4.062204
H	-0.277659	-3.977654	-1.751191
H	-1.833945	-3.351859	-2.324570
H	0.337633	-3.688982	0.424284
H	-0.647645	-2.668187	1.491825
H	-0.917989	-4.439981	1.417531
H	-2.717673	-3.197681	2.081786
H	-4.164765	-3.884260	1.331922
H	-6.114360	-0.977419	1.873970
H	-5.843905	-1.674719	0.259694
H	-6.101124	-2.739898	1.665024
H	0.943988	-0.086375	-4.219021
H	0.336633	0.471491	-2.648777
H	2.097591	2.404120	-2.088513
H	3.432602	2.540178	-3.260572
H	1.888173	1.879258	-3.786213
H	4.959794	1.330514	-2.133522
H	4.778989	-0.429579	-1.996030
H	6.922415	1.258805	0.541670
H	6.794894	-0.506551	0.737186
H	6.501193	0.233782	-0.840600
H	5.512574	0.387130	2.560976
H	4.343266	1.673520	2.216959
H	1.605911	-2.834005	2.544066
H	3.640670	-2.089190	0.106785
H	3.737030	-3.342458	1.380231
H	5.023760	-2.125970	1.251416

Table 51. Cartesian coordinates of the optimized DP5-Li-DMF cyclic structure.

Li	1.203503	0.034521	-1.118138
C	0.075741	1.123980	3.916869
N	0.217647	0.978441	2.473171
C	0.600086	-0.147594	1.847653
C	1.209333	-1.279032	2.685822
N	1.833204	-2.258610	1.825901
C	1.034970	-3.403062	1.392803
C	2.907442	-1.816934	1.113687
C	3.407472	-2.715129	-0.021463

Chapter 4. *Macrocyclic polypeptoids and their antimicrobial activity*

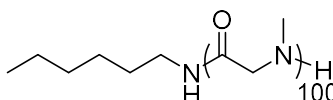
N	4.396755	-2.059122	-0.836881
C	3.967123	-0.945845	-1.574879
O	4.832147	-0.176441	-2.055315
O	2.705821	-0.829933	-1.726756
C	5.766317	-2.089461	-0.351885
O	3.447716	-0.741362	1.369449
O	0.496904	-0.277621	0.622015
C	-0.324981	2.046537	1.661048
C	-1.800497	1.805954	1.341602
N	-2.395508	2.713106	0.524958
C	-1.621248	3.698291	-0.226982
C	-3.709857	2.351624	0.041167
C	-3.605205	1.146123	-0.899065
N	-4.746299	0.460893	-1.161743
C	-6.065474	0.886425	-0.699267
C	-4.605240	-0.765093	-1.939172
C	-3.611687	-1.702566	-1.324470
O	-2.635378	-2.232981	-2.035191
C	-1.801967	-3.032800	-1.161525
O	-0.824743	-3.608737	-1.644773
C	-2.407559	-2.906823	0.078011
N	-3.525463	-2.085225	-0.077046
C	-4.410186	-1.683232	1.013885
O	-2.524835	0.792633	-1.363517
O	-2.411269	0.844792	1.807297
H	-0.981510	1.260802	4.163166
H	0.642744	1.994156	4.257443
H	0.440240	0.241785	4.437543
H	0.427247	-1.766853	3.274040
H	1.952370	-0.865273	3.370686
H	0.391711	-3.705759	2.220577
H	0.415739	-3.161333	0.520520
H	1.682354	-4.247346	1.152530
H	2.553355	-3.000223	-0.639777
H	3.834906	-3.631744	0.401207
H	6.432055	-1.737071	-1.138055
H	5.900693	-1.457037	0.536155
H	6.032069	-3.118924	-0.096016
H	-0.210209	2.989864	2.205225
H	0.244798	2.115338	0.728480
H	-1.041442	3.225324	-1.027532
H	-2.312328	4.420184	-0.661910
H	-0.950990	4.243733	0.439469
H	-4.147308	3.203699	-0.485902
H	-4.356599	2.104897	0.886996
H	-6.820934	0.477280	-1.370036
H	-6.272188	0.545260	0.321112
H	-6.147421	1.972932	-0.735648
H	-5.586165	-1.242058	-2.007736
H	-4.252045	-0.553697	-2.952865
H	-2.143227	-3.329557	1.031027
H	-4.070674	-0.726257	1.417913
H	-4.362783	-2.454126	1.781579
H	-5.433000	-1.612898	0.643743
O	1.546813	1.938329	-1.100184
C	2.741493	2.247255	-1.273208
N	3.249294	3.450762	-1.002364
C	2.428677	4.520647	-0.461114
C	4.665612	3.723317	-1.188671
H	3.466191	1.519276	-1.665680
H	2.585789	5.432158	-1.044063
H	2.698906	4.715299	0.581862
H	1.382303	4.224248	-0.518135
H	4.801593	4.531238	-1.913269
H	5.161244	2.822412	-1.554249
H	5.117010	4.020078	-0.237218

7.4 Cyclic homopolypeptoids synthesis

7.4.1 Poly(Nme) kinetics studies

Synthesis of hexylamine initiated polysarcosine (poly(sar) 44): The *N*-methylated NCA monomer (Sar-NCA, 0.1 g, 8.6×10^{-4} mol) was weighed in a glovebox under pure argon, introduced in a flame-dried Schlenk, and dissolved with 2 mL of anhydrous DMF. The solution was stirred for 5 min, and 17.3 μ L of hexylamine 0.5 M in DMF (8.6×10^{-6} mol) was added with an argon purged syringe. The solution was stirred at RT under argon until the disappearance of the peak around 1850 cm^{-1} by FTIR (**Figure 66**). The polymer was then recovered by precipitation in 20 mL of diethyl ether, centrifuged, and dried under high vacuum. Yield: 94% (0.058 g, white solid).

P(Nme) 44



$^1\text{H-NMR}$ in DMSO-d_6 (400 MHz, δ , ppm): 0.85 (s, 3H, CH_3 hexylamine), 1.23 (br, 10H, CH_2 hexylamine), 2.63-3.07 (m, 290H, CH_3), 3.83-4.45 (m, 182H, CH_2).

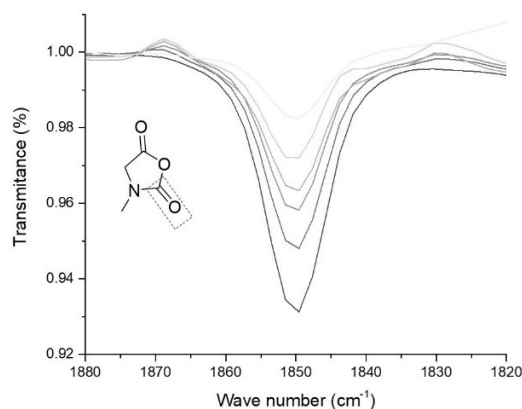


Figure 66. Kinetic experiments of Sar-NCA polymerization at $M/B = 100$: A) Decrease of the carbonyl stretching at 1850 cm^{-1} followed by FTIR

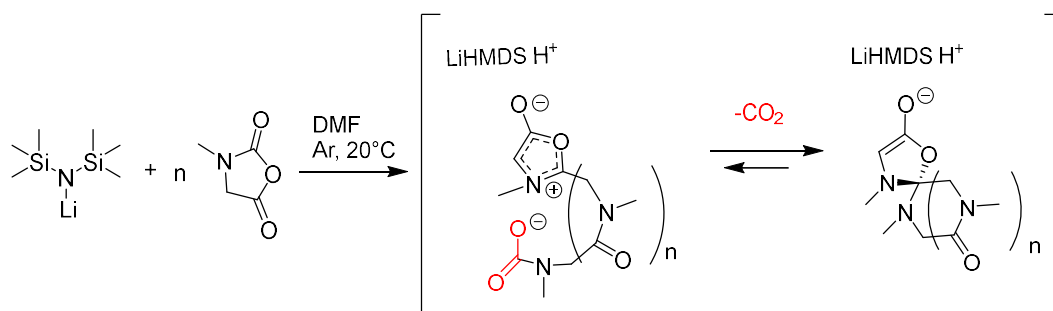
Synthesis of polysarcosine with LiHMDS and hexylamine (poly(sar) 45): The *N*-methylated NCA monomer (Sar-NCA, 0.1 g, 8.6×10^{-4} mol) was weighed in a glovebox under pure argon, introduced in a flame-dried Schlenk, and dissolved with 2 mL of anhydrous DMF. The solution was stirred for 5 min, then 17.3 μ L of hexylamine 0.5 M and LiHMDS 0.5M in THF (8.6

Chapter 4. Macrocylic polypeptoids and their antimicrobial activity

$\times 10^{-6}$ mol of hexylamine and 8.6×10^{-6} mol of LiHMDS) were added with an argon purged syringe. The solution was stirred at RT under argon until the disappearance of the peak around 1850 cm^{-1} by FTIR (**Figure 66**). The polymer was then recovered by precipitation in 20 mL of diethyl ether, centrifuged, and dried under high vacuum. Yield: 70% (0.043 g, yellowish solid).

$^1\text{H-NMR}$ in DMSO-d_6 (400 MHz, δ , ppm): 0.85 (br, CH_3 hexylamine), 1.23 (br, CH_2 hexylamine), 2.63-3.07 (m, 3H, CH_3), 3.83-4.45 (m, 2H, CH_2).

Synthesis of cyclic polysarcosine using LiHMDS M/I = 100 (poly(sar) 46). A typical procedure of synthesis is described at M/B = 100: The *N*-methylated NCA monomer (Sar-NCA, **Scheme 46**, 0.3 g, 2.6×10^{-3} mol) was weighed in a glovebox under argon, introduced in a flame-dried Schlenk, and dissolved with 6.5 mL of anhydrous DMF (0.4 M). A solution of LiHMDS 0.5 M in THF was prepared and 52 μL (2.6×10^{-5} mol) was added with an argon purged syringe. The solution was stirred at RT under argon until the disappearance of the peak around 1850 cm^{-1} by FTIR (**Figure 66**). The polymer was then recovered by precipitation in 60 mL of diethyl ether, centrifuged and dried under high vacuum. Yield: 97% (0.179 g, yellowish solid).



Scheme 46. Synthesis of cyclic polysarcosine in DMF at 0.4 M

$^1\text{H-NMR}$ of the polysarcosine backbone signals were observed in DMSO-d_6 (400 MHz, δ , ppm): 2.69-3.00 (m, 3H, CH_3), 3.84-4.44 (m, 2H, CH_2) 7.2-7.8 (m, 1H, $\text{CH}=\text{N}$ mesoionic oxazole).

7.4.2 Mechanism study

The M/I 2 using LiHMDS as initiator were prepared in order to elucidate by MALDI TOF and FTIR-ATR the mechanism of the polymerization, as an example the M/B = 1 was prepared as follows: the *N*-methylated NCA monomer (Sar-NCA 49.4 mg, 8.6×10^{-4} mol) was weighed in a glovebox under pure argon, introduced in a flame-dried Schlenk, and dissolved with 1 mL of anhydrous DMF. A second solution was prepared with LiHMDS (0.15 g, 8.6×10^{-4} mol) in

anhydrous THF at 0 °C. The NNCA solution was added to the LiHMDS solution with an argon purged syringe. The mixture was stirred for 10 min. and precipitated on 20 mL of diethyl ether and dried under vacuum. The dried powder was analyzed by mass spectroscopy and FTIR-ATR.

7.4.3 Stability assays: HBr/TFA and Propionylation

Synthesis of cyclic polysarcosine M/I = 35 (poly(sar) 47). A typical procedure of synthesis is described at M/B = 35: The *N*-methylated NCA monomer (Sar-NCA, 0.3 g, 2.6×10^{-3} mol) was weighed in a glovebox under argon, introduced in a flame-dried Schlenk, and dissolved with 6.5 mL of anhydrous DMF (0.4 M). A solution of LiHMDS 0.5 M in THF was prepared and 149.1 μ L (7.4×10^{-5} mol) was added with an argon purged syringe. The solution was stirred at RT under argon until the disappearance of the peak around 1850 cm^{-1} by FTIR. The polymer was then recovered by precipitation in 60 mL of diethyl ether, centrifuged, and dried under high vacuum. Yield: 95% (0.176 g, yellowish solid).

$^1\text{H-NMR}$ in DMSO- d_6 (400 MHz, δ , ppm): 2.69-3.00 (m, 3H, CH₃), 3.84-4.44 (m, 2H, CH₂), 7.2-7.8 (m, 1H, CH=N mesoionic oxazole).

$^{13}\text{C-NMR}$ of the polymer were observed in DMSO- d_6 (100 MHz, δ , ppm): 30.79 (CH₃), 32.36 (CH₃), 34.81-35.41 (CH₃), 35.88 (CH₃), 48.75-49.72 (CH₂), 51 (CH₂), 124.21 (C), 151.5 (C), 162.33 (C=N), 163.35 (C=N), 168.31-170.17 (NCO), 170.17 (COO), 171.55 (COO).

Acidic treatment using HBr/TFA: In a test tube, polysarcosine M/I = 35 (MW = 2090 g/mol) (poly(sar) 47), 20 mg, 9.5×10^{-6} mol) was dissolved in 0.5 mL TFA. Then, HBr 0.5 M in TFA (38 μ L, 1.9×10^{-5} mol) was added and the reaction was stirred first for 3 h at 20 °C. The polymer was precipitated in 10 mL of diethyl ether and dried under vacuum, dialyzed against water (MWCO 500 Da, RC membranes) and upon freeze-drying, a yellowish powder was obtained with a yield: 75%. (0.005 g, yellowish solid).

$^1\text{H-NMR}$ of the polysarcosine backbone signals were observed in DMSO- d_6 (400 MHz, δ , ppm): 2.69-3.00 (m, 3H, CH₃), 3.84-4.44 (m, 2H, CH₂), 7.2-7.8 (m, 1H, CH=N mesoionic oxazole).

$^{13}\text{C-NMR}$ of the polymer were observed in DMSO- d_6 (100 MHz, δ , ppm): 30.70 (CH₃), 32.35 (CH₃), 33.09 (CH₃), 34.81-35.41 (CH₃), 48.75-49.72 (CH₂), 50.99 (CH₂), 129.49 (C), 151.5 (C), 163.34 (C=N), 168.31-170.17 (NCO), 170.17 (COO), 206.52 (COOH).

Synthesis of linear polysarcosine analog (poly(sar) 47'). In a test tube, polysarcosine

Chapter 4. Macrocyclic polypeptoids and their antimicrobial activity

M/B = 35 (2090 g/mol) (poly(Nme), 70 mg, 3.3×10^{-5} mol) was dissolved in 1 mL anhydrous DMF. Then, propionic anhydride (7.6 μ L, 6.0×10^{-5} mol) was added and the reaction was stirred for 4 h at 20 °C. The polymer was precipitated in 20 mL of diethyl ether and dried under vacuum. Yield: 92% (0.067 g, yellowish solid).

$^1\text{H-NMR}$ in DMSO- d_6 (400 MHz, δ , ppm): 0.92-0.95 (m, 3H, CH₃, propionyl), 2.00-2.15 (m, 2H, CH₂), 2.17-2.35 (m, 2H, CH₂), 2.69-3.00 (m, 63H, CH₃), 3.84-4.44 (m, 40H, CH₂), 7.2-7.8 (m, 1H, CH=N).

Calculation of the polymerization degree was calculated using as reference the CH₃ of the propionylated extremity as follow:

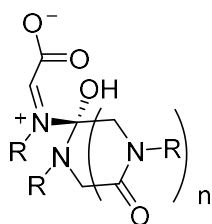
$$DP = \frac{I_{CH_2} + I_{CH_3}}{2}$$

Where I_{CH_2} and I_{CH_3} are the intensities of the polymer backbone

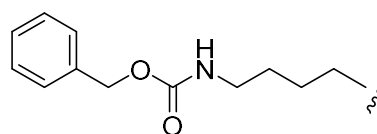
7.4.4 Cationic cyclic polypeptoids

As a polymeric analog of poly(lysine), our approach was used to synthesize a cyclic polypeptoid bearing cationic side chains: this new polymer (poly(Nlys)) was synthesized in two steps.

Step 1. Synthesis of cyclic poly((N'-(carbobenzyloxy)-N-aminobutyl)glycine) (P(ZNlys) 53). The ZLys-NNCA monomer (0.2 g, 6.5×10^{-4} mol) was weighed in a glovebox under argon, introduced in a flame-dried Schlenk, and dissolved with 1.6 mL of anhydrous DMF (0.4 M). A solution of LiHMDS 0.5 M in THF was prepared and 43.5 μ L (2.2×10^{-5} mol) was added with an argon purged syringe. The solution was stirred at RT under argon until the disappearance of the peak around 1850 cm^{-1} by FTIR. The polymer was then recovered by precipitation in 20 mL of diethyl ether, centrifuged, and dried under high vacuum. Yield: 58% (0.1 g, yellowish solid).



R=



Chapter 4. Macrocyclic polypeptoids and their antimicrobial activity

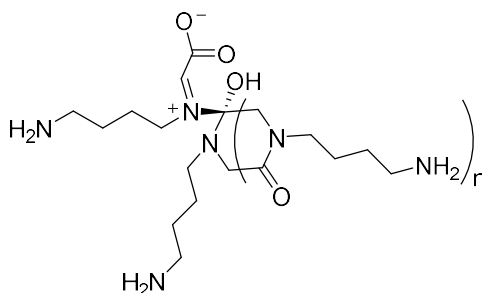
P(ZNlys)53 M/B = 30

Molar mass by SEC in DMF (using a calculated $dn/dc = 0.0922$): $M_n = 3200$ g/mol $\overline{M}_w = 1.02$

$^1\text{H-NMR}$ in CDCl_3 (400 MHz, δ , ppm): 1.02-1.93 (m, 4H, 2CH₂), 2.72-3.52 (m, 4H, 2CH₂), 3.62-4.62 (m, 2H, CH₂), 4.79-5.15 (m, 2H, CH₂), 7.25-5.50 (m, 5H, Ar).

^{13}C NMR in CDCl_3 (100 MHz, δ , ppm): 26.84 (m, 2CH₂), 40.53 (m, CH₂), 48.19 (m, 2CH₂), 66.56 (s, CH₂), 128.08 (s, 2CH), 128.51 (s, 3CH) 136 (m, C), 156.85 (s, 2NCO)

Step 2. Synthesis of cationic poly((*N*-aminobutyl)glycine) ((P(Nlys) 53D). 20 mg of Poly(ZNlys) were dissolved in 0.2 mL of TFA, 25 μL HBr in acetic acid 33% was added (2 equiv. based on Zlys unit MW = 262 g/mol, 1.4×10^{-4} mol) and stirred for 3 h. Then, the polymer was precipitated in diethyl ether, neutralized at pH = 7 using NaHCO_3 , dialyzed with water (MWCO 100-500 Da), and freeze-dried. Yield: 62% (5 mg, yellowish solid).

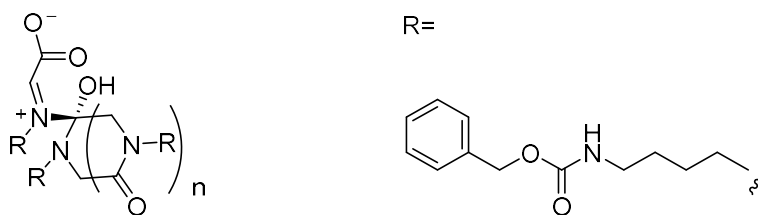


P(Nlys)53D M/B = 30

$^1\text{H-NMR}$ peaks in D_2O (400 MHz, δ , ppm): 1.34-1.59 (m, 4H, 2CH₂), 2.91-2.73 (br, 2H, CH₂), 3.10-3.35 (br, 2H, CH₂), 3.74-4.42 (m, 2H, CH₂).

Synthesis of poly((*N'*-(carbobenzyloxy)-*N*-aminobutyl)glycine) (PZNlys 54) M/B=50.

The ZLys-NNCA monomer (0.2 g, 6.5×10^{-4} mol) was weighed in a glovebox under argon, introduced in a flame-dried Schlenk, and dissolved with 1.5 mL of anhydrous DMF (0.4 M). A solution of LiHMDS 0.5 M in DMF was prepared and 26 μL (1.3×10^{-5} mol) was added with an argon purged syringe. The solution was stirred at room temperature under argon until the disappearance of the peak around 1850 cm^{-1} by FTIR. The polymer was then recovered by precipitation in 20 mL of diethyl ether, centrifuged, and dried under high vacuum. Yield: 56% (0.098 g, yellowish solid).

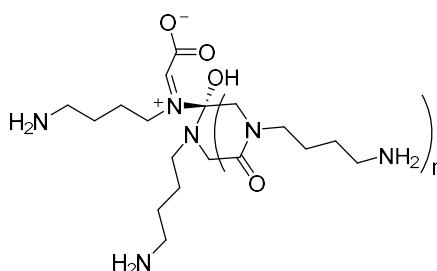


P(ZNlys)54 M/B = 50

Molar mass by SEC in DMF (using a calculated $dn/dc = 0.0922$): $M_n = 4900$ g/mol $\bar{M}_w = 1.08$

$^1\text{H-NMR}$ peaks in CDCl_3 (400 MHz, δ , ppm): 1.02-1.93 (m, 4H, 2CH_2), 2.72-3.52 (m, 4H, 2CH_2), 3.62-4.62 (m, 2H, CH_2), 4.79-5.15 (m, 2H, CH_2), 7.25-5.50 (m, 5H, Ar).

Synthesis of cationic poly((*N*-aminobutyl)glycine) (P(Nlys) 54D) M/B=50. 50 mg of Poly(ZNlys) were dissolved in 0.5 mL of TFA, 69 μL HBr in acetic acid 33% was added (2 equiv. based on Zlys unit MW = 262 g/mol, 3.8×10^{-4} mol) and stirred for 3 h (Step 2 in Scheme S5.1). Then, the polymer was precipitated in diethyl ether, neutralized at pH = 7 using NaHCO_3 , dialyzed with water (MWCO 100-500 Da), and freeze-dried. Yield: 65% (0.0361 g, yellowish solid).



P(Nlys)54D M/B=50

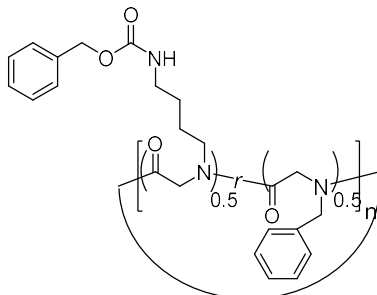
$^1\text{H-NMR}$ peaks in D_2O (400 MHz, δ , ppm): 1.34-1.59 (m, 4H, 2CH_2), 2.91-2.73 (br, 2H, CH_2), 3.10-3.35 (br, 2H, CH_2), 3.74-4.42 (m, 2H, CH_2).

7.5 Copolypeptoid preparation

Synthesis of cyclic poly[(*N'*-Cbz-*N*-aminobutyl)glycine]-random-(*N*-benzylglycine)] (c-P(ZNlys-*r*-Nphe) 59). A typical procedure for the synthesis is described at M/B = 50 and 50% hydrophobic content: The *N'*-Cbz-*N*-aminobutyl NCA monomer (ZLys-NNCA, 101 mg, 3.3×10^{-4} mol) and *N*-benzyl NCA (Phe-NNCA, 63 mg, 3.3×10^{-4} mol) were weighed in a glovebox under pure argon, introduced in a flame-dried Schlenk, and dissolved with 2 mL of anhydrous DMF. A solution of LiHMDS 0.5 M in DMF was prepared and 27 μL (1.3×10^{-5} mol) was added with an argon purged syringe. The solution was stirred at RT under argon until the disappearance of the

Chapter 4. Macrocyclic polypeptoids and their antimicrobial activity

peak around 1850 cm^{-1} by FTIR. The polymer was then recovered by precipitation in 20 mL of diethyl ether, centrifuged, and dried under high vacuum. Yield: 92% (0.126 g, yellowish solid).



P(ZNlys-*r*-Nphe)59 M/B=50

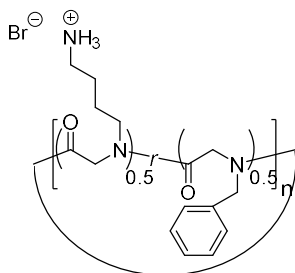
Hydrophobic content calculation by comparison of CH_2 Nphe (4.27-4.57 ppm) and 2CH_2 Nlys (1.35-1.90 ppm) according to:

$$\text{H/C}\% = \frac{\frac{X\text{H}_{\text{CH}_2 \text{Nphe}}}{5}}{\left(\frac{4\text{H}_{\text{CH}_2}}{4} + \frac{X\text{H}_{\text{Ar}}}{5}\right)} * 100$$

$$\text{H/C}\% = 50\%$$

$^1\text{H-NMR}$ in DMSO-d_6 (400 MHz, δ , ppm): 1.20-1.57 (m, 4H, 2CH_2 ZNlys), 2.87-3.28 (m, 4H, 2CH_2 ZNlys), 3.71-4.3 (m, 2H, CH_2 glycine backbone), 4.27-4.57 (m, 2H, CH_2 Nphe), 4.89-5.04 (m, 2H, CH_2 ZNlys), 7.00-7.46 (m, 11H, $2\text{Ar} + \text{NHCO}$).

Synthesis of cationic cyclic poly[(*N*-aminobutyl)glycine]-*random*-(*N*-benzyglycine)] [P(Nlys-*r*-Nphe) 59D]. Deprotection was carried out as mentioned before for poly(Nlys)53D yielding 46% (0.0417 g, yellowish solid).



P(Nlys-*r*-Nphe)59D M/B=50

Hydrophobic content calculation by comparison of Ar (7.10-7.56 ppm) and 2CH_2 (1.35-1.90 ppm) according to:

Chapter 4. Macrocyclic polypeptoids and their antimicrobial activity

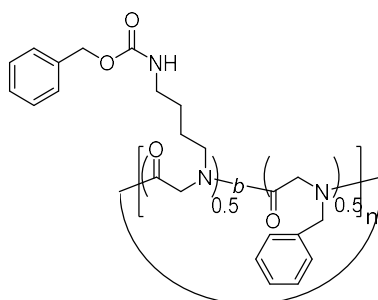
$$\text{H/C}\% = \frac{\frac{X_{H_{Ar}}}{5}}{\left(\frac{4H_{CH}}{4} + \frac{X_{H_{Ar}}}{5}\right)} * 100$$

$$\text{H/C}\% = 50\%$$

$^1\text{H-NMR}$ in D_2O (400 MHz, δ , ppm): 1.35-1.90 (m, 4H, 2CH_2 Nlys), 2.79-3.12 (m, 2H, CH_2 ZNlys), 3.17-3.51 (m, 2H, CH_2 Nlys), 3.62-4.42 (m, 2H, CH_2 glycine backbone), 4.40-4.73 (m, 2H, CH_2 Nphe), 7.10-7.56 (m, 5H, Ar Nphe).

Copolymers **55-58** and **55D-58D** were synthesized varying the concentration of both ZLys-NNCA and Phe-NNCA to afford the corresponding hydrophobic cation ratio from 10 to 40 % using the same protocol described for **59** and **59D** and no detailed information is provided.

Synthesis of cyclic poly[$((N'$ -Cbz- N -aminobutyl)glycine)-*block*-(N -benzylglycine)] [c-P(ZNlys-*b*-Nphe) **64].** A typical procedure for the synthesis is described at M/B = 50 and 50% hydrophobic content: The N' -Cbz- N -aminobutyl NCA monomer (ZLys-NNCA, 101 mg, 3.3×10^{-4} mol) was weighed in a glovebox under pure argon, introduced in a flame-dried Schlenk, and dissolved with 2 mL of anhydrous DMF. A solution of LiHMDS 0.5 M in DMF was prepared and 27 μL (1.3×10^{-5} mol) was added with an argon purged syringe. The solution was stirred at RT under argon until the disappearance of the peak around 1850 cm^{-1} by FTIR. Then, N -benzyl NCA (Phe-NNCA, 63 mg, 3.3×10^{-4} mol) was added and the reaction was monitored until the disappearance of the peak followed by FTIR. The polymer was precipitated in Et_2O and dried under vacuum. Yield: 50% yield (0.067 g, yellowish solid).



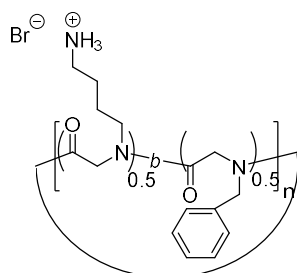
P(ZNlys-*b*-Nphe)64 M/B=50

Hydrophobic content calculation by comparison of CH_2 Nphe (4.27-4.57 ppm) and 2CH_2 Nlys (1.35-1.90 ppm) = 51%

Chapter 4. Macrocyclic polypeptoids and their antimicrobial activity

$^1\text{H-NMR}$ in DMSO-d_6 (400 MHz, δ , ppm): 1.20-1.57 (m, 4H, 2CH_2 ZNlys), 2.87-3.28 (m, 4H, 2CH_2 ZNlys), 3.71-4.3 (m, 2H, CH_2 glycine backbone), 4.27-4.57 (m, 2.1H, CH_2 Nphe), 4.89-7.46 (m, 10H, 2Ar + NHCO). The signals were in agreement with the random copolymer before deprotection.

Synthesis of cationic cyclic poly[(*N*-aminobutyl)glycine]-block-(*N*-benzylglycine)] [c-P(Nlys-*b*-Nphe) 64D]. Deprotection was carried out as mentioned before for poly(Nlys)53D. Yield: 91% yield (0.047 g, yellowish solid).



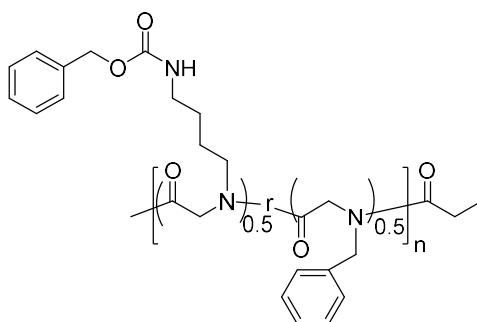
P(ZNlys-*b*-Nphe)64D M/B=50

Hydrophobic content calculation by comparison of Ar (7.10-7.56 ppm) and 2CH_2 (1.35-1.90 ppm) = 48%

$^1\text{H-NMR}$ in D_2O (400 MHz, δ , ppm): 1.35-1.90 (m, 4H, 2CH_2 Nlys), 2.79-3.12 (m, 2H, CH_2 ZNlys), 3.17-3.51 (m, 2H, CH_2 Nlys), 3.62-4.42 (m, 2H, CH_2 glycine backbone), 4.40-4.73 (m, 2H, CH_2 Nphe), 7.10-7.56 (m, 4.7H, Ar Nphe).

Copolymers 60-63 and 60D-63D were synthesized varying the concentration of both ZLys-NNCA and Phe-NNCA to afford the corresponding hydrophobic cation ratio from 10 to 40 % using the same protocol described for 64 and 64D and no detailed information is provided.

Synthesis of linear poly[(*N'*-Cbz-*N*-aminobutyl)glycine]-random-(*N*-benzylglycine)] using propionylation (I-P(ZNlys-*r*-Nphe) 65). In a test tube, poly(ZNlys-*r*-Nphe), M/B = 50 (5100 g/mol, 150 mg, 2.9×10^{-5} mol) was dissolved in 2 mL anhydrous DMF. Then, propionic anhydride (6.7 μL , 5.3×10^{-5} mol) was added and the reaction was stirred for 24 h at 20 °C. The polymer was precipitated in 40 mL of diethyl ether and dried under vacuum. Yield: 87%. (0.133 g, yellowish solid).



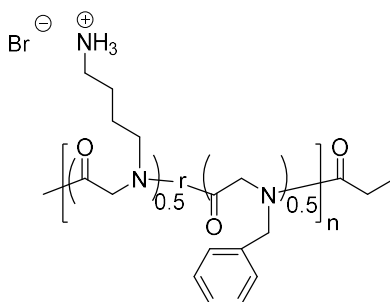
I-P(ZNlys-r-Nphe)65 M/B=50

Molar mass by SEC in DMF: $M_n = 6800$ g/mol $\bar{M}_w = 1.18$ using a $dn/dc = 0.0816$.

Hydrophobic content calculation by comparison of Ar (7.25-5.50 ppm) and 2CH_2 Nlys (1.35-1.90 ppm) = 48%

$^1\text{H-NMR}$ peaks in DMSO-d_6 (400 MHz, δ , ppm): 0.89 (br, 3H, CH_3), 1.17-1.61 (m, 4H, 2CH_2 ZNlys), 2.89-3.27 (m, 2H, 2CH_2 ZNlys), 3.74-4.48 (m, 2H, CH_2 glycine backbone), 4.90-5.11 (m, 4H, CH_2 ZNlys + CH_2 Nphe, 7.25-5.50 (m, 10H, Ar+NHCO) (**Figure 67**).

Synthesis of cationic linear poly[(N-aminobutyl)glycine]-random-(N-benzylglycine) [I-P(Nlys-r-Nphe) 65D] at 50% hydrophobic content and M/B = 50, Deprotection was carried out as mentioned before for poly(Nlys)53D. Yield: 80% (0.08 g, yellowish powder).



I-P(Nlys-r-Nphe)65D M/B=50

Hydrophobic content calculation by comparison of Ar (6.58-7.51 ppm) and 2CH_2 Nlys (1.35-1.90 ppm) = 54%

$^1\text{H-NMR}$ in D_2O (400 MHz, δ , ppm): 1.07 (br, 3H, CH_3), 1.47-1.89 (m, 4H, 2CH_2 Nlys), 2.81-3.47 (m, 4H, 2CH_2 ZNlys), 3.55-4.60 (m, 2H, CH_2 glycine backbone), 4.87-5.23 (m, 2H, CH_2 Nphe), 6.86-7.51 (m, 6H, Ar Nphe).

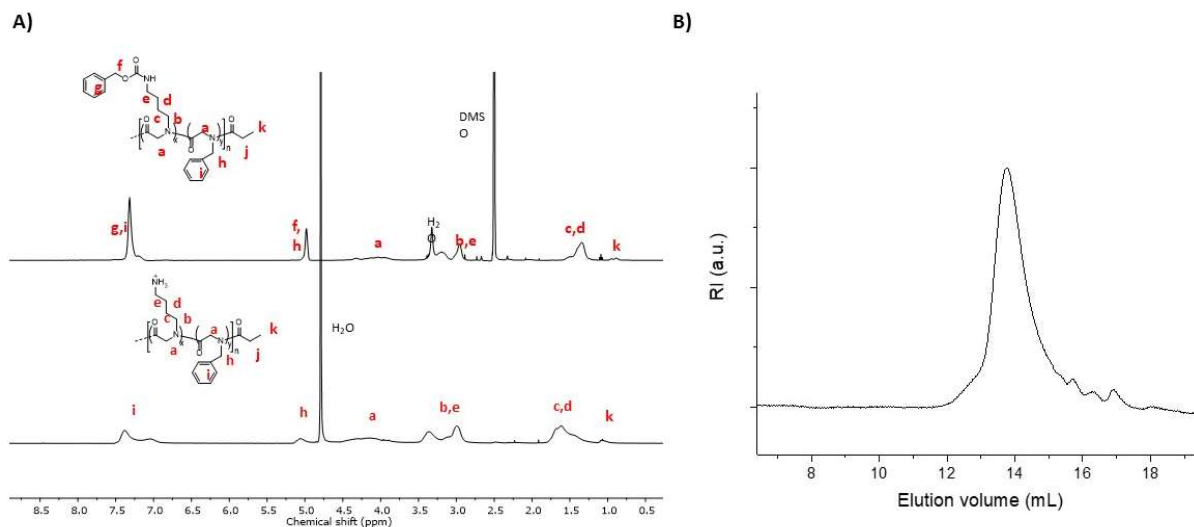


Figure 67. Characterization of *l*-P(Nlys-*r*-Nphe). a) ^1H -NMR spectra upon propionylation (up, **65**) and upon deprotection (down, **65D**). b) Refractive index trace from SEC performed in DMF.

7.6 Antimicrobial assay

The analyses were performed as it is described in chapter 3 (pp 186) for *C. difficile*.

To determine the MIC of the other gram positive or negative the experiments were carried on by FONDEREPHAR in Toulouse and the protocol was as follows:

Mother solutions of the polypeptoids under assay were prepared by adding 1 mL of sterile distilled water (SDW) directly in the Eppendorf containing the product, the solution was transfereed in a sterile tube. Eppendorf was rinsed 3 times (SDW) and the resulting solutions were added to the tube. The final volume was adjusted to a concentration of 500 $\mu\text{g}/\text{mL}$ with SDW. Shaking (4 times/h) during 1 h. Mother solutions were homogeneized and appear clear expected. Storage at -20°C .

Culture maintaining: *S. aureus*, *E. faecalis*, *L. monocytogenes*, *E. coli*, *A. baumannii*, *P. aeruginosa*: Muller Hinton agar, incubation 24 h at $36 \pm 1^\circ\text{C}$ under aerobiosis. *S. pneumoniae*: Muller Hinton agar, incubation 24 h at $36 \pm 1^\circ\text{C}$ under anaerobiosis. *B. fragilis*, *H. pylori*: Columbia agar + 5% sheep red cells, incubation 24 – 48 h at $36 \pm 1^\circ\text{C}$ under anaerobiosis for *B. fragilis* and under microaerophilic conditions for *H. pylori*.

Assays: *S. aureus*, *E. faecalis*, *L. monocytogenes*, *E. coli*, *A. baumannii*, *P. aeruginosa*: Muller Hinton broth, and agar, incubation 24 h at $36 \pm 1^\circ\text{C}$ under aerobiosis. *S. pneumoniae* :

Chapter 4. *Macrocyclic polypeptoids and their antimicrobial activity*

Muller Hinton broth, supplemented with 10% SVF and agar, incubation 24 h at $36 \pm 1^\circ\text{C}$ under anaerobiosis. *B. fragilis*: Muller Hinton broth and and agar, incubation 24 h at $36 \pm 1^\circ\text{C}$ under anaerobiosis. *H. pylori*: Muller Hinton broth, supplemented with 10% and Muller Hinton agar supplemented with 10% horse blood, incubation 24 h at $36 \pm 1^\circ\text{C}$ under microaerophilic conditions.

MIC (Minimal Inhibitory Concentration): Strains were maintained on agar specified above. A fresh suspension was prepared just before each assay in Tryptone salt and adjusted to 10^8 CFU/mL. Each well of a 96-well microtiter plate was filled with 100 μL of specify broth. Then, 100 μL of a mother solution were added to the first well of two lines of the microtiter plate and 2 fold dilutions were performed from well 1 to well 10. All the wells (except column 11 : sterility control) were inoculated with 1 to 3 μL of the tested suspension (multi inoculator Denley). Microplates were then incubated under conditions described above. MIC was determined as the lowest concentration without any visible growth versus positive control (column 12).

7.7 Cytotoxicity

The analyses were performed as described in chapter 3 (pp 187).

7.8 Liposome destabilization

The analyses were performed at the Centre d'Etudes et de Recherche sur le Médicament de Normandie (CERMN, Caen Normandie, France) by Dr. Marc Since. The procedure is described as follows.

Liposome mixtures of SPC:cholesterol (SPC:Chol) or DOPG:cholesterol (PG:Chol) in a molar ratio of 8:2 were formulated. Liposomes were formulated according to the adapted method of the thin lipid film hydration.⁵⁸ Lipid solutions in chloroform/methanol (4:1) were evaporated under nitrogen flow and left under vacuum for 2-3 h to form a lipid film. Carboxyfluoresceine (CF) was dissolved in phosphate buffer Saline (PBS) (137 mM NaCl, 2.7 mM KCl, 10 mM Na_2HPO_4 , 2 mM KH_2PO_4) to reach 70 μM , pH was adjusted with concentrated NaOH to 7.4. This thin lipid film was then hydrated in the CF solution and vortexed 1h. At RT the yielded multilamellar vesicles (MLVs) were then extruded 13 times with a mini-extruder (Avanti Polar Lipids, Inc., Alabaster, Alabama, USA) through polycarbonate membranes with a pore diameter of 100 nm (Avanti Polar Lipids, Inc.). The obtained LUVs were separated from possible unincorporated CF by passage through a Sepharose® CL-4B loaded (Sigma-Aldrich) column, using PBS buffer as eluent. The LUVs size was assessed by DLS (NanoZS®, Malvern Instruments, Worcestershire, UK) after a

Chapter 4. *Macrocyclic polypeptoids and their antimicrobial activity*

1:100 dilutions in the PBS buffer. Liposomes were stable within 4 month: SPC:Chol having a Z-average 153.1 ± 0.5 nm, PDI = 0.095 ± 0.02 and Z-potential -3.9 ± 0.9 ; PG:Chol having a Z-average 138.1 ± 1.7 nm with a PDI = 0.093 ± 0.04 and Z-potential -33.3 ± 2.2 . The entrapment of CF was measured by the dequenching of fluorescence after the addition of 2 μ L 20% (v/v) Triton X-100 measured with a Synergy 2 microplate reader (Biotek, Colmar, France) equipped with the appropriate filters ($\lambda_{\text{ex}}=485/20$ nm and $\lambda_{\text{em}}=528/20$ nm). CF release assay was performed in a final volume of 100 μ L, using 10 μ M LUVs in PBS buffer. Polypeptoids solubilized in PBS buffer were then added to the solution to reach a final concentration of 90 μ g/mL. The fluorescence was recorded immediately (F_0) and for 1.5 h at 25 °C. It was compared with that measured at the end of the experiment after the addition of 2 μ L of 20% Triton X-100 solution to achieve complete liposome leakage (F_{max}). The percentage of CF release was calculated according to the following equation:⁵⁹

$$\% \text{ CF leakage}_{(t)} = \frac{F_t - F_0}{F_{\text{max}} - F_0} \times 100$$

where F_t was the fluorescence intensity at time t , F_0 the initial fluorescence intensity, and F_{max} the final fluorescence intensity after adding Triton X-100. Fluorescences of PBS and polypeptoids alone at the same concentration were measured as negative controls.

7.9 Protease assay

The protocol was adapted from a known method for peptoid analysis.⁵¹ A polymer solution was prepared (0.1 mM) in 1 mL of NaHCO_3 buffer 50 mM pH = 7.8 equilibrated at 37 °C for 10 min and 47 μ L of trypsin 42 μ M (1 mg/mL) was added. At a certain time, 2.3 μ L of the reaction mixture were taken, placed in an Eppendorf tube, quenched with 200 μ L acetonitrile and 200 μ L sodium borate buffer 0.1 M and kept in an ice bath. 4-Fluoro-7-nitro-benzofurazan (NBDF) (10 μ L, acetonitrile solution 10 mM) was added, immediately the solution was incubated at 60 °C for 3 min and 500 rpm in the Eppendorf thermomixer R. The sample was placed on ice and 20 μ L of 3 N HCl were added to stabilize the 4-amino-7-nitro-benzofurazan product. The fluorescence was measured in a Spectra max M2 (Molecular devices) with $\lambda_{\text{ex}} = 470$ nm and $\lambda_{\text{em}} = 540$ nm. The values were adjusted using the appropriate blank. The raw data was obtained from SoftMaxPro V5 and analyzed in Origin2016 software.

7.10 Antimicrobial assay after trypsin treatment.

The analyses were performed at the Pasteur Institute (Paris, France) by PhD candidate Antoine Tronnet and Dr. Bruno Dupuy. The procedure is described as follows.

Chapter 4. *Macrocyclic polypeptoids and their antimicrobial activity*

Solution of **c-P(Nlys-r-Nphe)59D** was prepared in carbonate buffer 50 mM pH = 7.8 at 1 mg/mL with 0.3 mg/mL of trypsin (Sigma-Aldrich). Solution of LL-37 was prepared in sodium carbonate buffer 50 mM pH = 7.8 at 2 mg/mL with 0.6 mg/mL of trypsin. After 1h at 37°C, a twofold serial dilution of **59D** and LL-37 were prepared in carbonate buffer 50 mM pH = 7.8 to give a final concentration range of 1000 to 8 µg/mL for **59D** and 2000 to 16 µg/mL for LL-37 and 20 µL of each concentration was added to a 96-well plate. Solutions of **59D** and LL-37 in carbonate buffer 50 mM pH = 7.8 were also prepared without trypsin as control. Then, an overnight bacterial solution of *C. difficile* having an OD₆₀₀ between 0.450 and 0.600 (10⁷-10⁸ CFU/mL) was diluted in Brain Heart Infusion (BHI) at 10⁵ CFU/mL, each well was inoculated anaerobically with 180 µL and incubated at 37°C. MIC reported are the minimal drug concentration that suppressed totally the growth of bacteria after 24 h at 37°C and determined visually. The experiments were performed by triplicates. The uninoculated medium was used as a negative control to test for contamination of the growth medium. The positive control was inoculated with *C. difficile* but no antimicrobial compound was added.

8 References

- (1) Sprott, G. D. Structures of Archaeobacterial Membrane Lipids. *J. Bioenerg. Biomembr.* **1992**, *24* (6), 555–566.
- (2) Choi, J. S.; Joo, S. H. Recent Trends in Cyclic Peptides as Therapeutic Agents and Biochemical Tools. *Biomol. Ther.* **2020**, *28* (1), 18–24.
- (3) Nielsen, D. S.; Shepherd, N. E.; Xu, W.; Lucke, A. J.; Stoermer, M. J.; Fairlie, D. P. Orally Absorbed Cyclic Peptides. *Chem. Rev.* **2017**, *117* (12), 8094–8128.
- (4) National Institutes of Health (NIH). Clinical Trials.Gov. Clinical Trials.gov <https://clinicaltrials.gov/> (accessed Apr 13, 2021).
- (5) McGivern, J. G. Ziconotide: A Review of Its Pharmacology and Use in the Treatment of Pain. *Neuropsychiatr. Dis. Treat.* **2007**, *3* (1), 69–85.
- (6) Huang, H.; Damjanovic, J.; Miao, J.; Lin, Y. S. Cyclic Peptides: Backbone Rigidification and Capability of Mimicking Motifs at Protein-Protein Interfaces. *Phys. Chem. Chem. Phys.* **2021**, *23* (1), 607–616.
- (7) Abdel Monaim, S. A. H.; Somboro, A. M.; El-Faham, A.; de la Torre, B. G.; Albericio, F. Bacteria Hunt Bacteria through an Intriguing Cyclic Peptide. *ChemMedChem* **2019**, *14* (1), 24–51.
- (8) Pavithra, G.; Rajasekaran, R. Gramicidin Peptide to Combat Antibiotic Resistance: A Review. *Int. J. Pept. Res. Ther.* **2020**, *26* (1), 191–199.
- (9) Takada, Y.; Itoh, H.; Paudel, A.; Panthee, S.; Hamamoto, H.; Sekimizu, K.; Inoue, M. Discovery of Gramicidin A Analogues with Altered Activities by Multidimensional Screening of a One-Bead-One-Compound Library. *Nat. Commun.* **2020**, *11* (1), 1–10.
- (10) Taylor, S. D.; Palmer, M. The Action Mechanism of Daptomycin. *Bioorganic Med. Chem.* **2016**, *24* (24), 6253–6268.
- (11) Stone, K. J.; Strominger, J. L. Mechanism of Action of Bacitracin: Complexation with Metal Ion and C55-Isoprenyl Pyrophosphate. *Proc. Natl. Acad. Sci.* **1971**, *68* (12), 3223–3227.
- (12) Andrade, F. F.; Silva, D.; Rodrigues, A.; Pina-Vaz, C. Colistin Update on Its Mechanism of Action and Resistance, Present and Future Challenges. *Microorganisms* **2020**, *8* (11), 1–

- 12.
- (13) Ordooei Javan, A.; Shokouhi, S.; Sahraei, Z. A Review on Colistin Nephrotoxicity. *Eur. J. Clin. Pharmacol.* **2015**, *71* (7), 801–810.
- (14) Benson, M. A.; Shin, S. B. Y.; Kirshenbaum, K.; Huang, M. L.; Torres, V. J. A Comparison of Linear and Cyclic Peptoid Oligomers as Potent Antimicrobial Agents. *ChemMedChem* **2012**, *7* (1), 114–122.
- (15) Andreev, K.; Martynowycz, M. W.; Huang, M. L.; Kuzmenko, I.; Bu, W.; Kirshenbaum, K.; Gidalevitz, D. Hydrophobic Interactions Modulate Antimicrobial Peptoid Selectivity towards Anionic Lipid Membranes. *Biochim. Biophys. Acta - Biomembr.* **2018**, *1860* (6), 1414–1423.
- (16) Culkin, D. A.; Jeong, W.; Csihony, S.; Gomez, E. D.; Balsara, N. P.; Hedrick, J. L.; Waymouth, R. M. Zwitterionic Polymerization of Lactide to Cyclic Poly(Lactide) by Using *N*-Heterocyclic Carbene Organocatalysts. *Angew. Chem, Int. Ed.* **2007**, *46* (15), 2627–2630.
- (17) Honda, S.; Yamamoto, T.; Tezuka, Y. Topology-Directed Control on Thermal Stability: Micelles Formed from Linear and Cyclized Amphiphilic Block Copolymers. *J. Am. Chem. Soc.* **2010**, *132* (30), 10251–10253.
- (18) Honda, S.; Yamamoto, T.; Tezuka, Y. Tuneable Enhancement of the Salt and Thermal Stability of Polymeric Micelles by Cyclized Amphiphiles. *Nat. Commun.* **2013**, *4*.
- (19) Hoskins, J. N.; Grayson, S. M. Synthesis and Degradation Behavior of Cyclic Poly(ϵ -Caprolactone). *Macromolecules* **2009**, *42* (17), 6406–6413.
- (20) Haque, F. M.; Grayson, S. M. The Synthesis, Properties and Potential Applications of Cyclic Polymers. *Nat. Chem.* **2020**, *12* (5), 433–444.
- (21) Dove, A. P. Controlled Ring-Opening Polymerisation of Cyclic Esters: Polymer Blocks in Self-Assembled Nanostructures. *Chem. Commun.* **2008**, *48*, 6446.
- (22) Laurent, B. A.; Grayson, S. M. Synthetic Approaches for the Preparation of Cyclic Polymers. *Chem. Soc. Rev.* **2009**, *38* (8), 2202–2213.
- (23) Kricheldorf, H. R. Cyclic Polymers: Synthetic Strategies and Physical Properties. *J. Polym. Sci. Part A Polym. Chem.* **2010**, *48* (2), 251–284.
- (24) Iatrou, H.; Hadjichristidis, N.; Meier, G.; Frielinghaus, H.; Monkenbusch, M. Synthesis and

Chapter 4. *Macrocyclic polypeptoids and their antimicrobial activity*

- Characterization of Model Cyclic Block Copolymers of Styrene and Butadiene. Comparison of the Aggregation Phenomena in Selective Solvents with Linear Diblock and Triblock Analogues. *Macromolecules* **2002**, 35 (14), 5426–5437.
- (25) Schappacher, M.; Deffieux, A. α -Acetal- ω -Bis(Hydroxymethyl) Heterodifunctional Polystyrene: Synthesis, Characterization, and Investigation of Intramolecular End-to-End Ring Closure. *Macromolecules* **2001**, 34 (17), 5827–5832.
- (26) Schappacher, M.; Deffieux, A. Synthesis, Characterization, and Intramolecular End-to-End Ring Closure of α -Isopropylidene-1,1-Dihydroxymethyl- ω -Diethylacetal Polystyrene-Block-Polyisoprene Block Copolymers. *Macromol. Chem. Phys.* **2002**, 203 (17), 2463–2469.
- (27) Bielawski, C. W.; Benitez, D.; Grubbs, R. H. An “Endless” Route to Cyclic Polymers. *Science* **2002**, 297 (5589), 2041–2044.
- (28) Adachi, K.; Tezuka, Y. Topological Polymer Chemistry: Designing Unusual Macromolecular Architectures. *Kobunshi Ronbunshu* **2007**, 64 (11), 709–715.
- (29) Schappacher, M.; Deffieux, A. Synthesis of Macrocyclic Poly(2-Chloroethyl Vinyl Ether)S. *Macromol. Rapid Commun.* **1991**, 12, 447–453.
- (30) Laurent, B. A.; Grayson, S. M. An Efficient Route to Well-Defined Macrocyclic Polymers via “Click” Cyclization. *J. Am. Chem. Soc.* **2006**, 128 (13), 4238–4239.
- (31) Jeong, W.; Hedrick, J. L.; Waymouth, R. M. Organic Spirocyclic Initiators for the Ring-Expansion Polymerization of β -Lactones. *J. Am. Chem. Soc.* **2007**, 129 (27), 8414–8415.
- (32) Zhang, Y.; Liu, R.; Jin, H.; Song, W.; Augustine, R.; Kim, I. Straightforward Access to Linear and Cyclic Polypeptides. *Commun. Chem.* **2018**, 1 (1), 1–7.
- (33) Guo, L.; Zhang, D. Cyclic Poly(α -Peptoid)s and Their Block Copolymers from *N*-Heterocyclic Carbene-Mediated Ring-Opening Polymerizations of *N*-Substituted *N*-Carboxyanhydrides. *J. Am. Chem. Soc.* **2009**, 131 (50), 18072–18074.
- (34) Guo, L.; Lahasky, S. H.; Ghale, K.; Zhang, D. *N*-Heterocyclic Carbene-Mediated Zwitterionic Polymerization of *N*-Substituted *N*-Carboxyanhydrides toward Poly(α -Peptoid)s: Kinetic, Mechanism, and Architectural Control. *J. Am. Chem. Soc.* **2012**, 134 (22), 9163–9171.
- (35) Lee, C. U.; Smart, T. P.; Guo, L.; Epps, T. H.; Zhang, D. Synthesis and Characterization of

Chapter 4. *Macrocyclic polypeptoids and their antimicrobial activity*

- Amphiphilic Cyclic Diblock Copolypeptoids from *N*-Heterocyclic Carbene-Mediated Zwitterionic Polymerization of *N*-Substituted *N*-Carboxyanhydride. *Macromolecules* **2011**, *44* (24), 9574–9585.
- (36) Wu, Y.; Zhang, D.; Ma, P.; Zhou, R.; Hua, L.; Liu, R. Lithium Hexamethyldisilazide Initiated Superfast Ring Opening Polymerization of *Alpha*-Amino Acid *N*-Carboxyanhydrides. *Nat. Commun.* **2018**, *9* (1), 5297.
- (37) Boyd, G. V.; Wright, P. H.; Boyd, G. V.; Wright, P. H. Unstable Mesoionic Oxazolium-5-Oxides. *J. Chem. Society Perkin I* **1972**, No. 914, 914-918.
- (38) Gingrich, H. L.; Baum, J. S. Mesoionic Oxazoles. *Chemistry of Heterocyclic Compounds*. January 2, 1986, pp 731–961.
- (39) Aresta, M.; Dibenedetto, A.; Quaranta, E. Reaction of Alkali-Metal Tetraphenylborates with Amines in the Presence Of. *J. Chem. Society Dalt. Trans* **1995**, 3359–3363.
- (40) Discovery Studio; V17.2.0.16349; BIOVIA. Discovery Studio. Dassault Systèmes: San Diego 2016.
- (41) Sui, Q.; Borchardt, D.; Rabenstein, D. L. Kinetics and Equilibria of *Cis/Trans* Isomerization of Backbone Amide Bonds in Peptoids. *J. Am. Chem. Soc.* **2007**, *129* (39), 12042–12048.
- (42) Alberty, K. A.; Hogen-Esch, T. E.; Carlotti, S. Synthesis and Characterization of Macrocyclic Vinyl-Aromatic Polymers. *Macromol. Chem. Phys.* **2005**, *206* (10), 1035–1042.
- (43) Lutz, P.; McKenna, G.; Rempp, P.; Strazielle, C. Solution Properties of Ring-shaped Polystyrenes. *Die Makromol. Chemie, Rapid Commun.* **1986**, *7* (9), 599–605.
- (44) Guo, L.; Li, J.; Brown, Z.; Ghale, K.; Zhang, D. Synthesis and Characterization of Cyclic and Linear Helical Poly(α -Peptoid)s by *N*-Heterocyclic Carbene-Mediated Ring-Opening Polymerizations of *N*-Substituted *N*-Carboxyanhydrides. *Pept. Sci.* **2011**, *96* (5), 596–603.
- (45) Li, A.; Lu, L.; Li, X.; He, L. L.; Do, C.; Garno, J. C.; Zhang, D. Amidine-Mediated Zwitterionic Ring-Opening Polymerization of *N*-Alkyl *N*-Carboxyanhydride: Mechanism, Kinetics, and Architecture Elucidation. *Macromolecules* **2016**, *49* (4), 1163–1171.
- (46) Lahasky, S. H.; Serem, W. K.; Guo, L.; Garno, J. C.; Zhang, D. Synthesis and Characterization of Cyclic Brush-Like Polymers by *N*-Heterocyclic Carbene-Mediated Zwitterionic Polymerization of *N*-Propargyl *N*-Carboxyanhydride and the Grafting-to

Chapter 4. *Macrocyclic polypeptoids and their antimicrobial activity*

- Approach. *Macromolecules* **2011**, *44*, 9063–9074.
- (47) Lee, C.-U.; Li, A.; Ghale, K.; Zhang, D. Crystallization and Melting Behaviors of Cyclic and Linear Polypeptoids with Alkyl Side Chains. *Macromolecules* **2013**, *46* (20), 8213–8223.
- (48) Hemu, X.; Qiu, Y.; Nguyen, G. K. T.; Tam, J. P. Total Synthesis of Circular Bacteriocins by Butelase 1. *J. Am. Chem. Soc.* **2016**, *138* (22), 6968–6971.
- (49) Salas-Ambrosio, P.; Tronnet, A.; Verhaeghe, P.; Bonduelle, C. Synthetic Polypeptide Polymers as Simplified Analogues of Antimicrobial Peptides. *Biomacromolecules* **2021**, *22* (1), 57–75.
- (50) Lahasky, S. H.; Hu, X.; Zhang, D. Thermoresponsive Poly(α -Peptoid)s: Tuning the Cloud Point Temperatures by Composition and Architecture. *ACS Macro Lett.* **2012**, *1* (5), 580–584.
- (51) Miller, S. M.; Simon, R. J.; Ng, S.; Zuckermann, R. N.; Kerr, J. M. Comparison of the Proteolytic Susceptibilities of Homologous *L*-Amino Acid, *D*-Amino Acid and *N*-Substituted Glycine Peptide and Peptoid Oligomers. *Drug Dev. Res.* **1995**, *32*, 20–32.
- (52) Liu, R.; Suárez, J. M.; Weisblum, B.; Gellman, S. H.; McBride, S. M. Synthetic Polymers Active against *Clostridium difficile* Vegetative Cell Growth and Spore Outgrowth. *J. Am. Chem. Soc.* **2014**, *136* (41), 14498–14504.
- (53) Centers for Disease Control and Prevention (CDC). Antibiotic Resistance Threats in the United States. Antibiotic resistance threats in the United States <https://www.cdc.gov/drugresistance/biggest-threats.html> (accessed May 15, 2020).
- (54) Zhao, Y.; Truhlar, D. G. The M06 Suite of Density Functionals for Main Group Thermochemistry, Thermochemical Kinetics, Noncovalent Interactions, Excited States, and Transition Elements: Two New Functionals and Systematic Testing of Four M06-Class Functionals and 12 Other Function. *Theor. Chem. Acc.* **2008**, *120* (1–3), 215–241.
- (55) Gaussian 09, Revision D.01, M. J. Frisch, G. W. Trucks, H. B. Schlegel, G. E. Scuseria, M. A. Robb, J. R. Cheeseman, G. Scalmani, V. Barone, B. Mennucci, G. A. Petersson, H. Nakatsuji, M. Caricato, X. Li, H. P. Hratchian, A. F. Izmaylov, J. Bloino, G. Z. No Title. Wallingford CT 2013.
- (56) Cossi, M.; Barone, V.; Cammi, R.; Tomasi, J. Ab Initio Study of Solvated Molecules: A New Implementation of the Polarizable Continuum Model. *Chem. Phys. Lett.* **1996**, *255* (4), 327–

335.

- (57) Grimme, S.; Antony, J.; Ehrlich, S.; Krieg, H. A Consistent and Accurate Ab Initio Parametrization of Density Functional Dispersion Correction (DFT-D) for the 94 Elements H-Pu. *J. Chem. Phys.* **2010**, *132* (15), 154104.
- (58) Bangham, A. D.; Standish, M. M.; Watkins, J. C. Diffusion of Univalent Ions across the Lamellae of Swollen Phospholipids. *J. Mol. Biol.* **1965**, *13* (1), 238–252.
- (59) Jimah, J.; Schlesinger, P.; Tolia, N. Liposome Disruption Assay to Examine Lytic Properties of Biomolecules. *BIO-PROTOCOL* **2017**, *7* (15), 100–106.

Chapter 5. Macromolecular engineering of antimicrobial polypeptoids: star and drug-conjugate polymers

Synthetic polymers are certainly the best candidates to overcome the limitations posed by the production and use of AMPs.¹ In this direction, access to large amounts of material is an important asset of using polymer chemistry. Like AMPs, polymers are macromolecules, but unlike AMPs, they are polydisperse in size and constituted of monomer units whose sequence is not controlled. A very interesting point is that polymerization reaction paves the way to various topologies (cyclic, branched, conjugates, etc.) that would be difficult to implement using other preparation methods.

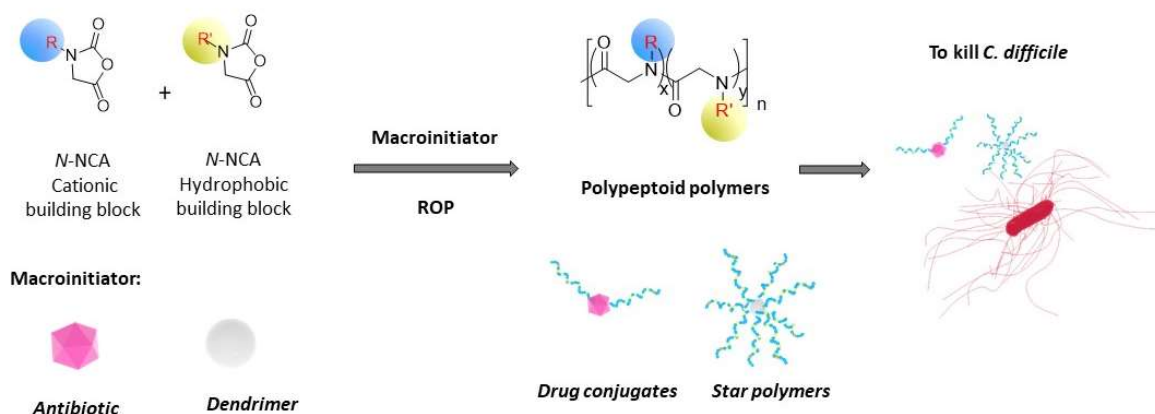
For instance, star-like polypeptides have shown impressive antimicrobial activities.² Star polymers are macromolecules with elongated polymeric arms using a core constituted of more than 3 arms³ and they are known to have the lowest entanglement as compared to cyclic and linear polymers.⁴ Previous studies revealed that star-like polymers greatly enhanced antimicrobial property as compared to linear polymers, meanwhile they decreased cell toxicity.^{2,5-7}

On another hand, macromolecular engineering is a unique tool to generate drug-polymer conjugates to protect the drug from the environment (i.e. enzymatic activity), to provide a controlled drug release and to reduce the side effects derived from a rapid release of the drug *in vivo*.⁸⁻¹⁰ In infectiology, a representative example of such drug-polymer conjugate is a copolymer based on penicillin V which demonstrated very low toxicity over human gingival fibroblasts, and an increase in bacterial inhibition growth even after salivary enzymatic exposure.¹¹

This overall Ph.D. research project aimed at developing polypeptoid polymers as analogs of AMPs with low protease susceptibility. In this chapter 5, the goal was to extend the use of polypeptoids to new macromolecular architectures: star-like polypeptoids and drug-polypeptoids conjugates. Following the SAR approach developed in chapter 3 on *C. difficile*, we based our design on copolypeptoids merging cationic (Lys-NNCA) and hydrophobic (Phe-NNCA) monomers using different macroinitiators (poly(amidoamine) (PAMAM) dendrimers, antibiotics such as vancomycin, amphotericin, nystatin, and sulfamethoxazole). The goal of this study was to evaluate if the use of macromolecular engineering enhanced the antimicrobial properties of

Chapter 5. Macromolecular engineering of antimicrobial polypeptoids: star and drug-conjugate polymers

polypeptoid polymers towards various bacteria including *C. difficile* (Scheme 47).



Scheme 47. Strategy to design star-like and drug-conjugates polypeptoids to kill *C. difficile*.

1 Star-like polypeptoids as antimicrobial agents

Star polymers are macromolecules consisting of a dendritic core from which at least three polymeric arms grow,³ and they are known to have the lowest entanglement as compared to cyclic and linear polymers.⁴ Due to low mobility, star polymers can increase the half-life time in blood circulation in comparison to linear polymers as it was demonstrated by E. Gilles *et al.* with branched poly(ethyleneoxide)s.¹² In infectiology, early studies involving branched copolymers constituted of methylmethacrylate and dimethylaminoethylmethacrylate demonstrated strong inhibition growth of *E. coli* and *S. aureus* in diffusion agar plates.¹³ Since then, similar works were developed to apply this property in the design of antimicrobial and antifouling surfaces.^{13–16}

A key work reported in 2016 by G. Qiao *et al.* was presenting the use of star-like polypeptides to kill multidrug-resistance bacteria (MIC = 1.7–7.0 $\mu\text{g}/\text{mL}$) with good stability *in vitro* and *in vivo*.² These star-like polypeptides were composed of several polymeric arms, containing lysine and valine, that have been grafted from poly(amidoamine)-dendrimers by ring-opening polymerization. The number of arms was either 16 or 32, keeping the ratio of lysine over valine ~2:1 with a polymerization degree DP = 30. Those star-shaped polypeptides were active in killing

Chapter 5. Macromolecular engineering of antimicrobial polypeptoids: star and drug-conjugate polymers

Gram-negative and Gram-positive bacteria including multidrug-resistant *P. aeruginosa* and *A. baumannii*. The copolymers presented enhanced selectivity (SI = 52 to 71) by comparing cytotoxicity with human embryonic cells (HEK293T) and rat hepatoma cells (H4IIE). The structure-activity relationship was investigated later by the same authors: they varied arm numbers (4-16) and arm length (5-30).⁶ They revealed that increasing arm number (16) and length (30) enhanced the antimicrobial activity (*E. coli* MIC = 4.4 $\mu\text{g/mL}$). However, this increase was associated with an increase in cytotoxicity. Another example of star-like polypeptides was recently published by I. Kim *et al.*: these authors prepared copolymers made of TFA-lysine and Cbz-glutamate monomer units by grafting from tris-(2-aminoethyl)amine initiators using ring-opening polymerization. Copolymers with 3 arms, having a polymerization degree of 30 and 20% of hydrophobic content were showing very good activity against *E. coli* and *B. subtilis* (MIC = 2-4 $\mu\text{g/mL}$) meanwhile keeping low hemolytic effects (HC₅₀ = 4000 $\mu\text{g/mL}$).¹⁷ Even more recently, J. Cai *et al.* reported the preparation of a star polymer with 8 arms constituted of mixed cationic side chains (lysine, ornithine, and diaminoheptylic acid) attached to polyethyleneimine dendrimers.⁷ The best properties were found with ornithine at M/I = 20 with improved activity against Gram-positive methicillin-resistant *S. aureus* and *S. epidermidis*, and *P. aeruginosa* (MIC = 9-15 $\mu\text{g/mL}$) and a very low hemolytic effect (HC₅₀ > 5000 $\mu\text{g/mL}$).

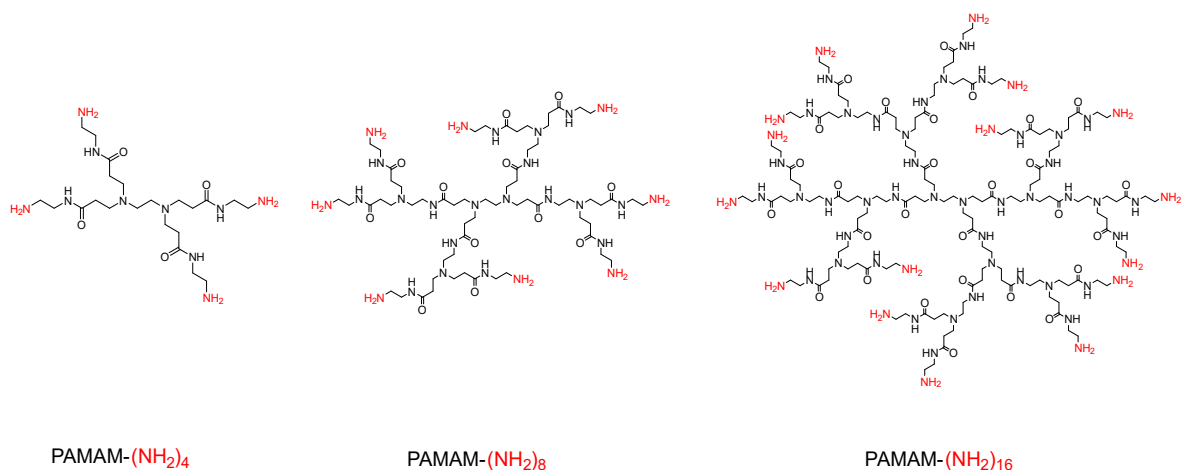
Overall, these recent examples revealed how star-like polypeptide enhanced antimicrobial efficacy: the chemical nature of the cationic side chain should be carefully designed,⁷ as well as the hydrophobic content,¹⁷ the number of arms and the polymerization degree.⁶ So far, no one has extended the use of this macromolecular engineering to star-like polypeptoids to design antibacterial scaffolds. This Ph.D. work is a pioneering study in this direction: we achieved this design and we evaluated the antimicrobial activity over various Gram-positive and Gram-negative bacteria, including *C. difficile*.

1.1 Preparation of star-like polypeptoids.

Several methodologies already enabled star-like polymers such as atom transfer radical polymerization (ATRP), reversible addition-fragmentation chain-transfer (RAFT) polymerization, living anionic polymerization, ring-opening metathesis polymerization and ring-opening polymerization (ROP).³ Usually, a dendritic core with “n” functional groups is used to promote polymerization growth.³ For instance, star-like polypeptides (from NCAs by ROP²) were successfully developed with PAMAM dendrimers that are displaying primary amines as terminal end groups. With NNCA, an early study already reported the preparation of polysarcosine from

Chapter 5. Macromolecular engineering of antimicrobial polypeptoids: star and drug-conjugate polymers

poly(trimethyleneimine) dendrimers with 64 primary amine groups.¹⁸ Here, we decided to employ PAMAM dendrimers macroinitiators to perform copolymerization of two other NNCA monomers (**Scheme 48**).

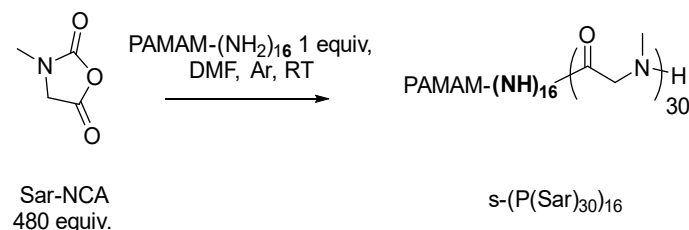


Scheme 48. PAMAM dendrimers used as macroinitiators to perform the ROP of NNCA in this thesis work.

In a first step, we optimized the ROP from PAMAM-(NH₂)₁₆ with Sar-NCA (as a model NNCA) targeting a DP = 30 (for each -NH₂ terminal group). According to already published procedures, we set up three different methodologies:

- Direct addition of initiator:* we prepared a Sar-NCA (480 equiv.) solution 0.4 M in anhydrous DMF and we added an aliquot of PAMAM-(NH₂)₁₆ (1 equiv., solution in DMF at 0.01 M).
- Direct addition of monomer:*² we prepared a solution of Sar-NCA (480 equiv.) that we added to a solution with PAMAM-(NH₂)₁₆ (1 equiv.) targeting a final concentration of 0.37 M in DMF (the volume ratio of DMF was 16:1 for monomer:initiator)
- Reduced concentration:* we prepared a solution of Sar-NCA (480 equiv.) that we added to a solution with PAMAM-(NH₂)₁₆ (1 equiv.) targeting a final concentration of 0.1 M in DMF (the volume ratio of DMF was 1:1 for monomer:initiator)

Chapter 5. Macromolecular engineering of antimicrobial polypeptoids: star and drug-conjugate polymers



Scheme 49. Synthesis of star-like poly(sarcosine) **66**.

The polymerizations were followed by FTIR monitoring the NNCA peak at 1850 cm⁻¹. Upon full conversion the s-(P(sar)₃₀)₁₆ were precipitated in Et₂O, dried under vacuum in good yields 78-87%. Then, we characterized the copolymers obtained from each method by SEC and ¹H-NMR (**Table 52** and **Figure 68**). From the SEC analyses in DMF, we characterized copolymers with numbered-molar masses (*M_n*) similar to the theoretical values (*M*/*I* theoretical, **Table 52**). Careful considerations of the MW values, and of dispersity made us concluded that the best methodology was the “method C” providing the lowest dispersity ($\mathcal{D}_M = 1.11$) and also, the highest yield (87%), polymer **66**.

Table 52. Comparison of SEC characterizations and yields obtained by analyzing s-(P(sar)₃₀)₁₆ from three methodologies studied.

	M/I theoretical	MW theo (g/mol)	<i>M_n</i> (g/mol) ^a	<i>M_w</i> (g/mol) ^a	\mathcal{D}_M	Yield (%)
Method A	30	37000	46900	52900	1.13	86
Method B	30	37000	36800	41200	1.12	78
Method C	30	37000	35000	39000	1.11	87

^a SEC performed in DMF. ^b Calculated from the ¹H-NMR spectrum in DMSO-d₆

We then characterized the s-(P(sar)₃₀)₁₆ by ¹H-NMR in DMSO-d₆ (**Figure 68**). We observed the characteristic peaks corresponding to poly(sarcosine) signals *a* and *b* (3.80-4.42 and 2.50-3.10 ppm) but we were not able to determine the DP_{NMR} because 1) the signals of the dendrimer initiator were overlapped by the signals of poly(sarcosine)¹⁹ and 2) the signals of the dendrimer initiator were very low due to the low proportion of the PAMAM protons as compared to the protons belonging to the copolymer arms (1:480). Despite this, SEC and NMR analyses provided clear evidence that we prepared successfully star-like polypeptoids in quantitative yields.

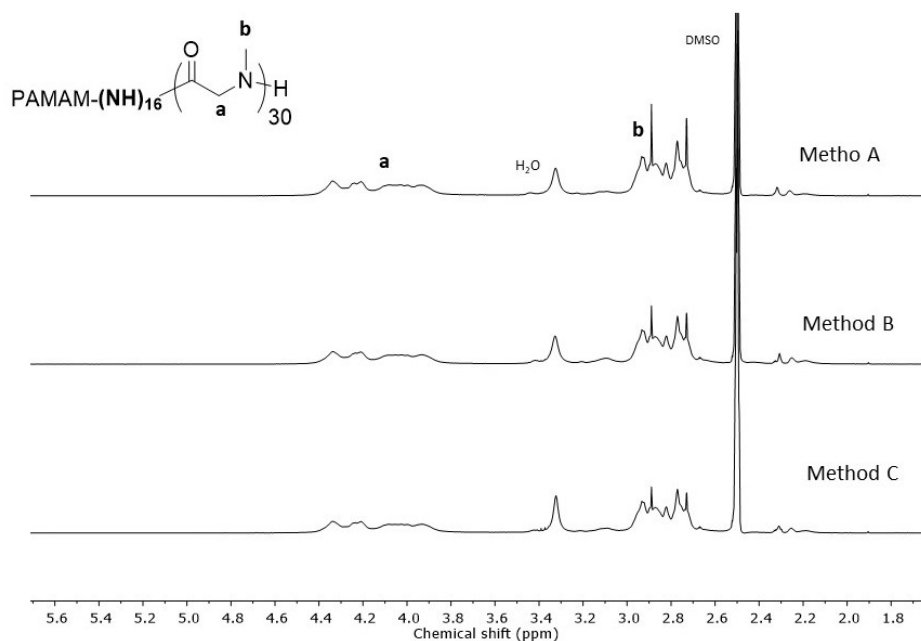


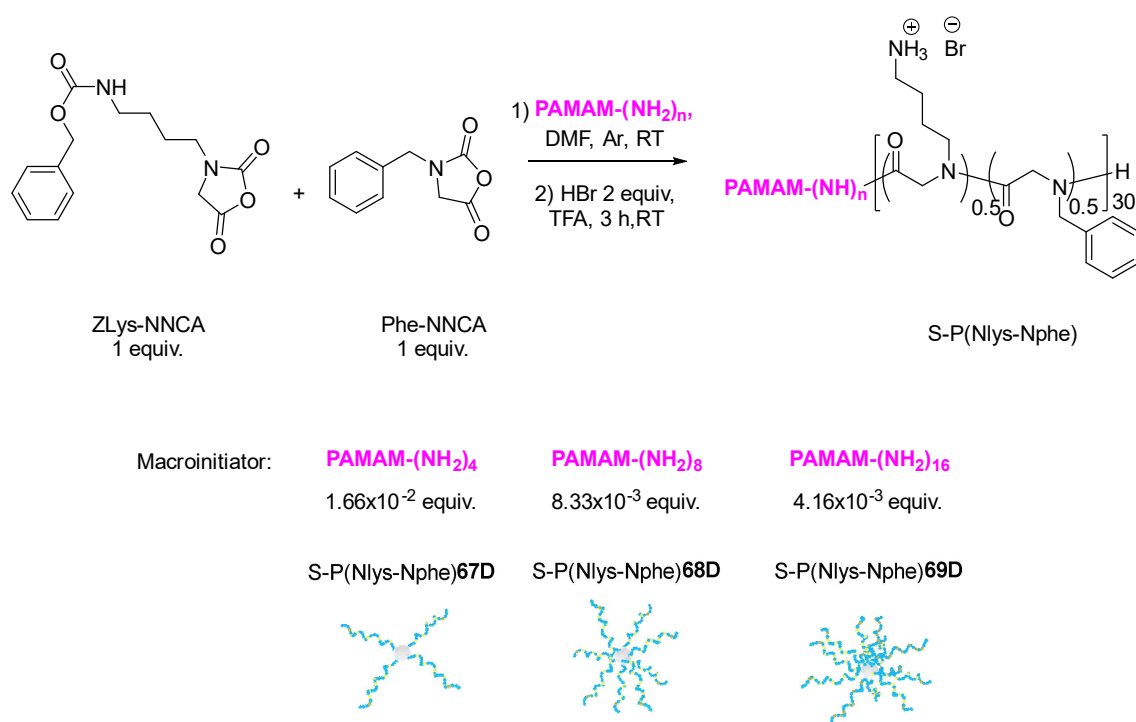
Figure 68. Comparison of the $^1\text{H-NMR}$ spectra of $s\text{-}(P(\text{sar})_{30})_{16}$ upon the three methodologies studied.

1.2 Star-like copolymers varying the arms number

To access antibacterial copolymers means preparing star-like polymers incorporating of cationic and hydrophobic side chains. Using the methodology established in section 1.1, we challenged the ROP of copolymers based on ZLys- and Phe-NNCAs using PAMAM dendrimers initiators. We performed the ROP from PAMAM having a different number of arms (PAMAM with 4, 8, 16 -NH_2 terminal groups) at $M/I = 30$ and 50% of hydrophobic content in DMF and under argon atmosphere (0.1 M at RT, step 1, **Scheme 50**).

We monitored the NNCA disappearance of the NCOO signal at 1850 cm^{-1} by FTIR until ROP completion (20 days). Then we isolated the star-protected copolymers S-P(ZNlys-Nphe)**67-69** by precipitation, dried under high vacuum in 40-45% yields and characterized them by SEC in DMF analyses (**Table 53** and **Figure 70**). We observed a 2-fold lower molar mass for the different star copolymers synthesized (**Table 53**). This result was not surprising because in the literature star polymers are known to elute at lower volume as compared to their linear counterparts, this elution behavior due to a difference on the hydrodynamic radius.²⁰

Chapter 5. Macromolecular engineering of antimicrobial polypeptoids: star and drug-conjugate polymers



Scheme 50. Synthesis of star-P(Nlys-Nphe) varying the number of arms: **67D**, a star-like polypeptoid with 4 arms; **68D**, a star-like polypeptoid with 8 arms and **69D**, a star-like polypeptoid with 16 arms.

Table 53. Star-P(ZNlys-Nphe) copolymers characterization: molar masses from SEC, hydrophobic content from ¹H-NMR and yields.

	Arms	M/I	Hydrophobic content theoretical (%)	MW theo (g/mol)	M _n (g/mol) ^a	M _w (g/mol)	Đ _M	Hydrophobic content (%) ^b	Yield (%)
S-P(ZNlys-Nphe)67	4	30	50	2.78x10 ⁴	1.20x10 ⁴	1.42x10 ⁴	1.18	49	45
S-P(ZNlys-Nphe)68	8	30	50	5.24x10 ⁴	1.75x10 ⁴	2.38x10 ⁴	1.36	51	43
S-P(ZNlys-Nphe)69	16	30	50	1.02x10 ⁵	3.59x10 ⁴	5.05x10 ⁴	1.40	52	40

^a SEC performed in DMF. ^b Calculated from the ¹H-NMR spectrum in DMSO-d₆.

The decrease in hydrodynamic radius was better evidenced by plotting the double logarithm of mean square radius (RMS radius) versus molar masses (MW) between linear and star-like polymers (**Figure 69**).²¹ Indeed, using the signal monitored by the MALS detector during the SEC analysis in DMF, we obtained the double logarithm plot 1) of a linear copolymer P(ZNlys-Nphe) initiated with allylamine at M/I = 30 and 2) of the star-like copolypeptoid S-P(ZNlys-Nphe)67

(Figure 69). The difference in slope values, in the case of the star-like copolymer, was in agreement with the difference expected for branched polymers (values of slope < 0.5).²² This result clearly demonstrated that we prepared star-like copolymers.

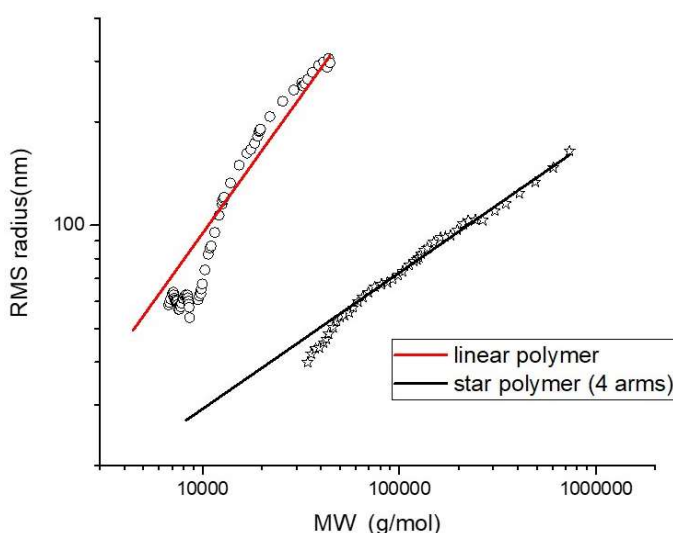


Figure 69. Double logarithm plot of the root means square radius plot versus molar masses of a linear copolypeptoid (*P*(ZNLys-Nphe)**42** with a *M*/*I* = 30 and the star-like polymer bearing 4 arms of *P*(ZNLys-Nphe)**67** *M*/*I* = 30. The slope for linear polymer was 0.8 ± 0.04 and for star polymer slope 0.4 ± 0.04 .

On another hand, we also observed a polymer dispersity that increased with the number of arms ($\mathcal{D}_M = 1.18$ for 4 arms and up to 1.40 for 16 arms), a characterization already reported with star-like polypeptides⁶ that we related to a more steric hindered structure.

Then, we characterized the copolymers by ¹H-NMR in DMSO-*d*₆ (Figure 70). We found signals attributable to the polymer backbone (CH₂, peak *a, a'*), signals attributable to the ZNLys moiety (peaks *b-h*) and signals attributable to Nphe moiety (peaks *i, j*). Using the integrations of those signals, we calculated a hydrophobic content in agreement with the stoichiometric ratio of the NNCA monomer involved in the copolymerization (Table 53). On another hand, we could not determine the DP_{NMR} due to the high monomer/initiator ratio (120:1 for PAMAM with 4 arms and even higher for PAMAM with 16 arms) and due to the PAMAM signals overlapped with the copolymer (peaks *b, e, a, a'*).

Chapter 5. Macromolecular engineering of antimicrobial polypeptoids: star and drug-conjugate polymers

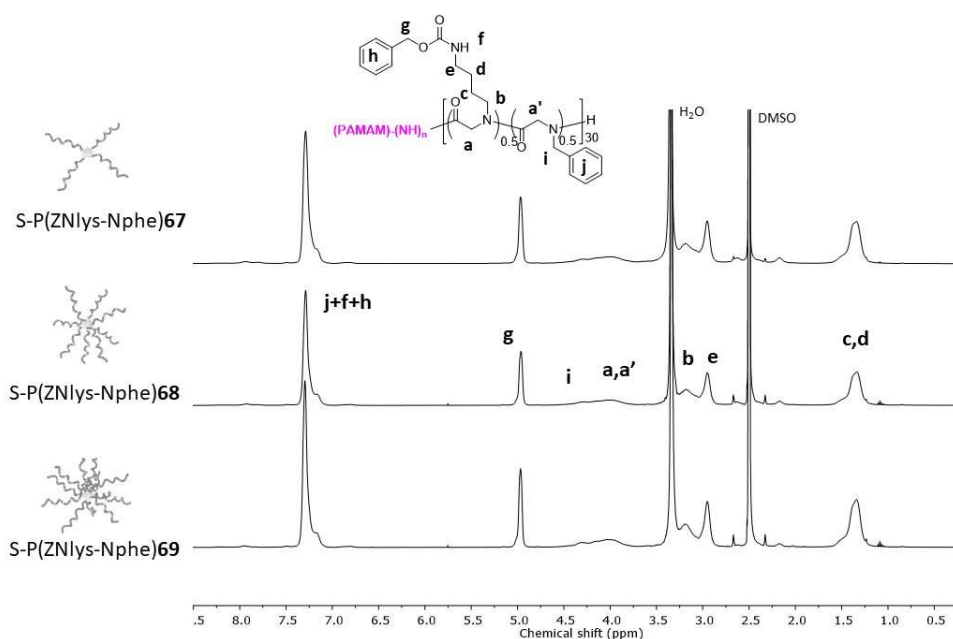


Figure 70. $^1\text{H-NMR}$ spectra in $\text{DMSO-}d_6$ of star- $[P(\text{ZNlys-Nphe})]$ having different number of arms: **67**, a star-like polypeptoid with 4 arms; **68**, a star-like polypeptoid with 8 arms and **69**, a star-like polypeptoid with 16 arms.

Then, we performed deprotection to the Z-Lys side chains using the procedure optimized for P(Nlys) in chapter 3 (section 2.1): the star-like copolymers were deprotected in TFA by adding 2 equivalents of HBr (relative to cationic side chains in TFA, RT). After 3 h, the copolymers (S-P(Nlys-Nphe)**67D-69D**) were isolated by precipitation in diethyl ether, dialyzed (MWCO = 10 kDa), and lyophilized (yields 21-62%, **Table 54**).

Table 54. Star- $[P(\text{Nlys-Nphe})]$ copolymers: hydrophobic content from $^1\text{H-NMR}$ and yields.

	Arms	M/I	Hydrophobic content theoretical (%)	Hydrophobic content (%) ^a	Yield (%)
S-P(Nlys-Nphe)67D	4	30	50	52	21
S-P(Nlys-Nphe)68D	8	30	50	55	41
S-P(Nlys-Nphe)69D	16	30	50	53	62

^a Calculated from the $^1\text{H-NMR}$ spectrum in D_2O

To determine the DP_{NMR} and the chemical composition in monomer units, we analyzed the samples by $^1\text{H-NMR}$ in D_2O (**Figure 71**). We found signals attributable to the polymer backbone (CH_2 , peak *a,a'*), signals attributable to the ZNlys moiety (peaks *b-e*) and signals attributable to Nphe moiety (peaks *i,j*). We calculated the hydrophobic content by carefully comparing the inte-

Chapter 5. Macromolecular engineering of antimicrobial polypeptoids: star and drug-conjugate polymers

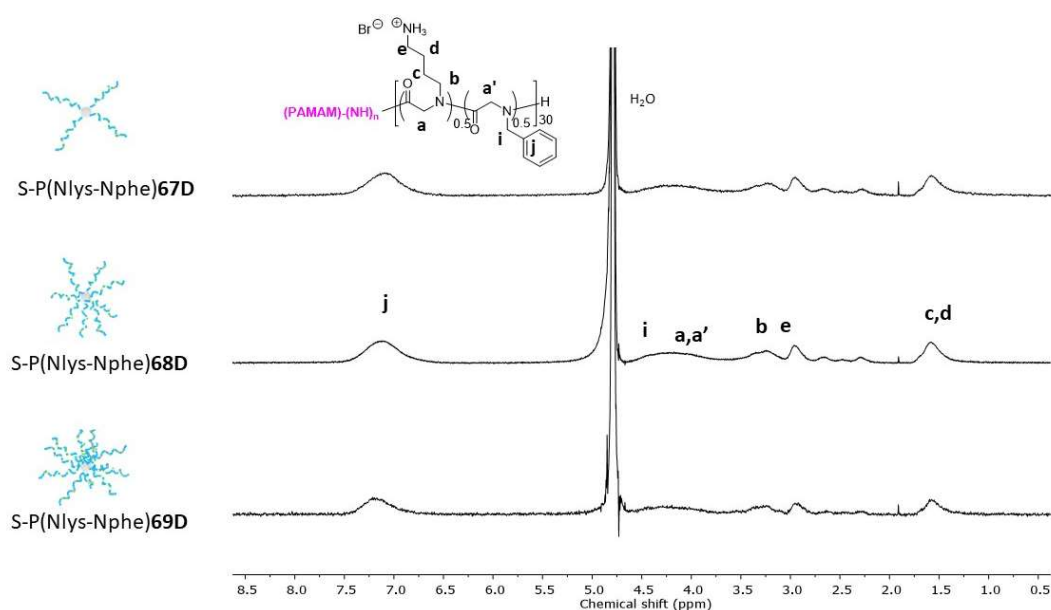


Figure 71. $^1\text{H-NMR}$ spectra in D_2O and upon deprotection of star- $[P(\text{Nlys-Nphe})]$ having different number of arms: **67D**, a star-like polypeptoid with 4 arms; **68D**, a star-like polypeptoid with 8 arms and **69D**, a star-like polypeptoid with 16 arms.

gration of Nlys (peaks *c, d*) and NPhe (peak *j*). Interestingly, we obtained hydrophobic content (52–55%) in agreement with the ones characterized before deprotection, confirming that the deprotection step did not modify the chemical composition. Finally, we could not determine the DP_{NMR} due to the high monomer/initiator ratio (120:1 for PAMAM with 4 arms and even higher for PAMAM with 16 arms) and due to the PAMAM signals overlapped with the copolymer (peaks *b, e, a, a'*).

This first series of copolymers were further studied in biology to evaluate their antimicrobial activity against *C. difficile* and a variety of representative pathogens: Gram-positive (*S. aureus*, *E. faecalis*, *L. monocytogenes* and *S. pneumoniae*) and Gram-negative bacteria (*E. coli*, *P. aeruginosa*, *A. baumannii*), including anaerobic bacteria (*B. fragilis* and *H. pylori*). The results are presented in **Table 55** and were compared to the linear polymer: we determined the MIC from the microdilution method bacteria (see the experimental section, approximately 10^5 CFU/mL) for 24–48 h with increasing concentrations of polypeptoids.

First, we observed that only the linear polypeptoid presented activity against *C. difficile* while all the star-like polypeptoids presented activity higher than $15.6 \mu\text{g/mL}$, this result was unfortunate since we expected to enhance the activity. Due to this result we also investigated the anti-infective

Chapter 5. Macromolecular engineering of antimicrobial polypeptoids: star and drug-conjugate polymers

activity in other microorganism and, we observed that the linear copolypeptoid presented MIC values above 62 µg/mL for the Gram-positive and negative bacteria tested, except for *L. monocytogenes*, *A. baumannii* and *B. fragilis* with MIC = 15.6 and 31.25 µg/mL. Then, we observed that star copolymers exhibited a relatively higher antimicrobial activity (Table 55). First, S-P(Nlys-Nphe)67D was active against the different Gram-positive and Gram-negative bacteria tested: the MIC was found below 62.5 µg/mL except for *S. pneumoniae* (MIC = 250 µg/mL, Table 55). which was not sensitive to this compound. The best antimicrobial activity was obtained against the anaerobic Gram-negative *B. fragilis* with a MIC in the range 7.8-15.6 µg/mL followed by the Gram-positive *L. monocytogenes* with a MIC in the range 15.6-31.25 µg/mL. Thus, with an enhanced antimicrobial activity fro *B. fragilis* but also a broader activity as compared to the linear 42D.

Table 55. Antimicrobial activity: the linear polypeptoid (42D) was compared to star-like copolymers (67D-69D) in assays involving Gram-positive and Gram-negative pathogens.

	Gram	Polypeptoid 42D		S-P(Nlys-Nphe)67D		S-P(Nlys-Nphe)68D		S-P(Nlys-Nphe)69D	
		MIC (µg/mL)	¹ MIC (10 ⁻⁶ M)	MIC (µg/mL)	² MIC (10 ⁻⁶ M)	MIC (µg/mL)	³ MIC (10 ⁻⁶ M)	MIC (µg/mL)	⁴ MIC (10 ⁻⁶ M)
<i>C. difficile</i>	+ (anaerobic)	15.6	2.5	62.5	6.1	250	17	>250	>8.2
<i>S. aureus</i> CIP 4.83	+	62.5	10	31.25-62.5	3.1-6.1	125	8.3	125	4.1
<i>S. aureus</i> ATCC33591	+	62.5	10	31.25	3.1	31.25	2.1	62.5	2
<i>E. faecalis</i> CIP 103015T	+	125	20	31,25 – 62,5	3.1-6.1	31.25-62.5	2.1-4.2	250	8.2
<i>L. monocytogenes</i> CIP 82110T	+	15.6	2.5	15.6-31.25	1.5-3.1	15.6-31.25	1.0-2.1	31.25	1
<i>S. pneumoniae</i> CIP 104471	+	250	40	250	25	250	17	250	8.2
<i>E. coli</i> CIP 53.126	-	62.5	10	62.5	6.1	125	8.3	125	4.1
<i>P. aeruginosa</i> CIP 82.118	-	62.5	10	31,25 – 62,5	3.1-6.1	62.5	4.2	62.5-125	2
<i>A. baumannii</i> CIP 70.34T	-	31.25	5	31.25	3.1	62.5	4.2	250	8.2
<i>B. fragilis</i> CIP 77.16	- (anaerobic)	15.6	2.5	7.8-15.6	0.76-1.5	7.8	0.52	31.25	1

¹ Calculated using MW = 6200 g/mol. ² Calculated using MW = 10200 g/mol. ³ Calculated using MW = 15000 g/mol. ⁴ Calculated using MW = 30500 g/mol. Values calculated from SEC in DMF.

Second, S-P(Nlys-Nphe)68D was comparatively less active against the different Gram-positive and Gram-negative bacteria tested with MIC values below 250 µg/mL (Table 55). However, we observed that copolymer 68D presented the same activity against *L.*

Chapter 5. Macromolecular engineering of antimicrobial polypeptoids: star and drug-conjugate polymers

monocytogenes (MIC in the range 15.6-31.25 µg/mL) with an enhancement of anti-*B. fragilis* activity (MIC = 7.8 µg/mL) as compared with **67D**.

Finally, S-P(Nlys-Nphe)**69D** was very similar to the 8 arms star-like polypeptoids: the copolymer was active against the different Gram-positive and Gram-negative bacteria tested with MIC values below 250 µg/mL (**Table 55**). The copolymer **69D** presented in general a preference for Gram-positive bacteria (MIC < 62.5 µg/mL) with more important antimicrobial efficacy against *L. monocytogenes* and *S. aureus*. Moreover, we observed that **69D** lost anti-*B. fragilis* activity reflected in 4 fold increase of the inhibitory concentration (MIC = 31.25 µg/mL) value as compared to the star-polymer with 8 arms.

Through these studies, we established that star-like polypeptoids can enhance the antibacterial properties with a broader spectrum of action as compared to the linear copolymer (with MIC < 62.5 µg/mL). Moreover, the number of arms was an important parameter to kill the anaerobic Gram-negative *B. fragilis* with the best value of MIC in a star copolymer with 8 arms and to kill effectively the Gram-positive *L. monocytogenes* having the best activity when the star-like polypeptoids had 16 arms.

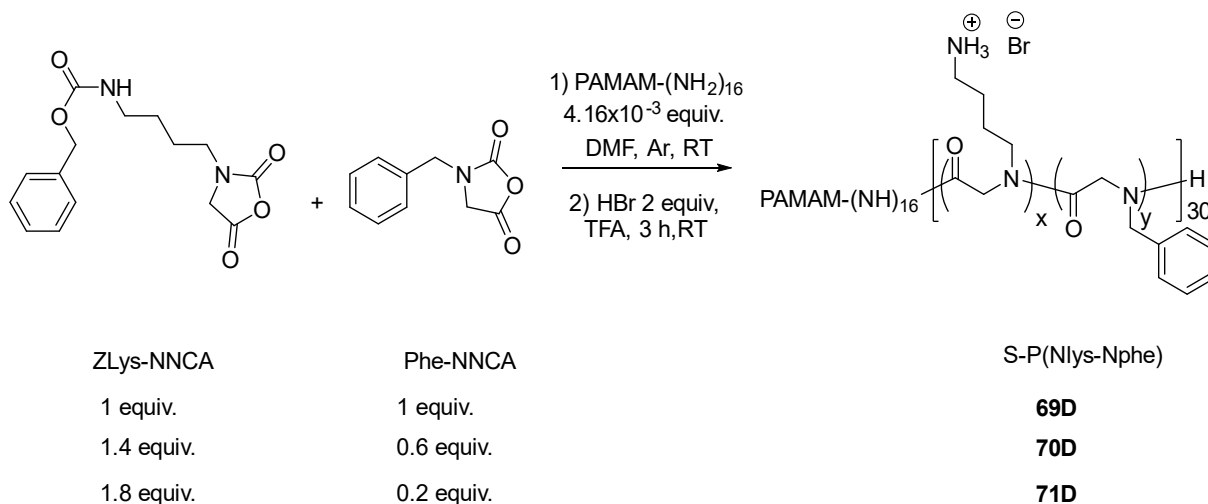
1.3 Star copolypeptoids varying the hydrophobic content

In section 1.2, the results obtained with the first series of copolymers did not clearly evidence a better antimicrobial activity when the star topology was compared to the linear polymer. To better understand these first results we decided to modify the cationic/hydrophobic ratio on the star-like topology to see if this could improve the antimicrobial efficacy. Indeed, the hydrophobic content is an important parameter when the antibacterial activity involves membrane destabilization as we already described in chapters 3 and 4. In this new study, we prepared a small series of star-P(ZNlys-Nphe) using a PANAM dendrimer having 16 (-NH₂) terminal functions because this topology was expected to present the lowest cytotoxicity.² We performed the polymerization using ZLys-NCA (1, 1.4 and 1.8 equiv.; 50, 70, 90 hydrophobic content) and Phe-NNCA (1, 0.6, 0.2 equiv.; 50, 30, 10% hydrophobic content) using PAMAM initiator at M/I = 30 (4.16x10⁻³ equiv.) in DMF 0.1 M at RT under argon atmosphere (step 1, **Scheme 51**).

We followed the conversion of the ROP by monitoring FTIR until reaction completion (NNCA stretching at 1850 cm⁻¹, 20 days). We purified the copolymers by precipitation in Et₂O, by drying

Chapter 5. Macromolecular engineering of antimicrobial polypeptoids: star and drug-conjugate polymers

under high vacuum and we recovered the different star-like copolymers in 39-45% yields. We first



Scheme 51. Synthesis route to prepare star-*P*(Nlys-Nphe) varying the hydrophobic content **69D-71D** using PAMAM with 16 arms.

characterized them by SEC analysis in DMF (**Table 56** and **Figure 72**). In marked contrast to these linear copolymers, we then calculated higher dispersity for the new star copolymers S-*P*(ZNlys-Nphe)**69-70** ($\bar{M}_w = 1.30-1.41$), a feature in agreement with copolymers from section 1.2 and with the previously reported star-like polypeptides.⁶

Table 56. Star-like *P*(ZNlys-Nphe) copolymers varying the hydrophobic content: molar masses from SEC, hydrophobic content from ¹H-NMR and yields.

	Arms	M/I	Hydrophobic content theoretical (%)	MW theo (g/mol)	M_n (g/mol) ^a	M_w (g/mol)	\bar{M}_w	Hydrophobic content NMR (%) ^b	Yield (%)
S- <i>P</i> (Nlys-Nphe) 69	16	30	50	1.02x10 ⁵	3.59x10 ⁴	5.05x10 ⁴	1.40	52	40
S- <i>P</i> (ZNlys-Nphe) 70	16	30	30	1.13x10 ⁵	3.62x10 ⁴	5.11x10 ⁴	1.41	51	39
S- <i>P</i> (ZNlys-Nphe) 71	16	30	10	1.24x10 ⁵	4.05x10 ⁴	5.28x10 ⁴	1.30	50	45

^a SEC performed in DMF. ^b Calculated from the ¹H-NMR spectrum in DMSO-d₆

Then, we characterized the copolymers by ¹H-NMR in DMSO-d₆ (**Figure 72**). We found signals attributable to the polymer backbone (CH₂, *peak a,a'*), signals attributable to the ZNlys moiety (peaks *b-h*) and signals attributable to Nphe moiety (peaks *i,j*). We determined the hydrophobic content by comparing integrations of the signals of the polymer backbone (-CH₂, peak *d,d'*, 3.8-4.5 ppm) to the signals from the side chains (*e-h*) and we calculated a hydrophobic content of around 50% in all the cases which were deviated from the expected values (**Table 56**).

Chapter 5. Macromolecular engineering of antimicrobial polypeptoids: star and drug-conjugate polymers

We could not determine the DP_{NMR} due to the high monomer/initiator ratio (120:1 for PAMAM with 4 arms and even higher for PAMAM with 16 arms) and due to the PAMAM signals overlapped with the copolymer (peaks *b*, *e*, *a*, *a'*).

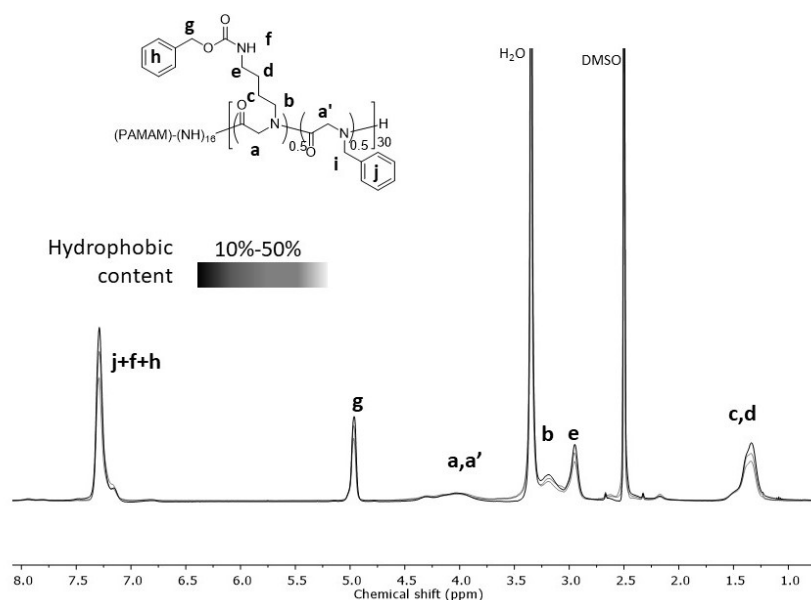


Figure 72. Overlay of the $^1\text{H-NMR}$ spectra of the different star- $\text{P}(\text{ZNlys-Nphe})$ in $\text{DMSO-}d_6$. The color scale indicates that a lighter color represents a higher hydrophobic content.

Then, we performed Z-Lys side chains deprotection using the procedure optimized for $\text{P}(\text{Nlys})$ in chapter 3 (section 2.1): the star-like copolymers were deprotected in TFA by adding 2 equivalents of HBr (relative to cationic side chains in TFA, RT). After 3 h, the copolymers were purified by precipitation in diethyl ether, dialyzed, and lyophilized (yields 42-62%, **Table 57**).

Table 57. Star- $\text{P}(\text{Nlys-Nphe})$ copolymers varying the hydrophobic content: hydrophobic content was evaluated from $^1\text{H-NMR}$ and yields.

	Arms	M/I	Hydrophobic content theoretical (%)	Hydrophobic content (%) ^a	Yield (%)
S- $\text{P}(\text{Nlys-Nphe})69\text{D}$	16	30	50	53	62
S- $\text{P}(\text{Nlys-Nphe})70\text{D}$	16	30	30	35	55
S- $\text{P}(\text{Nlys-Nphe})71\text{D}$	16	30	10	12	42

^a Calculated from the $^1\text{H-NMR}$ spectrum in D_2O

To determine the DP_{NMR} and the chemical composition in monomer units, we analyzed the samples by $^1\text{H-NMR}$ in D_2O (**Figure 73**). We calculated the hydrophobic content by carefully comparing the integration of signals belonging to Nlys side chains (peak *c,d*) and Nphe side chains (peak *j*) and we found values that were in agreement with the expected ones (**Table 57**).

Chapter 5. Macromolecular engineering of antimicrobial polypeptoids: star and drug-conjugate polymers

Moreover, this NMR characterization confirmed that the copolymers did not suffer from chemical modifications during the deprotection step and that copolymers containing Nlys and Nphe were prepared.

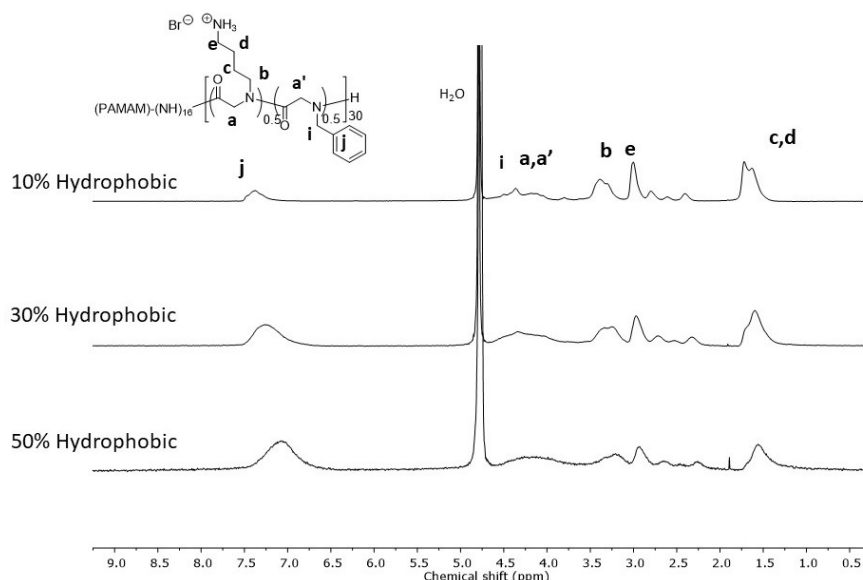


Figure 73. $^1\text{H-NMR}$ spectra in DMSO-d_6 of star-like $[P(\text{Nlys-Nphe})]$ having 16 arms at different hydrophobic content.

This new series of copolymers were then studied in biology to evaluate their antimicrobial activity against *C. difficile* and a variety of representative pathogens: Gram-positive (*S. aureus*, *E. faecalis*, *L. monocytogenes* and *S. pneumoniae*) and Gram-negative bacteria (*E. coli*, *P. aeruginosa*, *A. baumannii*), including anaerobic bacteria (*B. fragilis* and *H. pylori*). The results are presented in **Table 58**: we determined the MIC from the microdilution method bacteria (see the experimental section, approximately 10^5 CFU/mL) for 24-48 h with increasing concentrations of polypeptoids.

First, we observed that all the star-like polypeptoids were not active against *C. difficile* even at 50% of hydrophobic content. Then, our next step was to evaluate the star-like polymers in the other pathogenic bacteria. We observed that **70D**, with a hydrophobic content of 30%, was very active against *L. monocytogenes* with MIC values ranging from 15.6 to 31.25 $\mu\text{g/mL}$. However, MIC values obtained from other Gram-negative and Gram-positive bacteria tests were found significantly higher (MIC = 62.5 $\mu\text{g/mL}$) as compared to the copolymer with 50% of hydrophobic content (**69D**), where it was above this value, except against *B. fragilis* where the activity was

Chapter 5. Macromolecular engineering of antimicrobial polypeptoids: star and drug-conjugate polymers

preserved (MIC = 31.25 µg/mL).

Table 58. Antimicrobial activity: 16 arms star-like copolymers with different hydrophobic content were used in assays involving Gram-positive and Gram-negative pathogens.

	Gram	S-P(Nlys-Nphe)69D		S-P(Nlys-Nphe)70D		S-P(Nlys-Nphe)71D	
		MIC (µg/mL)	¹ MIC (10 ⁻⁶ M)	MIC (µg/mL)	² MIC (10 ⁻⁶ M)	MIC (µg/mL)	³ MIC (10 ⁻⁶ M)
<i>C. difficile</i>	+ (anaerobic)	>250	>8.2	250	8.7	250	8.6
<i>S. aureus</i> CIP 4.83	+	125	4.1	62.5	2.2	250	8.6
<i>S. aureus</i> ATCC33591	+	62.5	2	62.5	2.2	31.25	1.1
<i>E. faecalis</i> CIP 103015T	+	250	8.2	250	8.7	125	4.3
<i>L. monocytogenes</i> CIP 82110T	+	31.25	1	15.6-31.25	0.54-1.1	15.6-31.25	0.53-1.1
<i>S. pneumoniae</i> CIP 104471	+	250	8.2	>250	8.7	>250	8.6
<i>E. coli</i> CIP 53.126	-	125	4.1	62.5	2.2	250	8.6
<i>P. aeruginosa</i> CIP 82.118	-	62.5-125	2	62.5	2.2	125	4.3
<i>A. baumannii</i> CIP 70.34T	-	250	8.2	62.5	2.2	250	8.6
<i>B. fragilis</i> CIP 77.16	- (anaerobic)	31.25	1	31.25	1.1	250	8.6

¹Calculated using MW = 30500 g/mol. ²Calculated using MW = 28700 g/mol. ³Calculated using MW = 29200 g/mol. Values calculated from SEC in DMF.

Then, we evaluate the bacterial properties of the star-like copolymer with 10% of hydrophobic content (**71D**) and we found a MIC=15.6-31.25 µg/mL against *L. monocytogenes*. Surprisingly, we recovered the selectivity among the other bacteria, similarly to **69D**, where the MIC was above 62.5 µg/mL. From this study, we observed that star-like copolymers with a 30% of hydrophobic content presented a broader and better antimicrobial activity (MIC < 62.5 µg/mL) as compared to copolymers with 10 and 50%.

Furthermore, we assessed the cytotoxicity of the star-like copolymers (**67D-71D**) using the CaCO-2 cell line that are cells similar to the one encountered in the epithelium of the digestive tube and we compared the values with the linear copolymer **42D**. We observed an increase of the cytotoxicity for all the star-like copolypeptoids studied as it is depicted in **Table 59** in comparison with **42D**. Therefore, we could not decrease the cytotoxicity by the preparation of this particular topology as we expected with star-like polypeptides² even if we prepared 16-arm polypeptoids or with higher cationic content. However, we observed that star-like copolypeptoids

Chapter 5. Macromolecular engineering of antimicrobial polypeptoids: star and drug-conjugate polymers

can be an interesting approach for further investigations since we could reach selectivity indexes close to the one presented for **42D** (SI = 13.5) against *B. fragilis* by preparing either 4- or 8-arms polypeptoids (**67D** and **68D**) or against *L. monocytogenes* (**Table 59**).

Table 59. Cytotoxicity over CaCO-2 cells and selectivity indexes of star-like polypeptoids **67D-71D** and the linear polypeptoid **42D**.

	CaCO-2 CC ₅₀ (µg/mL)	MIC of <i>B. fragilis</i> (µg/mL)	SI (CC ₅₀ /MIC)	MIC of <i>L. monocytogenes</i> (µg/mL)	SI (CC ₅₀ /MIC)
42D	211.2±20	15.6	13.5	15.6	13.5
67D	79.9±3	7.8-15.6	10.2-5.1	15.6-31.25	5.1-2.5
68D	90.7±9	7.8	11.6	15.6-31.25	5.8-2.9
69D	138.4±5	31.25	4.4	31.25	4.4
70D	47.2±2	31.25	3.0	15.6-31.25	3.0-1.5
71D	42.9±3	250	>1	15.6-31.25	2.8-1.4

1.4 Liposome destabilization assay

The star-like polypeptoids prepared in this Ph.D. work are made of cationic and hydrophilic side chains and they can kill bacteria by destabilizing the bacterial membrane. Therefore we verified this possible mechanism by using an *in vitro* model: the destabilization of neutral or negatively charged liposomes containing carboxyfluorescein (CF). As we performed in the previous chapter 4, we used two different liposome models: 1) neutral liposome membranes constituted of soybean phosphatidylcholine and cholesterol (SPC:Chol, 8:2) with a zeta potential of $\zeta = -3.9 \pm 0.9$ mV and 2) negatively charged liposome membranes constituted of 1,2-dioleoyl-sn-glycero-3-phosphoglycerol (PG) and cholesterol (PG:Chol, 8:2) with a zeta potential of $\zeta = -33.3 \pm 2.2$ mV. The liposomes were first loaded with the fluorophore. Then, the star-like copolymers P(Nlys-Nphe) **67D-71D** and the linear one **42D** were prepared at a concentration of 90 µg/mL and mixed with the liposomes. Upon incubation (1.5 h), the concentration of released of carboxyfluorescein was measured by fluorimetry ($\lambda_{ex} = 485$ nm and $\lambda_{em} = 528$ nm) and reported in percentage of release (%CF release,). We clearly observed that copolymers having a hydrophobic content of 50% destabilized both negatively and neutrally charged liposome models in the case for the linear one **42D** it was 94% and 89%, respectively (**Figure 74**). Similar values were observed in the case of star-like polypeptoids even if we varied the number of arms (**67D-69D**). Interestingly, the lower the hydrophobic content in the 16-arm polypeptide was the lower ability to destabilize the liposomes we observed such as the case of **71D** (10% hydrophobic

Chapter 5. Macromolecular engineering of antimicrobial polypeptoids: star and drug-conjugate polymers

content) with 0% and 3% of CF release for neutral and negative liposome models as compared with **69D** (50% hydrophobic content) with 81% and 93% of CF release for neutral and negative liposome models. This membrane destabilization was in agreement with the MIC results shown against *B. fragilis* because **71D** had the lowest MIC (250 $\mu\text{g}/\text{mL}$) and also the lowest membrane destabilization.

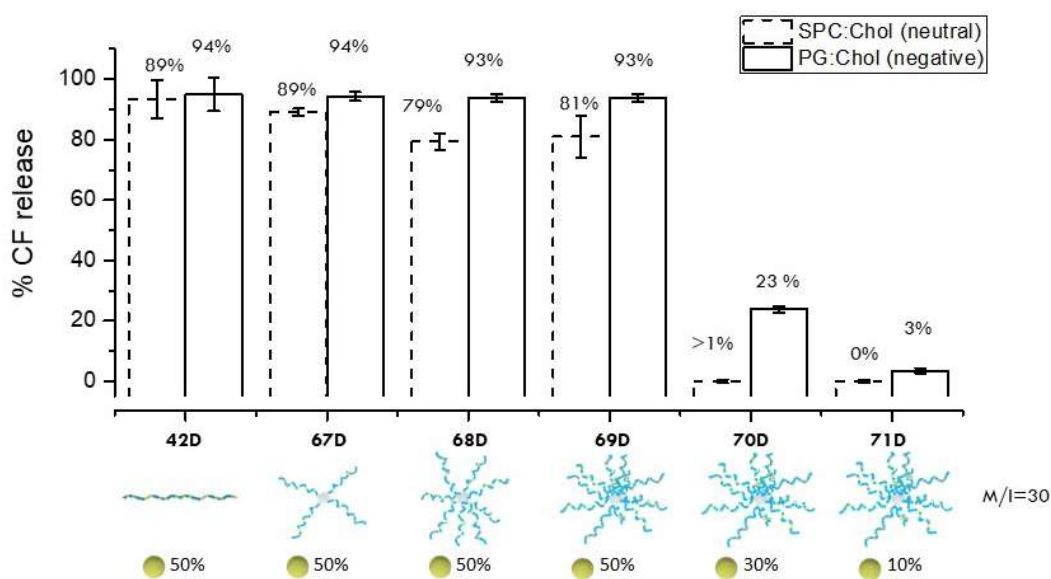


Figure 74. Membrane destabilization by active cyclic copolypeptoids using two different liposome models. SPC:Chol (8:2); PG:Chol (8:2).

Thus, by using artificial membranes, we showed that the star-like polypeptoids destabilized the lipid membranes in liposomes with an important related influence on the hydrophobic content.

In summary, by using dendrimers as macroinitiators during ROP of NNCAs, we accessed antimicrobial star-like polypeptoids with fine-tuning over the hydrophobic content and the number of arms. First, we established a methodology to prepare star-like polypeptoids in DMF at 0.1M under inert conditions. Then, we prepared copolymers varying the number of arms (4, 8 and 16 arms) and the hydrophobic content. In general, the star-like polypeptoids were obtained with good dispersity ($\text{Đ}_M < 1.4$), with a controlled hydrophobic content and with a preserved structure upon acidic treatment (HBr 2 equiv. in TFA). From this short structure-activity relationship study we established that star-like copolypeptoids were having a broader spectrum of activity as compared

Chapter 5. Macromolecular engineering of antimicrobial polypeptoids: star and drug-conjugate polymers

to the linear analogs but in general, they were better at killing Gram-positive germs, particularly *L. monocytogenes* with MIC values of 15.6-32.5 µg/mL. We concluded that 1) star-like copolypeptoids with 8 arms enhanced the antibacterial activity against the anaerobic Gram-negative *B. fragilis* in a star-like polypeptoid with (MIC = 7.8 µg/mL) and 2) the copolymers made from PAMAM with 16 arms were giving good antimicrobial properties at 50% hydrophobic content (*L. monocytogenes* with MIC = 15.6-32.5 µg/mL). Moreover, we also demonstrated that star-like polypeptoids destabilized liposome membranes with an important influence on the hydrophobic content.

2 Drug conjugates copolypeptoids as antimicrobial agents

Macromolecular engineering is a unique tool to bring a new life to commercial antibacterial agents via their conjugation to synthetic structures.²³ Using the right macromolecular chemistry, interesting properties have been obtained by conjugating lipids, nanoparticles, peptides, or even polymers with a wide variety of antimicrobial molecules.²³ For instance, the conjugation of malachite green with carbon nanotubes enhanced the inhibition of biofilm formation involving *P. aeruginosa* y *S. aureus*.²⁴ A major advantage of drug conjugation is the simple modulation of the drug lipophilicity, a property that is crucial to reach the best therapeutic effect with membrane permeation.²⁵ Lipids conjugates were for example good to enhance the antibacterial activity of neomycin against Gram-positive bacteria with a significant C₂₀ lipid tail (but less efficient against Gram-negative).²⁶ Closer to this work, another approach of drug conjugation involved antibiotics and peptides to modulate the cell penetration.²⁷ The resulting peptide-drug conjugates (PDCs) fused one or more drug molecules with a short peptide through biodegradable linkages. Using PDC, P. Khavari *et al.* improved the cell penetration of cyclosporin A by conjugation with arginine oligomers (7-mers).²⁸ They observed that the conjugate crossed the epidermis and dermis *in vivo* and *in vitro*, and decreased inflammation in a dermatitis model by controlled release of the drug (pH-responsive linker). Other works on PDC reported the improved cell-penetration (while killing dangerous pathogens) by conjugating of oligopeptides with triclosan (antiparasitic agent against *Toxoplasma gondii* tachyzoites),²⁹ methotrexate (against *L. monocytogenes*, *M. smegmatis* and *M. tuberculosis*),^{30,31} kanamycin (against *M. tuberculosis*, *Salmonella enteditidis* and *Brucella abortus*)³² or vancomycin (against *E. coli*, *Enterococcus* or *MRSA*).³³⁻³⁵ Another property that was enhanced by the drug conjugation was the controlled drug release mediated by polymers conjugates.³⁶ For instance, S. Gong *et al.* prepared a polymer-drug conjugate using aldehyde

Chapter 5. Macromolecular engineering of antimicrobial polypeptoids: star and drug-conjugate polymers

group of streptomycin and the amine pendant groups of biodegradable polyurea to release the antibiotic at a specific pH value of 7.4, killing MRSA *S. aureus* (MIC = 20 µg/mL) with low cytotoxicity towards HEK293 cells (CC₅₀ > 2000 µg/mL). Another example is the recent report of J. Cheng *et al.* involving the conjugation between vancomycin and polyglutamate oligomers synthesized by ROP (10-mers) bearing guanidinium side-chains: they demonstrated anti-infective activity against drug-resistant *S. aureus* and *Enterococcus* intracellular infections.³⁷

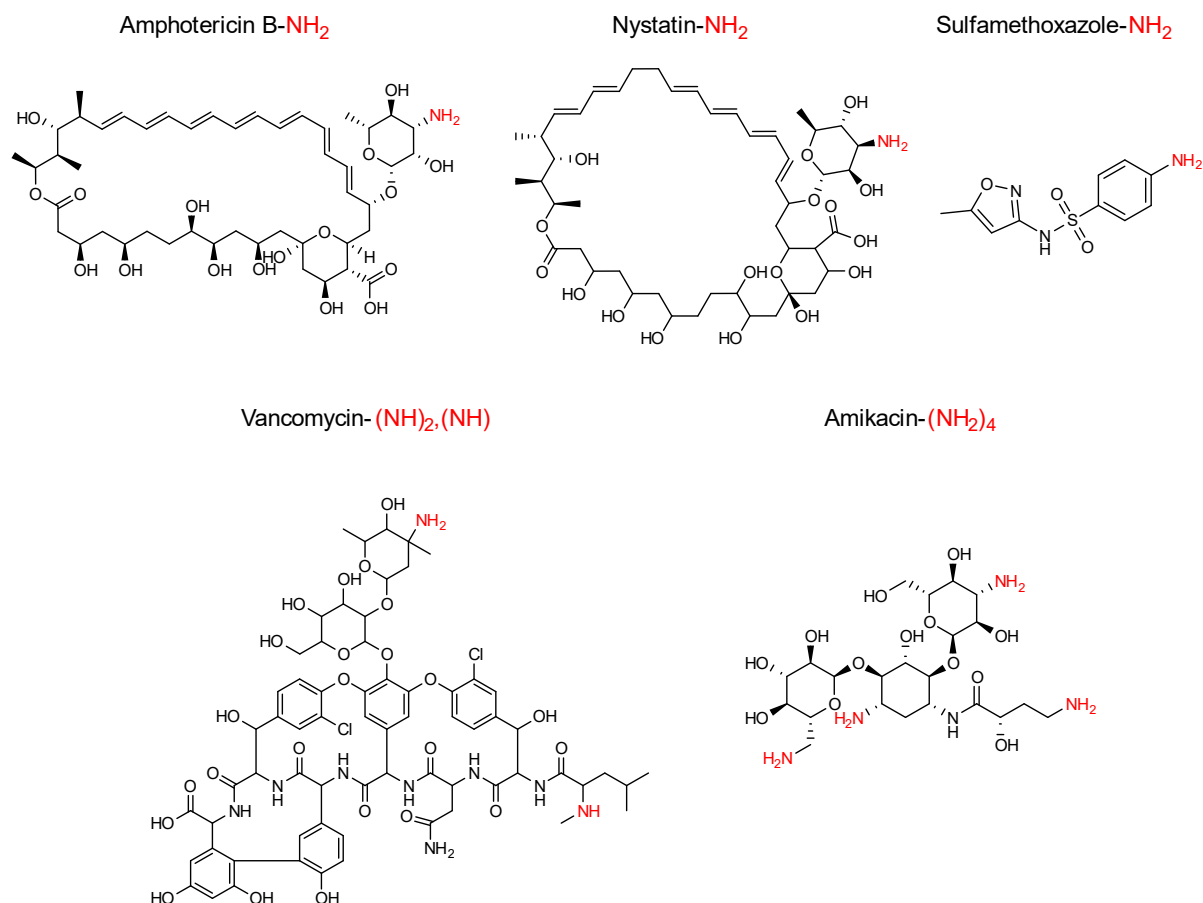
Overall, these examples revealed how drug conjugates enhanced antimicrobial efficacy by optimizing drug release and cell penetration. So far, no one has extended the use of this macromolecular engineering approach to polypeptoids. This Ph.D. work is a pioneering study in this direction: we achieved this design to the antimicrobial activity over various Gram-positive and Gram-negative bacteria, including *C. difficile*.

2.1 Preparation of polymer-drug conjugates

To prepare polymer-drug conjugates two routes are available: 1) coupling polymers (such as PEG, dextran, PAMAM, etc.) to the active molecule (grafting-to approach) sometimes using a stimuli-responsive linker^{36,38} and 2) preparing antibiotic with specific functionality and then using it in the polymerization process (grafting-from approach).³⁷ The grafting-from approach has been scarcely studied with other polymerization methods because of potential drawbacks such as antibiotic degradation during the process or the deprotection step. Here, we implemented this second grafting-from approach towards copolypeptoid-drug conjugates in two steps of synthesis: ROP of NNCA using antibiotics as macroinitiators followed by deprotection in acidic conditions to afford cationic conjugates.

Using the methodology established in section 1.1, we first challenged the ROP of copolymers based on ZLys- and Phe-NNCAs using various antibiotics as macroinitiators (**Scheme 52**). We for instance choose vancomycin to potentiate the antimicrobial activity against *C. difficile* by a synergic mechanism of action. We also selected sulfamethoxazole due to its bacteriostatic mechanism³⁹ and we decided to use amphotericin B⁴⁰ and nystatin⁴¹ because they are antibiotics (normally used for antifungal infections) with very limited solubility: we hypothesize that their enhanced solubility will increase the antibacterial efficacy. We finally included the antibiotic amikacin because of its glucosidic nature⁴¹ that could enhance synergically the antibacterial activity. Moreover, the number of arms (NH₂ groups) can allow the preparation of star polymers combining the star-polymer approach to the conjugate approach.

Chapter 5. Macromolecular engineering of antimicrobial polypeptoids: star and drug-conjugate polymers

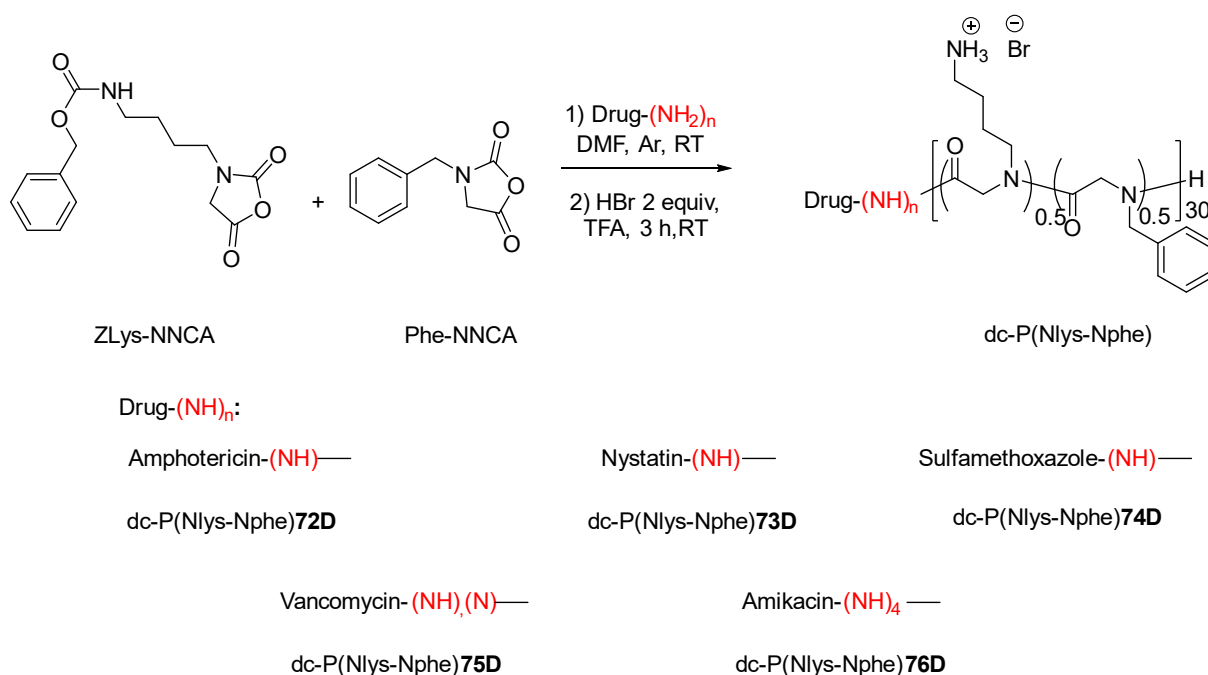


Scheme 52. Drug-polypeptoid conjugates: antibiotics used as initiator for the ROP of NNCA (The amine functions that initiate the polymerization are colored in red).

With all these drugs, we carried out the ROP of ZLys- and Phe-NNCA targeting the best chemical design described in chapter 3: 50% of hydrophobic content $M/I = 30$ (based on the amine-free groups). We performed the reactions in DMF at RT in anhydrous conditions (**Scheme 53**).

We monitored the NNCA disappearance of the NCOO signal at 1850 cm^{-1} by FTIR until full conversion (20 days). Then, we purified the protected drug-conjugate copolypeptoids (dc-P(ZNlys-NPhe)**72-76**) by precipitation in Et₂O, drying under high vacuum and recovered in 48-74% yields (**Table 60**). First, we characterized the compounds by SEC in DMF and we confirmed the formation of polymers (**Figure 75** and **Table 60**). For drug-conjugates dc-P(ZNlys-NPhe)**72-**

Chapter 5. Macromolecular engineering of antimicrobial polypeptoids: star and drug-conjugate polymers



Scheme 53. Synthesis route to prepare drug-conjugate-[P(Nlys-Nphe)] in two steps: the polymerization reaction (1) and the acidic deprotection (2) to obtain the water-soluble and cationic copolymer.

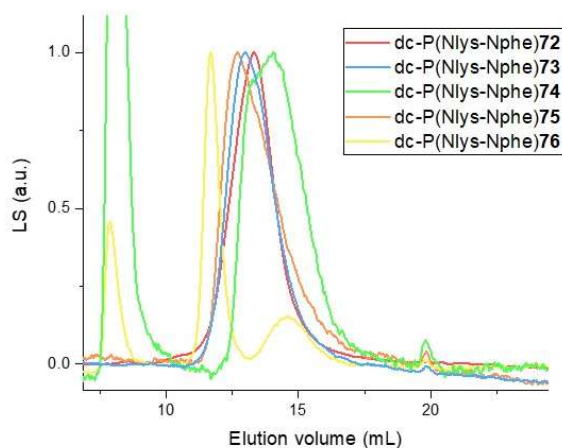


Figure 75. SEC chromatograms of the different P(Nlys-Nphe) drug-conjugates: **72**, amphotericin; **73**, nystatin; **74**, sulfamethoxazole; **75**, vancomycin; **76**, amikacin

75 we observed monomodal polymer distribution, while in dc-P(ZNlys-NPhe)**76** we observed a smaller molar mass that corresponded to a DP = 30 coming from possible impurity contained in the antibiotic. SEC analysis indicated that we obtained polymers with higher molar masses than

Chapter 5. Macromolecular engineering of antimicrobial polypeptoids: star and drug-conjugate polymers

the linear copolymers (initiated with allylamine at $M/I = 30$; $M_n = 5200$ g/mol $\bar{D}_M = 1.12$) demonstrating that our approach was successfully achieving polymer-drug conjugation. However, some polymer dispersity was found relatively high ($\bar{D}_M > 1.2$) a feature we attributed to limited solubility behaviors.

Table 60. Drug-conjugate P(ZNlys-Nphe) copolymers varying the hydrophobic content: molar masses from SEC, hydrophobic content from NMR and yields.

	Arms	M/I	Hydrophobic content theoretical (%)	MW theo (g/mol)	M_n (g/mol) ^a	M_w (g/mol)	\bar{D}_M	DP _{NMR} ^b	Hydrophobic content (%) ^b	Yield (%)
dc-P(ZNlys-Nphe) 72	1	30	50	7.0×10^3	6.9×10^3	8.1×10^3	1.17	30	37	68
dc-P(ZNlys-Nphe) 73	1	30	50	7.1×10^3	9.3×10^3	1.2×10^4	1.30	30	43	74
dc-P(ZNlys-Nphe) 74	1	30	50	6.4×10^3	5.6×10^3	7.4×10^3	1.31	54	49	66
dc-P(ZNlys-Nphe) 75	2	30	50	1.4×10^4	9.4×10^3	1.3×10^4	1.40	31	49	62
dc-P(ZNlys-Nphe) 76	4	30	50	2.8×10^4	2.0×10^4	2.2×10^4	1.13	-	50	48

^a SEC performed in DMF. ^b Calculated from the ¹H-NMR spectrum in DMSO-d₆

Then, we characterized the different copolymers by ¹H-NMR in DMSO-d₆ that we will describe one by one (Figure 76 - Figure 80).

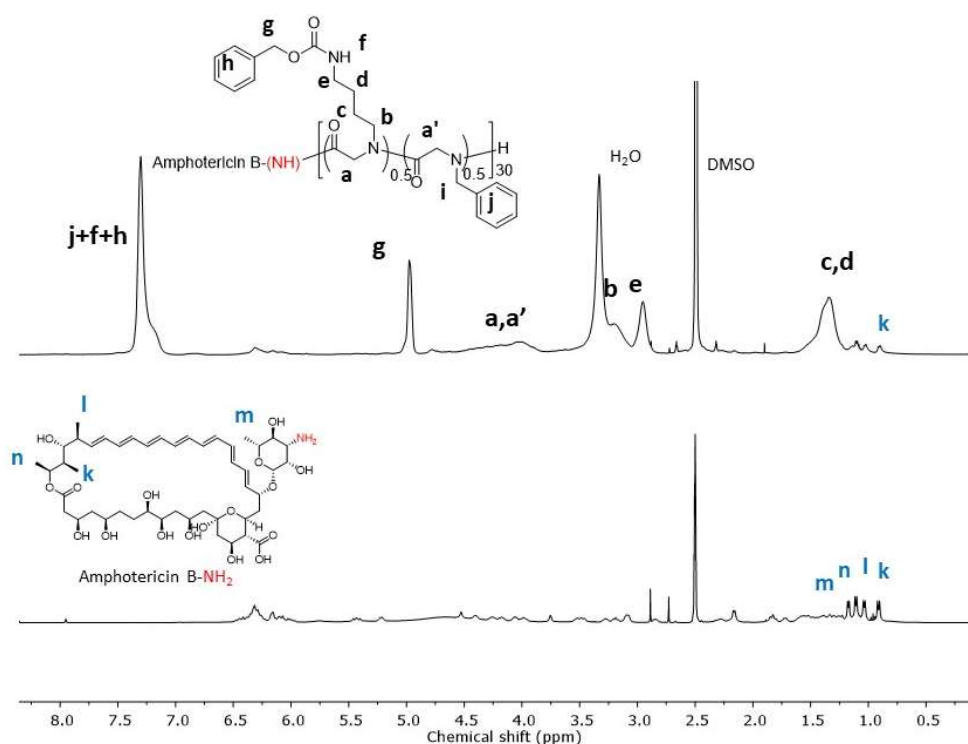


Figure 76. ¹H-NMR spectra of the amphotericin-P(ZNlys-Nphe) conjugate **72** (up) and of the amphotericin alone (down) in DMSO-d₆

For dc-P(ZNlys-Nphe)**72** we observed the peaks of the polymer backbone (CH₂, peak a,a'), ZNlys

Chapter 5. Macromolecular engineering of antimicrobial polypeptoids: star and drug-conjugate polymers

side chains (peaks *b-h*), Nphe side chains (peak *i,j*), and some peaks from the initiator such as the methyl groups (peaks *k-n*, 0.8-1.2 ppm) and aromatic protons (6.0-6.5 ppm) confirming the structure of the polymer-conjugates. We determined the DP_{NMR} comparing integrations of the signals of the polymer backbone ($-\text{CH}_2-$, peak *a,a'*) to the signals from the macroinitiator (CH_3 , 0.92 ppm, peak *k*) and we calculated an expected DP_{NMR} of 30 (**Table 60**). Then we determined the hydrophobic content by comparison of polymer backbone (CH_2- , peak *a,a'*) to the side chains (*b-j*). In fact, we were surprised to find a slightly lower hydrophobic content of 37% as compared to the expected 50%.

For dc-P(ZNlys-Nphe)**73**, we observed the peaks of the polymer backbone (CH_2 , peak *a,a'*), ZNlys side chains (peaks *b-h*), Nphe side chains (peak *i,j*) and the macroinitiator nystatin (methyl groups 0.90 ppm, specifically peaks *k, k'*, **Figure 77**). We determined the DP_{NMR} comparing integrations of the signals of the polymer backbone ($-\text{CH}_2-$, peak *a,a'*) to the signals from the macroinitiator (CH_3 , 0.90 ppm, peak *k,k'*) that was in agreement with the theoretical value ($DP_{\text{NMR}} = 30$, **Table 60**). Also, we determined the hydrophobic content by comparison of polymer backbone ($-\text{CH}_2-$, peak *a,a'*) to the side chains (*b-j*) and we found a hydrophobic content of 43% close to the 50% targeted.

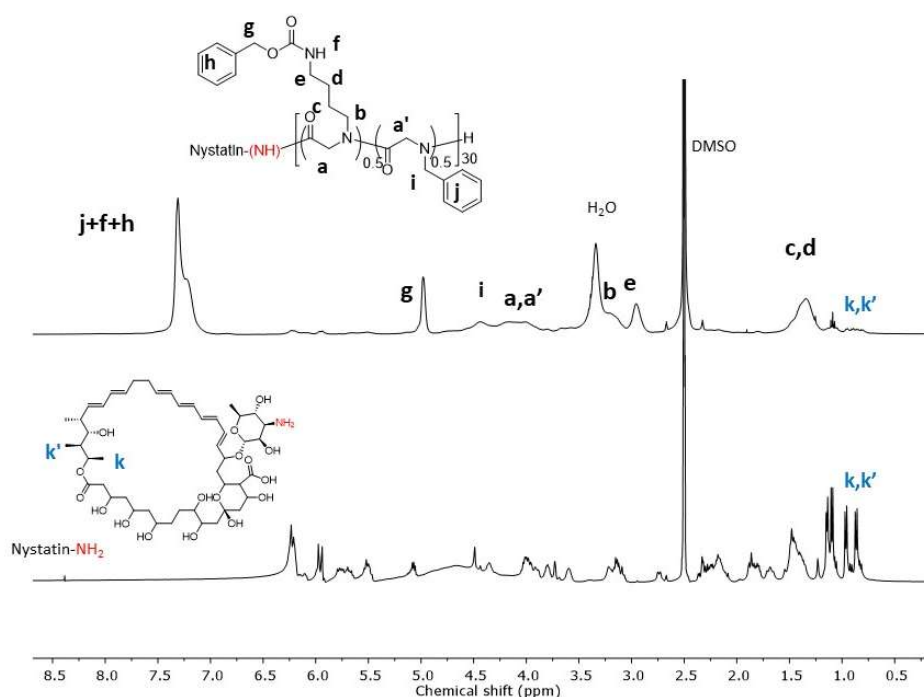


Figure 77. ¹H-NMR spectra of the nystatin-P(ZNlys-Nphe) conjugate **73** (up) and of the amphotericin alone (down) in DMSO-*d*₆

Chapter 5. Macromolecular engineering of antimicrobial polypeptoids: star and drug-conjugate polymers

For dc-P(ZNlys-Nphe)**74**, the $^1\text{H-NMR}$ spectrum in DMSO-d_6 revealed two small peaks at 2.11 and 5.38 ppm that we assigned to the initiator (peaks k,l). We also observed the typical signals for the polymer backbone (CH_2 peak a,a'), ZNlys (peaks $b-h$) and Nphe moieties (peaks i,j). Then, we tried to determine the DP_{NMR} comparing integrations of the signals of the polymer backbone (CH_2 , peak a,a' **Figure 78**) to the signals from the macroinitiator (CH_3 , 2.11 ppm, peak k and CH , 5.83 ppm, peak l) calculating a $\text{DP}_{\text{NMR}} = 54$ that was significantly higher than the theoretical one ($\text{DP} = 30$, **Table 60**). Moreover, we determined the hydrophobic content by comparing the signal intensities of the polymer backbone (CH_2 , peak a,a'), and of the side chains ($b-j$) and we found a hydrophobic content value of 49% that was expected.

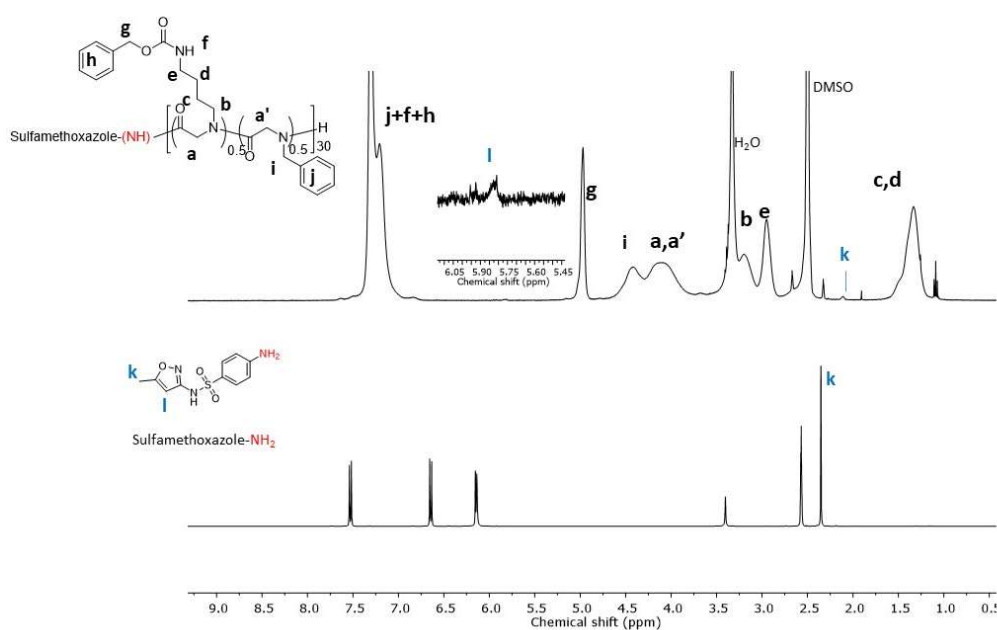


Figure 78. $^1\text{H-NMR}$ spectra of the sulfamethoxazole-P(ZNlys-Nphe) conjugate **74** (up) and of the amphotericin alone (down) in DMSO-d_6

Then, we analyzed dc-P(ZNlys-Nphe)**75** by $^1\text{H-NMR}$ in DMSO-d_6 and we found some signals corresponding to the macroinitiator, vancomycin, such as the methyl groups (CH_3 , 0.84 ppm, peak k,k'), we also observed signals of the polymer backbone (CH_2 , peak a,a') and the typical signals for ZNlys (peaks $b-h$) and Nphe moieties (peaks i,j , **Figure 79**). This signal allowed us to determine the DP_{NMR} by comparison of the integrations from the polymer backbone signal (CH_2 , peak a,a' , **Figure 79**) to the signals from the macroinitiator (CH_3 , 0.84 ppm, peak k,k') and we found a value of $\text{DP}_{\text{NMR}} = 31$ in agreement with the theoretical one (**Table 60**). Then, we

Chapter 5. Macromolecular engineering of antimicrobial polypeptoids: star and drug-conjugate polymers

determined the hydrophobic content by comparison of polymer backbone (CH_2 , peak a, a') to the side chains ($b-j$) and we found a hydrophobic content of 49% that was similar to the theoretical one.

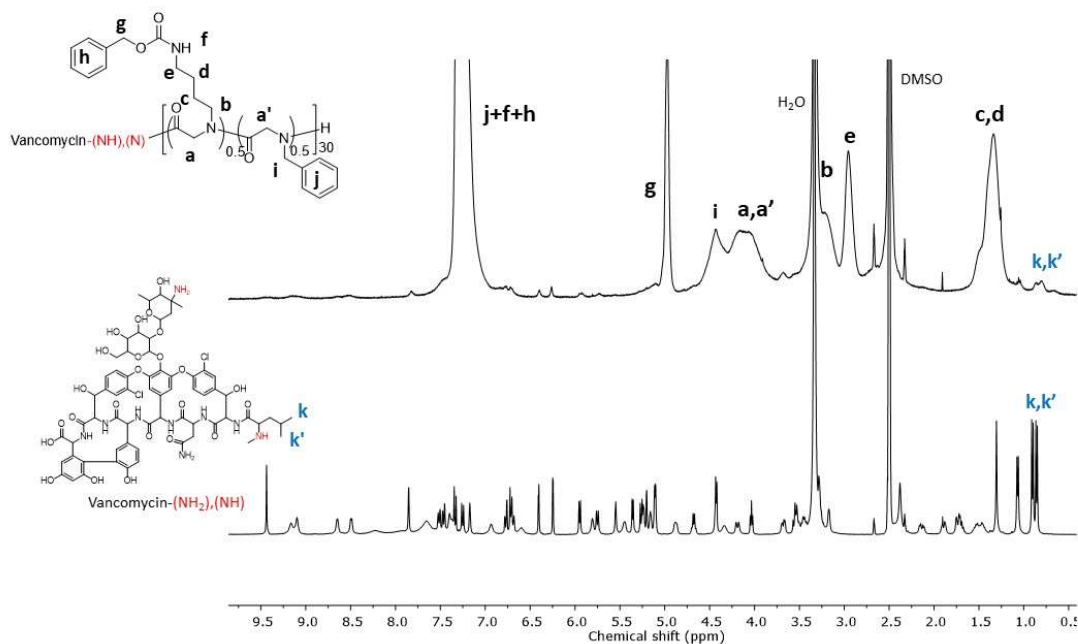


Figure 79. ^1H -NMR spectra of the vancomycin- $P(\text{ZNlys-Nphe})$ conjugate **75** (up) and of the amphotericin alone (down) in DMSO-d_6

Finally, we analyzed $\text{dc-P}(\text{ZNlys-Nphe})$ **76** by ^1H -NMR in DMSO-d_6 and we observed signals of the polymer backbone (CH_2 , peak a, a'), the typical signals for ZNlys (peaks $b-h$) and Nphe moieties (peaks i, j , **Figure 80**). However, we were not able to determine the DP_{NMR} because the signals of the macroinitiator were too weak due to the relation initiator:monomer instead of 1:30 was 1:120 (4 NH_2 terminal groups), and also because amikacin signals could be overlapped to the copolymer (**Figure 80**). Nevertheless, we successfully determined the hydrophobic content by comparing of integrations of the signals belonging to the polymer backbone ($-\text{CH}_2-$, peak a, a') to the integrations of the signals belonging to the side chains ($b-j$) and we found a hydrophobic content of 50% in agreement with the theoretical value (**Table 60**).

Overall, NMR and SEC analyses established that it was possible to copolymerize ZLys- and Nphe-NNCAs using antibiotics macroinitiators with controlled hydrophobic content, molar mass and relatively good dispersity $\text{Đ}_M < 1.4$.

Chapter 5. Macromolecular engineering of antimicrobial polypeptoids: star and drug-conjugate polymers

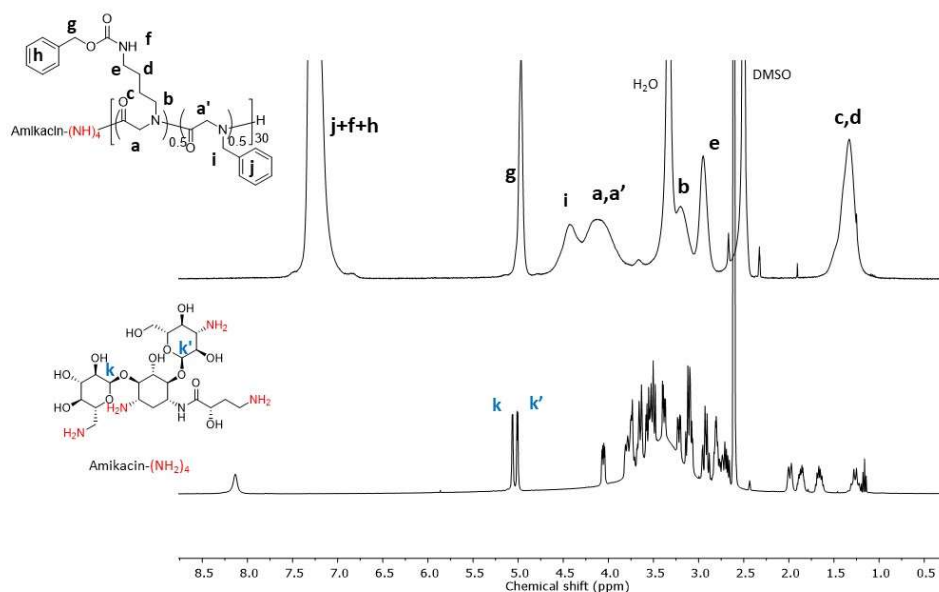


Figure 80. $^1\text{H-NMR}$ spectra of the amikacin- $\text{P}(\text{ZNlys-Nphe})$ conjugate **76** (up) and of the amphotericin alone (down) in DMSO-d_6

Later, we performed deprotection of the *Cbz* group in all our copolymers using the optimized protocol developed in chapter 3 (section 2.1). We mixed the drug-polymer conjugate in TFA and we added 2 equiv. of HBr (relative to cationic side chains). Upon deprotection (3 h), the copolymers were purified by precipitation in diethyl ether, dialyzed (MWCO 10kDa), lyophilized and recovered in 21-62% yields (**Table 61**).

Table 61. Drug conjugates-copolypeptoids upon deprotection: the hydrophobic content was evaluated from $^1\text{H-NMR}$ analysis.

	Arms	M/I	Hydrophobic content theoretical (%)	$\text{DP}_{\text{NMR}}^{\text{a}}$	Hydrophobic content (%) ^a	Yield (%)
dc-P(Nlys-Nphe) 72D	-	30	50	28	37	90
dc-P(Nlys-Nphe) 73D	-	30	50	30	44	96
dc-P(Nlys-Nphe) 74D	-	30	50	-	50	98
dc-P(Nlys-Nphe) 75D	2	30	50	28	51	98
dc-P(Nlys-Nphe) 76D	4	30	50	27	51	90

^a Calculated from the $^1\text{H-NMR}$ spectrum in D_2O

Then, we characterized the different copolymers by $^1\text{H-NMR}$ in D_2O that we will describe one by one: this analysis was used to evaluate the polymerization degree (**Figure 81 - Figure 85**). First, the copolymer initiated with amphotericin B **72D** only revealed the methyl group of the glycoside (peaks *m*, 1.28 ppm, **Figure 81**) and we did not observe the aromatic protons that we

Chapter 5. Macromolecular engineering of antimicrobial polypeptoids: star and drug-conjugate polymers

attributed before deprotection (6.0-6.5 ppm). Degradation of the aromatic part was discarded as the aqueous solution of this copolymer produced a clear brown coloration (data not shown) thus, we hypothesized the presence of nano aggregates in the solution due to the high hydrophobicity of the antibiotic. In addition, we observed the signals corresponding to the polymer backbone (peaks *a,a'*), Nlys side chains (peak *b-e*) and Nphe side chains (peak *i,j*). Then, we determined the DP_{NMR} comparing integrations of the signals of the polymer backbone ($-CH_2-$, peak *a,a'*) to the integrations of the signals from the macroinitiator (CH_3 , 1.28 ppm, peak *m*). We found a DP_{NMR} of 28 that was close to the expected one (**Table 61**). Then we determined the hydrophobic content by comparison of the signals of the Nlys moiety (peaks *c,d*) with the peak of the aromatic group in Nphe (peak *j*). Interestingly, we confirmed the hydrophobic content of 37% already established before deprotection on the 1H -NMR analysis performed in $DMSO-d_6$.

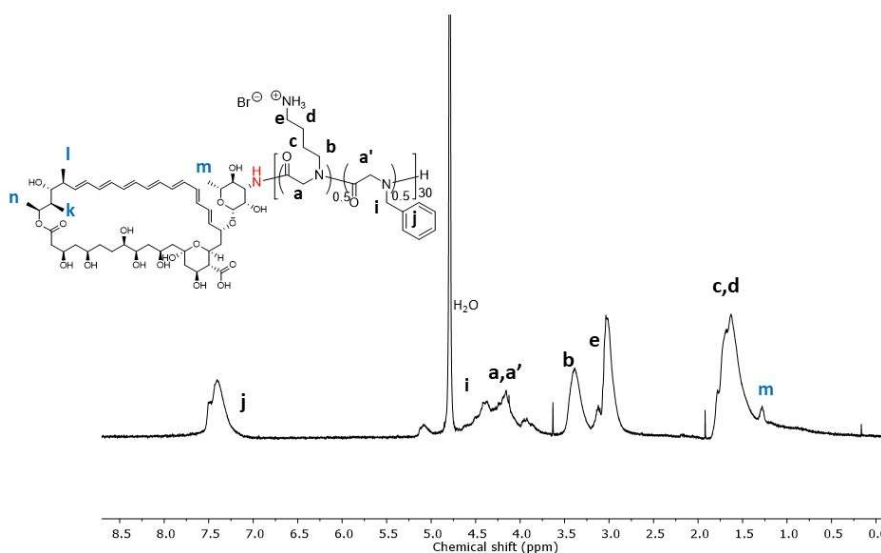


Figure 81. 1H -NMR spectra in D_2O of the amphotericin-*P*(Nlys-Nphe) conjugate **72D** (upon deprotection).

Then, we analyzed by 1H -NMR in D_2O the copolymer initiated with Nystatin (**73D**, **Figure 82**). We observed the signals corresponding to the polymer backbone (peaks *a,a'*), Nlys side chains (peak *b-e*) and Nphe side chains (peak *i,j*). We also observed the methyl group of the glucoside in nystatin (1.28 ppm, peak *m*, **Figure 82**) but we did not observe the expected aromatic protons (5.5-6.5 ppm, before deprotection). Degradation of the aromatic part was discarded as the aqueous solution of this copolymer produced a clear orange coloration (data not shown) thus, we hypothesized the presence of nano aggregates in the solution due to the high hydrophobicity of the antibiotic. We determined the DP_{NMR} by comparing integrations of the signals of the polymer

Chapter 5. Macromolecular engineering of antimicrobial polypeptoids: star and drug-conjugate polymers

backbone ($-\text{CH}_2-$, peak a,a') to the signals from the macroinitiator (CH_3 , 1.28 ppm, peak m) and we found a DP_{NMR} of 30 (**Table 61**) in agreement with the value before deprotection. Finally, we determined the hydrophobic content by comparing of the signals of the Nlys moiety (peaks c,d) with the peak of the aromatic group in Nphe (peak j). We calculated a hydrophobic content of 44% similar to the one obtained before deprotection.

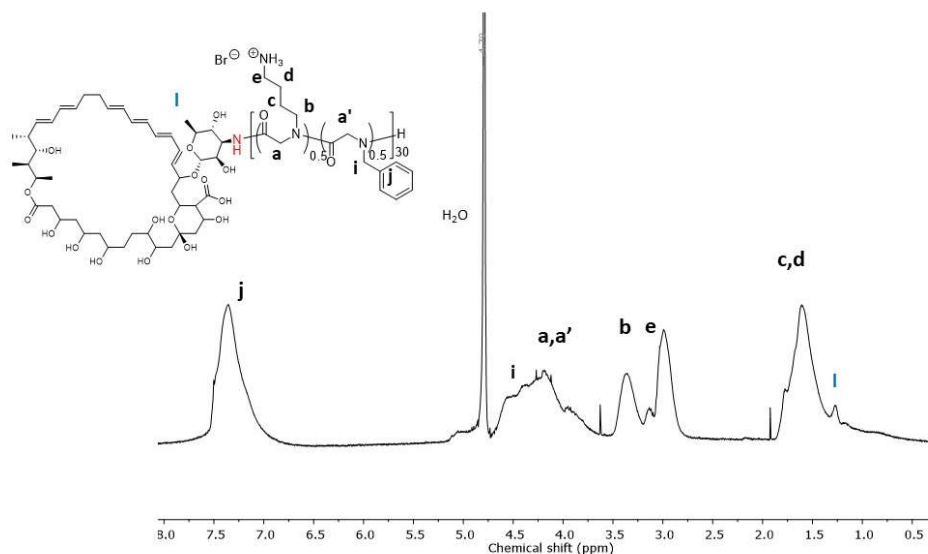


Figure 82. ^1H -NMR spectra in D_2O of the nystatin- $P(\text{Nlys-Nphe})$ conjugate **73D** (upon deprotection).

Analysis of the copolymer initiated with sulfamethoxazole (**74D**) in D_2O revealed signals corresponding to the polymer backbone (peaks a,a'), Nlys side chains (peak $b-e$) and Nphe side chains (peak i,j , **Figure 83**). However, we could not identify signals of the sulfamethoxazole initiator in contrast with the protected analog $\text{dc-P}(\text{ZNlys-Nphe})$ **74**. Then, we determined the hydrophobic content by comparison of the signals of the Nlys moiety (peaks c,d) with the peak of the aromatic group in Nphe (peak j) we found a value of hydrophobic content in agreement with the value before deprotection (50%, **Table 61**).

The copolymer initiated with vancomycin, **75D**, was also analyzed by ^1H -NMR in D_2O and we observed the signals corresponding to the polymer backbone (peaks a,a'), Nlys side chains (peak $b-e$) and Nphe side chains (peak i,j). We observed all the signals of vancomycin, the most representative were methyl groups (2CH_3 , 0.88 ppm, peak k,k' , **Figure 84**) demonstrating the conjugation antibiotic copolypeptoid. This signal allowed us to determine the DP_{NMR} by compari-

Chapter 5. Macromolecular engineering of antimicrobial polypeptoids: star and drug-conjugate polymers

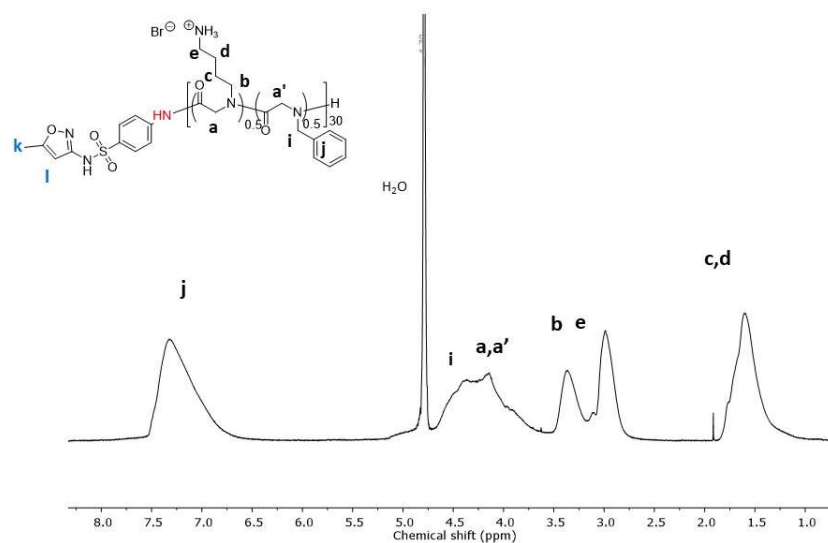


Figure 83. ¹H-NMR spectra in D₂O of the sulfamethoxazole-*P(Nlys-Nphe)* conjugate **74D** (upon deprotection).

son of the integrations from the polymer backbone signal (-CH₂-, peak *a, a'*) to the signals from the macroinitiator (peak *k, k'*) and we found a DP_{NMR} value of 28 in agreement with the value before deprotection (**Table 61**). Then, we determined the hydrophobic content by comparison of the Nlys moiety (peaks *c, d*) with the peak of the aromatic group in Nphe (peak *j*) and we found a hydrophobic content of 51% that was in agreement with the value obtained before deprotection.

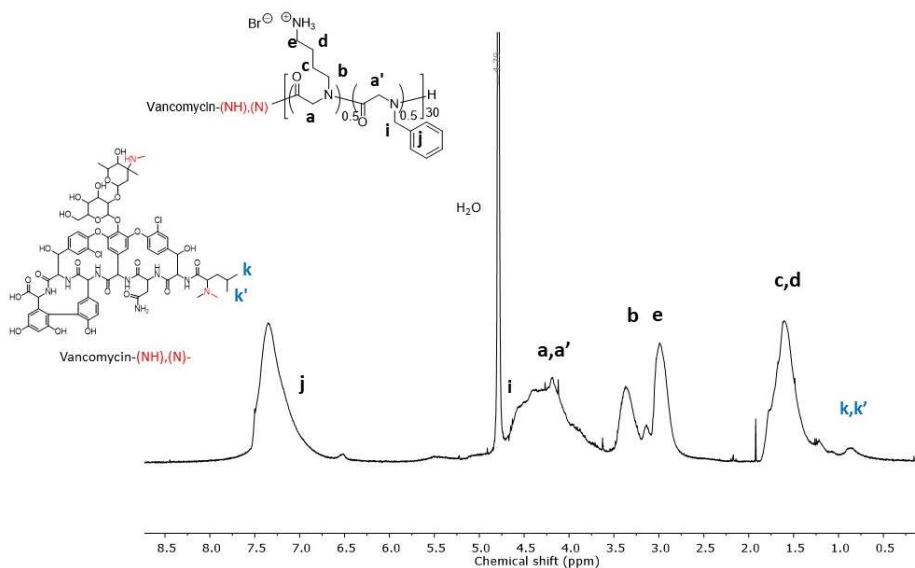


Figure 84. ¹H-NMR spectra in D₂O of the vancomycin-*P(Nlys-Nphe)* conjugate **75D** (upon deprotection).

Chapter 5. Macromolecular engineering of antimicrobial polypeptoids: star and drug-conjugate polymers

Then, we analyzed the copolymer initiated with amikacin **76D** by $^1\text{H-NMR}$ in D_2O and we observed the signals corresponding to the polymer backbone (peaks a, a'), Nlys side chains (peak $b-e$) and Nphe side chains (peak i, j). Interestingly, we observe signals of the macroinitiator amikacin corresponding to the methine protons (2CH , 5.53 and 5.17 ppm, peaks k, k' , **Figure 85**) thus confirming the conjugation. Then, we determined the DP_{NMR} by comparison of the integrations from the polymer backbone signal ($-\text{CH}_2-$, peak a, a') to the signals from the macroinitiator (peak k, k') and we found a value of $\text{DP}_{\text{NMR}} = 27$ in agreement with the value before deprotection (**Table 61**). Later, we determined the hydrophobic content by comparison of the Nlys moiety (peaks c, d) with the peak of the aromatic group in Nphe (peak j) and we found a hydrophobic content 51% that also was in agreement with the value before deprotection.

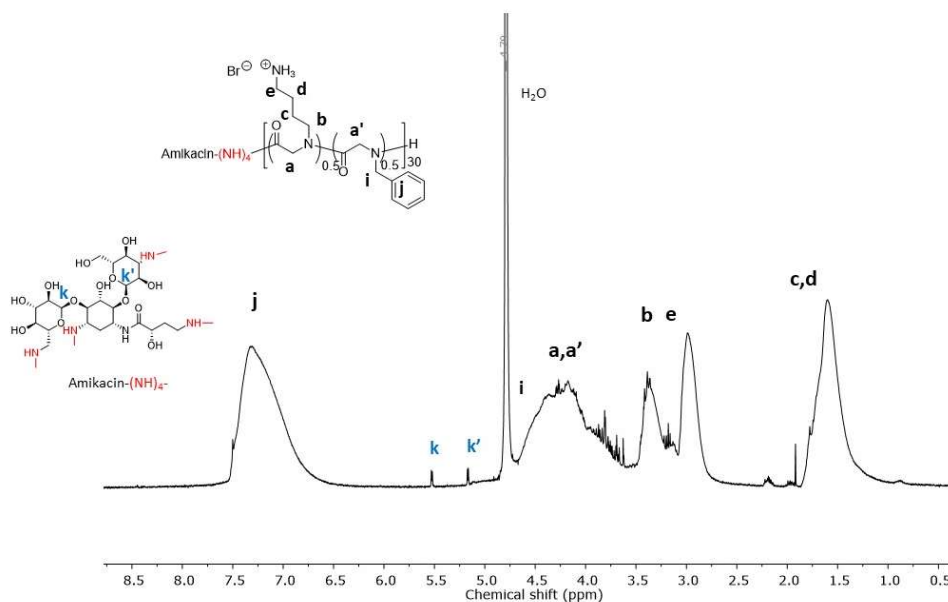


Figure 85. $^1\text{H-NMR}$ spectra in D_2O of the amikacin- $P(\text{Nlys-Nphe})$ conjugate **76D** (upon deprotection).

Finally, we determined the MIC against *C. difficile* and the cytotoxicity towards CaCO-2 cells as we previously studied in chapter 3 and we compared with the linear polypeptoid initiated with allylamine (**42D**) as it we showed in the **Figure 86**. First, the drug-conjugates initiated with sulfamethoxazole (**74D**), vancomycin (**75D**) and amikacin (**76D**) presented values of MIC = 7.8-16.5 $\mu\text{g/mL}$ that were close to the value of **42D**, while the drug-conjugate initiated with nystatin was slightly less active (MIC = 31.2 $\mu\text{g/mL}$) and even less active when we used amphotericin B as initiator (**72D** MIC >250 $\mu\text{g/mL}$). We attributed this low MIC value in **72D** due to the high hydrophobicity of the amphotericin B that could lead to the formation of nano aggregates limiting

Chapter 5. Macromolecular engineering of antimicrobial polypeptoids: star and drug-conjugate polymers

the interaction and destabilization of *C. difficile* membranes. Nonetheless, the values of the drug-conjugates were enough attractive to determine the cytotoxicity over CaCO-2 cells. We observed that the drug-conjugates **73D-76D** were more cytotoxic as compared to the one initiated with allylamine (**Figure 86**). But when we calculated the selectivity indexes, we found that vancomycin- (SI = 15.5) or amikacin-conjugates (SI = 12.2) with polypeptoids presented similar values to **42D**. These two drug-conjugates **75D** and **76D** are an interesting and novel approach to deliver the drugs while killing *C. difficile* and more studies will be carry on this sense.

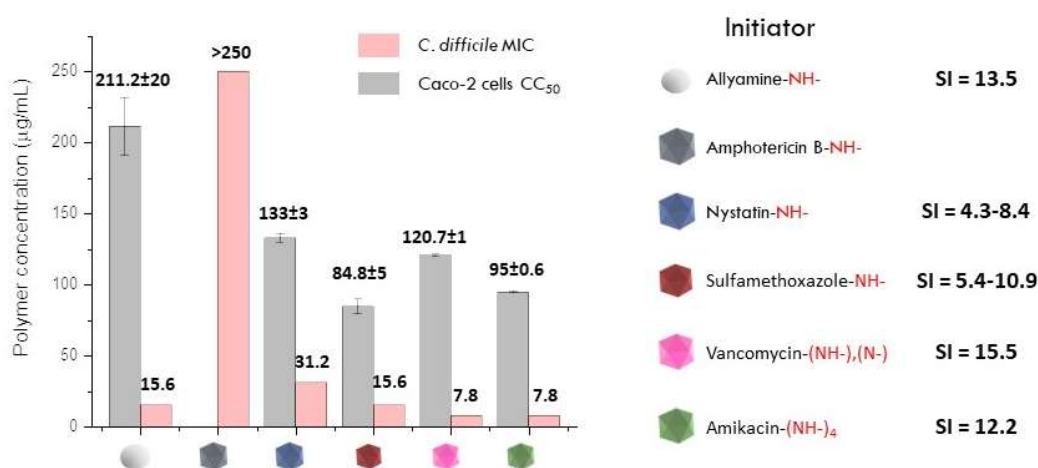


Figure 86. MIC and cytotoxic evaluation of the drug-conjugate polypeptoids, including the selectivity indexes (SI) using different antibiotics as macroinitiators: amphotericin B (**72D**), nystatin (**73D**), sulfamethoxazole (**74D**), vancomycin (**75D**), and amikacin (**76D**). The linear polypeptoid **42D** is also included as a benchmark.

Overall, these characterizations confirmed that we prepared copolymers using antibiotic conjugation by ROP with a controlled hydrophobic content of 50% for dc-P(ZNlys-Nphe)**73-76** and 37% for **72**, with increased molar masses ($M_n > 5000$ g/mol) and with polymer dispersity relatively low ($\mathcal{D}_M < 1.4$). Through the ¹H-NMR we identified that vancomycin and amikacin P(Nlys-Nphe)**75D** and **76D** were conjugated upon the acid deprotection. Furthermore, we found that vancomycin and amikacin as initiators are two platforms with anti-infective properties similar to the copolymer **42D** initiated with allylamine.

3 Conclusion

Overall, thanks to the ROP methodology we were able to prepare star and drug-conjugate copolypeptoids bearing hydrophobic and cationic side chains with potential use as anti-infective agents. First, we prepared star-shaped copolymers by establishing a methodology to perform ROP from PAMAM dendrimers using Sar-NCA. Using the same PAMAM macroinitiators, we prepared star-polymers varying the arm number and the hydrophobic (Nphe) and cationic (NIys) side chains ratio, a controlled hydrophobic content and relatively low polymer dispersity ($D_M < 1.4$). Upon deprotection in acidic conditions, the amphiphilic copolymers demonstrated broad antimicrobial activity. In general, MIC values were found in the range of 15.6-32.5 $\mu\text{g/mL}$ against the Gram-positive bacterium *L. monocytogenes* and a promising MIC of 7.8 $\mu\text{g/mL}$ was found against the anaerobic Gram-negative bacterium *B. fragilis* (with a star-like copolymer constituted of 8 arms, 50% H/C, M/I = 30) and they demonstrated to destabilize liposomal membranes. In a second time, we prepared drug-conjugated copolypeptoids by grafting from antibiotics with a controlled hydrophobic content and low dispersity ($D_M < 1.4$). These drug-conjugate polymers had anti-*C. difficile* activities similar to the benchmark **42D**, specifically the drug-conjugates initiated with vancomycin (**75D**) and amikacin (**76D**, MIC = 7.8 $\mu\text{g/mL}$) and similar selective indexes, SI = 15.6 and 12.2, respectively.

4 Materials and methods

4.1 Materials

All the chemicals and solvents in this work were purchased from Sigma Aldrich, Fluorochem, Acros, TCI, Strem and, unless otherwise described, were used without any purification. Dimethylformamide (DMF), tetrahydrofuran (THF) were obtained from a solvent system purificator (PureSolv, Innovative Technology), kept under argon atmosphere and freshly used. All the initiators were dried under high vacuum for 1 h and then 2 mL of anhydrous toluene was added and gently evaporated under high vacuum for 4 h. MiliQ water was obtained from a (Purelab Prima, ELGA).

4.2 Equipment and measurements

Glovebox

The monomers synthesized were stored at 4 °C under argon atmosphere and weighted in the glovebox Jacomex GP13 No. 2675 at the LCPO (Bordeaux, France).

Infrared (IR) spectroscopy

The IR spectra was recorded using the FTIR spectrometer (Vertex 70, Bruker), and the samples were measured with the ATR (GladiATR, Pike Technologies) from Fisher technologies performing 32 scans at the Laboratoire de Chimie des Polymères Organique (LCPO, Bordeaux, France). The raw data was obtained with the Opus7.5 software and processed using the Originlab 2016 software.

Size-exclusion chromatography (SEC)

Molar masses were determined using three different SEC systems according to the solubility.

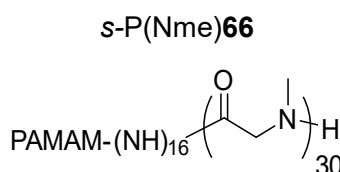
-Samples that were soluble in DMF were carried out using the system DMF/LiBr (1%), in an Ultimate 3000 HPLC System (Thermo Fisher Scientific, France) equipped with Asahipack gel columns (GF310 7.5x300 mm +GD510 7.5x300 mm) for extended temperature organic-based separations coupled to Wyatt-756rEX Refractive Index detector and Dawn Helos II MALS detector. The samples were dissolved in DMF (5 mg/mL) and were run at a flow rate of 0.5 mL/min

Chapter 5. Macromolecular engineering of antimicrobial polypeptoids: star and drug-conjugate polymers

at 50°C. The chromatograms were recorded with the Chromeleon 7.2 software and Astra 7.1.0 software and analyzed using the Originlab 2016 software. Either the molar mass was calculated using a calibration curve or the dn/dc value. The calibration curve was performed with polystyrene standards with molar masses in the range 0.9-364 kg/mol. The dn/dc was determined from the injection of samples dissolved in DMF at 5 mg/L.

4.3 Star-like polysarcosine

Synthesis of star-poly(*N*-methylglycine S-P(Nme)66. *N*-Methyl-NCA monomer (Sar-NCA, 0.1 g, 8.7×10^{-4} mol, 480 equiv.) was weighed in a glovebox under pure argon, introduced in a flame-dried Schlenck vessel, and dissolved with 4 mL of anhydrous DMF. In another Schlenck vessel PAMAM-(NH₂)₁₆ 29.5 mg (20% w/t in MeOH, 1.81×10^{-6} mol, 1 equiv.) was dried and dissolved with 4.7 mL of anhydrous DMF. The monomer solution was added to the initiator solution with vigorous stirring avoiding cloudiness during the addition. The mixture was stirred at room temperature under argon until completion and confirmed by FTIR. The polymer was then recovered by precipitation in diethyl ether and dried under high vacuum. Yield: 87% (0.059 g, white solid).



Molar mass (SEC in DMF, dn/dc = 0.0942): $M_n = 3.50 \times 10^4$ g/mol $D_M = 1.11$

¹H-NMR DMSO-d₆ 400MHz δ (ppm): 2.50-3.10 (m, 3H, CH₃), 3.80-4.42 (m, 2H, CH₂).

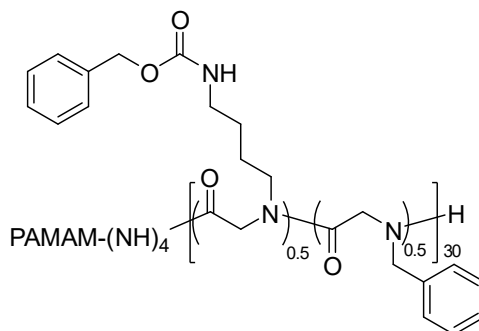
4.4 Star-copolymers preparation

Star-poly[(*Z*-*N*-aminobutylglycine)-(*N*-benzylglycine)] [S-P(ZNlys-Nphe)67]. *N*-(Cbz-(2-aminobutyl))-NCA (ZLys-NNCA, 0.2 g, 6.53×10^{-4} mol, 60 equiv.) and *N*-benzyl-NCA (Phe-NNCA, 124.8 mg, 6.53×10^{-4} mol, 60 equiv.) were weighed in a glovebox under pure argon, introduced in a flame-dried Schlenck vessel, and dissolved with 6 mL of anhydrous DMF. In another Schlenck vessel PAMAM-(NH₂)₄ 28.1 mg (20% w/w in MeOH, 1.09×10^{-5} mol, 1 equiv.) was dried and dissolved with 7 mL of anhydrous DMF. The monomer solution was added to the initiator solution with vigorous stirring avoiding cloudiness during the addition. The mixture was stirred at room temperature under argon until completion and confirmed by FTIR. The polymer was then recovered by precipitation in diethyl ether and dried under high vacuum. Yield: 45%

Chapter 5. Macromolecular engineering of antimicrobial polypeptoids: star and drug-conjugate polymers

(0.122 g, yellowish solid).

S-P(ZNlys-Nphe)**67**



SEC (DMF, dn/dc = 0.0816): 12000 g/mol, $\bar{M}_w = 1.18$

Hydrophobic content calculation by comparison of Ar (6.94-7.47 ppm) and 2CH₂ (1.12-1.65 ppm) according to:

$$\text{H/C}\% = \frac{\frac{XH_{Ar}}{6}}{\left(\frac{4H_{CH}}{4} + \frac{XH_{Ar}}{6}\right)} * 100$$

$$\text{H/C}\% = 49\%$$

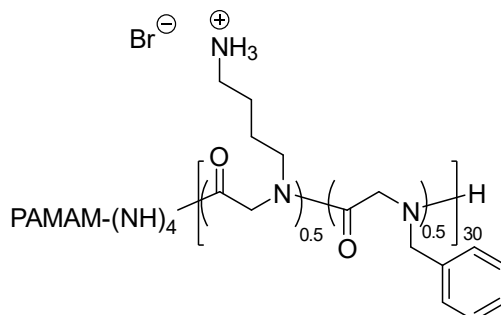
¹H-NMR DMSO-d₆ 400MHz δ (ppm): 1.12-1.65 (m, 4H, 2CH₂), 2.86-3.02 (m, 2H, CH₂), 3.07- 3.27 (m, 2H, CH₂), 3.75-4.48 (m, 2H, CH₂), 4.87-5.09 (m, 2H, CH₂), 6.94-7.47 (m, 5.84H, Ar+NHCO). We could not observe the CH₂ of the benzyl group approx. 4.5 ppm.

Deprotection method to prepare Star-poly[(N-aminobutylglycine)-(N-benzylglycine)].

In a test tube, 100 mg of S-ZPG1 (1.9×10^{-4} mol, MW = 262.32 g/mol monomer unit and taking into account as 50% mol) were completely dissolved with 1 mL of trifluoroacetic acid. To the polymer solution, 68.5 μ L of HBr 33% (3.8×10^{-4} mol) was added and the solution was stirred at 20 °C for 3 hours. Then, the polymer was precipitated on diethyl ether, centrifuged at 4000 rpm the supernatant was removed, the solid was resuspended in 1 mL of water and the pH was adjusted to pH = 7 with a NaHCO₃ saturated solution. The solutions were dialyzed using regenerated cellulose membranes (MWCO 10 kDa), the first time with Milli-Q water, followed by phosphates buffer pH = 7 (0.05 M) and two replacements with Milli-Q water. The solutions were freeze-dried (BenchTop Pro, SP Scientific). Upon freeze-drying, the copolymer was recovered as a yellowish powder in 21% yield (0.0185 g).

Chapter 5. Macromolecular engineering of antimicrobial polypeptoids: star and drug-conjugate polymers

S-P(Nlys-Nphe)67D



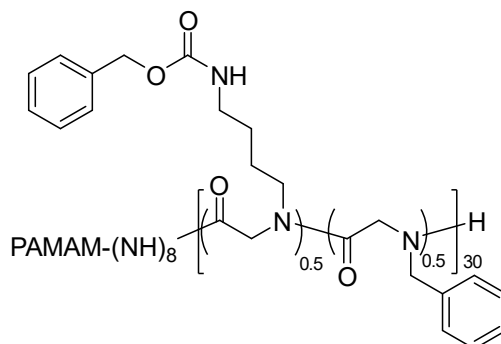
Calculated hydrophobic content by comparison of 2CH₂ (1.37-1.92 ppm) and Ar (6.93-7.39 ppm) according to:

$$H/C\% = \frac{\frac{XH_{Ar}}{5}}{\left(\frac{4H_{CH}}{4} + \frac{XH_{Ar}}{5}\right)} * 100$$

$$H/C\% = 52\%$$

¹H-NMR D₂O 400 MHz δ (ppm): 1.34-1.92 (m, 4H, 2CH₂), 2.75-3.04 (m, 2H, CH₂), 3.09-3.35 (m, 2H, CH₂), 3.373-4.63 (m, 4H, 2CH₂), 6.93-7.39 (m, 5.2H, Ar).

S-P(ZNlys-Nphe)68



Yield: 43% (0.118 g, yellowish solid)

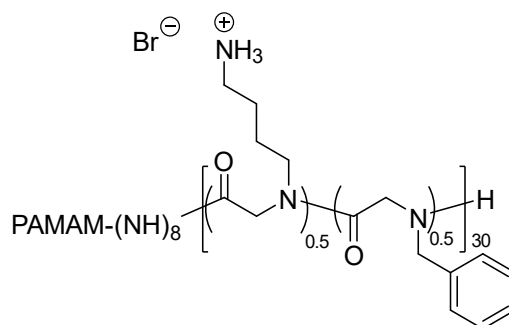
SEC (DMF, dn/dc = 0.0816): 17500 g/mol, Đ_M = 1.36

Hydrophobic content calculation by comparison of Ar (6.94-7.47 ppm) and 2CH₂ (1.12-1.65 ppm) = 51%.

Chapter 5. Macromolecular engineering of antimicrobial polypeptoids: star and drug-conjugate polymers

$^1\text{H-NMR}$ DMSO- d_6 400 MHz δ (ppm): 1.12-1.65 (m, 4H, 2CH₂), 2.86-3.02 (m, 2H, CH₂), 3.07- 3.27 (m, 2H, CH₂), 3.75-4.48 (m, 2H, CH₂), 4.87-5.09 (m, 2H, CH₂), 6.94-7.47 (m, 6.15H, Ar+NHCO). We could not observe the CH₂ of the benzyl group approx. 4.5 ppm.

S-P(NIlys-Nphe)**68D**

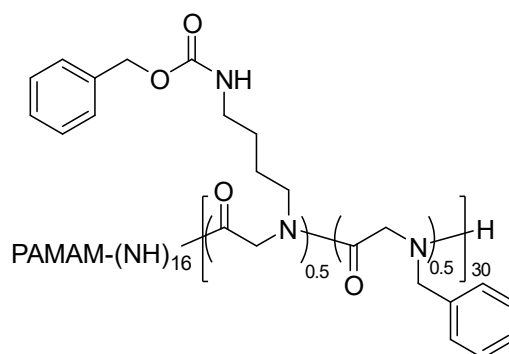


Yield: 41% (0.036 g, yellowish solid)

Calculated hydrophobic content by comparison of Ar (1.37-1.92 ppm) and 2CH₂ (6.93-7.39 ppm) = 55%

$^1\text{H-NMR}$ D₂O 400 MHz δ (ppm): 1.34-1.92 (m, 4H, 2CH₂), 2.75-3.04 (m, 2H, CH₂), 3.09-3.35 (m, 2H, CH₂), 3.373-4.63 (m, 4H, 2CH₂), 6.93-7.39 (m, 5.48H, Ar).

S-P(ZNIlys-Nphe)**69**



Yield: 40% (0.11 g, yellowish solid)

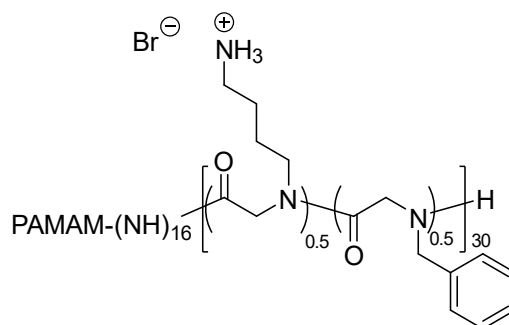
SEC (DMF, dn/dc = 0.0816): 35900 g/mol, $\bar{M}_w = 1.40$

Hydrophobic content calculation by comparison of Ar (6.94-7.47 ppm) and 2CH₂ (1.12-1.65 ppm) = 52%.

Chapter 5. Macromolecular engineering of antimicrobial polypeptoids: star and drug-conjugate polymers

$^1\text{H-NMR}$ DMSO- d_6 400 MHz δ (ppm): 1.12-1.65 (m, 4H, 2CH_2), 2.86-3.02 (m, 2H, CH_2), 3.07- 3.27 (m, 2H, CH_2), 3.75-4.48 (m, 2H, CH_2), 4.87-5.09 (m, 2H, CH_2), 6.94-7.47 (m, 6.42H, Ar+NHCO). We could not observe the CH_2 of the benzyl group approx. 4.5 ppm.

S-P(NIlys-Nphe)**69D**

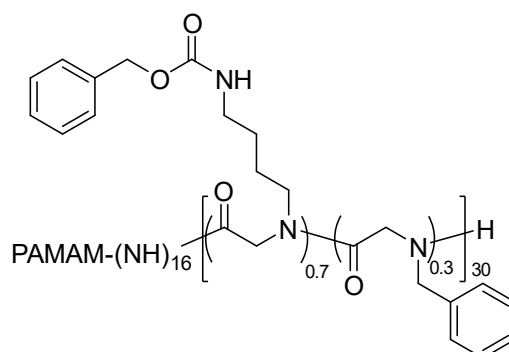


Yield: 62% (0.054 g, yellowish solid)

Calculated hydrophobic content by comparison of Ar (1.37-1.92 ppm) and 2CH_2 (6.93-7.39 ppm) = 53%

$^1\text{H-NMR}$ D₂O 400 MHz δ (ppm): 1.34-1.92 (m, 4H, 2CH_2), 2.75-3.04 (m, 2H, CH_2), 3.09-3.35 (m, 2H, CH_2), 3.373-4.63 (m, 4H, 2CH_2), 6.93-7.39 (m, 5.32H, Ar).

S-P(ZNIlys-Nphe)**70**



Yield: 39% (0.12 g, yellowish solid)

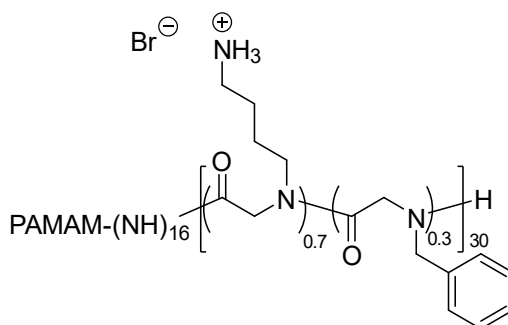
SEC (DMF, $dn/dc = 0.0816$): 36200 g/mol, $D_M = 1.41$

Hydrophobic content calculation by comparison of Ar (6.94-7.47 ppm) and 2CH_2 (1.12-1.65 ppm) = 51%.

Chapter 5. Macromolecular engineering of antimicrobial polypeptoids: star and drug-conjugate polymers

$^1\text{H-NMR}$ DMSO- d_6 400 MHz δ (ppm): 1.12-1.65 (m, 4H, 2CH₂), 2.86-3.02 (m, 2H, CH₂), 3.07- 3.27 (m, 2H, CH₂), 3.75-4.48 (m, 2H, CH₂), 4.87-5.09 (m, 2H, CH₂), 6.94-7.47 (m, 6.13H, Ar+NHCO). We could not observe the CH₂ of the benzyl group approx. 4.5 ppm.

S-P(NIlys-Nphe)70D

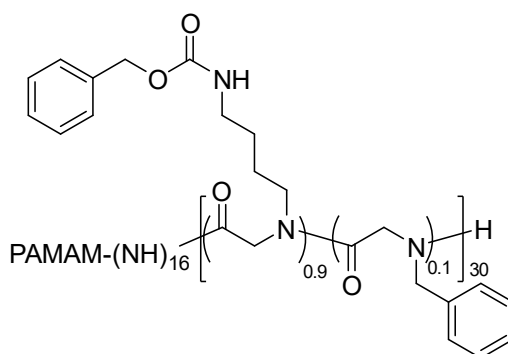


Yield: 55% (0.0486 g, yellowish solid)

Calculated hydrophobic content by comparison of Ar (1.37-1.92 ppm) and 2CH₂ (6.93-7.39 ppm) = 35%

$^1\text{H-NMR}$ D₂O 400 MHz δ (ppm): 1.34-1.92 (m, 4H, 2CH₂), 2.75-3.04 (m, 2H, CH₂), 3.09-3.35 (m, 2H, CH₂), 3.373-4.63 (m, 4H, 2CH₂), 6.93-7.39 (m, 3.47H, Ar).

S-P(ZNIlys-Nphe)71



Yield: 45% (0.148 g, yellowish solid)

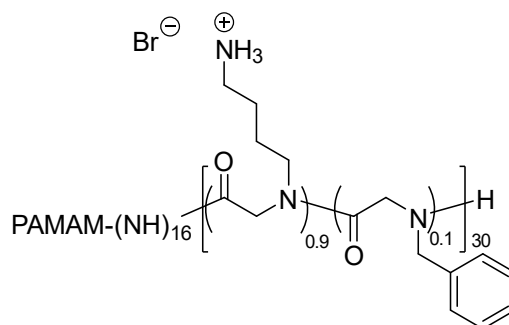
SEC (DMF, dn/dc = 0.0816): 40500 g/mol, $\bar{M}_w = 1.30$

Hydrophobic content calculation by comparison of Ar (6.94-7.47 ppm) and 2CH₂ (1.12-1.65 ppm) = 50%.

Chapter 5. Macromolecular engineering of antimicrobial polypeptoids: star and drug-conjugate polymers

$^1\text{H-NMR}$ DMSO- d_6 400 MHz δ (ppm): 1.12-1.65 (m, 4H, 2CH₂), 2.86-3.02 (m, 2H, CH₂), 3.07- 3.27 (m, 2H, CH₂), 3.75-4.48 (m, 2H, CH₂), 4.87-5.09 (m, 2H, CH₂), 6.94-7.47 (m, 5.97H, Ar+NHCO). We could not observe the CH₂ of the benzyl group approx. 4.5 ppm.

S-P(Nlys-Nphe)71D



Yield: 42% (0.0431 g, yellowish solid)

Calculated hydrophobic content by comparison of Ar (1.37-1.92 ppm) and 2CH₂ (6.93-7.39 ppm) = 12%

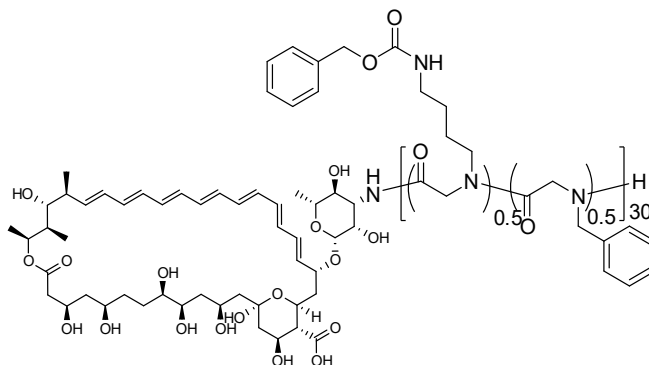
$^1\text{H-NMR}$ D₂O 400 MHz δ (ppm): 1.34-1.92 (m, 4H, 2CH₂), 2.75-3.04 (m, 2H, CH₂), 3.09-3.35 (m, 2H, CH₂), 3.373-4.63 (m, 4H, 2CH₂), 6.93-7.39 (m, 1.19H, Ar).

4.5 Drug conjugates-copolymers preparation

Amphotericin B-poly[(Z-N-aminobutylglycine)-(N-benzylglycine)] [dc-P(ZNlys-Nphe)72]. *N*-(Cbz-(2-aminobutyl))-NCA (ZLys-NNCA, 0.2 g, 6.53x10⁻⁴ mol, 15 equiv.) and *N*-benzyl-NCA (Phe-NNCA, 124.8 mg, 6.53x10⁻⁴ mol, 15 equiv.) were weighed in a glovebox under pure argon, introduced in a flame-dried Schlenk vessel, and dissolved with 6 mL of anhydrous DMF. In another Schlenk vessel Amphotericin-(NH₂) 47.3 mg (85%, 4.35x10⁻⁵ mol, 1 equiv.) was dried and dissolved with 7 mL of anhydrous DMF. The monomer solution was added to the initiator solution with vigorous stirring avoiding cloudiness during the addition. The mixture was stirred at room temperature under argon until completion and confirmed by FTIR. The polymer was then recovered by precipitation in diethyl ether and dried under high vacuum.

dc-P(ZNlys-Nphe)72

Chapter 5. Macromolecular engineering of antimicrobial polypeptoids: star and drug-conjugate polymers



Yield: 68% (0.209 g, brownish solid)

SEC (DMF, $dn/dc = 0.0816$): 6400 g/mol, $D_M = 1.17$

DP_{NMR} (from CH_2 signal at 3.80-4.54 ppm) = 30

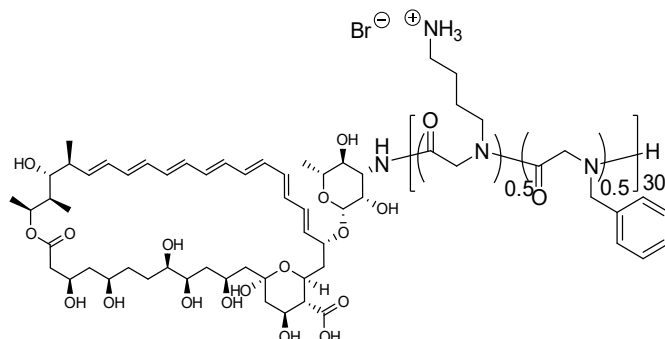
Hydrophobic content (from signals 1.20-1.62 ppm and 7.05-7.45 ppm) = 37%

1H -NMR DMSO- d_6 400 MHz δ (ppm): 0.91 (d, $J=6.7$ Hz, 3H, CH_3 initiator), 1.04 (d, $J=5.9$ Hz, 3H, CH_3 initiator), 1.09-1.14 (m, 3H, CH_3 initiator), 1.15 (s, 3H, CH_3 initiator), 1.20-1.62 (m, 107H, 2 CH_2), 1.72 (br, 1H CH initiator), 1.99 (br, 1H CH initiator), 2.16-2.28 (br, 3H initiator), 2.84-3.06 (m, 50H, CH_2), 3.06-3.25 (m, 45H, CH_2), 3.80-4.54 (m, 59H, CH_2), 4.90-5.08 (m, 46H, CH_2 initiator), 5.20 (br, 1H, CH initiator), 5.45 (br, 1H, CH initiator), 5.87-6.46 (m, 12H, CH initiator), 7.05-7.45 (m, 161H, 2Ar+NHCO). We could not observe several signals of the amphotericin B due to overlapping and we did not observe the CH_2 of the Nphe moiety.

Deprotection method to prepare amphotericin B-poly[(N-aminobutylglycine)-(N-benzylglycine)] [dc-P(Nlys-Nphe)72D]. In a test tube, 150 mg of S-ZPG1 (2.86×10^{-4} mol, MW = 262.32 g/mol monomer unit and taking into account as 50% mol) were completely dissolved with 1.5 mL of trifluoroacetic acid. To the polymer solution, 102.8 μ L of HBr 33% (5.72×10^{-4} mol, 2 equiv.) was added and the solution was stirred at 20 °C for 3 hours. Then, the polymer was precipitated on diethyl ether, centrifuged at 4000 rpm the supernatant was removed, the solid was resuspended in 1 mL of water and the pH was adjusted to pH = 7 with a $NaHCO_3$ saturated solution. The solutions were dialyzed using regenerated cellulose membranes (MWCO 10 kDa), the first time with Milli-Q water, followed by phosphates buffer pH = 7 (0.05 M) and two replacements with Milli-Q water. The solutions were freeze-dried (BenchTop Pro, SP Scientific). Upon freeze-drying, the copolymer was recovered as a brownish powder in 90% yield (0.12 g).

Chapter 5. Macromolecular engineering of antimicrobial polypeptoids: star and drug-conjugate polymers

dc-P(Nlys-Nphe)72D

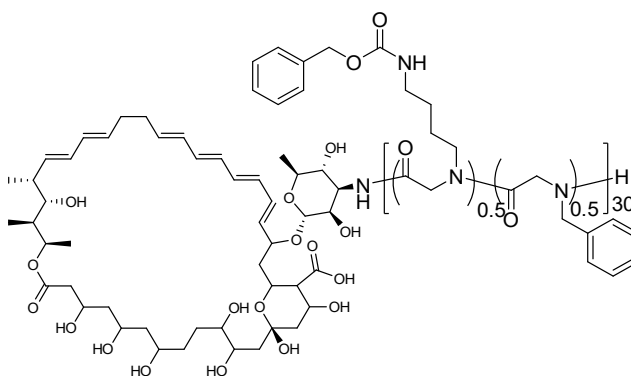


DP_{NMR} (from the signal 2CH₂ at 3.37-4.64 ppm) = 28

Hydrophobic content (from signals at 1.34-1.92 ppm and 7.00-7.64 ppm) = 37%

¹H-NMR D₂O 400 MHz δ (ppm): 1.28 (s, 3H, CH₃ initiator), 1.34-1.92 (m, 100H, 2CH₂), 2.75-3.09 (m, 89H, CH₂), 3.12 (m, 4H, CH), 3.26-3.57 (m, 59H, CH₂), 3.37-4.64 (m, 110H, 2CH₂), 5.08 (m, 8H, CH initiator), 7.00-7.64 (m, 74H, Ar). We could not observe several signals of the antibiotic due to overlapping and high hydrophobicity.

dc-P(ZNlys-Nphe)73



74% yield (0.198 g, orange solid)

SEC (DMF, dn/dc = 0.0816): 9300 g/mol, Đ_M = 1.30

DP_{NMR} (from the signal CH₂ at 3.73-4.38 ppm) = 30

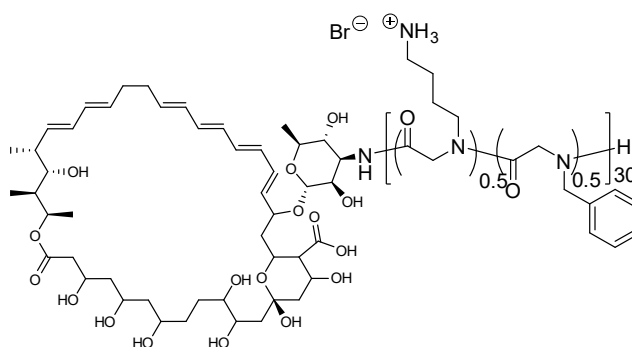
Hydrophobic content (from signals at 1.17-1.65 ppm and 6.91-7.70 ppm) = 43%

¹H-NMR DMSO-d₆ 400 MHz δ (ppm): 0.87 (m, 6H, 2CH₃ initiator), 1.01-1.16 (m, 6H, 2CH₃ initiator), 1.17-1.65 (m, 70H, 2CH₂), 1.80 (br, 2H, CH₂ initiator), 2.06-2.29 (m, 10H, 5CH₂+2CH

Chapter 5. Macromolecular engineering of antimicrobial polypeptoids: star and drug-conjugate polymers

initiator), 2.85-3.06 (m, 31H, CH₂), 3.06-3.25 (m, 31H, CH₂), 3.73-4.38 (m, 59H, 2CH₂ polymer), 4.40-4.70 (m, 30H, CH₂), 4.86-5.11 (m, 22H, CH), 5.43-5.74 (br, 4H, 4CH initiator), 5.83-6.03 (m, 4H, 4CH initiator), 6.05-6.32 (br, 4H, 4CH initiator), 6.91-7.70 (m, 147H, 2Ar+NHCO). We could not observe several signals due to overlapping.

dc-P(Nlys-Nphe)**73D**



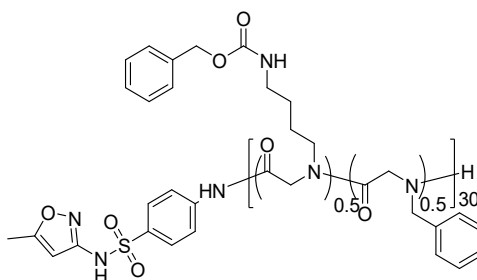
96% yield (0.15 g, yellowish solid)

DP_{NMR} (from the signal 2CH₂ at 3.37-4.64 ppm) = 30

Hydrophobic content (from signals at 1.34-1.92 ppm and 6.94-7.62 ppm) = 44%

¹H-NMR D₂O 400 MHz δ (ppm): 1.27 (s, 3H, CH₃ initiator), 1.34-1.92 (m, 100H, 2CH₂), 2.75-3.09 (m, 49H, CH₂ polymer), 3.13 (m, 5H, CH), 3.17-3.57 (m, 35H, CH₂), 3.37-4.64 (m, 120H, 2CH₂), 5.08 (m, 2H, CH), 6.94-7.62 (m, 98H, Ar). We could not observe several signals of the antibiotic due to overlapping and high hydrophobicity.

dc-P(ZNlys-Nphe)**74**



66% yield (0.175 g, yellowish solid)

SEC (DMF, dn/dc = 0.0816): 5600 g/mol, Đ_M = 1.31

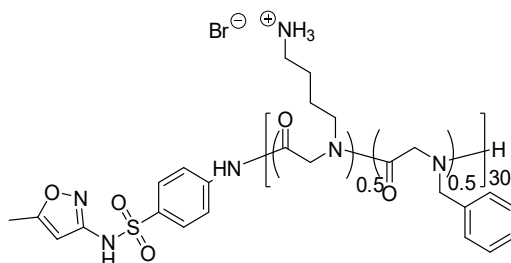
Chapter 5. Macromolecular engineering of antimicrobial polypeptoids: star and drug-conjugate polymers

DP_{NMR} (from the signal CH_2 at 3.73-4.38 ppm) = 54

Hydrophobic content (from signals at 1.15-1.65 ppm and 6.87-7.70 ppm) = 49%

1H -NMR DMSO- d_6 400 MHz δ (ppm): 1.15-1.65 (m, 121H, 2 CH_2), 2.11 (br, 3H, CH_3 initiator), 2.85-3.06 (m, 65H, CH_2), 3.06-3.25 (br, 44H, CH_2), 3.73-4.38 (m, 108H, CH_2), 4.40-4.70 (m, 59H, CH_2), 4.86-5.11 (m, 65H, CH), 5.81 (br, 1H, CH initiator), 6.87-7.70 (m, 327H, 2Ar+NHCO). We could not observe several signals due to overlapping.

dc-P(Nlys-Nphe)**74D**



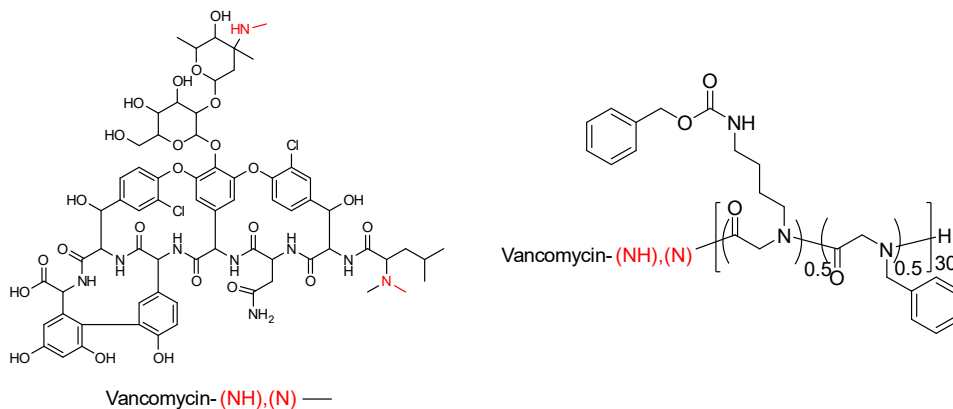
98% yield (0.133 g, yellowish solid)

No DP_{NMR} is given since we could not observe initiator signals

Hydrophobic content (from signals at 1.05-1.86 ppm and 6.57-7.74 ppm) = 50%

1H -NMR D_2O 400 MHz δ (ppm): 1.05-1.86 (m, 4H, 2 CH_2), 2.75-3.09 (m, 2H, CH_2), 3.17-3.57 (m, 2H, CH_2), 3.66-4.68 (m, 4H, 2 CH_2), 6.57-7.74 (m, 5H, Ar). We could not observe the signals of sulfamethoxazole.

dc-P(ZNlys-Nphe)**75**



Chapter 5. Macromolecular engineering of antimicrobial polypeptoids: star and drug-conjugate polymers

62% yield (0.165 g, yellowish solid)

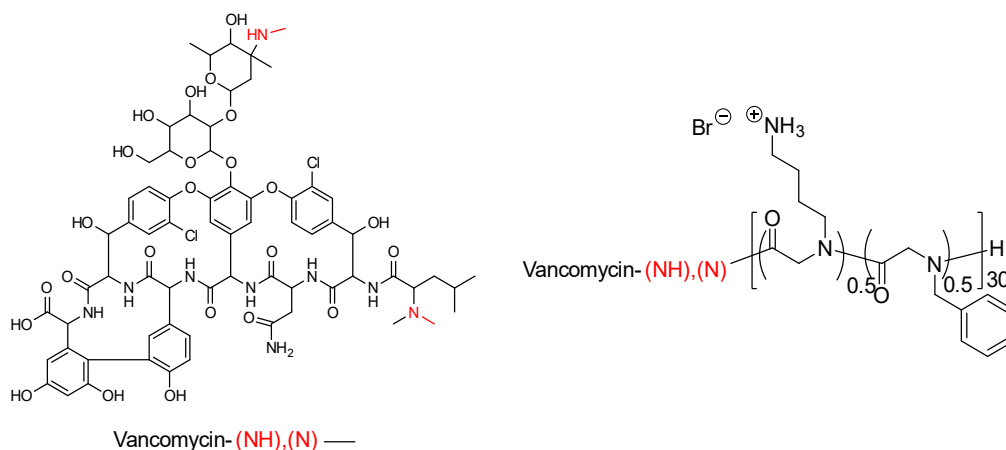
SEC (DMF, $dn/dc = 0.0816$): 9400 g/mol, $D_M = 1.40$

DP_{NMR} (from the signal $2CH_2$ at 3.74-4.29 ppm) = 31

Hydrophobic content (from signals at 1.19-1.56 ppm and 6.87-7.73 ppm) = 49%

1H -NMR DMSO- d_6 400 MHz δ (ppm): 0.84 (m, 6H, $2CH_3$ initiator), 1.19-1.56 (m, 143H, $2CH_2$), 2.81-3.06 (m, 82H, CH_2), 3.07-3.26 (m, 60H, CH_2), 3.74-4.29 (m, 123H, $2CH_2$), 4.40-4.70 (m, 74H, CH_2), 4.86-5.11 (m, 67H, CH), 6.87-7.73 (m, 384H, $2Ar+NHCO$). We could not observe several signals of vancomycin due to overlapping.

dc-P(Nlys-Nphe)**75D**



98% yield (0.125 g, yellowish solid)

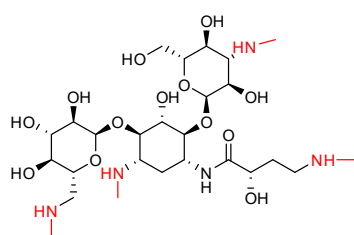
DP_{NMR} (from the signal $2CH_2$ at 3.62-4.65 ppm) = 28

Hydrophobic content (from signals at 1.28-1.92 ppm and 6.64-7.72 ppm) = 51%

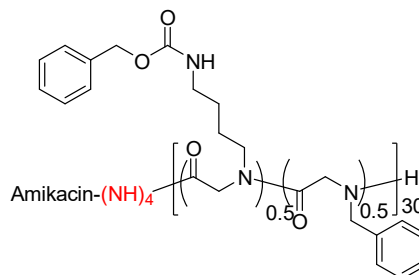
1H -NMR D_2O 400 MHz δ (ppm): 0.88 (s, 3H, CH_3 initiator), 1.28-1.92 (m, 167H, $2CH_2$), 2.75-3.09 (m, 85H, CH_2 polymer), 3.21-3.57 (m, 69H, CH_2), 3.62-4.65 (m, 227H, $2CH_2$), 5.47 (br, 3H, CH), 6.64-7.72 (m, 218H, Ar). We could not observe several signals of vancomycin due to overlapping.

dc-P(ZNlys-Nphe)**76**

Chapter 5. Macromolecular engineering of antimicrobial polypeptoids: star and drug-conjugate polymers



Amikacin-(NH)₄ —



48% yield (0.129 g, yellowish solid)

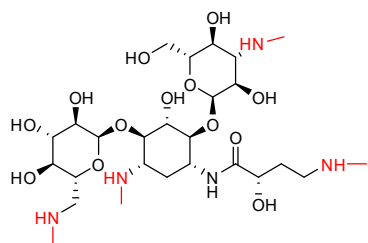
SEC (DMF, dn/dc = 0.0816): 20000 g/mol, $\bar{M}_n = 1.13$

No DP_{NMR} is given since we could not observe initiator signals

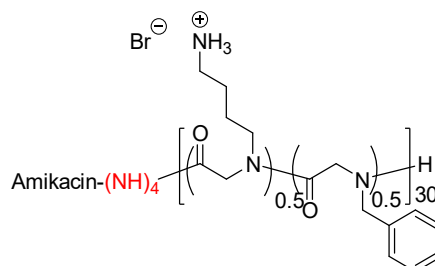
Hydrophobic content (from signals 1.12-1.65 ppm and 6.68-7.66 ppm) = 50%

¹H-NMR DMSO-d₆ 400 MHz δ (ppm): 1.12-1.65 (m, 4.6H, 2CH₂), 2.85-3.06 (m, 2.4H, CH₂), 3.08-3.25 (m, 1.8H, CH₂), 3.76-4.29 (m, 4H, 2CH₂), 4.30-4.77 (m, 2.4H, CH₂), 4.81-5.19 (m, 2.4H, CH), 6.68-7.66 (m, 12.7H, 2Ar+NHCO). We could not observe initiator signals due to overlapping.

dc-P(Nlys-Nphe)76D



Amikacin-(NH)₄ —



90% yield (0.094 g, yellowish solid)

DP_{NMR} (from the signal 2CH₂ at 3.62-4.68 ppm) = 27

Hydrophobic content (from signals 1.12-1.85 ppm and 6.55-7.66 ppm) = 51%

¹H-NMR D₂O 400 MHz δ (ppm): 0.88 (br, 1H, CH initiator), 1.12-1.85 (m, 305H, 2CH₂), 1.97 (m, 1H, CH initiator), 2.19 (m, 2H, CH₂), 2.71-3.11 (m, 168H, CH₂), 3.16-3.48 (m, 134H, CH₂), 3.62-4.68 (m, 435H, 2CH₂), 5.16 (s, 1H, CH initiator), 5.53 (s, 1H, CH initiator), 6.55-7.66 (m, 406H, Ar). We could not observe several signals of amikacin due to overlapping.

Chapter 5. *Macromolecular engineering of antimicrobial polypeptoids: star and drug-conjugate polymers*

4.1 Antimicrobial assay

The analyses were performed as it is described in chapter 3 (pp 186). And for the other bacteria as it is described in chapter 4 (pp 254).

4.2 Cytotoxicity

The analyses were performed as described in chapter 3 (pp 187).

5 References

- (1) Ergene, C.; Yasuhara, K.; Palermo, E. F. Biomimetic Antimicrobial Polymers: Recent Advances in Molecular Design. *Polym. Chem.* **2018**, *9* (18), 2407–2427.
- (2) Lam, S. J.; O'Brien-Simpson, N. M.; Pantarat, N.; Sulistio, A.; Wong, E. H. H.; Chen, Y.-Y.; Lenzo, J. C.; Holden, J. A.; Blencowe, A.; Reynolds, E. C.; Qiao, G. G. Combating Multidrug-Resistant Gram-Negative Bacteria with Structurally Nanoengineered Antimicrobial Peptide Polymers. *Nat. Microbiol.* **2016**, *1* (16162), 1–11.
- (3) Wu, W.; Wang, W.; Li, J. Star Polymers: Advances in Biomedical Applications. *Prog. Polym. Sci.* **2015**, *46*, 55–85.
- (4) Fox, M. E.; Szoka, F. C.; Fréchet, J. M. J. Soluble Polymer Carriers for the Treatment of Cancer: The Importance of Molecular Architecture. *Acc. Chem. Res.* **2009**, *42* (8), 1141–1151.
- (5) Chen, Y. F.; Lai, Y. Da; Chang, C. H.; Tsai, Y. C.; Tang, C. C.; Jan, J. S. Star-Shaped Polypeptides Exhibit Potent Antibacterial Activities. *Nanoscale* **2019**, *11* (24), 11696–11708.
- (6) Shirbin, S. J.; Insua, I.; Holden, J. A.; Lenzo, J. C.; Reynolds, E. C.; O'Brien-Simpson, N. M.; Qiao, G. G. Architectural Effects of Star-Shaped “Structurally Nanoengineered Antimicrobial Peptide Polymers” (SNAPPs) on Their Biological Activity. *Adv. Healthc. Mater.* **2018**, *7* (21), 1–12.
- (7) Pan, M.; Lu, C.; Zheng, M.; Zhou, W.; Song, F.; Chen, W.; Yao, F.; Liu, D.; Cai, J. Unnatural Amino Acid Based Star Shaped Poly(L -Ornithine)s as Emerging Long Term and Biofilm Disrupting Antimicrobial Peptides to Treat *Pseudomonas Aeruginosa* Infected Burn Wounds. *Adv. Healthc. Mater.* **2020**, *9* (19), 2000647.
- (8) Zhang, R.; Jones, M. M.; Moussa, H.; Keskar, M.; Huo, N.; Zhang, Z.; Visser, M. B.; Sabatini, C.; Swihart, M. T.; Cheng, C. Polymer-Antibiotic Conjugates as Antibacterial Additives in Dental Resins. *Biomater. Sci.* **2019**, *7* (1), 287–295.
- (9) Khandare, J.; Minko, T. Polymer-Drug Conjugates: Progress in Polymeric Prodrugs. *Prog. Polym. Sci.* **2006**, *31* (4), 359–397.
- (10) Duncan, R. Polymer Conjugates as Anticancer Nanomedicines. *Nat. Rev. Cancer* **2006**, *6*

- (9), 688–701.
- (11) Zhang, Z.; Jones, M. M.; Sabatini, C.; Vanyo, S. T.; Yang, M.; Kumar, A.; Jiang, Y.; Swihart, M. T.; Visser, M. B.; Cheng, C. Synthesis and Antibacterial Activity of Polymer-Antibiotic Conjugates Incorporated into a Resin-Based Dental Adhesive. *Biomater. Sci.* **2021**, *9* (6), 2043–2052.
- (12) Gillies, E. R.; Dy, E.; Fréchet, J. M. J.; Szoka, F. C. Biological Evaluation of Polyester Dendrimer: Poly(Ethylene Oxide) “Bow-Tie” Hybrids with Tunable Molecular Weight and Architecture. *Mol. Pharm.* **2005**, *2* (2), 129–138.
- (13) Vigliotta, G.; Mella, M.; Rega, D.; Izzo, L. Modulating Antimicrobial Activity by Synthesis: Dendritic Copolymers Based on Nonquaternized 2-(Dimethylamino)Ethyl Methacrylate by Cu-Mediated ATRP. *Biomacromolecules* **2012**, *13* (3), 833–841.
- (14) Yuan, H.; Yu, B.; Fan, L. H.; Wang, M.; Zhu, Y.; Ding, X.; Xu, F. J. Multiple Types of Hydroxyl-Rich Cationic Derivatives of PGMA for Broad-Spectrum Antibacterial and Antifouling Coatings. *Polym. Chem.* **2016**, *7* (36), 5709–5718.
- (15) Mortazavian, H.; Picquet, G. A.; Lejnieks, J.; Zaidel, L. A.; Myers, C. P.; Kuroda, K. Understanding the Role of Shape and Composition of Star-Shaped Polymers and Their Ability to Both Bind and Prevent Bacteria Attachment on Oral Relevant Surfaces. *J. Funct. Biomater.* **2019**, *10* (4).
- (16) Teper, P.; Chojniak-Gronek, J.; Hercog, A.; Oleszko-Torbus, N.; Płaza, G.; Kubacki, J.; Balin, K.; Kowalczyk, A.; Mendrek, B. Nanolayers of Poly(*N,N'*-Dimethylaminoethyl Methacrylate) with a Star Topology and Their Antibacterial Activity. *Polymers (Basel)*. **2020**, *12* (1), 230.
- (17) Zhang, Y.; Song, W.; Li, S.; Kim, D. K.; Kim, J. H.; Kim, J. R.; Kim, I. Facile and Scalable Synthesis of Topologically Nanoengineered Polypeptides with Excellent Antimicrobial Activities. *Chem. Commun.* **2020**, *56* (3), 356–359.
- (18) Aoi, K.; Hatanaka, T.; Tsutsumiuchi, K.; Okada, M.; Imae, T. Synthesis of a Novel Star-Shaped Dendrimer by Radial-Growth Polymerization of Sarcosine *N*-Carboxyanhydride Initiated with Poly(Trimethyleneimine) Dendrimer. *Macromol. Rapid Commun.* **1999**, *20* (7), 378–382.
- (19) Petersen, J. F.; Tortzen, C. G.; Pittelkow, M.; Christensen, J. B. Synthesis and Properties

- of Chiral Internally Branched PAMAM-Dendrimers. *Tetrahedron* **2015**, *71* (7), 1109–1116.
- (20) Ren, J. M.; McKenzie, T. G.; Fu, Q.; Wong, E. H. H.; Xu, J.; An, Z.; Shanmugam, S.; Davis, T. P.; Boyer, C.; Qiao, G. G. Star Polymers. *Chem. Rev.* **2016**, *116* (12), 6743–6836.
- (21) Podzimek, S.; Vlcek, T.; Johann, C. Characterization of Branched Polymers by Size Exclusion Chromatography Coupled with Multiangle Light Scattering Detector. I. Size Exclusion Chromatography Elution Behavior of Branched Polymers. *J. Appl. Polym. Sci.* **2001**, *81* (7), 1588–1594.
- (22) Podzimek, S.; Vlcek, T. Characterization of Branched Polymers by SEC Coupled with a Multiangle Light Scattering Detector. II. Data Processing and Interpretation. *J. Appl. Polym. Sci.* **2001**, *82* (2), 454–460.
- (23) Cal, P. M. S. D.; Matos, M. J.; Bernardes, G. J. L. Trends in Therapeutic Drug Conjugates for Bacterial Diseases: A Patent Review. *Expert Opin. Ther. Pat.* **2017**, *27* (2), 179–189.
- (24) Anju, V. T.; Paramanatham, P.; Siddhardha, B.; Lal, S. B. S.; Sharan, A.; Alyousef, A. A.; Arshad, M.; Syed, A. Malachite Green-Conjugated Multi-Walled Carbon Nanotubes Potentiate Antimicrobial Photodynamic Inactivation of Planktonic Cells and Biofilms of *Pseudomonas Aeruginosa* and *Staphylococcus Aureus*. *Int. J. Nanomedicine* **2019**, *14*, 3861–3874.
- (25) Ibrahim, M. A.; Panda, S. S.; Birs, A. S.; Serrano, J. C.; Gonzalez, C. F.; Alamry, K. A.; Katritzky, A. R. Synthesis and Antibacterial Evaluation of Amino Acid-Antibiotic Conjugates. *Bioorganic Med. Chem. Lett.* **2014**, *24* (7), 1856–1861.
- (26) Bera, S.; Zhanel, G. G.; Schweizer, F. Design, Synthesis, and Antibacterial Activities of Neomycin-Lipid Conjugates: Polycationic Lipids with Potent Gram-Positive Activity. *J. Med. Chem.* **2008**, *51* (19), 6160–6164.
- (27) Wang, Y.; Cheetham, A. G.; Angacian, G.; Su, H.; Xie, L.; Cui, H. Peptide–Drug Conjugates as Effective Prodrug Strategies for Targeted Delivery. *Adv. Drug Deliv. Rev.* **2017**, *110–111*, 112–126.
- (28) Rothbard, J. B.; Garlington, S.; Lin, Q.; Kirschberg, T.; Kreider, E.; McGrane, P. L.; Wender, P. A.; Khavari, P. A. Conjugation of Arginine Oligomers to Cyclosporin A Facilitates Topical Delivery and Inhibition of Inflammation. *Nat. Med.* **2000**, *6* (11), 1253–1257.
- (29) Samuel, B. U.; Hearn, B.; Mack, D.; Wender, P.; Rothbard, J.; Kirisits, M. J.; Mui, E.;

- Wernimont, S.; Roberts, C. W.; Muench, S. P.; Rice, D. W.; Prigge, S. T.; Law, A. B.; McLeod, R. Delivery of Antimicrobials into Parasites. *Proc. Natl. Acad. Sci. U. S. A.* **2003**, *100* (SUPPL. 2), 14281–14286.
- (30) Lei, E. K.; Pereira, M. P.; Kelley, S. O. Tuning the Intracellular Bacterial Targeting of Peptidic Vectors. *Angew. Chem, Int. Ed.* **2013**, *52* (37), 9660–9663.
- (31) Pereira, M. P.; Shi, J.; Kelley, S. O. Peptide Targeting of an Antibiotic Prodrug toward Phagosome-Entrapped Mycobacteria. *ACS Infect. Dis.* **2016**, *1* (12), 586–592.
- (32) Brezden, A.; Mohamed, M. F.; Nepal, M.; Harwood, J. S.; Kuriakose, J.; Seleem, M. N.; Chmielewski, J. Dual Targeting of Intracellular Pathogenic Bacteria with a Cleavable Conjugate of Kanamycin and an Antibacterial Cell-Penetrating Peptide. *J. Am. Chem. Soc.* **2016**, *138* (34), 10945–10949.
- (33) Antonoplis, A.; Zang, X.; Wegner, T.; Wender, P. A.; Cegelski, L. Vancomycin-Arginine Conjugate Inhibits Growth of Carbapenem-Resistant *E. Coli* and Targets Cell-Wall Synthesis. *ACS Chem. Biol.* **2019**, *14* (9), 2065–2070.
- (34) Mühlberg, E.; Umstätter, F.; Domhan, C.; Hertlein, T.; Ohlsen, K.; Krause, A.; Kleist, C.; Beijer, B.; Zimmermann, S.; Haberkorn, U.; Mier, W.; Uhl, P. Vancomycin-Lipopeptide Conjugates with High Antimicrobial Activity on Vancomycin-Resistant Enterococci. *Pharmaceuticals* **2020**, *13* (6).
- (35) Umstätter, F.; Domhan, C.; Hertlein, T.; Ohlsen, K.; Mühlberg, E.; Kleist, C.; Zimmermann, S.; Beijer, B.; Klika, K. D.; Haberkorn, U.; Mier, W.; Uhl, P. Vancomycin Resistance Is Overcome by Conjugation of Polycationic Peptides. *Angew. Chem, Int. Ed.* **2020**, *59* (23), 8823–8827.
- (36) Nicholas, D. S.; Michelle, A. O.; Kathryn, E. U. Antibiotic-Containing Polymers for Localized, Sustained Drug Delivery. *Adv. Drug Deliv. Rev.* **2014**, *1* (848), 77–87.
- (37) Jiang, Y.; Han, M.; Bo, Y.; Feng, Y.; Li, W.; Wu, J. R.; Song, Z.; Zhao, Z.; Tan, Z.; Chen, Y.; Xue, T.; Fu, Z.; Kuo, S. H.; Lau, G. W.; Luijten, E.; Cheng, J. “Metaphilic” Cell-Penetrating Polypeptide-Vancomycin Conjugate Efficiently Eradicates Intracellular Bacteria via a Dual Mechanism. *ACS Cent. Sci.* **2020**, *6* (12), 2267–2276.
- (38) Gauthier, M. A.; Klok, H. A. Peptide/Protein-Polymer Conjugates: Synthetic Strategies and Design Concepts. *Chem. Commun.* **2008**, No. 23, 2591–2611.

- (39) Lacey, R. W. Mechanism of Action of Trimethoprim and Sulphonamides: Relevance to Synergy *in Vivo*. *J. Antimicrob. Chemother.* **1979**, *5*, 75–83.
- (40) Charvalos, E.; Tzatzarakis, M. N.; Van Bambeke, F.; Tulkens, P. M.; Tsatsakis, A. M.; Tzanakakis, G. N.; Mingeot-Leclercq, M. P. Water-Soluble Amphotericin B-Polyvinylpyrrolidone Complexes with Maintained Antifungal Activity against *Candida* Spp. and *Aspergillus* Spp. and Reduced Haemolytic and Cytotoxic Effects. *J. Antimicrob. Chemother.* **2006**, *57* (2), 236–244.
- (41) Melkoumov, A.; Goupil, M.; Louhichi, F.; Raymond, M.; De Repentigny, L.; Leclair, G. Nystatin Nanosizing Enhances *in Vitro* and *in Vivo* Antifungal Activity against *Candida Albicans*. *J. Antimicrob. Chemother.* **2013**, *68* (9), 2099–2105.

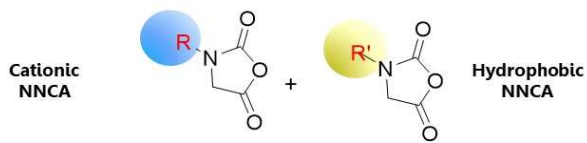
General conclusions

The goal of this Ph.D. thesis was to develop a medicinal chemistry approach to design antimicrobial polypeptoids capable of killing *C. difficile*. By mimicking the amphiphilic structure of AMPs, we prepared cationic copolymers combining lysine-like and phenylalanine-like monomer units to merge enhanced protease resistance with the ability to destabilize the membrane of *C. difficile*. Studying structure-activity relationships (SAR) we first varied the polymers hydrophobic content, the polymerization degree and the nature of the polymerization initiator to design active macromolecules through a rational design. Then, we pushed the use of polymer chemistry towards macromolecular engineering to compare the efficiency of antimicrobial polypeptoids in cyclic, star-like and drug-conjugates architectures.

All these amphiphilic copolymers were prepared by using the ring-opening polymerization (ROP) of *N*-alkylated *N*-carboxyanhydride (NNCA) monomers. We successfully prepared those NNCA building blocks in a gram scale with high yields by establishing a two-steps synthesis involving reductive amination followed by cyclization through the Leuchs method with *N*-Boc protected derivatives. We also performed a complete study of the NNCA ring-opening polymerization: first, the ROP kinetics showed that both the inductive effect and the steric hindrance of the *N*-alkylation influenced the kinetic rates. Second, copolymerization reactions combined with selective deprotection enabled us to prepare series of cationic copolymers varying different structural parameters (side chains, polymerization degree, initiator, etc.). Finally, we developed a simple route to cyclic poly(α -peptoids) from NNCA using LiHMDS promoted ring-expansion polymerization (REP) in DMF. This new method allowed the unprecedented use of lysine-like monomers in REP to design antimicrobial macrocycles.

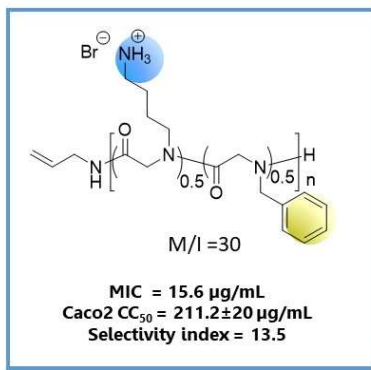
The series of amphiphilic copolypeptoids prepared in this research work were used to achieve a comprehensive SAR study against *C. difficile*: we found that both parameters, the hydrophobic content and the choice of the hydrophobic side chains, were crucial to prepare active compounds. Polypeptoids bearing Nphe and Nlys, having a polymerization degree of 30 and a hydrophobic content of 50%, were the most active linear copolymers (MIC = 15.6 μ g/mL) and the less toxic toward Caco-2 cells (CC₅₀ = 211 μ g/mL, selectivity index of SI = 13.5). The same monomer units were used to optimize the antimicrobial activity of cyclic copolymers and we obtained an even more active polypeptoid (MIC = 12.5 μ g/mL) that was also less toxic towards

Caco-2 cells ($CC_{50} = 208 \mu\text{g/mL}$, $SI = 17$). Those active macrocycles were built by mixing the monomer units randomly, at a hydrophobicity content of 50% and for a polymerization degree close to 30. Pushing the limits of ROP, we finally prepared star-like and drug conjugate polypeptoids bearing Nlys and Nphe monomer units to enhance the anti-*C. difficile* activity through macromolecular engineering and the studies demonstrated that they were not active against *C. difficile*. Moreover, an extension of the antibacterial studies towards other bacterial strains showed that star-like polypeptoids were active against the Gram-negative *B. fragilis* with a MIC value of $7.8 \mu\text{g/mL}$ (8 arms, polymerization degree of 30, 50% hydrophobic content). In the case of the drug-conjugates vancomycin was the most active having MIC value of $7.8 \mu\text{g/mL}$ and a selectivity index of $SI = 15.5$. Furthermore, this new polypeptoid platform demonstrated destabilization of bacterial membranes *in vitro* through the liposomal models and they presented resistance to trypsin.

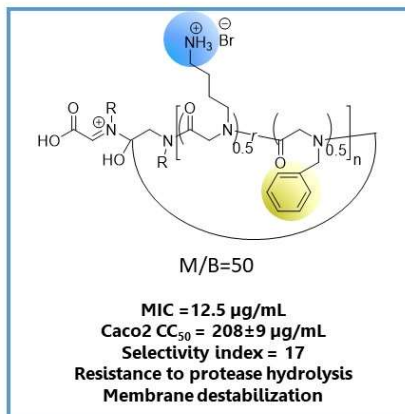


ROP SAR study REP SAR study ROP

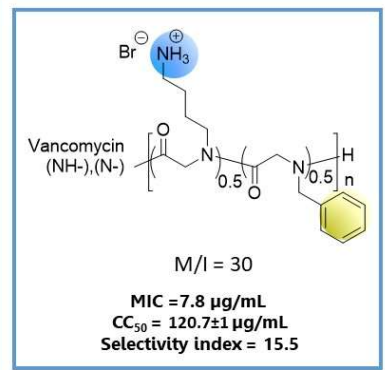
Polypeptides anti-*Clostridioides difficile*



Linear copolypeptides



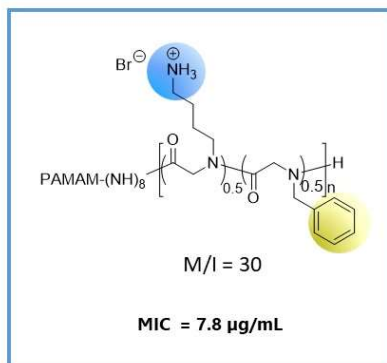
Cyclic copolypeptides



Drug-conjugate copolypeptides



Polypeptides anti-*B. fragilis*



Star-like copolypeptides



Perspectives

The ROP of NNCAAs was a versatile and facile polymerization route that allowed us to prepare a variety of macromolecules with antibacterial properties against serious pathogens such as *C. difficile*. Even if we performed a comprehensive study that afforded good antimicrobial efficacy, even more active or selective compounds could be prepared by implementing new studies with the following design: a) using new NNCAAs with other aromatic moieties such as naphthyl, b) using new NNCAAs with other cationic moieties such as guanidinium, c) using new NNCAAs with anionic precursors, d) better comparing statistical copolymers with block copolymers, e) targeting higher polymerization degree. These studies can be performed following the methodologies described in this Ph.D. work.

On another hand, in this study, we only explored the antimicrobial activity on the active form of *C. difficile* but it can be interesting to perform more studies on the dormant spores. Moreover, the first cytotoxic results showed sometimes low toxicity towards Caco-2 cells but *in vivo* studies are necessary to demonstrate that the polymers can be administered orally. This *in vivo* study should also involve an evaluation of the subacute and acute toxicity. Finally, we briefly presented an evaluation of the MIC selectivity by performing studies with a variety of Gram-negative and Gram-positive bacteria but it can be interesting to narrow this scope to evaluate the selectivity towards the intestinal microbiota. Moreover, if the molecules will present a large spectrum of action they can be useful for coating in medical devices, food packing and other applications.

From a more general perspective, the new macromolecular polypeptoids (linear, cyclic, star-like and drug conjugates) carried cationic and hydrophobic side chains. Thus, it is possible that among the copolymers synthesized in this Ph.D. work, some of them could present lower critical solubility temperature (LCST). Moreover, some of those copolypeptoids could be used as drug delivery systems, in particular the star-like polypeptoids.